Western Graduate&PostdoctoralStudies

Western University
Scholarship@Western

Electronic Thesis and Dissertation Repository

7-16-2024 10:00 AM

Exploring the Chemistry of Bis(azido)phosphine Chalcogenides and the Pursuit of Isolable Phosphinidene Chalcogenides

John Lortie, *Western University*

Supervisor: Ragogna, Paul J., *The University of Western Ontario*
A thesis submitted in partial fulfillment of the requirements for the Doctor of Philosophy degree in Chemistry

© John Lortie 2024

Follow this and additional works at: https://ir.lib.uwo.ca/etd

Part of the Inorganic Chemistry Commons

Recommended Citation

Lortie, John, "Exploring the Chemistry of Bis(azido)phosphine Chalcogenides and the Pursuit of Isolable Phosphinidene Chalcogenides" (2024). *Electronic Thesis and Dissertation Repository*. 10291.
https://ir.lib.uwo.ca/etd/10291

This Dissertation/Thesis is brought to you for free and open access by Scholarship@Western. It has been accepted for inclusion in Electronic Thesis and Dissertation Repository by an authorized administrator of Scholarship@Western. For more information, please contact wlswadmin@uwo.ca.

Abstract

The study of low-coordinate species and the pursuit of interesting bonding motifs has revealed new reactivity modes for main-group compounds, akin to transition metals, in the past two decades. An underexplored class of two-coordinate phosphorus compound is a phosphinidene sulfide, which has yet to be isolated in the solid-state with an accompanying crystal structure. This dissertation explores strategies towards the synthesis and reactivity of low-coordinate phosphinidene chalcogenide species, and related compounds supported by strongly pi-donating or weakly pi-donating environments. While the primary synthetic targets remained elusive, significant discoveries were made towards new methods of preparing electron rich phosphines, and the dual-reactivity modes of bis(diisopropylamino)cyclopropenone to generate a chlorophosphonate or cyclic phosphonates. **Chapter 2** outlines the strategies pursued for the generation of a phosphinidene sulfide utilizing a π-donating N-heterocyclic imine (NHI) ligand. Although synthesis of the desired species was not achieved, solid-state structures of new phosphorus-chalcogenide species were serendipitously obtained. These results suggested that the NHI was not adequate to stabilize a phosphinidene sulfide, and would require a bulkier ligand. **Chapter 3** explores a novel family of bis(azido)phosphines and their participation in chemoselective Staudinger reactions with secondary or tertiary phosphines to produce chiral phosphines. A tautomeric equilibrium of species was analyzed by ^{31}P-^{31}P nuclear Overhauser effect spectroscopy (NOESY). Thermogravimetric analysis (TGA) provided insights into the thermal stability of these compounds. Density functional theory (DFT) suggested that the observed chemoselectivity was a result of energetically inaccessible lowest unoccupied molecular orbitals (LUMOs) with appropriate N_3 π^* character. **Chapter 4** introduces a new synthetic approach for synthesis of a chlorophosphonate ($\mathbf{4.3_{BAC}}$) and cyclic phosphonates ($\mathbf{4.18_{Ph}}$ and $\mathbf{4.18_{Mes}}$), using $\boldsymbol{C_3O}$ and PCl_3 or $RP(O)Cl_2$. Pasteur separation allowed for structural characterization of $\mathbf{4.3_{BAC}}$ and $\mathbf{[}\boldsymbol{C_3Cl}\mathbf{]Cl}$ by-product, but an efficient separation method was not discovered. An intermediate $\mathbf{[4.6_{BAC}]^+}$ was detected and hydrolysis species were investigated. Reactivity of $\mathbf{4.3_{BAC}}$ with various Lewis acids was screened, and the *in situ* generation of monomeric dioxophosphoranes was reported.

This thesis highlights the complexities of isolating low-coordinate phosphorus chalcogenide species, while offering a new synthetic strategy for the synthesis of chiral phosphines and α-cationic dioxophosphoranes.

Keywords

Phosphorus • Chalcogen • Phosphinidene Chalcogenide • Phosphinidene Dichalcogenide • Dioxophosphorane • Phosphonate • Structure and Bonding • Main-Group Chemistry

Summary for Lay Audience

Phosphorus is an element that is ubiquitous all around us. It is found in biological systems, in everyday products like detergents, and in important chemicals such as herbicides, pesticides, and fertilizer. It is also important in the production of fine chemicals found in pharmaceuticals, and tailored ligands in catalysis. One reason that phosphorus is so versatile is the ability to adopt a diverse set of structural motifs, and easily bonds with group 16 elements like oxygen, sulfur, and selenium (known as chalcogens). Development of new methods for producing phosphorus-containing molecules can therefore impact many industries. To achieve this, such advancements can come from a greater understanding of the influence of structure and bonding on reactivity, which is why the isolation of highly reactive species can be of value. These highly reactive species are often fleeting (short-lived) intermediates, but can be challenging to detect. Strategies have thus been developed, using either bulky protecting groups or electron-rich groups to stabilize (and isolate) many highly reactive molecules.

In this thesis, a series of underexplored of phosphorus-chalcogenide motifs supported by either electron-rich or electron-poor groups were investigated. Although no evidence of the formation of the primary synthetic target of this work was found, two different motifs were each explored. The first motif was built of a phosphorus atom connected to groups of three-nitrogen atoms, in series, called an azide (N_3). Although two azide groups were present, only one of the azides could be converted by a known reaction. This selectivity was observed for each combination of reagents screened, therefore offering an easy method for tunability of the products. The final motif explored contained a phosphorus atom attached to two oxygen atoms, but was prepared by an unexpected exchange of an oxygen with two chlorine atoms. The method developed was also used for the preparation of other known and valuable products.

Co-Authorship Statement

The work described in chapters 2 and 4, including the synthesis and characterization of all compounds reported, initial and final drafts, and editing was performed by John L. Lortie. Paul J. Ragogna provided significant edits. Crystallographic solutions and refinements were performed by Paul D. Boyle.

The work described in chapter 3 was from a previously published manuscript, co-authored by John L. Lortie, Matthew Davies, Paul D. Boyle, Mikko Karttunen, and Paul J. Ragogna (*Inorganic Chemistry*, Published online March 22, 2024). JLL was responsible for the synthesis and characterization of all compounds reported, initial and final drafts, and editing. MD provided assistance with computational experiments. PDB was responsible for collection and refinement of all X-ray diffraction data. MK and PJR edited the manuscript. Solutions for high-resolution mass-spectrometry analyses were prepared by JLL then run by Chathu Pulukkody.

Acknowledgments

It has been a wild ride until now. I am here today due to the guidance, support, and sacrifices from so many friends, family, and supervisors. I would like start by thanking my supervisor Paul Ragogna for his support throughout my research. Paul continually encouraged me to develop my skills as a researcher and communicator, and I appreciate his patience during the hurdles of this research. I feel empowered to now say that Paul, you are wrong and carrot cake is in fact delicious! Thank you to Dr. Nikonov who instilled a love of inorganic chemistry and deconvoluting complex NMR spectra. I am grateful for the opportunities and respect offered to me. Thank you to my collaborators at Western: Paul Boyle, Mat Willans, Aruni Pulukkody, Mikko Karttunen. Your expertise has been invaluable to me during the completion of this degree.

To the Nikonov crew – I want you to know that I keep our old conference photos at my desk and I smile every time I see them! Now, thank you to the past and present students and post-docs of the Ragogna group. I am grateful to have had the pleasure of working with {*inhales deeply*}: Vanessa, Tristan, Linkin, Kelly, Alex W, Carmen, Justin, Jessica, Jeff, JW, Jeanette, Alex V, Blaine, Jordan, Golnoosh, Mehrnoosh, Ian, Monica, Sofia, Gabby, Scott, Yasmeen, Erica, Megan, Matt, Marco, and Ellie. From the discussing chemistry over Tims runs, chalk talks, and manuscript editing; to the happiness over sushi burritos, barbeques, and a murder mystery party, you all have been integral parts in my life over the past 5 years. Vanessa's "No Rules Friday" mantra resonated with me and led to the chemistry of my final chapter. Kelly, Jeanette, and Alex, our "BGS 2006" Spotify playlist is still in my personal rotation today. Thank you, Matt, for your expertise and time spent with me trying to troubleshoot DFT calculations. Thank you, Alex V. for your excellent advice, both in-lab and professionally. Thank you Jeff for always making sure the coffee maker was good-to-go with morning coffee. Thank you to the lab's fun enforcers, Justin and Jessica: you definitely made grad school much more bearable with the movie nights, kahoots, 3D printed doodads, and non-stop memes. Justin, you may have to take the torch for Secret Santa this year. Ian (a.k.a. Father ZAAC), I enjoyed our talks about music and music trivia. Thank you for introducing me to "bardcore", and sharing that the lead singer of the offspring has a PhD in molecular biology. Also, thank you to you and Gabby for the laughs over the Iggy Izalea look-alike.

Blaine, I am so happy that we really got to know each other at the CSC conference, our adventure to Stanley Park, and many conversations at the grad club. Thank you for being a good friend, indulging me with interesting chemistry problems, and always answering my “Hey Blaaaine…”.

Now to JW – our friendship started at back Brock and continued in the same lab at Western. It has been great to have a friend like you on the same wavelength, who I am free to be my quirky self. You brought me into your friend group with that fateful Shadowrun campaign, and I was humbled to be by your side at your wedding. You have always been a shoulder to lean on and my trusted confidant. I have seen your evolution into the clever and thoughtful researcher you are today. I wish great things for you in the future, and hopefully that includes a DnD campaign – I havn’t forgotten about it.

I would also like to extend my gratitude to my friends at Forst City Toastmasters to Toastmasters friends and supporters. It has been a pleasure knowing you and growing together. A special thank you to Jimmy Chien: you have been a wonderful role model and friend. Your motivation and friendship empowered me and helped improve confidence in myself.

A massive thank you to Joanne and Greg. You accepted me as family and did everything you could for Jen and I. You are examples of what can be achieved with a strong work ethic and an attention to detail. You helped us get our first house, were there for us when we needed help, and you brought the sweetest dogs, Mona and Waldo, into our lives.

To my wonderful girlfriend and partner-in-crime, Jen. I am eternally grateful to you and the sacrifices you made so we could come to London together. I know those early 3 AM starts couldn’t have been easy, but you never cease to amaze me with your drive and stick-to-itiveness. You are also so close to finishing your degree and I am so proud of you! Just remember, you’re strong, intelligent, and (maybe a little) hard-headed, but “this is your power”. I know you will achieve greatness and I am excited for the next chapter in our lives together. I love you.

To my family, and specifically Mom, Dad, Melissa, Grandma and Papa – I can finally say that I’m finished… it only took 15 years of post-secondary education to get here… I have so much gratitude for your financial and emotional support for as long as I can remember. You all placed me in your top priorities. Over the years it went from checking my homework, drives to and from school, and daily lunches; to the weekend trips, care packages, and phone calls that let me know you're thinking of me. I hope I have made you proud and earned all that you sacrificed for me.

Table of Contents

Abstract ii

Summary for Lay Audience iv

Co-Authorship Statement v

Acknowledgments vi

Table of Contents ix

List of Tables xiv

List of Figures xv

List of Schemes xxi

List of Appendices xxvi

List of Abbreviations xxxvii

Chapter 1 1

1 Introduction 1

- 1.1 Advancements in Fundamental Main Group Chemistry 1
- 1.2 Why Study Main Group Species? 3
- 1.3 Stabilizing Reactive Phosphorus Species 5
  - 1.3.1 General Considerations 5
  - 1.3.2 Classifying Bonding in Main Group Compounds 8
  - 1.3.3 Strong σ and π-Donating Ligands 10
  - 1.3.4 Strong σ-Donor, Poor π-Acceptor Ligands 12
- 1.4 Phosphinidene Chalcogenides (RPCh) 15
  - 1.4.1 Theory 15
  - 1.4.2 Generation 17
  - 1.4.3 Isolation 24
- 1.5 Dichalcogoxophosphroanes ($RPCh_2$) 31

1.5.1 Theory 31

1.5.2 Generation 35

1.5.3 Isolation 40

1.6 Structure and Aim of This Thesis 45

1.7 References 47

Chapter 2 66

2 Molecular Structures of N-heterocyclic Imine Supported Phosphine Chalcogenides $[IPrNPS]_2SO$ and $(IPrN)_2P(O)H$ 66

2.1 Introduction 66

2.2 Results and Discussion 69

2.2.1 Synthesis of Precursors 69

2.2.2 Transformation Pathway A 70

2.2.3 Transformation Pathway B 71

2.2.4 Transformation Pathways C to F 82

2.2.5 Transformation Pathway G 83

2.2.6 Structural Analysis of NHI-Supported Phosphine Compounds 85

2.3 Conclusion 86

2.4 Experimental Section 87

2.4.1 Modified Synthesis of $IPrNPCl_2$ (**2.6**) 88

2.4.2 Synthesis of **[2.7]Cl** 88

2.4.3 Synthesis of **2.8** 89

2.4.4 *In situ* generation of **[2.9]Cl** 89

2.4.5 $IPrNPCl_2$ and $S(SiMe_3)_2$ Reaction Mixture Analysis 90

2.4.6 Synthesis of $IPrNPSCl_2$ (**2.14**) 90

2.4.7 Attempted Synthesis of $IPrNPS(N_3)_2$ (**2.15**) *Via* Condensation of **2.14** With $SiMe_3N_3$ 91

2.4.8 Attempted Thermolysis of $IPrNPS(N_3)_2$ (**2.15**) 91

2.4.9 Photolysis of IPrNPS(N_3)$_2$ (**2.15**) 91

2.5 X-ray Crystallographic Details 92

2.6 References 95

Chapter 3 99

3 Chemoselective Staudinger Reactivity of Bis(azido)phosphines Supported With A π-Donating Imidazolin-2-Iminato Ligand 99

3.1 Introduction 99

3.2 Results and Discussion 102

3.2.1 Synthesis and Characterization of Bis(azido)phosphine Compounds 102

3.2.2 Staudinger Reactivity of Bis(azido)phosphines 105

3.3 X-ray Crystallography 108

3.4 Computational Investigation 110

3.5 Conclusions 112

3.6 Experimental Section 113

3.6.1 General Considerations 113

3.6.2 Modified Synthesis of IPrNPCl$_2$ 114

3.6.3 Synthesis of IPrNP(N_3)$_2$ (**3.2**) 115

3.6.4 Synthesis of IPrNP($NSiMe_3$)(N_3)$_2$ (**3.3**) 115

3.6.5 Synthesis of IPrNPS(N_3)$_2$ (**3.4S**) 116

3.6.6 Synthesis of IPrNPSe(N_3)$_2$ (**3.4Se**) 117

3.6.7 Synthesis of IPrNPO(N_3)$_2$ (**3.4O**) 117

3.6.8 Synthesis of IPrNP(S)(N_3)($NPMe_3$) (**3.5**$_{\mathbf{Me}}$) 118

3.6.9 Synthesis of IPrNP(S)(N_3)($NPCy_3$) (**3.5**$_{\mathbf{Cy}}$) 119

3.6.10 Synthesis of IPrNP(S)(N_3)($NPPh_3$) (**3.5**$_{\mathbf{Ph}}$) 120

3.6.11 Synthesis of IPrNP(S)(N_3)[NP(H)Cy_2] (**3.6a**) and IPrNP(S)(N_3)[N(H)PCy_2] (**3.6b**) 121

3.6.12 Synthesis of IPrNPN_3NPMe_3 (**3.7**) 123

3.6.13 Reaction of **3.7** with Excess S_8 To Generate **3.5$_{Me}$** 124

3.6.14 X-ray Crystallographic Data 124

3.7 References 127

Chapter 4 136

4 Facile Cyclopropenium Functionalization of PCl_3 and Redistribution of $RP(O)Cl_2$ Species with Bis(diisopropylamino)cyclopropenone 136

4.1 Introduction 136

4.2 Results and Discussion 142

4.2.1 Reaction of ***C$_3$O*** with *In Situ* Generated **[4.6$_{BAC}$]Cl** 142

4.2.2 Stages of Hydrolysis of **4.3$_{BAC}$** 146

4.2.3 Mechanistic Investigations 149

4.2.4 Reactivity of **4.3$_{BAC}$** 151

4.2.5 Comparison of ^{31}P NMR Spectroscopy Shifts of Related Onio-Substituted Oxo-Phosphorus Species 166

4.2.6 Application Towards Synthesis of $(ArPO_2)_3$ 168

4.3 Conclusions 171

4.4 Experimental Section 172

4.4.1 Modified Single Pot Procedure of ***C$_3$O*** Synthesis 172

4.4.2 Synthesis and Characterization of **4.3$_{BAC}$** and **[*C$_3$*Cl]Cl** 173

4.4.3 Synthesis and Characterization of **[4.21$_{mono}$]**Cl 175

4.4.4 Reactions of **4.3$_{BAC}$** and **[*C$_3$*Cl]Cl** With Lewis Bases 176

4.4.5 Synthesis and Characterization of **[4.17$_{DMAP}$]**Cl and **[4.24]Cl$_2$** 178

4.4.6 Reaction of **4.3$_{BAC}$** With $LiBF_4$ 180

4.4.7 Synthesis and Characterization of **[4.17$_{mono}$]OTf** and **[*C$_3$*Cl]**OTf 181

4.4.8 Synthesis of **[4.21$_{mono}$]OTf** 182

4.4.9 Reactions of **4.3$_{BAC}$** and BCF 182

4.4.10 *In Situ* Generation of **4.18$_{Ph}$** 184

    4.4.11 Synthesis of **4.18**$_{\mathbf{Mes}}$ 184

  4.5 X-ray Crystallographic Data 185

  4.6 References 187

Chapter 5 193

5 Conclusions and Future Work 193

  5.1 Summary and Conclusions 193

  5.2 Future Work 195

    5.2.1 Stabilization of Monomeric Phosphinidene Sulfide 195

    5.2.2 Reactivity of Bis(azido)phosphines 196

    5.2.3 Exploration of the Chemistry of Dichalcogoxophosphoranes and Dialkylcyclopropenones 197

  5.3 References 201

Appendices 204

Curriculum Vitae 288

List of Tables

Table 2-1. Summary of X-ray diffraction collection and refinement details for compounds **[2.7]Cl**, **2.10**, and **2.13**. 94

Table 3-1. Summary of X-ray diffraction collection and refinement details for compounds **3.2**, **3.4S**, **3.4Se**, and **3.5**$_{\mathbf{Cy}}$.. 126

Table 4-1. Table of related phosphine species (extended from reference[10]). Highlighted entries are species from this work.. 167

Table 4-2. Summary of X-ray diffraction collection and refinement details for compounds in chapter 4.. 186

List of Figures

Figure 1-1. The first examples of trivalent phosphorus species exhibiting multiple bond character (**1.1**, **1.2**, **1.3**$_{\textbf{Mes*}}$), and the first disilene (**1.4**).[7,8] 2

Figure 1-2. The first isolated example of a singlet carbene (**1.5**), first isolated N-heterocyclic carbene (NHC, **1.6**), and an early example of a heavy element analogue of a carbene (**1.7**)... 3

Figure 1-3. Low-coordinate phosphorus compounds: A) Sterically demanding diphosphenes; B) metal-coordinated phosphinidene; C) a room temperature stable singlet phosphinidene.[5,34–36] 6

Figure 1-4. Examples of canonical forms **[1.25]**$^{3+}$.[51] 9

Figure 1-5. Resonance structures for an ylide and isolobal relationships with other ligands. 10

Figure 1-6. Resonance structures contributing to stabilization of bis(amino)cyclopropenylidene and bis(amino)cyclopropenium.. 13

Figure 1-7. Sequence of energies (in eV) of the orbitals s and π, π* for HP=X, obtained from complete energy-optimized ab initio STO/3G calculations.[89] 17

Figure 1-8: Selected examples of precursors used to generate RP=S intermediates. 18

Figure 1-9. Examples of oligomeric dichalcogoxophosphoranes.[121,122,125,127,128] 33

Figure 1-10. Examples of base-stabilized chlorophosphonates.[133–136] 34

Figure 1-11. Structurally characterized cyclic phosphonates by Manners and co-workers.[121] 36

Figure 2-1. A) Selected examples of phosphinidene-sulfide precursors;[1,2,4,5,8] B) ylide-substituted thioxophosphanes reported by Schmidpeter and coworkers;[9] C) dimeric (Ar*PS)$_2$ reported by Ragogna group;[7] D) Lawesson's reagent.[10] 67

Figure 2-2. Stack plot of $^{31}P\{^{1}H\}$ NMR spectra of the reaction of **2.6** and Na_2S in CH_3CN. Aliquot taken after three days (top, green); after four days (middle, red); after seven days (bottom, blue). 72

Figure 2-3. $^{31}P\{^{1}H\}$ NMR spectra of the reaction of **2.6** with Na_2S, in different solvents, after 16 h: CH_2Cl_2/THF (top, red); acetonitrile (bottom, blue). 73

Figure 2-4. Side-by-side comparison of compound **2.6** (left) and the crude compound **2.8** (right). 73

Figure 2-5. Stack plot of $^{31}P\{^{1}H\}$ NMR spectra during different stages of isolation of **2.8**. (Top) Seven-day reaction aliquot of Na_2S, **2.6**, and DMF at room temperature; (Middle) Precipitate collected after cooling the reaction mixture to -30 °C in freezer over two days (CD_3CN); (Green) toluene-rinsed precipitate. 75

Figure 2-6. Reaction of **2.8** with sulfur in CD_3CN to generate the hypothetical species **2.8S**. 76

Figure 2-7. Selected examples of phosphorus-sulfur compounds. A) Neutral species reported by Dielmann and coworkers. B) Monomeric and dimeric dithioxophosphorane examples. Mox = 2,4-di-t-butyl-6-methoxyphenyl. C) Monomeric and dimeric NHI-supported species potentially formed after reaction with Na_2S. 77

Figure 2-8. $^{31}P\{^{1}H\}$ NMR spectrum of a sample of the crude reaction mixture of $IPrNPCl_2$ and PMe_3 in CH_2Cl_2 after 15 min. Unknown species denoted (*). 78

Figure 2-9. Stack plot of $^{31}P\{^{1}H\}$ and ^{31}P NMR spectra of products formed from the reaction of **2.6** and $S(SiMe_3)_2$. Reaction aliquot taken after 40 min (top, green); $^{31}P\{^{1}H\}$ (middle, red) and ^{31}P (bottom, blue) spectra of isolated material (**2.11** and **2.12**). 80

Figure 2-10. ^{1}H-^{1}H NOESY spectra of **2.11** and **2.12** after warming to room temperature (redissolved in $CDCl_3$). Cross peak in blue (positive phase) shows chemical exchange of broad resonances. Cross peaks in red (negative phase) show NOE signal enhancement. 81

Figure 2-11. $^{31}P\{^{1}H\}$ NMR spectrum of a reaction aliquot of **2.14** and $SiMe_3N_3$ after 72 h at 60 °C. Approximately 4 % conversion to $IPrNPS(N_3)_2$ (**2.15**; δ_P = 38.9 ppm) was observed. 83

Figure 2-12. Comparison of phosphinonitrene stabilizations. Stabilized phosphinonitrene[17] by delocalization through central phosphorus lone pair (top) and hypothetical nitrene intermediate lacking π-donation from central phosphorus atom (bottom). 84

Figure 2-13. Solid-state structures of **[2.7]Cl** (chloride anion omitted), IPrN$_2$P(O)H (**2.13**), and (IPrNPS)$_2$SO (**2.10**). Hydrogens have been omitted and Dipp substituents have been represented as wireframes for clarity, and ellipsoids shown at the 50% probability level..... 86

Figure 3-1. Mercury-rendered ORTEP style drawing of **3.2**, **3.4S**, **3.4Se** and **3.5$_{Cy}$**. Hydrogen atoms have been omitted for clarity and selected ellipsoids shown at the 50% probability level. Azido, imino, and phosphinimino nitrogen atoms, phosphorus atoms, and chalcogen labels have been displayed. 109

Figure 3-2. TGA plot of compounds **3.2**, **3.4S**, and **3.5$_{Me}$** [10 °C/min, performed in air under flow of N$_2$ (10 mL/min)]. 110

Figure 3-3. Molecular structures studied by DFT. 111

Figure 3-4. Kohn-Sham orbitals of **I** and **II** at B3LYP/Def2-TZVP level of theory[52–56] with D4 dispersion correction.[57,58] Yellow colour illustrates negative phase and blue illustrates positive phase of orbitals. The HOMO of **I** (A) and **II** (B). The N$_3$ π* character seen in **I** at the LUMO (-0.98 eV) level (C) is not observed until the LUMO+4 (-0.023 eV) level in **II** (D). Hydrogen atoms have been omitted for clarity. 112

Figure 4-1. Selected examples of stabilized PO and PO$_2$ species. 136

Figure 4-2. Examples of dichalcogoxophosphoranes. A) Monomeric dithioxophosphoranes and diselenoxophosphorane.[23,24] B) Dimeric Lawesson's reagent (LR) and Woolen's reagent (WR).[25,26] C) Dimeric dioxophosphorane.[21] 139

Figure 4-3. Resonance structures of BAC ligand. 140

Figure 4-4. ^{1}H NMR spectra of isolated **[*C*$_3$Cl]Cl** (block-like crystal, top) and **4.3$_{BAC}$** (needle-like crystal, bottom) in CDCl$_3$. 143

Figure 4-5. High-resolution mass spectrum of a sample containing **[*C*$_3$Cl]Cl** and **4.3$_{\text{BAC}}$**, redissolved in acetonitrile. 144

Figure 4-6. Mercury-rendered ORTEP style drawings of **[*C*$_3$Cl]ClHCl**, **[*C*$_3$Cl]PCl$_4$**, and **4.3$_{\text{BAC}}$**. Hydrogen atoms have been omitted for clarity and selected ellipsoids shown at the 50% probability level. 145

Figure 4-7. ^{1}H and ^{31}P{^{1}H} (inset) NMR spectra of **[4.21$_{\text{mono}}$]Cl** in CDCl$_3$, hydrolyzed in air. 147

Figure 4-8. ^{31}P{^{1}H} spectrum of a partially hydrolyzed sample of **4.3$_{\text{BAC}}$** and **[*C*$_3$Cl]Cl**, redissolved in CDCl$_3$ in a J-Young NMR tube. Image on the right contains zoomed in signal for **4.21$_{\text{di}}$**, and the labelled coupling values. 148

Figure 4-9. Plot of normalized ^{31}P{^{1}H} resonance integrations over time of a two-to-one reaction of bis(diisopropylamino)cyclopropenone (***C*$_3$*O***) and PCl$_3$.................................... 149

Figure 4-10. Stacked ^{31}P and ^{31}P{^{1}H} NMR spectra of the reaction of a 50:50 mixture of **4.3$_{\text{BAC}}$** and **[*C*$_3$Cl]Cl** with excess EtOH. Top: ^{31}P{^{1}H} NMR spectrum after 10 min. Middle: ^{31}P NMR spectrum (no decoupling) after 15 min. Bottom: ^{31}P{^{1}H} NMR spectrum after 5 d. 152

Figure 4-11. Stacked ^{31}P and ^{31}P{^{1}H} NMR spectra of the reaction of a 50:50 mixture of **4.3$_{\text{BAC}}$** and **[*C*$_3$Cl]Cl** with HN*i*-Pr$_2$. Asymmetric diphosphonate (**4.23$_{\text{Nipr2}}$**); dimeric (**4.21$_{\text{di}}$, !**) and trimeric (**4.21$_{\text{tri}}$,** †) hydrolysis products shown. 154

Figure 4-12. Stacked ^{31}P{^{1}H} NMR spectra of the reaction of a 50:50 mixture of **4.3$_{\text{BAC}}$** and **[*C*$_3$Cl]Cl** with excess pyridine. Possible pyridine adduct (*); Trimeric (**4.21$_{\text{tri}}$**, †) hydrolysis products shown. 155

Figure 4-13. Stacked ^{31}P and ^{31}P{^{1}H} NMR spectra of the reaction of a 50:50 mixture of **4.3$_{\text{BAC}}$** and **[*C*$_3$Cl]Cl** with excess H$_2$O. 156

Figure 4-14. Reactions of **4.3$_{\text{BAC}}$** and **[*C*$_3$Cl]Cl** with DMAP. 157

Figure 4-15. Stacked ^{1}H NMR spectra of reactions of DMAP with isolated crystals of **4.3$_{BAC}$** (top) or with the 50:50 mixture of **4.3$_{BAC}$** and **[*C$_3$*Cl]Cl** (bottom). Resonances for: **[4.17$_{DMAP}$]Cl** (*), **[4.24]Cl$_2$** (†), free DMAP (‡). 158

Figure 4-16. ^{1}H -^{1}H NOESY spectra of the crude mixture of **[4.17$_{DMAP}$]Cl** (*), **[4.24]Cl$_2$** (†) and free DMAP (‡). Correlation of DMAP (ortho protons) and cyclopropenium methyl fragments (left); Zoomed in region of **[4.17$_{DMAP}$]Cl** and DMAP exchange. NOE cross peaks (red) and EXSY cross peaks (blue).. 159

Figure 4-17. ^{31}P{^{1}H} NMR spectrum of a crude reaction mixture of **4.3$_{BAC}$** with SiMe$_3$OTf to generate **[4.17$_{mono}$]OTf**. Inset contains zoomed in spectrum showing ^{31}P-^{13}C coupling of monomeric **[4.17$_{mono}$]**. Sample contains other unidentified byproducts, which have been integrated and normalized.. 161

Figure 4-18. Mercury-rendered ORTEP style drawing of **[4.21$_{mono}$]OTf**. Triflate has been omitted for clarity and selected ellipsoids are shown at the 50% probability level............. 162

Figure 4-19. Stacked ^{31}P{^{1}H} NMR spectra of the reaction of **4.3$_{BAC}$** with LiBF$_4$ in CDCl$_3$ at room temperature. 163

Figure 4-20. ^{1}H NMR spectrum of the reaction mixture of **4.3$_{BAC}$** and BCF in CDCl$_3$, at 25 °C. 164

Figure 4-21. Stacked variable temperature ^{31}P{^{1}H} spectra of **4.26** and **[4.17$_{mono}$]ClBCF** in CD$_2$Cl$_2$... 165

Figure 4-22. Mercury-rendered ORTEP style drawing of **4.27**. Hydrogens have been omitted and BCF framework has been represented as wireframe for simplicity. Selected ellipsoids shown at the 50% probability level... 166

Figure 4-23. ^{31}P{^{1}H} NMR spectrum of crude reaction aliquot of ***C$_3$O*** and PhPOCl$_2$ to generate **4.18$_{Ph}$** (†). Unidentified species labelled with (*). 169

Figure 4-24. Stack plot ^{31}P{^{1}H} NMR spectra of 1 h reaction aliquots of MesPO$_2$Cl with ***C$_3$O*** in C$_6$D$_6$ (bottom), CDCl$_3$ (middle); after removal of toluene and redissolving the product in CDCl$_3$ (top). Uncharacterized intermediate formation at approximately δ_P = 18. 170

Figure 5-1. Bulky bidentate aminopyridine ligands reported by Kempe and co-workers.[1,2]196

Figure 5-2. Catalytic conversion of alcohols to chlorides. 199

Figure 5-3. Alkylation of **4.3$_{\mathbf{BAC}}$** (left) and structure of two acutely toxic chemical warfare agents (right). 199

Figure 5-4. Possible organophosphorus products by reactions with ***C$_3$S***. 200

List of Schemes

Scheme 1-1. Activations of H_2 at main group centres. A) Reaction of digermylene with H_2; B) Reaction of cAAC with H_2 or NH_3. 4

Scheme 1-2. Photolysis of phosphirane to triplet phosphinidene, and subsequent cycloaddition-trapped products.[28] 5

Scheme 1-3. Reactivity modes of phospha-Wittig reagents: A) general phospha-Wittig reaction scheme; B) *in situ* generation and reaction of phospha-Wittig reagent *via* reduction of bulky dichlorophosphines with PMe_3 and zinc, and reaction with benzaldehyde. 7

Scheme 1-4. Base-stabilized phosphorus nitrides supported by NHC and/or cAAC ligands. A) Canonical forms of one phosphorus nitride example; B) synthesis of a base-stabilized phosphorus nitride.[39,40] 8

Scheme 1-5. Selected examples of NHI-supported phosphines. A) formation of NHI-supported phosphine *via* Staudinger-type mechanism; B) single electron oxidation of phosphenium **[1.27]OTf**; C) synthesis of singlet phosphinonitrene. 11

Scheme 1-6. Recent examples of NHI-supported phosphorus species, reported by Dielmann and co-workers. 12

Scheme 1-7. Synthesis of isolable cyclopropylidene **1.38**. 13

Scheme 1-8. Contrasting reactivities of cyclopropenium species. 14

Scheme 1-9. Cycloaddition reactions of phosphinidene chalcogenides (**1.45Ch**) and surrogate species (**1.46**). 16

Scheme 1-10. Reactions of transient **$1.45O_{Ph}$** generated by thermolysis of **1.57**. 19

Scheme 1-11. Dehydrobromination method of release of **[$1.45S_{Ph}$]** and sequential reactions involving cyclobutadiene.[90] 20

Scheme 1-12. Divergent reactivity with 2,3-dimethyl-1,3-butadiene after thermal release of [RPS] from **1.53_R**.[83] 20

Scheme 1-13. Syntheses of oligomeric $(RPS)_3$ species, and related by-products. A) Unselective reduction of Mes*$PSCl_2$ with magnesium metal; B) sequential desulfurization reactions from a parent dithioxophosphorane.[101,102] 21

Scheme 1-14. Formations of $(RPS)_4$. A) Neutral oligomer synthesis; B) tetra-cationic oligomer supported by imidazolium ligands.. 22

Scheme 1-15. Reactions producing thiadiphosphiranes, selenodiphosphiranes, and related species. A) Metathesis reaction of dichlorodiphosphine 1.74tBu with $Ch(SnMe_3)_2$; B) reactions of terphenyl-supported phospha-Wittig reagent with chalcogen dioxide specices.[106,107].. 23

Scheme 1-16. Deselenation reactions of dichalcogoxophosphoranes to phosphinidene chalcogenides and subsequent decompositions, reported by Yoshifuji and co-workers.[108] ... 24

Scheme 1-17. Reduction of bis(Azido)phosphines to access phosphinidene chalcogenides. A) Photolysis performed in a frozen argon matrix at 10 K. B) Generation of methylphosphinidene oxide *via* isomerization of methoxyphosphinidene (**1.79**) or reduction of P(V) species **(1.80**).[109] 25

Scheme 1-18. Synthesis and oxidation of NHC-stabilized phosphinidene oxide.[110] 26

Scheme 1-19. Ylide stabilized species reported by Schmidpeter and co-workers.[88,111,113] 27

Scheme 1-20. Chemistry of a phosphinidene sulfide surrogate species (**$1.46S_{Ar*}$)**, reported by Ragogna and co-workers. A) Formation of dimeric **$1.46S_{Ar*}$**, base-stabilized **1.94**, and ring-expanded trimer (**$1.67S_{Ar*}$**). B) Cycloaddition reactions of **$1.46S_{Ar*}$**.[85] 29

Scheme 1-21. Reactions of a base-stabilized phosphinidene to produce a phosphinidene oxide, dioxophosphorane, phosphinidene sulfide, and phosphinidene imide, reported by the Nikonov group.[115] 31

Scheme 1-22. Generic oligomerization of $[RPCh_2]$ to four-coordinate phosphonate. 32

Scheme 1-23. Reactions of a dithioxophosphorane with alcohols, amines, and dimethylbutadiene.[102,131,132] 34

Scheme 1-24. Synthesis of **[1.110]OTf**, and demonstration of its utility as a phosphorylating agent.[137] 35

Scheme 1-25. General condensation reaction of a phosphonic acid and a phosphonic dichloride to generate oligomeric phosphonates. 36

Scheme 1-26. Photolysis of phenyl phosphirane and oxidation in a frozen matrix.[140] 37

Scheme 1-27. Flash vacuum pyrolysis reactions of phospholes.[141] 37

Scheme 1-28. Reactions of terphenyl-supported 1,3-dioxo-2-phospholane to generate base stabilized adduct of [RPO_2] and dioxophosphorane dimer.[122] 38

Scheme 1-29. Examples of dithioxophosphoranes and some reported reactions with alcohols.[142–144] 39

Scheme 1-30. Reactions of 2,4-di-tert-butyl-6-dimethylaminophenyl (Mx) supported phosphorus species, reported by Yoshifuji and co-workers.[108] 40

Scheme 1-31. NHC stabilized "$RPCh_2$" species.[110,146] 41

Scheme 1-32. Bis(NHC) stabilized P_2O_4.[147] 42

Scheme 1-33. Reactions of peri-substituted phosphorus species.[148,150] 43

Scheme 1-34. Depolymerization of $(PhPO_2)_n$ with DMAP, and coordination with BCF. 44

Scheme 1-35. Deoligomerization of tetra-cationic phosphorus-sulfur heterocycle and stabilization of dithioxophosphorane species.[97] 44

Scheme 2-1. Generalized routes towards the synthesis of an NHI-supported phosphinidene sulfide. 68

Scheme 2-2. Synthetic route to precursor **2.4**. 69

Scheme 2-3. Hypothesized routes towards IPrNPS from the $IPrNSiMe_3$ (**2.4**) precursor. Transformations are labelled A-G. 70

Scheme 2-4. Synthesis and canonical structures of bis(NHI) stabilized phosphenium **[2.7]Cl**. 71

Scheme 2-6. Reaction of **2.6** with PMe_3 to generate a proposed species **[2.9]Cl**. 78

Scheme 2-7. A standing solution of **2.6** and Na_2S over two weeks produced crystal of **2.10**, studied by SC-XRD. 79

Scheme 2-8. Recrystallization after the reaction of **2.6** with $S(SiMe_3)_2$ yielded a limited number of crystals, from which the solid-state structure of $(IPrN)_2P(O)H$ (**2.13**) was successfully determined using single crystal X-ray diffraction (SC-XRD)........................... 82

Scheme 3-1. General scheme for a Staudinger reaction to produce a phosphinimine with hydrolysis to an amine (A) and the aza-Wittig reaction (B). 99

Scheme 3-2. Comparative Staudinger reactivities of P(V) bis(azido)phosphines.[20,21] Bis(azido)phosphine in A) can react with two equivalents of PPh_3. Bis(azido)phosphine in B) can react with only one equivalent PPh_3. 101

Scheme 3-3. Select examples of transformations of Azidophosphines. 101

Scheme 3-4. Synthetic Routes to Bis(azido)phosphines **3.2**, **3.3**, and **3.4Ch** (Ch = O, S, Se). 103

Scheme 3-5. Staudinger reactivity of compound **3.4S** with tertiary and secondary phosphines (left) and example of tautomerization *via* hydride shift (right). 106

Scheme 3-6. Chemoselective Staudinger reactivity of **3.2** with PMe_3 and alternate synthetic route to **3.5_{Me}**. 107

Scheme 4-1. Selected examples of halogenated phosphonates and their proposed formations. 138

Scheme 4-2. Generic reaction of $RP(O)Cl_2$ and phosphonic acid to generate cyclic phosphonates. 140

Scheme 4-3. Examples of reactions with diphenylcyclopropenone.[32–34] 141

Scheme 4-4. Reactions of bis(diisopropylamino)cyclopropenone ***C_3O*** with PCl_3 or $ArPOCl_2$, and derivatization reactions of chlorophosphoante (**4.3_{BAC}**). 142

Scheme 4-5. Reaction of PCl_3 and bis(diisopropylamino)cyclopropenone (***C_3O***).............. 143

Scheme 4-6. Examples of chloride abstractions from chlorophosphines. A) Oxygen transfer and chloride abstraction of POCl3 with a urea.[11] B) chloride abstraction with an NHC.[36].. 146

Scheme 4-7. Hydrolysis of **4.3_{BAC}** to **$[4.21_{mono}]Cl$**. 147

Scheme 4-8. Two plausible pathways for the generation of **4.3_{BAC}** *via* Arbuzov style eliminations of **$[C_3Cl]Cl$**.. 150

Scheme 4-9. Pathway suggested for base-induced dismutation of $POCl_3$ by DMAP.[10]...... 151

Scheme 4-10. Species formed after **4.3_{BAC}** (top) and **$[C_3Cl]Cl$** (bottom) were mixed with $SiMe_3OTf$.. 160

Scheme 4-11. Proposed oligomerization and hydrolysis of **$[4.17_{mono}]^+$** cation.................. 162

Scheme 4-12. Proposed reaction of **4.3_{BAC}** with $LiBF_4$.. 163

Scheme 4-13. The reaction of **4.3_{BAC}** with BCF which resulted in the collection of X-ray diffraction data of **4.27**.. 166

Scheme 4-14. Screened reactions of **C_3O** with various chlorophosphines.......................... 168

Scheme 5-1. Cycloaddition reaction of **3.2**, and subsequent Staudinger reaction. 197

Scheme 5-2. Suggested proton-transfer reactions of **$[4.21_{mono}]^+$**. 198

Scheme 5-3. Deoxygenation of **4.3_{BAC}** to produce polycationic P-O heterocycles. 198

List of Appendices

Appendix A-1. ^{1}H NMR spectrum of **[2.7]Cl** crystals redissolved in $CDCl_3$. 204

Appendix A-2. ^{13}C{^{1}H} NMR spectrum of **[2.7]Cl** crystals redissolved in $CDCl_3$. 204

Appendix A-3. ^{31}P{^{1}H} NMR spectrum of **[2.7]Cl** crystals redissolved in $CDCl_3$. 205

Appendix A-4. ^{1}H NMR spectrum (CD_3CN) of crude mixture forming **2.8**. † Denotes unidentified impurity. 205

Appendix A-5. ^{13}C{^{1}H} NMR spectrum (CD_3CN) of crude mixture forming **2.8**. 206

Appendix A-6. ^{31}P{^{1}H} NMR spectrum (CD_3CN) of crude mixture forming **2.8**. † Denotes unidentified impurities. 207

Appendix A-7. ^{1}H-^{13}C HSQC spectrum of crude mixture of **2.8** in CD_3CN. 208

Appendix A-8. ^{1}H-^{13}C HMBC spectrum of crude mixture of **2.8** in CD_3CN. 208

Appendix A-9. Zoomed in stacked HMBC spectra of crude mixture of **2.8** in CD_3CN...... 209

Appendix A-10. ^{1}H NMR spectrum of mixture of **2.11** and **2.12** in $CDCl_3$. 209

Appendix A-11. ^{13}C{^{1}H} NMR spectrum of mixture of **2.11** and **2.12** in $CDCl_3$. 210

Appendix A-12. ^{31}P{^{1}H} NMR spectrum of mixture of **2.11** and **2.12** in $CDCl_3$. 210

Appendix A-13. ^{31}P NMR spectrum of mixture of **2.11** and **2.12** in $CDCl_3$. 211

Appendix A-14. ^{1}H -^{1}H COSY NMR spectrum of mixture of **2.11** and **2.12** in $CDCl_3$. 211

Appendix A-15. ^{1}H -^{1}H NOESY NMR spectrum of mixture of **2.11** and **2.12** in $CDCl_3$. .. 212

Appendix A-16. ^{1}H-^{13}C HSCQ NMR spectrum of **2.11** and **2.12** in $CDCl_3$. 212

Appendix A-17. ^{1}H-^{31}P HMBC NMR spectrum of mixture of **2.11** and **2.12** in $CDCl_3$. 213

Appendix A-18. FT-IR spectrum of crude mixture containing **2.11** and **2.12**. [Transmission mode, KBr pellet].. 213

Appendix A-19. ^{1}H NMR spectrum (C_6D_6) of **2.14** isolated after toluene extraction from reaction mixture. 214

Appendix A-20. ^{31}P{^{1}H} NMR spectrum of IPrNPSCl$_2$ (**2.14**) in C_6D_6. † Denotes unidentified impurity. 214

Appendix A-21. ^{31}P (^{1}H} NMR spectrum of the reaction of **2.14** (δ_P = 26) with SiMe$_3$N$_3$ at 60 °C after four h. Signal at 39 ppm is IPrNPS(N$_3$)$_2$ (*vide infra* Chapter 3). 215

Appendix A-22. ^{1}H NMR spectrum (C_6D_6) of the crude residue obtained after 20 h of heating at 115 °C in pressure tube. 215

Appendix A-23. ^{31}P{^{1}H} NMR spectrum (C_6D_6) of the crude residue obtained after 20 h of heating at 115 °C in a pressure tube. 216

Appendix A-24. ^{1}H NMR spectrum of **2.15** photolyzed for 1 h in C_6D_6 in a quartz NMR tube.. 216

Appendix A-25. ^{31}P{^{1}H} NMR spectrum of **2.15** photolyzed for 1 h in C_6D_6 in a quartz NMR tube.. 217

Appendix A-26. Stacked ^{31}P{^{1}H} spectra of **2.15** before (bottom) and after a 19 h low temperature photolysis experiment (top). 217

Appendix B-1. ^{1}H NMR spectrum of IPrNP(N$_3$)$_2$ (**3.2**) in C_6D_6.. 218

Appendix B-2. ^{13}C{^{1}H} NMR spectrum of IPrNP(N$_3$)$_2$ (**3.2**) in C_6D_6. 218

Appendix B-3. ^{31}P{^{1}H} NMR spectrum of IPrNP(N$_3$)$_2$ (**3.2**) in C_6D_6. 219

Appendix B-4. FT-IR spectrum of IPrNP(N$_3$)$_2$ (**3.2**) in KBr (Transmission mode). 219

Appendix B-5. ^{31}P{^{1}H} NMR of reaction of **3.1** with two and a half equivalents of Me$_3$SiN$_3$ in toluene after complete consumption of **3.1**.. 220

Appendix B-6. ^{1}H NMR spectrum of IPrNP(NSiMe$_3$)(N$_3$)$_2$ (**3.3**). 221

Appendix B-7. ^{13}C{^{1}H} NMR spectrum of compound IPrNP(NSiMe$_3$)(N$_3$)$_2$ (**3.3**). 221

Appendix B-8. ^{31}P{^{1}H} NMR spectrum of compound IPrNP(NSiMe$_3$)(N$_3$)$_2$ (**3.3**) in C$_6$D$_6$. 222

Appendix B-9. FT-IR spectrum of IPrNP(NSiMe$_3$)(N$_3$)$_2$ (**3.3**) (ATR mode). 222

Appendix B-10. ^{1}H NMR of IPrNPS(N$_3$)$_2$ (**3.4S**) in C$_6$D$_6$.. 223

Appendix B-11. ^{13}C{^{1}H} NMR spectrum of IPrNPS(N$_3$)$_2$ (**3.4S**) in C$_6$D$_6$.......................... 223

Appendix B-12. ^{31}P{^{1}H} NMR spectrum of IPrNPS(N$_3$)$_2$ (**3.4S**) in C$_6$D$_6$. 224

Appendix B-13. FT-IR spectrum of IPrNPS(N$_3$)$_2$ (**3.4S**) in air [ATR mode]...................... 224

Appendix B-14. ^{1}H NMR spectrum of IPrNPSe(N$_3$)$_2$ (**3.4Se**) in C$_6$D$_6$. † denotes residual pentane. ‡ denotes residual Et$_2$O. 225

Appendix B-15. ^{13}C{^{1}H} NMR spectrum of IPrNPSe(N$_3$)$_2$ (**3.4Se**) in C$_6$D$_6$. N*C*N carbon not detected. 225

Appendix B-16. ^{31}P{^{1}H} NMR spectrum of IPrNPSe(N$_3$)$_2$ (**3.4Se**) in C$_6$D$_6$....................... 226

Appendix B-17. FT-IR spectrum of IPrNPSe(N$_3$)$_2$ (**3.4Se**) (transmission mode). 226

Appendix B-18. ^{1}H NMR spectrum of *in situ* formation of IPrNPO(N$_3$)$_2$ (**3.4O**) in C$_6$D$_6$ solution in O$_2$ (g) pressurized J-Young NMR tube after seven days. 227

Appendix B-19. ^{13}C{^{1}H} NMR spectrum of *in situ* formation of IPrNPO(N$_3$)$_2$ (**3.4O**) in C$_6$D$_6$ solution in O$_2$ (g) pressurized J-Young NMR tube after seven days. 227

Appendix B-20. HSQC spectrum of IPrNPO(N$_3$)$_2$ (**3.4O**) in C$_6$D$_6$. 228

Appendix B-21. HMBC spectrum of IPrNPO(N$_3$)$_2$ (**3.4O**) in C$_6$D$_6$. 228

Appendix B-22. ^{31}P{^{1}H} NMR spectrum of *in situ* formation of IPrNPO(N$_3$)$_2$ (**3.4O**) by oxidation of **3.2** (*) with gaseous O$_2$ in C$_6$D$_6$ over six days at room temperature................ 229

Appendix B-23. $^{31}P\{^{1}H\}$ NMR spectrum of reaction of **3.2** with few crystals *m*-CPBA in C_6D_6, after ten min. Unreacted **3.2** can be observed at 123 ppm and IPrNPO(N_3)$_2$ (**3.4O**) at -11.2 ppm. Unknown species at 137.8 ppm. 229

Appendix B-24. ^{1}H NMR spectrum of IPrNP(S)(N_3)($NPMe_3$) (**3.5$_{Me}$**) in C_6D_6. 230

Appendix B-25. $^{13}C\{^{1}H\}$ NMR spectrum of IPrNP(S)(N_3)($NPMe_3$) (**3.5$_{Me}$**) in C_6D_6. 230

Appendix B-26. $^{31}P\{^{1}H\}$ NMR spectrum of IPrNP(S)(N_3)($NPMe_3$) (**3.5$_{Me}$**) in C_6D_6. 231

Appendix B-27. ^{31}P NMR spectrum of IPrNP(S)(N_3)($NPMe_3$) (**3.5$_{Me}$**) in C_6D_6. 231

Appendix B-28. FT-IR spectrum of IPrNP(S)(N_3)($NPMe_3$) (**3.5$_{Me}$**) (transmission mode). 232

Appendix B-29. ^{1}H NMR spectrum of IPrNP(S)(N_3)($NPCy_3$) (**3.5$_{Cy}$**) in $CDCl_3$. † denotes trace hexane. 232

Appendix B-30. $^{13}C\{^{1}H\}$ NMR spectrum of IPrNP(S)(N_3)($NPCy_3$) (**3.5$_{Cy}$**) in $CDCl_3$. 233

Appendix B-31. HSQC NMR spectrum of IPrNP(S)(N_3)($NPCy_3$) (**3.5$_{Cy}$**) in $CDCl_3$. 233

Appendix B-32. HMBC NMR spectrum spectrum of IPrNP(S)(N_3)($NPCy_3$) (**3.5$_{Cy}$**). 234

Appendix B-33. $^{31}P\{^{1}H\}$ NMR spectrum of IPrNP(S)(N_3)($NPCy_3$) (**3.5$_{Cy}$**) in $CDCl_3$. 234

Appendix B-34. ^{31}P NMR spectrum of IPrNP(S)(N_3)($NPCy_3$) (**3.5$_{Cy}$**), zoomed in. 235

Appendix B-35. FT-IR spectrum of IPrNP(S)(N_3)($NPCy_3$) (**3.5$_{Cy}$**) (transmission mode)... 235

Appendix B-36. Stacked $^{31}P\{^{1}H\}$ NMR spectra of the reaction of **3.4S** (δ_P = 40.7) with PCy_3 (δ_P = 9.9). Blue: complete consumption shown here after four days at room temperature in toluene-h8. Red: After three volumes of one milliliter triturations with hexanes, solids redissolved in $CDCl_3$. Green: recrystallized **3.5$_{Cy}$** from hot hexanes, redissolved in C_6D_6. 236

Appendix B-37. ^{1}H NMR spectrum of IPrNP(S)(N_3)($NPPh_3$) (**3.5$_{Ph}$**). Contains pentane and silicone grease impurities. 236

Appendix B-38. $^{13}C\{^1H\}$ NMR spectrum of IPrNP(S)(N_3)($NPPh_3$) (**3.5$_{Ph}$**). Pentane, hexane, and silicone grease impurities present in solvent. 237

Appendix B-39. HMBC NMR spectrum of IPrNP(S)(N_3)($NPPh_3$) (**3.5$_{Ph}$**) for assignment of N*C*N carbon. 237

Appendix B-40. $^{31}P\{^1H\}$ NMR spectrum of IPrNP(S)(N_3)($NPPh_3$) (**3.5$_{Ph}$**) in C_6D_6. 238

Appendix B-41. ^{31}P NMR spectrum of IPrNP(S)(N_3)($NPPh_3$) (**3.5$_{Ph}$**) in C_6D_6. 238

Appendix B-42. FT-IR spectrum of IPrNP(S)(N_3)($NPPh_3$) (**3.5$_{Ph}$**) (ATR mode). 239

Appendix B-43. Stacked $^{31}P\{^1H\}$ NMR spectra of the reaction of **3.4S** (δ_P = 40.7) and PPh_3 (δ_P = -5.9). Blue: after four days at room temperature (1.05 eq PPh_3 used). Red: After an additional equivalent of PPh_3 added and two additional days at room temperature. Green: complete consumption after one week. Purple: PPh_3 and $SPPh_3$ removed after precipitation from Et_2O/pentane at -30 °C, and 3 x 0.5 mL pentane triturations. 240

Appendix B-44. ^1H NMR spectrum of crystals of **3.6a**/**3.6b** dissolved in C_6D_6. Unambiguous assignment of aryl-, cyclohexyl-, and methyl- groups was not possible. Backbone, isopropyl, and P-H coupled protons have been explicitly labelled. Methyl groups have been assigned based on ^1H-^1H COSY. THF (*), pentane (‡), and silicone grease (†). 241

Appendix B-45. $^{13}C\{^1H\}$ NMR spectrum of **3.6a**/**3.6b** in C_6D_6 (full spectrum). 242

Appendix B-46. $^{13}C\{^1H\}$ NMR spectrum of **3.6a**/**3.6b** in C_6D_6 (zoomed in to 150 - 115 ppm). 242

Appendix B-47. $^{13}C\{^1H\}$ NMR spectrum of **3.6a**/**3.6b** in C_6D_6 (zoomed into 38 – 22 ppm). 243

Appendix B-48. $^{31}P\{^1H\}$ NMR spectrum of crystals of **3.6a**/**3.6b** dissolved in C_6D_6. First delay time set to six seconds. 244

Appendix B-49. ^{31}P NMR spectrum of crystals of **3.6a**/**3.6b** dissolved in C_6D_6. 244

Appendix B-50. ^1H-^1H COSY NMR spectrum of **3.6a**/**3.6b** dissolved in C_6D_6. 245

Appendix B-51. ^{1}H-^{1}H COSY NMR spectrum of **3.6a**/**3.6b** dissolved in C_6D_6 (zoomed in). 245

Appendix B-52. ^{1}H-^{13}C HSQC NMR spectrum of **3.6a**/**3.6b** dissolved in C_6D_6. 246

Appendix B-53. ^{1}H-^{13}C HSQC NMR spectrum of **3.6a**/**3.6b** dissolved in C_6D_6 (zoomed in). 247

Appendix B-54. ^{1}H-^{13}C HSQC NMR spectrum of **3.6a**/**3.6b** dissolved in C_6D_6 (zoomed in). 248

Appendix B-55. ^{1}H-^{13}C HMBC NMR spectrum of **3.6a**/**3.6b** dissolved in C_6D_6. 248

Appendix B-56. ^{1}H-^{13}C HMBC NMR spectrum of **3.6a**/**3.6b** dissolved in C_6D_6 (zoomed in). 249

Appendix B-57. ^{1}H-^{13}C HMBC NMR spectrum of **3.6a**/**3.6b** dissolved in C_6D_6 (zoomed in). 250

Appendix B-58. ^{1}H-^{13}C HMBC NMR spectrum of **3.6a**/**3.6b** dissolved in C_6D_6 (zoomed in). 251

Appendix B-59. ^{31}P-^{31}P EXSY NMR spectrum of reaction mixture containing **3.6a**/**3.6b** and residual dicyclohexylphosphine. 252

Appendix B-60. FT-IR spectrum of **3.6a**/**3.6b** (transmission mode). 252

Appendix B-61. ^{1}H NMR spectrum of $IPrNPN_3NPMe_3$ (**3.7**) in C_6D_6. 253

Appendix B-62. ^{13}C{^{1}H} NMR spectrum of $IPrNPN_3NPMe_3$ (**3.7**) in C_6D_6. 253

Appendix B-63. ^{31}P{^{1}H} NMR spectrum of $IPrNPN_3NPMe_3$ (**3.7**) in C_6D_6. 254

Appendix B-64. FT-IR spectrum of $IPrNPN_3NPMe_3$ (**3.7**) (transmission mode). 254

Appendix B-65. Stacked ^{1}H NMR spectra of **3.4S**, **3.7**, and the reaction of **3.7** with excess S_8. 255

Appendix B-66. Stacked $^{31}P\{^1H\}$ NMR spectra of **3.4S**, **3.7**, and a reaction of **3.7** with excess S_8. 256

Appendix B-67. Table of comparisons of low error ions measured by high-resolution mass spectrometry of $\mathbf{3.5_{Me}}$ produced by different methods. 256

Appendix B-68. ^1H NMR spectrum of isolated decomposition product in C_6D_6. 257

Appendix B-69. ^1H NMR spectrum of isolated decomposition product in C_6D_6. 257

Appendix B-70. ^{31}P NMR spectrum of decomposition product in C_6D_6. 258

Appendix B-71. $^{13}C\{^1H\}$ NMR spectrum of decomposition product in C_6D_6. 258

Appendix B-72. ^1H-^{13}C HMBC NMR spectrum spectrum of decomposition product in C_6D_6. 259

Appendix B-73. ^1H-^{31}P HMBC NMR spectrum of decomposition product. 259

Appendix B-74. ^1H-^1H NOESY NMR spectrum of decomposition product in C_6D_6.......... 260

Appendix B-75. ^1H-^1H COSY NMR spectrum of decomposition product in C_6D_6. 260

Appendix B-76. Structures investigated by DFT. 261

Appendix B-77. Visualized Kohn-Sham orbitals of **IV** corresponding to LUMO (A) and LUMO+12 (B). Yellow colour illustrates negative phase and blue illustrates positive phase of orbitals.. 261

Appendix B-78. Summary of calculated atomic charges for structures **I**, **II**, and **III** investigated by DFT... 262

Appendix B-79. ORTEP drawing of **3.2** asymmetric unit showing naming and numbering scheme. Ellipsoids are at the 50% probability level and hydrogen atoms were omitted for clarity. 263

Appendix B-80. ORTEP drawing of **3.2** coloured by symmetry operation. Ellipsoids are at the 50% probability level and hydrogen atoms were omitted for clarity. 264

Appendix B-81. Summary of Unit Cell parameters of Predominant and Minor Phases of **3.4S** 265

Appendix C-1. ^{1}H NMR spectrum of ***C_3O*** in $CDCl_3$... 266

Appendix C-2. ^{13}C{^{1}H} NMR spectrum of ***C_3O*** in $CDCl_3$. 266

Appendix C-3. FT-IR spectrum of ***C_3O*** [ATR-mode]. 267

Appendix C-4. ^{1}H NMR ($CDCl_3$) spectrum of crystals of **4.3_{BAC}** isolated by Pasteur separation. 267

Appendix C-5. ^{1}H NMR spectrum of crystals of **4.3_{BAC}** dissolved in CD_3CN. Residual PhF denoted with (*). 268

Appendix C-6. ^{13}C{^{1}H} NMR spectrum of isolated crystals of **4.3_{BAC}** in $CDCl_3$.............. 268

Appendix C-7. ^{31}P{^{1}H} NMR spectrum of isolated crystals of **4.3_{BAC}** in $CDCl_3$. 269

Appendix C-8. ^{31}P{^{1}H} NMR spectrum of **4.3_{BAC}** in CD_3CN. 269

Appendix C-9. ^{1}H NMR spectrum of 50:50 mixture of **4.3_{BAC}** (†) and **[*C_3*Cl]Cl** (*). 270

Appendix C-10. ^{13}C{^{1}H} NMR spectrum of 50:50 mixture of **4.3_{BAC}** and **[*C_3*Cl]Cl**. 270

Appendix C-11. ^{1}H- ^{13}C HSQC NMR spectra of **4.3_{BAC}** (†) and **[*C_3*Cl]Cl** (*) in $CDCl_3$. Left: Correlations of isopropyl groups. Right: Correlations of methyl groups. 271

Appendix C-12. ^{1}H - ^{13}C HMBC NMR spectra of **4.3_{BAC}** (†) and **[*C_3*Cl]Cl** (*) in $CDCl_3$. Left: correlations of isopropyl proton with cyclopropenium carbons. Right: correlations of isopropyl carbons with methyl protons. 271

Appendix C-13. ^{31}P{^{1}H} NMR spectrum of 50:50 mixture of **4.3_{BAC}** and **[*C_3*Cl]Cl** in $CDCl_3$. 272

Appendix C-14. FT-IR spectrum of **4.3_{BAC}** [transmission mode]. 272

Appendix C-15. FT-IR spectrum of mixture of **4.3_{BAC}** and **[*C_3*Cl]Cl** [transmission mode].273

Appendix C-16. ^{1}H NMR spectrum of **[4.21$_{\mathbf{mono}}$]Cl** in $CDCl_3$. 273

Appendix C-17. ^{13}C{^{1}H} NMR spectrum of **[4.21$_{\mathbf{mono}}$]Cl** in $CDCl_3$. Contains PhF. 274

Appendix C-18. ^{31}P{^{1}H} NMR spectrum of **[4.21$_{\mathbf{mono}}$]Cl** in $CDCl_3$. 274

Appendix C-19. ^{31}P{^{1}H} NMR spectrum of partial hydrolysis of **4.3$_{\mathbf{BAC}}$**. Intermediate hydrolysis species **[4.21$_{\mathbf{di}}$]$^{2+}$** detected at -19.7 ppm. 275

Appendix C-20. ^{1}H NMR spectrum of crude mixture of **[4.17$_{\mathbf{DMAP}}$]Cl** (*), **[4.24]Cl$_2$** (†), and DMAP (‡) in $CDCl_3$. 275

Appendix C-21. ^{13}C{^{1}H} NMR spectrum of mixture of **[4.17$_{\mathbf{DMAP}}$]Cl** and **[4.24]Cl** in $CDCl_3$. 276

Appendix C-22. ^{1}H – ^{1}H COSY NMR spectra of **[4.17$_{\mathbf{DMAP}}$]Cl**, **[4.24]Cl$_2$**, and DMAP ($CDCl_3$). 276

Appendix C-23. ^{1}H – ^{13}C HSQC NMR spectra of **[4.17$_{\mathbf{DMAP}}$]Cl**, **[4.24]Cl$_2$**, and DMAP... 277

Appendix C-24. ^{1}H - ^{13}C HMBC NMR spectra of **[4.17$_{\mathbf{DMAP}}$]Cl** and **[4.24]Cl$_2$**. 277

Appendix C-25. ^{31}P{^{1}H} NMR spectrum of crude reaction mixture containing **[4.17$_{\mathbf{DMAP}}$]Cl**, **[4.24]Cl**, and slight excess DMAP. 278

Appendix C-26. ^{1}H NMR spectrum of solids of **[4.17$_{\mathbf{DMAP}}$]Cl** precipitated from CH_2Cl_2/hexanes. 278

Appendix C-27. ^{31}C{^{1}H} NMR spectrum of isolated **[4.17$_{\mathbf{DMAP}}$]Cl** in $CDCl_3$. Note: cyclopropenium carbons were not detected. 279

Appendix C-28. ^{31}P{^{1}H} NMR spectrum of isolated crystals of **[4.17$_{\mathbf{DMAP}}$]Cl** (*) in $CDCl_3$. Spectrum contains free **4.3$_{\mathbf{BAC}}$** (‡). 279

Appendix C-29. ^{1}H NMR spectrum of **[4.17$_{\mathbf{mono}}$]OTf** and **[*C$_3$*Cl]OTf** in $CDCl_3$. Contains $SiMe_3Cl$ and $SiMe_3OTf$. 280

Appendix C-30. $^{13}C\{^1H\}$ NMR spectrum of **[4.17$_{mono}$]OTf** and **[*C$_3$*Cl]OTf** in $CDCl_3$. Sample contains $SiMe_3OTf$ and $SiMe_3Cl$. 280

Appendix C-31. $^{31}P\{^1H\}$ NMR spectrum of **[4.17$_{mono}$]OTf** and **[*C$_3$*Cl]OTf** in $CDCl_3$. 281

Appendix C-32. $^{19}F\{^1H\}$ NMR spectrum of **[4.17$_{mono}$]OTf** and **[*C$_3$*Cl]OTf** in $CDCl_3$. 281

Appendix C-33. ^1H - ^1H COSY NMR spectra of **[*C$_3$*Cl]OTf** and **[4.17$_{mono}$]OTf**. 282

Appendix C-34. ^1H - ^{13}C HSQC NMR spectra of **[*C$_3$*Cl]OTf** and **[4.17$_{mono}$]OTf** in $CDCl_3$. 282

Appendix C-35. ^1H - ^{13}C HMBC NMR spectra of **[*C$_3$*Cl]OTf** and **[4.17$_{mono}$]OTf** in $CDCl_3$. 283

Appendix C-36. ^1H NMR spectrum of reaction of **4.3$_{BAC}$** with $SiMe_3OTf$. Contains $SiMe_3Cl$ and $SiMe_3OTf$. 283

Appendix C-37. Stacked $^{13}C\{^1H\}$ NMR spectra of **[4.17$_{mono}$]OTf** generated *in situ*. Top: Mixture of **[4.17$_{mono}$]OTf** and **[*C$_3$*Cl]OTf**. Bottom: Prepared from isolated **4.3$_{BAC}$** (contains PhF). 284

Appendix C-38. $^{31}P\{^1H\}$ NMR spectrum of crude reaction mixture of **4.3$_{BAC}$** with $SiMe_3OTf$. Inset contains zoomed in spectrum showing P-C coupling of monomeric **[4.17$_{mono}$]$^+$**. 284

Appendix C-39. $^{31}P\{^1H\}$ NMR spectrum of crude reaction aliquot of ***C$_3$O*** and $PhPOCl_2$ to generate **4.18$_{Ph}$**. 285

Appendix C-40. ^1H NMR spectrum of solids isolated after reaction of ***C$_3$O*** and $MesPOCl_2$, redissolved in $CDCl_3$. Contains **[*C$_3$*Cl]Cl** (*). 285

Appendix C-41. $^{13}C\{^1H\}$ NMR spectrum of solids isolated after reaction of ***C$_3$O*** and $MesPOCl_2$. Contains **[*C$_3$*Cl]Cl** (*) and toluene (‡). 286

Appendix C-42. $^{31}P\{^1H\}$ NMR spectrum of precipitated **4.18$_{Mes}$**, redissolved in $CDCl_3$. .. 286

Appendix D-1. Screenshot of permission to use the previously published work, in chapter 3. 287

List of Abbreviations

$\{^1H\}$	Proton Decoupled
°	Degrees
°C	Degrees Celsius
Å	Angstrom
Ar	Aryl
Ar*	2,6-$(Mes)_2C_6H_3$
ATR	Attenuated Total Reflection
Avg	Average
B3LYP	Becke Three-Parameter Lee-Yang-Parr Functional
BAC	Bisaminocyclopropenylidene
BCF	Tris(Pentafluorophenyl)Borane; $B(C_6F_5)_3$
br	Broad
Bu	Butyl
C_3O	Bis(Diisopropylamino)Cyclopropenone
ca.	*Circa;* about
Ch	Chalcogen; Group 16 Element (O, S, Se, Te)
$cm\text{-}^1$	Wavenumbers
COSY	Correlational Spectroscopy
Cy	Cyclohexyl
d	Doublet
d	Days
D4	D4 London Dispersion Model
dd	Doublet Of Doublets
ddt	Doublet Of Doublet Of Triplets
Def2-TZVP	Triple Zeta Valence Polarization Basis Set
DFT	Density Functional Theory
Dipp	2,6-Diisopropylphenyl
DMAP	4-Dimethylaminopyridine
DMF	N,N-Dimethylformamide
dt	Doublet Of Triplets
e^-	Electron
e.g.	*Exempli Gratia;* For Example
EPR	Electron Paramagnetic Resonance
ESI-MS	Electrospray Ionization Mass Spectrometer
Et	Ethyl
et al.	*Et Alia;* And Others
Et_2O	Diethylether
eV	Electorn Volts
EXSY	Exchange Spectroscopy
FT	Fourier Transform
g	Gram
GOF	Goodness Of Fit
h	Hour
HMBC	Heteronuclear Multiple Bond Correlation
HOMO	Highest Occupied Molecular Orbital
HRMS	High Resolution Mass Spectrometer

HSQC	Heteronuclear Single Quantum Coherence
hν	Light
*i*Pr	Isopropyl
IPr	N,N’-Bis(2,6-Diisopropylphenyl)Imidazol-2-Ylidene
IPrN	N,N’-Bis(2,6-Diisopropylphenyl)Imidazol-2-Imino
IR	Infrared
J	Coupling Constant
K	Kelvin
LUMO	Lowest Unoccupied Molecular Orbital
M	Mass
m	Multiplet
m-	Meta
m/z	Mass To Charge Ratio
m-CPBA	Meta-Chloroperbenzoic Acid
Me	Methyl
Mes	Mesityl; 2,4,6-Trimethylphenyl
mg	Milligram
MHz	Megahertz
mL	Milliliter
mmol	Millimole
MO	Molecular Orbital
Mox	2,4-Diterybutyl-6-Methoxyphenyl
NHC	N-Heterocyclic Carbene
NHI	N-Heterocyclic Imine
NOE	Nuclear Overhauser Effect
NOESY	Nuclear Overhauser Effect Spectroscopy
o-	Ortho
OTf	Triflate; Trifluoromethyl Sulfonate; $SO_3CF_3^-$
p-	Para
Ph	Phenyl
ppm	Parts Per Million
q	Quartet
RT	Room Temperature
s	Singlet
SC-XRD	Singlet-Crystal X-Ray Diffraction
t	Triplet
t-Bu	Tert-Butyl
Ter	Terphenyl, 2,6-bis(phenyl)phenyl
TGA	Thermogravimetric Analysis
THF	Tetrahydrofuran
UV	Ultraviolet
V	Volume
VT	Variable Temperature
WBI	Wiberg Bond Index
Δ	Heat
δ	Proton Chemical Shift (ppm)
δ_F	Fluorine Chemical Shift (ppm)
δ_P	Phosphorus Chemical Shift (ppm)

λ	Wavelength
π	Pi Bonding
π^*	Pi Anti-Bonding
ρ	Density
σ	Sigma Bonding
σ^*	Sigma Anti-Bonding

Chapter 1

1 Introduction

1.1 Advancements in Fundamental Main Group Chemistry

Main group chemistry has evolved significantly in recent decades, propelled by the development and isolation of novel, highly reactive compounds. Pioneering contributions, such as those made by Georg Wittig, helped lay the foundation for modern phosphorus chemistry. Improvements to ligand design and analytical techniques, including X-ray crystallography and NMR spectroscopy, have facilitated these advancements and offer insights into the structure and bonding of such species. Key objectives in this field are to refine our understanding of structure and bonding by synthesizing novel compounds with unique bonding motifs, and to study new reactivity trends for use in novel chemical transformations.

Interest in main group chemistry over the past 25 years has grown due to discoveries that challenged traditional notions of multiple bonding and VSEPR non-compliance in p-block elements and revealed new reactivity modes. Transition metals experienced significant attention in the twentieth century featuring metal-based catalytic behaviour for many types of reactions. This is attributed to energetically close and partially filled valence d-orbitals with small differences in the energies of the highest occupied molecular orbital (HOMO) and lowest unoccupied molecular orbital (LUMO) levels. Main group chemistry has lagged significantly in catalytic reactions as the traditional understanding was that they possessed significant energy differences between the HOMO and LUMO orbitals.[1] When coupled with the inflexibile coordination numbers observed in early examples of p-block elements, key catalytic steps such as oxidative addition and reductive elimination remained elusive.[2] These limitations have been overcome using various main-group elements with the advancement of specific, customized stabilizing ligands for p-block centres.[3]

The "double bond rule" was an early misconception that heavy main group element bonds should have poor orbital overlap and prevent any formation of a double bond.[2] Violations of this rule have been shown for many elements including silicon, phosphorus, gallium, germanium, arsenic, tin, antimony, lead, and bismuth.[1,4–6] The first examples of multiple bonded, two-coordinate trivalent phosphorus species (**Figure 1-1**) were reported by Dimroth and Hoffman, who described the cationic phosphacyanine (**1.1**), and Markl, who reported triphenylphosphabenzene (**1.2**), but lacked structural characterization.[7,8] Yoshifuji *et al.* and West *et al.* reported the first structurally characterized diphosphene (**1.3$_{\text{Mes*}}$**) and disilene (**1.4**) in 1981, supported by bulky mesityl ligands (Mes*, 2,4,6-tri-*tert*-butylphenyl; and Mes, 2,4,6-trimethylphenyl) ligands. This then led to a wave of main group compounds which behave as transition metal mimics.[5,6]

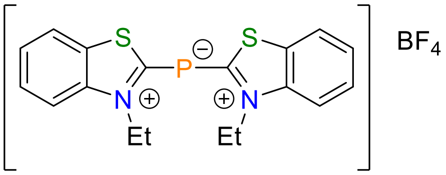

1.1

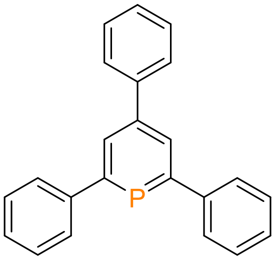

1.2

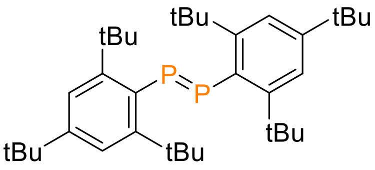

1.3$_{\text{Mes*}}$

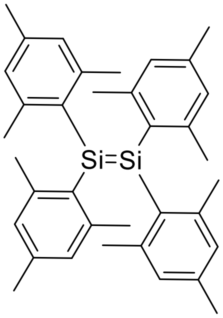

1.4

Figure 1-1. The first examples of trivalent phosphorus species exhibiting multiple bond character (**1.1**, **1.2**, **1.3$_{\text{Mes*}}$**), and the first disilene (**1.4**).[7,8]

1.2 Why Study Main Group Species?

Advances in fundamental main group chemistry can benefit many industries, as low-valent main group species can often exhibit bond-activation reactivity similar to transition metal complexes. This offers alternative strategies for transferring functional groups and synthesizing otherwise inaccessible compounds. One method for creating such species is the isolobal analogy. This theory compares the frontier molecular orbitals of different fragments, focusing on their symmetries, electron counts, and valence orbital energies. If two fragments have similar frontier orbitals, they are considered isolobal and may exhibit similar behavior.[9] Thus, strategies used to stabilize one reactive species can potentially stabilize others with similar frontier orbitals. Although the first isolated singlet carbene (**1.5**) was not achieved until 1988 and the first N-heterocyclic carbene (NHC, **1.6**) until 1991, heavier analogues such as plumbylene (**1.7**) were reported as early as the 1950s (**Figure 1-2**).[10–12] These species remain interesting because main group analogues of carbenes often display unique reactivities.[13]

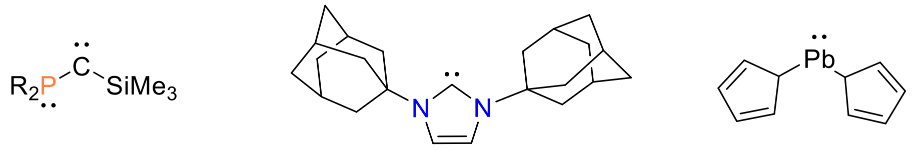

1.5 **1.6** **1.7**

Figure 1-2. The first isolated example of a singlet carbene (**1.5**), first isolated N-heterocyclic carbene (NHC, **1.6**), and an early example of a heavy element analogue of a carbene (**1.7**).

A heavy germanium alkyne analogue (**1.8**) with terphenyl ligands, reported in 2005, marked the first instance of a main-group element activating a dihydrogen bond in the condensed state (**Scheme 1-1**).[14] In 2007, Bertrand reported the activation of H_2 and NH_3 using cyclic and acyclic (amino)carbenes (*e.g.* **1.10**; **Scheme 1-1**).[15] This fundamental breakthrough expanded the understanding of main-group compounds which may behave like transition metals due to small energy separations of their frontier molecular orbitals with proper designs.[1]

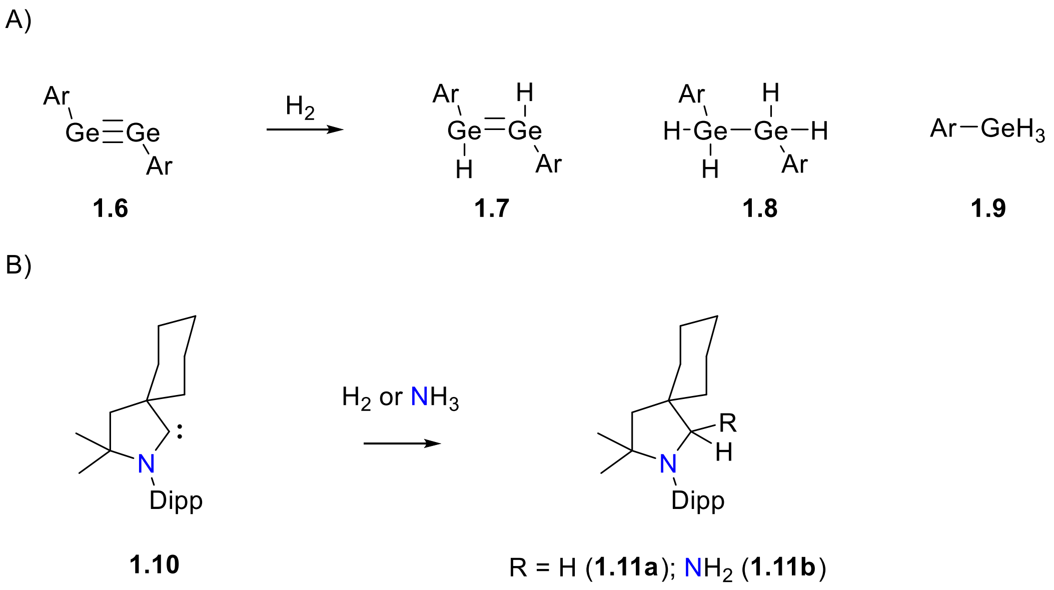

Scheme 1-1. Activations of H_2 at main group centres. A) Reaction of digermylene with H_2; B) Reaction of cAAC with H_2 or NH_3.

Low-valent compounds which are isolobal to carbenes are often reactive intermediates, whose existence is deduced from trapping experiments like cycloaddition or the formation of heterocyclic products. These reactive species are often ambiphilic and undergo self-quenching to form dimeric, trimeric, or higher-order oligomeric species. Isolation of reactive species therefore allows for more careful analysis of their structures and reactivities, which results in better understanding of how they may be useful in future applications.[1] Their ambiphilic nature combined with tailored and non-innocent ligands has also enabled reactivity akin to key reactions in catalytic cycles, such as oxidative additions and reductive eliminations.[33,16,17]

Phosphorus holds significant importance in various fields such as agriculture, medicinal chemistry, organic synthesis, and biological applications.[18–23] There is a dedicated branch within phosphorus chemistry focusing on its responsible utilization and stewardship.[24,25] The versatility of phosphorus also extends to use in pesticides and, unfortunately, as weaponized nerve agents.[26] There is also an impetus to isolate intermediates involved in chemical reactions, as this allows more effective exploration of reaction mechanisms. Particularly intriguing are highly reactive, low-coordinate phosphorus species, as they can lead to unusual and interesting bond activations.

1.3 Stabilizing Reactive Phosphorus Species

1.3.1 General Considerations

Phosphinidenes are monocoordinate phosphorus (I) species, whose existence was inferred, as early attempts at isolation resulted in the formation of ring and oligomeric compounds (*e.g.* triphosphirane **1.14_{Mes}**, **Scheme 1-2**).[27] A breakthrough came in 1994 when Gaspar *et al.* successfully trapped a triplet mesitylphosphinidene (**1.13**) in a frozen matrix that was detected by EPR spectroscopy (**Scheme 1-2**).[28] Compound **1.13** was reported to subsequently trimerize to **1.14_{Mes}**, or was reacted with an internal alkyne to generate a phosphirene (**1.15)**.

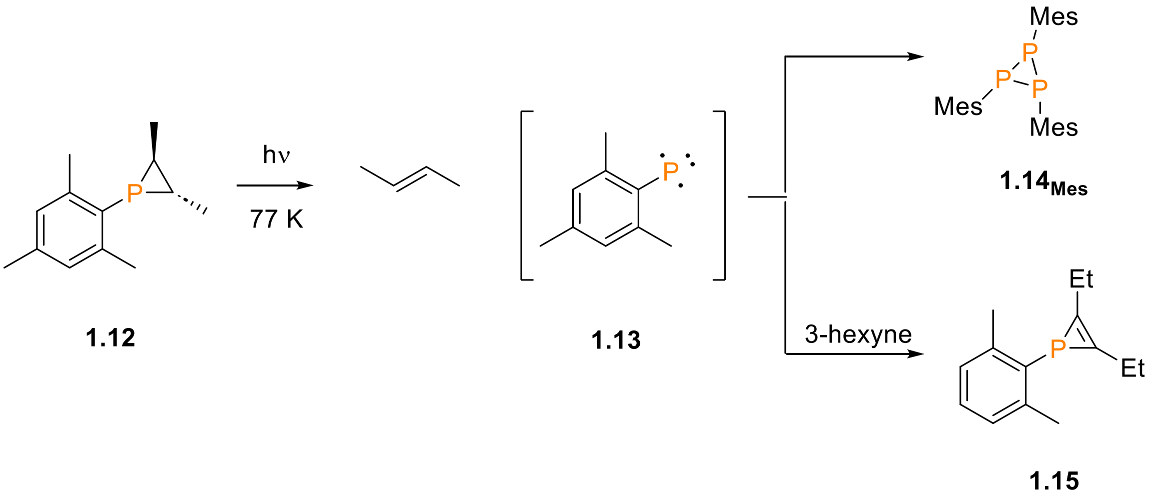

Scheme 1-2. Photolysis of phosphirane to triplet phosphinidene, and subsequent cycloaddition-trapped products.[28]

Phosphinidene and diphosphene compounds have been prepared within a metal coordination sphere, or stabilized by Lewis bases or sterically hindered ligands (**Figure 1-3**).[29–35] The first isolable singlet phosphinidene (**1.17**) was achieved by the combined stabilization of π-donation from an adjacent phosphorus atom and steric protection from an exceptionally bulky ligand.[36] Less bulky ligands in comparison were unable to stabilize the singlet phosphinidenes as they spontaneously dimerized to form diphosphenes.[36]

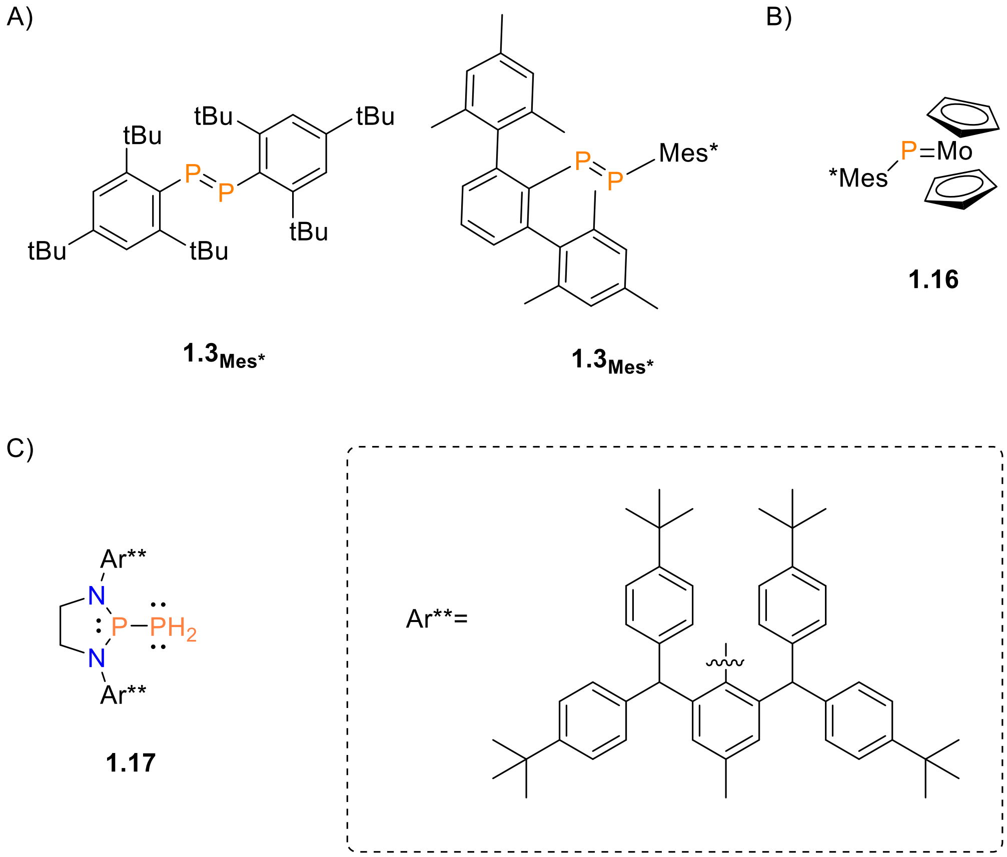

Figure 1-3. Low-coordinate phosphorus compounds: A) Sterically demanding diphosphenes; B) metal-coordinated phosphinidene; C) a room temperature stable singlet phosphinidene.[5,34–36]

Base-stabilized or strained heterocyclic species can serve as surrogates or precursors in solution for the "unprotected" counterparts. Phospha-Wittig reagents, also known as "masked phosphinidenes," exhibit reactivity similar to "free" phosphinidenes. Reactions involving a masked phosphinidene intermediate have proven useful in the selective synthesis of three-membered triphosphirane rings (**Scheme 1-3**).[37] Metal-assisted phospha-Wittig reactions, terminal phosphinidene complexes, and free phosphanylidene-σ^4-phosphoranes as phospha-Wittig reagents offer additional versatility in synthetic applications.[38]

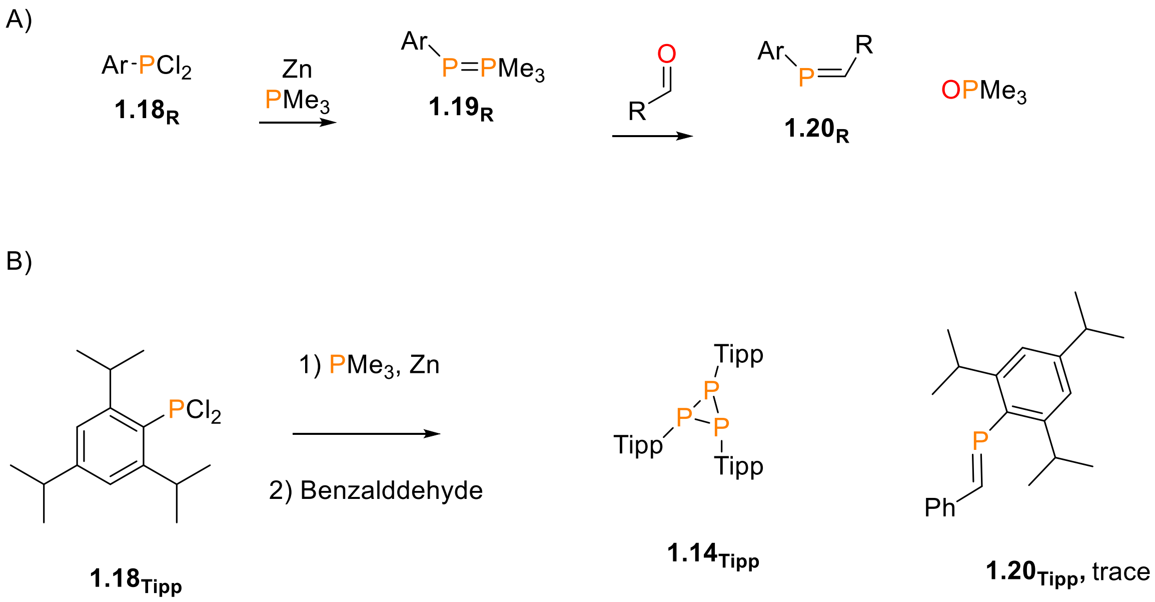
A)
Ar-PCl2
1.18R
Zn
PMe3
Ar
P=PMe3
1.19R
O
R
Ar
P
R
1.20R
OPMe3
B)
PCl2
1.18Tipp
1) PMe3, Zn
2) Benzalddehyde
Tipp
P
P
P
Tipp
Tipp
1.14Tipp
P
Ph
1.20Tipp, trace

Scheme 1-3. Reactivity modes of phospha-Wittig reagents: A) general phospha-Wittig reaction scheme; B) *in situ* generation and reaction of phospha-Wittig reagent *via* reduction of bulky dichlorophosphines with PMe_3 and zinc, and reaction with benzaldehyde.

NHCs and cAACs have been used for stabilizing low valent phosphorus species. NHCs exhibit poorer electron acceptance compared to cAAC ligands and are often better represented as forming a dative bond with phosphorus species. cAACs possess enhanced π-accepting character for back-donation, and feature shortened C-P distances, thus are more aptly described as phosphaalkenes. The reduction of $IPrNPCl_2$ (**1.22**, **Scheme 1-4**) in the presence of cAAC led to the isolation of base-stabilized phosphorus mononitride (P≡N, **1.21**). A similar strategy with an NHC was used to produce a set of P≡N and As≡N analogues (**1.22** – **1.24**).[39,40] The choice of weakly coordinating anion is important when isolating cationic main group cationic species.[41]

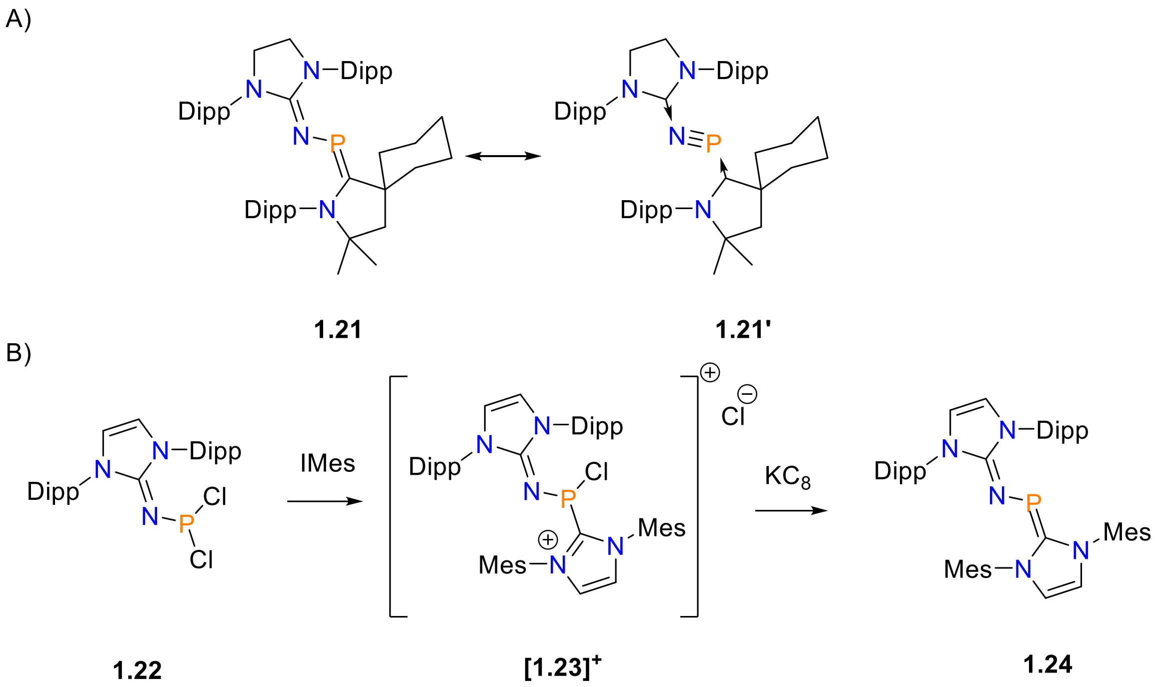
A)
N−Dipp
Dipp
N
N
P
Dipp−N
N−Dipp
Dipp
N
N≡P
Dipp−N
1.21
1.21'
B)
N−Dipp
Dipp
N
N
P
Cl
Cl
IMes
N−Dipp
Dipp
N
N
P
Cl
N
Mes
Mes−N
Cl
KC8
N−Dipp
Dipp
N
N
P
N
Mes
Mes−N
1.22
[1.23]+
1.24

Scheme 1-4. Base-stabilized phosphorus nitrides supported by NHC and/or cAAC ligands. A) Canonical forms of one phosphorus nitride example; B) synthesis of a base-stabilized phosphorus nitride.[39,40]

1.3.2 Classifying Bonding in Main Group Compounds

Understanding the nature of the compounds formed involved classifying them appropriately. When considering the bonding of adducts with a main group Lewis acid, questions arise about how to represent these structures accurately, namely as dative bonds[42] (donor-acceptor model) or covalent electron-sharing bonds.[43] This comparison may be found as dative bonds versus covalent bonds, but the term "covalent bond” refers to the energy lowering by the mixing of wavefunctions from two fragments that combine to give a molecule.[44–48] Dative bonds are distinguished from electron-sharing bonds by either heterolytic or homolytic cleavage, although their contributions has been suggested to exist in a continuum.[42,44] Dative arrows are therefore used to identify the flow of electrons from a donor to an acceptor, rather than a bond formation resulting from two atoms each contributing an electron.[47] This distinction is of value as there can be structural implications which fail to be explained by electron-sharing only models, such as the bent geometry of $C(PPh_3)_2$. [42]

A determination of the true nature of the bonding requires a holistic analysis of reactivity and of structural features in the solid state and *in-silico* models.[42,47] Energy decomposition analysis (EDA),[49] for example, is a computational method which breaks down an interpretation of a chemical bond into the individual components: an electrostatic interaction, repulsive Pauli exchange interaction, and covalent interactions; and for example, has been used to quantify metal backdonation to carbenes.[50] Himmel, Krossing, and Schnepf argued that the use of dative arrows in chemical structures should be avoided "*when one single conventional representation is entirely sufficient*".[43] While there is often a disparity between formal charges assigned in classical Lewis structures and partial atomic charges, canonical structures offer insights when structural parameters are intermediate between dative bonds and electron-sharing bonds.[44]

An example of this was in a report by the Alcarazo group who investigated N-centered cations, including **[1.25]$^{3+}$** (**Figure 1-4**).[51] They proposed two canonical structures with varying formal charges on the central nitrogen, electron-sharing to datively bonded models. Natural population analysis (NPA) calculations suggested the electronic structure was more closely related to **[1.25]$^{3+}$**, but the solid-state structure revealed a planar nitrogen with the cyclopropylidene ligands twisted out of the nitrogen coordination plane. This observation, along with calculated N-C bond orders, suggests minimal back donation from nitrogen into the rings.

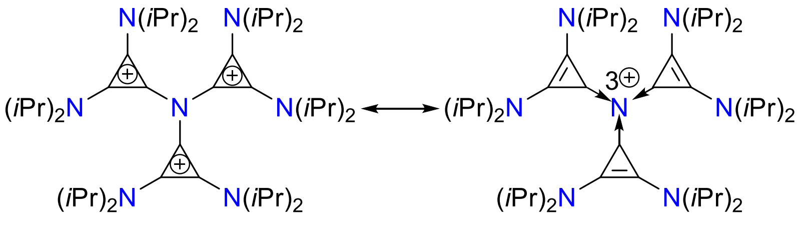

[1.25]$^{3+}$ **[1.25']$^{3+}$**

Figure 1-4. Examples of canonical forms **[1.25]$^{3+}$** .[51]

1.3.3 Strong σ and π-Donating Ligands

Ylidic substituents offer both σ and π- electron donation and have been effectively employed for zwitterionic stabilization of reactive phosphorus-chalcogenide species, without large a steric profile (see **Section 1.4.3**). Other ligands which offer comparable electronic stabilizations to phosphorus ylides are iminophosphines, N-heterocyclic imine (NHI), cyclic alkyl(amino)iminates, and N-heterocyclic olefin (NHO) ligands (**Figure 1-5**).[52–55] Furthermore, NHI ligands have been employed to stabilize various phosphorus and main group species. The coordination geometry of NHI ligands to acceptor atoms in solid-state structures, along with bond order calculations, indicates their capability to function as two, four, or six electron donors.[56]

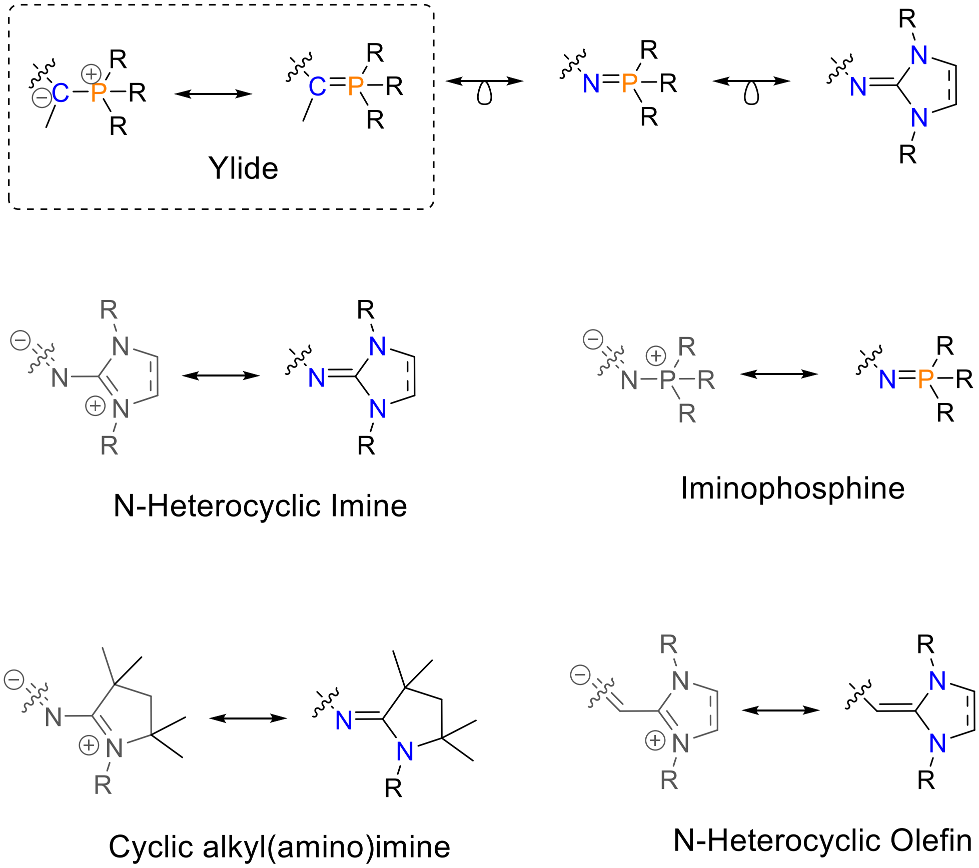

Figure 1-5. Resonance structures for an ylide and isolobal relationships with other ligands.

Phosphorus species supported by N-heterocyclic imine (NHI) ligands were first reported by Kuhn and co-workers in 1996, and later gained attention by 2010 by Bertrand and coworkers.[57] They demonstrated that [**1.27**]**OTf** (**Scheme 1-5**) could undergo a single-electron reduction to the isolable neutral phosphinyl radical **1.28**$^{\bullet}$, with significant localized spin density on phosphorus.[58] Many NHI-supported main group species have been prepared by reactions of a free NHC with $SiMe_3N_3$, followed by a condensation reaction with a respective element-halide bond.[56] Another reported route involved Staudinger-like rearrangement of an azido phosphorus-NHC adduct.[59] Access to diverse bulky NHC precursors has increased versatility of NHI-supported specices.[60]

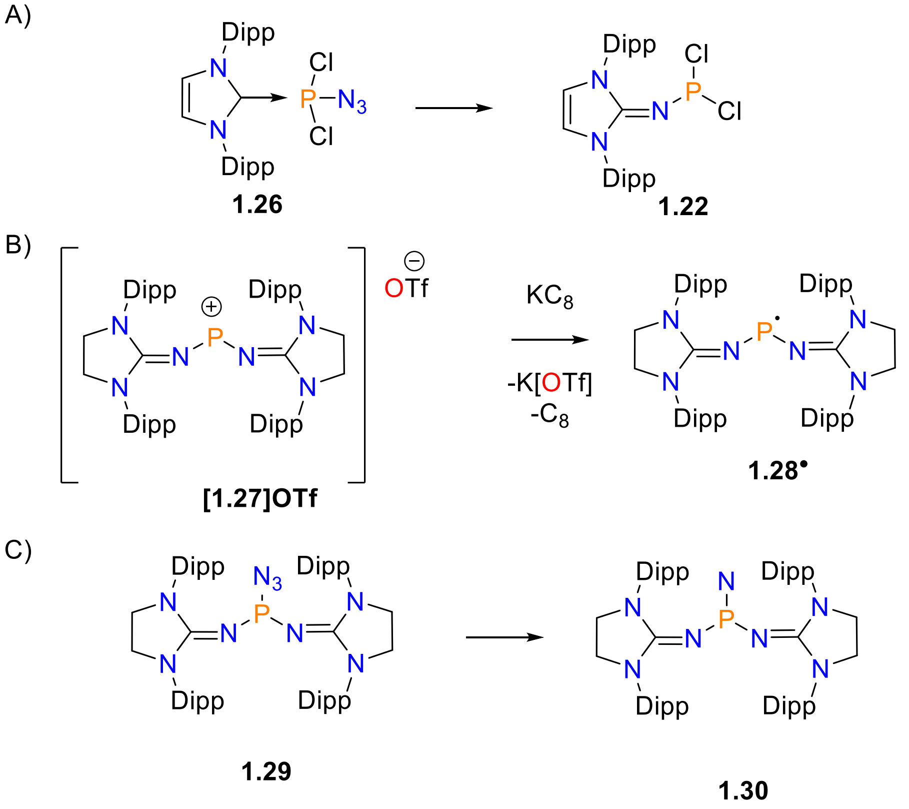
A)
Dipp
N
Cl
P
N3
Cl
N
Dipp
1.26
Dipp
Cl
N
N
P
Cl
N
Dipp
1.22
B)
Dipp
Dipp
N
P
N
N
N
N
N
Dipp
Dipp
OTf
[1.27]OTf
KC8
-K[OTf]
-C8
Dipp
Dipp
N
P
N
N
N
N
N
Dipp
Dipp
1.28•
C)
Dipp
N3
Dipp
N
P
N
N
N
N
N
Dipp
Dipp
1.29
Dipp
N
Dipp
N
P
N
N
N
N
N
Dipp
Dipp
1.30

Scheme 1-5. Selected examples of NHI-supported phosphines. A) formation of NHI-supported phosphine *via* Staudinger-type mechanism; B) single electron oxidation of phosphenium **[1.27]OTf**; C) synthesis of singlet phosphinonitrene.

Dielmann and Bertrand later reported conversion of an azidophosphine (**1.29**) to a stable and isolable phosphinonitrene (**1.30**, **Scheme 1-5**), and demonstrated nitrene-metal coordination and activations of small molecules.[61,62] Dielemann and co-workers expanded heavily into NHI-supported phosphorus species, including modified backbone substituents with a photo-switchable tail-group (**1.35**) or as a redox and pH sensitive ligand (**1.36**).[63–65] They also demonstrated cycloaddition reactions of cationic phosphorus oxide (**[1.31O]$^+$**) and phosphorus sulfide (**[1.31S]$^+$**) species (**Scheme 1-6**).[66–69]

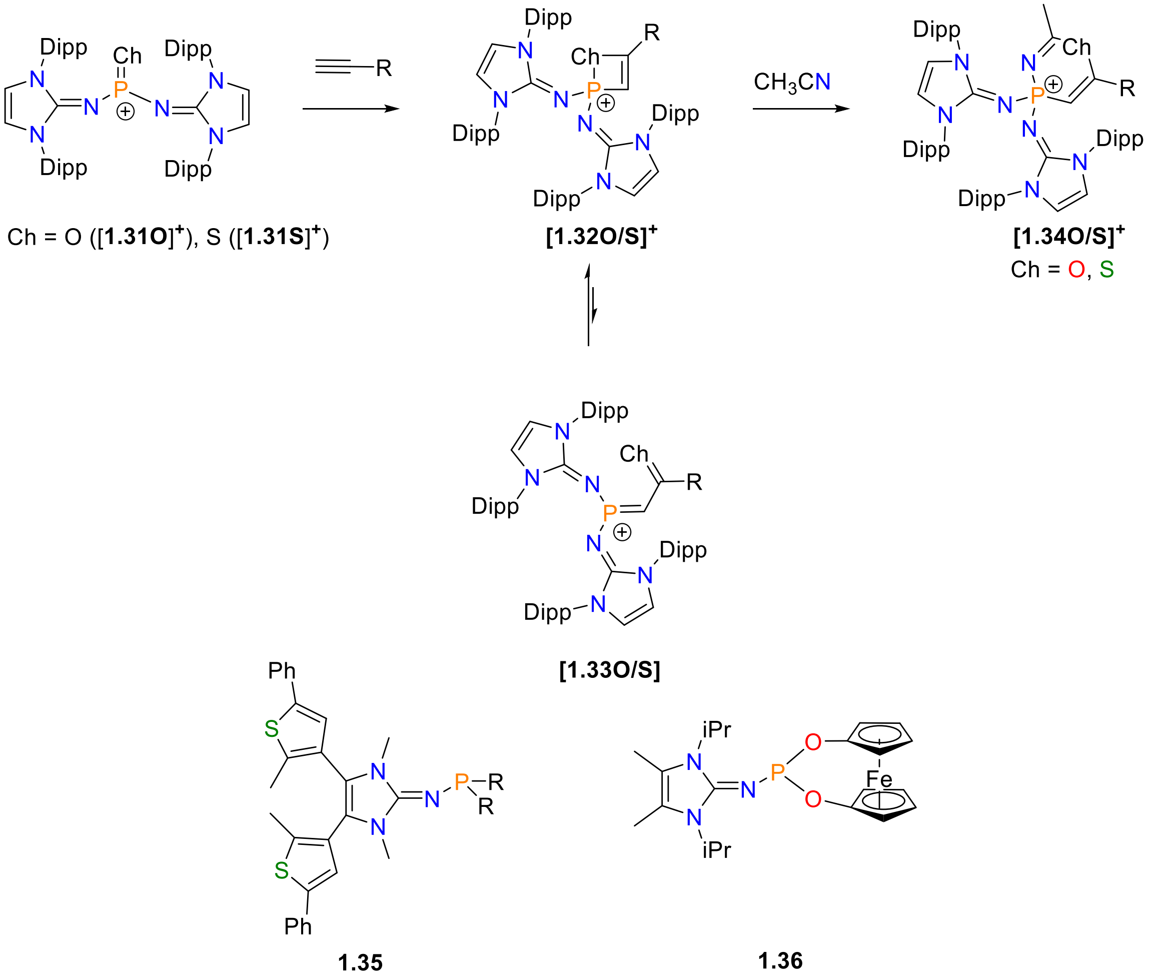

Ch = O ([**1.31O**]$^+$), S ([**1.31S**]$^+$)

[1.32O/S]$^+$

[1.34O/S]$^+$
Ch = O, S

[1.33O/S]

1.35

1.36

Scheme 1-6. Recent examples of NHI-supported phosphorus species, reported by Dielmann and co-workers.

1.3.4 Strong σ-Donor, Poor π-Acceptor Ligands

Ligands that offer strongly σ-donating properties, yet weak π-donation or acceptor properties, are important in main group chemistry. These ligands will often bear an adjacent partial positive charge (α-cation) when coordinated to an acceptor atom, while calculations and structural analysis may suggest minimal back-bonding and a low bond order. A highlighted example of this is the bis(diisopropylamino)cyclopropenylidene or bis(diisopropyl)cyclopropenium ligand (BAC, **Figure 1-6**).

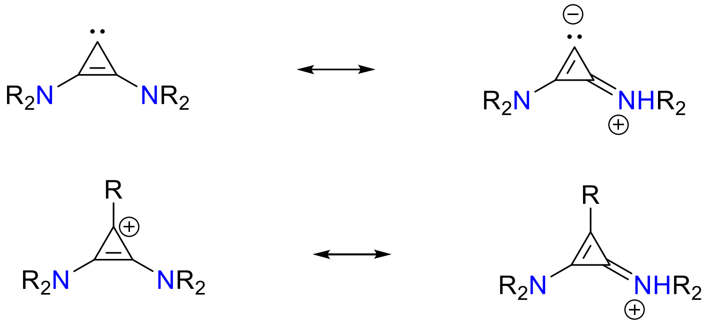

Figure 1-6. Resonance structures contributing to stabilization of bis(amino)cyclopropenylidene and bis(amino)cyclopropenium.

The first crystalline example of an isolated cyclopropylidene was reported by Bertrand using the bis(diisopropylamino) substitution pattern and demonstrated high thermal stability of 80 °C with only 10 % decomposition.[70] The unusual stability of the strained three-membered ring carbene is attributed to the donation form the flanking nitrogen lone pairs, which is more evident in cationic species than the free carbene.[70] Analysis by ^{1}H and ^{13}C variable temperature NMR spectroscopy revealed restricted rotation of isopropyl groups with a rotational barrier of 53 kJ/mol (**1.38**) while the parent protonated cyclopropenium (**[1.37]BF**$_4$, **Scheme 1-7**) has a C-N rotation barrier of 75 kJ/mol. This is in agreement with a stronger inductive effect from the nitrogen lone pairs into the ring of the positively charged species than the neutral species.

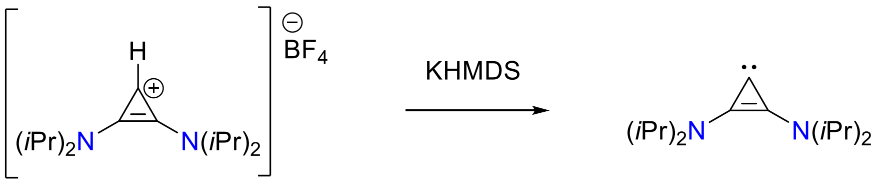

[1.37]BF$_4$

1.38

Scheme 1-7. Synthesis of isolable cyclopropylidene **1.38**.

The stabilizing effect of the amino groups can be demonstrated by comparing nucleophilic substitution reactions of 1,1-dichlorocyclopropenes (**1.39$_{Mes}$**) with 1-chlorocyclopropenium chloride (**[1.43]OTf**, **Scheme 1-8**). Nucleophilic substitution at the C-Cl bond of **[1.3]**$^+$ has been demonstrated using amines, alcohols, and PPh_3.[71–73] In contrast, **1.39$_{Mes}$** has been shown to react with PPh_3 in the presence of $SiMe_3OTf$ to yield a ring-opened species **[1.42$_{Mes}$]OTf**.[73]

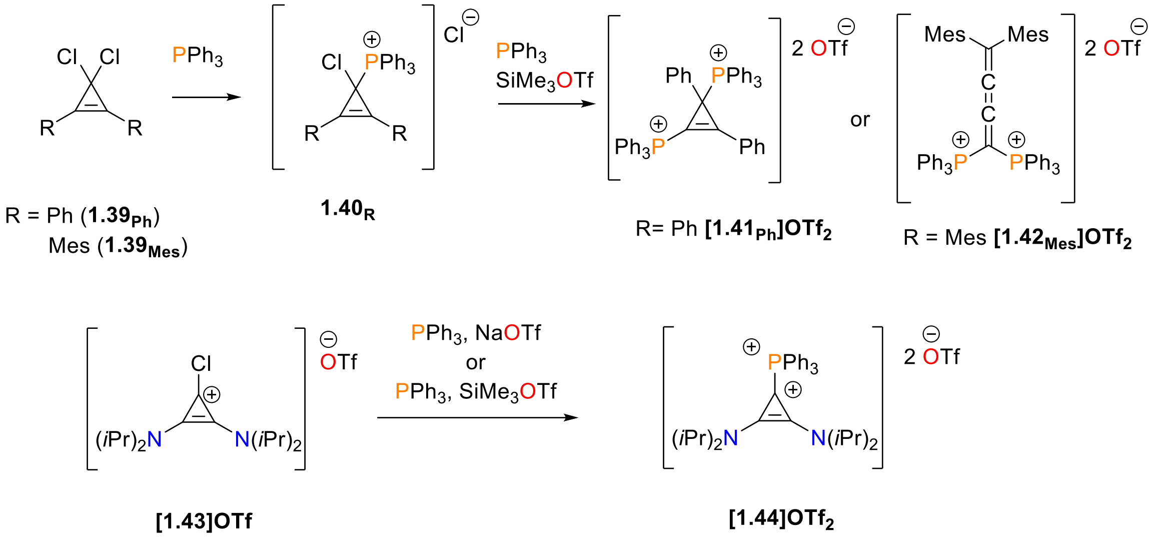
Cl
Cl
R
R
PPh3
Cl
PPh3
R
R
Cl
PPh3
SiMe3OTf
Ph
PPh3
Ph3P
Ph
2 OTf
or
Mes
Mes
C
C
Ph3P
PPh3
2 OTf
R = Ph (1.39Ph)
Mes (1.39Mes)
1.40R
R= Ph [1.41Ph]OTf2
R = Mes [1.42Mes]OTf2
Cl
(iPr)2N
N(iPr)2
OTf
PPh3, NaOTf
or
PPh3, SiMe3OTf
PPh3
(iPr)2N
N(iPr)2
2 OTf
[1.43]OTf
[1.44]OTf2

Scheme 1-8. Contrasting reactivities of cyclopropenium species.

The Alcarazo group has extensively studied α-cationic phosphines and arsines, including BAC-supported phosphines.[74,75] Several methods have been reported for the incorporation of a cyclopropenium ligand, including: reactions of the free carbene with low-valent species, salt metathesis, dehydrohalogenation, transfer metalation, and onio-transfer reactions.[76] Their analysis of DFT-calculated LUMOs for various cationic phosphine ($L\text{-}PPh_2^+$) species showed that cyclopropenium ligands have lower electron-accepting ability compared to NHC or pyridyl-based ligands.[77] This observation was based on the LUMO localization on either the cationic-ligand or the P-phenyl groups. They observed that excessive positive charge reduces the coordination ability of phosphorus species with metals. The decrease in nucleophilic character of phosphorus lone pairs in cationic organophosphines was attributed to the inductive effect toward positively charged ligands, while simultaneously demonstrating increased pi accepting ability from metal complexes due to their low lying P-C σ* orbitals.[77] Despite being generally poor ligands, dicationic phosphines, particularly those with BAC substituents, were able to form complexes with gold and platinum.[76]

1.4 Phosphinidene Chalcogenides (RPCh)

1.4.1 Theory

Phosphinidene-chalcogenides (R-P=Ch, **1.45Ch** where Ch = O, S, Se) are a class of highly reactive P^{III} compounds which offer synthetic value towards the production of phosphorus heterocycles *via* carbene or olefinic-like reactivity.[78–82] Unlike nitrosobenzenes (R-N=O), however, which have found application in organic transformations, the related two coordinate [R-P=Ch] species are not well understood due to their high reactivity. Phosphinidene oxides and sulfides have been studied as free transient intermediates or within a metal coordination sphere, stabilized by strong donor ligands, or with uniquely tailored ligands, as well as their reactivity towards unsaturated substrates for cycloaddition reactions (**Scheme 1-9**).[83–88] As discussed earlier with phospha-Wittig reagents, surrogates with behaviours akin to monomeric **1.45S** have been reported (**1.46S**).[85]

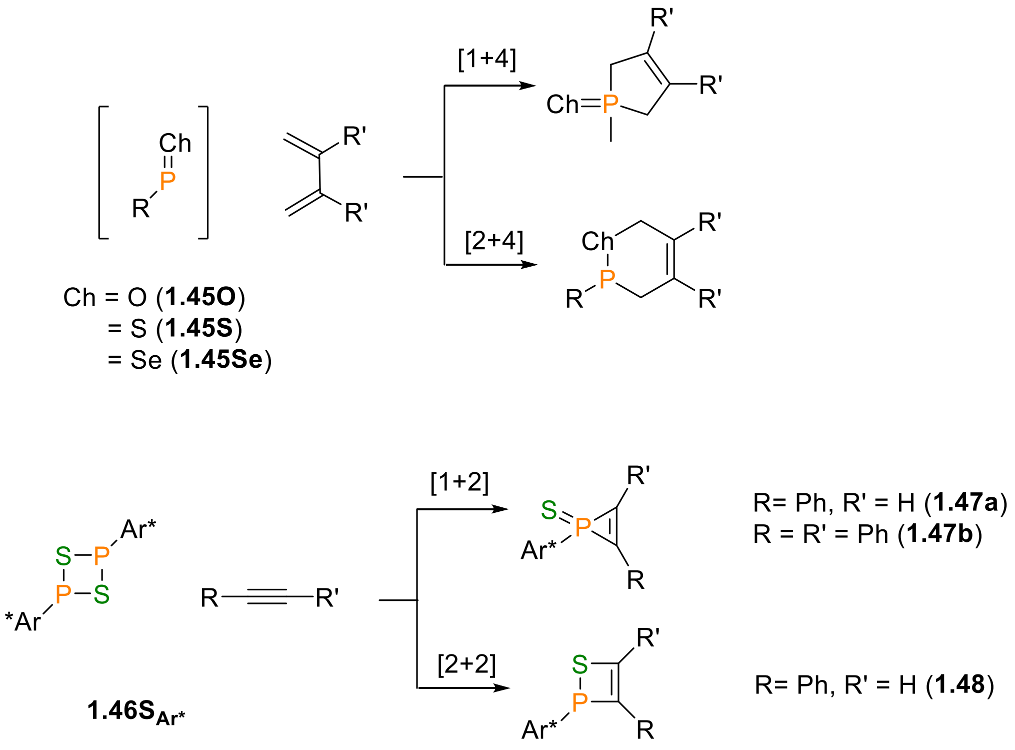
Ch
P
R
R'
R'
[1+4]
R'
Ch=P
R'
[2+4]
Ch
P
R
R'
R'
Ch = O (1.45O)
= S (1.45S)
= Se (1.45Se)
S
P
Ar*
P
S
*Ar
1.46S$_{Ar*}$
R
R'
[1+2]
S
P
Ar*
R'
R
R= Ph, R' = H (1.47a)
R = R' = Ph (1.47b)
[2+2]
S
P
Ar*
R'
R
R= Ph, R' = H (1.48)

Scheme 1-9. Cycloaddition reactions of phosphinidene chalcogenides (**1.45Ch**) and surrogate species (**1.46**).

Schoeller and Niecke compared frontier orbital energies of phosphaalkenes (**1.49**), iminophosphines (**1.50**), and phosphine-oxides (**1.45O**$_{\mathrm{H}}$). The HOMO of phosphaalkenes consisted of the P=C π bond, and the LUMO consisted of the P=C π* character. The symmetry calculated in the HOMO and LUMO suggested that RP=CR$_2$ will exhibit reactivity akin to olefins in [2+2] cycloadditions.[89] Replacement of the element bonded to phosphorus revealed that an increase in electronegativity or a π-accepting character, resulted in a HOMO which possessed more lone-pair character, akin to singlet carbenes.[89] Calculated frontier molecular orbitals of MeP=S (**1.45S**$_{\mathrm{Me}}$, **Figure 1-7**) revealed that the HOMO consisted of an in-plane phosphorus lone pair, P-C σ bond character, and in-plane P-S π bond character, while the HOMO-1 consisted largely of P=S π bond character.[90]

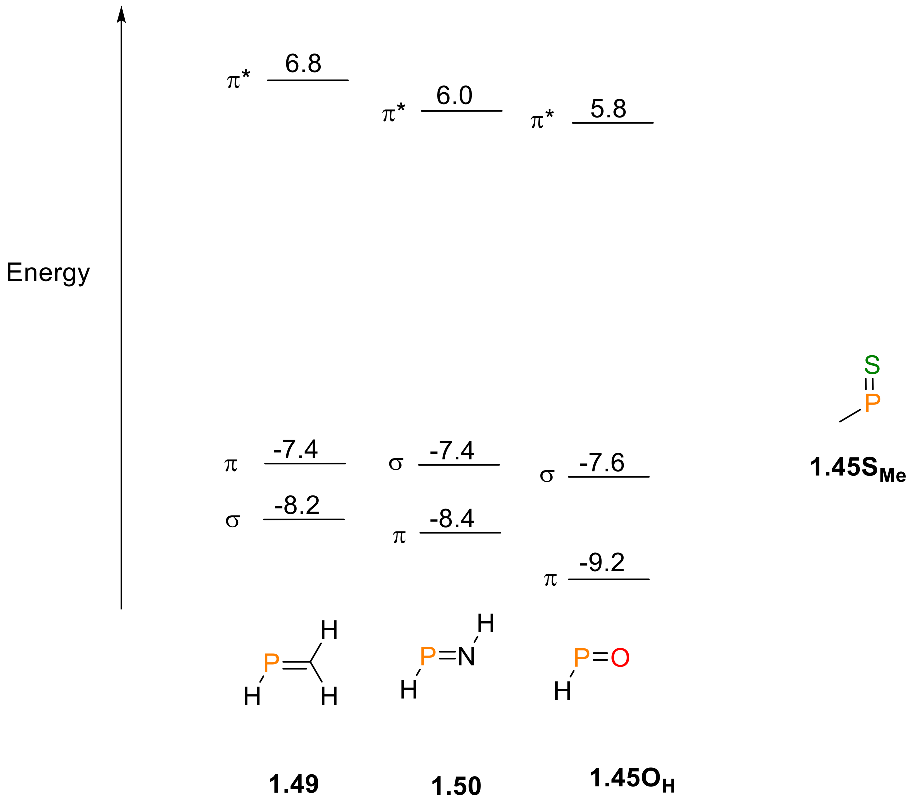

Figure 1-7. Sequence of energies (in eV) of the orbitals s and π, π* for HP=X, obtained from complete energy-optimized ab initio STO/3G calculations.[89]

1.4.2 Generation

Many methods have been reported to generate a [RPS] *in situ* by reductions with magnesium, thermolysis, or photolysis, or condensation with $S(SiMe_3)_2$ or Na_2S (**Figure 1-8**).[79,81,83,91–93] The [RP=S] unit is treated as reactive intermediate trapped by cycloaddition reactions, stabilized in solution by strong donor ligands, or prepared within the coordination sphere of a transition-metal complex.[85,86,94]

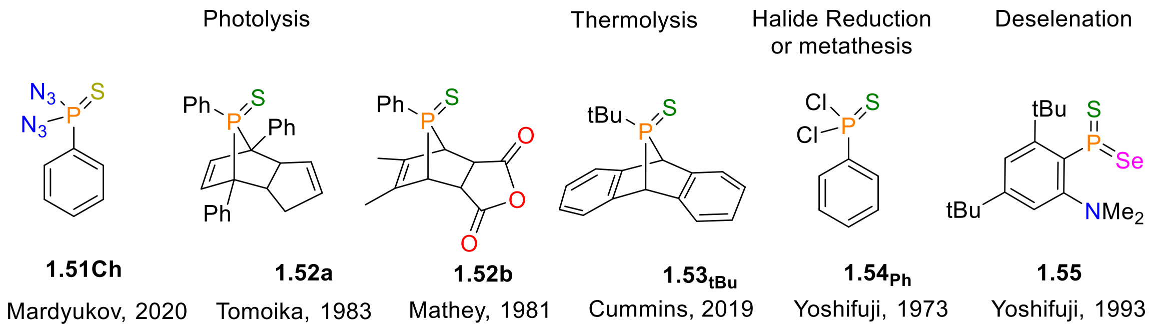
Photolysis
Thermolysis
Halide Reduction or metathesis
Deselenation
1.51Ch
Mardyukov, 2020
1.52a
Tomoika, 1983
1.52b
Mathey, 1981
1.53tBu
Cummins, 2019
1.54Ph
Yoshifuji, 1973
1.55
Yoshifuji, 1993

Figure 1-8: Selected examples of precursors used to generate RP=S intermediates.

The first reported example of a phosphinidene oxide *in situ* by Stille and co-workers could not be isolated in the solid state.[95] The authors prepared a P(V) phosphine oxide precursor which liberated tetraphenylnapthalene upon thermolysis. Decomposition of [PhPO] at 155 °C resulted in the formation of an oligomeric species $(PhPO)_{14}$ (**1.58**). They demonstrated reactions of both **[1.45O$_{Ph}$]** and **1.58** with methanol, $(EtS)_2$, and $CH_2{=}C(OEt)_2$ acetal to generate P(V) addition products (**1.59** – **1.61**, **Scheme 1-10**). The authors suggested that the formation occurred *via* addition of the phosphinidene oxide across the double bond, followed by rearrangements rather than a radical mechanism, as $CH_2{=}C(OEt)_2$ as a radical trap would be expected to add to the terminal carbon of the acetal instead.[95]

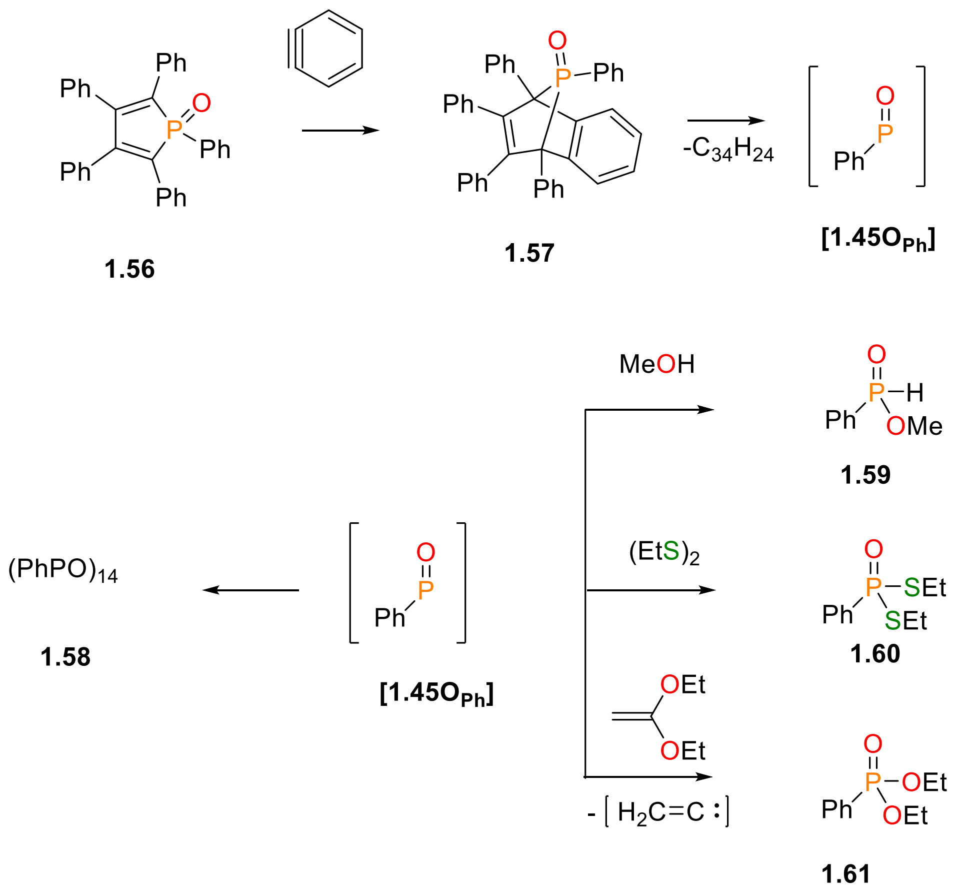
Ph
Ph
Ph
Ph
P
O
Ph
1.56
Ph
Ph
Ph
Ph
P
O
Ph
1.57
-C$_{34}$H$_{24}$
[1.45O$_{Ph}$]
MeOH
P
O
H
Ph
OMe
1.59
(PhPO)$_{14}$
1.58
[1.45O$_{Ph}$]
(EtS)$_2$
P
O
SEt
Ph
SEt
1.60
OEt
OEt
- [H$_2$C=C :]
P
O
OEt
Ph
OEt
1.61

Scheme 1-10. Reactions of transient **1.45O$_{Ph}$** generated by thermolysis of **1.57**.

Mathey and co-workers developed a series of precursors which generated phenylphosphinidene sulfide (**[1.45S$_{Ph}$]**) slowly *in situ* by dehydrobromination in the presence of a NEt$_3$ (**Scheme 1-11**). **[1.45S$_{Ph}$]** was trapped by either [4+2] cycloaddition reactions with 2,3-dimethyl-1,3-butadiene, or sequential reactions involving cyclopentadiene which produced a thiadiphospholane sulfide **1.65**. It was suggested that after the first [4+2] cycloaddition, a second equivalent of **[1.45S$_{Ph}$]** demonstrates carbene-like reactivity and inserted into the strained P-C bond.[90] The Cummins group reported a similar release of **[1.45S$_{Ph}$]** at 70 °C, but demonstrated divergent reactivity of **1.53$_{tBu}$** and **1.53$_{H}$** with 2,3-dimethyl-1,3-butadiene (**Scheme 1-12**). The expected [4+2] cycloaddition product (**1.66a**) was formed at 70 °C with **1.53$_{tBu}$**, but attempts to release and trap “HP=S” from **1.53$_{H}$** at 140 °C instead yielded an insoluble yellow polymeric (P$_2$S)$_n$ material (**1.66b**).[83]

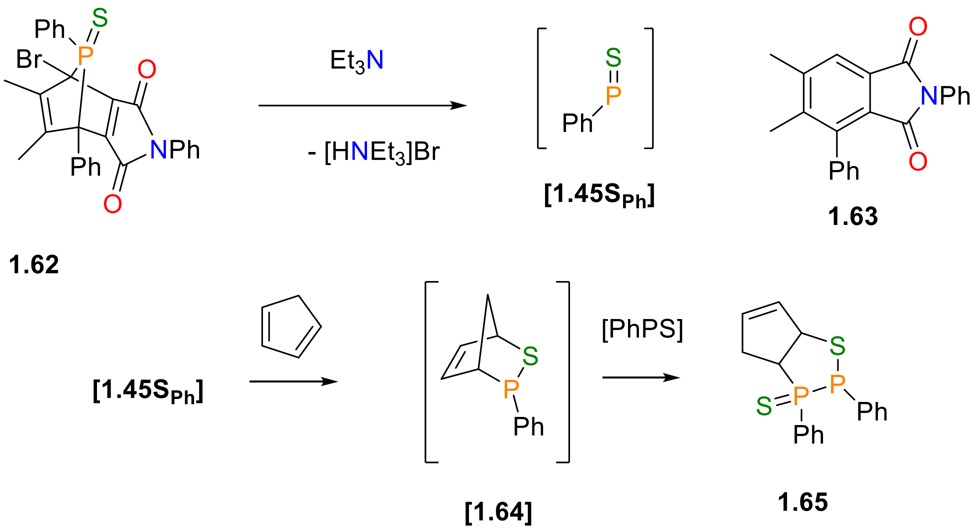
Et$_3$N
- [HNEt$_3$]Br
1.62
[1.45S$_{Ph}$]
1.63
[1.45S$_{Ph}$]
[PhPS]
[1.64]
1.65

Scheme 1-11. Dehydrobromination method of release of **[1.45S$_{Ph}$]** and sequential reactions involving cyclobutadiene.[90]

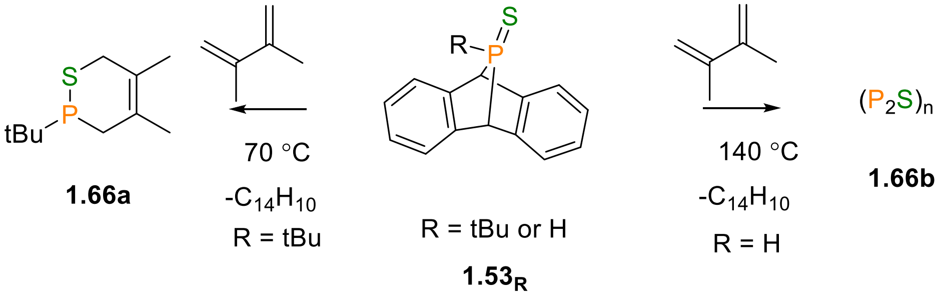
1.66a
70 °C
-C$_{14}$H$_{10}$
R = tBu
R = tBu or H
1.53$_R$
140 °C
-C$_{14}$H$_{10}$
R = H
(P$_2$S)$_n$
1.66b

Scheme 1-12. Divergent reactivity with 2,3-dimethyl-1,3-butadiene after thermal release of [RPS] from **1.53$_R$**.[83]

Oligomeric (RPS)$_n$ specices are also known to form in solution (n = 2, 3, or 4), although few have been structurally characterized.[85,96–100] Reduction of a bulky **1.54$_{Mes*}$** using Mg^0 was found to produce three isolable species, including an air stable thiadiphosphirane (**1.68S$_{Mes*}$**), diphosphene (**1.3$_{Mes*}$**), and a trimeric species [(Mes*PS)$_3$, **1.67S$_{Mes*}$**], separable *via* silica gel chromatography.[101] **1.67S$_{Mes*}$** has also been prepared *via* desulfurization of a dithiophosphorane (**1.69S$_{Mes*}$**), which was further reduced to the diphosphene (**1.3$_{Mes*}$**) by PPh$_3$ (**Scheme 1-13**).[102]

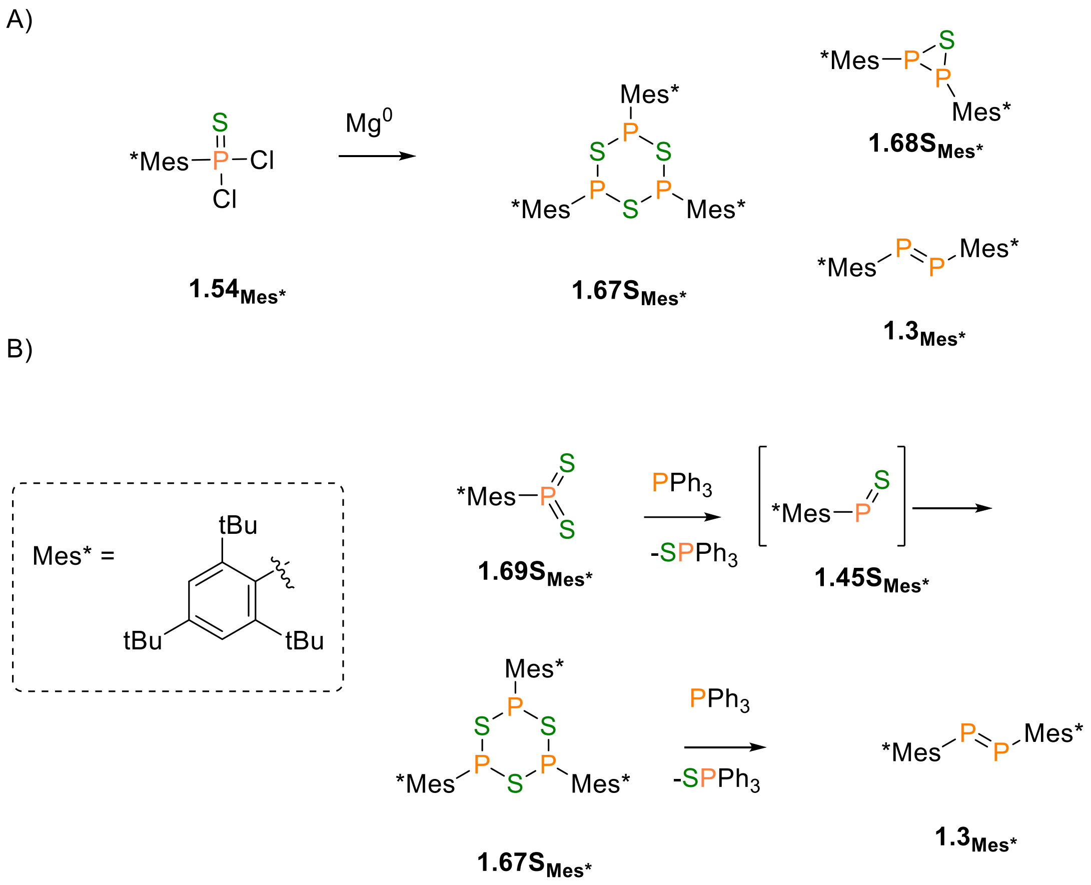
A)
Mg^0
*Mes–P(=S)(Cl)–Cl
1.54$_{\mathrm{Mes*}}$
1.67S$_{\mathrm{Mes*}}$
1.68S$_{\mathrm{Mes*}}$
1.3$_{\mathrm{Mes*}}$
B)
Mes* =
tBu
tBu
tBu
PPh$_3$
-SPPh$_3$
1.69S$_{\mathrm{Mes*}}$
1.45S$_{\mathrm{Mes*}}$
PPh$_3$
-SPPh$_3$
1.67S$_{\mathrm{Mes*}}$
1.3$_{\mathrm{Mes*}}$

Scheme 1-13. Syntheses of oligomeric (RPS)$_3$ species, and related by-products. A) Unselective reduction of Mes*PSCl$_2$ with magnesium metal; B) sequential desulfurization reactions from a parent dithioxophosphorane.[101,102]

A neutral tetrameric phosphorus-sulfur heterocycle (**1.70S$_{\mathrm{Mes}}$**) was isolated after reaction of the less bulky MesPCl$_2$ (**1.69S$_{\mathrm{Mes}}$**) with (SiMe$_3$)$_2$S (**Scheme 1-14**).[98] Analogous tetra-cationic imidazolium-supported phosphorus-sulfur heterocycles (**[1.73$_{\mathrm{R}}$]OTf$_4$**, **Scheme 1-14**) were prepared in high yields by condensation reaction of **[1.71$_{\mathrm{R}}$]OTf** with S(SiMe$_3$)$_2$, although an intermediate cationic two-coordinate phosphinidene sulfide (**1.72**) was not detected. VT-NMR and ^{31}P EXSY spectra of **[1.73$_{\mathrm{R}}$]OTf$_4$** revealed interconversion between a crown and boat shaped conformations.

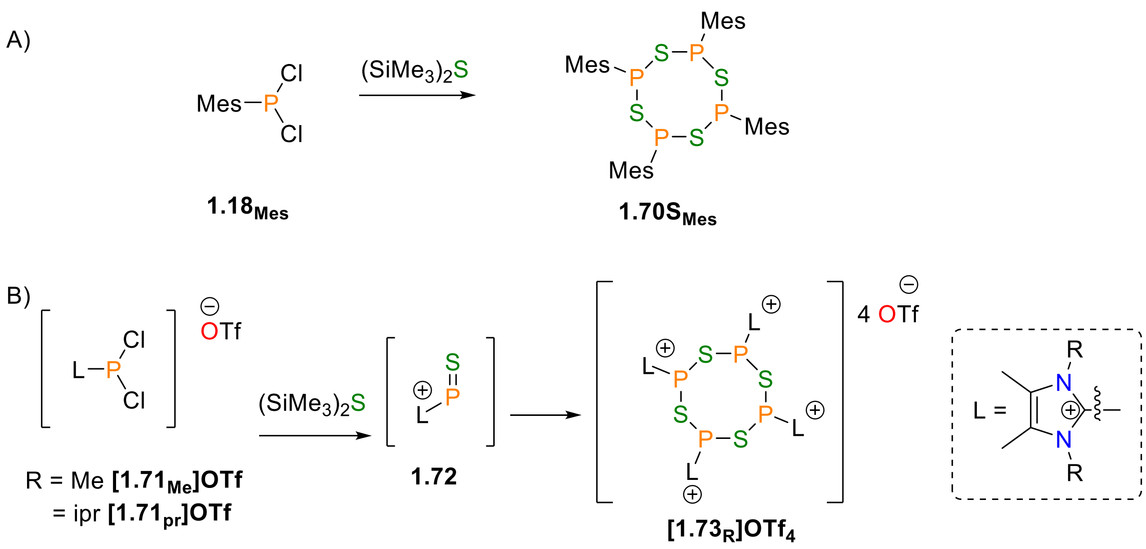
A)
Mes
Cl
Cl
(SiMe3)2S
1.18Mes
1.70SMes
B)
L
OTf
(SiMe3)2S
1.72
4 OTf
L =
N
R
R = Me [1.71Me]OTf
= ipr [1.71pr]OTf
[1.73R]OTf4

Scheme 1-14. Formations of (RPS)$_4$. A) Neutral oligomer synthesis; B) tetra-cationic oligomer supported by imidazolium ligands.

A family of heterocycles related to phosphinidene chalcogenides are chalcogendiphosphiranes (**1.68Ch**). Thiadiphosphiranes (**1.68S**) and selenodiphosphiranes (**1.68Se**) are often prepared *via* sub-stoichiometric sulfurization or selenation of diphosphenes.[102–105] They have also been reported as side products during reductions of dichlorophosphine sulfides (*e.g.***Scheme 1-13**), condensation of a P,P' dichlorodiphosphine (**1.74$_{\mathbf{tbu}}$**) with bis(trimethylstannyl) sulfide, or deoxygenation of EO$_2$ (E = S, Se) with a phospha-Wittig reagent (**Scheme 1-15**).[106,107]

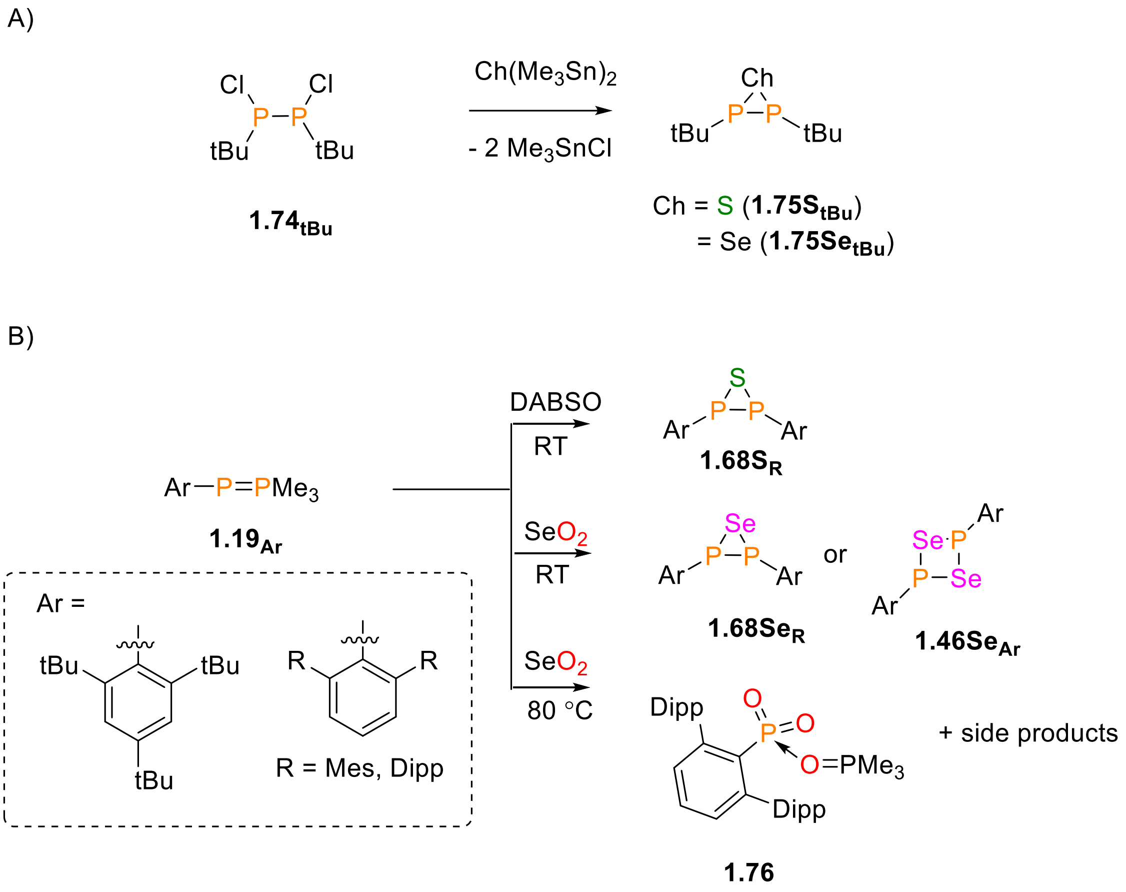
A)
Ch(Me$_3$Sn)$_2$
- 2 Me$_3$SnCl
1.74$_{tBu}$
Ch = S (1.75S$_{tBu}$)
= Se (1.75Se$_{tBu}$)
B)
Ar—P=PMe$_3$
1.19$_{Ar}$
DABSO
RT
SeO$_2$
RT
SeO$_2$
80 °C
1.68S$_R$
1.68Se$_R$
or
1.46Se$_{Ar}$
1.76
+ side products
Ar =
R = Mes, Dipp

Scheme 1-15. Reactions producing thiadiphosphiranes, selenodiphosphiranes, and related species. A) Metathesis reaction of dichlorodiphosphine 1.74tBu with Ch(SnMe$_3$)$_2$; B) reactions of terphenyl-supported phospha-Wittig reagent with chalcogen dioxide specices.[106,107]

The first account of [RP=S] to be stabilized in solution and studied by NMR spectroscopy was by Yoshifuji *et al.* (**Scheme 1-16**).[87] Deselenation of a mixed halogen selenoxothioxophosphorane (**1.55$_{Mx}$**) supported by a pendant σ-donor dimethylamino substituent using tris(dimethylamino)phosphine allowed for *in situ* detection of a phosphindiene sulfide[87] (**1.45S$_{Mx}$**, δ_P = 382), which decomposed to unidentified species. Analogous delsenenation of diselenophosphorane (**1.77$_{Mx}$**) resulted in transient formation of a phosphinidene selenide[108] (**1.45Se$_{Mx}$**, δ_P = 399), which decomposed *via* disproportonation to generate a diphosphene (**1.16$_{Mx}$**) and regenerate the diselenide (**1.77$_{Mx}$**, **Scheme 1-16**).

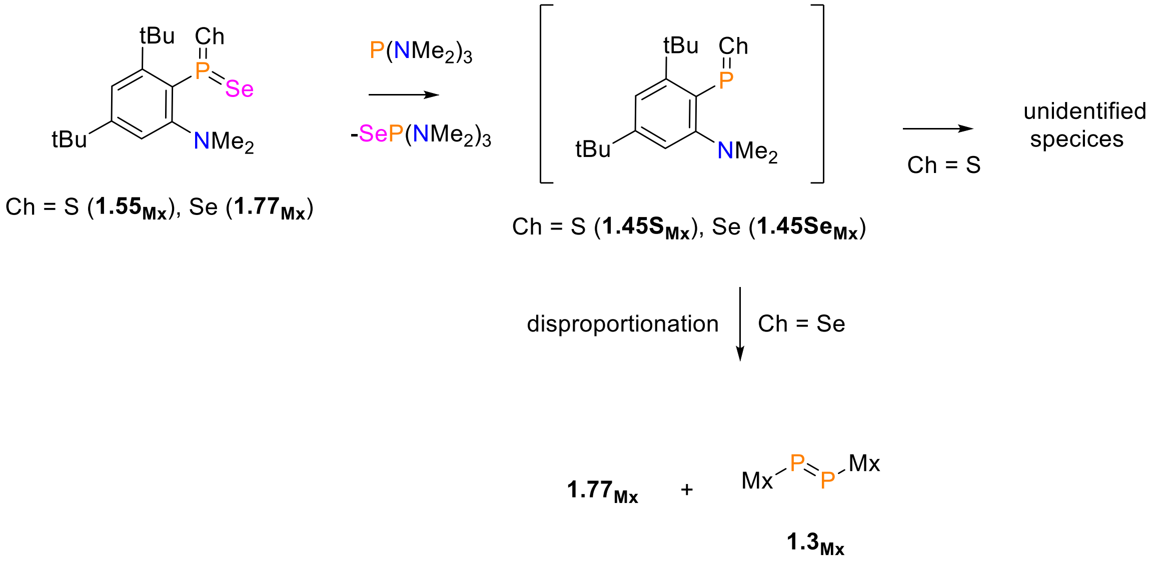
tBu
Ch
P
Se
tBu
NMe$_2$
Ch = S (**1.55$_{Mx}$**), Se (**1.77$_{Mx}$**)
P(NMe$_2$)$_3$
-SeP(NMe$_2$)$_3$
tBu
Ch
P
tBu
NMe$_2$
Ch = S (**1.45S$_{Mx}$**), Se (**1.45Se$_{Mx}$**)
Ch = S
unidentified species
disproportionation
Ch = Se
1.77$_{Mx}$
+
Mx
P
P
Mx
1.3$_{Mx}$

Scheme 1-16. Deselenation reactions of dichalcogoxophosphoranes to phosphinidene chalcogenides and subsequent decompositions, reported by Yoshifuji and co-workers.[108]

1.4.3 Isolation

Isolations of [PhP=S] and [PhP=O] were recently reported at low temperatures within frozen argon matrices (**Scheme 1-17**).[93] This allowed for spectroscopic characterization by IR and UV-vis. Recently PhP=O (**1.45O$_{Ph}$**) and PhP=S (**1.45S$_{Ph}$**) were observed by IR and UV-vis spectroscopies at 10 K in argon matrices by photolysis of their parent bis-azido molecules (**1.51Ch**).[93] Thermolysis or photolysis of $MeOP(N_3)_2$ (**1.78**) yielded phosphinidene (**1.79**), while light-induced isomerization generated MeP=O phosphinidene oxide (**1.45O$_{Me}$**) in a cryogenic H_2 or N_2 matrix. A nitrene intermediate was observable post-photolysis using EPR and IR spectroscopies.[109]

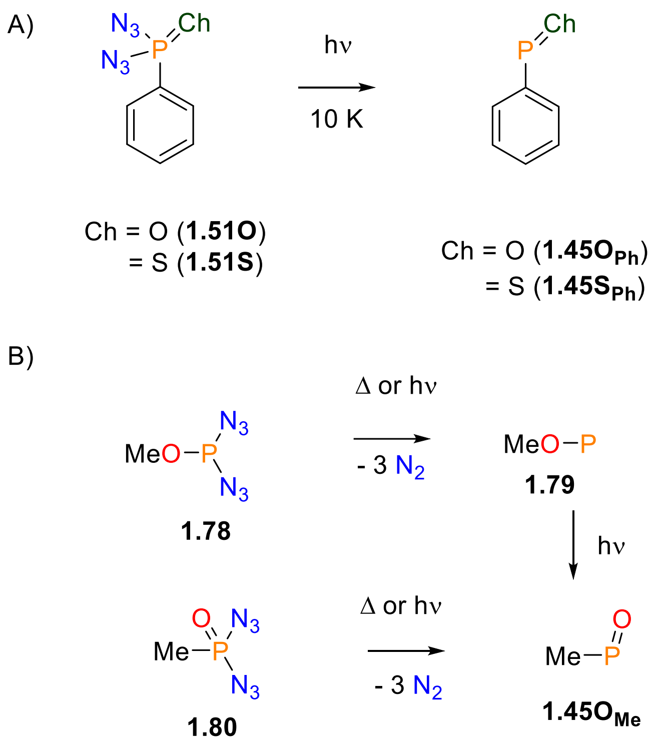
A)
N3
Ch
N3
P
hν
10 K
P
Ch
Ch = O (1.51O)
= S (1.51S)
Ch = O (1.45OPh)
= S (1.45SPh)
B)
Δ or hν
N3
MeO
P
N3
- 3 N2
MeO
P
1.79
1.78
hν
Δ or hν
O
N3
Me
P
N3
- 3 N2
O
Me
P
1.80
1.45OMe

Scheme 1-17. Reduction of bis(Azido)phosphines to access phosphinidene chalcogenides. A) Photolysis performed in a frozen argon matrix at 10 K. B) Generation of methylphosphinidene oxide *via* isomerization of methoxyphosphinidene (**1.79**) or reduction of P(V) species **(1.80**).[109]

The oxidation of an NHC-phosphinidene adduct (**1.81**$_{\mathbf{Ter}}$**)** with N_2O produced an NHC stabilized phosphinidene oxide (**1.82**, **Scheme 1-18**) which was structurally characterized by SC-XRD. The authors demonstrated single electron oxidation of **1.81** with KC_8 or $[NO]SbF_6$ to [**1.83**]SbF_6, supported by an *in situ* EPR spectrum that possessed a weak doublet, presumably for the radical intermediate **[1.83]**$^{\bullet}$. Isolation of the radical [**1.83**]SbF_6 was not possible due to spontaneous hydrogen abstraction and isomerization to **[1.85]**$\mathbf{SbF_6}$.[110]

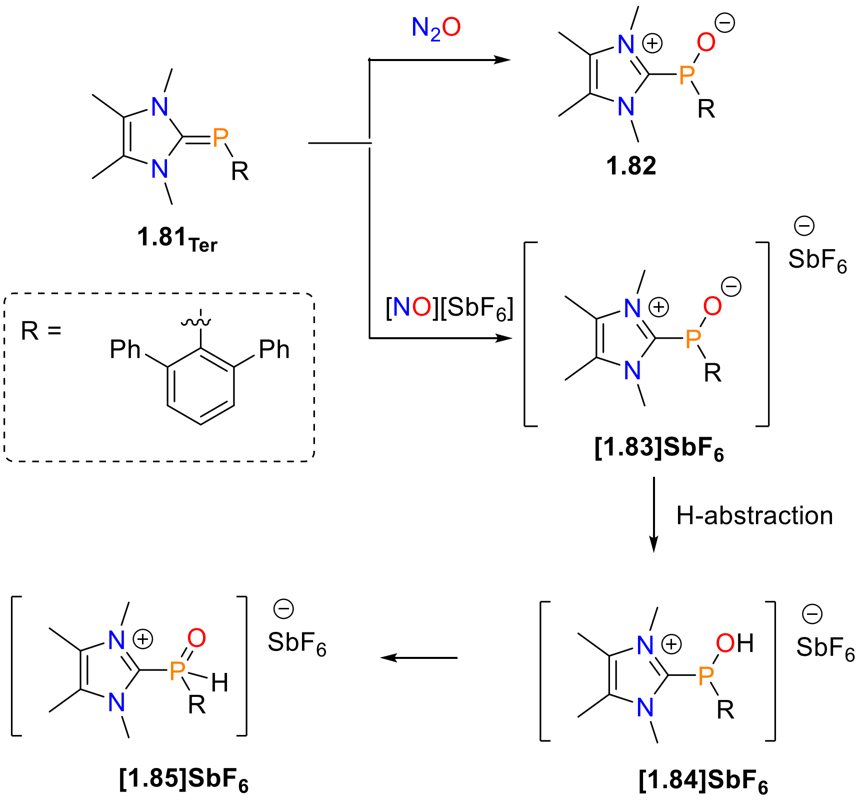

Scheme 1-18. Synthesis and oxidation of NHC-stabilized phosphinidene oxide.[110]

The first examples of diylide stabilized cationic chalcogeno(diorgano)phosphonium salts **[1.87]X** were reported by Schmidpeter and co-workers, who subsequently reported two coordinate ylide-stabilized [RPCh] species (**1.89S** and **1.89Se**, **Scheme 1-19**).[111] Condensation of the parent $RPCl_2$ (**1.88**) with Na_2Ch or $Ch(SiMe_3)_2$ stabilized by a phosphorus ylides without bulky substituents. The ^{31}P NMR chemical shifts for their ylide-stabilized RPS derivatives were recorded at 485 ppm. The length of the P-S bond of the ylide-stabilized RPS in the solid state was significantly elongated compared to accepted values of a P=S double bond. Nucleophilic character at the sulfur atom was demonstrated by an alkylation reaction with benzyl bromide to produce species **1.92**.[88] Sulfurization of phosphinidene sulfide **1.89S** with S_8 resulted in the formation of dithoxophosphorane **1.90S**, which was also generated by reaction of **1.88** with Na_2S_2. The reaction of the **1.89S** with phosphalkene **1.91** yielded unusual mixed P(III)/P(V) heterocycle. [112]

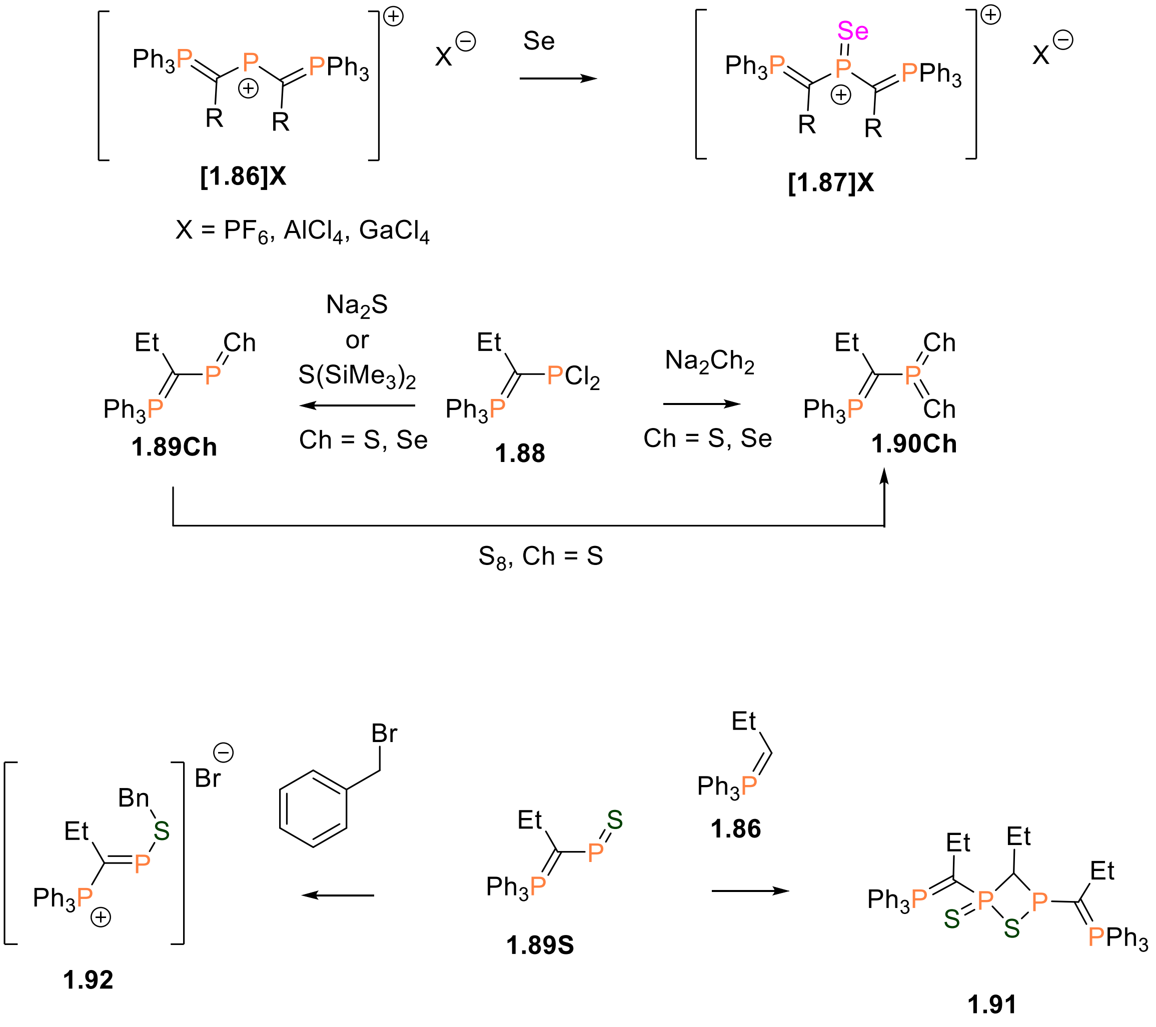
Ph3P
P
PPh3
R
R
X
Se
[1.86]X
X = PF6, AlCl4, GaCl4
[1.87]X
Et
Ch
P
Ph3P
1.89Ch
Na2S
or
S(SiMe3)2
Ch = S, Se
PCl2
1.88
Na2Ch2
Ch = S, Se
1.90Ch
S8, Ch = S
Bn
S
Br
1.92
1.89S
1.86
1.91

Scheme 1-19. Ylide stabilized species reported by Schmidpeter and co-workers.[88,111,113]

The Ragogna Group published a procedure for the isolation of the dimerized **1.46S**$_{\text{Ar*}}$ and **1.46Se**$_{\text{Ar*}}$ supported by a bulky terphenyl ligand.[85] Dissociation in solution was found to enable the dimer to function as a surrogate for monomeric "RP=S" *in situ* for cycloaddition reactions (**1.47a/b**, **1.48**, and **1.95Ch**; **Scheme 1-20**) or ring expansion reactions in the presence of DMAP (**1.67S**$_{\text{Ar*}}$, **Scheme 1-20**). [78,114] **1.46S**$_{\text{Ar*}}$ reacted with dimethylbutadiene to produce [2+4] cycloaddition products (**1.91Ch**), but divergent reactivity was observed with internal and alkynes. Carbene-like and olefinic-like reactivity was observed with phenylacetylene, which produced [1+2] and [2+2] cycloaddition products (**1.47**$_{\text{R}}$ and **1.48**, respectively), but only [1+2] cycloaddition product **1.47**$_{\mathbf{Ph}}$ was produced upon reaction with diphenylacetylene. Photolysis of phosphirene sulfide **1.47**$_{\mathbf{Ph}}$ was also found to behave surrogate source of "RP=S".

The Ragogna group also demonstrated that a reaction of **1.46S**$_{\mathbf{Ar*}}$ with an NHC (**1.93**) allowed for the first isolated example of a base-stabilized phosphinidene sulfide (**1.94**, **Scheme 1-20**), but the analogous phosphinidene selenide could not be isolated.[85] A comparison of solid-state and DFT-optimized structures suggested that the P-S bond of **1.94** was contracted (*ca.* 0.1 Å) and exhibited a slightly higher bond order relative to the dimeric **1.46S**$_{\mathbf{Ar*}}$ species. In both **1.46S**$_{\mathbf{Ar*}}$ and **1.46Se**$_{\mathbf{Ar*}}$ solid state structures, the P-Ch length of 2.1461(8) Å was similar to the single bond covalent radii for P and S of 2.14 Å.[85] This was also highlighted by a P-S Wiberg bond index calculation of 0.95. The DMAP catalyzed ring-expansion of **1.46S**$_{\mathbf{Ar*}}$ and **1.46Se**$_{\mathbf{Ar*}}$ was also explored computationally. Although DMAP was found to be less efficient at stabilizing "RP=S" than NHC **1.93**, a presence of DMAP allowed for a less endergonic ring expansion (44 kJ/mol) compared to non-base assisted ring expansion (118 kJ/mol).

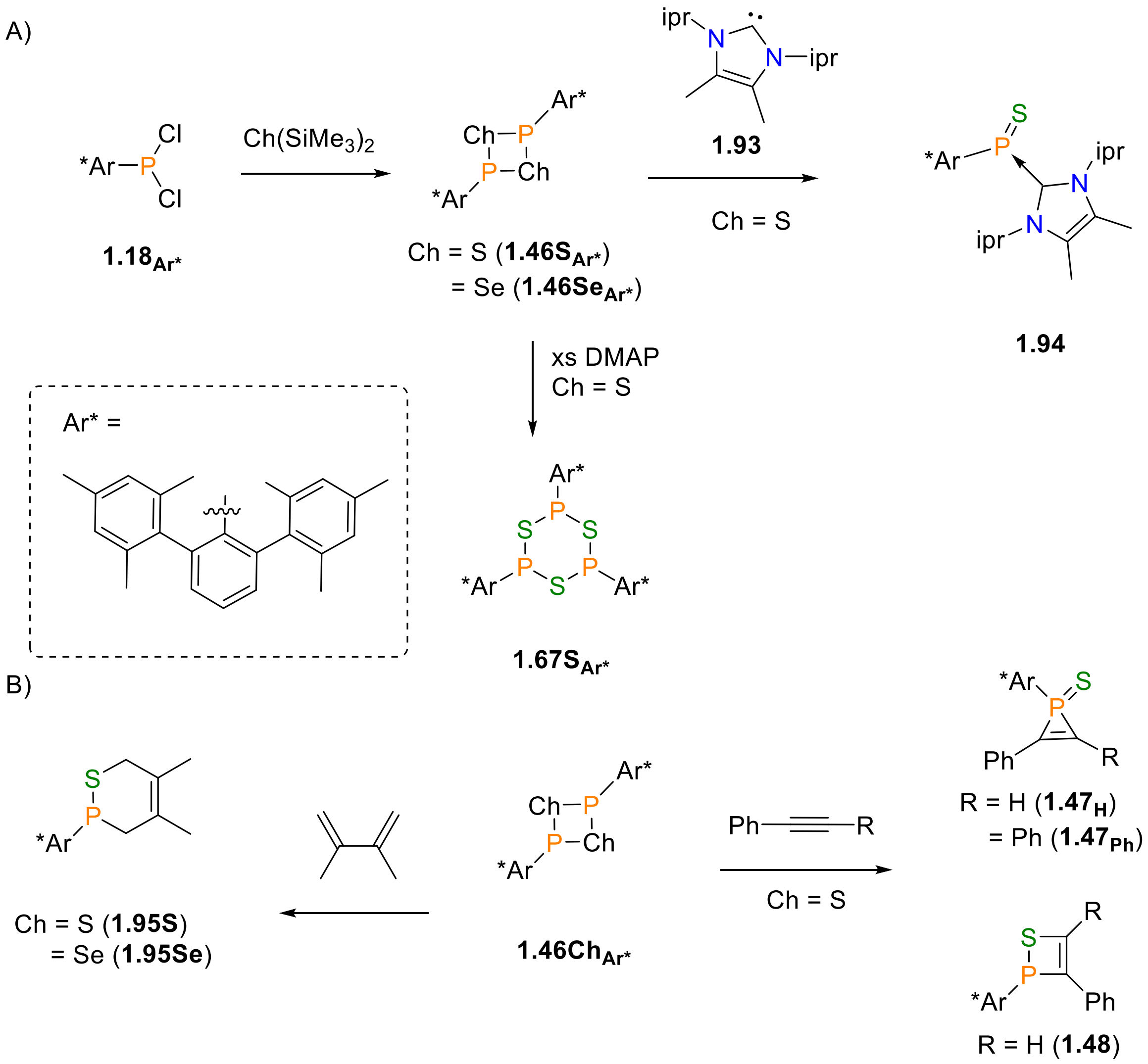
A)
1.18$_{Ar*}$
Ch(SiMe$_3$)$_2$
Ch = S (1.46S$_{Ar*}$)
= Se (1.46Se$_{Ar*}$)
1.93
Ch = S
1.94
xs DMAP
Ch = S
Ar* =
1.67S$_{Ar*}$
B)
Ch = S (1.95S)
= Se (1.95Se)
1.46Ch$_{Ar*}$
Ph—≡—R
Ch = S
R = H (1.47$_H$)
= Ph (1.47$_{Ph}$)
R = H (1.48)

Scheme 1-20. Chemistry of a phosphinidene sulfide surrogate species (**1.46S$_{Ar*}$**), reported by Ragogna and co-workers. A) Formation of dimeric **1.46S$_{Ar*}$**, base-stabilized **1.94**, and ring-expanded trimer (**1.67S$_{Ar*}$**). B) Cycloaddition reactions of **1.46S$_{Ar*}$**.[85]

The Nikonov group recently reported examples of a base-stabilized phosphinidene oxide (**1.97O**), phosphinidene sulfide (**1.97S**), and two phosphinidene imides (**1.99a/b**), by oxidation reactions of a parent phosphinidene (**1.96, Scheme 1-21**) with N_2O, S_8, trimethylsilyl azide, or *p*-tolylazide, respectively. Oxidation of the parent phosphinidene **1.96** was also performed using pyridine N-oxide (py-O) but resulted in the formation a dioxophosphorane (**1.98**). Phosphinidene oxide **1.97O** was detected *in situ* but oxidized further to a dioxophosphorane (**1.98**). An alternative oxidation strategy using pyridine N-oxide also resulted in the formation and isolation of the dioxophosphorane (**1.98**). Attempts to isolate the phosphinidene oxide by removal of volatiles revealed the species' instability.[115] The phosphinidene sulfide (**1.97S)** was found to possess a P-S bond length of 1.998(2) Å corresponding to a partial multiple bond character in the solid-state. Phosphinidene imides **1.99a/b** were generated by Staudinger reaction of the phosphinidene with the respective functionalized azide. Phosphinidene imide (**1.99b**) was not successfully isolated, but the formation was studied by periodic monitoring by low temperature $^{31}P\{^{1}H\}$ NMR spectroscopy. A resonance for a relatively stable azido-phosphinidene adduct which decomposed to the phosphinidene imide upon warming was detected. Although compound **1.99b** was not isolated, it was shown to react with *p*-tolylisocyanate to produce a urea-stabilized species (**1.100**).

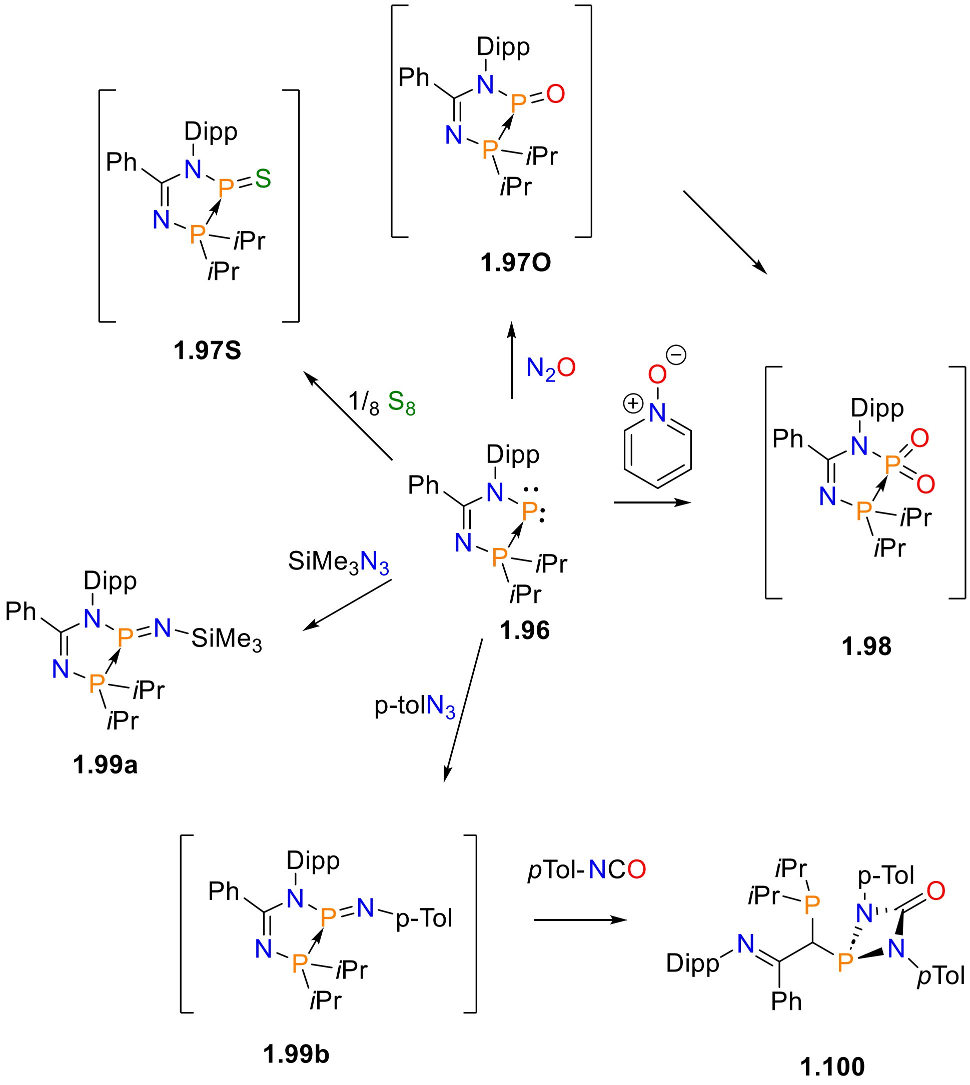
1.97S
1.97O
1.98
1/8 S8
N2O
SiMe3N3
p-tolN3
1.96
1.99a
1.99b
pTol-NCO
1.100

Scheme 1-21. Reactions of a base-stabilized phosphinidene to produce a phosphinidene oxide, dioxophosphorane, phosphinidene sulfide, and phosphinidene imide, reported by the Nikonov group.[115]

1.5 Dichalcogoxophosphroanes ($RPCh_2$)

1.5.1 Theory

Similar to phosphinidene chalcogenides, three-coordinate P(V) dichalcogenide species [$RPCh_2$] are highly reactive and rarely isolated.[116] [$RPCh_2$] species might be referred to as phosphinidene dichalcogenide, dichalcogoxophosphorane (*e.g.*

dioxophosphorane, dithioxophsophorane, diselenoxophosphorane), metaphosphonates, or anhydrides of the corresponding phosphonic acid. Sulfur and selenium derivatives have been studied to a greater extent compared to the lighter oxygen analogues, and is reflected in the relative abundance of examples contained in early reviews on the area.[116]

Oligomerization of [$RPCh_2$] may result in the formation of four-coordinate phosphonates which can be linear, branched, or cyclic, and can be fluxional in solution (**Scheme 1-22**).[117] The susceptibility to oligomerization and polymerization reactions of phosphonates is likely the cause of the difficulty encountered towards isolation of crystalline material or obtaining a product with suitable purity.[118] Early investigative studies relied on methods such as IR spectroscopy, elemental analysis, melting point analysis (or cryoscopy), or derivatization with alcohols, which yield exclusively phosphonic monoesters, for determination of molecular formulae.[119]

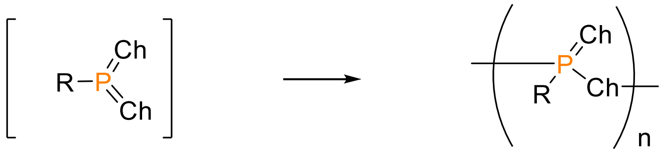

Scheme 1-22. Generic oligomerization of [$RPCh_2$] to four-coordinate phosphonate.

Phosphonates have been thermally treated to yield inorganic polymers and have applications in flame retardant materials.[120] Well defined cyclic phosphonates (Ch = O) remained structurally elusive until very recently,[121,122] although heavier dichalcogen analogues were structurally characterized much earlier. Few examples of kinetically stabilized dimers of $(RPCh_2)_2$ have been reported, often utilizing bulky ligands (**Figure 1-9**).[98,123] Lawessons and Woolens reagents are notable examples of sulfur and selenium analogues which have widespread application in organic syntheses reactions with ketones by their ability to exchange an oxygen for a heavier chalcogen. [124–126]

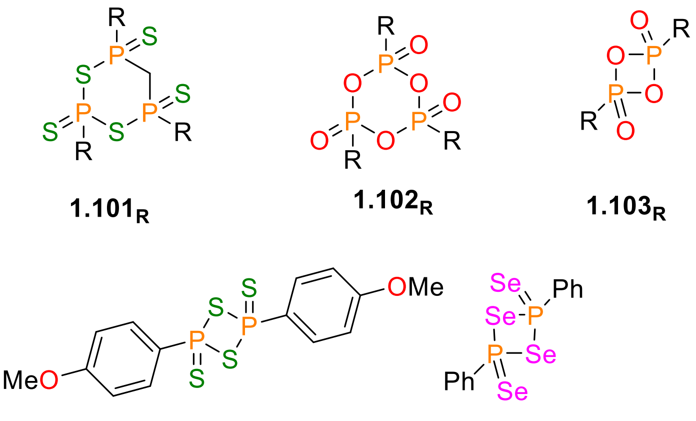

1.101$_R$ **1.102**$_R$ **1.103**$_R$

Lawesson's Reagent Woolen's Reagent

Figure 1-9. Examples of oligomeric dichalcogoxophosphoranes.[121,122,125,127,128]

Phosphonates and metaphosphonates are often sensitive to moisture, ambiphilic with Lewis acidic character at phosphorus and Lewis basic character at the terminal chalcogen, and also often exhibit an equilibrium of monomer and dimeric states.[107,129,130] Dioxophosphoranes react with nucleophiles such as alcohols similarly to phosphinidnene oxides, but reactions of dithioxophosphoranes with alcohols result in isomerization to the more stable phosphine oxide specices.[131] Dithioxophosphoranes have also demonstrated unexpected C-H activation of t-butyl groups when reacted with amines (**Scheme 1-23**).[132]

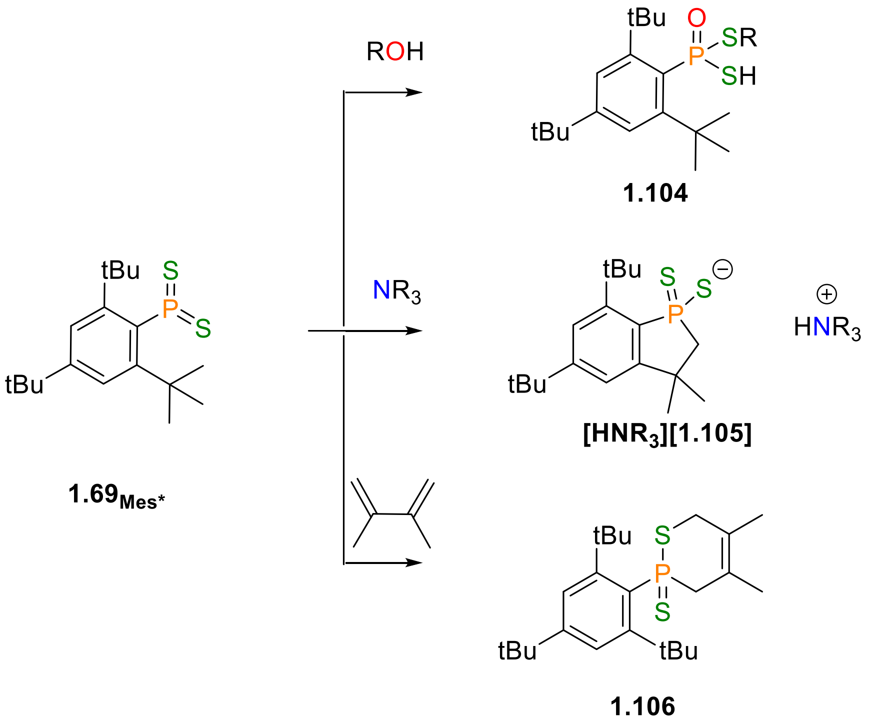
ROH
NR3
tBu
S
P
SR
SH
O
⊖
⊕
HNR3
1.69Mes*
1.104
[HNR3][1.105]
1.106

Scheme 1-23. Reactions of a dithioxophosphorane with alcohols, amines, and dimethylbutadiene.[102,131,132]

In addition to organophosphorus "$RPCh_2$", halogen adducts of PCh_2 and cationic $[PCh_2]^+$ fragments have been stabilized by Lewis bases (**Figure 1-10**). Lewis base adducts of PCh_2X have been prepared by mixing pyridine with P_4O_{10} or P_4S_{10} and $OPCl_3$ or $SPCl_3$, or by DMAP induced dismutation of $POCl_3$.[133,134] Stephan and co-workers have reported a fluoride analogue stabilized by bis(diisopropylamino)cyclopropenium.[135]

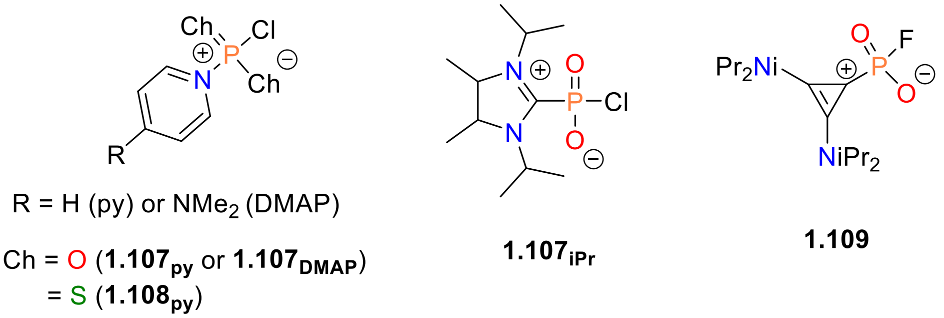
Ch
Cl
P
N
R
⊕
⊖
R = H (py) or NMe2 (DMAP)
Ch = O (1.107py or 1.107DMAP)
= S (1.108py)
N
O
Cl
1.107iPr
Pr2Ni
NiPr2
F
1.109

Figure 1-10. Examples of base-stabilized chlorophosphonates.[133–136]

A recent synthetic method of preparing a bis(pyridyl) was reported, demonstrating utility as a phosphorylating agent.[137] Combining pyridine with common industrial phosphorus waste products and triflic anhydride produced adduct **1.110** in high yields, and enabled high yield phosphorylation reactions to industrially relevant phosphonates (**Scheme 1-24**).[137]

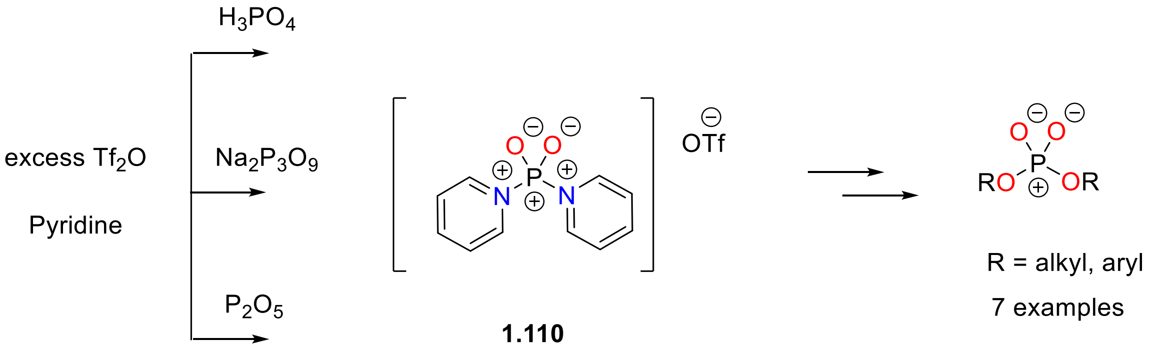

Scheme 1-24. Synthesis of **[1.110]OTf**, and demonstration of its utility as a phosphorylating agent.[137]

1.5.2 Generation

Condensation of a dichlorophosphonous oxide and phosphonic acid derivative is a a known method of generating $[RPO_2]_n$ species for over a century (**Scheme 1-25**). Michaelis and Rothe reported their synthesis of “$PhPO_2$” in 1892 as a white crystalline solid that matched combustion analysis for a species with a formula of $C_6H_5PO_2$.[138] More than 60 years later, analysis of the same reaction by melting point analysis (cryoscopy) revealed that when volatiles were removed below 65 °C, the melting point of 103 - 105 °C was consistent with a dimeric formula. When removal of volatiles was performed at an elevated temperature of 90 °C, the melting point of 209 - 212 °C was consistent with a trimeric species.[139]

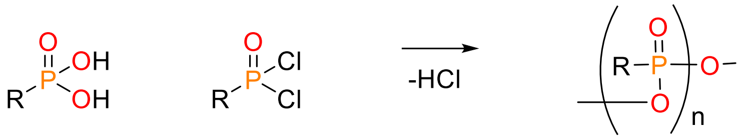

Scheme 1-25. General condensation reaction of a phosphonic acid and a phosphonic dichloride to generate oligomeric phosphonates.

The first structurally characterized examples of trimeric cyclic phosphonates were reported in 2019 by the Manners group, which included an unexpected hexameric, phenyl substituted species (**Figure 1-11**).[121] Condensation of aryl-supported phosphonic acid and phosphonic dichlorides was used to synthesize the rings and were recrystallized at low temperature. $^{31}P\{^{1}H\}$ NMR spectra of $(MesPO_2)_3$ in C_6D_6 revealed a doublet and a *pseudo* triplet for the two phosphorus environments of an A_2B spin system, while the resonances converged to approximately a singlet in $CDCl_3$, which demonstrated the fluxional nature of such rings in solution. They also demonstrated that the thermally ring-opened polymers were dynamic in solution, contained high molecular weight chains, and could be depolymerized in dilute solutions.[121]

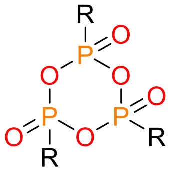

1.102_R

R = 4-tBu(C_6H_4)
= Mes
= 2,6-Me-4-tBu(C_6H_2)

$(PhPO_2)_6$

1.111

Figure 1-11. Structurally characterized cyclic phosphonates by Manners and co-workers.[121]

Photolysis of phenyl phosphirane (**1.112)** in a frozen matrix has been used to isolate a triplet phosphinidene (**1.113**), which was oxidized with O_2 to an intermediate 3-phenyl-1,2,3-dioxaphosphirane that decomposed to phenyldioxophosphorane (**1.114_{Ph}**) by irradiation (λ = 465 nm, **Scheme 1-26**).[140] Pyrolysis of phosphole precursors has also been used to generate $[RPO_2]$ *in situ*. $[PhPO_2]$ reportedly oligomerized to generate

$(PhPO_2)_3$, but reaction with methanol produced the expected monoester, which was in support of a product containing "$PhPO_2$" connectivity. Another mode of decomposition of a dioxophosphorane was observed when the biphenyl derivative was pyrolyzed. Decomposition of the intermediate **1.114$_{BP}$** to a tricyclic species **1.117** was suggested to occur *via* intramolecular C-H activation (**Scheme 1-27**).[141] Similar thermolysis of a bulky-terphenyl supported 1,3-dioxa-2-phospholate (**1.115$_{DippTer}$**) at 150 °C allowed for the isolation of the first example of dioxophosphorane dimer (**1.103**,**Scheme 1-28**).[122]

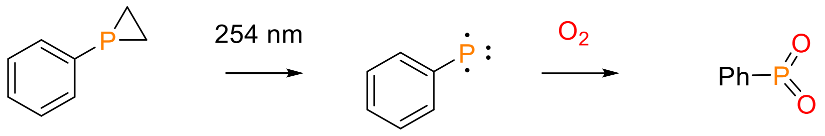
254 nm
P
P
O2
Ph
P
O
O

1.112 **1.113** **1.114$_{Ph}$**

Scheme 1-26. Photolysis of phenyl phosphirane and oxidation in a frozen matrix.[140]

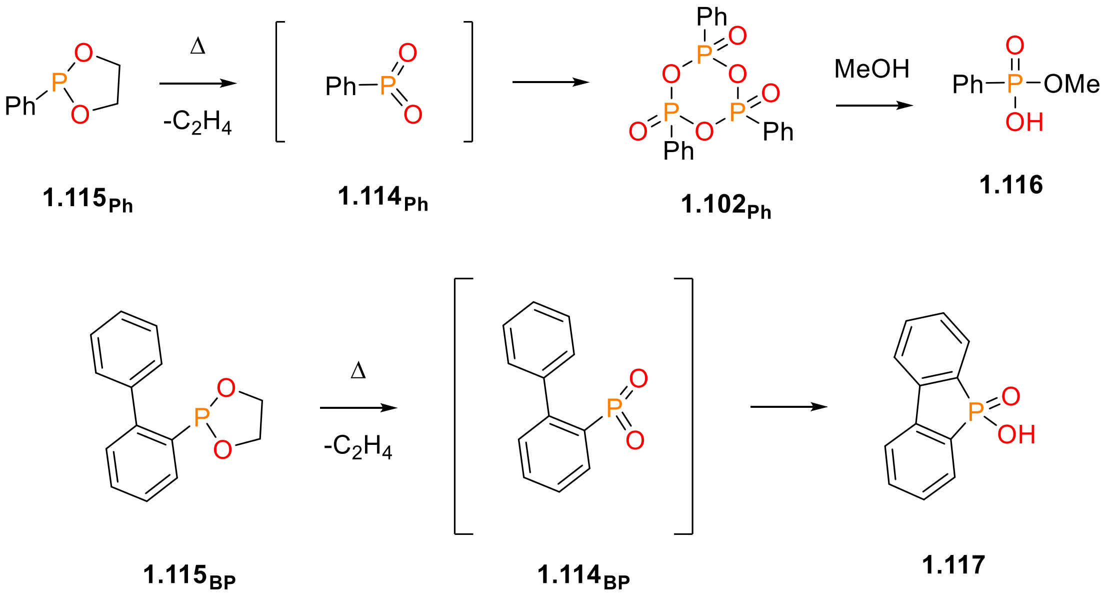
Ph
P
O
O
Δ
-C2H4
Ph
P
O
O
Ph
P
O
O
O
O
P
P
O
O
Ph
Ph
MeOH
Ph
P
OMe
O
OH
1.115Ph
1.114Ph
1.102Ph
1.116
P
O
O
Δ
-C2H4
P
O
O
P
O
OH
1.115BP
1.114BP
1.117

Scheme 1-27. Flash vacuum pyrolysis reactions of phospholes.[141]

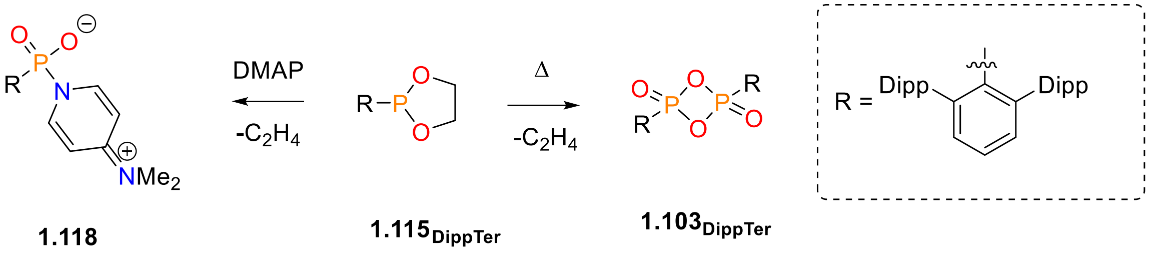

Scheme 1-28. Reactions of terphenyl-supported 1,3-dioxo-2-phospholane to generate base stabilized adduct of [RPO_2] and dioxophosphorane dimer.[122]

$PhPCl_2$ reportedly reacted with H_2S_2 to generate dimeric $(PhPS_2)_2$ (**1.119**) along with elimination of HCl, suggested by molecular weight calculations by cryoscopic determination (**Scheme 1-29**, B).[142] The first example of an isolated dithioxophosphorane (**1.69$_{Mes*}$**) in the solid state was by Appel *et al.* and Navech *et al.* independently in 1983 (**Scheme 1-29**, C).[143,144] Appel and co-workers reported the reaction of bistrimethylsilylphosphine with S_2Cl_2.[143] Similar to the oxygen analogues and $(PhPS_2)_2$, Mes*PS_2 (**1.69$_{Mes*}$**) also reacted with alcohols to generate a monoester of the formula Mes*P(S)(SH)(OR) (**1.121**).[143] As depicted in the previous section (**Scheme 1-19**), sulfurization or selenation of ylide-stabilzied RPCh has also resulted in formation of ylide stabilized $RPS_2$and $RPSe_2$.[88,113,145]

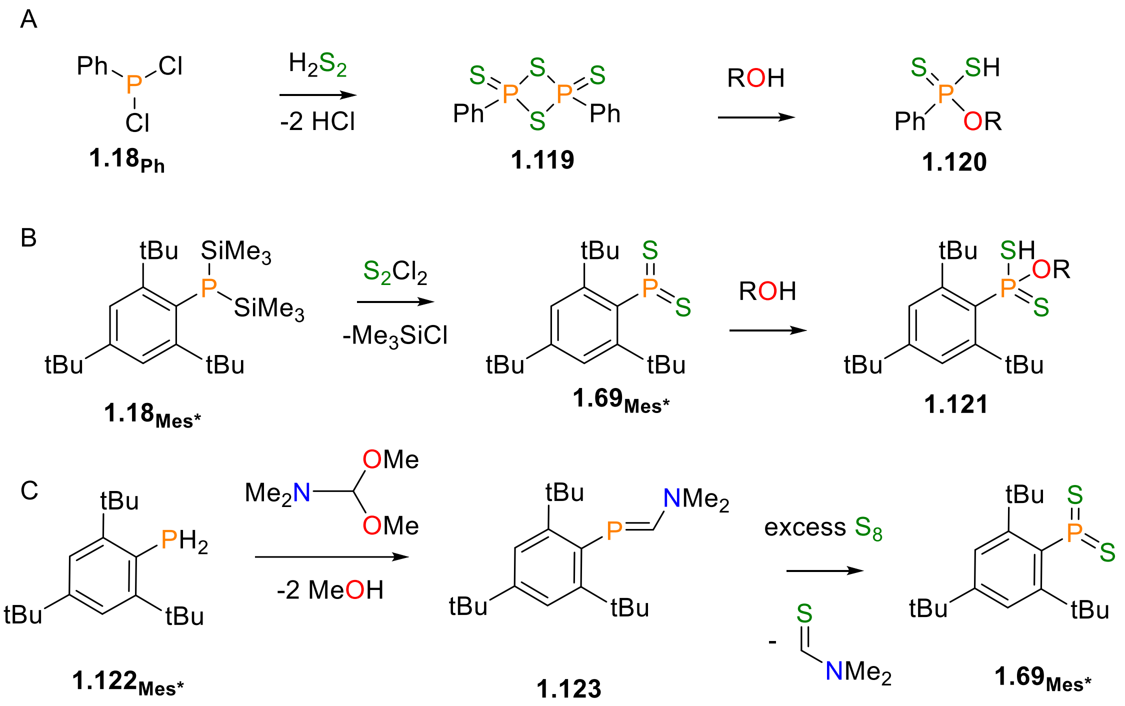
A
Ph
P
Cl
Cl
1.18Ph
H2S2
-2 HCl
S
P
S
P
S
Ph
S
Ph
1.119
ROH
S
SH
P
Ph
OR
1.120
B
tBu
SiMe3
P
SiMe3
tBu
tBu
1.18Mes*
S2Cl2
-Me3SiCl
tBu
S
P
S
tBu
tBu
1.69Mes*
ROH
tBu
SH
OR
P
S
tBu
tBu
1.121
C
tBu
PH2
tBu
tBu
1.122Mes*
Me2N
OMe
OMe
-2 MeOH
tBu
NMe2
P
tBu
tBu
1.123
excess S8
-
S
NMe2
tBu
S
P
S
tBu
tBu
1.69Mes*

Scheme 1-29. Examples of dithioxophosphoranes and some reported reactions with alcohols.[142–144]

Chalcogenization reactions of a diphosphene or sulfurization of the RPH_2 species in the presence of a base has been used as a method for producing $RPCh_2$ (Ch = S, Se) supported by bulky ligands with a flanking dialkylamino group (Mx = 2,4-di-tert-butyl-6-dimethylaminophenyl, **Scheme 1-30**).[108] The chemical shift of the Mx supported dithioxophosphorane (**1.69_{Mx}**) was upfield by over 100 ppm in ^{31}P NMR spectra compared to the Mes* derivative (**1.69_{Mes*}**).[108,142–144] In the solid state, the P-S bonds of **1.69_{Mx}** were elongated compared to the tris(t-butyl)phenyl analogue, indicating a decrease in P-S bond multiple bond character upon coordination of amino group.[145]

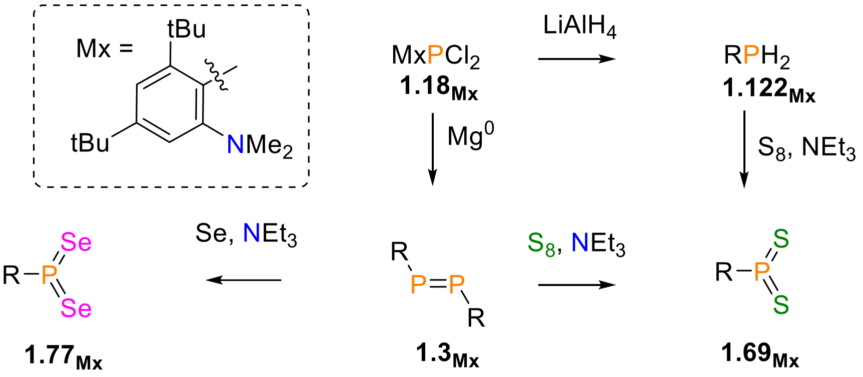

Scheme 1-30. Reactions of 2,4-di-tert-butyl-6-dimethylaminophenyl (Mx) supported phosphorus species, reported by Yoshifuji and co-workers.[108]

1.5.3 Isolation

The first example of a base-stabilized organodioxophosphorane (**1.124**) was reported *via* oxidation an NHC-stabilized phosphinidene (**Scheme 1-31**).[146] Analogous oxidations of the parent NHC-adduct with S_8 or Se_{grey} resulted in the isolation of the respective dithioxophosphorane (**1.125**) and diselenoxophosphoranes (**1.126**).[146] Similarly, oxidation of NHC-phosphinidene oxide adduct supported by a terphenyl ligand using N_2O was used to isolate dioxophosphorane species in the solid-state.[110] A recent example of a phospha-Wittig reagent (**1.19$_{\mathbf{DipTer}}$**) was also shown to produce an unusual $OPMe_3$ stabilized dioxophosphorane (**1.127**) reaction by deoxygenation of SeO_2 at elevated temperatures (**Scheme 1-15**).[107]

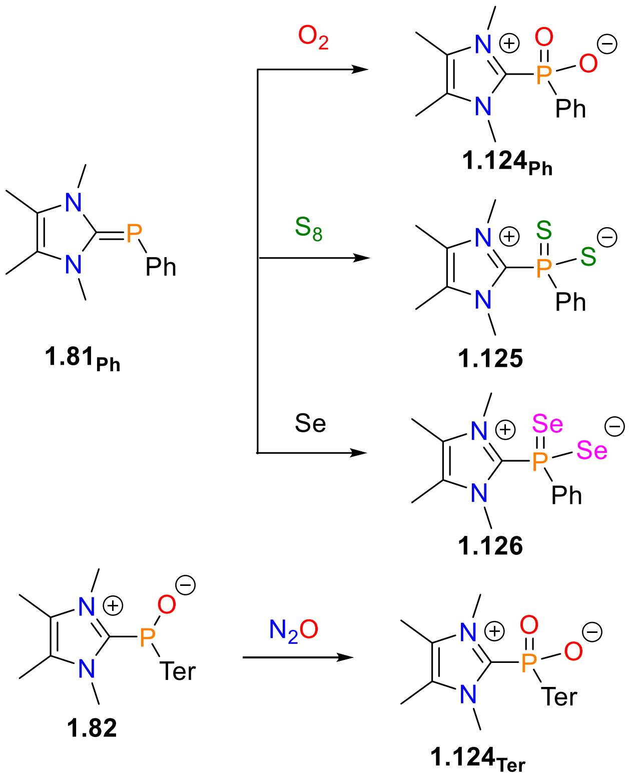

Scheme 1-31. NHC stabilized “$RPCh_2$” species.[110,146]

Oxidation of a diphosphene supported by two-NHC ligands (**1.128**) has also been used to access stabilized P_2O_4 species (**1.129, Scheme 1-32**).[147] Compared to the precursor, the P-P and P-C Wiberg bond index (WBI) of the tetroxide species was lower indicing a weaker P-C bond, while the P-O bonds had average WBI of 1.14, indicating partial multiple bond character. Charge analysisa also revealed that the phosphorus bares a large positive charge (+1.8) while the oxygens had negative charges of -1.1, indicating dative bond character as a contributing resonance structure.

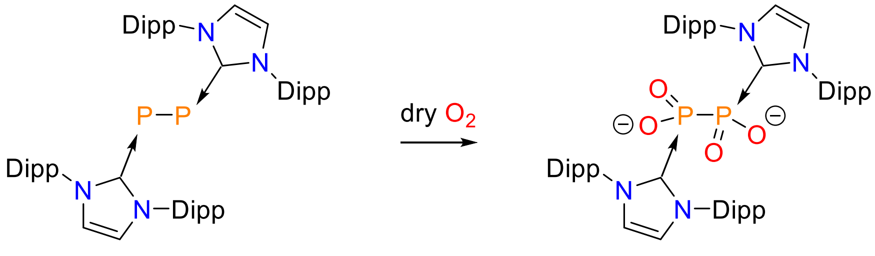

1.128

1.129

Scheme 1-32. Bis(NHC) stabilized P_2O_4.[147]

Ligands have been designed for intramolecular stabilization, including peri-substituted aromatics.[148–150] Oxidation reactions of various peri-stabilized phosphinidenes have been used to access various phosphinidene chalcogenides and dichalcogoxo phosphoranes of oxygen through tellurium (*e.g.* **Scheme 1-33**).[148] Mixed oxide/sulfide (**1.132S**) or oxide/selenides (**1.132Se**) have been accessed by reaction of a parent bis-aminophosphine (**1.131**) and methanol, followed by S_8 or Se.[150] A reaction of the parent phosphinidene with excess S_8 reportedly generated a specices containing two P^V atoms and three total sulfur atoms (**1.136**). The bridging sulfur atom demonstrated significantly different P-S bond lengths between the two phosphorus centers, which the authors suggested could indicate a dative bond character of sulfur lone pair to the PS_2 moiety. Calculated WBI values of the P-S bonds (0.53 and 1.13) and the localized negative charges on terminal sufur atoms (-0.33 and -0.53) were suggestive of a dative interaction. The authors also suggested the posibility that the difference in interatomic distances may simply be attributed to the different electronic environments of the two phosphorus atoms.

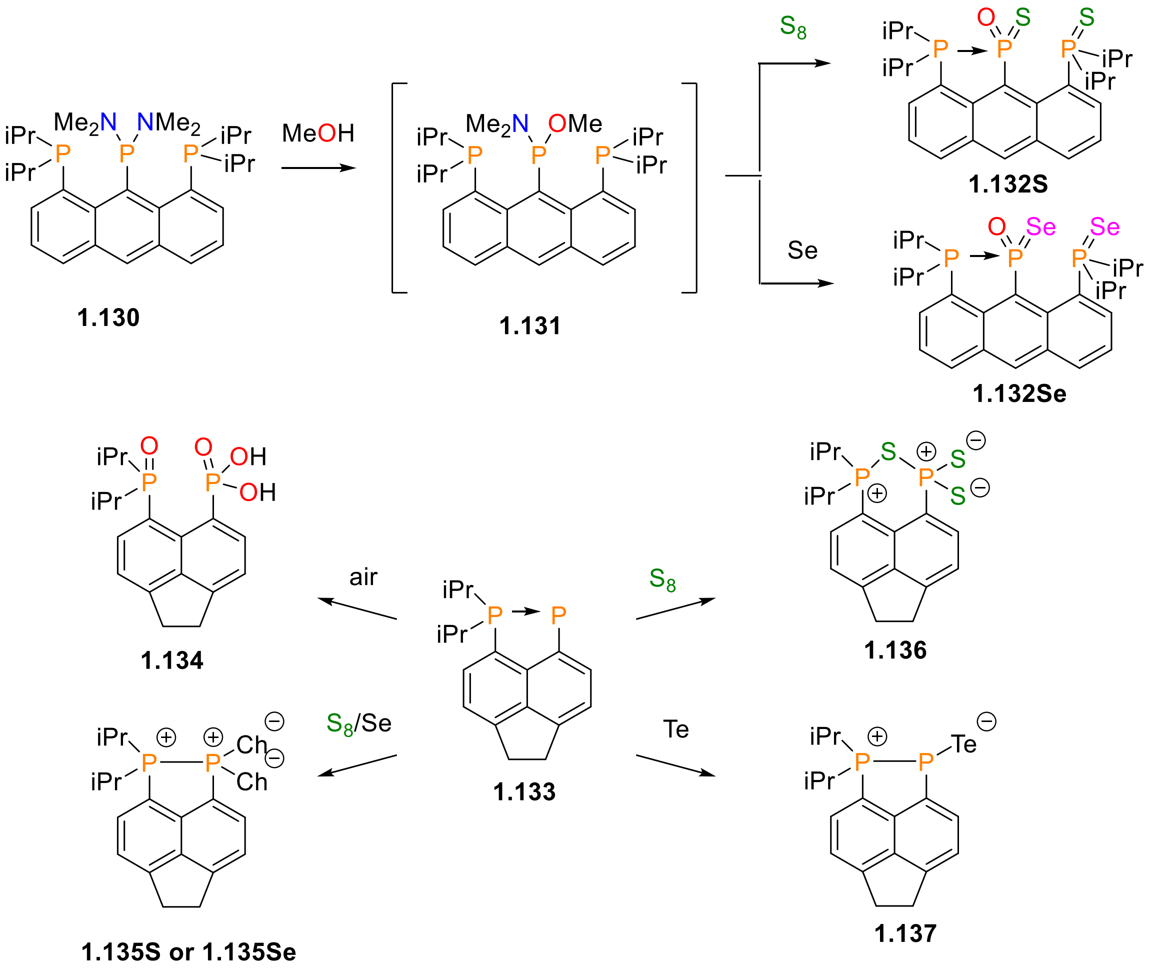

Scheme 1-33. Reactions of peri-substituted phosphorus species.[148,150]

Depolymerization of cyclic phosphonates has been demonstrated using DMAP for $(RPO_2)_n$ (n = 2, 3, and 4) and allowed isolation of base-stabilized dioxophosphoranes (**Scheme 1-34**).[97,121,122] Deoligomerization of **[1.73$_{\mathrm{R}}$]OTf$_4$** was also shown to occur in the presence of DMAP (**Scheme 1-35**). This pathway initially proceeded via formation of DMAP-adduct (**1.140)**, then underwent subsequent dismutation to the bis(imidazolium) species (**1.141$_{\mathrm{R}}$**) and dithioxophosphorane (**1.142$_{\mathrm{R}}$**). The structure of bis(DMAP) adduct (**1.143$_{\mathrm{R}}$**) was confirmed by SC-XRD, and equilibrium of the disulfide was observed with excess DMAP or triflate coordination scrambling in acetonitrile.[97]

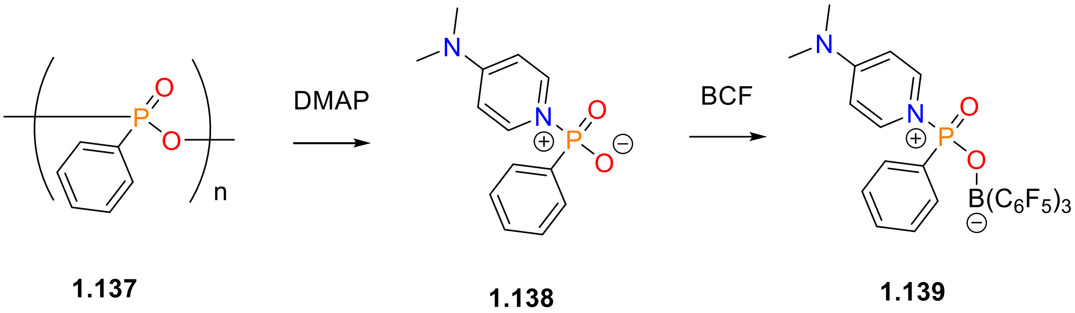
DMAP
BCF
n
1.137
1.138
1.139

Scheme 1-34. Depolymerization of $(PhPO_2)_n$ with DMAP, and coordination with BCF.

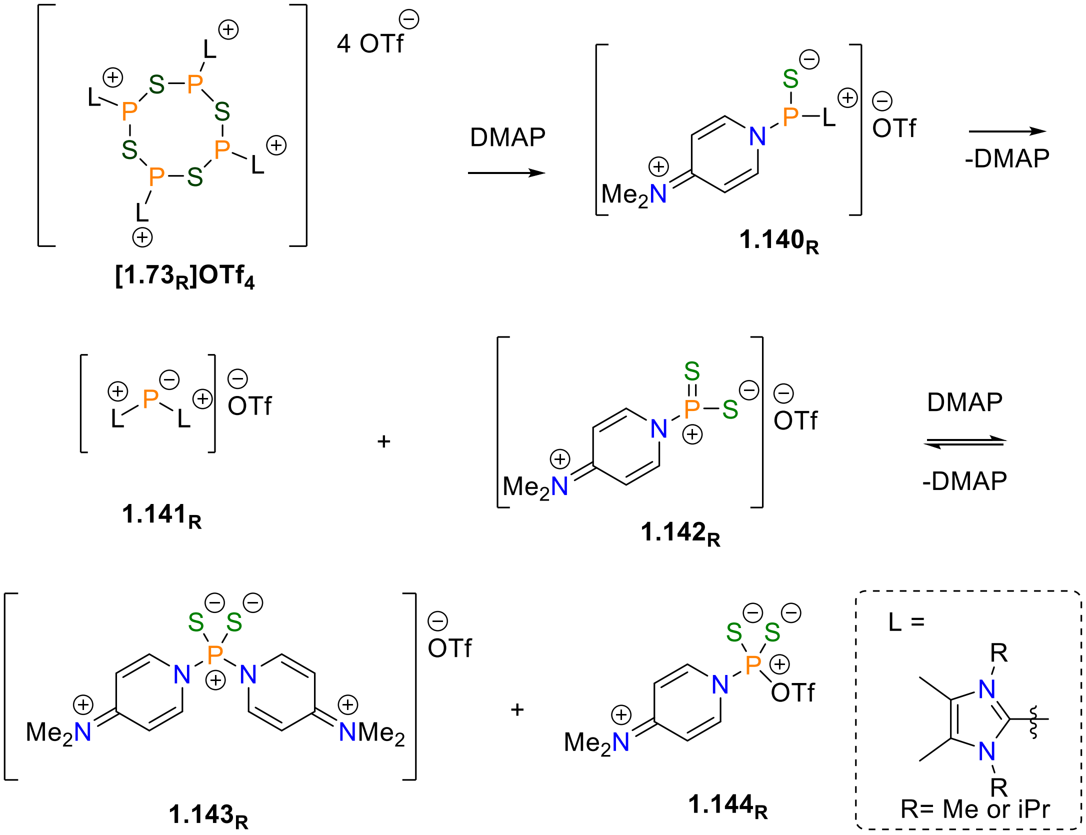
4 OTf
DMAP
-DMAP
[1.73R]OTf4
1.140R
1.141R
1.142R
DMAP
-DMAP
1.143R
1.144R
L =
R= Me or iPr

Scheme 1-35. Deoligomerization of tetra-cationic phosphorus-sulfur heterocycle and stabilization of dithioxophosphorane species.[97]

1.6 Structure and Aim of This Thesis

Apart from the ylide-stabilized phosphinidene-chalcogenides documented by Schmidpeter and co-workers, most instances of phosphinidene chalcogenides and dichalcogoxo phosphoranes to date have relied on support from bulky aromatic groups or additional donor atoms like NHCs or DMAP.[88,113] Considering the diverse methods reported for generating various phosphinidene-chalcogenides, the objective of this work was to evaluate their effectiveness while altering the electronic properties of the ligands.

In chapter 2, the aim was to explore the effect of a strongly pi-donating N-heterocyclic imine (NHI) ligand towards efforts to stabilize a monomeric phosphinidene-chalcogenide, and assess the most common methods in the relevant literature towards the viability of synthesis of a phosphinidene sulfide supported by an NHI ligand. Efforts were made towards the establishment of a route towards the generation of a phosphindine sulfide from a novel bis(azido)phosphine precursor. While no strong evidence of the formation of a phosphindine-sulfide supported by the NHI ligand was encountered, novel phosphorus-chalcogen heterocycles were obtained, and an unexpected ligand scrambling of a bis(NHI)phosphenium was explored.

Chapter 3 explores the versatility and modifications of a novel family of P(III) and P(V) bis(azido)phosphines, with a primary focus on their application in chemoselective Staudinger reactions as a means to modulate properties of a mono(azido)phosphine. The work presented in this chapter was published in *Inorganic Chemistry*.

Chapter 4 explores the attempted synthesis of an α-cationic $[RPOCl_2]Cl$ which resulted in facile generation of a zwitterionic RPO_2Cl. The unexpected divergent reactivity of bis(diisopropylamino)cyclopropenone with either PCl_3 or $RP(O)Cl_2$ was also explored. While the reactions proceed quite rapidly, separation of products was not trivial. The reactions presented in this chapter serve as a novel route towards the formation of new P-O and P-C bonds, as well as demonstrated the novel utility of the cyclopropenone to facilitate oxygen/chlorine exchange for the *in situ* generation of known cyclic phosphonates.

Chapter 5 outlines future work related to the study of phosphorus chalcogenide species as it pertains to the current work, and the appendix includes additional supporting spectra for chapters 2-4.

1.7 References

(1) Power, P. P. Main-Group Elements as Transition Metals. *Nature* **2010**, *463* (7278), 171–177. https://doi.org/10.1038/nature08634.

(2) Jutzi, P. New Element-Carbon (p-p)π Bonds. *Angew. Chem. Int. Ed.* **1975**, *14* (4), 232–245. https://doi.org/10.1002/anie.197502321.

(3) Chu, T.; Nikonov, G. I. Oxidative Addition and Reductive Elimination at Main-Group Element Centers. *Chem. Rev.* **2018**, *118* (7), 3608–3680. https://doi.org/10.1021/acs.chemrev.7b00572.

(4) Robinson, G. H. *Main Group: Multiple Bonding*; Major Reference Works; 2011. https://doi.org/10.1002/9781119951438.eibc0273.

(5) Yoshifuji, M.; Shima, I.; Inamoto, N.; Hirotsu, K.; Higuchi, T. Synthesis and Structure of Bis(2,4,6-Tri-Tert-Butylphenyl)Diphosphene: Isolation of a True Phosphobenzene. *J. Am. Chem. Soc.* **1981**, *103* (15), 4587–4589. https://doi.org/10.1021/ja00405a054.

(6) West, R.; Fink, M. J.; Michl, J. Tetramesityldisilene, a Stable Compound Containing a Silicon-Silicon Double Bond. *Science* **1981**, *214* (4527), 1343 LP – 1344. https://doi.org/10.1126/science.214.4527.1343.

(7) Dimroth, K.; Hoffmann, P. Phosphacyanines, a New Class of Compounds Containing Trivalent Phosphorus. *Angew. Chem. Int. Ed.* **1964**, *3* (5), 384. https://doi.org/10.1002/anie.196403841.

(8) Märkl, G. 2,4,6-Triphenylphosphabenzene. *Angew. Chem. Int. Ed.* **1966**, *5* (9), 846–847. https://doi.org/10.1002/anie.196608463.

(9) Hoffmann, R. Building Bridges Between Inorganic and Organic Chemistry (Nobel Lecture). *Angew. Chem. Int. Ed.* **1982**, *21* (10), 711–724. https://doi.org/10.1002/anie.198207113.

(10) Igau, A.; Grutzmacher, H.; Baceiredo, A.; Bertrand, G. Analogous α,α’-Bis-Carbenoid, Triply Bonded Species: Synthesis of a Stable λ^3-Phosphino Carbene-λ^5-Phosphaacetylene. *J. Am. Chem. Soc.* **1988**, *110* (19), 6463–6466. https://doi.org/10.1021/ja00227a028.

(11) Arduengo, A. J. I. I. I.; Harlow, R. L.; Kline, M. A Stable Crystalline Carbene. *J. Am. Chem. Soc.* **1991**, *113* (1), 361–363. https://doi.org/10.1021/ja00001a054.

(12) Fischer, E. O.; Grubert, H. Über Aromatenkomplexe von Metallen. IV. Di-Cyclopentadienyl-Blei. *Z. Anorg. Allg. Chem.* **1956**, *286* (5–6), 237–242. https://doi.org/10.1002/zaac.19562860507.

(13) Driess, M.; Grützmacher, H. Main Group Element Analogues of Carbenes, Olefins, and Small Rings. *Angew. Chem. Int. Ed.* **1996**, *35* (8), 828–856. https://doi.org/10.1002/anie.199608281.

(14) Spikes, G. H.; Fettinger, J. C.; Power, P. P. Facile Activation of Dihydrogen by an Unsaturated Heavier Main Group Compound. *J. Am. Chem. Soc.* **2005**, *127* (35), 12232–12233. https://doi.org/10.1021/ja053247a.

(15) Frey, G. D.; Lavallo, V.; Donnadieu, B.; Schoeller, W. W.; Bertrand, G. Facile Splitting of Hydrogen and Ammonia by Nucleophilic Activation at a Single Carbon Center. *Science* **2007**, *316* (5823), 439–441. https://doi.org/10.1126/science.1141474.

(16) McCarthy, S. M.; Lin, Y.-C.; Devarajan, D.; Chang, J. W.; Yennawar, H. P.; Rioux, R. M.; Ess, D. H.; Radosevich, A. T. Intermolecular N–H Oxidative Addition of Ammonia, Alkylamines, and Arylamines to a Planar σ^3-Phosphorus Compound via an Entropy-Controlled Electrophilic Mechanism. *J. Am. Chem. Soc.* **2014**, *136* (12), 4640–4650. https://doi.org/10.1021/ja412469e.

(17) Dunn, N. L.; Ha, M.; Radosevich, A. T. Main Group Redox Catalysis: Reversible P^{III}/P^{V} Redox Cycling at a Phosphorus Platform. *J. Am. Chem. Soc.* **2012**, *134* (28), 11330–11333. https://doi.org/10.1021/ja302963p.

(18) Urso, J. H.; Gilbertson, L. M. Atom Conversion Efficiency: A New Sustainability Metric Applied to Nitrogen and Phosphorus Use in Agriculture. *ACS Sustain. Chem. Eng.* **2018**, *6* (4), 4453–4463. https://doi.org/10.1021/acssuschemeng.7b03600.

(19) Rodriguez, J. B.; Gallo-Rodriguez, C. The Role of the Phosphorus Atom in Drug Design. *ChemMedChem* **2019**, *14* (2), 190–216. https://doi.org/10.1002/cmdc.201800693.

(20) Pradere, U.; Garnier-Amblard, E. C.; Coats, S. J.; Amblard, F.; Schinazi, R. F. Synthesis of Nucleoside Phosphate and Phosphonate Prodrugs. *Chem. Rev.* **2014**, *114* (18), 9154–9218. https://doi.org/10.1021/cr5002035.

(21) Cadogan, J. I. G.; Mackie, R. K. Tervalent Phosphorus Compounds in Organic Synthesis. *Chem. Soc. Rev.* **1974**, *3* (1), 87–137. https://doi.org/10.1039/CS9740300087.

(22) Ozturk, T.; Ertas, E.; Mert, O. A Berzelius Reagent, Phosphorus Decasulfide (P_4S_{10}), in Organic Syntheses. *Chem. Rev.* **2010**, *110* (6), 3419–3478. https://doi.org/10.1021/cr900243d.

(23) Fernández-García, C.; Coggins, A. J.; Powner, M. W. A Chemist's Perspective on the Role of Phosphorus at the Origins of Life. *Life* **2017**, *7* (3). https://doi.org/10.3390/life7030031.

(24) Geeson, M. B.; Cummins, C. C. Let's Make White Phosphorus Obsolete. *ACS Cent. Sci.* **2020**, *6* (6), 848–860. https://doi.org/10.1021/acscentsci.0c00332.

(25) Schipper, W. Phosphorus: Too Big to Fail. *Eur. J. Inorg. Chem.* **2014**, *2014* (10), 1567–1571. https://doi.org/10.1002/ejic.201400115.

(26) Costanzi, S.; Machado, J.-H.; Mitchell, M. Nerve Agents: What They Are, How They Work, How to Counter Them. *ACS Chem. Neurosci.* **2018**, *9* (5), 873–885. https://doi.org/10.1021/acschemneuro.8b00148.

(27) Baudler, M.; Glinka, K. Monocyclic and Polycyclic Phosphanes. *Chem. Rev.* **1993**, *93* (4), 1623–1667. https://doi.org/10.1021/cr00020a010.

(28) Li, X.; Weissman, S. I.; Lin, T.-S.; Gaspar, P. P.; Cowley, A. H.; Smirnov, A. I. Observation of a Triplet Phosphinidene by ESR Spectroscopy. *J. Am. Chem. Soc.* **1994**, *116* (17), 7899–7900. https://doi.org/10.1021/ja00096a058.

(29) Marinetti, A.; Mathey, F.; Fischer, J.; Mitschler, A. Stabilization of 7-Phosphanorbornadienes by Complexation; X-Ray Crystal Structure of 2,3-Bis(Methoxycarbonyl)-5,6-Dimethyl-7-Phenyl-7-Phosphanorbornadiene(Pentacarbonyl)-Chromium. *J. Chem. Soc. Chem. Commun.* **1982**, No. 12, 667–668. https://doi.org/10.1039/C39820000667.

(30) Marinetti, A.; Mathey, F. The Carbene-like Behavior of Terminal Phosphinidene Complexes toward Olefins. A New Access to the Phosphirane Ring. *Organometallics* **1984**, *3* (3), 456–461. https://doi.org/10.1021/om00081a021.

(31) Marinetti, A.; Mathey, F. The Chemistry of Free and Complexed Phosphirenes: Reactivity toward Electrophiles, Nucleophiles, and Conjugated Dienes. *J. Am. Chem. Soc.* **1985**, *107* (16), 4700–4706. https://doi.org/10.1021/ja00302a016.

(32) Allen, D. W. Chapter 1 Phosphines and Related P–C-Bonded Compounds. In *Organophosphorus Chemistry: Volume 43*; The Royal Society of Chemistry, 2014; Vol. 43, pp 1–51. https://doi.org/10.1039/9781782623977-00001.

(33) Yoshifuji, M. Protecting Groups for Stabilization of Inter-Element Linkages. *J. Organomet. Chem.* **2000**, *611* (1), 210–216. https://doi.org/10.1016/S0022-328X(00)00458-7.

(34) Smith, R. C.; Urnezius, E.; Lam, K.-C.; Rheingold, A. L.; Protasiewicz, J. D. Syntheses and Structural Characterizations of the Unsymmetrical Diphosphene DmpPPMes* (Dmp = 2,6-$Mes_2C_6H_3$, Mes* = 2,4,6-$^tBu_3C_6H_2$) and the Cyclotetraphosphane $[DmpPPPh]_2$. *Inorg. Chem.* **2002**, *41* (20), 5296–5299. https://doi.org/10.1021/ic025759l.

(35) Hitchcock, P. B.; Lappert, M. F.; Leung, W.-P. The First Stable Transition Metal (Molybdenum or Tungsten) Complexes Having a Metal–Phosphorus(III) Double Bond: The Phosphorus Analogues of Metal Aryl- and Alkyl-Imides; X-Ray Structure of [Mo(η-C_5H_5)$_2$(=PAr)](Ar = $C_6H_2Bu^t{}_3$-2,4,6). *J. Chem. Soc. Chem. Commun.* **1987**, No. 17, 1282–1283. https://doi.org/10.1039/C39870001282.

(36) Liu, L.; Ruiz, D. A.; Munz, D.; Bertrand, G. A Singlet Phosphinidene Stable at Room Temperature. *Chem* **2016**, *1* (1), 147–153. https://doi.org/10.1016/j.chempr.2016.04.001.

(37) Schumann, A.; Reiß, F.; Jiao, H.; Rabeah, J.; Siewert, J.-E.; Krummenacher, I.; Braunschweig, H.; Hering-Junghans, C. A Selective Route to Aryl-Triphosphiranes and Their Titanocene-Induced Fragmentation. *Chem. Sci.* **2019**, *10* (34), 7859–7867. https://doi.org/10.1039/C9SC02322D.

(38) Shah, S.; Protasiewicz, J. D. ‘Phospha-Variations’ on the Themes of Staudinger and Wittig: Phosphorus Analogs of Wittig Reagents. *Coord. Chem. Rev.* **2000**, *210* (1), 181–201. https://doi.org/10.1016/S0010-8545(00)00311-8.

(39) Kinjo, R.; Donnadieu, B.; Bertrand, G. Isolation of a Carbene-Stabilized Phosphorus Mononitride and Its Radical Cation ($PN^{+\cdot}$). *Angew. Chem. Int. Ed.* **2010**, *49* (34), 5930–5933. https://doi.org/10.1002/anie.201002889.

(40) Bockfeld, D.; Tamm, M. Isolation of N-Heterocyclic Carbene-Stabilized Phosphorus and Arsenic Mononitride. *Z. Anorg. Allg. Chem.* **2020**, *646* (13), 866–872. https://doi.org/10.1002/zaac.202000094.

(41) Engesser, T. A.; Lichtenthaler, M. R.; Schleep, M.; Krossing, I. Reactive P-Block Cations Stabilized by Weakly Coordinating Anions. *Chem. Soc. Rev.* **2016**, *45* (4), 789–899. https://doi.org/10.1039/C5CS00672D.

(42) Frenking, G. Dative Bonds in Main-Group Compounds: A Case for More Arrows! *Angew. Chem. Int. Ed.* **2014**, *53* (24), 6040–6046. https://doi.org/10.1002/anie.201311022.

(43) Himmel, D.; Krossing, I.; Schnepf, A. Dative Bonds in Main-Group Compounds: A Case for Fewer Arrows! *Angew. Chem. Int. Ed.* **2014**, *53* (2), 370–374. https://doi.org/10.1002/anie.201300461.

(44) Haaland, A. Covalent versus Dative Bonds to Main Group Metals, a Useful Distinction. *Angew. Chem. Int. Ed.* **1989**, *28* (8), 992–1007. https://doi.org/10.1002/anie.198909921.

(45) Hellmann, H. Zur Rolle Der Kinetischen Elektronenenergie Für Die Zwischenatomaren Kräfte. *Z. Phys.* **1933**, *85* (3), 180–190. https://doi.org/10.1007/BF01342053.

(46) Ruedenberg, K. The Physical Nature of the Chemical Bond. *Rev. Mod. Phys.* **1962**, *34* (2), 326–376. https://doi.org/10.1103/RevModPhys.34.326.

(47) Zhao, L.; Hermann, M.; Holzmann, N.; Frenking, G. Dative Bonding in Main Group Compounds. *Coord. Chem. Rev.* **2017**, *344*, 163–204. https://doi.org/10.1016/j.ccr.2017.03.026.

(48) Nordholm, S.; Bacskay, G. B. The Basics of Covalent Bonding in Terms of Energy and Dynamics. *Molecules* **2020**, *25* (11), 2667.

(49) Zhao, L.; von Hopffgarten, M.; Andrada, D. M.; Frenking, G. Energy Decomposition Analysis. *WIREs Comput. Mol. Sci.* **2018**, *8* (3), e1345. https://doi.org/10.1002/wcms.1345.

(50) Tonner, R.; Heydenrych, G.; Frenking, G. Bonding Analysis of N-Heterocyclic Carbene Tautomers and Phosphine Ligands in Transition-Metal Complexes: A Theoretical Study. *Chem. Asian J.* **2007**, *2* (12), 1555–1567. https://doi.org/10.1002/asia.200700235.

(51) Kozma, Á.; Gopakumar, G.; Farès, C.; Thiel, W.; Alcarazo, M. Synthesis and Structure of Carbene-Stabilized N-Centered Cations $[L_2N]^+$, $[L_2NR]^{2+}$, $[LNR_3]^{2+}$, and $[L_3N]^{3+}$. *Chem. Eur. J.* **2013**, *19* (11), 3542–3546. https://doi.org/10.1002/chem.201204186.

(52) Loh, Y. K.; Melaimi, M.; Munz, D.; Bertrand, G. An Air-Stable “Masked” Bis(Imino)Carbene: A Carbon-Based Dual Ambiphile. *J. Am. Chem. Soc.* **2023**, *145* (4), 2064–2069. https://doi.org/10.1021/jacs.2c12847.

(53) Huynh, S.; Arrowsmith, M.; Meier, L.; Dietz, M.; Härterich, M.; Michel, M.; Gärtner, A.; Braunschweig, H. Cyclic Alkyl(Amino)Iminates (CAAIs) as Strong 2σ,4π-Electron Donor Ligands for the Stabilisation of Boranes and Diboranes(4): A Synthetic and Computational Study. *Dalton Trans.* **2023**, *52* (12), 3869–3876. https://doi.org/10.1039/D3DT00298E.

(54) G, M.; Sharma, D.; Dandela, R.; Dhayalan, V. Synthetic Strategies of N-Heterocyclic Olefin (NHOs) and Their Recent Application of Organocatalytic Reactions and Beyond. *Chem. Eur. J.* **2023**, *29* (70), e202302106. https://doi.org/10.1002/chem.202302106.

(55) Roy, M. M. D.; Rivard, E. Pushing Chemical Boundaries with N-Heterocyclic Olefins (NHOs): From Catalysis to Main Group Element Chemistry. *Acc. Chem. Res.* **2017**, *50* (8), 2017–2025. https://doi.org/10.1021/acs.accounts.7b00264.

(56) Ochiai, T.; Franz, D.; Inoue, S. Applications of N-Heterocyclic Imines in Main Group Chemistry. *Chem. Soc. Rev.* **2016**, *45* (22), 6327–6344. https://doi.org/10.1039/C6CS00163G.

(57) Kuhn, N.; Fawzi, R.; Steimann, M.; Wiethoff, J. Derivate Des Imidazols, XVII. Synthese Und Eigenschaften von Dichlor(1,3-Dimethyl-2-Imidazol-2-Ylidenimino)-Phosphan – Ein Methylenamino-Substituent Mit Ungewöhnlichen Donoreigenschaften. *Chem. Ber.* **1996**, *129* (4), 479–482. https://doi.org/10.1002/cber.19961290418.

(58) Back, O.; Donnadieu, B.; von Hopffgarten, M.; Klein, S.; Tonner, R.; Frenking, G.; Bertrand, G. N-Heterocyclic Carbenes versus Transition Metals for Stabilizing Phosphinyl Radicals. *Chem. Sci.* **2011**, *2* (5), 858–861. https://doi.org/10.1039/C1SC00027F.

(59) Roy, M. M. D.; Miao, L.; Ferguson, M. J.; McDonald, R.; Rivard, E. An Unexpected Staudinger Reaction at an N-Heterocyclic Carbene-Carbon Center. *Can. J. Chem.* **2018**, *96* (6), 543–548. https://doi.org/10.1139/cjc-2017-0607.

(60) Kuhn, N.; Göhner, M.; Grathwohl, M.; Wiethoff, J.; Frenking, G.; Chen, Y. 2-Iminoimidazoline — Starke Stickstoffbasen Als Koordinationspartner in Der Anorganischen Chemie. *Z. Anorg. Allg. Chem.* **2003**, *629* (5), 793–802. https://doi.org/10.1002/zaac.200390141.

(61) Dielmann, F.; Andrada, D. M.; Frenking, G.; Bertrand, G. Isolation of Bridging and Terminal Coinage Metal–Nitrene Complexes. *J. Am. Chem. Soc.* **2014**, *136* (10), 3800–3802. https://doi.org/10.1021/ja5007355.

(62) Dielmann, F.; Bertrand, G. Reactivity of a Stable Phosphinonitrene towards Small Molecules. *Chem. Eur. J.* **2015**, *21* (1), 191–198. https://doi.org/10.1002/chem.201405430.

(63) Buß, F.; Das, M.; Janssen-Müller, D.; Sietmann, A.; Das, A.; Wilm, L. F. B.; Freitag, M.; Seidl, M.; Glorius, F.; Dielmann, F. Photoswitchable Electron-Rich Phosphines: Using Light to Modulate the Electron-Donating Ability of Phosphines. *Chem. Commun.* **2023**, *59* (80), 12019–12022. https://doi.org/10.1039/D3CC04050J.

(64) Birenheide, B. S.; Krämer, F.; Bayer, L.; Mehlmann, P.; Dielmann, F.; Breher, F. Multistimuli-Responsive [3]Dioxaphosphaferrocenophanes with Orthogonal Switches. *Chem. Eur. J.* **2021**, *27* (61), 15067–15074. https://doi.org/10.1002/chem.202101969.

(65) Mehlmann, P.; Dielmann, F. Switching the Electron-Donating Ability of Phosphines through Proton-Responsive Imidazolin-2-Ylidenamino Substituents. *Chem. Eur. J.* **2019**, *25* (9), 2352–2357. https://doi.org/10.1002/chem.201805540.

(66) Löwe, P.; Feldt, M.; Wünsche, M. A.; Wilm, L. F. B.; Dielmann, F. Oxophosphonium–Alkyne Cycloaddition Reactions: Reversible Formation of 1,2-

Oxaphosphetes and Six-Membered Phosphorus Heterocycles. *J. Am. Chem. Soc.* **2020**, *142* (21), 9818–9826. https://doi.org/10.1021/jacs.0c03494.

(67) Wünsche, M. A.; Witteler, T.; Dielmann, F. Lewis Base Free Oxophosphonium Ions: Tunable, Trigonal-Planar Lewis Acids. *Angew. Chem. Int. Ed.* **2018**, *57* (24), 7234–7239. https://doi.org/10.1002/anie.201802900.

(68) Löwe, P.; Feldt, M.; Röthel, M. B.; Wilm, L. F. B.; Dielmann, F. Thiophosphonium–Alkyne Cycloaddition Reactions: A Heavy Congener of the Carbonyl–Alkyne Metathesis. *Inorg. Chem.* **2021**, *60* (19), 14509–14514. https://doi.org/10.1021/acs.inorgchem.1c02076.

(69) Löwe, P.; Witteler, T.; Dielmann, F. Lewis Base-Free Thiophosphonium Ion: A Cationic Sulfur Atom Transfer Reagent. *Chem. Commun.* **2021**, *57* (41), 5043–5046. https://doi.org/10.1039/D1CC01273H.

(70) Lavallo, V.; Canac, Y.; Donnadieu, B.; Schoeller, W. W.; Bertrand, G. Cyclopropenylidenes: From Interstellar Space to an Isolated Derivative in the Laboratory. *Science* **2006**, *312* (5774), 722–724. https://doi.org/10.1126/science.1126675.

(71) Bandar Tristan H., J. S. . L. Aminocyclopropenium Ions: Synthesis, Properties, and Applications. *Synthesis* **2013**, *45* (18), 2485–2498. https://doi.org/10.1055/s-0033-1338516.

(72) Wilson, R. M.; Lambert, T. H. Cyclopropenium Ions in Catalysis. *Acc. Chem. Res.* **2022**, *55* (20), 3057–3069. https://doi.org/10.1021/acs.accounts.2c00546.

(73) Taakili, R.; Duhayon, C.; Lugan, N.; Canac, Y. Reactivity vs. Stability of Cyclopropenium Substituted Phosphonium Salts. *Eur. J. Inorg. Chem.* **2019**, *2019* (36), 3982–3989. https://doi.org/10.1002/ejic.201900867.

(74) Alcarazo, M. α-Cationic Phosphines: Synthesis and Applications. *Chem. Eur. J.* **2014**, *20* (26), 7868–7877. https://doi.org/10.1002/chem.201402375.

(75) Dube, J. W.; Zheng, Y.; Thiel, W.; Alcarazo, M. α-Cationic Arsines: Synthesis, Structure, Reactivity, and Applications. *J. Am. Chem. Soc.* **2016**, *138* (21), 6869–6877. https://doi.org/10.1021/jacs.6b03500.

(76) Mehler, G.; Linowski, P.; Carreras, J.; Zanardi, A.; Dube, J. W.; Alcarazo, M. Bis(Cyclopropenium)Phosphines: Synthesis, Reactivity, and Applications. *Chem. Eur. J.* **2016**, *22* (43), 15320–15327. https://doi.org/10.1002/chem.201601759.

(77) Alcarazo, M. Synthesis, Structure, and Applications of α-Cationic Phosphines. *Acc. Chem. Res.* **2016**, *49* (9), 1797–1805. https://doi.org/10.1021/acs.accounts.6b00262.

(78) Graham, C. M. E.; Macdonald, C. L. B.; Boyle, P. D.; Wisner, J. A.; Ragogna, P. J. Addressing the Nature of Phosphinidene Sulfides via the Synthesis of P−S Heterocycles. *Chem. Eur. J.* **2018**, *24* (3), 743–749. https://doi.org/10.1002/chem.201705198.

(79) Yoshifuji, M.; Nakayama, S.; Okazaki, R.; Inamoto, N. Phosphinidenes and Related Intermediates. Part I. Reactions of Phosphinoylidenes (R–P=O) and Phosphinothioylidenes (R–P=S) with Diethyl Disulphideand Benzil. *J. Chem. Soc. Perkin Trans. 1* **1973**, No. 0, 2065–2068. https://doi.org/10.1039/P19730002065.

(80) Santini, C. C.; Fischer, J.; Mathey, F.; Mitschler, A. Phosphole [2 + 2] and [4 + 2] Dimerizations around Metal Carbonyl Moieties. Structure and Chemistry of a New Type of Exo [4 + 2] Dimers. *J. Am. Chem. Soc.* **1980**, *102* (18), 5809–5815. https://doi.org/10.1021/ja00538a018.

(81) Gaspar, P. P.; Qian, H.; Beatty, A. M.; André D’Avignon, D.; Kao, J. L. F.; Watt, J. C.; Rath, N. P. 2,6-Dimethoxyphenylphosphirane Oxide and Sulfide and Their Thermolysis to Phosphinidene Chalcogenides - Kinetic and Mechanistic Studies. *Tetrahedron* **2000**, *56* (1), 105–119. https://doi.org/10.1016/S0040-4020(99)00779-6.

(82) Nakayama, S.; Yoshifuji, M.; Okazaki, R.; Inamoto, N. Reactions of

Phosphinothioylidene (R–P=S) as Intermediate. *J. Chem. Soc. D Chem. Commun.* **1971**, No. 19, 1186–1187. https://doi.org/10.1039/C29710001186.

(83) Transue, W. J.; Nava, M.; Terban, M. W.; Yang, J.; Greenberg, M. W.; Wu, G.; Foreman, E. S.; Mustoe, C. L.; Kennepohl, P.; Owen, J. S.; Billinge, S. J. L.; Kulik, H. J.; Cummins, C. C. Anthracene as a Launchpad for a Phosphinidene Sulfide and for Generation of a Phosphorus-Sulfur Material Having the Composition P_2S, a Vulcanized Red Phosphorus That Is Yellow. *J. Am. Chem. Soc.* **2019**, *141* (1), 431–440. https://doi.org/10.1021/jacs.8b10775.

(84) Graham, T. W.; Udachin, K. A.; Carty, A. J. Synthesis of σ-π-Phosphinidene Sulfide Complexes $[Mn_2(CO)_n(\mu\text{-}\eta^1,\eta^2\text{-}P(NR_2)S)]$ (N=8,9) via Direct Sulfuration of Electrophilic μ-Phosphinidenes and Photochemical Transformation to a Trigonal Prismatic $Mn_2P_2S_2$ Cluster. *Inorganica Chim. Acta* **2007**, *360* (4), 1376–1379. https://doi.org/10.1016/j.ica.2006.02.022.

(85) Graham, C. M. E.; Pritchard, T. E.; Boyle, P. D.; Valjus, J.; Tuononen, H. M.; Ragogna, P. J. Trapping Rare and Elusive Phosphinidene Chalcogenides. *Angew. Chem. Int. Ed.* **2017**, *56* (22), 6236–6240. https://doi.org/10.1002/anie.201611196.

(86) Pritchard, T. E. Exploring the Chemistry of Asymmetric Phosphines & Phosphinidene Sulfides. *Electron. Thesis Diss. Repos.* **2018**, *5664*.

(87) Yoshifuji, M.; Sangu, S.; Hirano, M.; Toyota, K. A Stabilized Phosphinothioylidene Generated by Deselenation of a Selenoxothioxophosphorane. *Chem. Lett.* **1993**, *22* (10), 1715–1718. https://doi.org/10.1246/cl.1993.1715.

(88) Jochem, G.; Nöth, H.; Schmidpeter, A. Ylide-Substituted Thioxophosphanes and Dithioxophosphoranes. *Angew. Chem. Int. Ed.* **1993**, *32* (7), 1089–1091. https://doi.org/10.1002/anie.199310891.

(89) Schoeller, W. W.; Niecke, E. Frontier Orbital Crossing and Ambident Reactivity in Phosphorus(III) Systems with (p–p)π-Bonds. *J. Chem. Soc. Chem. Commun.* **1982**,

No. 11, 569–570. https://doi.org/10.1039/C39820000569.

(90) Wang, L.; Ganguly, R.; Mathey, F. Revisiting the Chemistry of Phosphinidene Sulfides. *Organometallics* **2014**, *33* (19), 5614–5617. https://doi.org/10.1021/om500828n.

(91) Tomioka, H.; Miura, S.; Izawa, Y. Synthesis and Photochemical Reaction of Diels-Alder Adduct of Phosphole Oxide and Cyclopentadiene. *Tetrahedron Lett.* **1983**, *24* (32), 3353–3356. https://doi.org/10.1016/S0040-4039(00)86268-1.

(92) Holand, S.; Mathey, F. New Method for Building Carbon-Phosphorus Heterocycles. *J. Org. Chem.* **1981**, *46* (22), 4386–4389. https://doi.org/10.1021/jo00335a013.

(93) Mardyukov, A.; Keul, F.; Schreiner, P. R. Isolation and Characterization of the Free Phenylphosphinidene Chalcogenides $C_6H_5P{=}O$ and $C_6H_5P{=}S$, the Phosphorous Analogues of Nitrosobenzene and Thionitrosobenzene. *Angew. Chem. Int. Ed.* **2020**, *59* (30), 12445–12449. https://doi.org/10.1002/anie.202004172.

(94) Lindner, E.; Auch, K.; Hiller, W.; Fawzi, R. Methyl(Thioxo)Phosphane: Generation and Trapping Reaction with $Mn_2(CO)_{10}$. *Angew. Chem. Int. Ed.* **1984**, *23* (4), 320. https://doi.org/10.1002/anie.198403201.

(95) Stille, J. K.; Eichelberger, J. L.; Higgins, J.; Freeburger, M. E. Phenylphosphinidene Oxide. Thermal Decomposition of 2,3-Benzo-1,4,5,6,7-Pentaphenyl-7-Phosphabicyclo[2.2.1]Hept-5-Ene Oxide. *J. Am. Chem. Soc.* **1972**, *94* (13), 4761–4763. https://doi.org/10.1021/ja00768a071.

(96) Çetinkaya, B.; Hitchcock, P. B.; Lappert, M. F.; Thorne, A. J.; Goldwhite, H. Synthesis and Characterisation of 2, 4, 6-Tri-t-Butylphenylphosphines; X-Ray Structure of $[P(C_6H_2Bu^t{}_3\text{-}2,4,6)S]_3$. *J. Chem. Soc. Chem. Commun.* **1982**, No. 12, 691–693. https://doi.org/10.1039/C39820000691.

(97) Henne, F. D.; Watt, F. A.; Schwedtmann, K.; Hennersdorf, F.; Kokoschka, M.;

Weigand, J. J. Tetra-Cationic Imidazoliumyl-Substituted Phosphorus–Sulfur Heterocycles from a Cationic Organophosphorus Sulfide. *Chem. Commun.* **2016**, *52* (10), 2023–2026. https://doi.org/10.1039/C5CC08182C.

(98) Lensch, C.; Sheldrick, G. M. Preparation and Crystal Structures of Two Phosphorus–Sulphur Rings: $(RPS)_4$ and $(RPS_2)_2(R = C_6H_2Me_3\text{-}2,4,6)$. *J. Chem. Soc. Dalton Trans.* **1984**, No. 12, 2855–2857. https://doi.org/10.1039/DT9840002855.

(99) Yoshifuji, M.; Toyota, K.; Ando, K.; Inamoto, N. Isolation And Characterization Of A Stable Dithioxophosphorane. *Chem. Lett.* **1984**, *13* (3), 317–318. https://doi.org/10.1246/cl.1984.317.

(100) Baudler, M.; Koch, D.; Vakratsas, T.; Tolls, E.; Kipker, K. Beiträge Zur Chemie Des Phosphors. 59. Zur Synthese Und Struktur von $(C_6H_5PS)_3$. *Z. Anorg. Allg. Chem.* **1975**, *413* (3), 239–251. https://doi.org/10.1002/zaac.19754130304.

(101) Yoshifuji, M.; Ando, K.; Shibayama, K.; Inamoto, N.; Hirotsu, K.; Higuchi, T. The First X-Ray Structure Analysis of a Thiadiphosphirane. *Angew. Chem. Int. Ed.* **1983**, *22* (5), 418–419. https://doi.org/10.1002/anie.198304181.

(102) Navech, J.; Revel, M.; Kraemer, R. Etude de La Reactivite Du Tris(Tertiobutyl)Phenyldithiophosphorane. *Tetrahedron Lett.* **1985**, *26* (2), 207–210. https://doi.org/10.1016/S0040-4039(00)61881-6.

(103) Yoshifuji, M.; Shibayama, K.; Inamoto, N.; Hirotsu, K.; Higuchi, T. Reaction of the Diphosphene ArP=PAr (Ar = $2,4,6\text{-}Bu^t{}_3C_6H_2$) with Sulphur: Isolation and X-Ray Structure of the Diphosphene Monosulphide. *J. Chem. Soc. Chem. Commun.* **1983**, No. 16, 862–863. https://doi.org/10.1039/C39830000862.

(104) Sasamori, T.; Sakagami, M.; Tokitoh, N. Step-Wise Sulfurization of Stable 1,2-Bis(Ferrocenyl)Diphosphene. *J. Sulfur Chem.* **2013**, *34* (6), 677–683. https://doi.org/10.1080/17415993.2013.795224.

(105) Yoshifuji, M.; Shibayama, K.; Inamoto, N. Reaction Of Diphosphenes With

Elemental Selenium. Isolation And Characterization Of Selenadiphosphiranes And Diselenoxophosphorane. *Chem. Lett.* **1984**, *13* (4), 603–606. https://doi.org/10.1246/cl.1984.603.

(106) Baudler, M.; Suchomel, H.; Fürstenberg, G.; Schings, U. Di- Tert-Butylthia- and -Selenadiphosphirane. *Angew. Chem. Int. Ed.* **1981**, *20* (12), 1044–1045. https://doi.org/10.1002/anie.198110441.

(107) Dankert, F.; Gupta, P.; Wellnitz, T.; Baumann, W.; Hering-Junghans, C. Deoxygenation of Chalcogen Oxides EO_2 (E = S, Se) with Phospha-Wittig Reagents. *Dalton Trans.* **2022**, *51* (48), 18642–18651. https://doi.org/10.1039/D2DT03703C.

(108) Yoshifuji, M.; Hirano, M.; Toyota, K. Stable Dithioxophosphorane, Diselenoxophosphorane, and Selenoxophosphine Bearing 2,4-Di-t-Butyl- 6-(Dimethylamino)Phenyl Group as a New Sterically Protecting Auxiliary. *Tetrahedron Lett.* **1993**, *34* (6), 1043–1046. https://doi.org/10.1016/S0040-4039(00)77487-9.

(109) Chu, X.; Yang, Y.; Lu, B.; Wu, Z.; Qian, W.; Song, C.; Xu, X.; Abe, M.; Zeng, X. Methoxyphosphinidene and Isomeric Methylphosphinidene Oxide. *J. Am. Chem. Soc.* **2018**, *140* (42), 13604–13608. https://doi.org/10.1021/jacs.8b09201.

(110) Dhara, D.; Pal, P. K.; Dolai, R.; Chrysochos, N.; Rawat, H.; Elvers, B. J.; Krummenacher, I.; Braunschweig, H.; Schulzke, C.; Chandrasekhar, V.; Priyakumar, U. D.; Jana, A. Synthesis and Reactivity of NHC-Coordinated Phosphinidene Oxide. *Chem. Commun.* **2021**, *57* (75), 9546–9549. https://doi.org/10.1039/D1CC04421D.

(111) Schmidpeter, A.; Jochem, G.; Karaghiosoff, K.; Robl, C. Phosphorus(V) Selenides with Phosphorus in a Trigonal-Planar Environment. *Angew. Chem. Int. Ed.* **1992**, *31* (10), 1350–1352. https://doi.org/10.1002/anie.199213501.

(112) Jochem, G.; Schmidpeter, A.; Kulzer, F.; Dick, S. Ylidyl 1,2,4-Thiadiphosphetane

and 1,2,4-Selenadiphosphetane Sulfides and Selenides. *Chem. Ber.* **1995**, *128* (10), 1015–1020. https://doi.org/10.1002/cber.19951281009.

(113) Jochem, G.; Karaghiosoff, K.; Plank, S.; Schmidpeter, S. D. U. A. Ylidylphosphorsulfide, -Selenide, -Disulfide, -Sulfidselenide Und -Diselenide. *Chem. Ber.* **1995**, *128* (12), 1207–1219. https://doi.org/10.1002/cber.19951281212.

(114) Graham, C. M. E. E.; Valjus, J.; Pritchard, T. E.; Boyle, P. D.; Tuononen, H. M.; Ragogna, P. J. Phosphorus-Chalcogen Ring Expansion and Metal Coordination. *Inorg. Chem.* **2017**, *56* (21), 13500–13509. https://doi.org/10.1021/acs.inorgchem.7b02217.

(115) Baradzenka, A. G.; Vyboishchikov, S. F.; Pilkington, M.; Nikonov, G. I. Base-Stabilized Phosphinidene Oxide, Imide and Sulfide. *Chem. Eur. J.* **2023**, *29* (59), e202301842. https://doi.org/10.1002/chem.202301842.

(116) Romanenko, V. D.; Sanchez, M. Recent Developments in the Chemistry of Three-Coordinate Pentavalent Phosphorus Compounds ($\sigma^3\lambda^5$-Phosphoranes). *Coord. Chem. Rev.* **1997**, *158*, 275–324. https://doi.org/10.1016/S0010-8545(97)90061-8.

(117) Jessen, H. J.; Dürr-Mayer, T.; Haas, T. M.; Ripp, A.; Cummins, C. C. Lost in Condensation: Poly-, Cyclo-, and Ultraphosphates. *Acc. Chem. Res.* **2021**, *54* (21), 4036–4050. https://doi.org/10.1021/acs.accounts.1c00370.

(118) Fuchs, S.; Schmidbaur, H. Phosphonic Acid Anhydrides $[RPO_2]_n$: Oligomerization and Structure. *Z. Naturforsch. B* **1995**, *50b*, 855. https://doi.org/10.1515/znb-1995-0601.

(119) Cherbuliez, E.; Weber, G.; Rabinowitz, J. Note Sur Les Anhydrides et Monoesters Méthanephosphoniques et Dodécanephosphoniques. *Helv. Chim. Acta* **1963**, *46* (6), 2461. https://doi.org/10.1002/hlca.19630460668.

(120) Ranganathan, T.; Zilberman, J.; Farris, R. J.; Coughlin, E. B.; Emrick, T. Synthesis and Characterization of Halogen-Free Antiflammable Polyphosphonates

Containing 4,4’-Bishydroxydeoxybenzoin. *Macromolecules* **2006**, *39* (18), 5974. https://doi.org/10.1021/ma0614693.

(121) Arz, M. I.; Annibale, V. T.; Kelly, N. L.; Hanna, J. V; Manners, I. Ring-Opening Polymerization of Cyclic Phosphonates: Access to Inorganic Polymers with a P^V–O Main Chain. *J. Am. Chem. Soc.* **2019**, *141* (7), 2894–2899. https://doi.org/10.1021/jacs.8b13435.

(122) English, L. E.; Pajak, A.; McMullin, C. L.; Lowe, J. P.; Mahon, M. F.; Liptrot, D. J. A Terphenyl Supported Dioxophosphorane Dimer: The Light Congener of Lawesson’s and Woollins’ Reagents. *Chem. Eur. J.* **2022**, *28* (28), e202200376. https://doi.org/10.1002/chem.202200376.

(123) Lensch, C.; Clegg, W.; Sheldrick, G. M. Preparation and Crystal Structures of Two Phosphorus–Sulphur Rings: $(PhP)_3S_3$ and $(PhP)_2S_4$. *J. Chem. Soc. Dalton Trans.* **1984**, No. 4, 723–725. https://doi.org/10.1039/DT9840000723.

(124) Cherkasov, R. A.; Kutyrev, G. A.; Pudovik, A. N. Tetrahedron Report Number 186: Organothiophosphorus Reagents in Organic Synthesis. *Tetrahedron* **1985**, *41* (13), 2567–2624. https://doi.org/10.1016/S0040-4020(01)96363-X.

(125) Gray, I. P.; Bhattacharyya, P.; Slawin, A. M. Z.; Woollins, J. D. A New Synthesis of $(PhPSe_2)_2$ (Woollins Reagent) and Its Use in the Synthesis of Novel P–Se Heterocycles. *Chem. Eur. J.* **2005**, *11* (21), 6221–6227. https://doi.org/10.1002/chem.200500291.

(126) Woollins, J. D. How Not to Discover a New Reagent. the Evolution and Chemistry of Woollins’ Reagent. *Synlett* **2012**, *23* (8), 1154–1169. https://doi.org/10.1055/s-0031-1290665.

(127) Fluck, E.; Reinisch, R. M. Die Reaktion von Phenylphosphin Mit Dischwefeldichlorid. *Chem. Ber.* **1962**, *95* (6), 1388–1390. https://doi.org/10.1002/cber.19620950611.

(128) Yde, B.; Yousif, N. M.; Pedersen, U.; Thomsen, I.; Lawesson, S.-O. Studies on

Organophosphorus Compounds XLVII Preparation of Thiated Synthons of Amides, Lactams and Imides by Use of Some New p,s-Containing Reagents. *Tetrahedron* **1984**, *40* (11), 2047–2052. https://doi.org/10.1016/S0040-4020(01)88445-3.

(129) Harsági, N.; Keglevich, G. The Hydrolysis of Phosphinates and Phosphonates: A Review. *Molecules* **2021**, *26* (10). https://doi.org/10.3390/molecules26102840.

(130) Beckmann, H.; Großmann, G.; Ohms, G.; Sieler, J. New Perthiophosphonic Acid Anhydrides and the Direct Indication of the Dimer-Monomer Equilibrium. NMR and X-Ray Studies. *Heteroat. Chem.* **1994**, *5* (1), 73–83. https://doi.org/10.1002/hc.520050113.

(131) Navech, J.; Revel, M.; Kraemer, R. Etude De L'action Du Soufre Sur La Tris(Tertiobutyl)Phenylphosphine. *Phosphorus Sulfur Relat. Elem.* **1984**, *21* (1), 105–110. https://doi.org/10.1080/03086648408073132.

(132) Navech, J.; Et, M. R.; Mathieu, S. Etude De L'action Des Nucleophiles Sur Le Tris(Tert-Butyl)-2,4,6′ Phenyldithophosphorane-λ^5, [Sgrave]^3. *Phosphorus Sulfur Relat. Elem.* **1988**, *39* (1–2), 33–43. https://doi.org/10.1080/03086648808072852.

(133) Meisel, M.; Bock, H.; Solouki, B.; Kremer, M. Generation and Ionization Pattern of the Iso(Valence)Electronic Compounds $ClP(=O)_2$ and $ClP(=S)_2$. *Angew. Chem. Int. Ed.* **1989**, *28* (10), 1373–1376. https://doi.org/10.1002/anie.198913731.

(134) Rovnaník, P.; Kapička, L.; Taraba, J.; Černík, M. Base-Induced Dismutation of $POCl_3$ and $POBr_3$: Synthesis and Structure of Ligand-Stabilized Dioxophosphonium Cations. *Inorg. Chem.* **2004**, *43* (7), 2435–2442. https://doi.org/10.1021/ic0354163.

(135) Zhou, J.; Liu, L. L.; Cao, L. L.; Stephan, D. W. Base-Stabilized $[PO]^+/[PO_2]^+$ Cations. *Angew. Chem. Int. Ed.* **2019**, *58* (50), 18276–18280. https://doi.org/10.1002/anie.201912009.

(136) Kuhn, N.; Ströbele, M.; Walker, M. A Stable Carbene Phosphenic Chloride

Complex: First Structural Characterization of a PO_2Cl Base Adduct [1]. *Z. Anorg. Allg. Chem.* **2003**, *629* (2), 180–181. https://doi.org/10.1002/zaac.200390026.

(137) Schneider, T.; Schwedtmann, K.; Fidelius, J.; Weigand, J. J. Redox-Neutral Conversion of Ubiquitous P^V Sources to a Versatile PO_2^+ Phosphorylation Reagent. *Nat. Synth.* **2023**, *2* (10), 972–979. https://doi.org/10.1038/s44160-023-00344-0.

(138) Michaelis, A.; Rothe, F. Über Die Den Nitroverbindungen Entsprechenden Phosphorderivate. *Ber. Dtsch. Chem. Ges.* **1892**, *25*, 1747.

(139) Cherbuliez, E.; Baehler, B.; Hunkeler, F.; Rabinowitz, J. Recherches Sur La Formation et La Transformation Des Esters XXVIII. Sur La Phosphonylation Des Alcools Par Les Oxydes Phosphoniques. *Helv. Chim. Acta* **1961**, *44* (6), 1812. https://doi.org/10.1002/hlca.19610440644.

(140) Mardyukov, A.; Niedek, D.; Schreiner, P. R. Preparation and Characterization of Parent Phenylphosphinidene and Its Oxidation to Phenyldioxophosphorane: The Elusive Phosphorus Analogue of Nitrobenzene. *J. Am. Chem. Soc.* **2017**, *139* (14), 5019. https://doi.org/10.1021/jacs.7b01639.

(141) Bracher, S.; Cadogan, J. I. G.; Gosney, I.; Yaslak, S. The Generation and Trapping of a Monomeric Aryldioxophosphorane (‘Metaphosphonate’). *J. Chem. Soc., Chem. Commun.* **1983**, 857. https://doi.org/10.1039/C39830000857.

(142) Baudler, M.; Valpertz, H.-W. Notizen: Beiträge Zur Chemie Des Phosphors XXXV. Reaktion von Organyl-Dichlor-Phosphinen Mit Disulfan. *Z. Naturforsch. B* **1967**, *22* (2), 222–223. https://doi.org/10.1515/znb-1967-0224.

(143) Appel, R.; Knoch, F.; Kunze, H. The First Organodithioxophosphorane. *Angew. Chem. Int. Ed.* **1983**, *22* (12), 1004–1005. https://doi.org/10.1002/anie.198310041.

(144) Navech, J.; Majoral, J. P.; Kraemer, R. Synthesis of the First Stable Metadithiophosphonate. *Tetrahedron Lett.* **1983**, *24* (52), 5885–5886. https://doi.org/10.1016/S0040-4039(00)94227-8.

(145) Yoshifuji, M.; Sangu, S.; Kamijo, K.; Toyota, K. Preparation and Structure of Dithioxo- and Diselenoxophosphoranes Stabilized by Intramolecular Coordination with a Dialkylamino Group. *Chem. Ber.* **1996**, *129* (9), 1049–1055. https://doi.org/10.1002/cber.19961290912.

(146) Bockfeld, D.; Bannenberg, T.; Jones, P. G.; Tamm, M. N-Heterocyclic Carbene Adducts of Phenyldioxophosphorane and Its Heavier Sulfur and Selenium Analogues. *Eur. J. Inorg. Chem.* **2017**, *2017* (28), 3452. https://doi.org/10.1002/ejic.201700494.

(147) Wang, Y.; Xie, Y.; Wei, P.; Schaefer, H. F. I. I. I.; Schleyer, P. von R.; Robinson, G. H. Splitting Molecular Oxygen En Route to a Stable Molecule Containing Diphosphorus Tetroxide. *J. Am. Chem. Soc.* **2013**, *135* (51), 19139–19142. https://doi.org/10.1021/ja411667f.

(148) Surgenor, B. A.; Chalmers, B. A.; Athukorala Arachchige, K. S.; Slawin, A. M. Z.; Woollins, J. D.; Bühl, M.; Kilian, P. Reactivity Profile of a Peri-Substitution-Stabilized Phosphanylidene-Phosphorane: Synthetic, Structural, and Computational Studies. *Inorg. Chem.* **2014**, *53* (13), 6856–6866. https://doi.org/10.1021/ic500697m.

(149) Kilian, P.; Parveen, S.; Fuller, A. L.; Slawin, A. M. Z.; Derek Woollins, J. Structure and Reactivity of Phosphorus-Selenium Heterocycles with Peri-Substituted Naphthalene Backbones. *Dalton Trans.* **2008**, No. 14, 1908–1916. https://doi.org/10.1039/B718853F.

(150) Kilian, P.; Slawin, A. M. Z. 1,8,9-Substituted Anthracenes, Intramolecular Phosphine Donor Stabilized Metaphosphonate and Phosphenium. *Dalton Trans.* **2007**, No. 30, 3289–3296. https://doi.org/10.1039/B705286C.

Chapter 2

2 Molecular Structures of N-heterocyclic Imine Supported Phosphine Chalcogenides $[IPrNPS]_2SO$ and $(IPrN)_2P(O)H$

2.1 Introduction

The isolation and stabilization of low-valent phosphorus compounds are pivotal endeavors that enable researchers to delve into the study of highly reactive species and provide crucial mechanistic insights into their transformations. One such significant functional group in this context is the phosphinidene-sulfide [RP=S], representing a formally two-coordinate phosphorus (III) species. Phosphinidene sulfides have been prepared and reacted *in situ* by various routes (**Figure 2-1**, A) including dehalogenation,[1] deselenation,[2] photolysis,[3–5] and heat induced retro-cycloaddition reactions.[6] A recently reported photolytic reduction within a frozen argon matrix allowed for the isolation and spectroscopic analysis of phosphinidene-chalcogenide species.[5] Coordination of phosphinidene sulfide units to metal complexes has also emerged as an effective strategy for stabilization. Previous efforts towards the isolation of a free monomeric [RP=S] predominantly employed bulky aryl ligands[7] or additional stabilization through donating ligands;[2] however an isolated monomeric phosphinidene sulfide in the solid-state has proven elusive.

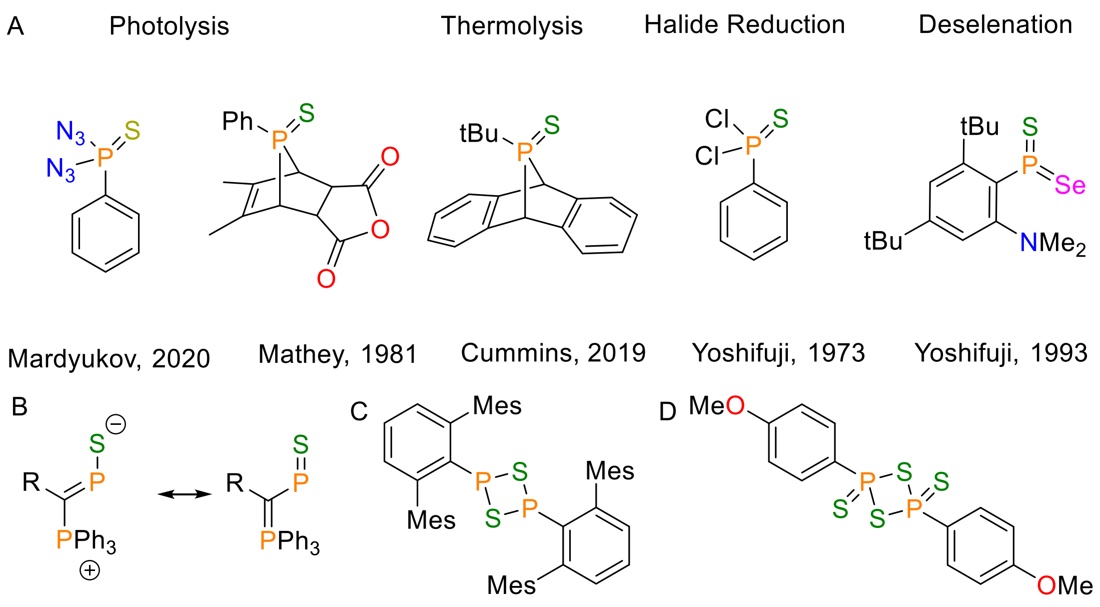

Figure 2-1. A) Selected examples of phosphinidene-sulfide precursors;[1,2,4,5,8] B) ylide-substituted thioxophosphanes reported by Schmidpeter and coworkers;[9] C) dimeric (Ar*PS)$_2$ reported by Ragogna group;[7] D) Lawesson's reagent.[10]

Illustrative examples of isolable two-coordinate phosphinidene sulfides are the ylide-substituted thioxophosphanes reported by Schmidpeter and coworkers[9] (**Figure 2-1**, B), wherein the P-S bond was observed to be elongated compared to typical P=S double-bonded species. The Ragogna group additionally contributed to the exploration of phosphinidene-sulfides by reporting the synthesis of terphenyl-supported heterocyclic phosphorus chalcogenide (Ch = S and Se) species *via* condensation of Ar*PCl$_2$ (Ar* = bis(2,4,6-trimethylphenyl)phenyl) with Ch(SiMe$_3$)$_2$, resulting in a species with a P$_2$Ch$_2$ heterocyclic core (**Figure 2-1**, C). The dimeric (Ar*PS)$_2$ behaved as a surrogate for monomeric phosphinidene sulfide by participating in cycloaddition reactions with unsaturated substrates in solution.[11]

Phosphorus (V) chalcogenides, such as disulfides and mixed P(V) chalcogenides, are also of importance as these reagents may be used in organic transformations and chalcogenide transfer reactions. Lawesson's reagent (RPS$_2$)$_2$ (R = 4-methoxyphenyl; LR, **Figure 2-1**, D), for example, has been used extensively for sulfurization reactions in organic chemistry by the transformation of a ketone to a thioketone, producing mixed phosphine chalcogenide heterocyclic byproducts with the driving force being the formation of a stronger P=O bond.[12,13] LR is known to be sensitive to moisture and so any resulting hydrolysis leads to a mixture of phosphine chalcogenide species *in situ*.[14]

Ylide-substituted thioxophosphanes[9] (**Figure 2-1**, B) prompted us to consider the use of bulky π-donating ligands for the stabilization of a phosphinidene sulfide. The N-heterocyclic imine ligand (NHI) has been effectively used to stabilize many reactive main group compounds,[15] including organophosphorus species,[16–19] but the effect on the chemistry of phosphinidene sulfides or $(RPS)_n$ heterocycles has not been reported. Condensation reactions of $RPCl_2$ and photolysis reactions of bis(azido)phosphine chalcogenides to access phosphinidene chalcogenides have precedence in reported literature, so the impetus was the development of a synthetic route for the preparation of a phosphinidene sulfide *via* either a condensation of $IPrNPCl_2$ with Na_2S or $S(SiMe_3)_2$, or reduction of a novel bis(azido)phosphine sulfide precursor (**Scheme 2-1**). The work presented in this chapter describes the strategies taken to generate a phosphinidene sulfide and the precursor species, which despite best efforts for the exclusion of water/O_2 succumbed to difficulties which arose because of the presence of moisture. Serendipitously isolated crystals and solid-state structures of the mixed phosphorus chalcogenide species $(IPrNPS)_2SO$ (**2.10**) and a neutral phosphine oxide $(IPrN)_2P(O)H$ (**2.13**), as well as unsuccessful reduction methods of $IPrNP(S)(N_3)_2$ (**2.15**) will be discussed.

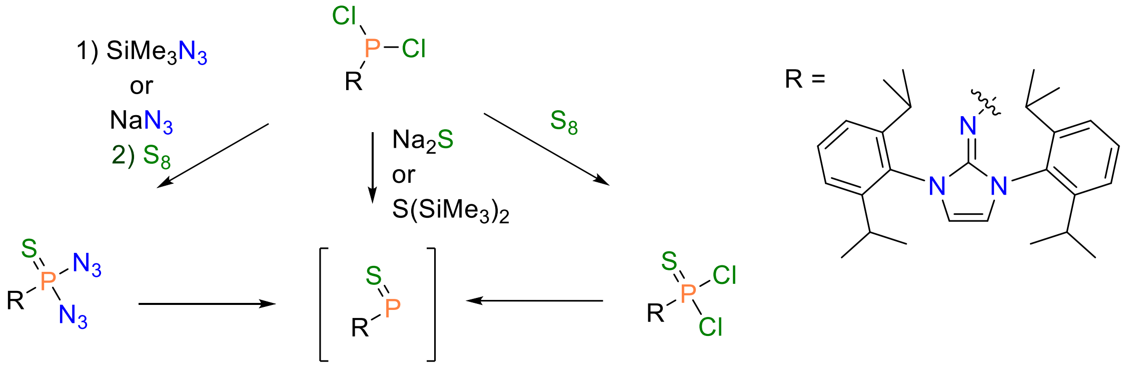

Scheme 2-1. Generalized routes towards the synthesis of an NHI-supported phosphinidene sulfide.

2.2 Results and Discussion

2.2.1 Synthesis of Precursors

The synthesis of the imidazolin-2-iminato species **2.4** (**Scheme 2-2**) from 2,6-diisopropylaniline was performed following established procedures,[20,21] including an optimization for the imidazolium salt **2.2** using $SiMe_3Cl$ as a chloride source.[22] A solution of **2.3** with $SiMe_3N_3$ in toluene was heated to reflux for 48 h under high-purity argon, then subsequently concentrated to dryness under vacuum. The N-heterocyclic imine (NHI) **2.4** was extracted from the crude mixture with toluene. When the same procedure was performed under nitrogen, significant hydrolysis to **2.5** was encountered. This was possibly a result of pervasive moisture introduced from the "medical grade" nitrogen which was not effectively dried by the in-line drying tube containing Drierite ($CaSO_4$). From the N-heterocyclic imine, multiple potential routes towards the synthesis of an NHI-stabilized phosphinidene sulfide were envisioned (A – G, **Scheme 2-3**).

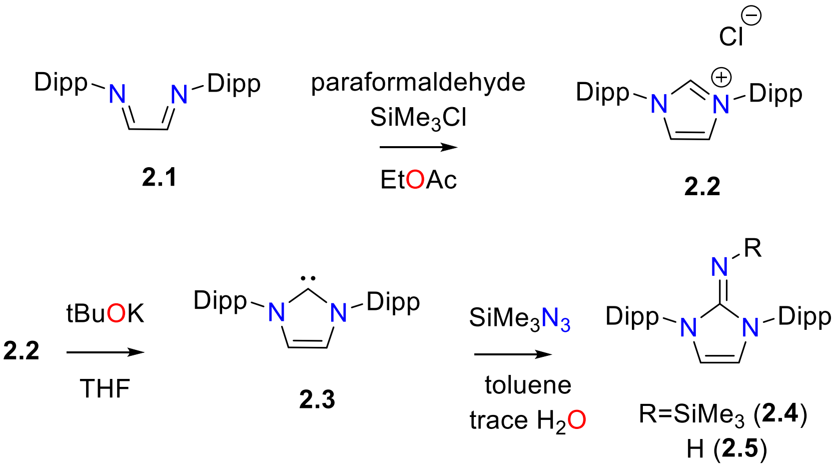
Dipp
N
N
Dipp
2.1
paraformaldehyde
SiMe3Cl
EtOAc
Cl
Dipp
N
N
Dipp
2.2
2.2
tBuOK
THF
Dipp
N
N
Dipp
2.3
SiMe3N3
toluene
trace H2O
N
R
Dipp
N
N
Dipp
R=SiMe3 (2.4)
H (2.5)

Scheme 2-2. Synthetic route to precursor **2.4**.

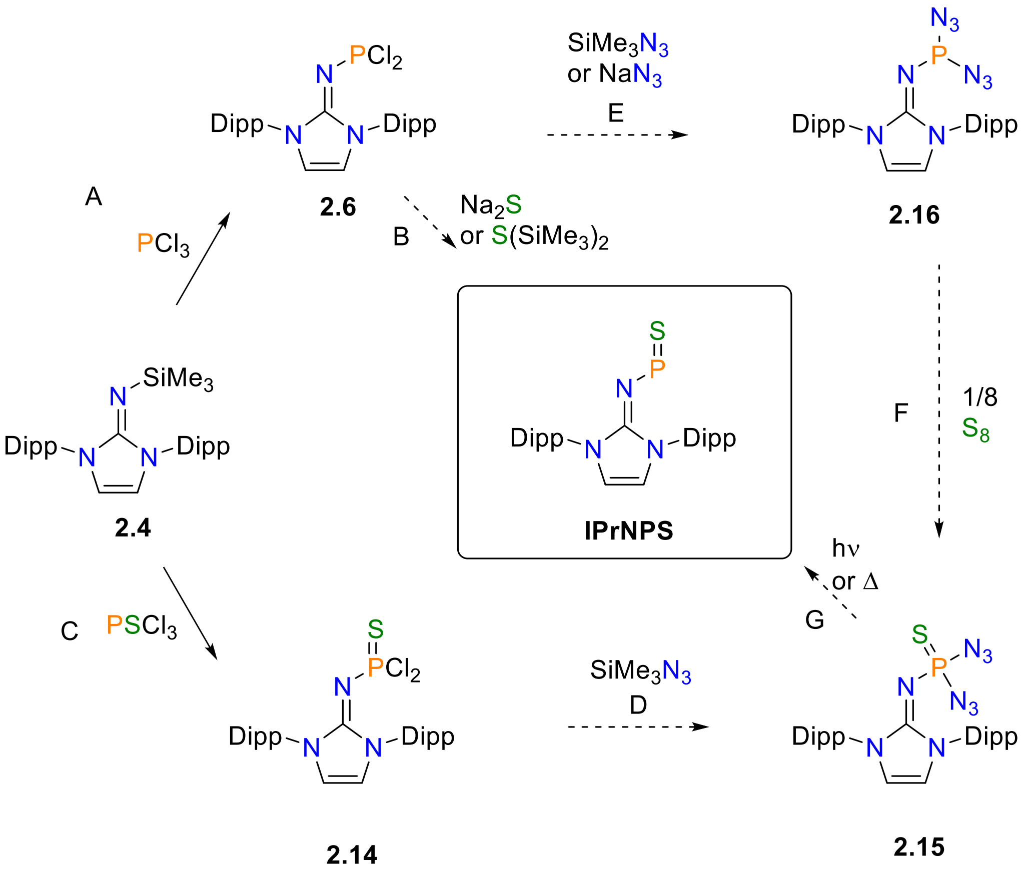

Scheme 2-3. Hypothesized routes towards IPrNPS from the IPrNSiMe$_3$ (**2.4**) precursor. Transformations are labelled A-G.

2.2.2 Transformation Pathway A

Regardless of the purity, mixtures of partially hydrolyzed **2.4** & **2.5** were effectively utilized for the preparation of **2.6** through condensation reactions with PCl$_3$ when NEt$_3$ was used as a proton scavenger. The addition of PCl$_3$ to concentrated solutions of **2.4** and NEt$_3$ in toluene resulted in the rapid precipitation of **[2.7]Cl** (δ_P = 309, CDCl$_3$, **Figure 2-2**) as a bright yellow solid (**Scheme 2-4**). Prolonged stirring in a dilute conditions gradually facilitated redissolution and disappearance of colour due to a ligand redistribution of **[2.7]Cl** with PCl$_3$, leading to the production of two stoichiometric equivalents of **2.6** (δ_P = 163, CDCl$_3$; 183, CD$_3$CN). Structural confirmation of the **[2.7]Cl** intermediate was obtained through single-crystal X-ray diffraction (SC-XRD) of bright yellow crystals isolated from a concentrated THF solution *vide infra* (**Figure 2-13**), and is consistent with the analogous **[2.7][B((CF$_3$)$_2$C$_6$H$_3$)$_4$)]** reported by Dielmann (δ_P = 308).[19]

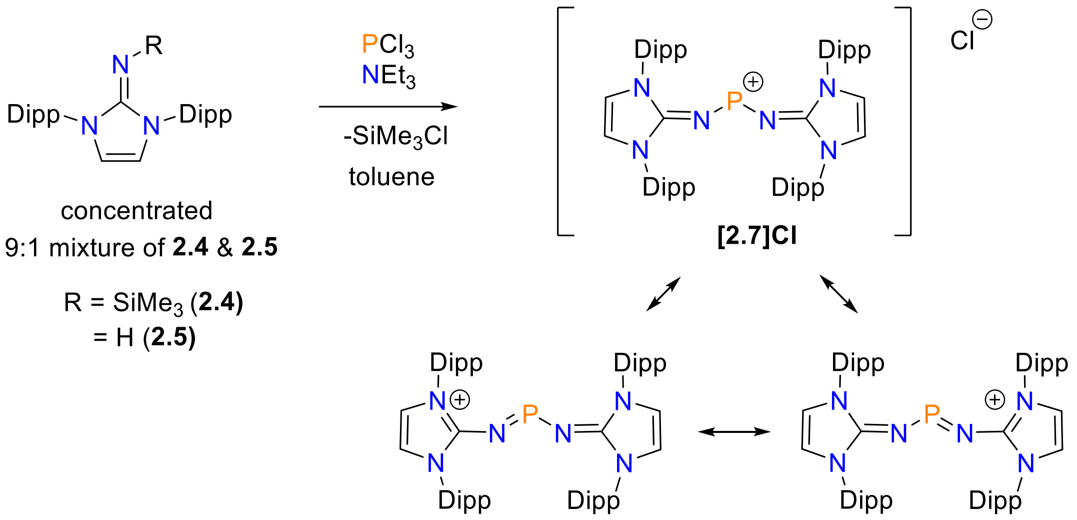
R
N
Dipp
N
N
Dipp
concentrated
9:1 mixture of **2.4** & **2.5**
R = SiMe$_3$ (**2.4**)
= H (**2.5**)
PCl$_3$
NEt$_3$
-SiMe$_3$Cl
toluene
Dipp
Dipp
N
N
P
N
N
N
N
Dipp
Dipp
Cl
[2.7]Cl
Dipp
Dipp
Dipp
Dipp
Dipp
Dipp
Dipp
Dipp

Scheme 2-4. Synthesis and canonical structures of bis(NHI) stabilized phosphenium **[2.7]Cl**.

2.2.3 Transformation Pathway B

A stirred solution of **2.2** in acetonitrile with Na_2S at room temperature resulted in a distinct signal at δ_P = 310 (referred herein as compound **2.8, Figure 2-2)**. The reaction was also observed to proceed to the same product, although more sluggishly, in a mixture of THF and CH_2Cl_2 (**Figure 2-3**), and was accompanied by the formation of a yellow color in each experiment (see **Figure 2-4**). **2.8** notably appeared at the same chemical shift position in $^{31}P\{^1H\}$ NMR experiments as **[2.7]Cl**, which suggested that **[2.7]Cl** was being formed instead of the target compound in these reactions. These observations were unexpected as the ylide-stabilized phosphinidene sulfide reported by Schmidpeter and co-workers[9] was dark red and significantly further downfield relative to compound **2.8** ($\Delta\delta_P$ ≈ 170).[9] While the identity of **2.8** was not confirmed, the observed colour change, NMR spectroscopic data, and reactivity with sulfur (*vide infra*) correlate an identity of **2.8** to plausibly be **[2.7]Cl**.

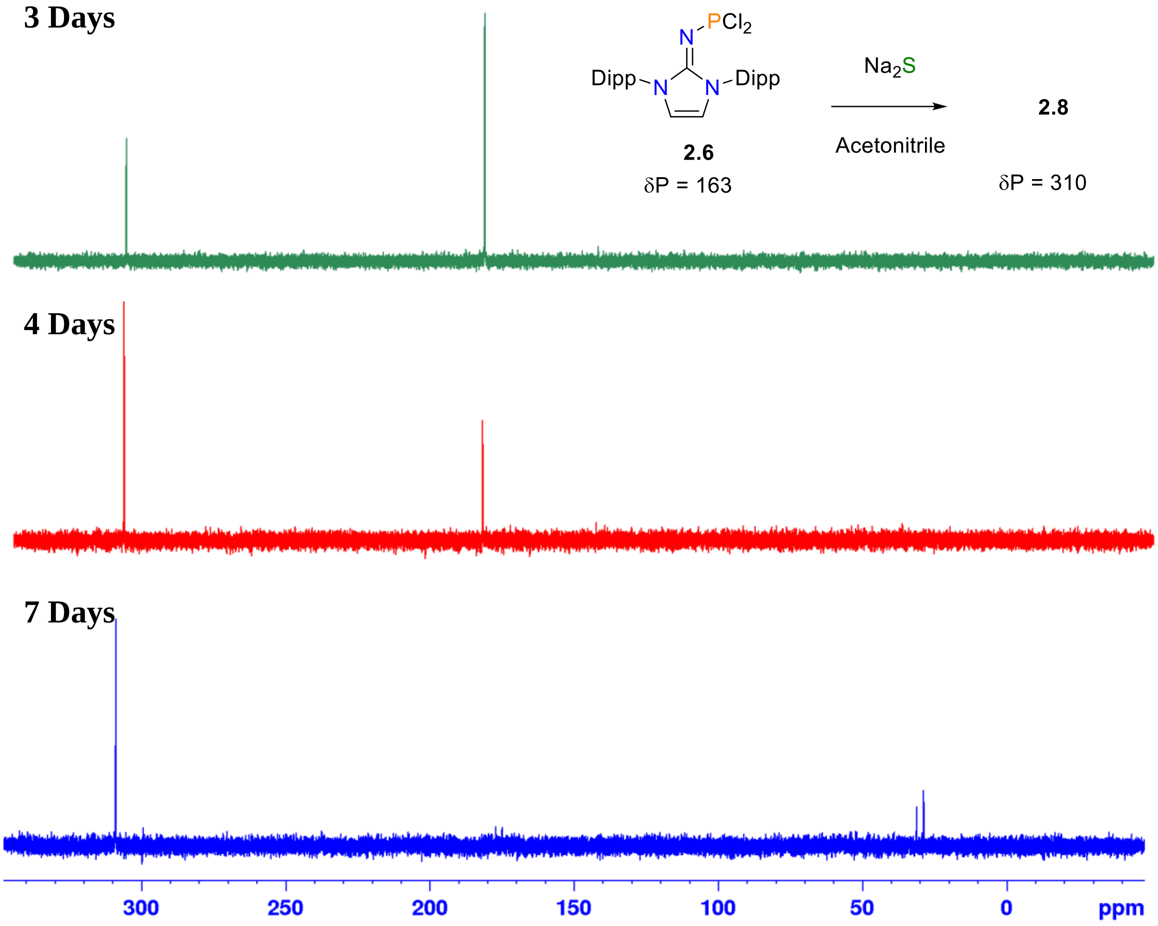

Figure 2-2. Stack plot of $^{31}P\{^{1}H\}$ NMR spectra of the reaction of **2.6** and Na_2S in CH_3CN. Aliquot taken after three days (top, green); after four days (middle, red); after seven days (bottom, blue).

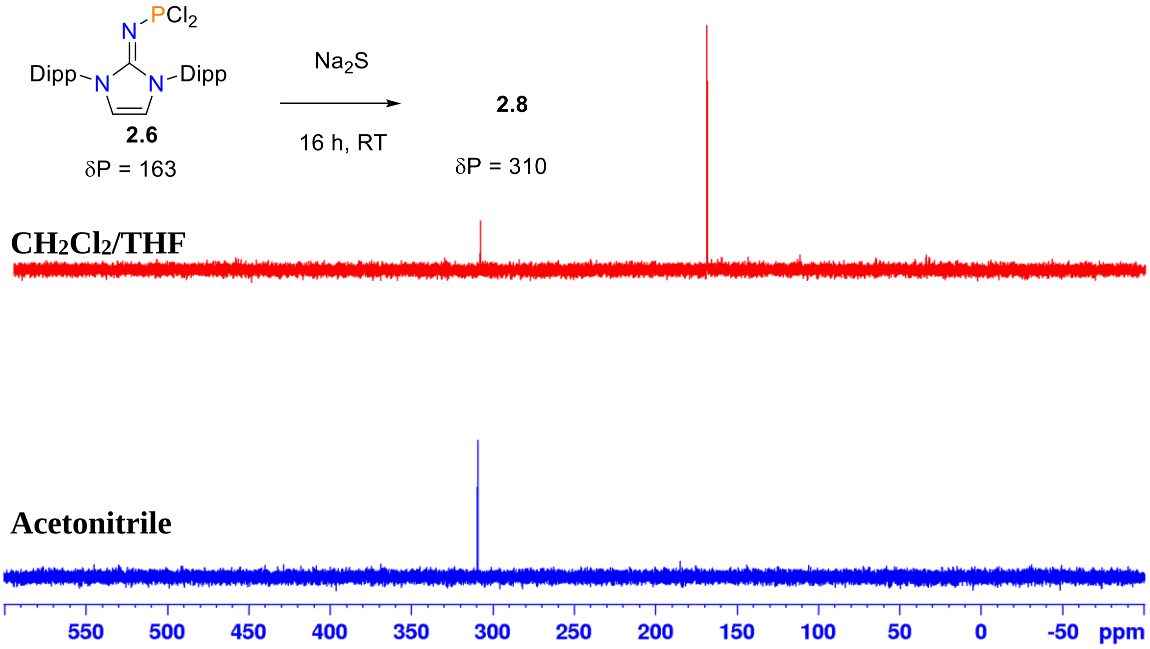

Figure 2-3. $^{31}P\{^1H\}$ NMR spectra of the reaction of **2.6** with Na_2S, in different solvents, after 16 h: CH_2Cl_2/THF (top, red); acetonitrile (bottom, blue).

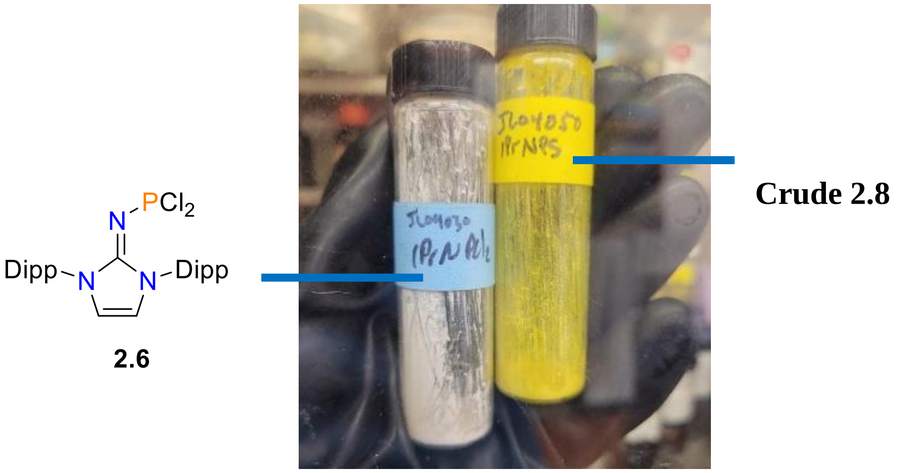
Crude 2.8
PCl2
N
Dipp
N
N
Dipp
2.6
JL04050
IPrNPS
JL04030
IPrNPCl2

Figure 2-4. Side-by-side comparison of compound **2.6** (left) and the crude compound **2.8** (right).

Scaling up the reaction to target the unidentified species **2.8** required a substantial increase in reaction time to ensure the complete consumption of the Na_2S starting material, monitored by $^{31}P\{^1H\}$ NMR spectroscopy. These reaction times were often more than a week. The slow reactivity was hypothesized to be caused by the low solubility of Na_2S in acetonitrile. The addition of small quantities of N,N-dimethylformamide (DMF) was postulated to increase the solubility of Na_2S, and subsequently increase the rate of reaction. A $^{31}P\{^1H\}$ NMR spectrum obtained 15 min following dissolution of a sample of crude residue of **2.8** in DMF did not suggest a rapid reaction occured. $^{31}P\{^1H\}$ NMR spectra (*e.g.,* **Figure 2-5**) revealed that an addition of DMF to a reaction mixture over prolonged periods of time resulted in formations of other uncharacterized phosphorus species. The addition was optimized such that only 1-3 drops of DMF were used when performing the reaction on a 0.5 mmol scale. This allowed for more rapid formation of **2.8** and limited the formation of undesirable side-products. This modified procedure led to the isolation of a product with an estimated purity of approximately 80 %, as assessed by both $^{31}P\{^1H\}$, ^1H, and $^{13}C\{^1H\}$ NMR spectroscopy, which showed only minor amounts of side products containing the N-heterocyclic imine ligand. The ^1H and $^{13}C\{^1H\}$ NMR experiments confirmed the predominating signals were a result of compound **2.8**.

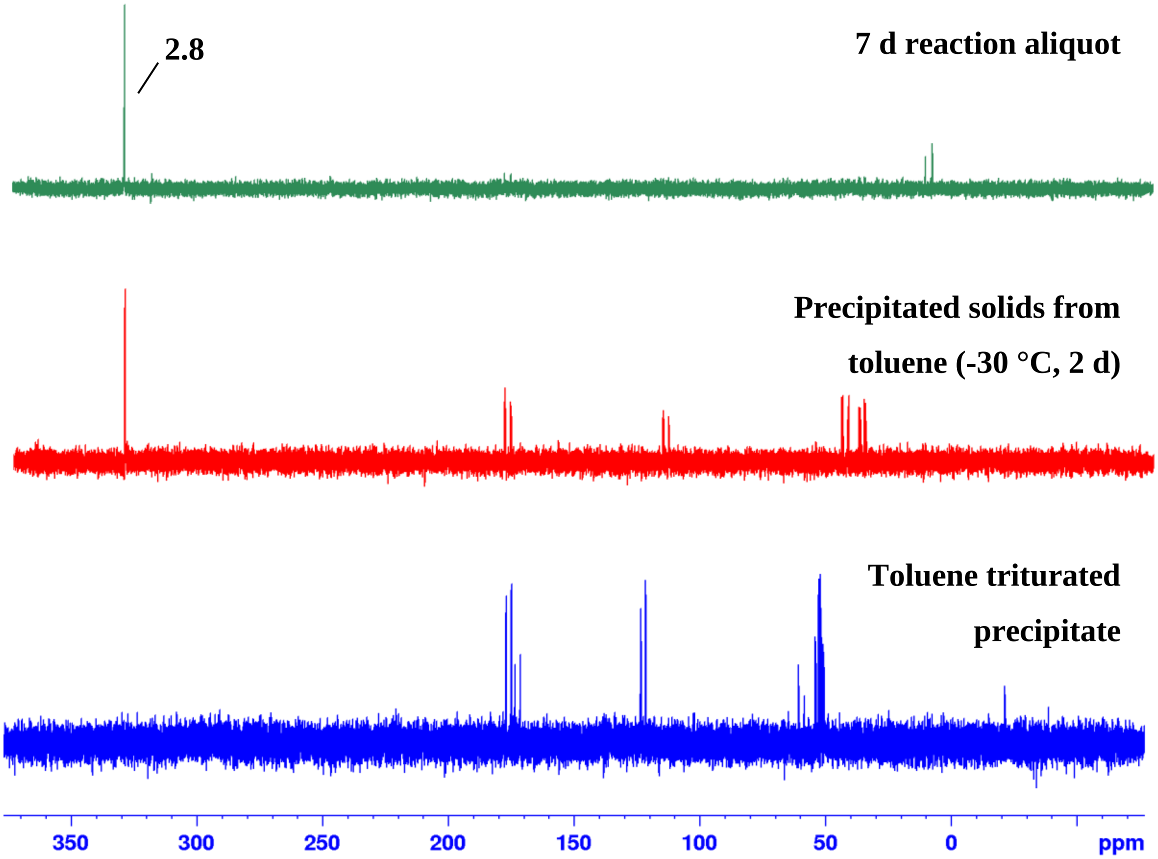

Figure 2-5. Stack plot of $^{31}P\{^1H\}$ NMR spectra during different stages of isolation of **2.8**. (Top) Seven-day reaction aliquot of Na_2S, **2.6**, and DMF at room temperature; (Middle) Precipitate collected after cooling the reaction mixture to -30 °C in freezer over two days (CD_3CN); (Green) toluene-rinsed precipitate.

Attempts to purify **2.8**, including recrystallization at -30 °C and trituration with toluene, were unsuccessful at providing a method for isolation of a single species. The unpurified material thus remained characterized and tentative assignments of species formed in the reaction were reliant on analysis of ^1H and $^{31}P\{^1H\}$ NMR spectroscopic techniques. Unfortunately the ^1H NMR spectra of **[2.7]Cl** and **2.8** were recorded in different solvents deuterated solvents ($CDCl_3$ and CD_3CN, respectfully), which limited a direct comparison. Based on the physical description and $^{31}P\{^1H\}$ resonance observed in $CDCl_3$, the current hypothesis suggests that **[2.7]Cl** was the major species detected. Phosphinidene sulfides and phosphinidene oxides have been previously shown to react with benzil ((PhCO)$_2$) to form four-coordinate phosphorus species,[1,6] but no reaction was observed between **2.8** and a four-fold excess of benzil in acetonitrile. A reaction of **2.8** with elemental sulfur resulted in the formation of a new a major signal at δ_P = 24.3 (**2.8S**, **Figure 2-6**), indicating a nucleophilic phosphorus centre, and was consistent with the published values for the formation of (IPrN)$_2$P(S)Cl (δ_P = 25.9, C_6D_6; **Figure 2-7**).[19]

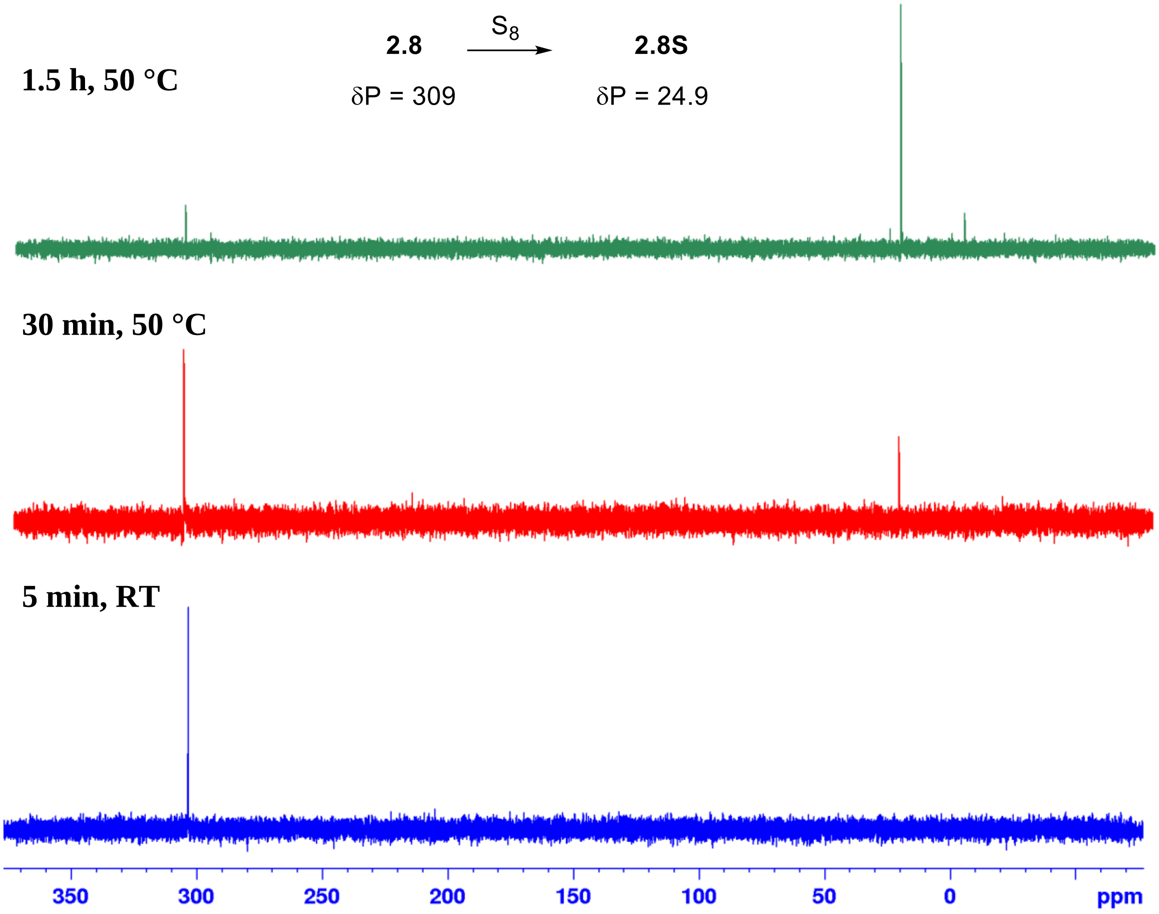

Figure 2-6. Reaction of **2.8** with sulfur in CD_3CN to generate the hypothetical species **2.8S**.

However unlikely, the identical $^{31}P\{^1H\}$ resonances of **[2.7]Cl** and **2.8** may be coincidental, and the formation of a monomeric RPS at δ_P = 309 cannot be explicitly ruled out with the current information (**Figure 2-7**, C). Sulfurization of a monomeric phosphinidene sulfide can also give rise to a dithioxophosphorane species[9] (RPS$_2$), which spontaneously dimerize to species $(RPS_2)_2$ with similarly up-field shifted resonances ($\delta_P \approx$ 30, **Figure 2-7**, B).[10,14]

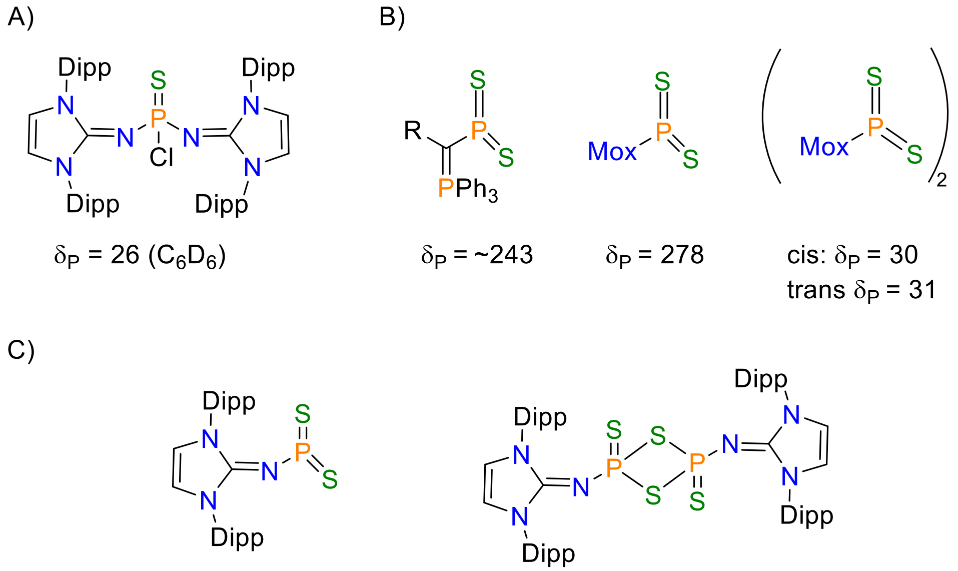
A)
Dipp
S
Dipp
N
P
N
N
N
N
Cl
N
Dipp
Dipp
δ_P = 26 (C_6D_6)
B)
S
R
P
S
PPh3
S
Mox
P
S
S
Mox
P
S
2
δ_P = ~243
δ_P = 278
cis: δ_P = 30
trans δ_P = 31
C)
Dipp
S
N
N
P
S
N
Dipp
Dipp
Dipp
N
N
S
S
P
N
P
N
S
S
N
N
Dipp
Dipp

Figure 2-7. Selected examples of phosphorus-sulfur compounds. A) Neutral species reported by Dielmann and coworkers. B) Monomeric and dimeric dithioxophosphorane examples. Mox = 2,4-di-t-butyl-6-methoxyphenyl. C) Monomeric and dimeric NHI-supported species potentially formed after reaction with Na_2S.

The origin of the observed redistribution of **2.6** in polar solvents can only be speculated, as there was not enough evidence to define which mechanism or reagents were involved in the transformation. One explanation may be that trace water allowed for cleavage of a P-N bond which subsequently reacted with another phosphorus center. An alternative theory is that the scrambling was facilitated by the coordination of a polar solvent, such as acetonitrile. Notably, the $^{31}P\{^1H\}$ NMR spectrum of **2.6** in $CDCl_3$ displayed the expected chemical shift of δ_P = 163, which shifted downfield to δ_P = 183 in CD_3CN. This downfield shift was suggestive of the electrophilic nature of **2.6** and the potential coordination of acetonitrile to the phosphorus center. The electrophilic character was probed by a preliminary reaction with PMe_3. This reaction resulted in the formation of a species with an AB spin system observable by $^{31}P\{^1H\}$ NMR spectrum (δ_P = 120.0 and 21.4, $^1J_{P\text{-}P}$ = 301 Hz, **Scheme 2-5** and **Figure 2-8**) in CH_2Cl_2. This species was tentatively assigned as $[IPrNPCl(PMe_3)]Cl$ (**[2.9]Cl**).

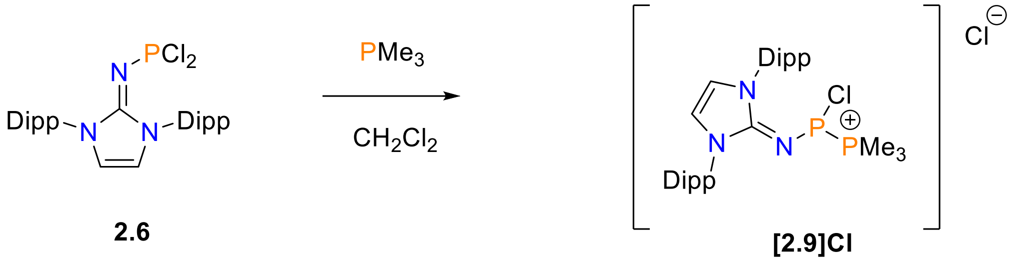

Scheme 2-5. Reaction of **2.6** with PMe_3 to generate a proposed species **[2.9]Cl**.

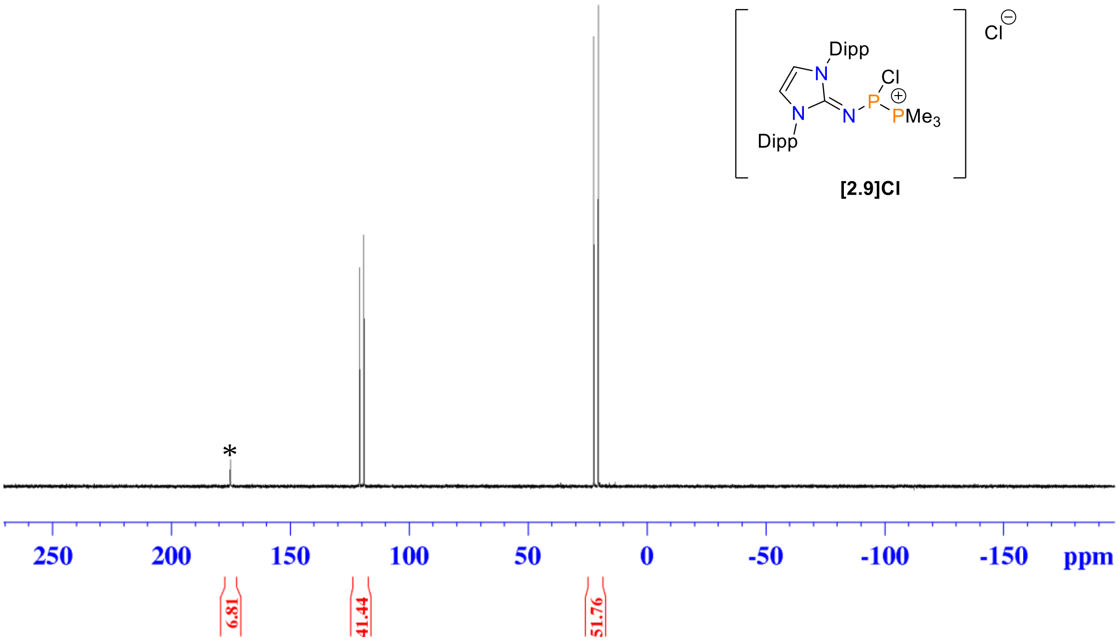

Figure 2-8. $^{31}P\{^{1}H\}$ NMR spectrum of a sample of the crude reaction mixture of $IPrNPCl_2$ and PMe_3 in CH_2Cl_2 after 15 min. Unknown species denoted (*).

A standing solution of **2.6** with Na_2S in acetonitrile/DMF produced few single crystals, and one was suitable for SC-XRD, and was identified as the mixed chalcogen compound $(IPrN)_2PS_3O$ (**2.10**;**Scheme 2-6**), rather than the expected phosphinidene-sulfide monomer or dimer. Solid-state data collected of $(IPrN)_2PS_3O$ provided some chemical insights for the reaction: 1) Na_2S is potentially a suitable source of sulfur for the formation of a P-S bond; 2) The sulfur-to-phosphorus ratio is greater than one in the solid-state, which suggested that over oxidation or disproportionation reactions may also occur in solution upon reaction with Na_2S; and, 3) the incorporation of oxygen in the solid state structure of the a mixed chalcogenide species **2.10** system, may have occurred from deoxygenation of DMF, reaction with trace water, or by contamination by air.

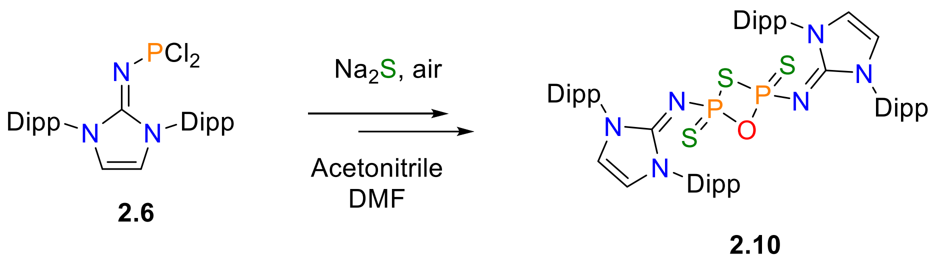

Scheme 2-6. A standing solution of **2.6** and Na_2S over two weeks produced crystal of **2.10**, studied by SC-XRD.

Initial attempts to perform a condensation reaction of $IPrNPCl_2$ (**2.6**) with $S(SiMe_3)_2$ at room temperature resulted in rapid generation of a yellow solution but contained an unassignable mixture of species observed by ${}^{31}P\{{}^{1}H\}$ analysis of a reaction mixture aliquot. An addition of $S(SiMe_3)_2$ to a solution of **2.6** at -78 °C produced numerous new signals detectable in a ${}^{31}P\{{}^{1}H\}$ NMR spectrum after 40 min, but reduced to two upon warming the entire reaction mixture to room temperature (**Figure 2-9**). After concentrating the mixture to dryness under vacuum, the residue possessed a major species with a chemical shift of $\delta_P = 7.5$ (${}^{1}J_{PH} = 688$ Hz) and a minor species at $\delta_P = -3$ (${}^{1}J_{PH} = 700$ Hz) in a 98:2 integration ratio.

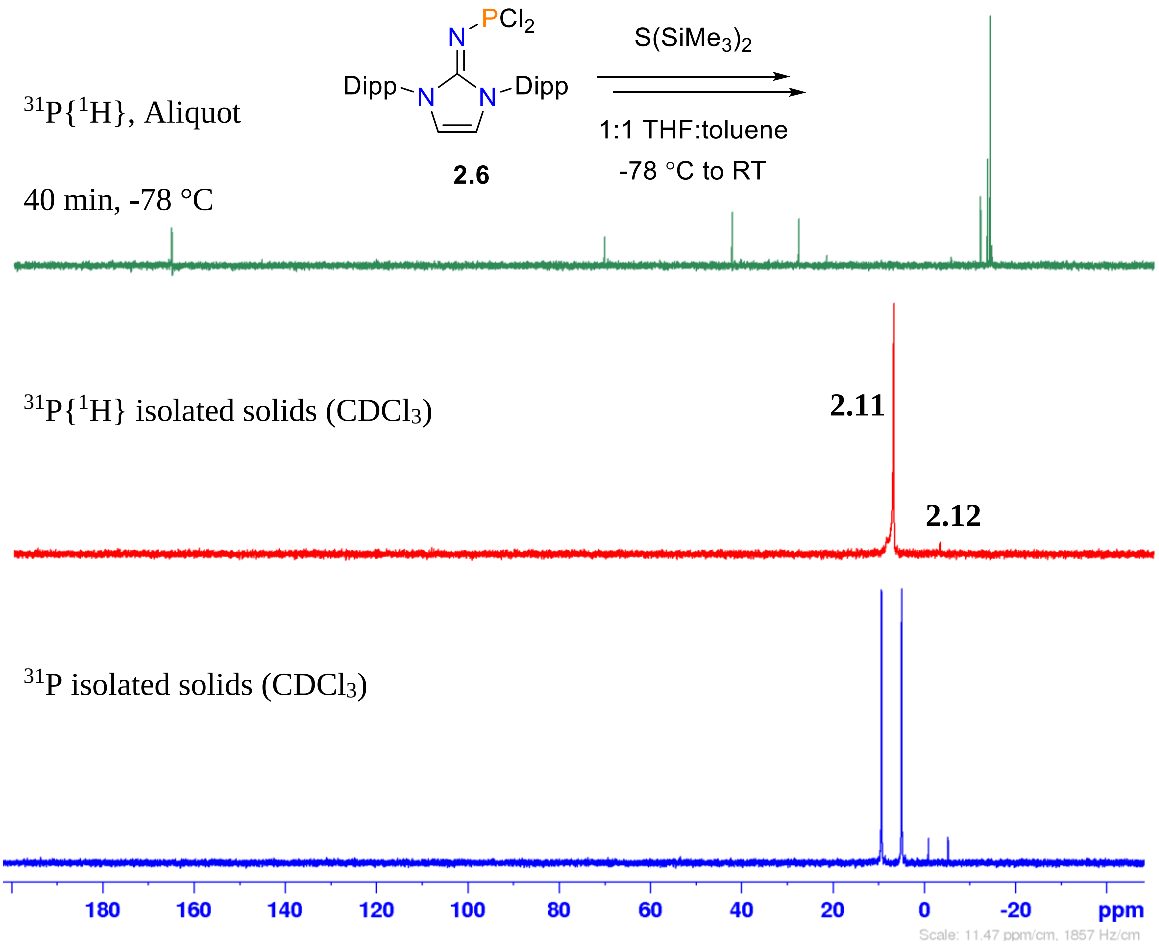

Figure 2-9. Stack plot of ^{31}P{^{1}H} and ^{31}P NMR spectra of products formed from the reaction of **2.6** and S(SiMe$_3$)$_2$. Reaction aliquot taken after 40 min (top, green); ^{31}P{^{1}H} (middle, red) and ^{31}P (bottom, blue) spectra of isolated material (**2.11** and **2.12**).

Multinuclear NMR spectroscopic analyses were conducted for the resulting mixture, with $^1J_{P\text{-}H}$ coupling confirmed in both the ^{31}P ($\delta_P = 7$, $^1J_{P\text{-}H} = 688$ Hz; **Figure 2-9**) and ^{1}H spectrum ($\delta = 6.37$, $^1J_{P\text{-}H} = 688$ Hz, **Appendix A-10**). The major species appeared as a doublet in the ^{31}P NMR spectrum indicating one P-H bond was present, while integration of the major resonances and P-H coupled proton in the ^{1}H NMR spectrum support a structure possessing one IPrN ligand and one P-H bond. A definitive structural characterization could not be determined due to the appearance of two unassigned additional broad resonances at approximately 11 ppm and at 7.4 ppm, which each integrate for approximately two protons. A ^{1}H - ^{1}H NOESY experiment (**Figure 2-10**) performed on this sample revealed cross peaks with phasing indicative of chemical exchange of these two resonances, which is characteristic of acidic hydrogens on heteroatoms (such as O and N). The same spectrum may also contains low intensity (and low resolution), alternately phased cross-peaks of the broad signals with the backbone, isopropyl, and methyl protons which suggested they could be associated with the same species in solution. These broad resonances were suggestive of the generation acidic protons *via* hydrolysis by infiltration of moist air. This theory of hydrolysis was additionally supported by the solid-state structure revealing an inclusion of oxygen atom.

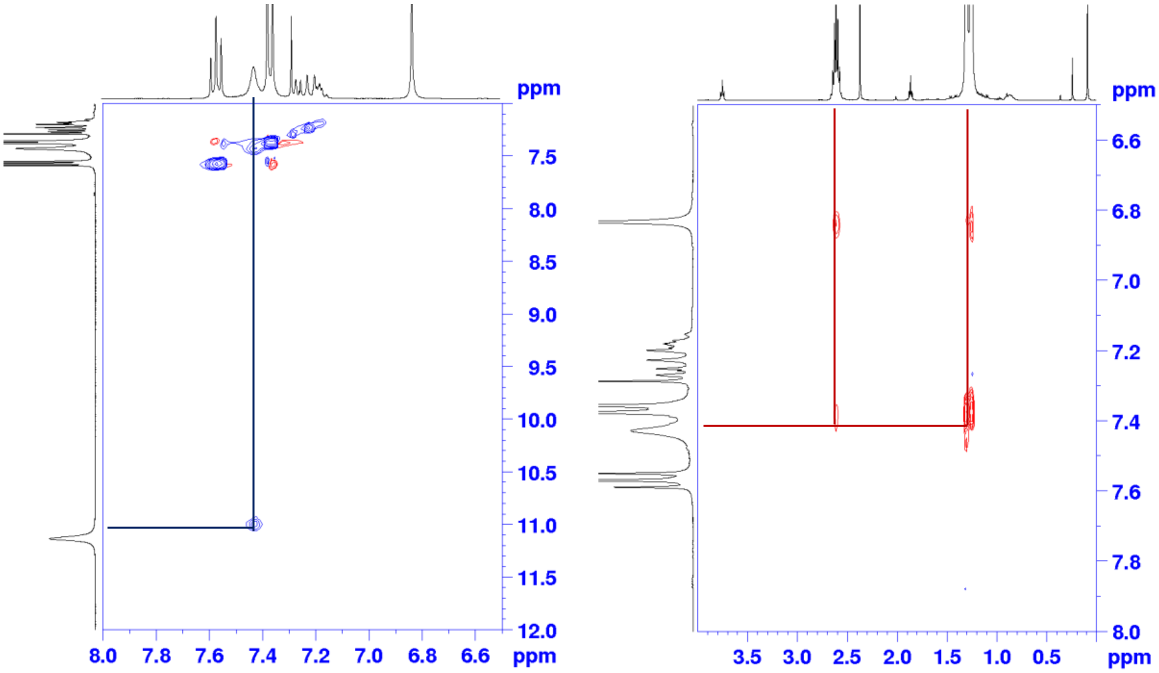

Figure 2-10. ^{1}H-^{1}H NOESY spectra of **2.11** and **2.12** after warming to room temperature (redissolved in CDCl$_3$). Cross peak in blue (positive phase) shows chemical exchange of broad resonances. Cross peaks in red (negative phase) show NOE signal enhancement.

The mixture of **2.11** and **2.12** was subjected to recrystallization at -30 °C over three months and yielded a limited number of single crystals suitable for X-ray diffraction. SC-XRD analysis revealed the selected crystal to be $(IPrN)_2P(O)H$ (**2.13**, **Scheme 2-7**), indicative of a byproduct of hydrolysis and redistribution. This unexpected outcome was further supported by the FT-IR spectrum, which exhibited a P-H bond stretching frequency at 2418 cm^{-1}.

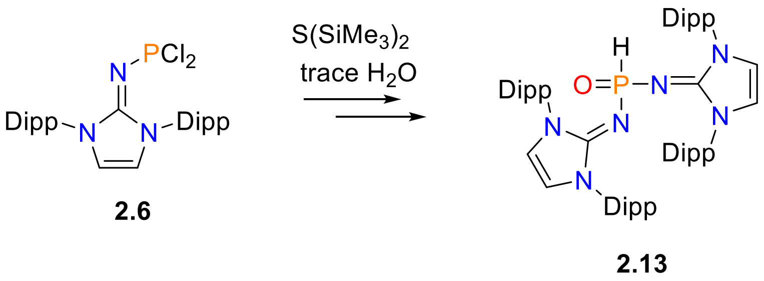

Scheme 2-7. Recrystallization after the reaction of **2.6** with $S(SiMe_3)_2$ yielded a limited number of crystals, from which the solid-state structure of $(IPrN)_2P(O)H$ (**2.13**) was successfully determined using single crystal X-ray diffraction (SC-XRD).

2.2.4 Transformation Pathways C to F

The next approach taken towards a synthesis of a phosphinidene sulfide (RPS) was to generate the bis(azido)phosphine sulfide $RP(S)(N_3)_2$ (**2.15**) then reduce the P(V) center to P(III) by liberation of three stoichiometric equivalents of N_2. Inspiration for the synthesis of $IPrNP(S)Cl_2$ (**2.14**) precursor was taken from the reported reaction of $POCl_3$ with **2.4** to generate the related $IPrNPOCl_2$ species.[18] The compound $IPrNP(S)Cl_2$ (**2.14**) was generated by replacement with $PSCl_3$ in the same manner. ^1H and $^{31}P\{^1H\}$ NMR spectra of the crude material obtained was in agreement with data reported by the Dielmann lab for this compound.[19]

Efforts to generate $IPrNPS(N_3)_2$ (**2.15**) by metathesis of $IPrNPSCl_2$ (**2.14**) with $SiMe_3N_3$ in heated pressure tubes in THF resulted in only ca. 4 % conversion after 72 h at 60 °C ($\delta_P = 39$, **Figure 2-11**). The synthetic approach was deemed not viable, so the salt metathesis reaction of **2.6** with an excess of NaN_3 to generate a P(III) bis(azido)phosphine (**2.16**), followed by sulfurization to generate the target IPrNPS(N_3)$_2$ was pursued (**2.15**; *vide infra*, see Chapter 3).

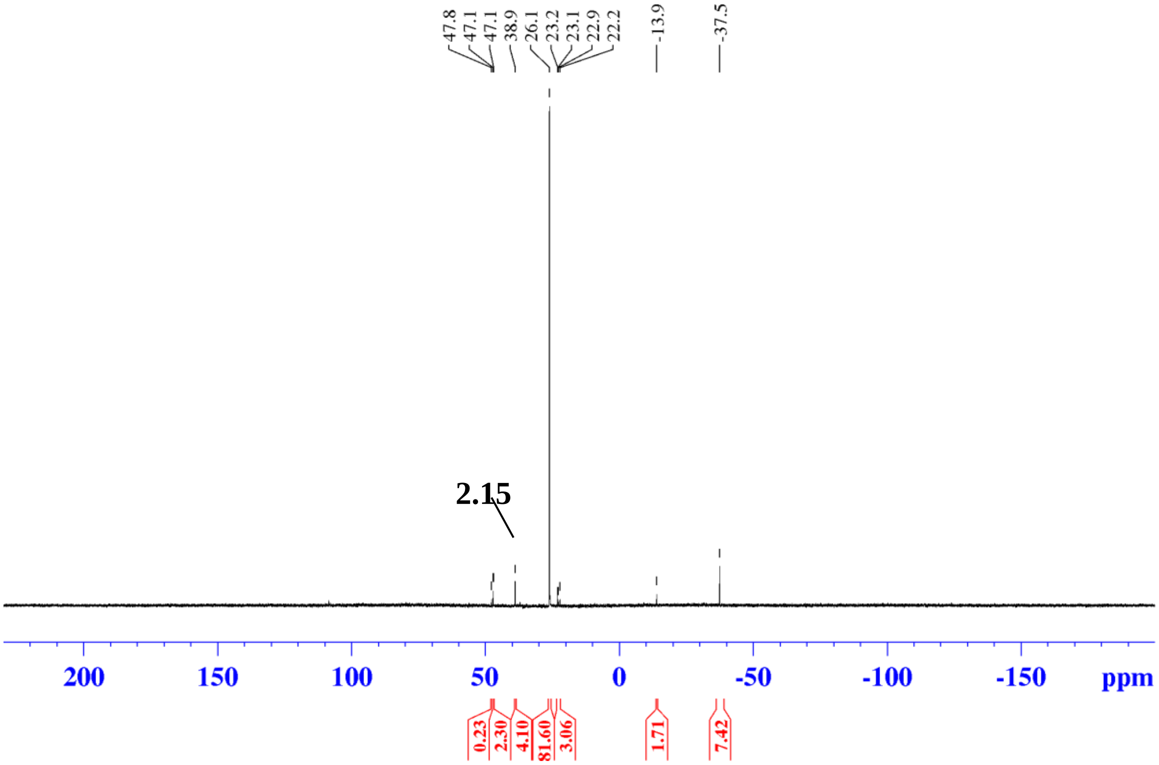

Figure 2-11. $^{31}P\{^1H\}$ NMR spectrum of a reaction aliquot of **2.14** and $SiMe_3N_3$ after 72 h at 60 °C. Approximately 4 % conversion to IPrNPS(N_3)$_2$ (**2.15**; δ_P = 38.9 ppm) was observed.

2.2.5 Transformation Pathway G

Thermal reduction of **2.15** was attempted at 115 °C over four days in a pressure tube, which resulted in the formation of a dark-colored solution that contained multiple species, as observed by $^{31}P\{^1H\}$ NMR spectroscopy. Analysis using TGA later demonstrated that IPrNPS(N_3)$_2$ had a $T_{95\%}$ = 185 °C, exemplifying high thermal stability (*vide infra*, see Chapter 3). This suggested that the reaction performed in a pressure tube may have been affected by air leakage as a cause of the multiple species formed.

Compound **2.15** was found to react under photolytic conditions at room temperature and at -50 °C with a (λ_{max} = 254 nm, broad spectrum) in toluene or C_6D_6, but afforded a dark-colored solution with no discernable phosphorus signals besides residual starting material (**Appendix A-25** and **Appendix A-26**). The numerous, broad NHI-backbone protons were also observable in the ^{1}H NMR spectrum (**Appendix A-24**). Previous work by Bertrand and Dielman demonstrated that two NHI ligands could stabilize a phosphinonitrene after photolysis of the mono(azido)phosphine species, and subsequently demonstrated the reactivity of the nitrene with other small molecules. An apparent lack of control during reduction experiments of **2.15** may be rationalized by poor electronic stabilization of a nitrene intermediate, as a hypothetical tetrahedral P(V) phosphinonitrene intermediate may not offer as much π-stabilization from phosphorus when compared to the Dielman system (**Figure 2-12**).

Stabilized Phosphinonitrene

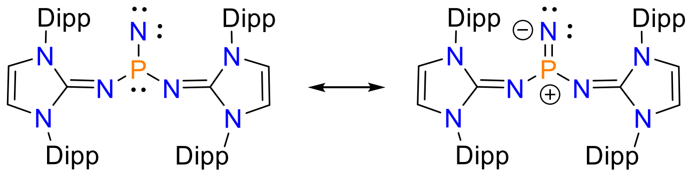

Hypothetical Unstabilized thiophosphinonitrene

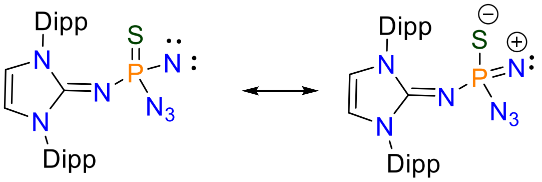

Figure 2-12. Comparison of phosphinonitrene stabilizations. Stabilized phosphinonitrene[17] by delocalization through central phosphorus lone pair (top) and hypothetical nitrene intermediate lacking π-donation from central phosphorus atom (bottom).

As a result of poor selectivity of the preliminary reduction methods attempted from the bis(aizdo)phosphine sulfide **2.15**, no further attempted reductions were performed. A possible improvement to stabilize any reactive species formed may be to use a bulkier N-aryl group which may offer more steric protection. Future work involving reactions of **2.6** with Na_2S should be accompanied by a stability test of the reagents in the selected solvent. Solvents bearing a carbonyl group (such as DMF), which have been shown to react with phosphorus-sulfur heterocycles[10] and act as a potential source of oxygen, should be avoided.

2.2.6 Structural Analysis of NHI-Supported Phosphine Compounds

Solid state structures of **[2.7]Cl**, **2.10**, and **2.13** were obtained from single-crystal X-ray diffraction experiments, and shown in **Figure 2-13**. **[2.7]Cl** crystallized in orthorhombic C222 space group with two half-molecules in the asymmetric unit, on different rotation axes. The phosphorus atom adopted a bent geometry, with an NPN angle of 105.5(3) °. The N-C-N-P dihedral angle of 82.8(7) ° underscored the phosphorus atom as being twisted out of the plane of the imidazolium core, while the nearly coplanar N-P-N-C dihedral angle is 175.7(6) °. The P-N bond length of 1.569(5) Å is contracted as compared to $IPrNPCl_2$ (P-N=1.602(2) Å), indicative of partial multiple bond character.

2.10 possessed two P=S bonds and bridging sulfur and oxygen atoms and crystallized in the Cc space group. A comparison of this structure to the previously reported 4-bis(2,4,6-tri-isopropylphenyl)-2,4-dithioxo-l,3,2,4-oxathiadiphosphetane revealed that both structures adopted a *trans* configuration. The exocyclic P=S bond length average (1.9232(15) Å was longer by ~0.4 Å in the NHI-species, which can be explained by a partial zwitterionic character with partial charge accumulation on the exocyclic sulfur and the π-donating NHI ring. P-S bond lengths of the bridging sulfur atom of 1.9252(15) Å and 1.9213(15) Å were not statistically significantly different from the reported aryl functionalized mix chalcogen species, while the P-O bond length average (1.639(2)) was slightly contracted by ~0.03 Å.

2.13 co-crystallized in monoclinic Cc space group with one molecule of CH_3CN. The central phosphorus atom adopted a tetrahedral geometry, with an NPN angle of

102.7(2) °, and NPO angles of 116.0(2) ° and 114.5(2) °. This contrasts with the $[IPrN_2PO]^+$ cation reported by Dielmann which was trigonal planar at phosphorus and had NPN angle of 108.92 ° and NPO angles of 125.99 ° and 125.09 ° ($\Sigma_{\angle NPN \text{ and } \angle NPO}$ = 360 °).[18] Further comparisons made with the cationic $[IPrN_2PO]^+$ reveal that the measured slightly elongated P-N_{avg} (0.024 Å) and P=O (0.040 Å) and C=N_{avg} bond contraction (0.044 Å) lengths are not statistically significant.

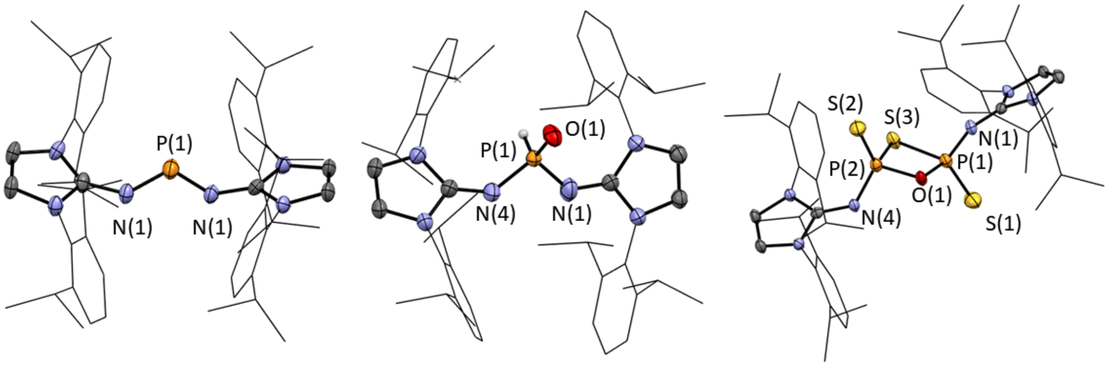

Figure 2-13. Solid-state structures of **[2.7]Cl** (chloride anion omitted), $IPrN_2P(O)H$ (**2.13**), and $(IPrNPS)_2SO$ (**2.10**). Hydrogens have been omitted and Dipp substituents have been represented as wireframes for clarity, and ellipsoids shown at the 50% probability level.

2.3 Conclusion

Multiple methods were used towards the attempted syntheses of a phosphinidene sulfide, which were ultimately unsuccessful. Ligand exchange reactions were likely encountered in polar solvents, as the physical appearance and $^{31}P\{^1H\}$ resonance was identical to phosphenium **[2.7]Cl** which was independently prepared and isolated. Solid-state structures of $[IPrNPS]_2SO$ and $IPrN_2POH$ were obtained and demonstrated oxygen incorporation. This was suggestive that contamination was either occurring via trace moisture present, or that side reactions were occurring upon prolonged reactions in the presence of DMF. The incorporation of sulfur observed in the solid-state structure of **2.10** indicates that sodium sulfide undergoes a reaction with **2.6** in solution in the presence of

DMF;[10] however, the formation of the numerous species demonstrates the inefficiency of this strategy to access a single species. $S(SiMe_3)_2$ was found to react very rapidly with **2.6**, which upon workup was found to produce at least two species which possess a P-H bond. Additional proton resonances present in the ^1H NMR spectrum which could not be explained, and oxygen incorporation in the solid-state structure obtained of **2.13** indicate that there was an unaccounted-for contaminant in the reaction and maybe an indication of a presence of moisture. Only partial characterization and identification of these species was achieved due to available resources and limited materials.

2.4 Experimental Section

All reactions were carried out under nitrogen atmosphere using standard Schlenk techniques with nitrogen sourced from medical grade nitrogen cylinders dried through a tube containing Drierite ($CaSO_4$), or the use of a nitrogen filled glovebox with a high-pressure liquid nitrogen dewar source of N_2 gas was used unless otherwise noted. All glassware was either flame dried or oven-dried at 170 °C for at least 60 min. Unless otherwise noted, all solvents were dried and stored over 4 Å molecular sieves, except for acetonitrile which was dried using 3 Å sieves. Unless otherwise specified, syntheses of **2.1**[20], **2.2**[20,22], **2.3**[20], and **2.4**[20], were performed following literature procedures. Detailed experimental procedures and characterization data of $IPrNP(N_3)_2$ (**2.16**) and $IPrNPS(N_3)_2$ (**2.15**) can be found in Chapter 3 (*vide infra*). All NMR spectra were obtained on either Bruker or INOVA 400 MHz or 600 MHz spectrometers. NMR data was processed in either Bruker TopSpin 4.0.7, or in MestReNova 1.13. ^1H and $^{13}C\{^1H\}$ spectra were referenced to the solvent signal (trace proteo-solvent in the case of ^1H spectra). $^{31}P\{^1H\}$ spectra were referenced to an 85 % H_3PO_4 external standard at 0.0 ppm. FT-IR spectra were collected with Bruker Alpha II spectrometer in transmission mode. Photolysis experiments were performed in a UV-box from Ace Glass Incorporated (Vineland, NJ, USA) equipped with a 400 W Mercury Bulb. FT-IR spectra were collected with a Bruker ALPHA II FTIR spectrometer in air, in either ATR-mode (attenuated total reflection) or in transmission mode as a KBr pellet, and the collection method was noted for each respective sample.

2.4.1 Modified Synthesis of IPrNPCl$_2$ (**2.6**)

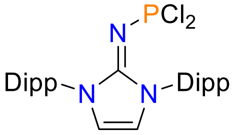

2.6

Following a procedure adapted from Roy *et al.*,[23] IPrNSiMe$_3$ (2.19 g, 4.59 mmol) was dissolved in toluene (30 mL), followed by the addition of PCl$_3$ (0.50 mL, 5.7 mmol). NEt$_3$ (0.2 mL, 1.4 mmol) was then added dropwise. The formation of a bright yellow solid forms initially but prolonged stirring results in gradual colour change to an off-white slurry. The mixture was stirred for 16 h at room temperature, then the volatiles were removed *in vacuo*. The residue was reconstituted in THF (15 mL), centrifuged, decanted, and then washed again with an additional portion of THF (5 mL). The decanted THF solutions were combined, the volatiles were removed resulting in the isolation of an off-white powder (1.89 g, 3.75 mmol, 79 % yield). The purity of the resulting off-white powder was determined by ^{1}H and ^{31}P{^{1}H} NMR spectroscopy to be suitable for further reactions in most syntheses. Recrystallization from concentrated THF solutions at -30 °C could be performed to increase purity if necessary.

^{1}H and ^{31}P{^{1}H} NMR spectra of this material matched with known literature data.[23]

2.4.2 Synthesis of **[2.7]Cl**

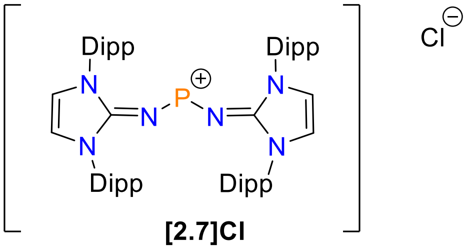

[2.7]Cl

In a one pot reaction, 4.96 g (12.8 mmol) of **2.3** was dissolved in toluene (55 mL) the set to reflux with SiMe$_3$N$_3$ (3 mL, 20 mmol) over 2 days under argon, then volatiles were removed under vacuum. The residue was resuspended in toluene (30 mL) and NEt$_3$ (200 µL, 1.4 mmol) was added to the flask. PCl$_3$ (1.2 mL, 13.7 mmol) was then rapidly added to the stirring flask. The formation of a bright yellow solid rapidly occurred, which was stirred overnight at room temperature. The mixture was stirred for 16 h at room temperature, then volatiles were removed in vacuo. Approximately 80 mg of the residue was portioned and used for further purification. The portion was slurried with THF (15 mL), centrifuged, decanted, then washed again with a further portion of THF (5 mL). The THF washings were combined, concentrated under vacuum to incipient crystallization, then placed in a -30 °C freezer overnight. Several crystals were portioned for SC-XRD analysis, and the remaining crystals were decanted and dried in vacuo. Subsequent recrystallization from the mother liquor resulted in isolation of an additional bright yellow crystals (Total isolated yield: 45 mg, 0.052 mmol).

^{1}H NMR (400 MHz, CDCl$_3$) δ = 7.43 (t, 4H, *p*-Ar, 7.6 Hz), 7.14 (d, 8H, *m*-Ar, 7.6 Hz), 6.97 (s, 4H, N(C*H*)$_2$N), 2.36 (sept, 8H, *i*-Pr, 6.8 Hz), 1.14 (d, 24H, CH$_3$, 6.8 Hz), 0.80 (d, 24H, CH$_3$, 6.8 Hz). **^{13}C{^{1}H} NMR (100.6 MHz, CDCl$_3$)** δ = 147.1 (d, 27 Hz, N*C*N), 146.2 (*o*-Ar), 131.1 (*p*-Ar), 129.7 (*ipso*-Ar), 124.4 (*m*-Ar), 118.8 (N*CC*N), 28.8 (*i*-Pr), 24.2 (CH$_3$), 23.1 (CH$_3$). **^{31}P{^{1}H} NMR (162 MHz, CDCl$_3$)** δ = 310.

2.4.3 Synthesis of **2.8**

A slurry of Na$_2$S (51.4 mg, 0.659 mmol, 1.15 eq) in acetonitrile (15 mL) was stirred while a suspension of **2.6** (290 mg, 0.576 mmol) was added in two portions of acetonitrile (3 mL) and two drops of DMF were added. Volatiles were removed after seven days *in vacuo*, and the solids were extracted with two portions of THF (10 mL). The solution was concentrated and placed in a -30 °C freezer. The precipitate from the freezer was dried under vacuum. Isolated 120 mg of bright yellow powder, approximately 80% purity by ^{31}P{^{1}H} NMR in CD$_3$CN.

Major component **2.8**: **^{1}H NMR (400 MHz, CD$_3$CN)** δ = 7.47 (t, 4H overlapped with impurities, *p*-Ar, 7.8 Hz), 7.18 (d, 8H, *m*-Ar, 7.8 Hz), 7.08 (s, 4H, N(C*H*)$_2$N), 2.35 (multiplet, 8H overlapped with impurities, *i*-Pr), 1.09 (d, 24H, CH$_3$, 7.1 Hz), 0.81 (d, 24H, CH$_3$, 7.1 Hz). **^{13}C{^{1}H} NMR (100.6 MHz, CD$_3$CN)** δ = Note: signal-to-noise ratio for NCN carbon too low. 147.2 (*o*-Ar), 132.0 (*p*-Ar), 130.8 (*ipso*), 125.3 (*m*-Ar), 118.3 (NCCN), 29.7 (*i*-Pr), 24.3 (CH$_3$), 23.5 (CH$_3$). **^{31}P{^{1}H} NMR (162 MHz, CD$_3$CN)** δ = 308.4.

2.4.4 *In situ* generation of **[2.9]Cl**

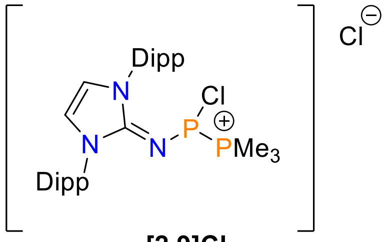

[2.9]Cl

To an NMR tube containing IPrNPCl$_2$ (20 mg, 0.04 mmol) in CH$_2$Cl$_2$ (0.5 mL), neat PMe$_3$ (4 µL, 0.04 mmol) was added in one portion. $^{31}P\{^{1}H\}$ NMR spectrum was obtained after 15 min at room temperature, which revealed complete consumption of PMe_3. Normalization of resonances at 175 ppm and 120 ppm to 100 demonstrated a conversion of approximately 85% to **[2.9]Cl** within 15 mins.

$^{31}P\{^{1}H\}$ NMR (162 MHz, CD_3CN) δ = 120 (d, $^{1}J_{P\text{-}P}$ = 301 Hz, N-*P*(Cl)-P), 21 (d, 301 Hz, N-P-*P*$(CH_3)_3$).

2.4.5 IPrNPCl$_2$ and S(SiMe$_3$)$_2$ Reaction Mixture Analysis

Prepared a solution of $IPrNPCl_2$ in a 1:1 mixture of THF and toluene (2 mL) in one Schlenk tube and prepared a solution of $S(SiMe_3)_2$ in THF 2.5 mL). Both flasks were then then transferred to a Schlenk line and cooled to -78 °C. The solution containing $S(SiMe_3)_2$ was added dropwise over 25 min then stirred at -78 °C for 1 h before warming to room temperature overnight. Volatiles were then removed under reduced pressure and a white residue was collected. A small portion was used for NMR analysis and the remaining portion was set up for recrystallization. The sample was redissolved in THF, concentrated then placed in the freezer. Minimal recrystallization occurred and the few crystals were not weighed (estimated mass less than 5 mg) and were used for SC-XRD analysis.

Major species: **^{1}H NMR (400 MHz, $CDCl_3$)** δ = 11.13 (broad singlet, 2H, **unassigned**), 7.57 (t, 8.4 Hz, *p*-Ar), 7.43 (broad singlet, 2H, **unassigned**), 7.37 (d, 4H, *m*-Ar, 8.4 Hz), 6.83 (s, 2H, $N(CH)_2N$), 6.37 (d, 1H, P-H, 688.9 Hz), 2.61 (septet, 4H, *i*-Pr, 6.8 Hz), 1.30 (d, 12H, CH_3, 6.8 Hz), 1.25 (d, 12H, CH_3, 6.8 Hz). **$^{13}C\{^{1}H\}$ NMR (100.6 MHz, $CDCl_3$)** δ = 147.2 (NCN), 146.4 (*o*-Ar), 132.3 (*p*-Ar), 127.62 (ipso), 125.4 (*m*-Ar), 117.7 (NCCN), 29.2 (*i*-Pr), 24.3 (CH_3), 23.4 (CH_3). **$^{31}P\{^{1}H\}$ NMR (162 MHz, $CDCl_3$)** δ = 7.1 ppm (s). **^{31}P NMR (162 MHz, $CDCl_3$)** δ = 7.1 (d, 689 Hz).

2.4.6 Synthesis of IPrNPSCl$_2$ (**2.14**)

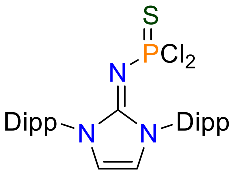

2.14

The following procedure was adapted from a report from the Dielmann group in 2018 for the synthesis of $IPrNP(O)Cl_2$,[18] but a similar synthesis of IPrNP(S)Cl_2 was subsequently reported by the Dielmann group in 2021.[19]

Prepared solutions of IPrNTMS/IPrNH (500 mg, approximately 0.78 mmol : 0.32 mmol) mixture with NEt_3 (45 µL, 0.32 mmol) in 20 mL toluene, and $PSCl_3$ (0.33 mL, 3.3 mmol) in 5 mL toluene. The solutions were cooled to -78 °C then $PSCl_3$ solution was added dropwise over 15 min. The stirred mixture was allowed to warm to room temperature overnight. The solution was transferred to a receiving flask *via* filter cannula then volatiles were removed under reduced pressure. 0.433 g of off-white solids were collected then were extracted with benzene (7 mL). 0.343 g (ca. 0.64 mmol, 58 % yield) of a grey powder was collected, but still contained trace impurities by inspection of ^1H NMR spectrum. The ^1H and $^{31}P\{^1H\}$ NMR resonances in C_6D_6 were in agreement with the reported values of IPrNP(S)Cl_2,[19] and this material was subsequently used for test reactions with $SiMe_3N_3$.

2.4.7 Attempted Synthesis of IPrNPS(N_3)$_2$ (**2.15**) *Via* Condensation of **2.14** With $SiMe_3N_3$

A pressure tube containing a solution of IPrNP(S)Cl_2 (50 mg, 0.1 mmol) and $SiMe_3N_3$ (130 uL, 1.0 mmol) in THF (1 mL) was heated at 60°C for 3 days. Small aliquots were taken periodically to monitor the reaction by $^{31}P\{^1H\}$ NMR spectroscopy.

2.4.8 Attempted Thermolysis of IPrNPS(N_3)$_2$ (**2.15**)

IPrNP(S)(N_3)$_2$ (11 mg, 0.02 mmol) was dissolved in toluene (1 mL) and transferred to a pressure tube. The pressure tube was heated at 110 °C for 20 h, then volatiles were removed under reduced pressure. The residue was redissolved in C_6D_6 and analyzed by ^1H and $^{31}P\{^1H\}$ NMR spectroscopy.

2.4.9 Photolysis of IPrNPS(N_3)$_2$ (**2.15**)

Procedure one: IPrNP(S)(N_3)$_2$ (11 mg, 0.02 mmol) was dissolved in C_6D_6 (0.5 mL) and transferred to a quartz NMR tube, and wrapped with electrical tape and a strip of aluminum foil around the cap. The tube was then placed in a UV-light box and irradiated for 1 h.

Procedure 2: 10 mg IPrNPS$(N_3)_2$ was dissolved in 1 mL toluene-H_8 and transferred to a J-Young tube and foil was placed around the cap. The sample was then cooled to -50 °C and photolyzed (λ_{max} = 254 nm) for 19 h as the solution turned dark brown. A comparison of the relative intensities of $^{31}P\{^1H\}$ spectra before and after photolysis with the same number of scans suggested consumption of starting material, occurred but no discernable major species was detected between +650 - -150 ppm.

2.5 X-ray Crystallographic Details

A summary of X-ray diffraction collection and refinement data can be found in **Table 2-1**. Unless otherwise specified each sample was mounted on a Mitegen polyimide micromount with a small amount of Paratone N oil. X-ray measurements were made on a Bruker Kappa Axis Apex2 diffractometer at a temperature of -163 °C. The data collection strategy ω and φ scans, and data was collected up to 2θ values found in **Table 2-1**. The frame integrations were performed using SAINT.[24] The resulting raw data was scaled and absorption corrected using a multi-scan averaging of symmetry equivalent data using SADABS.[24,25] Unless otherwise stated, the structures were solved by using a dual space methodology using the SHELXT program.[26] All non-hydrogen atoms were obtained from the initial solution. The hydrogen atoms were introduced at idealized positions and were allowed to ride on the parent atom. The structural models were fit to the data using full matrix least-squares based on F^2. The calculated structure factors included corrections for anomalous dispersion from the usual tabulation. The structures were refined using the SHELXL program from the SHELX suite of crystallographic software.[26] Graphic plots were produced using the Mercury program.[27]

Structure Solution and Refinement: Unless otherwise stated, the structures were solved by using a dual space methodology using the SHELXT program.[26] All non-hydrogen atoms were obtained from the initial solution. The hydrogen atoms were introduced at idealized positions and were allowed to ride on the parent atom. The structural models were fit to the data using full matrix least-squares based on F^2. The calculated structure factors included corrections for anomalous dispersion from the usual tabulation. The structures were refined using the SHELXL program from the SHELX suite of crystallographic software.[26] Graphic plots were produced using the Mercury program.[27]

To test whether the X-ray diffraction measured bond lengths of two sets of bonds were statistically different, a z-test for comparing two means was performed using the formula $z = \frac{mean_1 - mean_2}{\sqrt{\sigma_1^2 + \sigma_2^2}}$. The z-score was compared to a z-table to find the corresponding p-value, which allowed for the determination of the statistical significance of the difference between the bond lengths. Depending on the p-value, no significant difference ($p > 0.05$), possible difference ($0.01 < p < 0.05$), or significant difference ($p < 0.01$) was assigned.[28]

Table 2-1. Summary of X-ray diffraction collection and refinement details for compounds **[2.7]Cl**, **2.10**, and **2.13**.

Formula	$C_{54}H_{72}ClN_6P$ **[2.7]Cl**	$C_{58}H_{78}N_8OP_2S_3$ **(2.10)**	$C_{56}H_{76}N_7OP$ **(2.13)**
Formula Weight (g/mol)	871.59	1061.40	894.20
Crystal Color and Habit	yellow prism	colourless needle	colourless prism
Crystal System	orthorhombic	tetragonal	monoclinic
Space Group	C 2 2 2	I 41/a	C c
Temperature, K	110	110	110
a, Å	26.214(8)	44.62(2)	17.617(6)
b, Å	26.654(8)	44.620	19.004(7)
c, Å	16.875(5)	12.023(5)	16.068(4)
a,°	90	90	90
b,°	90	90	98.98(2)
g,°	90	90	90
V, Å^3	11790(6)	23937(24)	5313(3)
Z	8	16	4
F(000)	3760	9088	1936
ρ (g/cm)	0.982	1.178	1.118
λ, Å, (MoKα)	0.71073	0.71073	0.71073
μ, (cm^{-1})	0.127	0.222	0.096
Max 2θ for data collection, °	40.21	41.224	47.15
Measured fraction of data	0.995	0.998	0.995
R_{merge}	0.1286	0.1114	0.0593
R_1	0.0409	0.0377	0.0435
wR_2	0.1108	0.0857	0.1117
R_1 (all data)	0.0447	0.0547	0.0468
wR_2 (all data)	0.113	0.0961	0.1143
GOF	1.077	1.028	1.040

$R_1 = \Sigma \mid |F_o| - |F_c| \mid / \Sigma F_o$; $wR_2 = [\Sigma(w(F_o^2 - F_c^2)^2) / \Sigma w(F_o^4)]^{½}$; $GOF = [\Sigma(w(F_o^2 - F_c^2)^2) / (\text{No. of reflns.} - \text{No. of params.})]^{½}$

2.6 References

(1) Yoshifuji, M.; Nakayama, S.; Okazaki, R.; Inamoto, N. Phosphinidenes and Related Intermediates. Part I. Reactions of Phosphinoylidenes (R–P=O) and Phosphinothioylidenes (R–P=S) with Diethyl Disulphideand Benzil. *J. Chem. Soc. Perkin Trans. 1* **1973**, No. 0, 2065–2068. https://doi.org/10.1039/P19730002065.

(2) Yoshifuji, M.; Sangu, S.; Hirano, M.; Toyota, K. A Stabilized Phosphinothioylidene Generated by Deselenation of a Selenoxothioxophosphorane. *Chem. Lett.* **1993**, *22* (10), 1715–1718. https://doi.org/10.1246/cl.1993.1715.

(3) Tomioka, H.; Miura, S.; Izawa, Y. Synthesis and Photochemical Reaction of Diels-Alder Adduct of Phosphole Oxide and Cyclopentadiene. *Tetrahedron Lett.* **1983**, *24* (32), 3353–3356. https://doi.org/10.1016/S0040-4039(00)86268-1.

(4) Holand, S.; Mathey, F. New Method for Building Carbon-Phosphorus Heterocycles. *J. Org. Chem.* **1981**, *46* (22), 4386–4389. https://doi.org/10.1021/jo00335a013.

(5) Mardyukov, A.; Keul, F.; Schreiner, P. R. Isolation and Characterization of the Free Phenylphosphinidene Chalcogenides $C_6H_5P{=}O$ and $C_6H_5P{=}S$, the Phosphorous Analogues of Nitrosobenzene and Thionitrosobenzene. *Angew. Chem. Int. Ed.* **2020**, *59* (30), 12445–12449. https://doi.org/10.1002/anie.202004172.

(6) Gaspar, P. P.; Qian, H.; Beatty, A. M.; André D’Avignon, D.; Kao, J. L. F.; Watt, J. C.; Rath, N. P. 2,6-Dimethoxyphenylphosphirane Oxide and Sulfide and Their Thermolysis to Phosphinidene Chalcogenides - Kinetic and Mechanistic Studies. *Tetrahedron* **2000**, *56* (1), 105–119. https://doi.org/10.1016/S0040-4020(99)00779-6.

(7) Graham, C. M. E.; Pritchard, T. E.; Boyle, P. D.; Valjus, J.; Tuononen, H. M.;

Ragogna, P. J. Trapping Rare and Elusive Phosphinidene Chalcogenides. *Angew. Chem. Int. Ed.* **2017**, *56* (22), 6236–6240. https://doi.org/10.1002/anie.201611196.

(8) Transue, W. J.; Nava, M.; Terban, M. W.; Yang, J.; Greenberg, M. W.; Wu, G.; Foreman, E. S.; Mustoe, C. L.; Kennepohl, P.; Owen, J. S.; Billinge, S. J. L.; Kulik, H. J.; Cummins, C. C. Anthracene as a Launchpad for a Phosphinidene Sulfide and for Generation of a Phosphorus-Sulfur Material Having the Composition P_2S, a Vulcanized Red Phosphorus That Is Yellow. *J. Am. Chem. Soc.* **2019**, *141* (1), 431–440. https://doi.org/10.1021/jacs.8b10775.

(9) Jochem, G.; Nöth, H.; Schmidpeter, A. Ylide-Substituted Thioxophosphanes and Dithioxophosphoranes. *Angew. Chem. Int. Ed.* **1993**, *32* (7), 1089–1091. https://doi.org/10.1002/anie.199310891.

(10) Yde, B.; Yousif, N. M.; Pedersen, U.; Thomsen, I.; Lawesson, S.-O. Studies on Organophosphorus Compounds XLVII Preparation of Thiated Synthons of Amides, Lactams and Imides by Use of Some New p,s-Containing Reagents. *Tetrahedron* **1984**, *40* (11), 2047–2052. https://doi.org/10.1016/S0040-4020(01)88445-3.

(11) Graham, C. M. E.; Macdonald, C. L. B.; Boyle, P. D.; Wisner, J. A.; Ragogna, P. J. Addressing the Nature of Phosphinidene Sulfides via the Synthesis of P−S Heterocycles. *Chem. Eur. J.* **2018**, *24* (3), 743–749. https://doi.org/10.1002/chem.201705198.

(12) Beckmann, H.; Ohms, G.; Großmann, G.; Krüger, K.; Klostermann, K.; Kaiser, V. Synthesis, Crystal Structure, and NMR Spectroscopy of a 1,3,2λ^5,4λ^5-Oxathiadiphosphetane. *Heteroat. Chem.* **1996**, *7* (2), 111–118. https://doi.org/10.1002/(SICI)1098-1071(199603)7:2<111::AID-HC2>3.0.CO;2-G.

(13) Yoshifuji, M.; An, D.-L.; Toyota, K.; Yasunami, M. Preparations and Sulfurization Reactions of (2,4-Di-t-Butyl-6-Methoxyphenyl)Phosphine and 1-(2,4-Di-t-Butyl-6-Methoxyphenyl)-2-(2,4,6-Tri-t-Butylphenyl)Diphosphene. *Chem. Lett.* **1993**, *22*

(12), 2069–2072. https://doi.org/10.1246/cl.1993.2069.

(14) Przychodzeń, W. Mechanism of the Reaction of Lawesson's Reagent with N-Alkylhydroxamic Acids. *Eur. J. Org. Chem.* **2005**, *2005* (10), 2002–2014. https://doi.org/10.1002/ejoc.200400727.

(15) Ochiai, T.; Franz, D.; Inoue, S. Applications of N-Heterocyclic Imines in Main Group Chemistry. *Chem. Soc. Rev.* **2016**, *45* (22), 6327–6344. https://doi.org/10.1039/C6CS00163G.

(16) Böhme, M. D.; Eder, T.; Röthel, M. B.; Dutschke, P. D.; Wilm, L. F. B.; Hahn, F. E.; Dielmann, F. Synthesis of N-Heterocyclic Carbenes and Their Complexes by Chloronium Ion Abstraction from 2-Chloroazolium Salts Using Electron-Rich Phosphines. *Angew. Chem. Int. Ed.* **2022**, *61* (28), e202202190. https://doi.org/10.1002/anie.202202190.

(17) Dielmann, F.; Back, O.; Henry-Ellinger, M.; Jerabek, P.; Frenking, G.; Bertrand, G. A Crystalline Singlet Phosphinonitrene: A Nitrogen Atom-Transfer Agent. *Science* **2012**, *337* (6101), 1526–1528. https://doi.org/10.1126/science.1226022.

(18) Wünsche, M. A.; Witteler, T.; Dielmann, F. Lewis Base Free Oxophosphonium Ions: Tunable, Trigonal-Planar Lewis Acids. *Angew. Chem. Int. Ed.* **2018**, *57* (24), 7234–7239. https://doi.org/10.1002/anie.201802900.

(19) Löwe, P.; Witteler, T.; Dielmann, F. Lewis Base-Free Thiophosphonium Ion: A Cationic Sulfur Atom Transfer Reagent. *Chem. Commun.* **2021**, *57* (41), 5043–5046. https://doi.org/10.1039/D1CC01273H.

(20) Jafarpour, L.; Stevens, E. D.; Nolan, S. P. A Sterically Demanding Nucleophilic Carbene: 1,3-Bis(2,6-Diisopropylphenyl)Imidazol-2-Ylidene). Thermochemistry and Catalytic Application in Olefin Metathesis. *J. Organomet. Chem.* **2000**, *606* (1), 49–54. https://doi.org/10.1016/S0022-328X(00)00260-6.

(21) Tamm, M.; Randoll, S.; Herdtweck, E.; Kleigrewe, N.; Kehr, G.; Erker, G.; Rieger, B. Imidazolin-2-Iminato Titanium Complexes: Synthesis, Structure and

Use in Ethylene Polymerization Catalysis. *Dalton Trans.* **2006**, No. 3, 459–467. https://doi.org/10.1039/B511752F.

(22) Hintermann, L. Expedient Syntheses of the N-Heterocyclic Carbene Precursor Imidazolium Salts IPr·HCl, IMes·HCl and IXy·HCl. *Beilstein J. Org. Chem.* **2007**, *3*, 22. https://doi.org/10.1186/1860-5397-3-22.

(23) Roy, M. M. D.; Miao, L.; Ferguson, M. J.; McDonald, R.; Rivard, E. An Unexpected Staudinger Reaction at an N-Heterocyclic Carbene-Carbon Center. *Can. J. Chem.* **2018**, *96* (6), 543–548. https://doi.org/10.1139/cjc-2017-0607.

(24) Bruker-AXS, SAINT Version 2013.8, 2013, Bruker-AXS, Madison, WI 53711, USA.

(25) Bruker-AXS, SADABS Version 2012.1, 2012, Bruker-AXS, Madison, WI 53711, USA.

(26) Sheldrick, G. M. SHELXT - Integrated Space-Group and Crystal-Structure Determination. *Acta Cryst. A* **2015**, *71* (1). https://doi.org/10.1107/S2053273314026370.

(27) Macrae, C. F.; Bruno, I. J.; Chisholm, J. A.; Edgington, P. R.; McCabe, P.; Pidcock, E.; Rodriguez-Monge, L.; Taylor, R.; Van De Streek, J.; Wood, P. A. Mercury CSD 2.0 - New Features for the Visualization and Investigation of Crystal Structures. *J. Appl. Cryst*. 2008. https://doi.org/10.1107/S0021889807067908.

(28). Kooijman H. *Interpretation of crystal structure determinations*. Utrecht University. 2005.

Chapter 3

3 Chemoselective Staudinger Reactivity of Bis(azido)phosphines Supported With A π-Donating Imidazolin-2-Iminato Ligand

3.1 Introduction

Phosphinimines ($R_3P=N-R'$) have been exploited both as ligands for stabilizing main group compounds, and for their utility as intermediates in organic syntheses.[1,2] Hydrolysis of the P=N bond offers a mild method of reducing azides to primary amines, while a reaction of a phosphinimine with a carbonyl compound can provide access to C=N bond formation *via* an aza-Wittig reaction (**Scheme 3-1**).[3] The electronic structure and multiple bond character resulting from negative hyperconjugation of a phosphinimine P-N bond is comparable to a P-C bond in a phosphonium ylide, while the nitrogen atom of phosphinimines also bears a similar basicity with the class of strongly π-donating N-heterocyclic imines (NHI).[1,4–6]

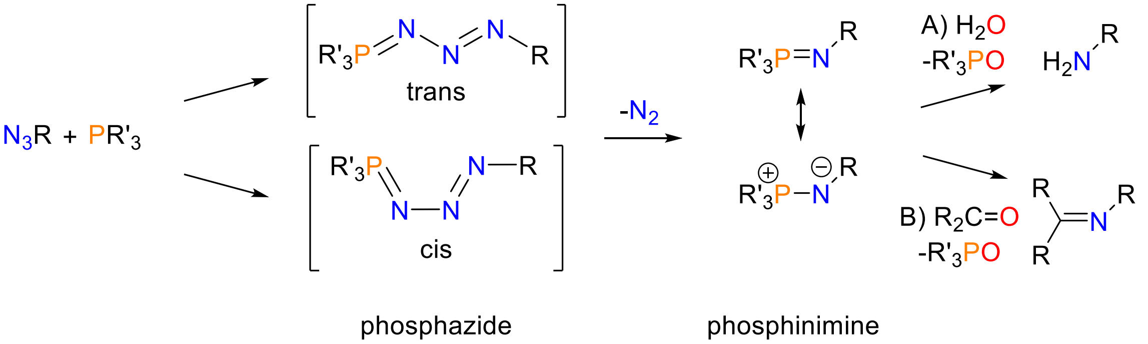

Scheme 3-1. General scheme for a Staudinger reaction to produce a phosphinimine with hydrolysis to an amine (A) and the aza-Wittig reaction (B).

Arguably the most versatile reaction for the synthesis of phosphinimines is the Staudinger reaction of organic azides with tertiary phosphines.[7,8] Computational and experimental evidence suggests the Staudinger reaction often proceeds *via* ring-closure of a cis-phosphazide ($R_3P^+-N=N-N^--R'$) intermediate to a 4-membered transition state, followed by liberation of N_2 as the key enthalpic and entropic driving force for the reaction.[7,9–15] An alternative one-step pathway has also been suggested in some instances involving electron deficient phosphines.[9] The use of an electron deficient azide, more nucleophilic phosphine, or more polar solvents have all been demonstrated to increase the reaction rate, while electron donating groups on the azide hinder the reaction.[10] Staudinger reactions of P(III) (azido)phosphines (R_2P-N_3) have also been reported, but their ambiphilic nature can result in spontaneous decomposition to oligomeric phosphazenes $(RP{=}N)_n$, and the reactivity can be attenuated by steric protection or by electron delocalization.[16] The ambiphilic nature of azidophosphines is also demonstrated by their ability to form a R_2P-$N{=}PR_3$ motif, or their reaction with an electrophilic azide to produce $R_2P(NPh)(N_3)$.[8,16,17] Bis(azido)phosphines are scarcely reported due to poor thermal stability, but have been isolated either using N-aryl[18] or cationic imidazolium ligands.[19] Phosphorus(V) bis(azido)phosphines are intriguing because the conversion of the first azide to a strongly π-donating phosphinimine has been reported to influence the ability of the remaining azide to perform a subsequent Staudinger reaction. For example (**Scheme 3-2**), $Et_2N(N_3)_2P{=}NPh$ may perform two subsequent unimpeded Staudinger reactions with PPh_3 to produce $Et_2N(N{=}PPh_3)_2P{=}NPh$,[20] whereas $SP(N_3)_2(NPPh_3)$ will react with only one more equivalent of PPh_3 to produce $SP(N{=}Ph_3)_2(N_3)$,[21] which bears an azide resilient to subsequent Staudinger reactivity.

Azidophosphines have functioned as precursors to interesting phosphorus species (**Scheme 3-3**), including an NHI-supported phosphine[22], a bis(NHI)-supported phosphinonitrene ($R_2P{\equiv}N$),[23–25] phosphinidene (R-P),[26] phosphinidene chalcogenide ($RP{=}Ch$),[27] phosphorus mono-nitride ($P{\equiv}N$),[28–30] and a phosphorus-substituted triazole *via* a click-reaction.[29]

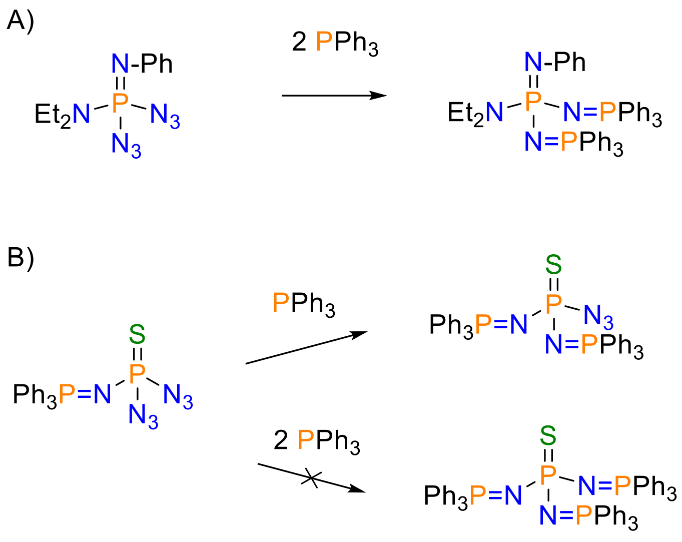
A)
2 PPh3
B)
PPh3
2 PPh3

Scheme 3-2. Comparative Staudinger reactivities of P(V) bis(azido)phosphines.[20,21] Bis(azido)phosphine in A) can react with two equivalents of PPh_3. Bis(azido)phosphine in B) can react with only one equivalent PPh_3.

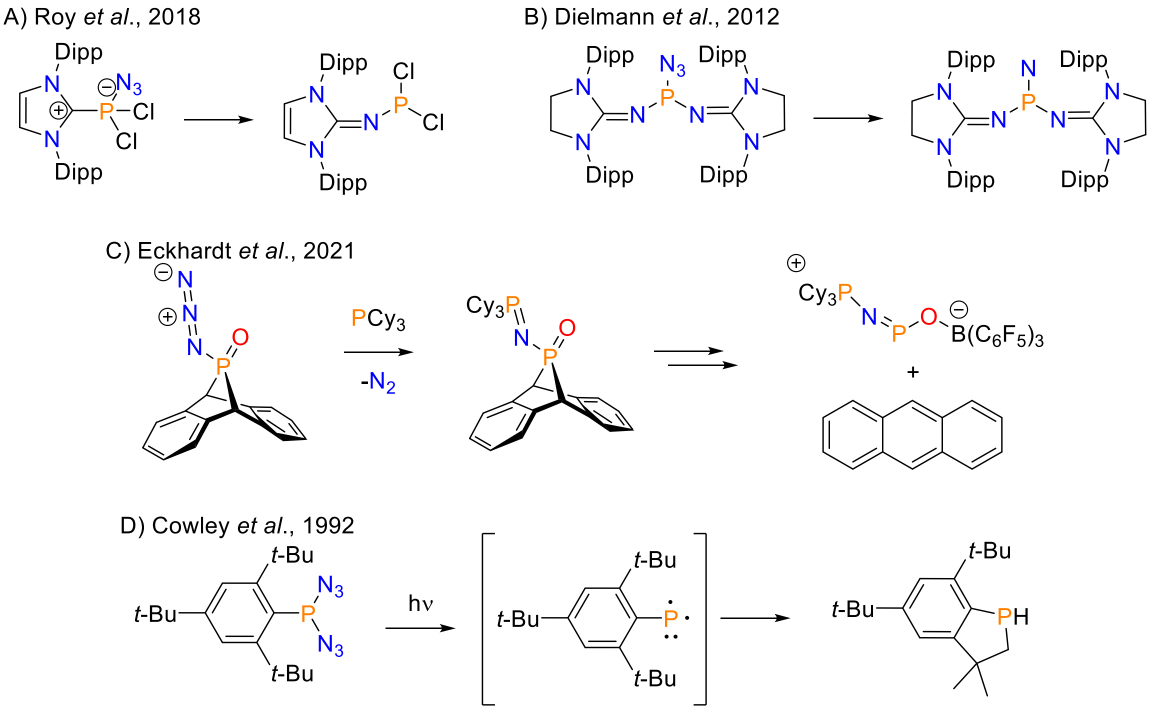
A) Roy et al., 2018
B) Dielmann et al., 2012
C) Eckhardt et al., 2021
PCy3
-N2
D) Cowley et al., 1992
hν

Scheme 3-3. Select examples of transformations of Azidophosphines.

This investigation sought to explore the synthesis of phosphorus species containing both a π-donating phosphinimine ligand, and a bulky, π-donating NHI ligand to prepare electron-rich phosphines. Electron-rich phosphine ligands have already demonstrated their application as ligands in catalytic transformations,[31,32] and P-stereogenic phosphines further hold promise as ligands in asymmetric catalysis.[33] This work demonstrates the potential of NHI-supported bis(azido)phosphines to undergo chemoselective Staudinger reactions with both tertiary or secondary phosphines to generate modular mono(azido)phosphines. A combination of DFT optimized structures, Kohn-Sham orbitals, and charge analyses reveal subtle changes that explain the observed chemoselectivity in the P(V) family. This work highlights the stabilizing nature of the bulky NHI-ligand for bottleable bis(azido)phosphines and provides an approach for preparing P-chiral phosphines bearing an azide handle.

3.2 Results and Discussion

3.2.1 Synthesis and Characterization of Bis(azido)phosphine Compounds

A series of P(III) and P(V) bis(azido)phosphines were prepared (**Scheme 3-4**). Salt metathesis reactions of IPrNPCl$_2$ (**3.1**) with an excess of NaN$_3$ in acetonitrile, followed by an extraction using benzene allowed for the facile production and isolation of IPrNP(N$_3$)$_2$ (**3.2**). Trimethylsilylazide (Me$_3$SiN$_3$) was also explored as a method of synthesizing compound **3.2**, but was found to concurrently generate mixtures of **3.2** (δ_P = 123), a transient species IPrP(N$_3$)Cl (**3.2’**; δ_P = 148), and a bis(azido)(trimethylsilyliminyl)phosphine **3.3** (IPrNP(NSiMe$_3$)(N$_3$)$_2$; δ_P = -28).[16,34] The ambiphilic nature of **3.2** was noted by the spontaneous decomposition to a complex mixture of species in THF, likely containing oligomers of P-(N-P)$_n$ motifs *via* Staudinger reactions, while decomposition of **3.2** was much slower in less polar aromatic solvents (*i.e.* benzene or toluene). Using aromatic solvents allowed for longer timescale reactions to be performed at or below room temperature (*i.e.* in the syntheses of **3.4Ch** and **3.7**).

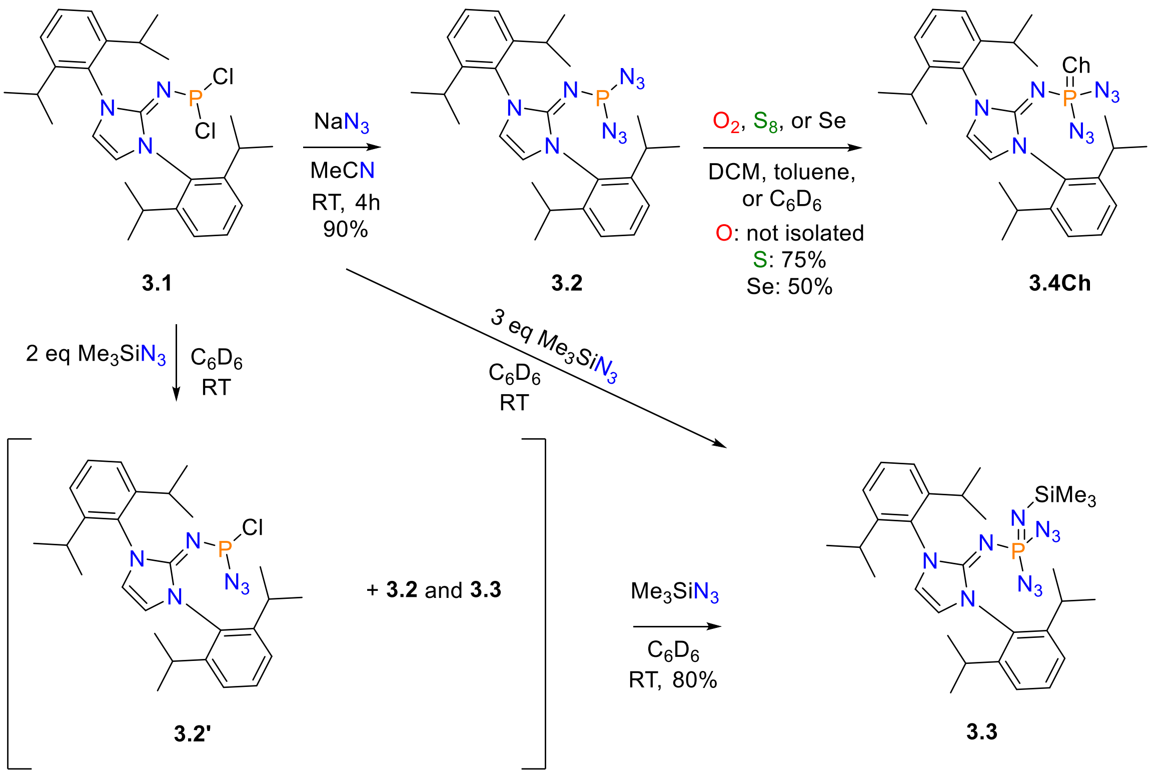

3.1
NaN_3
MeCN
RT, 4h
90%
3.2
O_2, S_8, or Se
DCM, toluene, or C_6D_6
O: not isolated
S: 75%
Se: 50%
3.4Ch
2 eq Me_3SiN_3
C_6D_6
RT
3 eq Me_3SiN_3
C_6D_6
RT
3.2'
+ 3.2 and 3.3
Me_3SiN_3
C_6D_6
RT, 80%
3.3

Scheme 3-4. Synthetic Routes to Bis(azido)phosphines **3.2**, **3.3**, and **3.4Ch** (Ch = O, S, Se).

Bis(azido)phosphine chalcogenides (**3.4Ch**, **Scheme 3-4**) were subsequently prepared. Compound **3.4S** was prepared by sulfurization of a standing solution of **3.2** in toluene using one-eighth molar equivalents of S_8 at -30 °C for 5 days. In an analogous manner, selenation of **3.2** was performed in toluene but over 7 days of stirring at room temperature due to the low solubility of elemental selenium in toluene. Sulfurization of **3.2** to **3.4S** was later optimized to small batches (< 500 mg) in CH_2Cl_2 at room temperature, requiring only 30 min of reaction time for complete conversion.[35] Removal of trace unreacted sulfur from **3.4S** required successive triturations with pentane, cyclohexane, and Et_2O, followed by recrystallization of the bulk material from Et_2O. The poor solubility of elemental selenium allowed for the isolation of **3.4Se** simply by filtration and recrystallization from Et_2O. Fourier transform infrared spectroscopy (FT-IR) spectra of **3.2**, **3.3** and **3.4Ch** confirmed the presence of azides with asymmetric stretching bands between 2083 and 2140 cm^{-1} (See **Appendix B**).[26] To detect any unreacted sulfur in the crude reaction mixture of **3.4S** in CH_2Cl_2, a qualitative assay was employed wherein PPh_3 was introduced to a disposable sample. The emergence of $SPPh_3$ ($\boldsymbol{\delta}_P = 43$) within 15 min served as an indication of the presence of residual sulfur. Isolated yields of **4S** were subsequently improved by the incorporation of this qualitative test, by which small quantities of either S_8 or **3.2** were added to the principal reaction mixture until a tested assay showed no detectable trace of either $SPPh_3$ or **3.2** by $^{31}P\{^1H\}$ NMR spectroscopy.

Following an initial attempt at oxidation of **3.2** using pyridine N-oxide, which was extremely sluggish and resulted in the formation of multiple new phosphorus species in solution, dry gaseous O_2 or *m*CPBA were explored as oxidants. Further resistance to oxidation by O_2 was noted of compound **2** following a brief exposure *via* bubbling of dry O_2 into a solution of **3.2** in C_6D_6 for 10 min, which did not result in any detectable change by $^{31}P\{^1H\}$ NMR spectroscopy. Nevertheless, pressurizing a J-Young NMR tube containing a degassed C_6D_6 solution of **3.2** with O_2 (1.5 atm) slowly resulted in approximately 50 % conversion to **3.4O** after 6 days ($\boldsymbol{\delta}_P$ = -11) with concomitant formation of multiple minor unidentifiable species (**Appendix B-22**). Compound **3.4O** was also identified as the major product by oxidation of **3.2** using *m*CPBA, though it could not be isolated as a pure compound. Oxidation of NHI-supported phosphines has been demonstrated to proceed cleanly with N_2O.[36] The slow oxidation of **3.2** can be rationalized from the large P-Se coupling constant of **3.4Se** ($^1J_{P\text{-}Se}$ = 990 Hz), which suggests that the parent compound **3.2** may be even less basic than $P(OMe)_3$.[37]

Oxidation of **3.2** to **3.4Ch** was accompanied by a phosphorus resonance shifted to lower frequency (**3.2**: $\boldsymbol{\delta}_P = 123$; **4S**: $\boldsymbol{\delta}_P = 41$; **3.4Se**: $\boldsymbol{\delta}_P = 30$, $^1J_{P\text{-}Se}$= 990 Hz; **3.4O**= $\boldsymbol{\delta}_P$ = -11, *c.f.* $OP(NMe_2)_3$ $\boldsymbol{\delta}_P = -23.4$[38]) and an NHI-backbone proton resonance shifted to higher frequency (**3.2**: $\boldsymbol{\delta} = 5.91$; **3.4S**: $\boldsymbol{\delta} = 6.06$; **3.4Se** $\boldsymbol{\delta} = 6.07$; **3.4O**: $\boldsymbol{\delta} = 6.04$). This resulted from an increased π-donation from the NHI and exocyclic nitrogen in **3.4Ch**, as the NHC ring accumulated aromatic and zwitterionic character. Oxidation with $SiMe_3N_3$ to **3.3** resulted in an even more deshielded phosphorus centre ($\boldsymbol{\delta}_P$ = -28), without appreciable change to **3.2** in the NHI-backbone resonance ($\boldsymbol{\delta} = 5.93$) and was indicative of a lower degree of zwitterionic character.

3.2.2 Staudinger Reactivity of Bis(azido)phosphines

Racemic mixtures of chiral phosphines **3.5$_{\mathbf{R}}$** were prepared from benzene solutions of compound **3.4S** by the addition of stoichiometric equivalents of PR_3 (where R = Me, Cy, or Ph) at room temperature. The rate of reaction for each derivative was correlated with the nucleophilicity of the respective phosphine.[39] Higher than stoichiometric tertiary phosphine loadings at ambient temperature resulted in an increased reaction rate, and surprisingly, did not induce a second Staudinger reaction in any of the experiments conducted. The selective formation of products **3.5$_{\mathbf{R}}$** resulting from a single Staudinger reaction were confirmed *via* multiple spectroscopic methods (see appendix chapter Appendix B): (a) A comparison of NHI-backbone protons' resonance with the phosphinimine substituents' ($N{=}P\mathit{R_3}$) integrations in the ^1H NMR spectra; (b) Integration of the $^{31}P\{^1H\}$ spectra that characteristically contained two doublets in a 1 : 1 ratio, with coupling constants consistent with a $^2J_{P\text{-}P}$ coupling[40]; (c) Stretching modes of unreacted azide functional groups using FT-IR spectroscopy; (d) *via* Electrospray-ionization Mass spectroscopy (ESI-MS) detection of the expected molecular ion peak and Na^+/K^+ adducts; and, (e) Structural confirmation of **3.5$_{\mathbf{Cy}}$** by SC-XRD (*vide infra*, **Figure 3-1**) along with the ^1H and $^{31}P\{^1H\}$ NMR spectroscopic fingerprinting of the crystals compared with the bulk powder. For the synthesis of **3.5$_{\mathbf{Me}}$**, excess PMe_3 was removed *in vacuo*; however, the removal of non-volatile phosphines from **3.5$_{\mathbf{Cy}}$** and **3.5$_{\mathbf{Ph}}$** necessitated multiple triturations, which contributed to low isolated yields, despite their near quantitative conversion as noted by $^{31}P\{^1H\}$ NMR spectroscopy of reaction mixture samples (**Appendix B-36** and **Appendix B-43**). PCy_3 was found to be sufficiently nucleophilic to achieve complete conversion of **3.4S** to **3.5$_{\mathbf{Cy}}$** within two days when a stoichiometric loading was used. An alternative purification method discovered for species **3.5$_{\mathbf{Cy}}$**, **3.5$_{\mathbf{Ph}}$**, and **3.6a/3.6b** (*vide infra*) that consisted of a recrystallization from their respective concentrated hot pentane or hexane solutions. Reactions of **3.4S** with phosphines containing a P-Cl bond were not selective, likely because of N_3^-/Cl^- exchange that resulted in the formation of complex mixtures.[41]

$HPCy_2$ was also evaluated for Staudinger-type reactivity with **3.4S,** and the reaction was found to give rise to two species in solution (**3.6a** and **3.6b**). 1D- and 2D-

NMR spectroscopic experiments supported the identities of compounds **3.6a** and **3.6b,** which were formed in approximately 2:1 ratio in solution. The P(V)-N=P(V)(H) functionality of **3.6a** is hallmarked by a doublet-of-doublet-of triplets in the ^{1}H NMR spectrum at δ=6.27 ($^{1}J_{\text{P-H}}$ = 432 Hz; $^{3}J_{\text{P-H}}$ = 12.2 Hz; $^{3}J_{\text{H-H}}$ = 3.2 Hz), while the N-H signal of the tautomerized species **3.6b** with P(V)-N(H)-P(III) connectivity, appeared as a broad doublet of doublets at δ=2.77 (**Appendix B-44**). Signals for **3.6b** in the ^{31}P{^{1}H} and ^{31}P NMR spectra (**Appendix B-48** and **Appendix B-49**) are at higher frequency than **3.6a** and exhibited greater P-P coupling ($\boldsymbol{\delta}_{\text{P}}$ = 45 and 43, $^{2}J_{\text{P-P}}$ = 56 Hz) than **3.6a** ($\boldsymbol{\delta}_{\text{P}}$ = 39 and 24, $^{2}J_{\text{P-P}}$ = 12 Hz), also exhibited larger coupling than the P(V)-N-P(V) coupled compounds **3.5** - **3.7**,[42,43] and is slightly lower than P(V)-N-P(III) coupled compound **3.7** ($^{2}J_{\text{P-P}}$ = 69 Hz).[44–46] P-H connectivity of **3.6a** was evident in the ^{31}P NMR spectrum by pair of broad resonances about 24.4 ppm separated by 432 Hz (**Appendix B-49**). Chemical exchange of **3.6a** and **3.6b** was observed by cross peaks in ^{31}P-^{31}P EXSY at room temperature (**Appendix B-59**), supporting the proposed tautomerization. Examples of imine/amine isomerization have been reported for P-alkoxyphosphaazo- compounds that readily rearrange,[8] tautomerization of bis(amino)cyclodiphosph(V)azene and bis(imino)cyclophosph(V)azane *via* 1,3-hydride shift (**Scheme 3-5**, right),[47] and P,O-chelating sulfonamidophosphorus ligands[48,49]

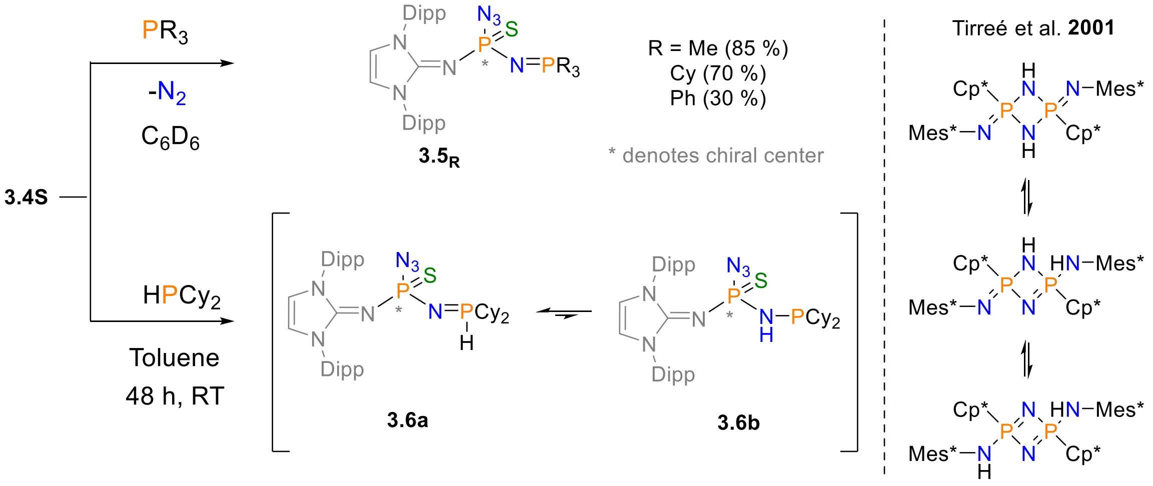

Scheme 3-5. Staudinger reactivity of compound **3.4S** with tertiary and secondary phosphines (left) and example of tautomerization *via* hydride shift (right).

Compound **3.2** was observed to undergo Staudinger reactions with exogenous PMe_3 to generate compound **3.7** in solution *via* a single Staudinger reaction (**Scheme 3-6**). Acknowledging the ambiphilic nature and instability of **3.2** in solution, the decomposition *via* oligomerization was attenuated with the addition of a large excess (approximately twenty molar equivalents) of PMe_3, which allowed for complete consumption of **3.2** within three hours at room temperature to produce **3.7** as the major species (approximately 80 % of normalized $^{31}P\{^1H\}$ NMR integrations). Attempts to purify compound **3.7** using hexanes washes were complicated by the thermal decomposition of **3.7** to an unknown major species containing a P-H bond ($^1J_{P\text{-}H}$ = 560 Hz) (See section **B2** in appendix). Lyophilization from a frozen benzene matrix could be used to remove excess PMe_3 from the sample while minimizing thermal decomposition of **3.7**, although a few minor uncharacterized species remain detectable in the baseline of the $^{31}P\{^1H\}$ NMR spectra (**Appendix B-63**). Compound **3.7** readily dissolved in chlorinated solvents but was unstable and rapidly decomposed to a mixture of phosphorus-containing species. A sample of **3.7** in C_6D_6 was stored in a foil-wrapped, J-Young NMR tube at ambient temperature, and monitored periodically over 3 days. In the absence of PMe_3, the species gradually decomposed to yield the same $^{31}P\{^1H\}$ signals encountered after the washing of crude **3.7** with hexanes. FT-IR spectroscopic analysis of lyophilized material confirmed that compound **3.7** is an azidophosphine by the presence of an intense N_3-asymmetric stretching band at 2127 cm^{-1} with two accompanying combination bands at 2064 cm^{-1} and 1999 cm^{-1} (**Appendix B-64**).

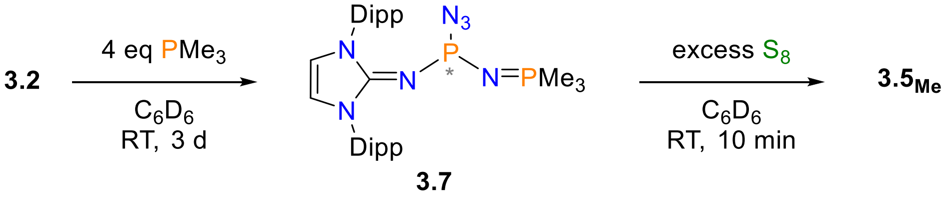

* denotes chiral center

Scheme 3-6. Chemoselective Staudinger reactivity of **3.2** with PMe_3 and alternate synthetic route to **3.5$_{Me}$**.

Unlike the species **3.2** - **3.6** which were stable in acetonitrile for ESI-HRMS analysis, the apparent instability of **3.7** in polar solvents resulted in an evasion of the expected molecular ion fragments from detection. The ambiphilic nature of **3.7** resulted in the detection of a molecular ion fragment that matched for the product of a Staudinger reaction of two stoichiometric equivalents of **3.7** ([**3.2** + **3.7** - N_2]$^+$), in addition to [**3.7** - N_3]$^+$. To provide more evidence towards the identity of **3.7**, a 50-fold excess of S_8 was added to **3.7** in C_6D_6 to produce two-doublets in ^{31}P**{**^{1}H} NMR spectrum matching for **3.5$_{Me}$** within 10 min (**Appendix B-65** and **Appendix B-66**). Gratifyingly, the dilution of this reaction mixture using acetonitrile and a subsequent filtration of the cloudy mixture allowed for the detection of the characteristic molecular ion signals for **3.5$_{Me}$** *via* ESI-HRMS (**Appendix B-67**). This experiment also confirmed that the central phosphorus atom of **3.7** adopted some nucleophilic character.

3.3 X-ray Crystallography

The family of P(III) (**3.2**) and P(V) (**3.4S** or **3.4Se**) bis(azido)phosphines, as well as the Staudinger product **3.5$_{Cy}$** were analyzed *via* single crystal X-ray diffraction and are visualized in **Figure 3-1**. Compound **3.2** exhibited tetrahedral geometry, while **3.4S** and **3.4Se** exhibited trigonal pyramidal geometries at the central phosphorus. The average P-N_{azide} bond length for **3.2** was 1.77 Å, while the more electron deficient P(V) species **3.4S** and **3.4Se** possessed average P-N_{azide} lengths of 1.72 Å. This suggested the bis(azido)phosphine species developed a slightly higher P-N_{azide} bond order upon oxidation. More significant contractions of the P-N_{NHI} bond lengths were apparent when comparing **3.2** (1.6290(15) Å) to the oxidized species **3.4S** and **3.4Se** (1.5750(13) and 1.5758(16) Å, respectively as compared to the P-N bonds in triphenylphosphonium substituted phosphinimines that range from 1.54 to 1.64 Å ($\sum$ (covalent radii) P=N = 1.62 Å).[40] Compounds **3.2**, **3.4S** and **3.4Se** clearly exhibited P-N_{NHI} multiple bond character.

The structure and chirality of **3.5$_{Cy}$** was confirmed as the species crystallized as a racemic mixture within the *P2$_1$/n* space group. Comparing the structures of **3.5Cy** to **3.4S** revealed an elongated P-S (0.028 Å), P-N_{NHI} (0.025 Å) and P-N_{N3} (ca. 0.042 Å, averaged), while the remaining P-N bond (which underwent an azide to phosphinimine conversion) experienced a significant contraction by 0.15 Å (averaged). The electronic similarity of the phosphinimine and NHI ligands is evident in both the P-N_{NHI} and P-

N_{PCy3} bond lengths (1.6001(11) Å and 1.5933(11) Å) and in the P-N-C and P-N-P bond angles of (132.41(8) ° and 137.94(7) °).

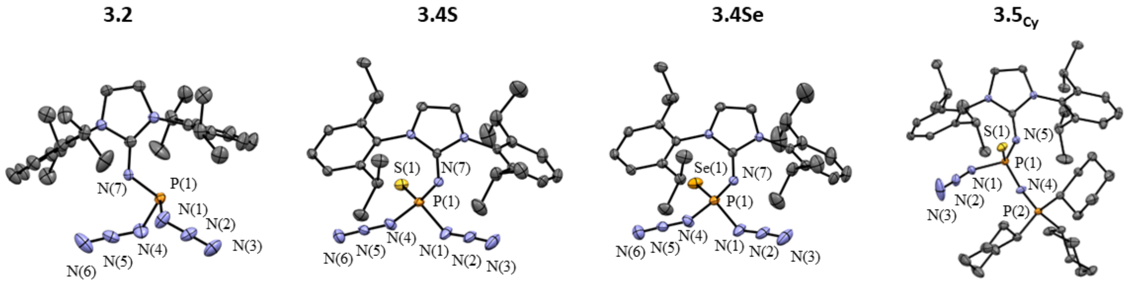

Figure 3-1. Mercury-rendered ORTEP style drawing of **3.2**, **3.4S**, **3.4Se** and **3.5_{Cy}**. Hydrogen atoms have been omitted for clarity and selected ellipsoids shown at the 50% probability level. Azido, imino, and phosphinimino nitrogen atoms, phosphorus atoms, and chalcogen labels have been displayed.

Thermogravimetric analysis (TGA, **Figure 3-2**) of compound **3.2** revealed that a rapid mass loss of 16.5 % occurred at 93 °C and is consistent with the loss of three stoichiometric equivalents of N_2 (Theoretical = 16.2 %). Following this event, the mass remained constant (< ± 0.5 %) until approximately 194 °C. This suggested that compound **3.2** may be used as a precursor for phosphinidene chemistry in subsequent studies.[26,50] Compounds **3.4S** and **3.5_{Me}** were observed to undergo a mass loss equivalent to one N_2 moiety at higher temperatures than **3.2** (186 °C and 196 °C, respectively), and the traces for **3.4S** and **3.5_{Me}** did not suggest the formation of a stable intermediate *via* N_2 evolution. A melting point analysis of **3.4S** in a sealed capillary resulted in darkening between 135 – 145 °C that was indicative of decomposition. In comparison to bulky azidophosphines (R_2P-N_3) supported by tetramethylpiperidyl and/or dimethylpiperidyl ligands, which were reported to decompose between 50 and 60 °C,[51] species **3.2** and **3.4Ch** are considerably more thermally stable.

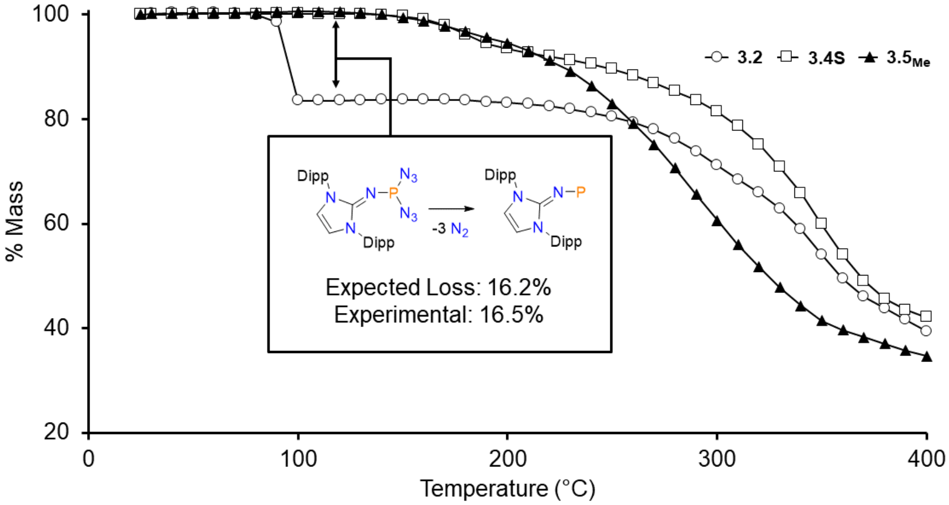

Figure 3-2. TGA plot of compounds **3.2**, **3.4S**, and **3.5Me** [10 °C/min, performed in air under flow of N_2 (10 mL/min)].

3.4 Computational Investigation

A computational study was undertaken on the progression of species **3.4S** from its initial bisazide state (labelled **I**) to the monoazide state **3.5Me** (labelled **II**), and finally, into the hypothetical, doubley reacted, species **III** (**Figure 3-3**). As might be expected, both azide groups of **I** were equally favourable to initiate the reaction, with no notable differences between the two species, such that the selectivity cannot be explained through a single predetermined preferential azide available attack by the PMe_3. This is in agreement with the crystalographic results which show both enantiomers of monoazide species **3.5Me** are produced.

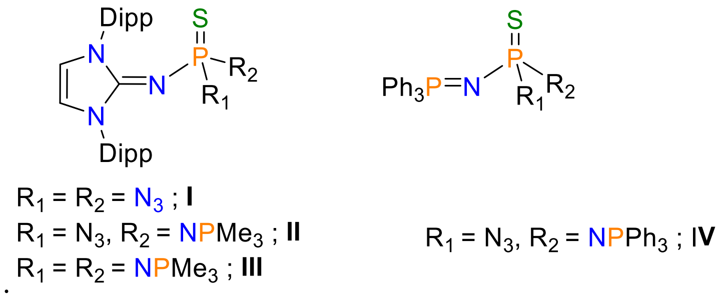
Dipp
S
N
N
P
R_2
R_1
N
Dipp
$R_1 = R_2 = N_3$; I
$R_1 = N_3$, $R_2 = NPMe_3$; II
$R_1 = R_2 = NPMe_3$; III
S
$Ph_3P{=}N$
P
R_1
R_2
$R_1 = N_3$, $R_2 = NPPh_3$; IV

Figure 3-3. Molecular structures studied by DFT.

Optimized structures **I-III** possessed a P-S bond that was twisted nearly 90° out of the plane of the NHI moiety. The highest occupied molecular orbital (HOMO) for species **I** (-5.992 eV) and **II** (-5.246 eV) were all found to be comprised of NHI π-symmetric and sulfur lone pair character (**Figure 3-4**, A and B), which suggests a nucleophilic sulfur may be amenable to further functionalization. The distinct difference between species **I** and **II** is in the N_3 π* and P-S σ* character found in the LUMO level (-0.98 eV) of **I**, but not until LUMO+4 (-0.023 eV) in **II** (**Figure 3-4**, C and D). This suggested that the electronic inaccessibility of this N_3 π* system was the main driver of the observed chemoselectivity. To test this hypothesis further, the resilient azide species **IV**[21] (**Figure 3-3**) was also investigated. This analysis revealed no significant N_3 π* system was until the LUMO+12 (0.081 eV; section **B4** in appendix).

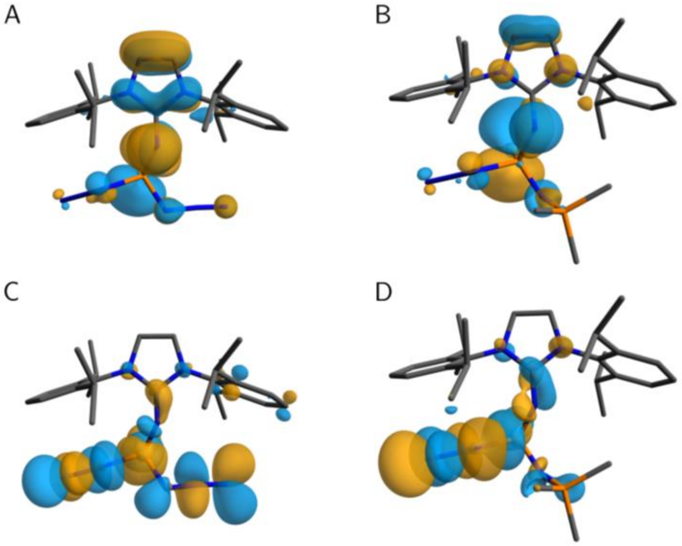

Figure 3-4. Kohn-Sham orbitals of **I** and **II** at B3LYP/Def2-TZVP level of theory[52–56] with D4 dispersion correction.[57,58] Yellow colour illustrates negative phase and blue illustrates positive phase of orbitals. The HOMO of **I** (A) and **II** (B). The N_3 π* character seen in **I** at the LUMO (-0.98 eV) level (C) is not observed until the LUMO+4 (-0.023 eV) level in **II** (D). Hydrogen atoms have been omitted for clarity.

3.5 Conclusions

This work demonstrated the formation of P(III) and P(V) bis(azido)phosphine and bis(azido)phosphine chalcogenides, which undergo chemoselective Staudinger reactions to produce chiral (NHI)(azido)(phosphinimine)phosphine or (NHI)(azido)(phosphinimine)phosphine chalcogenide at room temperature. The reactions of both **3.2** and **3.4S** with stoichiometric excessive loadings of PMe_3 were found to selectively react only once to produce **3.7** and **3.5$_{Me}$**. Cy_2PH was nucleophilic enough to react with **3.4S**, and the equilibrium nature of the product was confirmed by ^{31}P-^{31}P EXSY NMR experiment. Species **3.5$_R$** and **3.6** were more thermally resilient than species **3.7**, which allowed recrystallization and purification from hot pentane/hexanes. Compound **3.7** decomposed at room temperature and generated an unknown species containing a P-H bond, as indicated by coupling constant of 560 Hz. DFT calculations were used to offer reasoning for the chemoselectivity of **3.4S** with PMe_3. Kohn-Sham orbitals of the mono- and bis(azido) species reveal a sharp contrast in energetic accessibility of N_3 anti-bonding character of the two species. The inaccessibility of the resilient azide of **II** was also found for the known literature example of species **V** and explains the observed chemoselectivity of **3.4S** with various aryl and alkyl phosphines.

3.6 Experimental Section

3.6.1 General Considerations

All manipulations were conducted under an inert atmosphere using a nitrogen-filled glovebox or using standard Schlenk techniques. All glassware was oven-dried prior to use. All solvents were purchased from Caledon, Sigma-Aldrich, or Alfa-Aesar and dried using a MBraun controlled atmosphere solvent purification system, then stored in a N_2 filled glovebox atmosphere over 3 Å or 4 Å molecular sieves. C_6D_6 and $CDCl_3$ were purchased from Sigma Aldrich and pre-dried by refluxing over CaH_2, followed by distillation, and degassing by multiple freeze-pump-thaw cycles, and finally stored over 4 Å molecular sieves under an N_2 atmosphere. Synthesis of IPr*HCl,[59,60] IPr,[59] IPrNSiMe$_3$[61] were prepared following literature procedures and recrystallized from concentrated solutions of ethanol, toluene, and pentane respectively. Synthesis of IPrNPCl$_2$ was prepared and isolated using a slightly modified procedure.[22] All NMR spectra were collected on a Bruker 400 MHz, Bruker 600 MHz, or INOVA 600 MHz spectrometer. NMR data as processed in either Bruker TopSpin 4.0.7, or in MestReNova 1.13. ^1H and $^{13}C\{^1H\}$ spectra were referenced to the solvent signal (trace proteo-solvent in the case of ^1H spectra). $^{31}P\{^1H\}$ spectra were referenced to an 85 % H_3PO_4 external standard at 0.0 ppm. Electrospray Ionization – Mass Spectrometry was used to analyze samples in acetonitrile at a concentration of 0.05 mg/mL, unless otherwise specified. FT-IR spectra were collected with a Bruker ALPHA II FTIR spectrometer in air, in either ATR-mode (attenuated total reflection) or in transmission mode as a KBr pellet, and the collection method was noted for each respective sample. Samples were prepared inside a nitrogen-filled glovebox and quickly measured either as a solid or as a KBr pellet of approximately 1 mg sample/100 mg KBr concentration. High-Resolution Mass-

Spectrometry of acetonitrile solutions were performed using a Bruker MicrOTOF-II-focus instrument in positive polarity mode.

Safety Statement! *Covalent azides pose an explosion risk and should be handled with extreme caution! Rigorous exclusion of water from samples should be prioritized and use of halogenated solvents should be avoided when possible due to the possibility of forming hydrazoic acid or di(azido)methane.*[62] *All syntheses were performed on sub-millimole scale for safety. While no ignition or detonation was encountered while handling these species, cautions should be taken to minimize exposure to shock, spark, or light. The use of a plastic spatula, electrical grounding, and a general avoidance of ground glass joints while handling these materials is recommended. The following reactions should not be scaled up without appropriate information regarding the shock or abrasion sensitivity of the azidophosphines.*

All computational simulations were undertaken with the ORCA (v5.0.4) software.[63] Geometry optimizations were performed using the Becke three-parameter Lee-Yang-Parr (B3LYP) density functional[52–55] and the def2-TZVP basis set.[56] Atom-pairwise dispersion correction (D4) was used.[57,58] Optimized structures were confirmed to be local minima by ensuring no imaginary frequencies were obtained. The initial structure for I was taken from the CIF file of compound **3.2**. Initial structures of II and III were generated by editing the optimized structure I in Avogadro.[64] Hirshfield, Mulliken, Löwdin and dipole corrected Becke charges were all calculated using Multiwfn (v3.6).[65]

3.6.2 Modified Synthesis of IPrNPCl$_2$

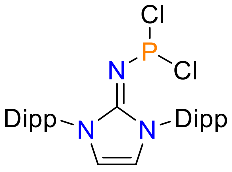

Following a procedure adapted from Roy *et al.*,[22] IPrNSiMe$_3$ (1.47 g, 3.08 mmol) was dissolved in 20 mL toluene, followed by PCl$_3$ (0.30 mL, 3.4 mmol). NEt$_3$ (0.04 mL 0.3 mmol) was then added dropwise. The formation of a bright yellow solid forms initially but prolonged stirring results in gradual colour change to an off-white slurry. Mixture was stirred for 16 h at room temperature, then volatiles removed. The residue was reconstituted in 15 mL THF, centrifuged, decanted, and washed again with THF (5 mL). Decanted THF solutions were combined, and volatiles were removed again, resulting in isolation of an off-white, slightly yellow powder (1.4 g, 2.8 mmol, 92% yield). The purity of the resulting off-white powder was assessed by ^{1}H and ^{31}P{^{1}H} NMR spectroscopy to be suitable for further reactions. Recrystallization from concentrated THF solutions at -30 °C could also be performed to increase purity, if deemed necessary.

3.6.3 Synthesis of IPrNP(N$_3$)$_2$ (**3.2**)

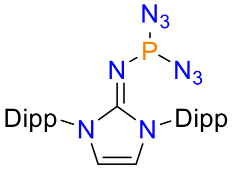

Method 1: IPrNPCl$_2$ (1.00 g, 1.98 mmol) was dissolved in 20 mL acetonitrile then sodium azide (0.50 g, 7.7 mmol) was added in portions to a stirring solution. After 4 h, volatiles were removed then residue was then resuspended in 10 mL benzene, centrifuged, and decanted. Removal of volatiles results in isolation of a white powder (0.78 g, 76% yield).

Method 2: IPrNPCl$_2$ (0.400 g, 0.900 mmol) was dissolved in 15 mL toluene at room temperature and neat SiMe$_3$N$_3$ (240 µL 1.8 mmol) was added dropwise over 5 min. The mixture was allowed to stir at room temperature for 3 days while periodically monitoring the reaction progress *via* ^{31}P{^{1}H} NMR spectroscopy). Note A) IPrNP(N$_3$)Cl (**3.2'**) formed *in situ* can be detected at δ = 149 ppm). Note B) the crude product obtained via this method consistently formed with concurrent generation of **3.3** at -28 ppm [IPrNP(NSiMe$_3$)(N$_3$)$_2$].

^{1}H NMR (400 MHz, C$_6$D$_6$) δ = 7.23 (t, 2H, *p*-H, 7.8 Hz), 7.08 (d, 4H, *m*-H, 7.8 Hz), 5.91 (s, 2H, N(C*H*)$_2$N). 2.88 (sept, 4H, C*H*(CH$_3$)$_2$, 6.8 Hz), 1.37 (d, 12H, CH$_3$, 6.8 Hz), 1.09 (d, 12H, CH$_3$, 6.8 Hz). **^{13}C{^{1}H} NMR (100.6 MHz, C$_6$D$_6$)** δ = 147.7 (d, N*C*(NP)N), 27 Hz), 146.9 (*o*-C), 131.9 (*ipso*-C), 130.6 (*p*-C), 124.0 (*m*-C), 115.7 (N(*C*H)$_2$N), 29.0 (*C*H(CH$_3$)$_2$), 24.4 (*C*H$_3$), 22.6 (*C*H$_3$). **^{31}P{^{1}H} NMR (162 MHz, C$_6$D$_6$)** δ = 123.1. **FT-IR (KBr pellet, cm^{-1})** 2110 & 2083 (N$_3$ stretches). **ESI-MS (m/z)** 518.2885 [**3.2 + H:** 518.2904 expected], 540.2705 [**3.2 + Na:** 540.2723 expected].

3.6.4 Synthesis of IPrNP(NSiMe$_3$)(N$_3$)$_2$ (**3.3**)

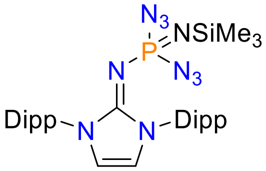

To a stirred solution of IPrNPCl$_2$ (71.1 mg, 0.139 mmol) in 5 mL toluene, an excess of SiMe$_3$N$_3$ (74 µL, 0.556 mmol) was added dropwise. The resulting mixture was then stirred at room temperature over 4 days with periodic monitoring *via* ^{31}P NMR spectroscopy. Removal of volatiles under reduced pressure resulted in isolation of white powder of suitable purity by ^{1}H and ^{31}P{^{1}H} NMR spectroscopy (0.0954 g, 0.12 mmol, 84 % yield).

^{1}H NMR (400 MHz, C_6D_6) δ = 7.22 (t, 2H, *p*-H, 7.7 Hz), 7.10 (d, 4H, *m*-H, 7.6 Hz), 5.93 (s, 2H, N(C*H*)2N), 2.88 (sept, 4H, C*H*(CH_3)$_2$, 6.8 Hz), 1.43 (d, 12H, CH_3, 6.8 Hz), 1.07 (d, 12H, CH_3, 6.8 Hz). **^{13}C{^{1}H} NMR (100.6 MHz, C_6D_6)** δ = 146.6 (*o*-C), 131.9 (ipso-C), 130.5 (*p*-C), 124.0 (*m*-C), 116.3 (N(*C*H)$_2$N), 28.9 (CH(CH_3)2), 24.4 (CH_3), 23.0 (CH_3), 3.48 (d, Si(CH_3)$_3$, $^{3}J_{P\text{-}C}$ = 5.3 Hz). [N*C*N not observed]. **^{31}P{^{1}H} NMR (162 MHz, C_6D_6)** δ = -28.9. **FT-IR (ATR, cm^{-1})** 2140 & 2116 (N_3 stretches) **ESI-MS (m/z)** 605.3387 [**3.3** + **H:** 605.3408 expected], 627.3221 [**3.3** + **Na:** 627.3228 expected], 643.2963 [**3.3** + **K:** 643.2967 expected].

3.6.5 Synthesis of IPrNPS(N_3)$_2$ (**3.4S**)

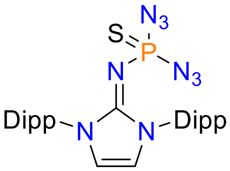

A solution of S_8 (21.0 mg, 0.0820 mmol) in 2 mL CH_2Cl_2 was added to a solution of **3.2** (0.342g, 0.661 mmol) in 12 mL CH_2Cl_2, and vial was rinsed with one additional mL CH_2Cl_2. The mixture was stirred at room temperature for 30 min then volatiles were removed. Residue rinsed with 5 mL cyclohexane, decanted and volatiles removed. (0.353 g, 0.642 mmol, 95 % yield).

Method 2: S_8 (31.2 mg, 0.122 mmol) was added to a solution of **3.2** (0.479 g, 0.926 mmol) in 15 mL toluene, and mixture was allowed to sit at -30 °C for 7 days, monitoring conversion by ^{31}P NMR aliquots. Volatiles were then removed, and the solids were triturated with 0.5 mL portions of cold Et_2O and pentane, and recrystallized from Et_2O. (0.28 g, 0.51 mmol, 55% yield).

As an aside, a qualitative test for the presence of residual sulfur to be addition of PPh_3 to a $CDCl_3$ or CH_2Cl_2 solution of a sacrificial sample of **3.4S** which will lead to rapid development of $SPPh_3$ (δ_P = 42.7) if any unreacted sulfur remains.[35]

^{1}H NMR (400 MHz, C_6D_6) δ = 7.21 (dd, 2H, *p*-H, 7.7 Hz), 7.09 (d, 4H, *m*-H, 7.7 Hz), 6.06 (s, 2H, N(C*H*)$_2$N), 2.95 (sept, 4H, C*H*(CH$_3$)$_2$, 6.9 Hz), 1.45 (d, 12H, CH$_3$, 6.8 Hz), 1.04 (d, 12H, CH$_3$, 6.8 Hz). **^{13}C{^{1}H} NMR (100.6 MHz, C_6D_6)** δ = 146.7 (*o*-C), 145.8 (d, NCN, 12 Hz), 131.5 (ipso), 130.7 (*p*-H), 124.2 (*m*-C), 117.0 (N(*C*H)$_2$)N), 28.9 (*C*H(CH$_3$)$_2$), 24.9 (*C*H$_3$), 23.1 (*C*H$_3$). **^{31}P{^{1}H} NMR (162 MHz, C_6D_6)** δ = 40.7. **FT-IR (KBr pellet, cm^{-1})** 2134 (N$_3$ stretch). **ESI-MS (m/z)** 572.2455 [**3.4S** + **Na:** 572.2444 expected], 588.2216 [**3.4S** + **K:** 588.2148 expected] **Elemental Analysis** Calculated C 59.00; H 6.60; N 22.93; S 5.83. Found C 59.52; H 6.45; N 22.1; S 5.44.

3.6.6 Synthesis of IPrNPSe(N$_3$)$_2$ (**3.4Se**)

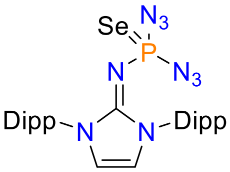

Selenium powder (85 mg, 1.1 mmol) was added in portions to a stirred solution of **3.2** (520 mg, 0.17 mol) in 5 mL toluene. The mixture was allowed to stir at room temperature for 7 days. Solution was filtered and volatiles were removed in vacuo. Recrystallization from Et$_2$O/pentane resulted in isolation of clear-colourless crystals suitable for X-ray diffraction studies. (45 mg, 0.075 mmol, 45 % yield).

^{1}H NMR (400 MHz, C_6D_6) δ = 7.25-7.08 (multiplet, 2H, *p*-H), 7.09 (multiplet, 4H, *m*-H), 6.07 (s, 2H, N(C*H*)$_2$N), 2.97 (septet, 4H, C*H*(CH$_3$)$_2$, 6.8 Hz), 1.47 (d, 12H, CH(C*H$_3$*)$_2$, 6.8 Hz), 1.03 (d, 12H, CH(C*H$_3$*)$_2$, 6.8 Hz). **^{13}C{^{1}H} NMR (100.6 MHz, C_6D_6)** δ = 146.6 (*o*-C), 131.5 (ipso), 130.7(*p*-C), 124.3 (*m*-C), 117.2 (N(*C*H)$_2$N), 28.9 (*C*H(CH$_3$)$_2$), 25.0 (*C*H$_3$), 23.2 (*C*H$_3$). **^{31}P{^{1}H} NMR (162 MHz, C_6D_6)** δ = 30.0 ($^1J_{P\text{-}Se}$ = 891 Hz). **FT-IR (KBr pellet, cm^{-1})** 2132 (N$_3$ stretch). **ESI-MS (m/z)** 598.2050 [**3.4Se** + **H:** 598.2069 expected], 620.1909 [**3.4Se** + **Na:** 620.1889 expected], 636.1659 [**3.4Se** + **K:** 636.1628 expected].

3.6.7 Synthesis of IPrNPO(N$_3$)$_2$ (**3.4O**)

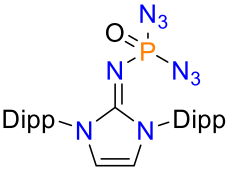

Method 1: a 0.5 mL C_6D_6 solution of **3.2** (10 mg, 0.19 mmol) was charged in a J-Young NMR tube. The sample was frozen and degassed three times, and tube was evacuated a final time. O$_2$ gas was purged for 10 min passed over CaH$_2$ drying tube before

connecting the J-young NMR tube and pressurizing J-Young with 1.5 atm O_2. Reaction was left at room temperature, wrapped in foil, for 1 week.

Method 2: A solution of **3.2** in C_6D_6 was prepared in a nitrogen filled glovebox and was exposed to air momentarily outside the glovebox while adding a couple of crystals of *m*CPBA via spatula to the open NMR tube. NMR spectrum was collected within 15 min at room temperature and shows formation of two major species. Sample decomposed to crystalline $[IPrNH_2]^+$ salts upon attempts to recrystallize species.

^{1}H NMR (400 MHz, C_6D_6) δ = 7.23 (t, 2H, *p*-H, 7.5 Hz), 7.11 (d, 4H, *m*-H, 7.5 Hz), 6.04 (s, 2H, N(CH)$_2$N), 2.85 (septet, 4H, C*H*(CH$_3$)$_2$, 6.4 Hz), 1.44 (d, 12H, CH(CH$_3$)$_2$, 6.4 Hz), 1.07(d, 12H, CH(CH$_3$)$_2$, 6.4 Hz). **^{13}C{^{1}H} NMR (100.6 MHz, C_6D_6)** δ = 146.8 (*o*-C), 145.8 (NCN, $^2J_{P\text{-}C}$ = 10.9 Hz), 131.4 (ipso), 130.7(*p*-H), 124.1 (*m*-C), 116.5 (N(*C*H)$_2$N), 29.0 (*C*H(CH$_3$)$_2$), 24.5 (*C*H$_3$), 22.8 (*C*H$_3$). **^{31}P{^{1}H} NMR (162 MHz, C_6D_6)** δ = -11.3.

3.6.8 Synthesis of IPrNP(S)(N$_3$)(NPMe$_3$) (**3.5$_{Me}$**)

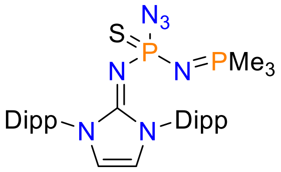

To a solution of **3.4S** (0.055 g, 0.10 mmol) in 2 mL toluene, PMe$_3$ (32 µL, 0.32 mmol) was added neat and allowed to stir at room temperature until complete consumption of **3.4S** was determined by ^{31}P NMR analysis. The removal of volatiles *in vacuo*, followed by trituration with a minimal amount of pentane, resulted in the isolation of an off-white, sticky residue (0.041 g, 69 % yield).

^{1}H NMR (400 MHz, C_6D_6) δ = 7.22 (multiplet, 2H, *p*-H), 7.15 (multiplet, 4H, *m*-H), 6.11 (s, 2H, N(CH)$_2$N), 3.28 (septet, 4H, C*H*(CH$_3$)$_2$, 6.6 Hz), 1.62 (d, 6H, CH$_3$, 6.6 Hz), 1.58 (d, 6H, CH$_3$, 6.6 Hz), 1.74 (d, 6H*, CH$_3$, 6.8 Hz), 1.15 (d, 6H*, CH$_3$, 6.8 Hz) {*= overlapped doublets; integration total equals 12 protons)}, 0.78 (9H, d, P(CH$_3$)$_3$, 13.3 Hz). **^{13}C{^{1}H} NMR (100.6 MHz, C_6D_6)** δ = 147.6 (*o*-C), 147.4 (*o*-C), 145.0 (d, N*C*N, 10.6 Hz), 133.5 (ipso), 129.6 (*p*-C), 123.8 (*m*-C), 123.8 (*m*-C), 116.1 (N(*C*H)$_2$)N), 28.81 (CH$_3$), 28.79 (CH$_3$), 25.01 (CH$_3$), 24.99 (CH$_3$), 23.5 (d, P(CH$_3$)$_3$, 10.4 Hz). **^{31}P{^{1}H} NMR (162 MHz, C_6D_6)** δ = 36.3 ([N]*P*(N$_3$)(NPMe$_3$), 17 Hz), 15.3 ([N]P(N$_3$)(N*P*Me$_3$), 17 Hz). **FT-IR (KBr pellet, cm^{-1})**: 2113 (N$_3$ stretch) **ESI-MS (m/z)** 598.3006 [**3.5$_{Me}$ + H:**

598.3005 expected], 620.2837 [**3.5$_{Me}$ + Na:** 620.2825 expected], 636.2580 [**3.5$_{Me}$ + K:** 636.2564 expected]. **Elemental Analysis** Calculated C 60.28; H 7.59; N 16.40; S 5.36. Found C 60.71; H 7.47; N 15.20; S 5.06.

3.6.9 Synthesis of IPrNP(S)(N_3)($NPCy_3$) (**3.5$_{Cy}$**)

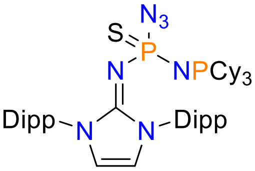

To a solution of **3.4S** (55 mg, 0.10 mmol) in two mL benzene, PCy_3 (30 mg, 0.11 mmol) was added as a solution in two mL benzene and stirred at room temperature over two days. Removal of volatiles resulted in isolation of crude colourless sticky-oily residue. Recrystallization was performed by suspension of the sticky residue in eight mL of pentane, followed by gentle heating, hot filtration through a celite filter pipette, concentrating the solution to approximately four mL *in vacuo*, and then finally allowing the solution to sit undisturbed at -30 °C for one week. A few crystals were isolated and used for X-ray analysis. The remaining crystals were decanted and dried under reduced pressure (31 mg, 0.039 mmol. 39 % yield).

^{1}H NMR (400 MHz, $CDCl_3$) δ = 7.40 (t, 2H, *p*-H, 7.8 Hz), 7.28-7.24 (m, 4H, overlapped partially with $CHCl_3$ signal, *m*-H), 6.52 (s, 2H, N(C*H*)$_2$N), 3.15-3.01 (m, 4H, C*H*(CH_3)$_2$), 1.98-1.83 (m, 3H, P-C*H*(C_5H_{10})), 1.77-1.50 (m, 15H, Cy), 1.47-1.36 (overlapped doublets, 12H, 6.6 Hz, C*H$_3$*), 1.23-1.16 (overlapped doublets, 12H, 4.18 Hz, C*H$_3$*). **^{13}C{^{1}H} NMR (100.6 MHz, C_6D_6)** δ = 147.4 (*o*-C), 147.2 (*o*-C), 143.3 (N*C*N,[detected by heteronuclear multiple bond correlation (HMBC) spectroscopy]), 133.3 (*ipso*), 129.4 (*p*-C), 123.71 (*m*-C), 123.67 (*m*-C), 116.3 (N(*C*H)$_2$N), 34.6 (dd, P-Cy(H), $^{1}J_{P\text{-}C}$ = 58.3; $^{3}J_{P\text{-}C}$ = 5.2 Hz), 26.9 (d, Cy, $^{3}J_{P\text{-}C}$ = 11.4 Hz), 26.4 (dd, Cy, $^{2}J_{P\text{-}C}$ = 6.4 Hz, $^{4}J_{P\text{-}C}$ = 1.8 Hz), 26.0 (P-CH(CH_2)$_2$*C*H$_2$), 25.12 & 25.09 (CH_3), 23.5 & 23.2 (CH_3). **^{31}P{^{1}H} NMR (162 MHz, C_6D_6)** δ = 25.5 (d, *P*Cy$_3$, 30 Hz) 25.1 (d, *P*(S)-N=P, 30 Hz). **FT-IR (KBr pellet, cm^{-1})** 2117 (N_3 stretch) **ESI-MS (m/z)** 802.4895 [**3.5$_{Cy}$ + H:** 802.4883 expected], 803.4925 [**3.5$_{Cy}$ + 2H:** 803.4961 expected], 824.4699 [**3.5$_{Cy}$ + Na:** 824.4703 expected], 840.4438 [**3.5$_{Cy}$ + K:** 840.4442 expected].

3.6.10 Synthesis of IPrNP(S)(N_3)($NPPh_3$) (**3.5$_{Ph}$**)

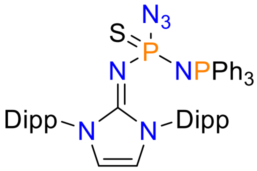

Method 1: in 1 mL solution of PPh_3 in C_6D_6 was added to **3.4S** and sealed in a J-Young NMR tube. The reaction was monitored periodically by $^{31}P\{^1H\}$ NMR spectroscopy and the sample was heated at 70 °C in an oil bath until complete consumption of starting PPh_3 and **4S** evident *via* $^{31}P\{^1H\}$ NMR spectroscopy. Volatiles were removed under vacuum to result in isolation of a sticky-oily residue. Trituration of this residue with 5 x 1 mL of pentane resulted in collection of a fine white powder. Method 2: Solid PPh_3 (42 mg, 0.16 mmol) was added to a stirring solution of **3.4S** (55 mg, 0.10 mmol) in 2 mL toluene at room temperature for 3 weeks. Two sequential recrystallizations from concentrated pentane solutions at -30 °C for 16 h and 2 h respectively, allowed for the isolation of a fine white powder free of PPh_3. (25 mg, 34 % yield).

^{1}H NMR (400 MHz, C_6D_6) δ = 7.62 (dd, 4H, *o*-Ph, 6.9 Hz and 17.2 Hz), 7.26 (t, 2H, *p*-H 7.6 Hz), 7.22 (d, 2H, *o*-H, 7.6 Hz), 7.15 (partially overlapped with solvent signal, 2H, *o*-H), 7.02 (partially overlapped with PPh_3, 3H), 6.98 (td, 6H, *m*-Ph, 2.8 Hz & 7.6 Hz), 6.14 (s, 2H, N(C*H*$_2$)$_2$N), 3.36 (septet, 2H, C*H*(CH_3)$_2$, 6.8 Hz), 3.29 (septet, 2H, C*H*(CH_3)$_2$, 6.8 Hz), 1.60 (d, 6H, CH_3, 6.8 Hz), 1.55 (d, 6H, CH_3, 6.8 Hz), 1.18 (d, 6H, CH_3, 7.6 Hz), 1.16 (d, 6H, CH_3, 7.6 Hz). **$^{13}C\{^1H\}$ NMR (100.6 MHz, C_6D_6)** δ = 147.5 (*o*-Dipp), 147.3(*o*-Dipp), 144.7 (confirmed by HMBC, N*C*N), 133.3 (ipso-Dipp), 133.0 (d, *o*-Ph, $^2J_{P\text{-}C}$ = 10.6 Hz), 131.1 (d, $^3J_{P\text{-}C}$ = 3.0 Hz, *m*-Ph), 129.6 (*p*-Dipp), 128.2 (d, *ipso*-Ph, $^1J_{P\text{-}C}$ = 17.0 Hz), 128.0 (br s, *p*-Ph), 124.0 (*m*-Dipp), 123.9 (*m*-Dipp), 116.2 (N(*C*H)$_2$N), 128.91 (*C*H(CH_3)$_2$), 128.89 (*C*H(CH_3)$_2$), 25.02 (CH(*C*H$_3$)$_2$), 24.97 (CH(*C*H$_3$)$_2$), 23.6 (CH(*C*H$_3$)$_2$), 23.5 (CH(*C*H$_3$)$_2$). **$^{31}P\{^1H\}$ NMR (162 MHz, C_6D_6)** δ = 31.1 (d, 36 Hz), 5.0 (d, 36 Hz). **FT-IR (KBr pellet, cm^{-1})** 2116 **ESI-MS (m/z)** 784.3520 [**3.5$_{Ph}$** + **H:** 784.3475 expected], 785.3549 [**3.5$_{Ph}$** + **2H**: 785.3553 expected], 806.3330 [**3.5$_{Ph}$** + **Na**: 806.3294 expected], 807.3371 [**3.5$_{Ph}$** + **H** + **Na**: 807.3372 expected].

3.6.11 Synthesis of IPrNP(S)(N_3)[NP(H)Cy_2] (**3.6a**) and IPrNP(S)(N_3)[N(H)PCy_2] (**3.6b**)

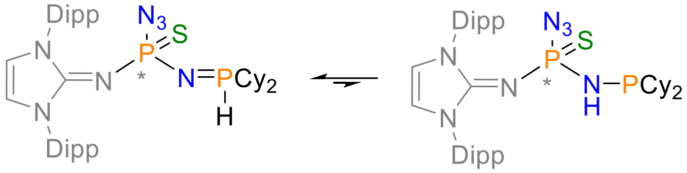

6a **6b**

$HPCy_2$ was added to a solution of **3.4S** in benzene and allowed to stir at room temperature over two days. Complete consumption of **3.4S** was determined *via* $^{31}P\{^1H\}$ NMR analysis. The volatiles were removed *in vacuo,* followed by a resuspension of the sticky residue in 8 mL hot pentane. Hot filtration was performed through a celite filter pipette, and the filtrate was subsequently concentrated approximately 4 mL *in vacuo*. Storage of the turbid solution at -30 °C for 1 week resulted in the formation of spherical crystals which were unsuitable for X-ray diffraction studies. Note: Due to the equilibrium of **3.6a** and **3.6b** in solution, the unambiguous assign each signa could not be performed, and resonances for the aryl, methyl, and the cyclohexyl groups for both species are overlapping. Fortunately, the backbone protons and P-H coupled signals are well separated and easily observed. A combination of 2-D NMR experimental spectra allowed for the partial assignment of individual isopropyl groups. **3.6a** and **3.6b** appear in a 2: 1 ratio in C_6D_6. Due to the flexible nature and the complexity of signals assigning cyclohexyl carbons, not all carbon signals could be unambiguously assigned. Unambiguous signals assignable *via* 2-D correlational spectra are reported below for their respective compounds. Ambiguously assigned "*C*H_2" cyclohexyl carbons were validated by phasing in heteronuclear single quantum coherence (HSQC) experiment: **$^{13}C\{^1H\}$ NMR (151 MHz, C_6D_6)** δ 27.50, 27.48, 27.42, 27.40, 27.37, 27.33, 27.29, 27.25, 27.21, 27.16, 26.91, 26.86, 26.76, 26.64, 26.53, 26.52, 26.45, 26.42, 26.34, 26.26, 26.25, 26.18, 25.97, 25.85. **FT-IR (KBr pellet, cm^{-1})** 2124 (N_3 stretch). **ESI-MS (m/z)** 720.4078 [**3.6 + H**: expected 720.4101], 742.3898 [**3.6 + Na**: expected 742.3920], 758.3637 [**3.6 + K**: expected 758.3659]. **Elemental Analysis** Calculated C 65.05; H 8.26; N 13.62; S 4.45. Found C 66.07; H 8.34; N 13.44; S 4.07.

3.6a: **^1H NMR (600 MHz, C_6D_6)** δ = 7.29 - 7.23 (m (overlapped with **3.6b**), 2H, *p*-Dipp), 7.22 - 7.12 (m (overlapped with 6b), 4H, *m*-Dipp), 6.27 (ddt, 1H, P-N=P(*H*), $^1J_{P\text{-}H}$ = 435.2 Hz, $^3J_{P\text{-}H}$ = 12.0 Hz, $^3J_{H\text{-}H}$ = 3.4 Hz), 6.13 (s, 2H, (NC*H*)$_2$), 3.38 (sept, 2H, C*H*(CH$_3$)$_{2,}$ 6.7 Hz), 3.25 (sept, 2H, C*H*(CH$_3$)$_{2,}$ 6.8 Hz), 1.66 (d (overlapped with Cy resonances), 6H, CH$_3$, 6.8 Hz), 1.58 (d (overlapped with Cy resonances), 6H, CH$_3$, 6.8 Hz), 1.17 (d (overlapped with Cy and **3.6b** methyl resonances), 6H, CH$_3$, 6.8 Hz), 1.15 (d (overlapped with Cy resonances), 6H, CH$_3$, 6.8 Hz), 1.92-0.38 (m (overlapped with methyl and pentane signals, 22H + 24H [43H found when excluding known regions of n-hexane and pentane). **^{13}C{^{1}H} NMR (151 MHz, C$_6$D$_6$)** δ = 147.9 (*o*-Dipp), 147.7 (*o*-Dipp), 145.8 (dd, N*C*N, ${}^2J_{\text{P-C}}$ = 11.2 Hz and ${}^4J_{\text{P-C}}$ = 2.8 Hz), 133.8 (*ipso*-Dipp), 130.05 (*p*-Dipp), 124.3 (overlapped with **3.6b**, *m*-Dipp), 124.1 (*m*-Dipp), 116.7 (N(*C*H)$_2$N), 33.8 – 33.4, multiplet, P-C$_{\text{cy}}$’ ${}^1J_{\text{P-C}}$ approximately 28 Hz, ${}^3J_{\text{P-C}}$ approximately 4 Hz), 33.1 (dd, P-C$_{\text{cy,}}$ ${}^1J_{\text{P-C}}$ = 31.6 Hz and ${}^3J_{\text{P-C}}$ = 4.3 Hz), 29.7 (d, P-CH(*C*H$_2$)$_2$, ${}^2J_{\text{P-C}}$ = 20.1 Hz), 29.3 ([overlapped with **3.6b**], *C*H(CH$_3$)$_2$), 29.1 ([overlapped with **3.6b**], *C*H(CH$_3$)$_2$), 28.9 (d, P-CH(*C*H$_2$)$_2$, ${}^2J_{\text{P-C}}$ = 20.1 Hz), 25.6 (CH$_3$), 25.5 (CH$_3$), 25.5(CH$_3$), 25.3(CH$_3$), 24.1 (CH$_3$), 23.8 (CH$_3$). **^{31}P{^{1}H} (243 MHz, C$_6$D$_6$)** δ = 39.1 (d, 1P, *P*(S), ${}^2J_{\text{P-P}}$ =12.8 Hz), 24.4 (d, 1P, *P*(H)Cy$_{2,}$ ${}^2J_{\text{P-P}}$ =12.8 Hz). **^{31}P (243 MHz, C$_6$D$_6$)** δ = 39.1 (dd, 1P, *P*(S), ${}^2J_{\text{P-P}}$ =12.8 Hz, ${}^3J_{\text{P-H}}$ = 12.1 Hz), 24.4 (broad d, 1P, *P*(H)Cy$_2$, ${}^1J_{\text{P-H}}$ = 434 Hz).

3.6b: **^{1}H NMR (600 MHz, C$_6$D$_6$)** δ = 7.29 - 7.23 (m (overlapped with 6a), 2H, *p*-Dipp), 7.22 - 7.12 (m (overlapped with **3.6a**), 4H, *m*-Dipp), 6.08 (s, 2H, (NC*H*)$_2$), 3.20 (sept, 2H, C*H*(CH$_3$)$_{2,}$ 6.8 Hz), 3.12 (sept, 2H, C*H*(CH$_3$)$_{2,}$ 6.8 Hz), 2.77 (dd, 1H, PN(*H*)P, ${}^2J_{\text{P-H}}$ = 9.8 Hz & ${}^2J_{\text{P-H}}$ = 6.8 Hz), 1.60 (d (overlapped with Cy resonances), 6H, CH$_3$, 6.8 Hz), 1.57 (d (overlapped with Cy resonances), 6H, CH$_3$, 6.8 Hz), 1.12 (d (overlapped with Cy and **3.6a** methyl resonances), 6H, CH$_3$, 6.8 Hz), 1.09 (d (overlapped with Cy resonances), 6H, CH$_3$, 6.8 Hz), 1.69-1.06 (m (overlapped with methyl and pentane signals, 22H). **^{13}C{^{1}H} NMR (151 MHz, C$_6$D$_6$)** δ = 147.6 (*o*-Dipp), 147.4 (*o*-Dipp), 147.1 (d, N*C*N, ${}^2J_{\text{P-C}}$ = 11.0 Hz), 133.1 (*ipso*-Dipp), 130.6 (*p*-Dipp), 124.5 (*m*-Dipp), 124.3 (overlapped with **3.6a**, *m*-Dipp), 117.3 (N(*C*H)$_2$N), 36.5 (dt, P-C$_{\text{cy}}$, ${}^1J_{\text{P-C}}$ = 16.3 Hz and ${}^3J_{\text{P-C}}$ = 4.7 Hz), 32.6 (d, P-CH(*C*H$_2$)$_2$, ${}^2J_{\text{P-C}}$ = 19.0 Hz), 30.2 (d, P-CH(*C*H$_2$)$_2$, ${}^2J_{\text{P-C}}$ = 10.1 Hz), 29.3 ([overlapped with **3.6a**], *C*H(CH$_3$)$_2$), 29.1 ([overlapped with **3.6a**], *C*H(CH$_3$)$_2$), 25.6 (CH$_3$), 25.6 (CH$_3$), 25.2 (CH$_3$), 24.1 (CH$_3$), 24.0 (CH$_3$), 23.4 (CH$_3$). **^{31}P{^{1}H} (243 MHz, C$_6$D$_6$)** δ = 45.7 (d, 1P, *P*(S), ${}^2J_{\text{P-P}}$ = 56.5 Hz), 43.8(d, 1P, *P*Cy$_2$, ${}^2J_{\text{P-P}}$ = 56.5 Hz). **^{31}P (243 MHz, C$_6$D$_6$)** δ = 45.7 (dd, 1P, *P*(S), ${}^2J_{\text{P-P}}$ = 56.5 Hz, ${}^2J_{\text{P-H}}$ = 9.6 Hz), 43.8 (broad d, 1P, *P*Cy$_2$, ${}^2J_{\text{P-P}}$ = 56.5 Hz).

3.6.12 Synthesis of IPrNPN$_3$NPMe$_3$ (**3.7**)

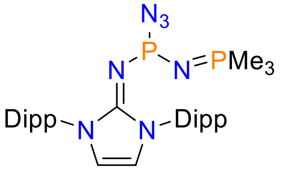

Method 1) to a solution of **3.2** (0.040 g, 0.077 mmol) in 2 mL benzene, a large excess of PMe$_3$ (ca. 150 μL, 1.5 mmol) was added neat to the stirred solution. The reaction progress was monitored by taking small aliquots for ^{31}P{^{1}H} NMR spectroscopic analysis. Complete consumption of **3.2** was reached within 3 h at room temperature, then the solution was subsequently placed into a freezer at -30 °C for 5 min. The frozen mixture was quickly placed under vacuum within a pre-cooled cold well, and the excess PMe$_3$ and solvent were removed while maintaining a low temperature, resulting in the isolation of a very pale yellow solid (0.030 g, 69 % yield). Note: Attempts to isolate **3.7** following analogous procedures to **3.5**$_{\mathbf{R}}$ using hexanes washes resulted in decomposition. Both the undissolved residue and the hexanes rising contained the same decomposition product as the major species, determined by ^{31}P{^{1}H} NMR spectroscopy.

^{1}H NMR (400 MHz, C$_6$D$_6$) δ = 7.23 (t, 2H, *p*-Dipp, 7.0 Hz), 7.14-7.05 (m, 4H, *m*-Dipp), 5.96 (s, 2H, N(*C*H$_2$)$_2$N), 3.33-3.17 (br m, 2H, C*H*(CH$_3$)$_2$), 3.17-3.04 (br m, 2H, C*H*(CH$_3$)$_2$), 1.52-1.43 (br m, 12H, CH$_3$, 9.2 Hz), 1.17 (d, 12 H, CH$_3$, 7.1 Hz), 0.80 (d, 9H, NP(C*H*$_3$)$_3$, 13.7 Hz). **^{13}C{^{1}H} NMR (100.6 MHz, C$_6$D$_6$)** δ = 147.9 (br s, *o*-Dipp), 147.2 (br s, *o*-Dipp), 146.7 (d, N*C*N, 18.1 Hz), 134.2 (s, *ipso*-Dipp), 129.5 (s, *p*-Dipp), 123.6 (br s, *m*-Dipp), 123.5 (br s, *m*-Dipp), 115.1 (N(*C*H$_2$)$_2$N), 28.9 (br s, *C*H(CH$_3$)$_2$), 24.6 (s, CH$_3$), 22.9 (br s, CH$_3$), 22.6 (br s, CH$_3$), 17.7 (dd, NP(*C*H$_3$)$_3$, $^{1}J_{\text{P-C}}$ = 65.7 Hz, $^{3}J_{\text{P-C}}$ = 5.7 Hz). **^{31}P{^{1}H} NMR (162 MHz, C$_6$D$_6$)** 133.1 (d, IPrN-*P*, $^{2}J_{\text{PP}}$ = 67 Hz), 11.4 (d, N*P*(CH$_3$)$_3$, $^{2}J_{\text{PP}}$ = 67 Hz). **FT-IR (KBr pellet, cm^{-1})** 2127 (antisymmetric N$_3$ stretch), 2064 (combination band of antisymmetric N$_3$ stretch: 1260 & 803 cm^{-1}), 1999 (combination band of antisymmetric N$_3$ stretch: 1260 & 739 cm^{-1} **ESI-MS (m/z)** 523.3126 [**3.7** - N$_3$: 523.3114 expected], 524.3158 [**3.7** + H - N$_3$: 524.3192 expected], 1103.6465 [2***3.7** + H - N$_2$: 1103.6435].

3.6.13 Reaction of **3.7** with Excess S_8 To Generate **3.5**$_{\mathbf{Me}}$

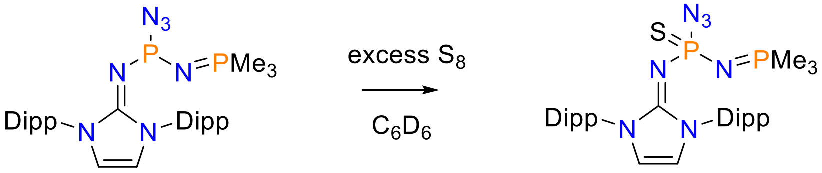

S_8 (12.0 mg, 0.0468 mmol) was weighed into a vial and was dissolved in 1 mL C_6D_6 then added to a vial containing minimally decomposed **3.7** (4.0 mg, 0.0071 mmol). The solution was transferred into an NMR tube and analyzed by ^{1}H and ^{31}P{^{1}H} NMR spectroscopy within 10 min of mixing. 200 μL of this solution was added to 800 μL of acetonitrile, then was filtered through filter pipette. 50 μL of this solution was then diluted to 1 mL in acetonitrile for ESI-MS analysis **(Appendix B-67**).

3.6.14 X-ray Crystallographic Data

A summary of X-ray diffraction collection and refinement data can be found in **Table 3-1**. Unless otherwise specified each sample was mounted on a Mitegen polyimide micromount with a small amount of Paratone N oil. X-ray measurements for compounds **3.2**, **3.4S**, and **3.4Se** were made on a Bruker Kappa Axis Apex2 diffractometer at a temperature of -163 °C, while X-ray measurements for **3.5**$_{\mathbf{Cy}}$ were made on a Bruker D8 Venture diffractometer at a temperature of -169 °C. The data collection strategy ω and φ scans, and data was collected up to 2θ values found in **Table 3-1**. The frame integrations were performed using SAINT.[66] The resulting raw data was scaled and absorption corrected using a multi-scan averaging of symmetry equivalent data using SADABS.[66,67] Unless otherwise stated, the structures were solved by using a dual space methodology using the SHELXT program.[68] All non-hydrogen atoms were obtained from the initial solution. The hydrogen atoms were introduced at idealized positions and were allowed to ride on the parent atom. The structural models were fit to the data using full matrix least-squares based on F^2. The calculated structure factors included corrections for anomalous dispersion from the usual tabulation. The structures were refined using the SHELXL program from the SHELX suite of crystallographic software.[68] Graphic plots were produced using the Mercury program.[69]

Structure Solution and Refinement: Unless otherwise stated, the structures were solved by using a dual space methodology using the SHELXT program.[68] All non-hydrogen atoms were obtained from the initial solution. The hydrogen atoms were introduced at idealized positions and were allowed to ride on the parent atom. The structural models were fit to the data using full matrix least-squares based on F^2. The calculated structure factors included corrections for anomalous dispersion from the usual tabulation. The structures were refined using the SHELXL program from the SHELX suite of crystallographic software.[68] Graphic plots were produced using the Mercury program.[69]

Table 3-1. Summary of X-ray diffraction collection and refinement details for compounds **3.2**, **3.4S**, **3.4Se**, and **3.5**$_{\mathrm{Cy}}$.

Formula	$C_{27}H_{36}N_9P$ **(3.2)**	$C_{27}H_{36}N_9PS$ **(3.4S)**	$C_{27}H_{36}N_9PSe$ **(3.4Se)**	$C_{45}H_{69}N_7P_2S$ **(3.5Cy)**
Formula Weight (g/mol)	517.62	549.68	596.58	802.07
Crystal Dimensions (mm)	0.367 × 0.231 × 0.179	0.348 × 0.134 × 0.133	0.310 × 0.214 × 0.096	0.300 × 0.295 × 0.082
Crystal Color and Habit	colourless prism	colourless prism	colourless prism	colourless plate
Crystal System	monoclinic	triclinic	triclinic	monoclinic
Space Group	C 2/c	P -1	P -1	P 21/n
Temperature, K	110	110	110	104
a, Å	16.898(5)	9.016(5)	9.031(3)	19.043(7)
b, Å	9.415(3)	9.366(4)	9.319(3)	13.049(4)
c, Å	17.739(6)	21.187(9)	21.348(6)	20.801(6)
a,°	90	92.568(10)	92.649(10)	90
b,°	90.651(12)	99.542(7)	99.111(8)	116.550(11)
g,°	90	114.087(18)	113.257(8)	90
V, Å^3	2822.0(15)	1598.1(13)	1617.9(8)	4624(3)
Z	4	2	2	4
F(000)	1104	584	620	1736
ρ (g/cm)	1.218	1.142	1.225	1.152
λ, Å, (MoKα)	0.71073	0.71073	0.71073	0.71073
μ, (cm^{-1})	0.13	0.182	1.24	0.177
Max 2θ for data collection, °	67.498	62.08	59.192	67.508
Measured fraction of data	0.998	0.998	0.999	0.999
R_{merge}	0.0474	0.0697	0.0588	0.0905
R_1	0.0448	0.0462	0.0407	0.0463
wR_2	0.1251	0.1168	0.0948	0.1146
R_1 (all data)	0.0596	0.0639	0.0582	0.0654
wR_2 (all data)	0.1372	0.1264	0.1018	0.1291
GOF	1.035	1.035	1.047	1.029

$R_1 = \Sigma \mid |F_o| - |F_c| \mid / \Sigma F_o$; $wR_2 = [\Sigma(w(F_o^2 - F_c^2)^2) / \Sigma w(F_o^4)]^{½}$; $GOF = [\Sigma(w(F_o^2 - F_c^2)^2) / (\text{No. of reflns.} - \text{No. of params.})]^{½}$

3.7 References

(1) Dehnicke, K.; Weller, F. Phosphorane Iminato Complexes of Main Group Elements. *Coord. Chem. Rev.* **1997**, *158*, 103–169. https://doi.org/10.1016/S0010-8545(97)90055-2.

(2) Palacios, F.; Aparicio, D.; Rubiales, G.; Alonso, C.; de los Santos, M. J. Synthetic Applications of Intramolecular Aza-Wittig Reaction for the Preparation of Heterocyclic Compounds. *Cur. Org. Chem.* **2009**, 810–828. https://doi.org/10.2174/138527209788167196.

(3) Lao, Z.; Toy, P. H. Catalytic Wittig and Aza-Wittig Reactions. *Beilstein J. Org. Chem.* **2016**, *12*, 2577–2587. https://doi.org/10.3762/bjoc.12.253.

(4) Ochiai, T.; Franz, D.; Inoue, S. Applications of N-Heterocyclic Imines in Main Group Chemistry. *Chem. Soc. Rev.* **2016**, *45* (22), 6327–6344. https://doi.org/10.1039/C6CS00163G.

(5) Kuhn, N.; Fawzi, R.; Steimann, M.; Wiethoff, J.; Bläser, D.; Boese, R. Synthese Und Struktur von 2-Imino-1,3-Dimethylimidazolin / Synthesis and Structure of 2-Imino-1,3-Dimethylimidazoline. *Z. Naturforsch. B.* **1995**, *50* (12), 1779–1784. https://doi.org/10.1515/znb-1995-1202.

(6) Kuhn, N.; Fawzi, R.; Steimann, M.; Wiethoff, J. Derivate Des Imidazols, XVII. Synthese Und Eigenschaften von Dichlor(1,3-Dimethyl-2-Imidazol-2-Ylidenimino)-Phosphan – Ein Methylenamino-Substituent Mit Ungewöhnlichen Donoreigenschaften. *Chem. Ber.* **1996**, *129* (4), 479–482. https://doi.org/10.1002/cber.19961290418.

(7) Staudinger, H.; Meyer, J. Über Neue Organische Phosphorverbindungen III. Phosphinmethylenderivate Und Phosphinimine. *Helv. Chim. Acta* **1919**, *2* (1), 635–646. https://doi.org/10.1002/hlca.19190020164.

(8) Gololobov, Y. G.; Zhmurova, I. N.; Kasukhin, L. F. Sixty Years of Staudinger

Reaction. *Tetrahedron* **1981**, *37* (3), 437–472. https://doi.org/10.1016/S0040-4020(01)92417-2.

(9) Tian, W. Q.; Wang, Y. A. Mechanisms of Staudinger Reactions within Density Functional Theory. *J. Org. Chem.* **2004**, *69* (13), 4299–4308. https://doi.org/10.1021/jo049702n.

(10) Leffler, J. E.; Temple, R. D. Staudinger Reaction between Triarylphosphines and Azides. Mechanism. *J. Am. Chem. Soc.* **1967**, *89* (20), 5235–5246. https://doi.org/10.1021/ja00996a027.

(11) Bebbington, M. W. P.; Bourissou, D. Stabilised Phosphazides. *Coord. Chem. Rev.* **2009**, *253* (9), 1248–1261. https://doi.org/10.1016/j.ccr.2008.08.009.

(12) Hinz, A.; Schulz, A.; Villinger, A.; Wolter, J.-M. Cyclo-Pnicta-Triazanes: Biradicaloids or Zwitterions? *J. Am. Chem. Soc.* **2015**, *137* (11), 3975–3980. https://doi.org/10.1021/jacs.5b00959.

(13) Seidl, M.; Kuntz, C.; Bodensteiner, M.; Timoshkin, A. Y.; Scheer, M. Reaction of Tungsten–Phosphinidene and –Arsinidene Complexes with Carbodiimides and Alkyl Azides: A Straightforward Way to Four-Membered Heterocycles. *Angew. Chem. Int. Ed.* **2015**, *54* (9), 2771–2775. https://doi.org/10.1002/anie.201410191.

(14) Alexandrova, A. V; Mašek, T.; Polyakova, S. M.; Císařová, I.; Saame, J.; Leito, I.; Lyapkalo, I. M. Synthesis of Electron-Rich Sterically Hindered P_1 Phosphazene Bases by the Staudinger Reaction. *Eur. J. Org. Chem.* **2013**, *2013* (9), 1811–1823. https://doi.org/10.1002/ejoc.201201400.

(15) Bock, H.; Schnöller, M. Proof of $N_\gamma N_\beta$-Elimination from Staudinger Adducts $R_3P{=}N_\gamma$-N_β-N_α-X by ^{15}N-Isotopic Labeling. *Angew. Chem. Int. Ed.* **1968**, *7* (8), 636. https://doi.org/10.1002/anie.196806361.

(16) Riesel, L.; Friebe, R.; Sturm, D. Synthesis and Reactivity of N-Phosphanyl Phosphazenes. *Phosphorus. Sulfur. Silicon Relat. Elem.* **1993**, *76* (1–4), 207–210. https://doi.org/10.1080/10426509308032395.

(17) Widauer, C.; Grützmacher, H.; Shevchenko, I.; Gramlich, V. Insights into the Staudinger Reaction: Experimental and Theoretical Studies on the Stabilization of Cis-Phosphazides. *Eur. J. Inorg. Chem.* **1999**, *1999* (10), 1659–1664. https://doi.org/10.1002/(SICI)1099-0682(199910)1999:10<1659::AID-EJIC1659>3.0.CO;2-I.

(18) Wilson, W. W.; Clough, A. J.; Haiges, R.; Rahm, M.; Christe, K. O. Syntheses of Diphenylaminodiazidophosphane and Diphenylaminofluoroazidophosphane. *Inorg. Chem.* **2015**, *54* (24), 11859–11867. https://doi.org/10.1021/acs.inorgchem.5b02097.

(19) Weigand, J. J.; Feldmann, K.-O.; Henne, F. D. Carbene-Stabilized Phosphorus(III)-Centered Cations $[LPX_2]^+$ and $[L_2PX]^{2+}$ (L = NHC; X = Cl, CN, N_3). *J. Am. Chem. Soc.* **2010**, *132* (46), 16321–16323. https://doi.org/10.1021/ja106172d.

(20) Riesel, L.; Friebe, R.; Bergemann, A.; Detlef/Sturm. Azidophosphanes: Attractive Starting Materials for the Preparation of Phosphazenes. *Heteroat. Chem.* **1991**, *2* (4), 469–472. https://doi.org/10.1002/hc.520020408.

(21) Götz, N.; Herler, S.; Mayer, P.; Schulz, A.; Villinger, A.; Weigand, J. J. On the Staudinger Reaction of $SP(N_3)_3$ with PPh_3 and$(Me_3Si)_2N–(Me_3Si)N–PPh_2$. *Eur. J. Inorg. Chem.* **2006**, *2006* (10), 2051–2057. https://doi.org/10.1002/ejic.200501131.

(22) Roy, M. M. D.; Miao, L.; Ferguson, M. J.; McDonald, R.; Rivard, E. An Unexpected Staudinger Reaction at an N-Heterocyclic Carbene-Carbon Center. *Can. J. Chem.* **2018**, *96* (6), 543–548. https://doi.org/10.1139/cjc-2017-0607.

(23) Dielmann, F.; Back, O.; Henry-Ellinger, M.; Jerabek, P.; Frenking, G.; Bertrand, G.; Fabian, D.; Olivier, B.; Martin, H.-E.; Paul, J.; Gernot, F.; Guy, B. A Crystalline Singlet Phosphinonitrene: A Nitrogen Atom–Transfer Agent. *Science* **2012**, *337* (6101), 1526–1528. https://doi.org/10.1126/science.1226022.

(24) Schoeller, W.; Rozhenko, A. B. On the Stabilisation of a Singlet Nitrene by the Phosphaniminato and Related Imine-Type Substituents, a Quantum Chemical Investigation. *Eur. J. Inorg. Chem.* **2001**, *2001* (3), 845–850. https://doi.org/10.1002/1099-0682(200103)2001:3<845::AID-EJIC845>3.0.CO;2-N.

(25) Dielmann, F.; Bertrand, G. Reactivity of a Stable Phosphinonitrene towards Small Molecules. *Chem. Eur. J.* **2015**, *21* (1), 191–198. https://doi.org/10.1002/chem.201405430.

(26) Cowley, A. H.; Gabbai, F.; Schluter, R.; Atwood, D. New Approaches to the Generation of Phosphinidenes. *J. Am. Chem. Soc.* **1992**, *114* (8), 3142–3144. https://doi.org/10.1021/ja00034a073.

(27) Mardyukov, A.; Keul, F.; Schreiner, P. R. Isolation and Characterization of the Free Phenylphosphinidene Chalcogenides $C_6H_5P=O$ and $C_6H_5P=S$, the Phosphorous Analogues of Nitrosobenzene and Thionitrosobenzene. *Angew. Chem. Int. Ed.* **2020**, *59* (30), 12445–12449. https://doi.org/10.1002/anie.202004172.

(28) Eckhardt, A. K.; Riu, M.-L. Y.; Müller, P.; Cummins, C. C. Frustrated Lewis Pair Stabilized Phosphoryl Nitride (NPO), a Monophosphorus Analogue of Nitrous Oxide (N_2O). *J. Am. Chem. Soc.* **2021**, *143* (50), 21252–21257. https://doi.org/10.1021/jacs.1c11426.

(29) Eckhardt, A. K.; Riu, M.-L. Y.; Müller, P.; Cummins, C. C. Staudinger Reactivity and Click Chemistry of Anthracene (A)-Based Azidophosphine N_3PA. *Inorg. Chem.* **2022**, *61* (3), 1270–1274. https://doi.org/10.1021/acs.inorgchem.1c03753.

(30) Eckhardt, A. K.; Riu, M.-L. Y.; Ye, M.; Müller, P.; Bistoni, G.; Cummins, C. C. Taming Phosphorus Mononitride. *Nat. Chem.* **2022**, *14* (8), 928–934. https://doi.org/10.1038/s41557-022-00958-5.

(31) Wünsche, M. A.; Mehlmann, P.; Witteler, T.; Buß, F.; Rathmann, P.; Dielmann, F.

Imidazolin-2-Ylidenaminophosphines as Highly Electron-Rich Ligands for Transition-Metal Catalysts. *Angew. Chem. Int. Ed.* **2015**, *54* (40), 11857–11860. https://doi.org/10.1002/anie.201504993.

(32) Witteler, T.; Darmandeh, H.; Mehlmann, P.; Dielmann, F. Dialkyl(1,3-Diarylimidazolin-2-Ylidenamino)Phosphines: Strongly Electron-Donating, Buchwald-Type Phosphines. *Organometallics* **2018**, *37* (18), 3064–3072. https://doi.org/10.1021/acs.organomet.8b00439.

(33) Cabré, A.; Riera, A.; Verdaguer, X. P-Stereogenic Amino-Phosphines as Chiral Ligands: From Privileged Intermediates to Asymmetric Catalysis. *Acc. Chem. Res.* **2020**, *53* (3), 676–689. https://doi.org/10.1021/acs.accounts.9b00633.

(34) Eckart, A.; Lux, K.; Karaghiosoff, K. Iminophosphoranyl Dichlorophosphines R_3PNPCl_2. *Z. Anorg. Allg. Chem.* **2014**, *640* (5), 962–967. https://doi.org/10.1002/zaac.201300518.

(35) Nguyen, T. B. Convenient Synthesis of Triphenylphosphine Sulfide from Sulfur and Triphenylphosphine. *Clean Technologies*. **2022**, 234–238. https://doi.org/10.3390/cleantechnol4020013.

(36) Buß, F.; Rotering, P.; Mück-Lichtenfeld, C.; Dielmann, F. Crystalline, Room-Temperature Stable Phosphine–SO_2 Adducts: Generation of Sulfur Monoxide from Sulfur Dioxide. *Dalton Trans.* **2018**, *47* (31), 10420–10424. https://doi.org/10.1039/C8DT01484A.

(37) McFarlane, W.; Rycroft, D. S. Studies of Organophosphorus Selenides by Heteronuclear Magnetic Triple Resonance. *J. Chem. Soc. Dalton Trans.* **1973**, No. 20, 2162–2166. https://doi.org/10.1039/DT9730002162.

(38) Muller, N.; Lauterbur, P. C.; Goldenson, J. Nuclear Magnetic Resonance Spectra of Phosphorus Compounds. *J. Am. Chem. Soc.* **1956**, *78* (15), 3557–3561. https://doi.org/10.1021/ja01596a002.

(39) Maraval, A.; Magro, G.; Maraval, V.; Vendier, L.; Caminade, A.-M.; Majoral, J.-

P. Functionalized Phosphorus Derivatives of Salpen-like Compounds: Synthesis and Preliminary Complexation Studies. *J. Organomet. Chem.* **2006**, *691* (7), 1333–1340. https://doi.org/10.1016/j.jorganchem.2005.12.022.

(40) Johnson, A. W. *Ylides and Imines of Phosphorus*; A Wiley-Interscience publication; Wiley, 1993.

(41) Paciorek, K. L. Preparation of Linear Phosphonitrilic Derivatives. *Inorg. Chem.* **1964**, *3* (1), 96–100. https://doi.org/10.1021/ic50011a020.

(42) Cupertino, D. C.; Keyte, R. W.; Slawin, A. M. Z.; Woollins, J. D. Synthesis and Coordination Chemistry of Tetrabutyldithioimidodiphosphinates. *Polyhedron* **1999**, *18* (5), 707–716. https://doi.org/10.1016/S0277-5387(98)00343-X.

(43) Currie, I.; Sleebs, B. E. Synthesis of Acyl Phosphoramidates Employing a Modified Staudinger Reaction. *Org. Lett.* **2021**, *23* (2), 464–468. https://doi.org/10.1021/acs.orglett.0c03987.

(44) Colquhoun, I. J.; McFarlane, W. Studies of Phosphorus–Phosphorus Nuclear-Spin Coupling in Species with Phosphorus–Nitrogen Bonds. *J. Chem. Soc. Dalton Trans.* **1977**, No. 17, 1674–1679. https://doi.org/10.1039/DT9770001674.

(45) Bhattacharyya, P.; Slawin, A. M. Z.; Williams, D. J.; Woollins, J. D. Monoxidised Sulfur and Selenium Derivatives of Bis(Diphenyl-Phosphino)Amine: Synthesis and Co-Ordination Chemistry. *J. Chem. Soc. Dalton Trans.* **1995**, No. 19, 3189–3194. https://doi.org/10.1039/DT9950003189.

(46) Ghisolfi, A.; Fliedel, C.; Rosa, V.; Pattacini, R.; Thibon, A.; Yu. Monakhov, K.; Braunstein, P. Solvent-Dependent Reversible Ligand Exchange in Nickel Complexes of a Monosulfide Bis(Diphenylphosphino)(N-Thioether)Amine. *Chem. Asian J.* **2013**, *8* (8), 1795–1805. https://doi.org/10.1002/asia.201300687.

(47) Tirreé, J.; Gudat, D.; Nieger, M.; Niecke, E. Reversible Tautomeric Transformation between a Bis(Amino)Cyclodiphosph(V)Azene and a Bis(Imino)Cyclodiphosph(V)Azane. *Angew. Chem. Int. Ed.* **2001**, *40* (16), 3025–

3028. https://doi.org/10.1002/1521-3773(20010817)40:16<3025::AID-ANIE3025>3.0.CO;2-E.

(48) Patureau, F. W.; Kuil, M.; Sandee, A. J.; Reek, J. N. H. METAMORPhos: Adaptive Supramolecular Ligands and Their Mechanistic Consequences for Asymmetric Hydrogenation. *Angew. Chem. Int. Ed.* **2008**, *47* (17), 3180–3183. https://doi.org/10.1002/anie.200705212.

(49) Terrade, F. G.; Lutz, M.; van der Vlugt, J. I.; Reek, J. N. H. Synthesis, Coordination Chemistry, and Cooperative Activation of H_2 with Ruthenium Complexes of Proton-Responsive METAMORPhos Ligands. *Eur. J. Inorg. Chem.* **2014**, *2014* (10), 1826–1835. https://doi.org/10.1002/ejic.201301215.

(50) Chu, X.; Yang, Y.; Lu, B.; Wu, Z.; Qian, W.; Song, C.; Xu, X.; Abe, M.; Zeng, X. Methoxyphosphinidene and Isomeric Methylphosphinidene Oxide. *J. Am. Chem. Soc.* **2018**, *140* (42), 13604–13608. https://doi.org/10.1021/jacs.8b09201.

(51) Tirrée, J.; Ruban, A. V; Nieger, M.; Li, C.; Nyulászi, L.; Niecke, E. Overcrowded Aminophospanitrenes: A Case Study. *Z. Naturforsch. B* **2017**, *72* (11), 865–871. https://doi.org/10.1515/znb-2017-0124.

(52) Becke, A. D. Density-Functional Exchange-Energy Approximation with Correct Asymptotic Behavior. *Phys. Rev. A* **1988**, *38* (6), 3098–3100. https://doi.org/10.1103/PhysRevA.38.3098.

(53) Lee, C.; Yang, W.; Parr, R. G. Development of the Colle-Salvetti Correlation-Energy Formula into a Functional of the Electron Density. *Phys. Rev. B* **1988**, *37* (2), 785–789. https://doi.org/10.1103/PhysRevB.37.785.

(54) Becke, A. D. A New Mixing of Hartree–Fock and Local Density-functional Theories. *J. Chem. Phys.* **1993**, *98* (2), 1372–1377. https://doi.org/10.1063/1.464304.

(55) Becke, A. D. Density-functional Thermochemistry. III. The Role of Exact Exchange. *J. Chem. Phys.* **1993**, *98* (7), 5648–5652.

https://doi.org/10.1063/1.464913.

(56) Weigend, F.; Ahlrichs, R. Balanced Basis Sets of Split Valence, Triple Zeta Valence and Quadruple Zeta Valence Quality for H to Rn: Design and Assessment of Accuracy. *Phys. Chem. Chem. Phys.* **2005**, *7* (18), 3297–3305. https://doi.org/10.1039/B508541A.

(57) Caldeweyher, E.; Bannwarth, C.; Grimme, S. Extension of the D3 Dispersion Coefficient Model. *J. Chem. Phys.* **2017**, *147* (3), 34112. https://doi.org/10.1063/1.4993215.

(58) Caldeweyher, E.; Ehlert, S.; Hansen, A.; Neugebauer, H.; Spicher, S.; Bannwarth, C.; Grimme, S. A Generally Applicable Atomic-Charge Dependent London Dispersion Correction. *J. Chem. Phys.* **2019**, *150* (15), 154122. https://doi.org/10.1063/1.5090222.

(59) Jafarpour, L.; Stevens, E. D.; Nolan, S. P. A Sterically Demanding Nucleophilic Carbene: 1,3-Bis(2,6-Diisopropylphenyl)Imidazol-2-Ylidene). Thermochemistry and Catalytic Application in Olefin Metathesis. *J. Organomet. Chem.* **2000**, *606* (1), 49–54. https://doi.org/10.1016/S0022-328X(00)00260-6.

(60) Hintermann, L. Expedient Syntheses of the N-Heterocyclic Carbene Precursor Imidazolium Salts IPr·HCl, IMes·HCl and IXy·HCl. *Beilstein J. Org. Chem.* **2007**, *3*, 22. https://doi.org/10.1186/1860-5397-3-22.

(61) Tamm, M.; Randoll, S.; Herdtweck, E.; Kleigrewe, N.; Kehr, G.; Erker, G.; Rieger, B. Imidazolin-2-Iminato Titanium Complexes: Synthesis, Structure and Use in Ethylene Polymerization Catalysis. *Dalton Trans.* **2006**, No. 3, 459–467. https://doi.org/10.1039/B511752F.

(62) Bräse, S.; Gil, C.; Knepper, K.; Zimmermann, V. Organic Azides: An Exploding Diversity of a Unique Class of Compounds. *Angew. Chem. Int. Ed.* **2005**, *44* (33), 5188–5240. https://doi.org/10.1002/anie.200400657.

(63) Neese, F.; Wennmohs, F.; Becker, U.; Riplinger, C. The ORCA Quantum

Chemistry Program Package. *J. Chem. Phys.* **2020**, *152* (22), 224108. https://doi.org/10.1063/5.0004608.

(64) Hanwell, M. D.; Curtis, D. E.; Lonie, D. C.; Vandermeersch, T.; Zurek, E.; Hutchison, G. R. Avogadro: An Advanced Semantic Chemical Editor, Visualization, and Analysis Platform. *J. Cheminform.* **2012**, *4* (1), 17. https://doi.org/10.1186/1758-2946-4-17.

(65) Lu, T.; Chen, F. Multiwfn: A Multifunctional Wavefunction Analyzer. *J. Comput. Chem.* **2012**, *33* (5), 580–592. https://doi.org/10.1002/jcc.22885.

(66) Bruker-AXS, SAINT Version 2013.8, 2013, Bruker-AXS, Madison, WI 53711, USA.

(67) Bruker-AXS, SADABS Version 2012.1, 2012, Bruker-AXS, Madison, WI 53711, USA.

(68) Sheldrick, G. M. SHELXT - Integrated Space-Group and Crystal-Structure Determination. *Acta Cryst A* **2015**, *71* (1). https://doi.org/10.1107/S2053273314026370.

(69) Macrae, C. F.; Bruno, I. J.; Chisholm, J. A.; Edgington, P. R.; McCabe, P.; Pidcock, E.; Rodriguez-Monge, L.; Taylor, R.; Van De Streek, J.; Wood, P. A. Mercury CSD 2.0 - New Features for the Visualization and Investigation of Crystal Structures. *J. Appl. Cryst.* **2008**. https://doi.org/10.1107/S0021889807067908.

(70) Calculations Were Performed by the LATTAN (Lattan.Py) Lattice Analysis Program Written by Paul D. Boyle. Unpublished (2022).

(71) Spek, A. L. PLATON SQUEEZE: A Tool for the Calculation of the Disordered Solvent Contribution to the Calculated Structure Factors. *Acta Crystallogr. Sect. C Struct. Chem.* **2015**, *71*. https://doi.org/10.1107/S2053229614024929.

Chapter 4

4 Facile Cyclopropenium Functionalization of PCl_3 and Redistribution of $RP(O)Cl_2$ Species with Bis(diisopropylamino)cyclopropenone

4.1 Introduction

Extensive studies have been conducted on isolable nitrogen-oxide species, including NO, N_2O, and NO_2, although the corresponding heavier Group 15 analogues such as PO and PO_2 have yet to be isolated as free compounds. Few higher order oxides, such as P_4O_6 have been characterized in the solid state,[1–3] while anhydrides like P_2O_5 have found application as desiccants given their strong affinity for water. Few examples of monomeric phosphenic chlorides have been isolated, but they have been studied in the vapour phase[4] and in frozen argon matrixies.[5] Stabilization of PO and phosphinidene oxides has been achieved within the coordination sphere of transition metals,[6] Lewis bases,[7] or as cationic phosphine oxides supported by two Lewis donors (**Figure 4-1**).

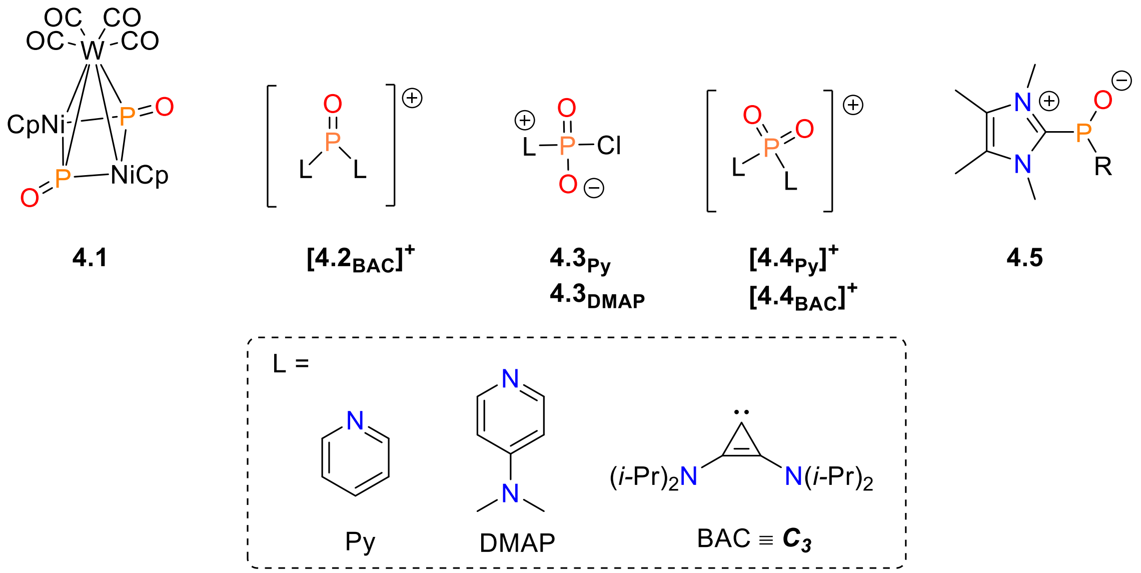
OC
CO
OC
W
CO
CpNi
P
O
P
NiCp
O
4.1
O
P
L
L
[4.2BAC]+
O
L
P
Cl
O
4.3Py
4.3DMAP
O
P
O
L
L
[4.4Py]+
[4.4BAC]+
N
N
P
O
R
4.5
L =
N
Py
N
N
DMAP
(i-Pr)2N
N(i-Pr)2
BAC ≡ C3

Figure 4-1. Selected examples of stabilized PO and PO_2 species.

Phosphoryl chloride ($POCl_3$) is a commonly employed precursor for preparing functionalized phosphine oxides. While there have been examples of "PO" or "PO_2" by reactions of $POCl_3$ with Lewis bases such as pyridine (**4.3_{Py}** or [**4.4_{Py}**]$^+$, **Figure 4-1**) and N,N-dimethylaminopyridine (DMAP; **4.3_{DMAP}** or **[4.4_{DMAP}]$^+$**, **Figure 4-1**),[8–10] these reports often lacked complete characterization often due to the inherent low solubilities of the poly-cationic species.[11] [**$4.4O_{DMAP}$]$^+$** was structurally characterized *via* single crystal X-ray diffraction (SC-XRD) analysis.[10] Despite the availability of precursor materials, further reactivity of these poly(onio)- PO and PO_2 stabilized cations remained under explored until Zhou *et al*. demonstrated ambiphilic reactivity of PO^+ and PO_2^+ cations supported by two bis(diisopropylamino)cyclopropylidene ligands (BAC; **[4.2_{BAC}]$^+$** and **[4.4_{BAC}]$^+$,** respectively; **Figure 4-1**).

The first example of a base-stabilized halogenated betaine (**4.3_R**) was obtained following the combination of $POCl_3$ and an NHC (NHC = 1,3-bis(isopropyl)-4,5-dimethylimidazol-2-ylidene) to yield [**4.6_{NHC}]Cl**, which then underwent a suggested partial hydrolysis to zwitterion **4.3_{NHC}** (**Scheme 4-1**).[12] A similar reaction between $POCl_3$ and DMAP was later shown to undergo base-induced dismutation to yield the analogous DMAP-adduct **$4.2O_{DMAP}$** without invoking a hydrolysis pathway.[10] This motif was also accessed by an unusual rearrangement and elimination of CH_3Cl (**$4.2Ch_R$**),[13,14] or by fluoride substitution of a cyclopropenium ligand from [**4.4_{BAC}]BF_4** to **4.9** (**Scheme 4-1)**.[15]

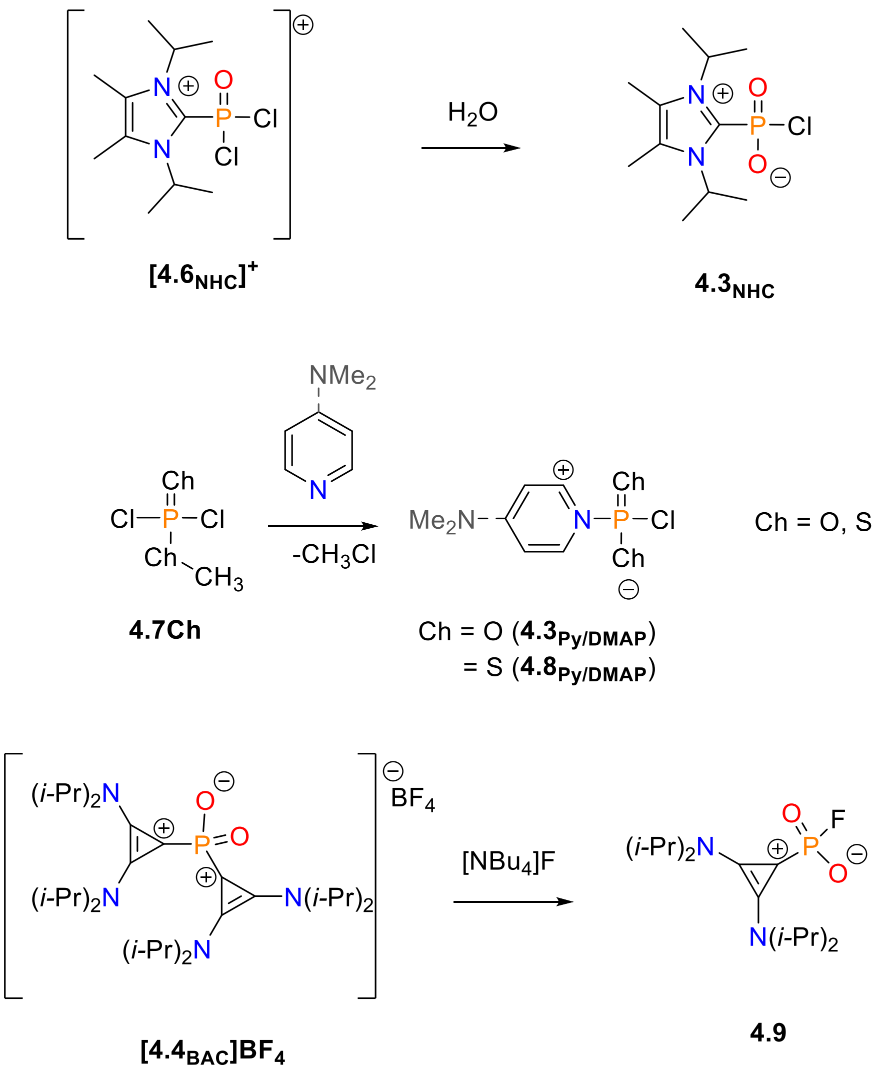

Scheme 4-1. Selected examples of halogenated phosphonates and their proposed formations.

Dioxophosphoranes (RPO_2), dithioxophosphoroanes (RPS_2), and diselenoxophosphoranes ($RPSe_2$) are three-coordinate phosphorus dichalcogenide species which often form oligomeric species (*e.g.* cyclic phosphonates). The most common route for the synthesis of cyclic phosphonates is by condensation reactions of $RP(O)(OH)_2$ and $RP(O)Cl_2$ (**Scheme 4-2**). Although only a few examples of cyclic phosphonates have been structurally characterized,[16–18] cyclic phosphonates have demonstrated versatility in ring opening polymerization or depolymerization reactions.[18–22] Monomeric RPS_2 and $RPSe_2$ species have been observed spectroscopically and structurally characterized (*e.g.*

4.10, **Figure 4-2**);[23,24] however, an analogous RPO_2 species remains elusive. Lawesson's reagent[25] (**LR**) and Woollin's reagent[26] (**WR**) possess a four-membered P_2Ch_4 core in the solid state and have been employed as sulfur and selenium transfer reagents with ketones to generate new C=Ch (where Ch = S, Se) bonds. The thionization mechanism with Lawesson's reagent has been determined to go through a highly reactive coordinatively unsaturated monomeric intermediate (**LR')**. A lighter oxygen analogue (**4.11**, **Figure 4-2**) was only recently reported in 2022, supported with bulky-terphenyl ligands.[21]

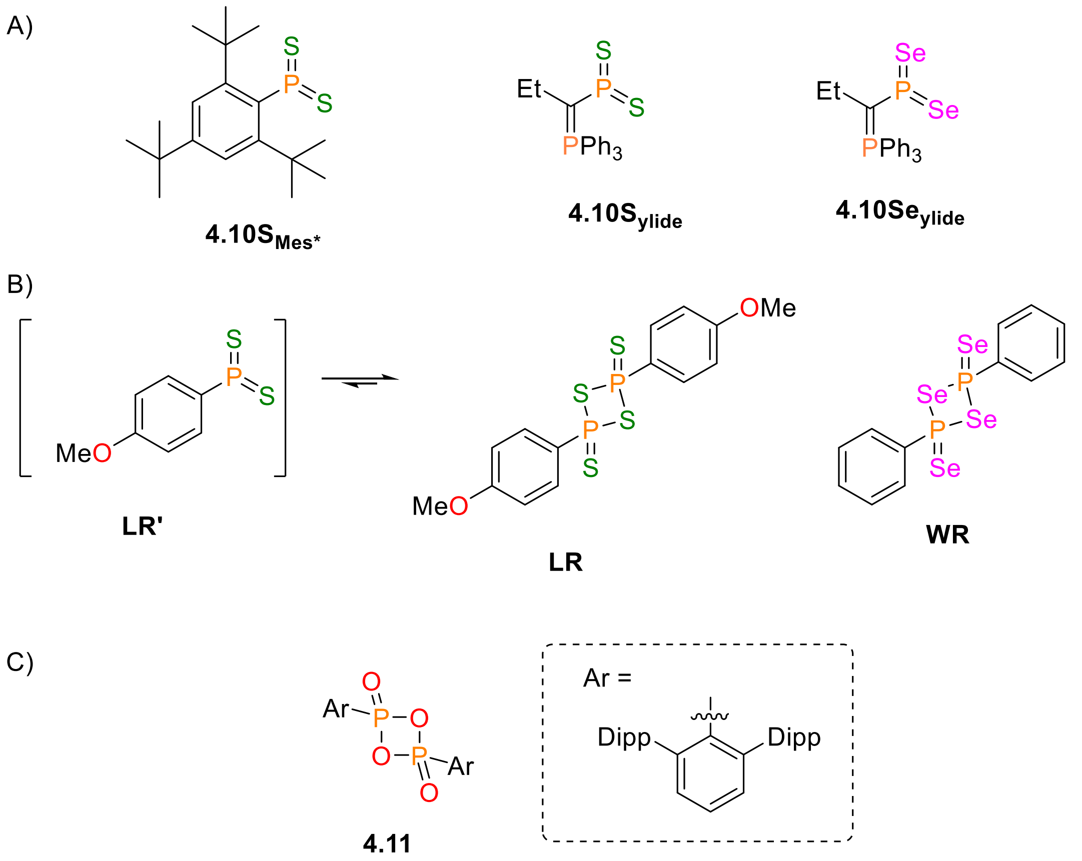
A)
S
P
S
4.10S$_{Mes*}$
S
Et
P
S
PPh$_3$
4.10S$_{ylide}$
Se
Et
P
Se
PPh$_3$
4.10Se$_{ylide}$
B)
S
P
S
MeO
LR'
OMe
S
S
P
S
P
S
MeO
LR
Se
P
Se
Se
P
Se
WR
C)
O
Ar
P
O
O
P
Ar
O
4.11
Ar =
Dipp
Dipp

Figure 4-2. Examples of dichalcogoxophosphoranes. A) Monomeric dithioxophosphoranes and diselenoxophosphorane.[23,24] B) Dimeric Lawesson's reagent (LR) and Woolen's reagent (WR).[25,26] C) Dimeric dioxophosphorane.[21]

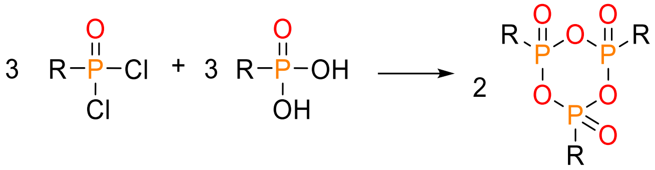

Scheme 4-2. Generic reaction of $RP(O)Cl_2$ and phosphonic acid to generate cyclic phosphonates.

An interesting class of ligands that have gained notoriety in transition metal complexes and bear an similar electronic structure to phosphorus-ylides (*i.e.* used to stabilize **4.10S$_{\mathbf{ylide}}$**, **Figure 4-2**) are bis(dialkylamino)cyclopropeniums (BAC).[27] The three-membered ring is uniquely stable due to the high symmetry, Hückel aromaticity, and resonance delocalization through the nitrogen atoms (**Figure 4-3**).[28] As a result of the unique stability, there have been multiple examples of isolated BAC transition-metal coordination complexes, while some complexes have been shown to participate in cyclopropylidene transfer reactions.[29,30] A previous study documented the deoxygenation of a diphenylcyclopropenone to generate a metallo-cyclopropylidene species (**4.13**,**Scheme 4-3**).[31] After careful literature searches, no examples of reactions between (dialkylamino)cyclopropenones and phosphines were found. Conversely, diphenylcyclopropenones undergo ring-open upon addition of PPh_3 as a nucleophile (**4.14**,**Scheme 4-3**).[32] The generation of an (amino)phosphinidene in the presence of an excess of the cyclopropenone resulted in multiple sequential ring-opening reactions (**4.16**, **Scheme 4-3**, bottom).[33] α-Cationic BAC coordinated phosphorus species have been explored for potential applications in catalysis.[34]

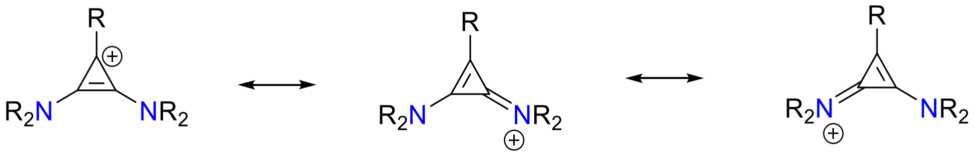

Figure 4-3. Resonance structures of BAC ligand.

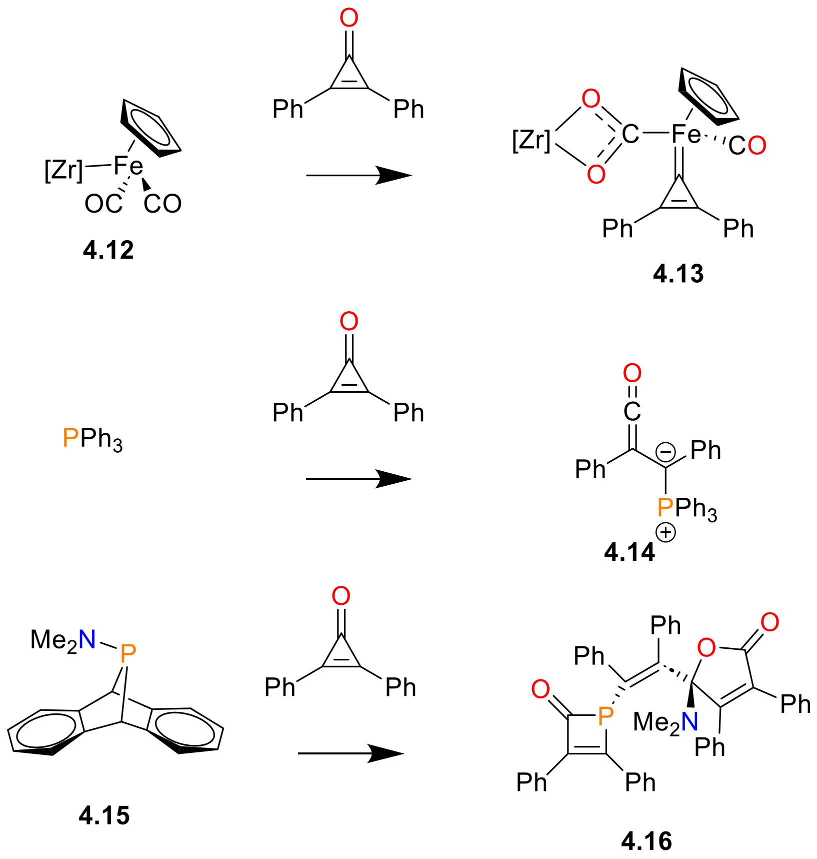

Scheme 4-3. Examples of reactions with diphenylcyclopropenone.[32–34]

In this chapter, the reactivity of bis(diisopropylamino)cyclopropenone (***C*$_3$*O***) and PCl_3 to generate a chlorophosphonate (**4.3**$_{\mathrm{BAC}}$) by sequential P-C bond formation and O/Cl_2 exchange is described. Expanding the application of this O/Cl_2 exchange methodology to simple aryl(dichloro)phosphine oxides resulted in the formation of cyclic phosphonates $(ArPO_2)_3$ (Ar = phenyl or 2,4,6-trimethylphenyl, **4.18**$_{\mathrm{Ar}}$). Preliminary reactivity studies of mixtures of **4.3**$_{\mathrm{BAC}}$ and **[*C*$_3$Cl]Cl**, as well as select reactions with purified **4.3**$_{\mathrm{BAC}}$ were performed (**Scheme 4-4**). ^1H and $^{31}P\{^1H\}$ NMR spectroscopies suggest that reactions between **4.3**$_{\mathrm{BAC}}$ and **[*C*$_3$Cl]Cl** with 4-dimethylaminopyridine (DMAP) or trimethylsilyl trifluoromethanesulfonate ($SiMe_3OTf$) produce a single phosphorus containing species; however, a general and reliable purification remained elusive.

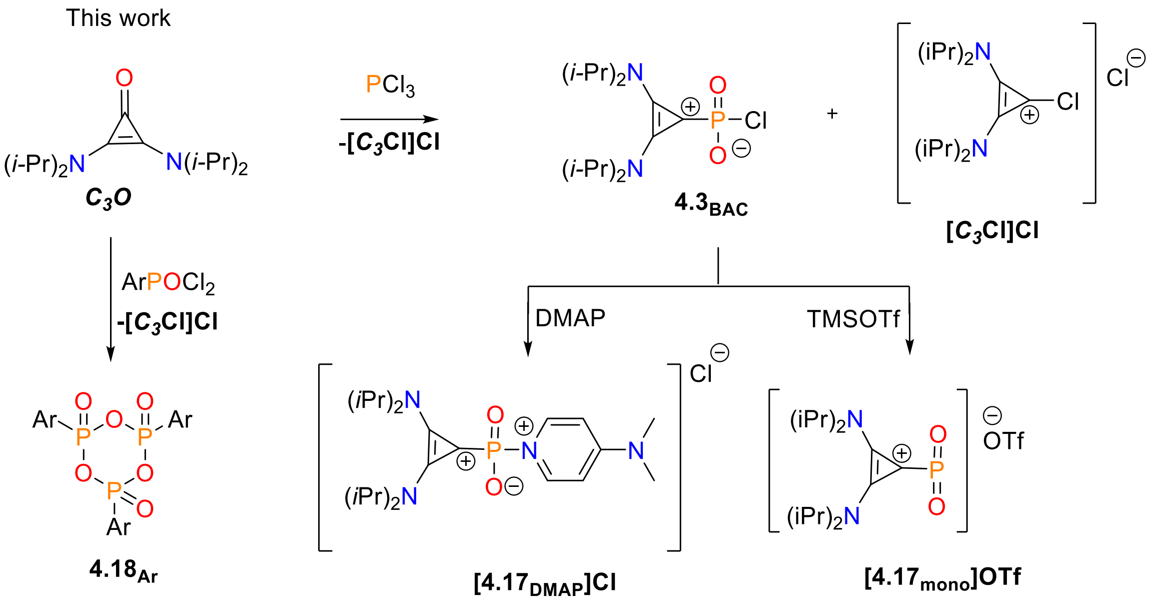

Scheme 4-4. Reactions of bis(diisopropylamino)cyclopropenone ***C_3O*** with PCl_3 or $ArPOCl_2$, and derivatization reactions of chlorophosphoante (**4.3BAC**).

4.2 Results and Discussion

4.2.1 Reaction of ***C_3O*** with *In Situ* Generated **[4.6BAC]Cl**

A new method for the synthesis of an α-cationic phosphoryl dichloride using cyclopropenone ***C_3O*** as a source for both an oxygen atom and the cyclopropylidene functional group was investigated. This approach aimed to establish a novel pathway for constructing modifiable phosphine-oxides supported by an α-cationic cyclopropenium ligand. PCl_3 was added to a toluene solution of ***C_3O***, which rapidly resulted in the precipitation of a white solid of a one-to-one ratio of betaine **4.3BAC** and **[*C_3*Cl]Cl** (**Scheme 4-5**). The reaction was successfully carried out on gram scale, without any notable impact on yield. A small portion of crystals of **4.3BAC** were isolated by Pasteur separation (*vide infra*, **Figure 4-4**), which allowed for definite assignment of resonances in the ^{1}H and $^{31}P\{^{1}H\}$ NMR spectra. Only the aliphatic carbon resonances were detected in the $^{13}C\{^{1}H\}$ NMR spectrum of isolated crystals of **4.3BAC** due to the low sensitivity of the carbon nuclei, but complete assignments were performed from concentrated samples containing a mixture of **4.3$_{\text{BAC}}$** and **[*C*$_3$Cl]Cl**. based on appearances of P-C coupling. ^{1}H and ^{13}C{^{1}H} NMR spectra aligned with reported resonances for **[*C*$_3$Cl]Cl**.[35]

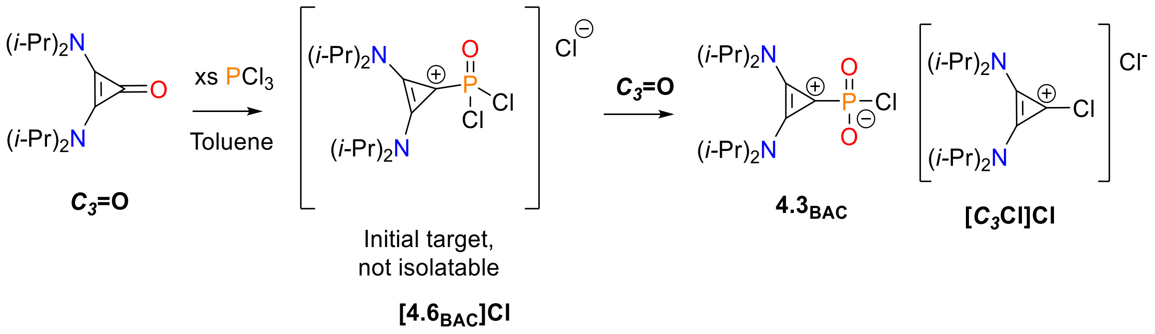
(i-Pr)2N
(i-Pr)2N
O
C3=O
xs PCl3
Toluene
(i-Pr)2N
(i-Pr)2N
O
P
Cl
Cl
Cl
Initial target,
not isolatable
[4.6BAC]Cl
C3=O
(i-Pr)2N
(i-Pr)2N
O
P
Cl
O
4.3BAC
(i-Pr)2N
(i-Pr)2N
Cl
Cl-
[C3Cl]Cl

Scheme 4-5. Reaction of PCl$_3$ and bis(diisopropylamino)cyclopropenone (***C*$_3$*O***).

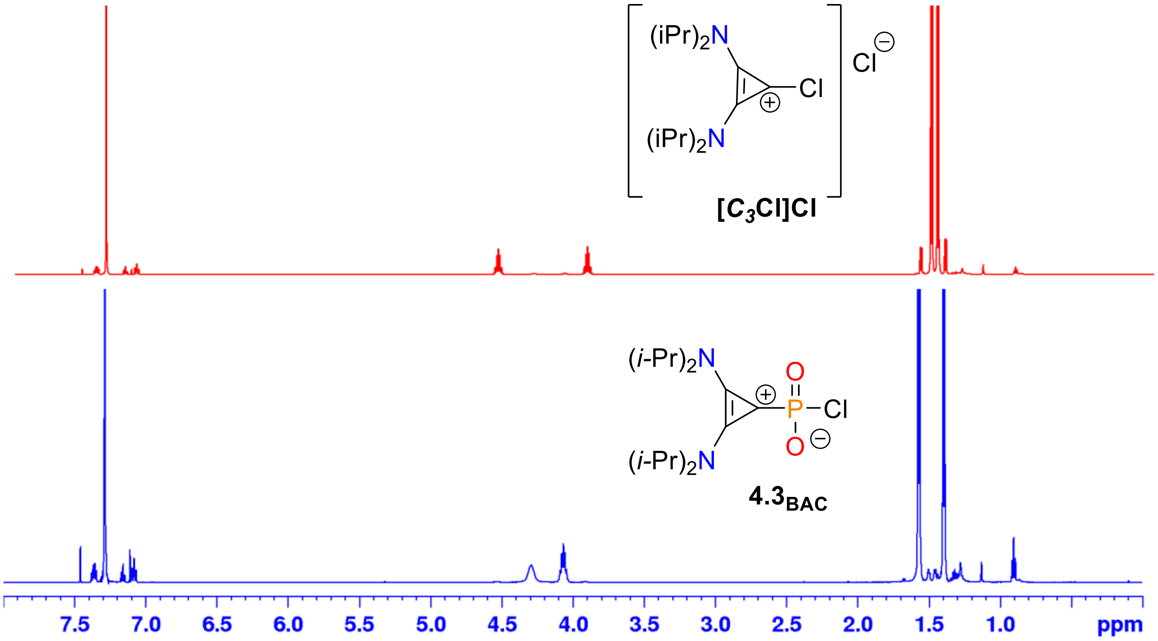

Figure 4-4. ^{1}H NMR spectra of isolated **[*C*$_3$Cl]Cl** (block-like crystal, top) and **4.3$_{\text{BAC}}$** (needle-like crystal, bottom) in CDCl$_3$.

Analysis of the mixture of by high-resolution ESI-MS (**Figure 4-5**) revealed a mass fragment for [**4.3$_{\text{BAC}}$ - Cl]$^+$** (*i.e.* **4.17$_{\text{mono}}$**, *vide infra*) and **[*C*$_3$Cl]$^+$**. Additionally, an adduct of ***C*$_3$*O*** and the intermediate **4.6$_{\text{BAC}}$** ([***C*$_3$*O*** + **4.6$_{\text{BAC}}$**]$^{+,}$ 605.35 m/z), along with monomeric and oligomeric hydrolysis products (**4.21$_{\text{mono}}$**, **4.21$_{\text{di}}$**, and **4.21$_{\text{tri}}$**, *vide infra*) were detected.

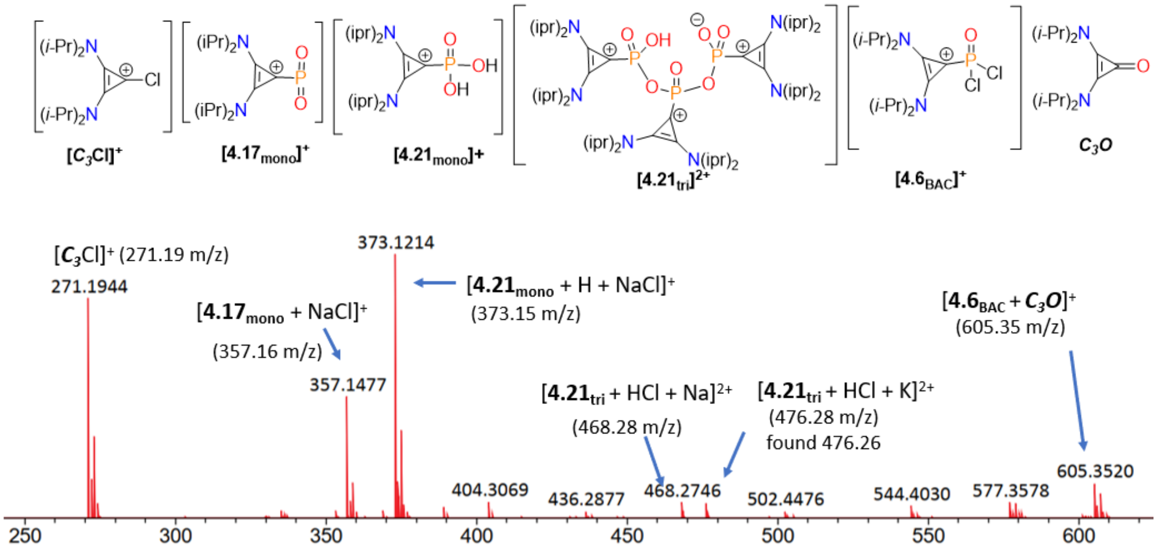

Figure 4-5. High-resolution mass spectrum of a sample containing **[*C*$_3$Cl]Cl** and **4.3BAC**, redissolved in acetonitrile.

Both **4.3BAC** and **[*C*$_3$Cl]Cl** demonstrated comparable solubilities in common organic solvents, specifically high solubility in polar aprotic solvents such as CH_3CN, $CHCl_3$, CH_2Cl_2, and THF. **4.3BAC** and **[*C*$_3$Cl]Cl** showed limited solubility in aromatic solvents, and were insoluble in aliphatic solvents. Crystals obtained through recrystallization of **4.3BAC** and **[*C*$_3$Cl]Cl** from concentrated fluorobenzene (PhF) solutions were manually separated. Careful inspection of the transparent, colourless crystal habits under a magnifying glass revealed that crystals of **[*C*$_3$Cl]Cl** often grew larger in three dimensions (block-like), while co-crystals of **4.3BAC·PhF** typically grew as single needles or plates. An additional qualitative feature used for separation was that crystals of **4.3BAC·PhF** turned cloudy during separation, likely due to desolvation of the co-crystallized fluorobenzene. Pasteur separation and sequential recrystallization allowed for isolation of 115 mg (9.9 % isolated yield) of **4.3BAC**. A more practical separation by dropwise addition of hexanes to a concentrated solution of **4.3BAC** in α,α,α-trifluorotoluene offered sporadic consistency in separation efficiency, but was inconsistent and a robust and highly repeatable procedure for efficient separation was not established. Employing the described method as an initial separation and a subsequent recrystallization from fluorobenzene afforded 80 mg of **4.3BAC**.

The presence and connectivity of both **4.3$_{\text{BAC}}$** and **[*C*$_3$Cl]Cl** were established directly and indirectly, with the collection of solid-state structures of **[*C*$_3$Cl]ClHCl**, **[*C*$_3$Cl]PCl$_4$**, and **4.3$_{\text{BAC}}$** (**Figure 4-6**). SC-XRD data of **[*C*$_3$Cl]ClHCl** revealed the basic nature of **[*C*$_3$Cl]Cl** and was plausibly formed following hydrolysis of the P-Cl bonds of **4.3$_{\text{BAC}}$,** which liberated HCl to form the three-center-four electron bonded $ClHCl^-$ ion. Recrystallization from a THF solution which contained residual PCl_3 resulted in the collection of a solid product. SC-XRD analysis of this product gave the solid-state structure of **[*C*$_3$Cl]PCl$_4$** with a hypervalent PCl_4^- anion. The equilibrium of $Cl^- + PCl_3 \rightleftharpoons PCl_4^-$ lies to the left in CH_2Cl_2 but the $^{31}P\{^1H\}$ resonance for PCl_4^- was observed in THF.

In the solid-state, the phosphonate species crystallizes as the neutral **4.3$_{\text{BAC}}$** with a weakly associated fluorobenzene. A comparison of the structure of **4.3$_{\text{BAC}}$** with the NHC adduct reported by Kuhn *et al*. was performed.[12] A negligible difference in the P-O bond lengths was observed; however, **4.3$_{\text{BAC}}$** possessed a contracted P-C bond (~0.27 Å) and an elongated P-Cl bond (~0.25 Å). This suggested that the BAC is a stronger σ-donor than the NHC. A subsequent comparison of **4.3$_{\text{BAC}}$** with the fluoride derivative (**4.9**) reported by Zhou *et al.* reveal negligible differences, besides a contracted P-X of the fluoride derivative.[15]

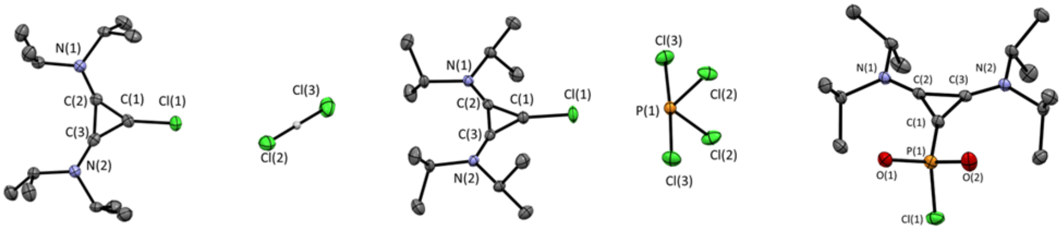

[*C*$_3$Cl]ClHCl **[*C*$_3$Cl]PCl$_4$** **3.4$_{\text{BAC}}$**

Figure 4-6. Mercury-rendered ORTEP style drawings of **[*C*$_3$Cl]ClHCl**, **[*C*$_3$Cl]PCl$_4$**, and **4.3$_{\text{BAC}}$**. Hydrogen atoms have been omitted for clarity and selected ellipsoids shown at the 50% probability level.

Structural confirmation of the neutral species **4.3_{BAC}** also demonstrated the utility of the cyclopropenone ***C_3O*** to generate a new P-C and two new P-O bonds (**Scheme 4-6**). Precedence for the formation of a P-C bond through the exchange of oxygen and chloride has been reported with tetramethyl urea and $POCl_3$.[11] The use of a sacrificial NHC to abstract two chlorides has also been used for generating E-C bonds of a cationic phosphenium ([**4.20_{NHC}]**Cl, **Scheme 4-6**).[36]

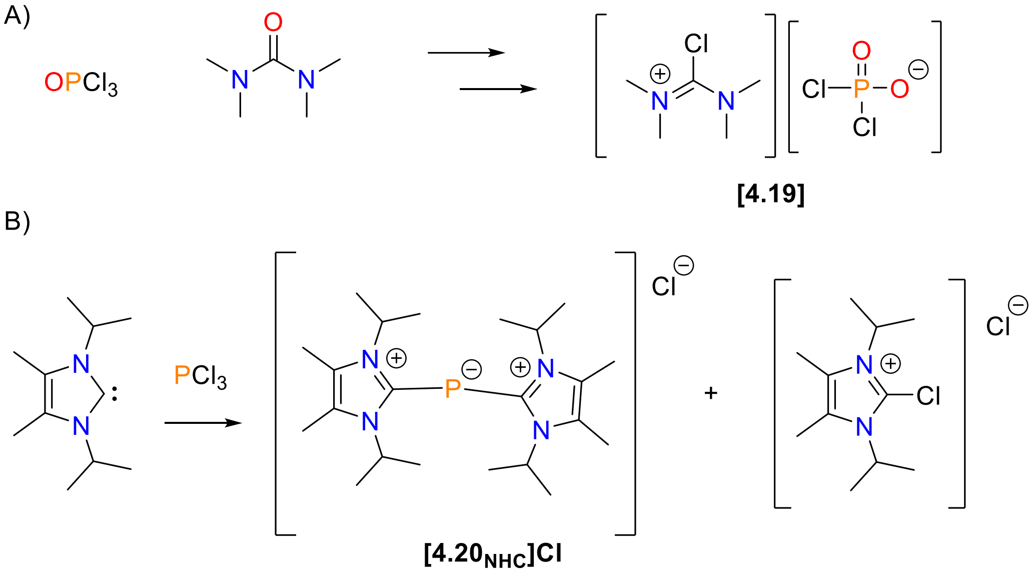

Scheme 4-6. Examples of chloride abstractions from chlorophosphines. A) Oxygen transfer and chloride abstraction of POCl3 with a urea.[11] B) chloride abstraction with an NHC.[36]

4.2.2 Stages of Hydrolysis of **4.3_{BAC}**

Compound **4.3_{BAC}** was sensitive to the presence of moisture, where samples dissolved in $CDCl_3$ slowly decomposed to **[4.21_{mono}]Cl** (δ_P = -8; **Scheme 4-7** and **Figure 4-7**) by exposure to air. Structural confirmation of the related **[4.21_{mono}]OTf** salt was also obtained during the course of this work (*vide infra*).

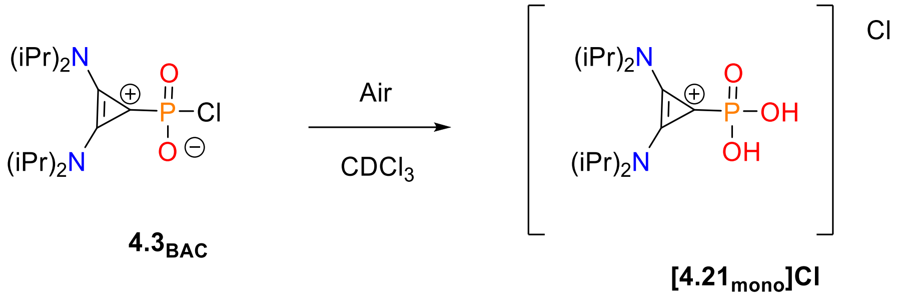
(iPr)$_2$N
(iPr)$_2$N
P
O
Cl
O
Air
CDCl$_3$
OH
OH
Cl
4.3$_{BAC}$
[4.21$_{mono}$]Cl

Scheme 4-7. Hydrolysis of **4.3$_{BAC}$** to **[4.21$_{mono}$]Cl**.

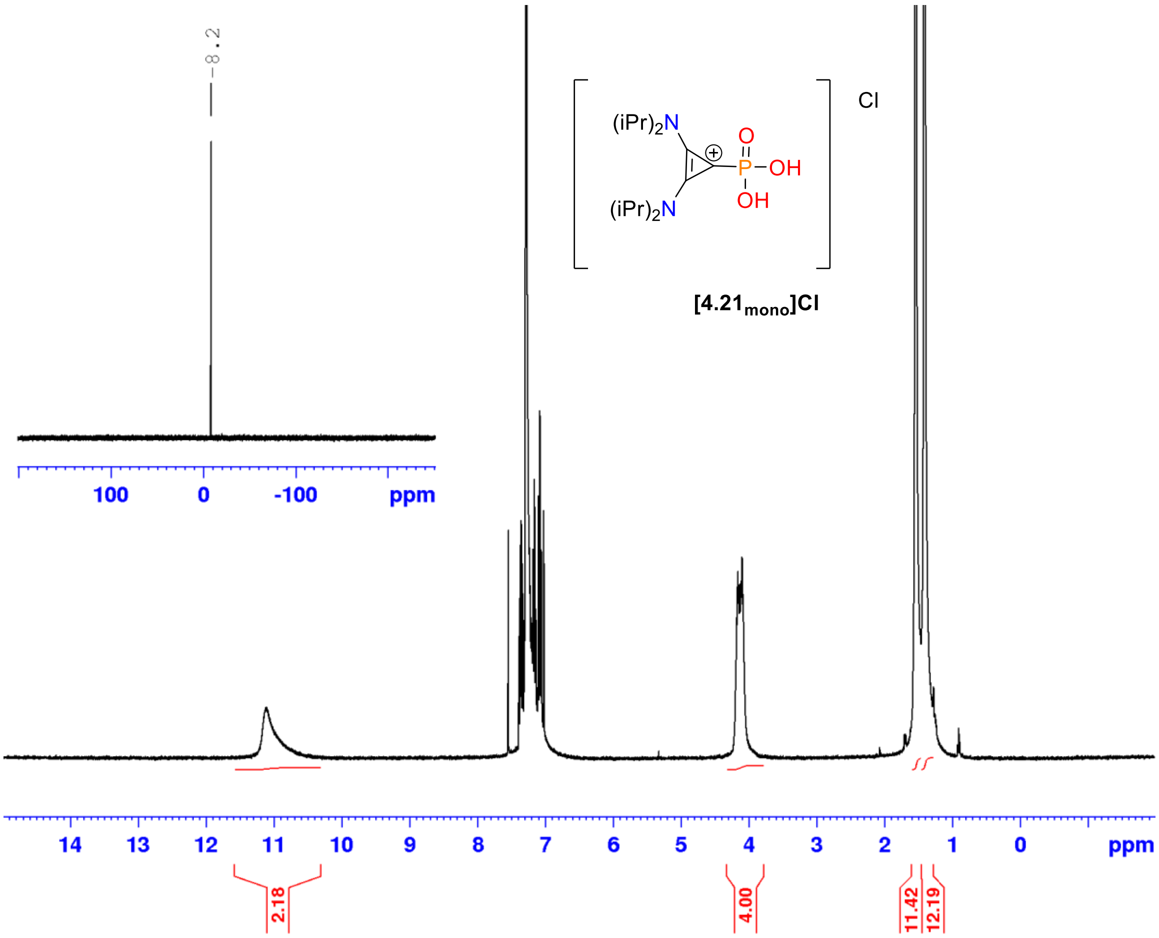

Figure 4-7. ^{1}H and ^{31}P{^{1}H} (inset) NMR spectra of **[4.21$_{mono}$]Cl** in CDCl$_3$, hydrolyzed in air.

^{1}H and ^{31}P{^{1}H} NMR spectroscopic analysis were caried out on a highly concentrated mixture of partially hydrolyzed **4.3$_{BAC}$** and **[*C*$_3$Cl]Cl**. The presence of a partially hydrolyzed species (**4.21$_{di}$**) was supported by a broad singlet at δ = 14.1 that corresponded to an acidic proton environment. Two major resonances belonging to **4.3**$_{\mathrm{BAC}}$ (δ_P = -14.3, 46 %) and **4.21**$_{\mathrm{di}}$ (δ_P = -19.5, 49 %), with four additional minor resonances were detected in a $^{31}P\{^{1}H\}$ experiment with 1024 scans. The ^{31}P-^{13}C satellites of the two major species were well defined and allowed for further structural distinction in solution (**Figure 4-8**). As expected from the solid-state structure of **4.3**$_{\mathrm{BAC}}$, the singlet at δ_P = -14.3 ppm is coupled to a ^{13}C nuclei only ($^{1}J_{31P\text{-}13C}$ =175 Hz), which suggested that **4.3**$_{\mathrm{BAC}}$ existed as a monomer in $CDCl_3$ at room temperature. The resonance for **4.21**$_{\mathrm{di}}$ (δ_P = -19.5) demonstrated a slightly larger P-C coupling constant ($^{1}J_{31P\text{-}13C}$ = 215 Hz) but was coupled to an additional phosphorus nuclei ($^{3}J_{31P\text{-}31P'}$ = 21 Hz). This phenomenon was a result of the low abundance of ^{13}C nuclei (ca. 1 % natural abundance) which induced a magnetic-inequivalence of chemically-equivalent phosphorus atoms. This magnetic inequivalence allowed for the indirect measurement of a P-P coupling constant from the ^{31}P-^{13}C-$^{31}P'(^{12}C)$ spin system in the symmetric species.[37] It was concluded that the partially hydrolyzed species **4.21**$_{\mathrm{di}}$ was present as a dimer in solution.

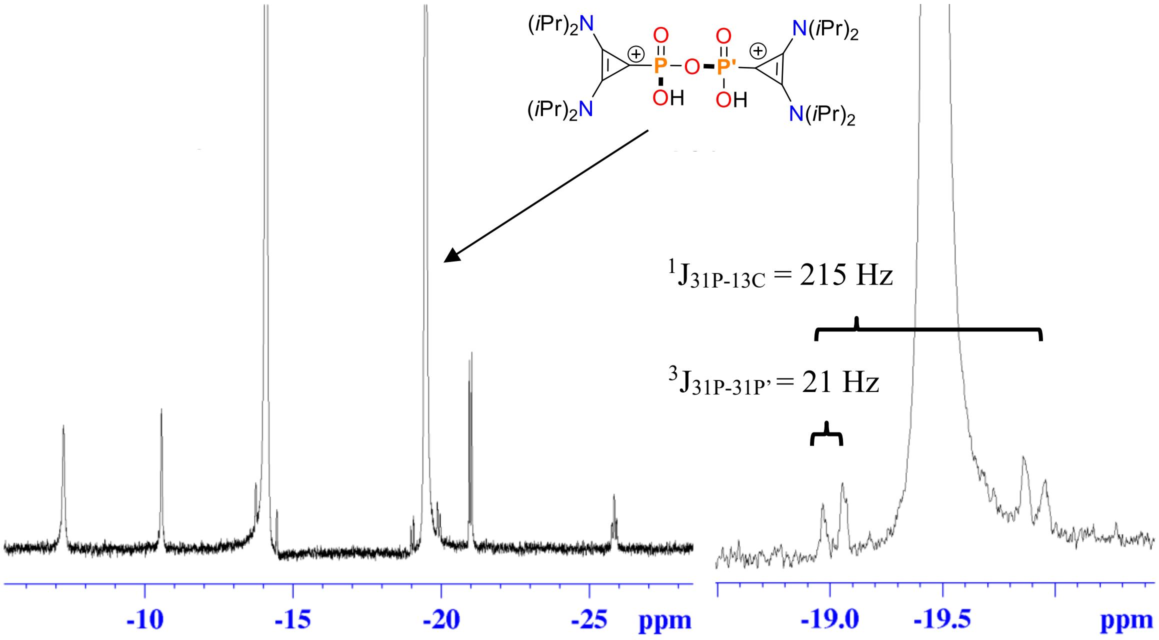

Figure 4-8. $^{31}P\{^{1}H\}$ spectrum of a partially hydrolyzed sample of **4.3**$_{\mathrm{BAC}}$ and **[C_3Cl]Cl**, redissolved in $CDCl_3$ in a J-Young NMR tube. Image on the right contains zoomed in signal for **4.21**$_{\mathrm{di}}$, and the labelled coupling values.

4.2.3 Mechanistic Investigations

The reaction of PCl_3 with two stoichiometric equivalents of ***C*₃*O*** was tracked by $^{31}P\{^1H\}$ NMR spectroscopy over 45 h (**Figure 4-9**) in $CDCl_3$ for which three resonances were detected: PCl_3 (δ_P = 219), an intermediate species (**[4.6BAC]Cl**, δ_P = -13.4), and **4.3BAC** (δ_P = -14.3). The concentration of the intermediate [**4.6BAC**]Cl was observed to increase to a maximum value after approximately 3 h, then decreased in concentration as the signal for **4.3BAC** continued to increase.

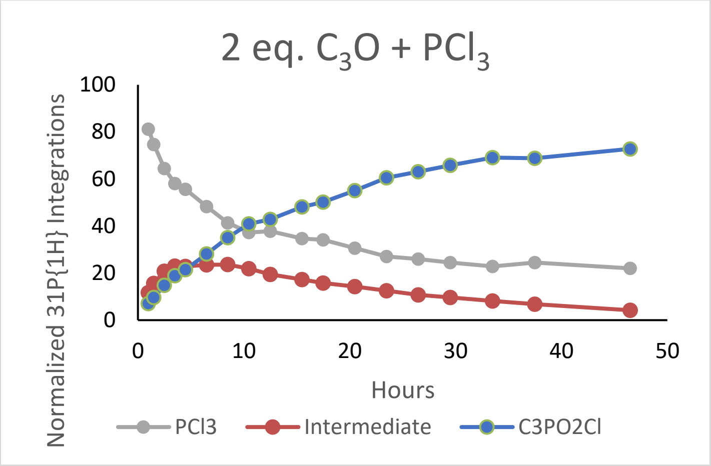

Figure 4-9. Plot of normalized $^{31}P\{^1H\}$ resonance integrations over time of a two-to-one reaction of bis(diisopropylamino)cyclopropenone (***C*₃*O***) and PCl_3.

Based on the detection of a single intermediate **[4.6BAC]Cl** in $CDCl_3$ and pathways known for phosphonate syntheses, it was suspected that the formation of **4.3BAC** proceeded *via* an Arbuzov type mechanism.[38,39] Two different pathways for the generation of **4.3BAC** (**Scheme 4-8**) were suggested. Pathway A would have involved a stoichiometric equivalent of **[4.6BAC]Cl**, which reacts with another stoichiometric equivalent of ***C*₃*O*** to generate a short-lived monomeric or dimeric species. A chloride may then attack the cyclopropenium bound to oxygen, which released a $[C_3Cl]^+$ as a leaving group. Pathway B involved dimerization of **[4.6BAC]Cl**. Rovnaník *et al.* reported base-induced dismutation of $POCl_3$ with DMAP in SO_2 which generated an analogous **4.3DMAP**.[10] The authors suggested that ionization of $POCl_3$ with DMAP generated [**4.6DMAP**]Cl (δ_P = 13), which exchanged with a second stoichiometric equivalent of

$POCl_3$ to generate **4.3$_{\text{DMAP}}$** (δ_P = -9) and PCl_5 (**Scheme 4-9**). It is worth recognizing both BAC and DMAP are strong σ-donating onio ligands.[10,12,15,36] Applying a similar treatment and proposal of transition state involving two phosphorus species, a plausible pathway involved an exchange of chloride and oxygen, that released PCl_3. Unlike the report by Rovnaník *et al.*, there was no evidence that the generation of **4.3$_{\text{BAC}}$** involved any generation of $POCl_3$, rather a redox-reaction and generation of PCl_3.

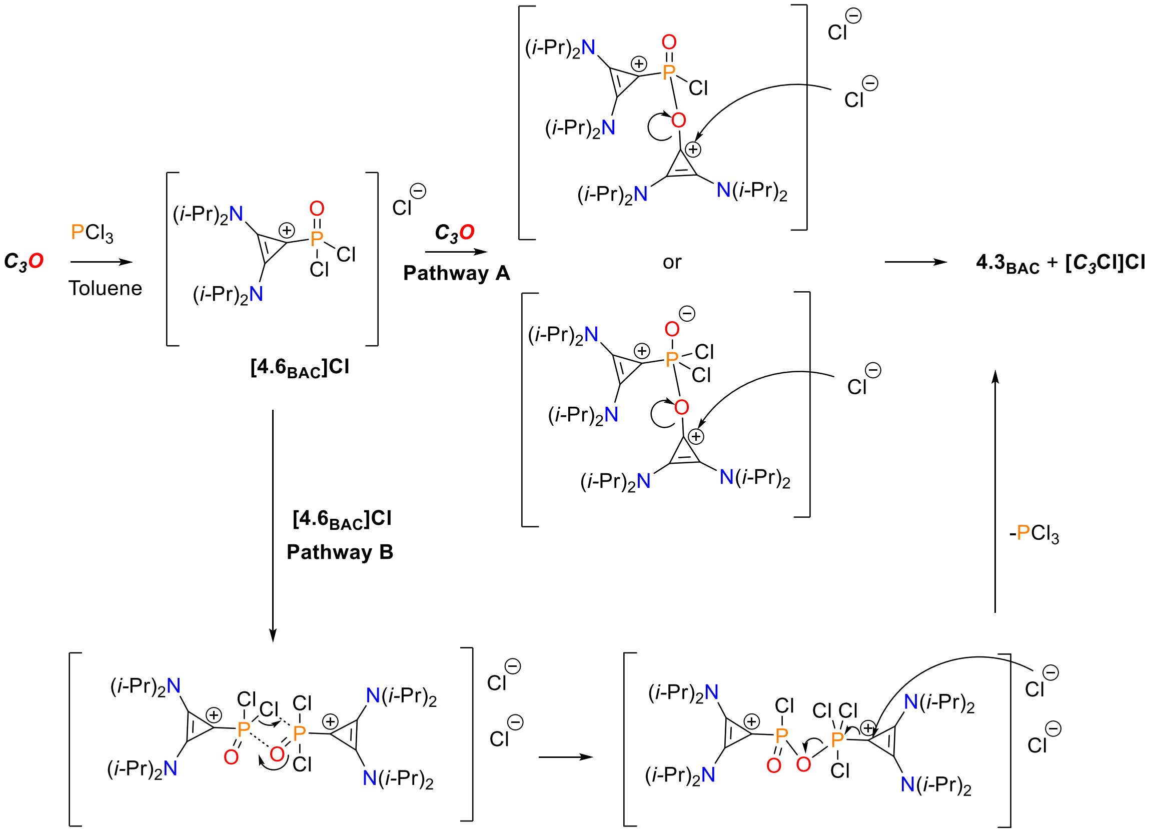
C3O
PCl3
Toluene
[4.6BAC]Cl
C3O
Pathway A
or
4.3BAC + [C3Cl]Cl
[4.6BAC]Cl
Pathway B
-PCl3
(i-Pr)2N
N(i-Pr)2
Cl
O
P

Scheme 4-8. Two plausible pathways for the generation of **4.3$_{\text{BAC}}$** *via* Arbuzov style eliminations of **[*C*$_3$Cl]Cl**.

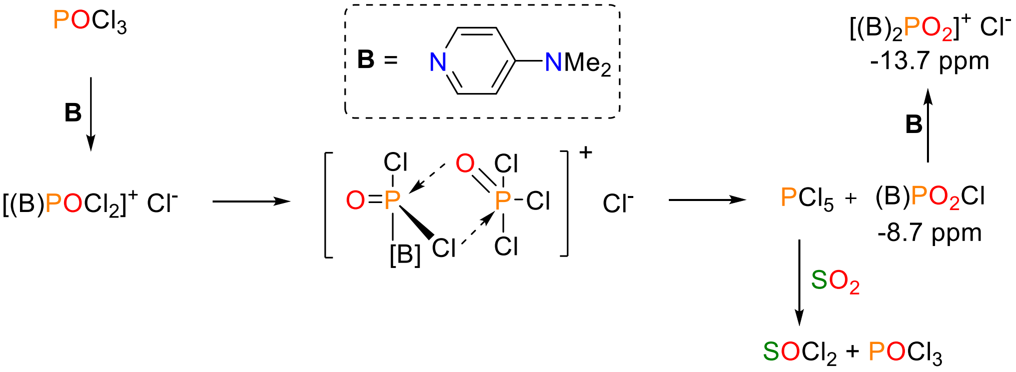

Scheme 4-9. Pathway suggested for base-induced dismutation of $POCl_3$ by DMAP.[10]

4.2.4 Reactivity of $\mathbf{4.3_{BAC}}$

In the absence of a robust separation method for species $\mathbf{4.3_{BAC}}$ and **[*C*₃Cl]Cl**, reactions of the 50:50 mixture of $\mathbf{4.3_{BAC}}$ and $\mathbf{[}\boldsymbol{C_3}\mathbf{Cl]Cl}$ were initially conducted, while selected reactions were later performed using isolated crystals of $\mathbf{4.3_{BAC}}$ (*vide infra*). This approach aimed to investigate the behaviour of the species in solution and explore a method of selective functionalization that could assist in the separation of the species. It is crucial to note that $\mathbf{[}\boldsymbol{C_3}\mathbf{Cl]Cl}$ had been reported to be stable to water but readily reacts with protic nucleophiles in the presence of a base, producing various monocationic bis- or tris-(dialkylamino)cyclopropenium species,[11] as well as reaction with nucleophiles such as PPh_3 to produce a dicationic species.[40] The reactivity of $\mathbf{[}\boldsymbol{C_3}\mathbf{Cl]Cl}$ was theorized to be independent of $\mathbf{4.3_{BAC}}$ for the initial reagents chosen. Changes in the $^{31}P\{^1H\}$ spectra were studied only to develop a relationship between chemical shift and possible structures of intermediates and products formed. The analysis of ^1H NMR spectra was not performed because of overlapping signals between multiple species and an inability to provide clarity into the chemistry at the phosphorus center.

Addition of *ca.* 1.1 stoichiometric equivalents of 95 % ethanol with the mixture of $\mathbf{4.3_{BAC}}$ and $\mathbf{[}\boldsymbol{C_3}\mathbf{Cl]Cl}$ resulted in the rapid consumption of the signal attributed to $\mathbf{4.3_{BAC}}$, and formation of a singlet in $^{31}P\{^1H\}$ spectrum (δ_P = -8, $\mathbf{4.22_{OEt}}$; **Figure 4-10**). This singlet expectedly split into a triplet ($^3J_{P\text{-}H}$ = 7.9 Hz) in a proton coupled experiment, consistent with generation of a P-OEt moiety. The formation of partially hydrolyzed ($\delta_P \approx$

-19, [**4.21$_{\mathbf{di}}$**]) and fully hydrolyzed **[4.21$_{\mathbf{mono}}$]Cl** ($\delta_P \approx$ -10, **[4.21$_{\mathbf{mono}}$]Cl**) were also detected (**Figure 4-10**).

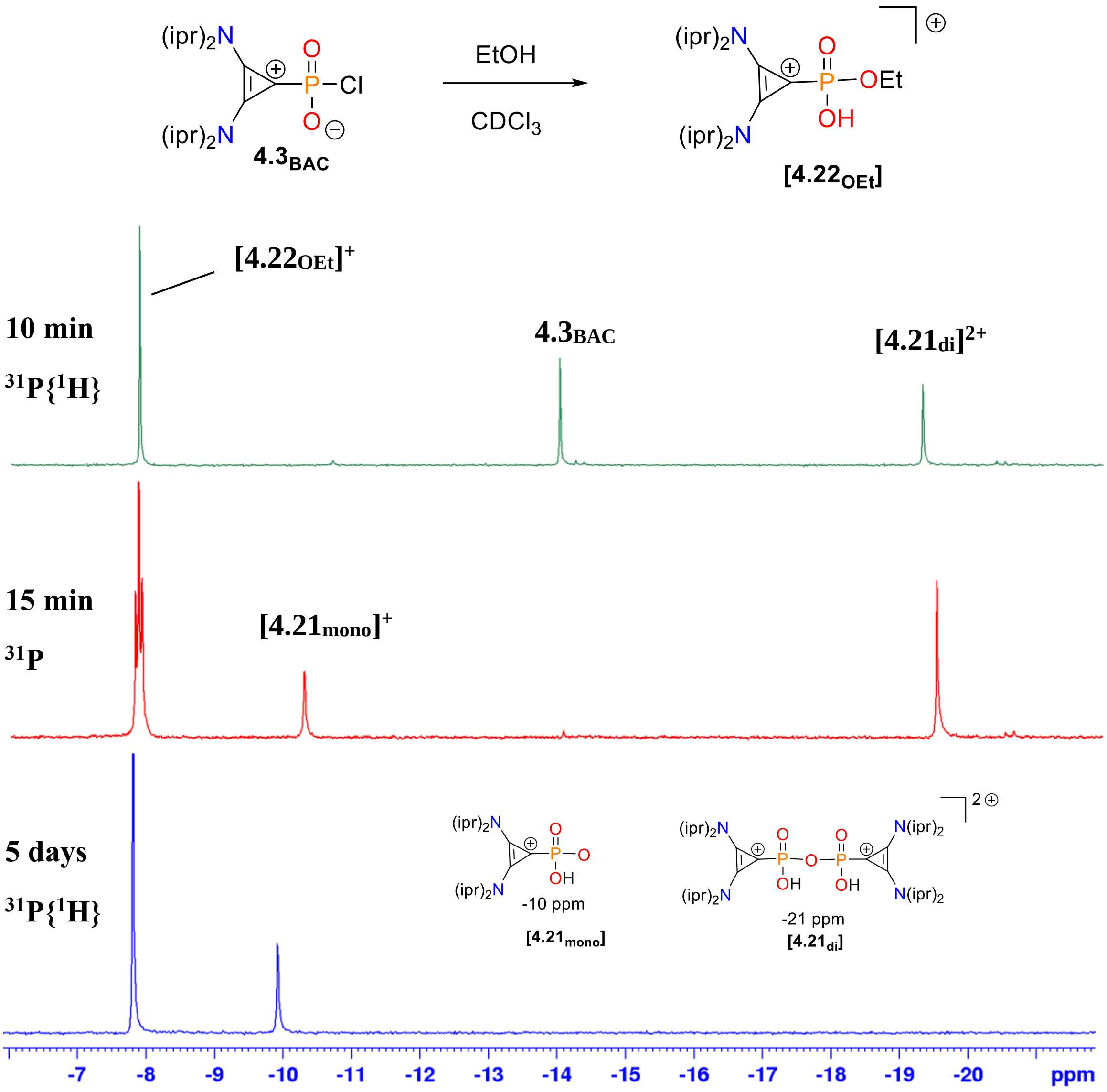

Figure 4-10. Stacked ^{31}P and ^{31}P{^{1}H} NMR spectra of the reaction of a 50:50 mixture of **4.3$_{\mathbf{BAC}}$** and **[*C*$_3$Cl]Cl** with excess EtOH. Top: ^{31}P{^{1}H} NMR spectrum after 10 min. Middle: ^{31}P NMR spectrum (no decoupling) after 15 min. Bottom: ^{31}P{^{1}H} NMR spectrum after 5 d.

The reaction of **4.3$_{\mathbf{BAC}}$** and **[*C*$_3$Cl]Cl** with an excess of diisopropylamine at 50 °C overnight resulted in the formation of an asymmetric diphosphonate, in addition to hydrolysis products (**Figure 4-11**). The asymmetric diphosphonate with one diisopropylamino substituent appeared as two doublets (δ_P = -8 and -22, $^2J_{P\text{-}P}$ = 27 Hz) in the $^{31}P\{^1H\}$ spectrum. Phosphorus NMR spectroscopy revealed P-H coupling from the diisopropylamino group of **4.23$_{Nipr2}$** to the resonance at -8 ppm, which split into a doublet of triplets ($^2J_{P\text{-}P}$ = 27 Hz; $^3J_{P\text{-}H}$ = 20 Hz). A trimeric phosphonate hydrolysis species (**4.21$_{tri}$**) was also observed (δ_P = -21.2 (d) and -25.8 (t), $^2J_{P\text{-}P}$ = 20.6 Hz; **Figure 4-12)**. These results demonstrated that the P-Cl bond of **4.3$_{BAC}$** is amenable to nucleophilic attack by alcohols and amines and may react further to form oligomeric structures (**Figure 4-11**).

Reactions of compound **4.3$_{BAC}$** with pyridine resulted in little change of the $^{31}P\{^1H\}$ NMR spectra at ambient temperature. NMR tubes containing $CDCl_3$ solutions of **4.3$_{BAC}$** and **[*C$_3$*Cl]Cl** heated in an oil bath resulted in the formation of an oligomeric triphosphonate species (**4.21$_{tri}$**, **Figure 4-12)**. Addition of pyridine resulted in an additional broad signal at δ_P = -11 which may be attributed to a weakly coordinated pyridine adduct. Previous work to stabilize “[PO]” adducts with pyridine demonstrated pyridine was a poor nucleophile and required substitution of weaker P-Br bonds for adduct formation.[10] A similarly reported pyridine adduct formation with $[PO_2Cl]$ did not proceed well, but a pyridine adduct was reported with the more acidic $[PS_2Cl]$ as the first example of a base-stabilized $[PCh_2Cl]$ fragment.[41] A follow up set of experiments of pyridine and the mix of **4.3$_{BAC}$** and **[*C$_3$*Cl]Cl** performed simultaneously in either a J-Young tube or a standard NMR tube (no special precautions taken to exclude moisture) revealed that the trimeric species (**4.21$_{tri}$**) was only present after heating in the standard NMR tube. This suggested that trace moisture was the cause of the extended trimeric phosphonate (**4.21$_{tri}$**) and is a related hydrolysis by-product (**Figure 4-12**).

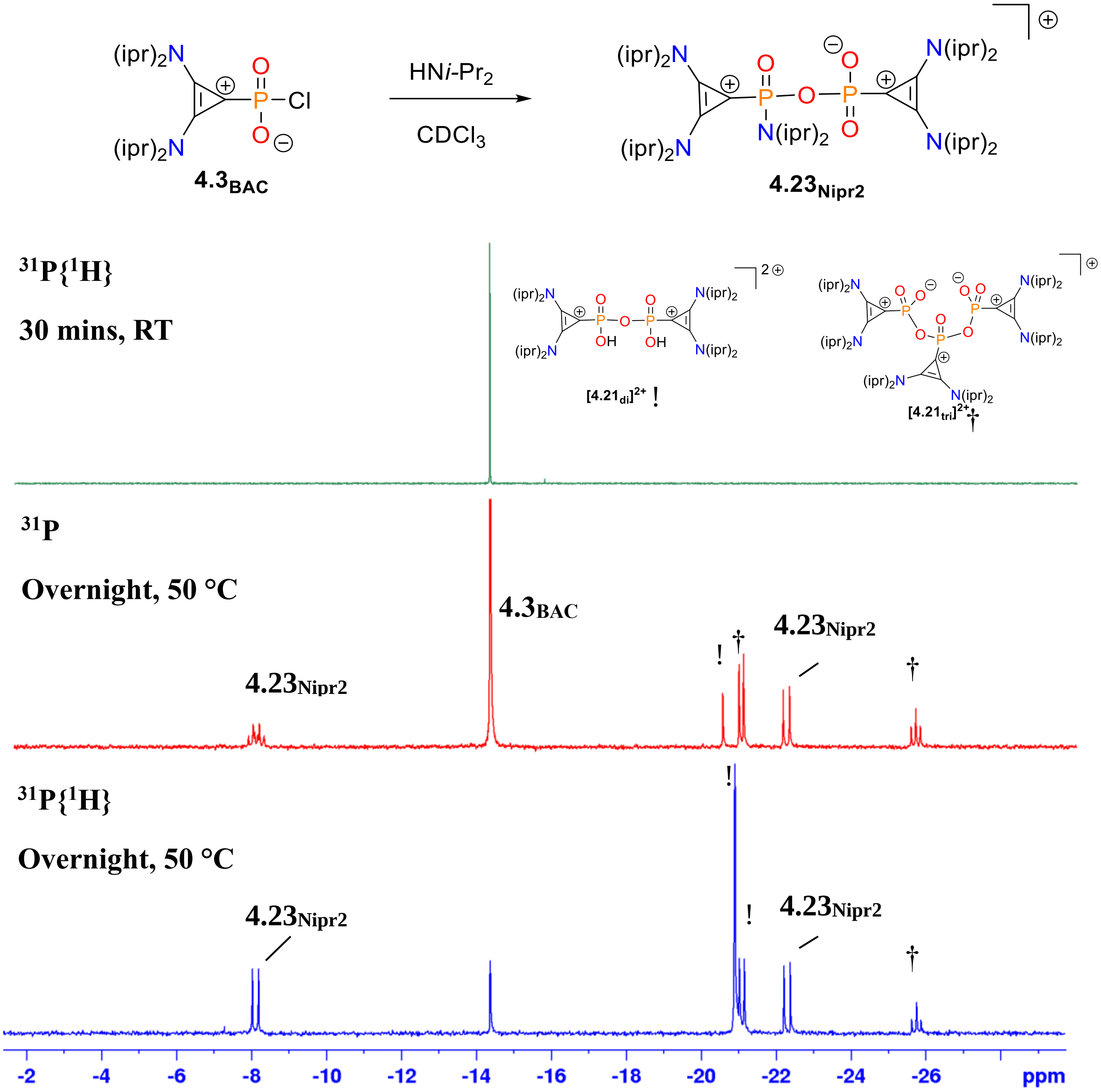

Figure 4-11. Stacked ^{31}P and ^{31}P{^{1}H} NMR spectra of the reaction of a 50:50 mixture of **4.3$_{BAC}$** and **[*C*$_3$Cl]Cl** with HN*i*-Pr$_2$. Asymmetric diphosphonate (**4.23$_{Nipr2}$**); dimeric (**4.21$_{di}$, !**) and trimeric (**4.21$_{tri}$, †**) hydrolysis products shown.

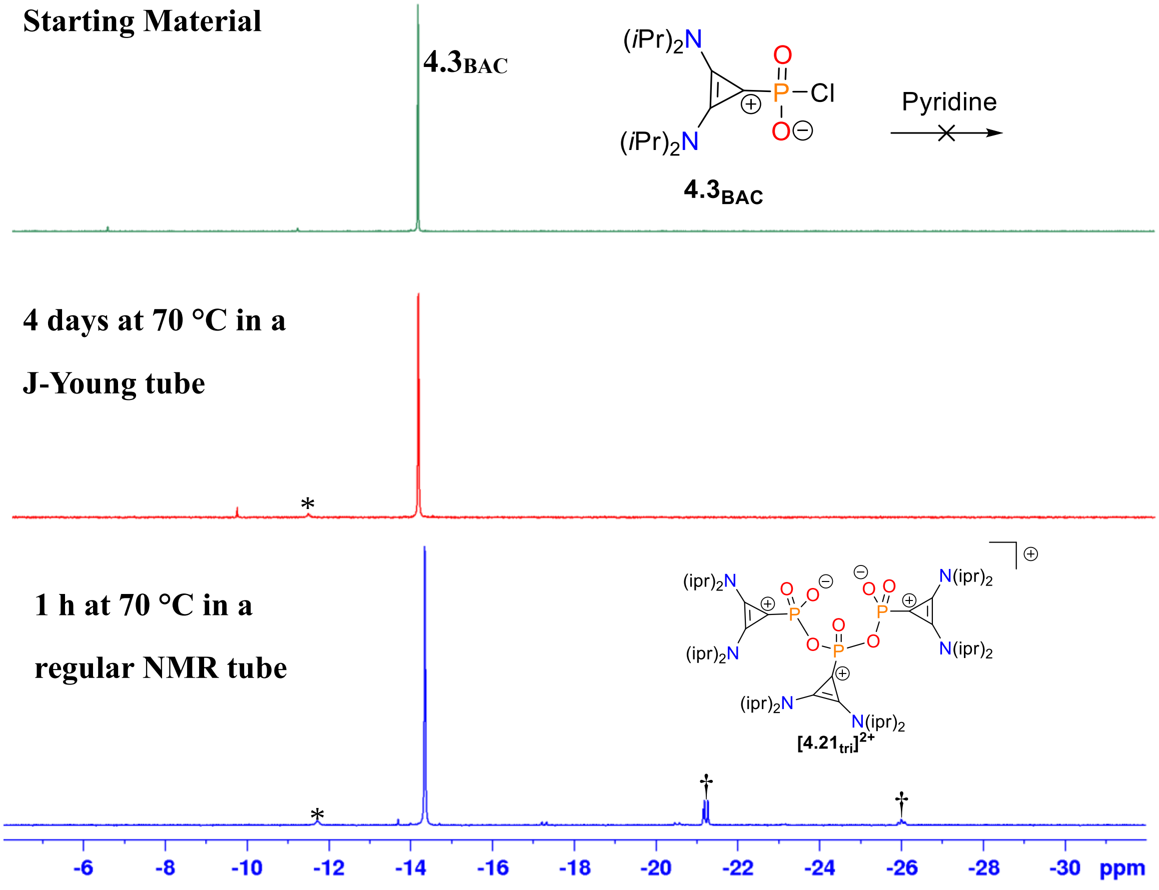

Figure 4-12. Stacked $^{31}P\{^1H\}$ NMR spectra of the reaction of a 50:50 mixture of **4.3$_{BAC}$** and **[*C*$_3$Cl]Cl** with excess pyridine. Possible pyridine adduct (*); Trimeric (**4.21$_{tri}$**, †) hydrolysis products shown.

An addition of distilled water initially produced a singlet at $\delta_P \approx -21$ (**4.21$_{di}$**), followed by a second singlet resonance of a decomposition product at $\delta_P \approx -8$ (**4.21$_{mono}$, Figure 4-13**). This pattern of hydrolysis stages was consistent among many samples of **4.3$_{BAC}$**, which slowly hydrolyzed due to leakage of air. In the absence of a base (*e.g.*, diisopropylamine; pyridine), both resonances that resulted from hydrolysis were each accompanied by a broad signal slightly up field ($\Delta\delta_P = 0.5$), likely attributed to an equilibrium of proton migration between **[*C*$_3$Cl]Cl** and the P-O-H resulting from a hydrolyzed P-Cl bond. This hypothesis, and the basicity of **[*C*$_3$Cl]Cl**, were supported by solid-state structure obtained of **[*C*$_3$Cl]ClHCl** (**Figure 4-6**).

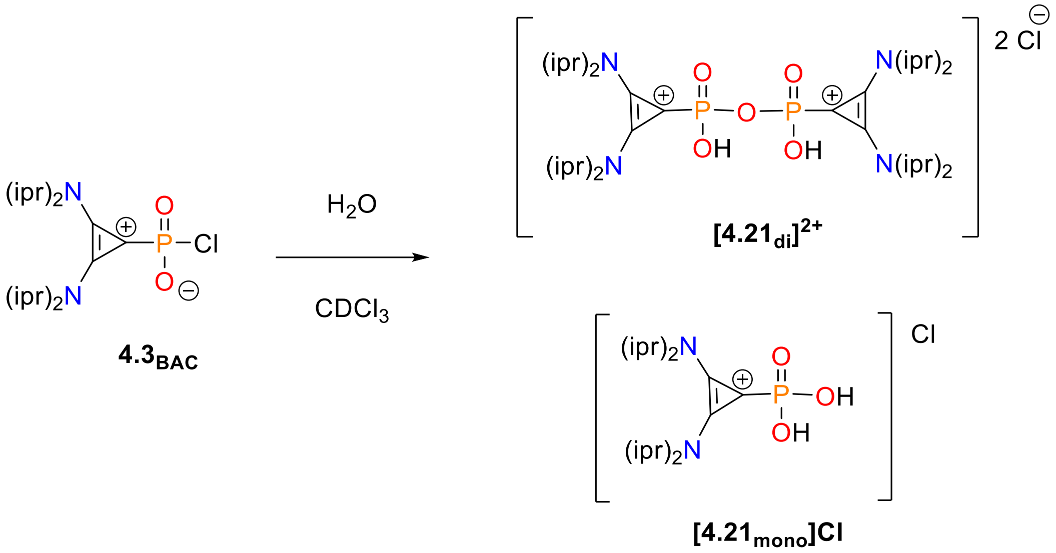
(ipr)$_2$N
(ipr)$_2$N
O
P
Cl
O
4.3$_{BAC}$
H$_2$O
CDCl$_3$
(ipr)$_2$N
(ipr)$_2$N
O
P
O
P
OH
OH
N(ipr)$_2$
N(ipr)$_2$
2 Cl
[4.21$_{di}$]$^{2+}$
(ipr)$_2$N
(ipr)$_2$N
O
P
OH
OH
Cl
[4.21$_{mono}$]Cl

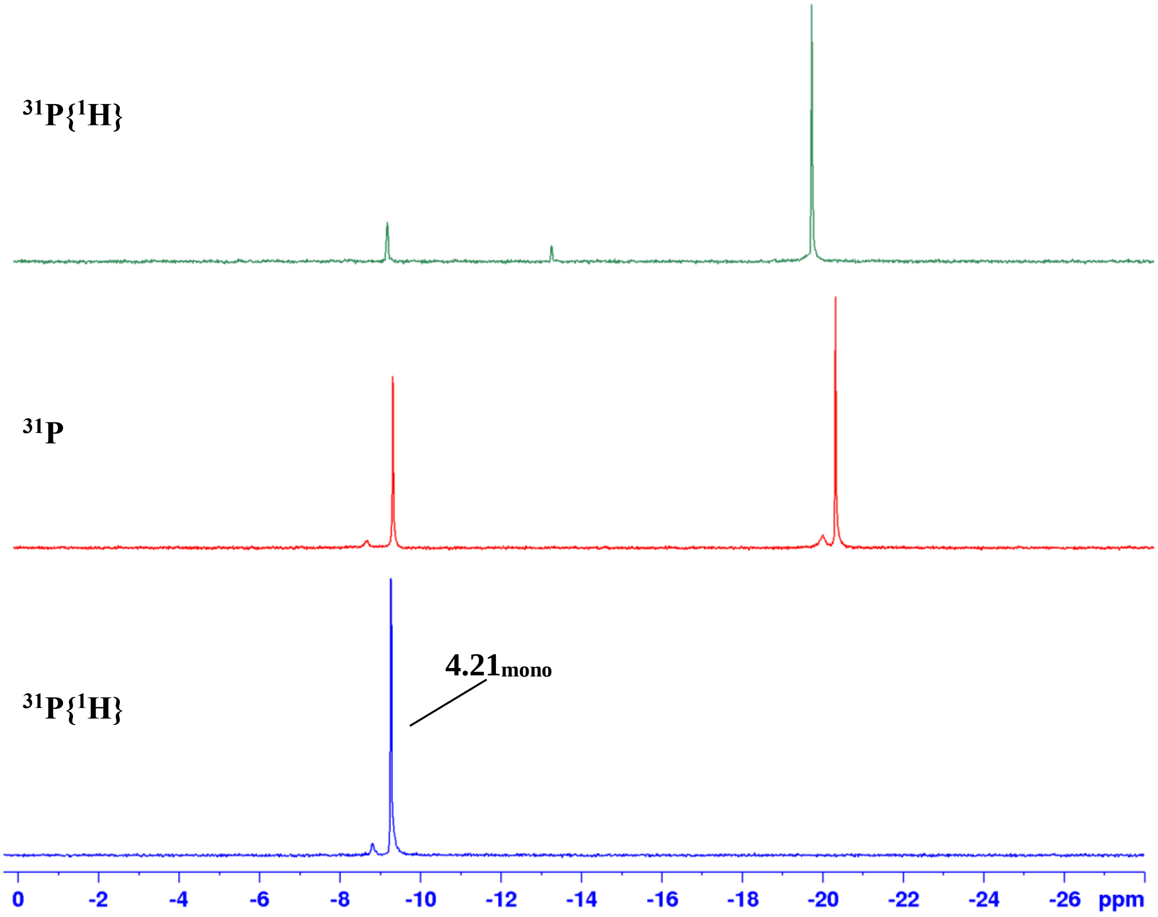

Figure 4-13. Stacked ^{31}P and ^{31}P{^{1}H} NMR spectra of the reaction of a 50:50 mixture of **4.3$_{BAC}$** and **[C_3Cl]Cl** with excess H_2O.

As none of the trial reactions described above successfully produced a single phosphorus containing species, attempts to separate the phosphorus species from the non-phosphorus containing species were not made. However, reactions involving the 50:50 mixture of **4.3BAC** and **[C_3Cl]Cl** with either DMAP or SiMe$_3$OTf could consistently generate a single phosphorus-containing species in solution (*vide infra*). Due to the inherent difficulty in isolating appreciable quantities of **4.3BAC** required for detecting the ring carbons, reactions from the 50:50 mixtures could be used for obtaining better ^{13}C{^{1}H} NMR data for the low-intensity ring carbon resonances.

Synthesis of a “PO_2^+” cation stabilized by two ligands was explored next (**[4.17DMAP]Cl**, **Figure 4-14**). Isolated crystals of **4.3BAC** were reacted with DMAP in CDCl$_3$ to produce a single phosphorus resonance at δ_P = 16 (**[4.17DMAP]Cl**). Combining DMAP with a 50:50 mixture of **4.3BAC** and **[C_3Cl]Cl** generated the same ^{31}P{^{1}H} resonance, and ^{1}H NMR spectrum contained a mixture of **[4.24]Cl$_2$** and **[4.17DMAP]Cl (Figure 4-15).** This underscores the electrophilic character of both **4.3BAC** and **[C_3Cl]Cl**. Compound **[4.17DMAP]Cl** is isoelectronic with the bis-ligated known species **[4.4DMAP]**$^+$ [15] and **[4.4BAC]**$^+$ [10,38], while the formation of **[4.24]Cl$_2$** is consistent with the known reactivity of **[C_3Cl]Cl** with PPh$_3$ to generate a dicationic species.[40]

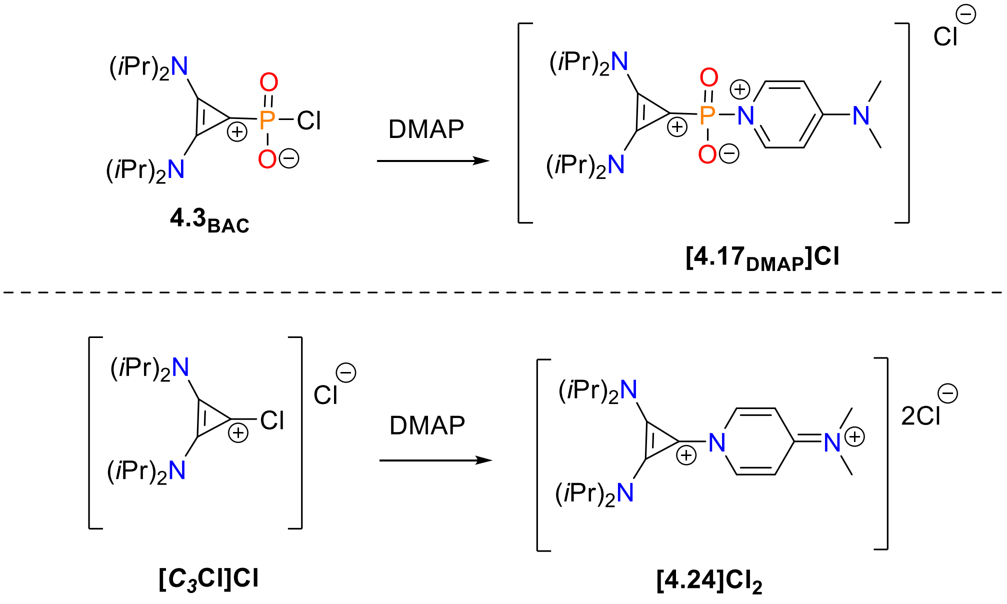

Figure 4-14. Reactions of **4.3BAC** and **[C_3Cl]Cl** with DMAP.

Deconvolution of ^{1}H, ^{13}C{^{1}H}, and ^{31}P{^{1}H} NMR spectra of a 50:50 mixture of **[4.17DMAP]Cl** and **[4.24]Cl$_2$** was done using multinuclear correlation experiments, and comparisons to the NMR spectra of the reaction of isolated phosphonate crystals (**4.3BAC**) with DMAP. Despite multiple washings with toluene and recrystallization from CH_2Cl_2/hexanes, ^{1}H NMR spectroscopy revealed free DMAP was present in solution, which suggested that the free and associated forms may exist in an equilibrium in solution. Low intensity exchange cross peaks of DMAP protons were observed in a ^{1}H - ^{1}H NOESY experiment (**Figure 4-16**).

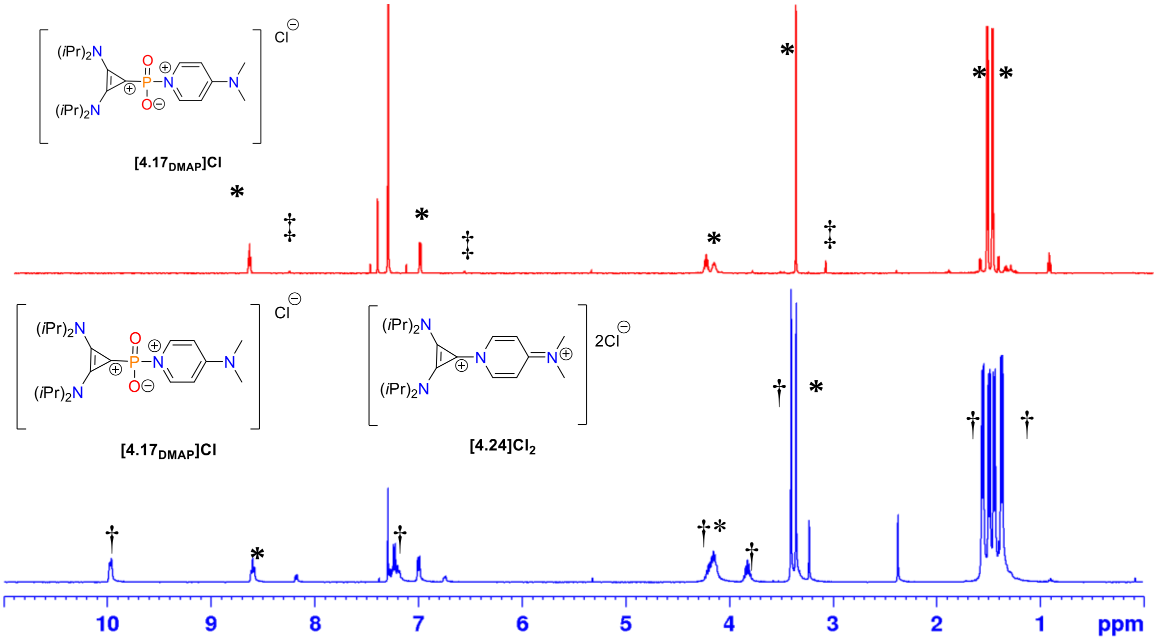

Figure 4-15. Stacked ^{1}H NMR spectra of reactions of DMAP with isolated crystals of **4.3BAC** (top) or with the 50:50 mixture of **4.3BAC** and **[*C*$_3$Cl]Cl** (bottom). Resonances for: **[4.17DMAP]Cl** (*), **[4.24]Cl$_2$** (†), free DMAP (‡).

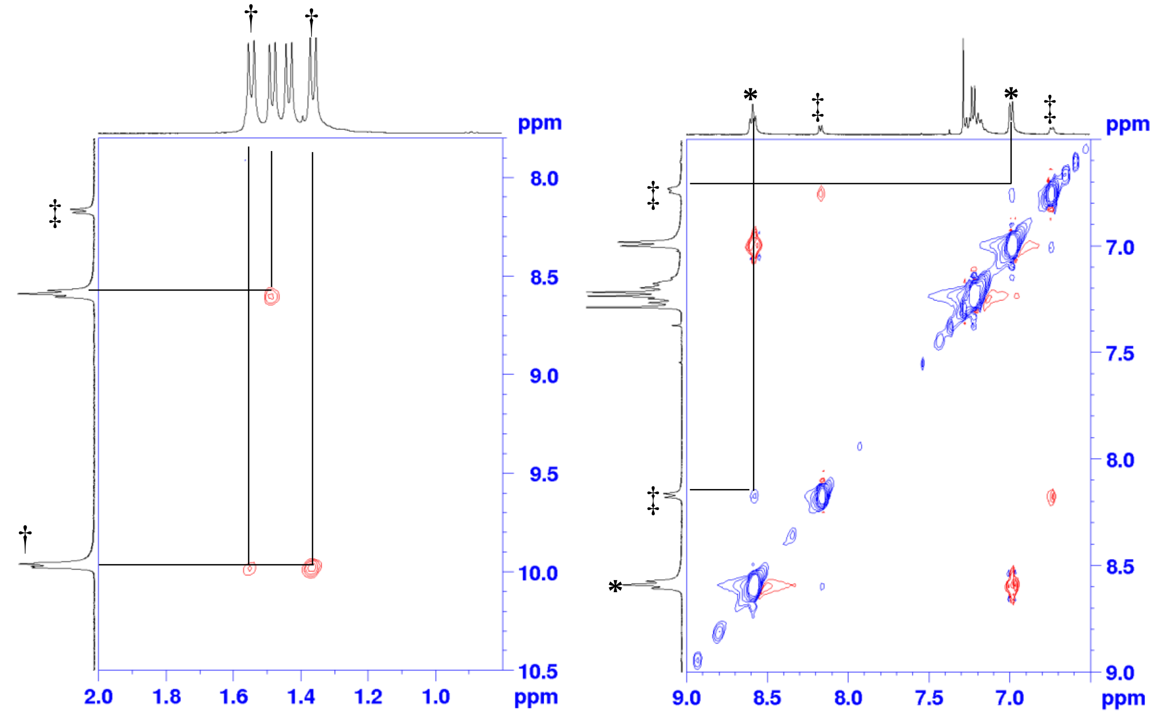

Figure 4-16. ^{1}H -^{1}H NOESY spectra of the crude mixture of **[4.17$_{DMAP}$]Cl** (*), **[4.24]Cl$_2$** (†) and free DMAP (‡). Correlation of DMAP (ortho protons) and cyclopropenium methyl fragments (left); Zoomed in region of **[4.17$_{DMAP}$]Cl** and DMAP exchange. NOE cross peaks (red) and EXSY cross peaks (blue).

The formation of a three-coordinate cationic [RPO$_2$]$^+$ species was explored using halogen abstraction and replacement with a weakly associating counter anion (**Scheme 4-10**). Isolated crystals of **4.3$_{BAC}$** or a 50:50 mixture of **4.3$_{BAC}$** and **[*C*$_3$Cl]Cl** were mixed with SiMe$_3$OTf and rapidly produced **[4.17$_{mono}$]OTf** (δ_P = -9) or both **[4.17$_{mono}$]OTf** and the known species **[*C*$_3$Cl]OTf**[42] when an excess of SiMe$_3$OTf was added in CDCl$_3$ or CH$_2$Cl$_2$ **Scheme 4-10**). Confirmation of the monomeric nature of **[4.17$_{mono}$]OTf** was confirmed by analysis of ^{31}P-^{13}C sidebands ($^2J_{P\text{-}C}$ = 278 Hz, **Figure 4-17**) as discussed (See Section **4.2.2**) for **4.3$_{BAC}$** and the dimeric hydrolysis product. Analysis of the ^{19}F NMR spectra of the initial mixture showed only one resonance, which indicated that a triflate-bound cyclopropenium was not formed. The data for **[*C*$_3$Cl]OTf**[42] was confirmed by comparison to reported data and **[4.17$_{mono}$]** was characterized *in situ* by NMR spectroscopy immediately after formation. HSQC and HMBC NMR spectroscopy experiments were used to correlate signals in ^{1}H and ^{13}C{^{1}H} NMR spectroscopy experiments to the respective compounds. The *ipso* carbons could not be assigned by HMBC, so assignments were made based on the presence or absence of presumed P-C coupling, and by comparison to other known values of bridgehead carbons in related compounds. One final resonance in the ^{13}C{^{1}H} NMR spectrum a (δ_P = 172) could not be correlated to any other resonances using correlation experiments, and the origin of this signal is unclear.

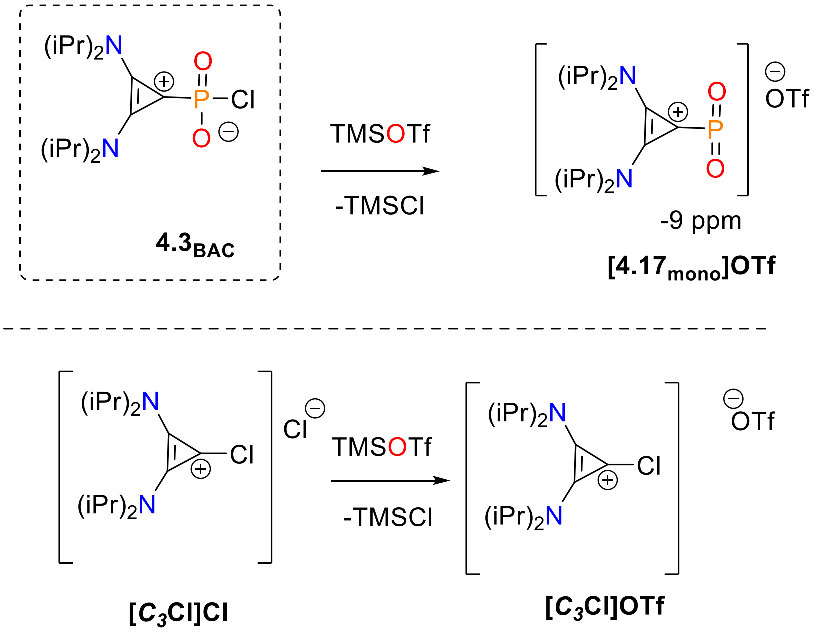
(iPr)$_2$N
(iPr)$_2$N
P
Cl
O
O
4.3$_{BAC}$
TMSOTf
-TMSCl
OTf
-9 ppm
[4.17$_{mono}$]OTf
Cl
[C_3Cl]Cl
[C_3Cl]OTf

Scheme 4-10. Species formed after **4.3$_{BAC}$** (top) and **[*C*$_3$Cl]Cl** (bottom) were mixed with SiMe$_3$OTf.

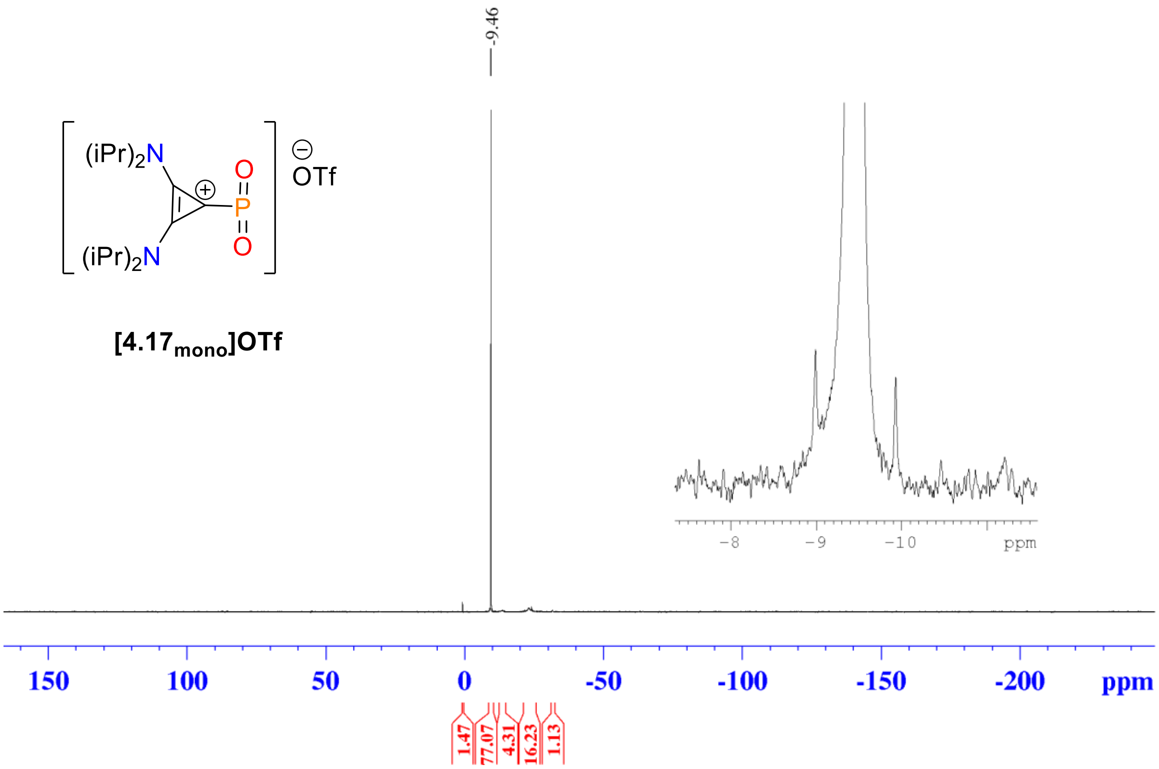

Figure 4-17. ^{31}P{^{1}H} NMR spectrum of a crude reaction mixture of **4.3$_{\text{BAC}}$** with SiMe$_3$OTf to generate **[4.17$_{\text{mono}}$]OTf**. Inset contains zoomed in spectrum showing ^{31}P-^{13}C coupling of monomeric **[4.17$_{\text{mono}}$]**. Sample contains other unidentified byproducts, which have been integrated and normalized.

Structural confirmation of **[4.17$_{\text{mono}}$]** *via* SC-XRD was not achieved although X-ray diffraction data of the hydrolysis product **[4.21$_{\text{mono}}$]OTf** was obtained (**Figure 4-18**). Purification attempts *via* trituration with fluorobenzene resulted in a change from a powder to gum-like consistency, accompanied by a pronounced insolubility in CDCl$_3$. It was hypothesized that the observed physical behaviour resulted from the lack of steric protection offered by the cyclopropenium ligand, which allowed for a decomposition pathway where the three coordinate species ambiphilic **[4.17$_{\text{mono}}$]$^+$** may form oligomeric mixtures of four-coordinate phosphorus species and become coordinately saturated (**Scheme 4-11**).

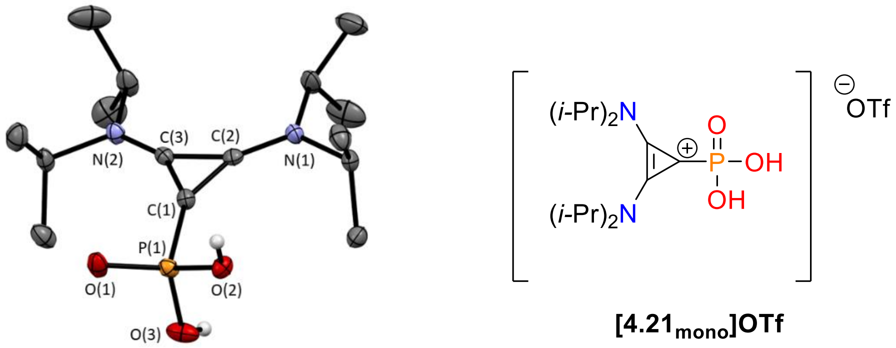

[4.21$_{mono}$]OTf

Figure 4-18. Mercury-rendered ORTEP style drawing of **[4.21$_{mono}$]OTf**. Triflate has been omitted for clarity and selected ellipsoids are shown at the 50% probability level

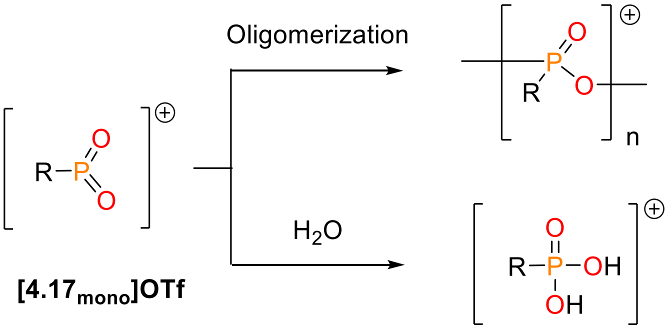

[4.17$_{mono}$]OTf

[4.21$_{mono}$]OTf

Scheme 4-11. Proposed oligomerization and hydrolysis of **[4.17$_{mono}$]$^+$** cation.

Additional evidence for the Lewis acidic nature of **[4.17$_{mono}$]$^+$** cation was observed during a reaction of **4.3$_{BAC}$** with $NaBF_4$. An initial chloride abstraction *via* salt metathesis from **4.3$_{BAC}$** using $NaBF_4$ was suggestive by an immediate broadening and gradual shift to δ_P = -10.4 after 18 h (re: **[4.17$_{mono}$]OTf**), but was found in $^{31}P\{^1H\}$ and ^{19}F spectroscopy experiments to gradually decompose to a species with distinctive $^1J_{P\text{-}F}$ coupling of 991 Hz. The detected resonances at δ_P = -19.0 and δ_F = 53.9 in the $^{19}F\{^1H\}$ spectrum do not match reported data for (BAC)PO_2F (**4.9**, δ_P = -14.9 and δ_F = 45.3, $^1J_{P\text{-}F}$ = 945 Hz),[15] and thus were hypothesized to be from the formation of a BF_3 adduct **4.25 (Scheme 4-12** and **Figure 4-19)**.

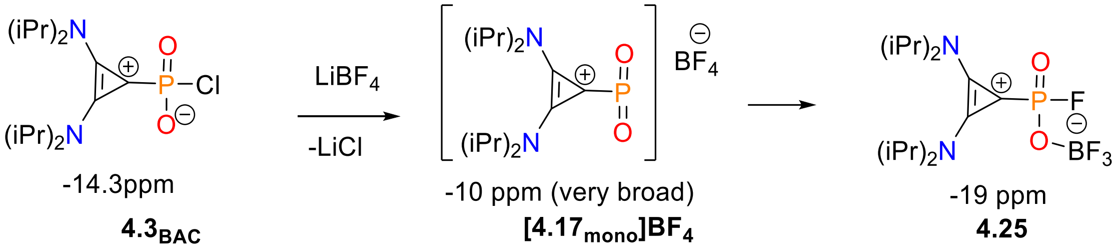
(iPr)2N
P−Cl
LiBF4
-LiCl
BF4
P−F
BF3
-14.3ppm
4.3BAC
-10 ppm (very broad)
[4.17mono]BF4
-19 ppm
4.25

Scheme 4-12. Proposed reaction of **4.3$_{\mathbf{BAC}}$** with LiBF$_4$.

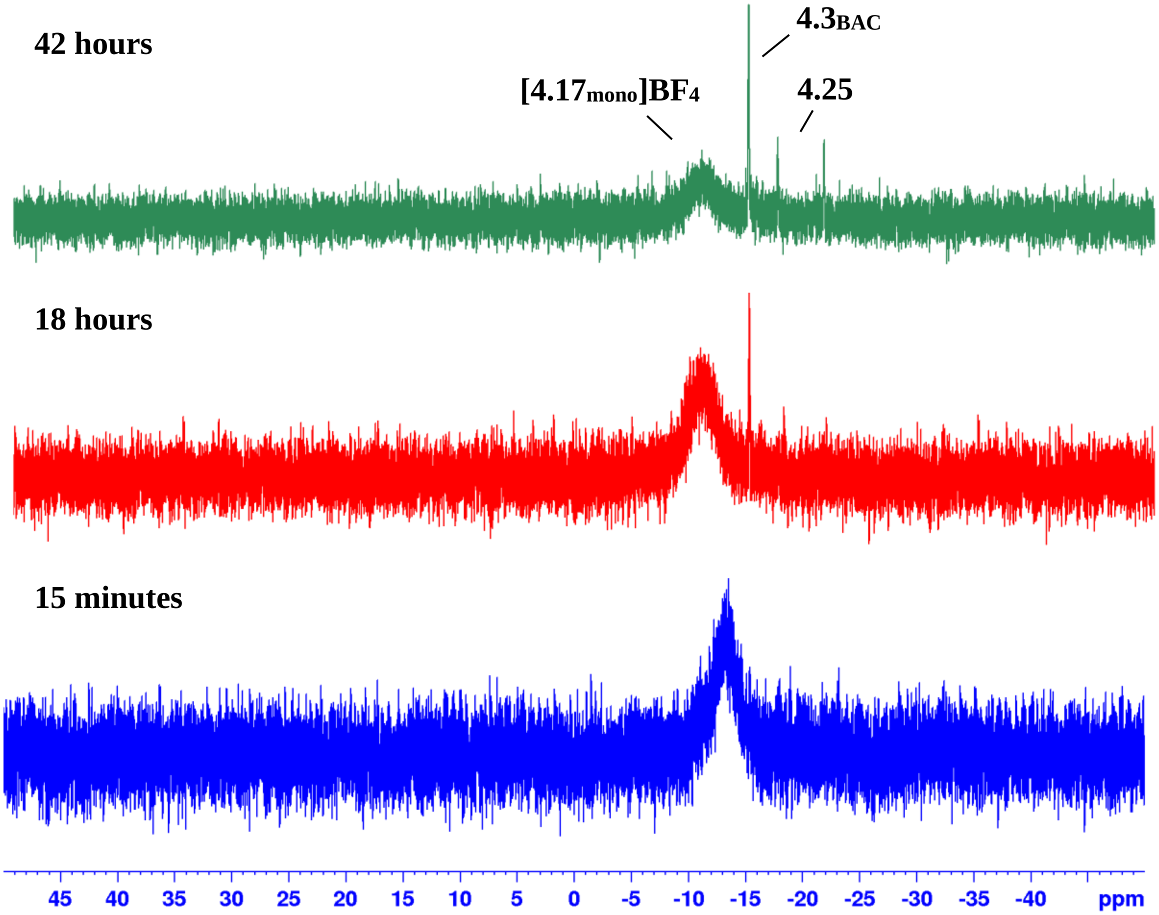

Figure 4-19. Stacked ^{31}P{^{1}H} NMR spectra of the reaction of **4.3$_{\mathbf{BAC}}$** with LiBF$_4$ in CDCl$_3$ at room temperature.

A small-scale reaction (ca. 0.004 g) of isolated phosphonate crystals with one stoichiometric equivalent of tris(pentafluorophenyl)borane (BCF) resulted in no significant change by ^{31}P{^{1}H} NMR spectroscopy, but a reaction was evident by a coalescence of isopropyl signals in a ^{1}H NMR spectrum (**Figure 4-20**).

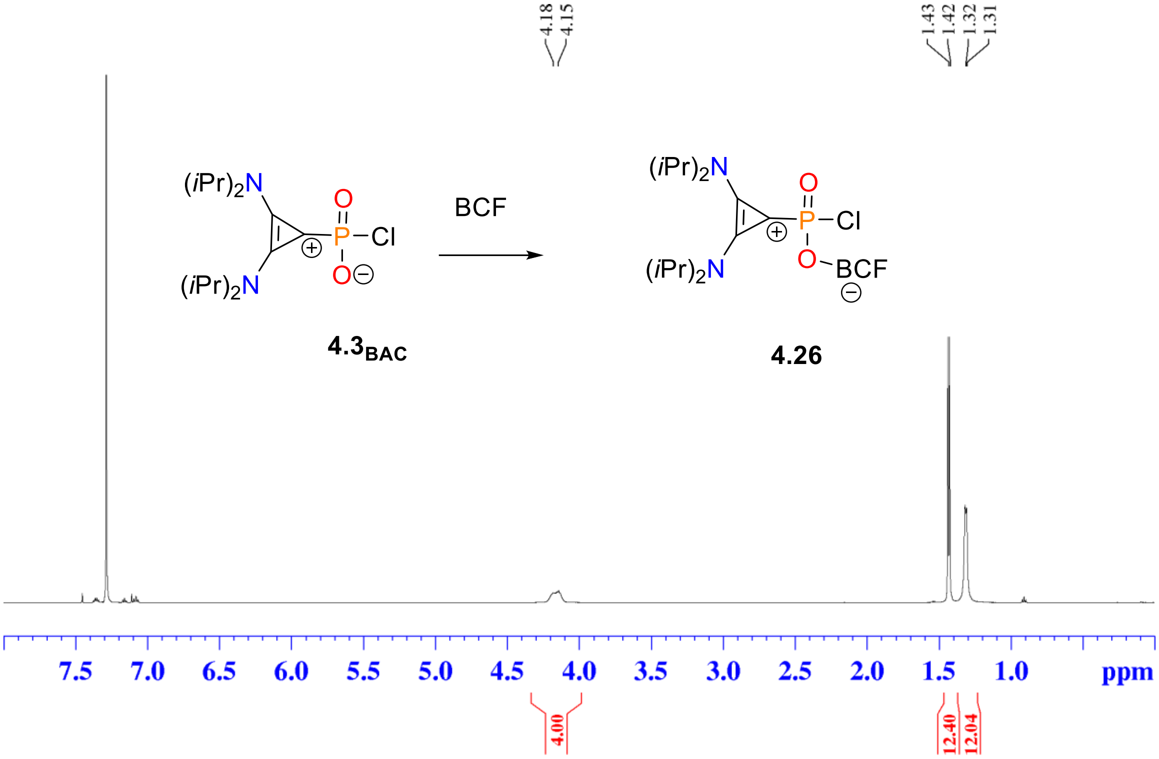

Figure 4-20. ^{1}H NMR spectrum of the reaction mixture of **4.3$_{\mathbf{BAC}}$** and BCF in $CDCl_3$, at 25 °C.

A follow up experiment was performed using a J-Young tube, where one molar equivalent of BCF and **4.3$_{\mathbf{BAC}}$** (0.020 g) were combined in CH_2Cl_2, recrystallized from hot PhF, and washed with pentane. The solubility of the recrystallized material was unexpectedly poor in CD_2Cl_2, but may be attributed to oligomerization of **[4.17$_{\mathbf{mono}}$]$^+$**. To determine the structure of the afforded material, variable temperature multinuclear NMR spectroscopy experiments were conducted despite the sample having contained undissolved material. Lowering the temperature to -50 °C (**Figure 4-21**) resulted in a separation of resonances in ^{31}P{^{1}H} spectrum into two resonances, tentatively assigned as **[4.17$_{\mathbf{mono}}$]Cl·BCF** (δ_P = -10) and **4.26** (δ_P = –17). ^{11}B NMR spectroscopy experiments were unable to resolve any boron signal, but the ^{19}F{^{1}H} NMR spectrum was significantly sharpened and resolved at low temperatures.

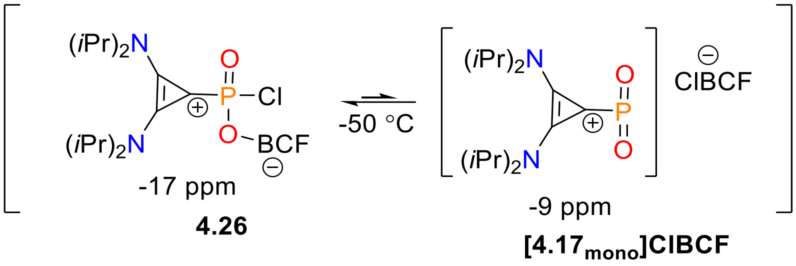
(iPr)2N
(iPr)2N
O
P
Cl
O
BCF
-17 ppm
4.26
-50 °C
(iPr)2N
(iPr)2N
O
P
O
ClBCF
-9 ppm
[4.17mono]ClBCF

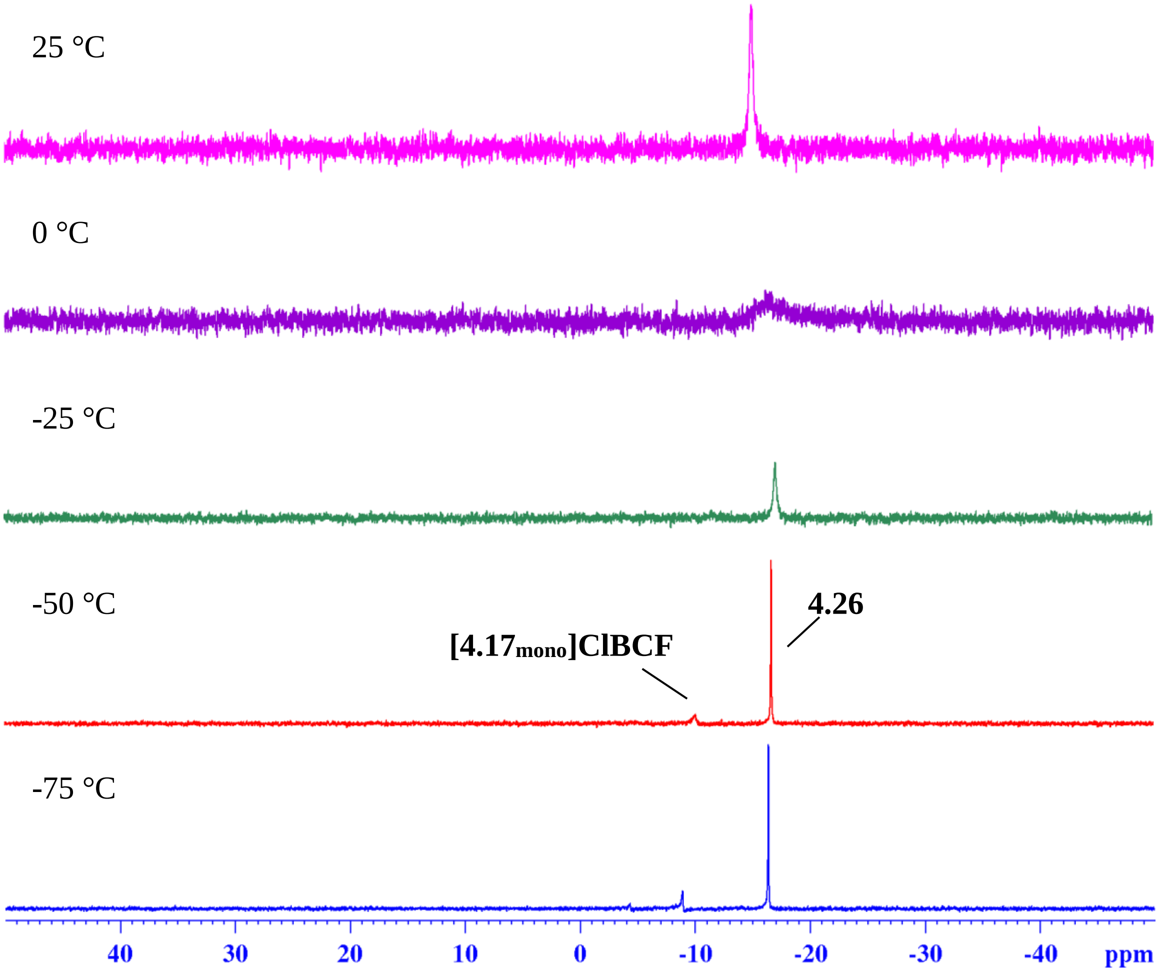

Figure 4-21. Stacked variable temperature $^{31}P\{^{1}H\}$ spectra of **4.26** and **[4.17$_{mono}$]ClBCF** in CD_2Cl_2.

The crystal which was analyzed by SC-XRD from the reaction of **4.3_{BAC}** with BCF was of **4.27** (**Scheme 4-13** and **Figure 4-22**), containing two BCF moieties per phosphonate. This could mean there was a more complex equilibrium of BCF adducts from zero to two stoichiometric equivalents.

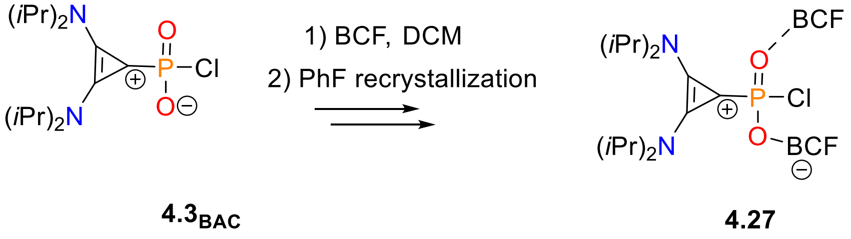

Scheme 4-13. The reaction of **4.3_{BAC}** with BCF which resulted in the collection of X-ray diffraction data of **4.27**.

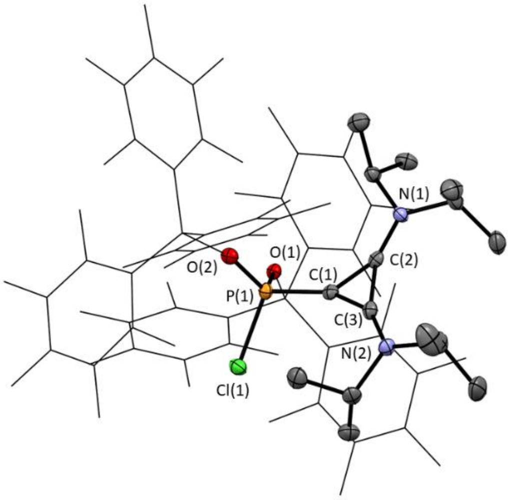

Figure 4-22. Mercury-rendered ORTEP style drawing of **4.27**. Hydrogens have been omitted and BCF framework has been represented as wireframe for simplicity. Selected ellipsoids shown at the 50% probability level.

4.2.5 Comparison of ^{31}P NMR Spectroscopy Shifts of Related Onio-Substituted Oxo-Phosphorus Species

The intermediate signal assigned as **[4.6_{BAC}]Cl** (δ_P = -13.7, $CDCl_3$) appeared to be significantly different than the related intermediate detected in the reaction of DMAP and

$POCl_3$ (**[4.6$_{DMAP}$]Cl**; δ_P = 13.0, SO_2,[10]). Quantum chemical calculations to predicted the chemical shift of **[4.6$_{DMAP}$]$^+$** conformers to be δ_P = 24.3 and δ_P = 17.1, in agreement with the experimentally measured signal. To rationalize the discrepancy between the $^{31}P\{^1H\}$ chemical shifts of the proposed speciation of **[4.6$_{BAC}$]Cl** with **[4.6$_{DMAP}$]$^+$**, a survey of the literature of directly related species was carried out (**Table 4-1**). Within each class of species, $^{31}P\{^1H\}$ resonances for DMAP adducts were downfield relative to species with a BAC ligand.

Table 4-1. Table of related phosphine species (extended from reference[10]). Highlighted entries are species from this work.

Entry	Species	δ_P	Solvent
1	**[4.20$_{BAC}$]BF_4**	-93.1[15]	$CDCl_3$
2	**[4.20$_{DMAP}$]OTf**	-20.06[38]	CD_3NO_2
3	**[4.6$_{BAC}$]Cl**	-13.7	$CDCl_3$
4	**[4.6$_{DMAP}$]$^+$**	+13.0[10]	SO_2
5	**4.3$_{BAC}$**	-14.3	$CDCl_3$
7	**4.3$_{DMAP}$**	-8.7[10]	SO_2
9	**[4.4$_{BAC}$]BF_4**	-22.94[15]	$CDCl_3$
10	**[4.17$_{DMAP}$]Cl**	-16	$CDCl_3$
11	**[4.4$_{Py}$]$^+$**	-14.2[10]	SO_2
12		-14.6[10]	SO_2
13	**[4.4$_{DMAP}$]$^+$**	-13.7[10]	SO_2

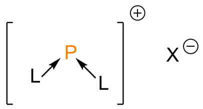
[4.20$_L$]X

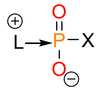
4.3$_L$

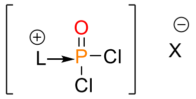
[4.6$_L$]X

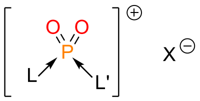
[4.4L]X, L=L'
[4.17DMAP]Cl, L=BAC; L'=DMAP

4.2.6 Application Towards Synthesis of $(ArPO_2)_3$

A report from the Manners Group presented thorough characterization data, solid-state structures, and comments on the solubility of various cyclic phosphonates of $[ArPO_2]_3$ (**4.18$_{Ar}$**, Ar = 4-*t*-butylphenyl, Mes, and 2,6-dimethyl-4-*t*-butylphenyl) or $(PhPO_2)_6$, which were prepared by condensations of phosphonic dichlorides $RPOCl_2$ and phosphonic acids $RPO(OH)_2$.[18] Given the proposed and unexpected reaction of the **[4.6$_{BAC}$]Cl** intermediate with **C_3O**, reactions with $ArPOCl_2$ were explored to generate $[ArPO_2]_n$ *in situ* by a halogen abstraction and oxygen transfer (**Scheme 4-14**).

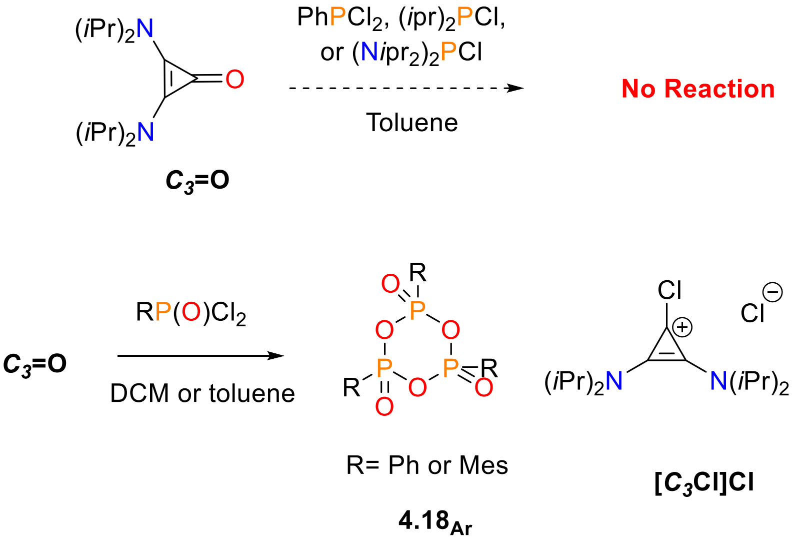

Scheme 4-14. Screened reactions of **C_3O** with various chlorophosphines.

No reaction was observed between **C_3O** and P(III) chlorides (**Scheme 4-14**), but rapid reactions occurred upon mixing **C_3O** with phenylphosphoryl chloride ($PhPOCl_2$) or mesityl phosphoryl chloride ($MesPOCl_2$). Upon reaction with $PhPOCl_2$ in $CDCl_3$ (**Figure 4-23**), complete consumption of **C_3O** was accompanied by the formation of the six-membered cyclic phosphonate (δ_P = 3.0 (t) and 1.4 (d)), as well as trace amounts an unidentified impurity (δ_P = 19). The analogous reaction of **C_3O** with $MesPOCl_2$ (**Figure 4-24**) resulted also resulted in the appearance of a six-membered cyclic phosphonate **4.18$_{Mes}$** as the major species, and an intermediate resonance (δ_P = 18), which converged to the major product ($\delta_P \approx -1$) in a standing solution of C_6D_6 at room temperature. The identities of the unassigned species ($\delta_P \approx 17$) were assigned to the dimeric cyclic phosphonate $(RPO_2)_2$.[21] Only one example of an isolated dimeric phosphonate has been reported, and was supported by a bulky terphenyl ligand ($\delta_P = 17$).[21] An appearance of other minor by-products in repeated synthesis ($\delta_P = -0.2$ and $\delta_P = -5$) was suggestive of formations of higher oligomeric systems.[18] The previous report of $(MesPO_2)_3$ also described the fluxional nature of the compound in $CDCl_3$ which resulted in a pseudo-singlet, and a slower exchange in C_6D_6 resulting in second-order phosphorus resonances which resolved into approximately a doublet and triplet. The ^1H and $^{31}P\{^1H\}$ chemical shifts, second-order coupling patterns, $^2J_{P\text{-}P}$ coupling (40 Hz), relative behavior and solubilities in $CDCl_3$ and C_6D_6, were all in agreement with previously reported species.[18]

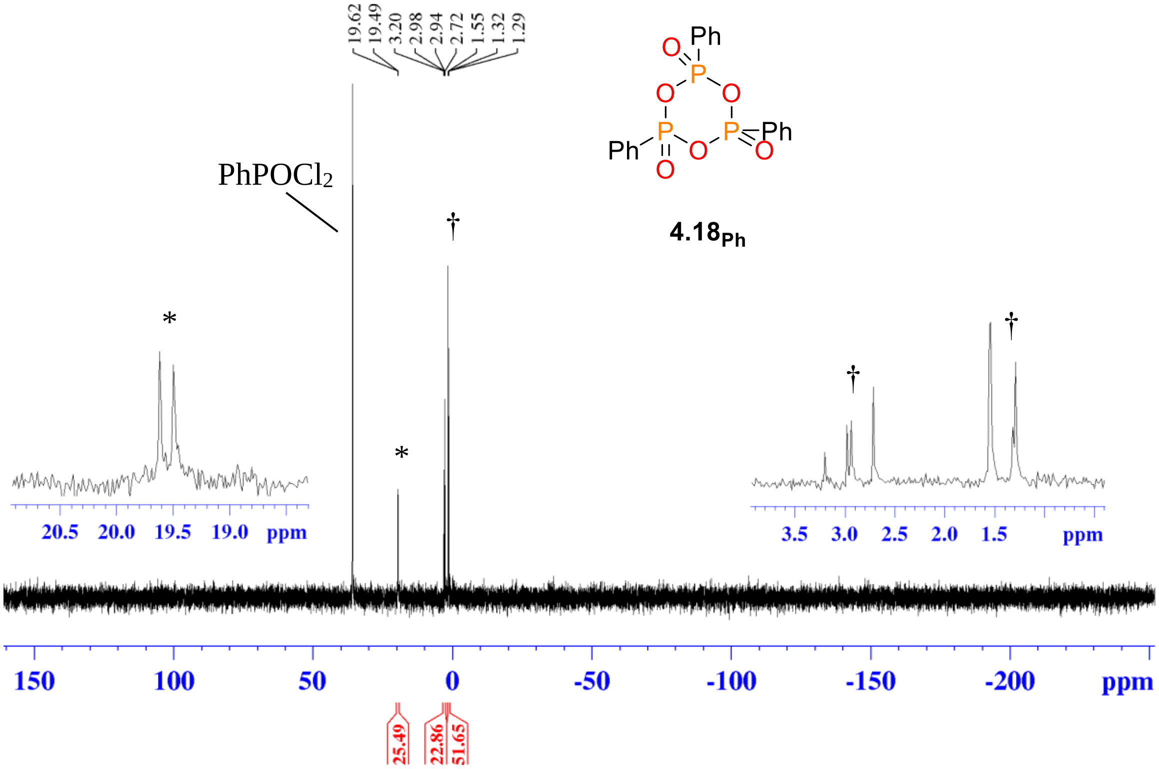

Figure 4-23. $^{31}P\{^1H\}$ NMR spectrum of crude reaction aliquot of ***C_3O*** and $PhPOCl_2$ to generate **4.18_{Ph}** (†). Unidentified species labelled with (*).

Although the synthesis of **4.18_{Ph}** proceeded quickly, separation of **4.18_{Ph}** and **[C_3Cl]Cl** was not achieved. A separation of **4.18_{Ph}** and **[C_3Cl]Cl** that showed some potential involved layering a DCM reaction mixture with hexanes and storing at -30 °C. Crystalline solids of **[C_3Cl]Cl** formed at the bottom of the NMR tube but were found to rapidly dissolve upon warming to room temperature. A rapid decanting using a canula needle and syringe was successful in recovery of 20 mg (40 % yield) **[C_3Cl]Cl**, with only trace amounts (ca. 1 % by integration) of **4.18$_{Ph}$** detected by ^{1}H NMR spectroscopy.

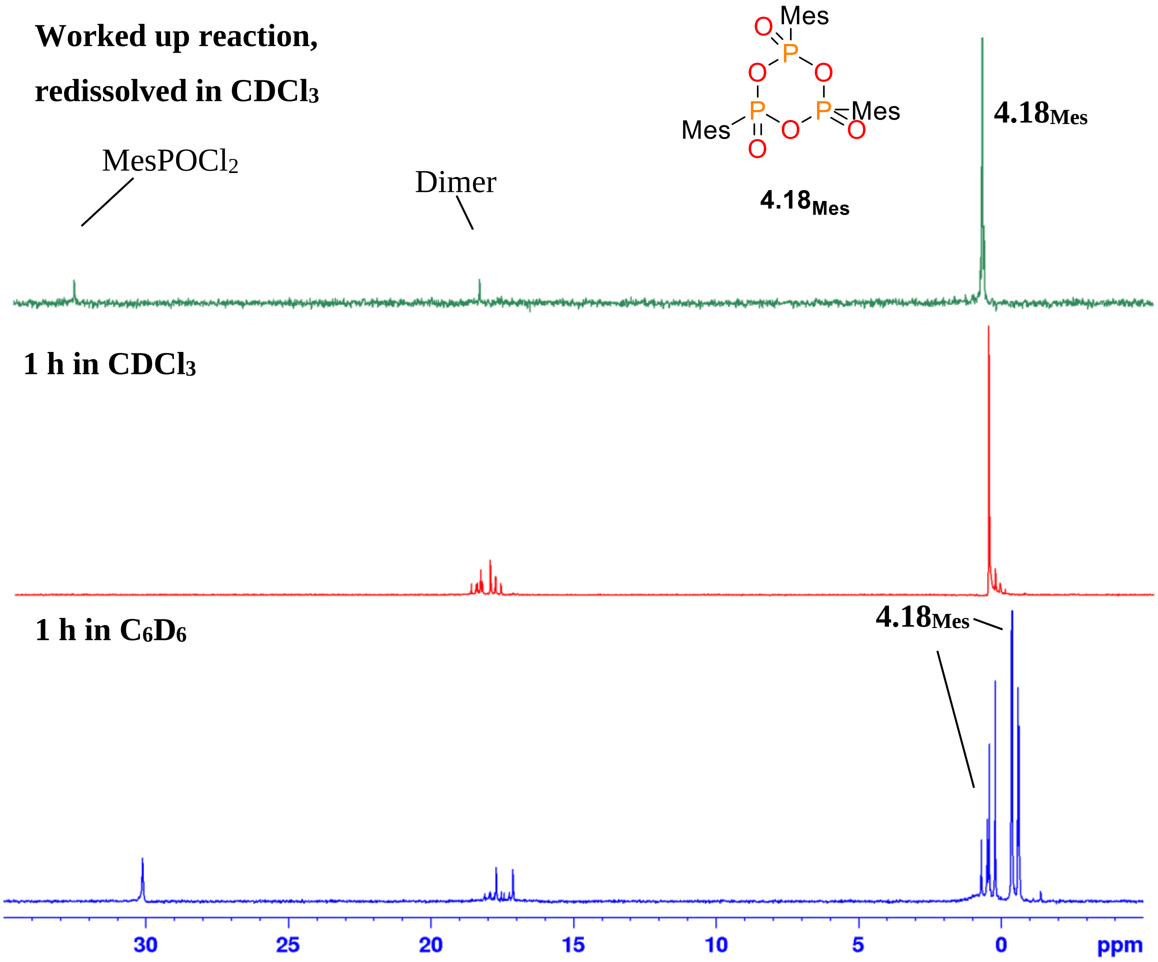

Figure 4-24. Stack plot ^{31}P{^{1}H} NMR spectra of 1 h reaction aliquots of MesPO$_2$Cl with ***C_3O*** in C_6D_6 (bottom), $CDCl_3$ (middle); after removal of toluene and redissolving the product in $CDCl_3$ (top). Uncharacterized intermediate formation at approximately δ_P = 18.

Since **[C_3Cl]Cl** has a low solubility in aromatic solvents and reports show that **4.18$_{Mes}$** was significantly more soluble in aromatic solvents than **4.18$_{Ph}$,**[18] it was suspected that separation by liquid extraction would be simple as a proof-of-principle. The reaction proceeded slower in $CDCl_3$ than in aromatic solvents, possibly due to the precipitation of **[*C₃*Cl]Cl** as a thermodynamic driving force. In an effort to aid separation of **4.22$_{\mathbf{Mes}}$** and **[*C₃*Cl]Cl**, a preliminary filtration after *ca.* 45 min allowed for recovery of approximately 70 % of the expected **[*C₃*Cl]Cl** cleanly. Allowing the reaction mixture to stir at room temperature for 16 h further resulted in significant precipitation of both species. Validation for the identification of the product was achieved by analysis of C_6D_6 and $CDCl_3$ solutions.

4.3 Conclusions

A new pathway towards the generation of a cyclopropenium-supported chlorophosphonate (**4.3$_{\mathbf{BAC}}$**) with concurrent generation of **[*C₃*Cl]Cl** by-product was demonstrated. Although a consistent separation method was not established, parallel reactions performed on Pasteur separated crystals and on a 50:50 mixture of **4.3$_{\mathbf{BAC}}$** and **[*C₃*Cl]Cl** allowed for the dissemination of electrophilic character and halogen abstraction. Evidence of a dimeric hydrolyzed species was demonstrated by a measured $^{31}P{\sim}^{31}P{\sim}^{13}C$ spin system, but confirmation *via* SC-XRD remains elusive. Evidence of the formation of **[4.17$_{\mathbf{mono}}$]$^+$** cations was ascertained *via* comparable shifts in $^{31}P\{^1H\}$ spectra from reactions of **4.3$_{\mathbf{BAC}}$** with $SiMe_3OTf$, $NaBF_4$, and BCF. Isolation and structural characterization of **[4.17$_{\mathbf{mono}}$]$^+$** was complicated by a sensitivity to hydrolysis and decomposition *via* a proposed oligomerization of monomeric three-coordinate **[4.17$_{\mathbf{mono}}$]$^+$** species to four-coordinate phosphorus species. ***C₃O*** was also demonstrated to act as an oxygen donor and dihalogen abstractor for a new synthetic route towards cyclic phosphonates from $ArPOCl_2$ (Ar = Ph and Mes). A higher solubility of **4.22$_{\mathbf{Mes}}$** compared to **4.22$_{\mathbf{Ph}}$** in aromatic solvents aided in separation from **[*C₃*Cl]Cl** by-product, but complete separation of cyclic phosphates **4.22$_{\mathbf{Ph}}$** or **4.22$_{\mathbf{Mes}}$** from **[*C₃*Cl]Cl** was not achieved.

4.4 Experimental Section

Compound **[*C₃*Cl]Cl** was prepared *in situ via* a reported procedure.[35] Compound ***C₃*O** was prepared using a slightly modified procedure.[35]. Modifications are detailed in specific procedures below. Unless otherwise noted, all manipulations were carried out under an inert atmosphere using a nitrogen filled MBraun Labmaster 130 glovebox or using standard Schlenk techniques. All glassware was oven-dried prior to use. All solvents were pre-dried and degassed using a MBraun controlled atmosphere solvent purification systems and stored over 4 Å molecular sieves under N_2. $CDCl_3$ and CD_3CN were purchased from Sigma Aldrich. $CDCl_3$ was dried first by refluxing over CaH_2, then distilled and degassed by multiple freeze-pump-thaw cycles, and stored over 4 Å molecular sieves. CD_3CN was stored over 3 Å molecular sieves for multiple days prior to use. Ethanol was used as supplied. Diisopropylamine was dried by refluxing over CaH_2 then distillation. Pyridine was stored over 4 Å molecular sieves for 3 days prior to use. Molecular sieves were activated at 350 °C. All NMR spectra were collected on a Bruker 400 MHz, Bruker 600 MHz, or INOVA 600 MHz spectrometer. NMR data as processed in either Bruker TopSpin 4.0.7, or in MestReNova 1.13. ^1H and $^{13}C\{^1H\}$ spectra were referenced to the solvent signal (trace proteo-solvent in the case of ^1H spectra). $^{31}P\{^1H\}$ spectra were referenced to an 85 % H_3PO_4 external standard at 0.0 ppm. Electrospray Ionization – Mass Spectrometry was used to analyze samples in acetonitrile at a concentration of 0.05 mg/mL, unless otherwise specified. FT-IR spectra were collected with a Bruker ALPHA II FTIR spectrometer in air, in either ATR-mode (attenuated total reflection) or in transmission mode as a KBr pellet, and the collection method was noted for each respective sample. Samples were prepared inside a nitrogen-filled glovebox and quickly measured either as a solid or as a KBr pellet of approximately 1 mg sample/100 mg KBr concentration. High-Resolution Mass-Spectrometry of acetonitrile solutions were performed using a Bruker MicrOTOF-II-focus instrument in positive polarity mode.

4.4.1 Modified Single Pot Procedure of ***C₃O*** Synthesis

Procedure was adapted from Strater *et. al.*[35].

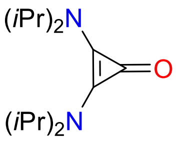

***C*$_3$O**

No special precautions were taken to exclude air or moisture. Around bottom flask containing C_3Cl_5H (5.0 mL, *ca*. 28 mmol) in CH_2Cl_2 (250 mL) were cooled to 0 ° C, then a solution of diisopropylamine (ca. 40 mL, 285 mmol) in CH_2Cl_2 (40 mL) were added dropwise over 1 h. The solution was allowed to stir at 0 °C for 4 h. The crude mixture was brought to near complete dryness *in vacuo*. To the same round-bottom flask containing the crude residue, MeOH (100 mL) was added, and the mixture stirred until all the solids were dissolved. The flask was gently cooled with an ice bath. Solid KOH pellets (12 g, 214 mmol) were then added to the stirred methanolic solution in one portion. After stirring for 10 min at 0 °C, the ice bath was removed and allowed to stir at room temperature for 4 h. Volatiles were removed *in vacuo*. The residue was reconstituted in CH_2Cl_2 (150 mL), followed by the addition of distilled water (150 mL) to separate the organic layer. The aqueous layer was then extracted with CH_2Cl_2 (3 x 30 mL). The combined organic layers were then dried with Na_2SO_4, filtered, and volatiles removed *in vacuo*. The solids were then redissolved in boiling ethyl acetate and allowed to slowly cool to room temperature over 2 h. After large needle-like crystals had formed, the mixture was then placed in a -30 °C freezer to allow further crystallization over 16 h. The white-to-pale-yellow needle-like solids were then collected in a Buchner funnel and dried under vacuum. A second batch of crystals were collected from the mother liquor. (3.5 g, 14 mmol, 50 % yield).

^{1}H NMR spectrum of this material matched with known literature data.[35]

4.4.2 Synthesis and Characterization of **4.3$_{BAC}$** and **[*C*$_3$Cl]Cl**

4.4.2.1 Reaction of ***C*$_3$*O*** and PCl_3

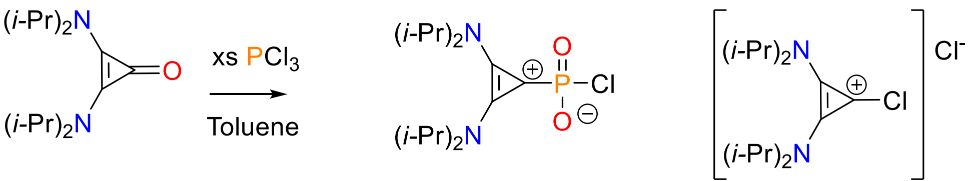

***C*$_3$O**

4.3$_{BAC}$

[*C*$_3$Cl]Cl

In a typical experiment, ***C_3O*** (1.00 g, 3.95 mmol) was weighed into a vial and toluene (5 mL) was added. The suspension was stirred vigorously until almost completely dissolved, at which point PCl_3 (1.6 mL, 18.3 mmol) was added rapidly neat. The mixture rapidly went cloudy after about 1 min of stirring and was allowed to stir for another hour. The suspension was centrifuged and decanted. The precipitate was washed four more times with toluene (10 mL), then the pellet was extracted with CH_2Cl_2 (3 mL) and transferred to a pre-weighed vial and volatiles were then removed in vacuo for 3 h. Analysis of the solids by ^{1}H NMR spectroscopy showed an approximate ratio of **4.3$_{\mathrm{BAC}}$**: **[*C_3*Cl]Cl** to be 50:50 by integration of the isopropyl signals. ^{31}P{^{1}H} NMR spectrum was free of detectable PCl_3 (δ_P = 220). The crude yield after washing had approximately 1:1 ratio of **4.3$_{\mathrm{BAC}}$** and **[*C_3*Cl]Cl** by ^{1}H NMR spectroscopy. (Yield 1.4 g, 90 % mass recovery).

Separation method A): The crude mixture (from reaction of 3.5 mmol of ***C_3O*** with excess PCl_3) was dissolved in hot fluorobenzene and allowed to cool to room temperature undisturbed for 24 h. The mother liquor was decanted, and the solids were carefully spread on a petri dish divided into two hemispheres A survey of crystals grown from this solution were individually tested by ^{1}H NMR in CH_2Cl_2 or $CDCl_3$. Needle-like and platelike crystals (**4.3$_{\mathrm{BAC}}$·PhF**) were manually separated from blocklike crystals (**[*C_3*Cl]Cl**). The crystals (0.187 mg; 87:13 ratio of **4.3$_{\mathrm{BAC}}$**: **[*C_3*Cl]Cl** by ^{1}H NMR integration) were initially were subsequently redissolved in hot PhF (2.5 mL), decanted, then separated (95.4 mg, 8.1 %). Further crystallization from the mother liquor resulted in a third collection of **4.3$_{\mathrm{BAC}}$** (20 mg, 1.7 % yield). Total combined yield = 120 mg, 9.9 %.

Separation method b): The crude mixture (500 mg) was dissolved in α,α,α-trifluorotoluene (11 mL) and stirred vigorously. Over 15 min, hexanes (6 mL) was added dropwise until slight precipitation was noted. The solution was allowed to stir for 5 min and then was filtered. The solvent was decanted, volatiles were removed, and a white powder was collected (50 mg, 88 % **4.3$_{\mathrm{BAC}}$** by ^{1}H NMR integration; ~20 % recovery of **4.3$_{\mathrm{BAC}}$**) was obtained from the first batch. Note: Solids collected *via* this initial separation method were frequently up to 85 % **4.3$_{\mathrm{BAC}}$** by ^{1}H integration, although this separation was not consistent.

4.4.2.2 Characterization of **[C_3Cl]Cl**

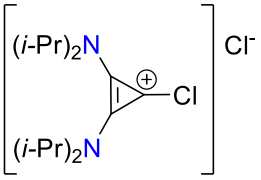

[C_3Cl]Cl

^{1}H NMR and ^{13}C{^{1}H} spectrum of this material matched with known literature data.[35]

^{1}H NMR (CDCl$_3$, 400 MHz) δ = 4.45 (sept, $^3J_{H-H}$ = 6.9 Hz, 2H, C*H*(CH$_3$)$_2$), 3.91 (sept, $^3J_{H-H}$ = 6.7 Hz, 2H, C*H*(CH$_3$)$_2$), 1.47 (d, $^3J_{H-H}$ = 6.7 Hz, 12H, CH(C*H$_3$*)$_2$, 1.43 (d, $^3J_{H-H}$ = 6.7 Hz, 12H, CH(C*H$_3$*)$_2$). **^{13}C{^{1}H} NMR (CDCl$_3$, 100 MHz)** δ = 132.5 (s, *C*-Cl), 92.6 (s, (*C)*$_2$C-Cl), 58.1 (s, *i*-Pr), 48.3 (s, *i*-Pr), 22.6 (s, Me), 21.0 (s, Me).

4.4.2.3 Characterization of **4.3$_{BAC}$**

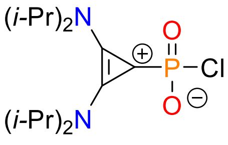

4.3$_{BAC}$

^{1}H NMR (CDCl$_3$, 400MHz) δ = 4.40 - 4.20 (br s, 2H, C*H*(CH$_3$)$_2$), 4.07 (sept, $^3J_{H-H}$ = 7.0 Hz, 2H, C*H*(CH$_3$)$_2$), 1.54 (d, $^3J_{H-H}$ = 7.0 Hz, 12H, CH(C*H$_3$*)$_2$), 1.38 (d, $^3J_{H-H}$ = 7.0 Hz, 12H, CH(C*H$_3$*)$_2$*)*. **^{1}H NMR (CD$_3$CN, 600MHz)** δ = 4.13 - 4.02 (m, 4H, *i*-Pr), 1.53 (d, 12H, $^3J_{H-H}$ = 6.9 Hz, CH$_3$), 1.35 (d, 12H, $^3J_{H-H}$ = 6.7 Hz, CH$_3$).**^{13}C{^{1}H} NMR (CDCl$_3$, 100 MHz)** δ = 133.7 (d, $^2J_{P-C}$ = 4.5 Hz, P-C-*C*-N), 109.5 (d, $^1J_{P-C}$ = 170 Hz, P-*C*), 58.1 (s, P-C-C-N-*C*), 53.2 (br s, P-C-C-N-*C*), 52.3 (br s, P-C-C-N-*C*), 21.5 (s, CH$_3$), 20.7 (s, CH$_3$). **^{31}P{^{1}H} NMR (CDCl$_3$,** 161.8 MHz) δ = -14.3. **^{31}P{^{1}H} NMR** (**CD$_3$CN, 242.3 MHz**) δ = -13.7.

4.4.3 Synthesis and Characterization of **[4.21$_{mono}$]**Cl

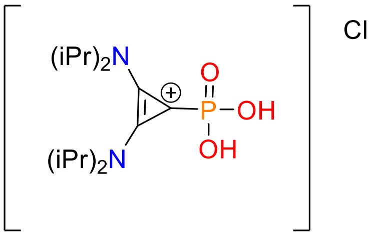

[4.21$_{mono}$]Cl

A CDCl$_3$ solution of **4.3$_{BAC}$** (4 mg) at room temperature was allowed to slowly react with atmospheric moisture in an NMR tube. Periodic monitoring by ^{31}P NMR revealed that the first hydrolysis product had a ^{31}P{^{1}H} NMR spectroscopy signal at -19.7 ppm which slowly converted to -8.2 ppm (**Appendix C-19**). Product was not isolated but quantitative conversion was observed by ^{31}P{^{1}H} NMR spectroscopy.

^{1}H NMR (400 MHz, CDCl$_3$) δ = 11.5 - 10.5 (br s, 2H, P(O*H*)$_2$), 4.4 - 3.8 (multiplet, 4H, *i*-Pr), 1.53 (d, 12H, $^3J_{H\text{-}H}$ = 6.9 Hz, CH$_3$), 1.41 (d, 12H, $^3J_{H\text{-}H}$ = 6.9 Hz, CH$_3$). **^{13}C{^{1}H} NMR (100.6 MHz, CDCl$_3$)** δ = Note: Ring carbons were not confirmed. 53.8 (br s, *i*-Pr), 52.4 (br s), 21.4 (CH$_3$), 20.7 (CH$_3$). **^{31}P{^{1}H} NMR (162 MHz, CDCl$_3$)** δ = -8.4 ppm.

4.4.4 Reactions of **4.3$_{BAC}$** and **[*C$_3$*Cl]Cl** With Lewis Bases

4.4.4.1 Reaction of **4.3$_{BAC}$** and **[*C$_3$*Cl]Cl** With EtOH

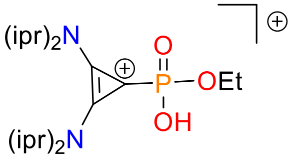

[4.22$_{OEt}$]

A solution of ~50:50 mixture of **4.3$_{BAC}$** and **[*C$_3$*Cl]Cl** (40 mg, ~0.06 mmol each) was prepared in CDCl$_3$ (1 mL) in a nitrogen filled glovebox, and transferred into an NMR tube sealed with a rubber septum. Outside of the glovebox, EtOH (5 µL, 0.9 mmol) was added *via* syringe through the septum then monitored periodically by NMR spectroscopy.

^{31}P{^{1}H} NMR (162 MHz, CDCl$_3$) δ = -7.7. **^{31}P NMR (162 MHz, CDCl$_3$)** δ = 7.7 (t, $^2J_{P\text{-}H}$ = 8 Hz).

4.4.4.2 Reaction of **4.3$_{BAC}$** and **[*C$_3$*Cl]Cl** With HN*i*Pr$_2$

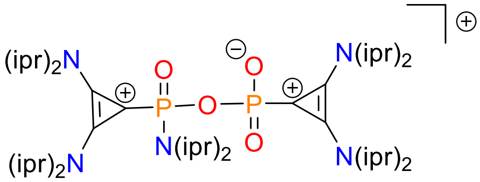

4.23$_{Nipr2}$

A solution of ~50:50 mixture of **4.3$_{BAC}$** and **[*C$_3$*Cl]Cl** (40 mg, ~0.06 mmol each) was prepared in CDCl$_3$ (1 mL) in a nitrogen filled glovebox, and transferred into an NMR tube sealed with a rubber septum. Outside of the glovebox, HN*i*-Pr$_2$ (20 µL, 0.14 mmol) was added *via* syringe through the septum then monitored periodically by NMR spectroscopy. The NMR tube was heated in an oil bath at 50 °C when the sample was outside of the spectrometer.

^{31}P{^{1}H} NMR (162 MHz, CDCl$_3$) δ = -8.1 (d, 1P, $^2J_{P\text{-}P}$ = 27 Hz), -22.3 (d, 1P, $^2J_{P\text{-}P}$ = 27 Hz). **^{31}P NMR (162 MHz, CDCl$_3$)** δ = -8.1 (dt, $^2J_{P\text{-}P}$ = 27 Hz and $^2J_{P\text{-}H}$ = 8 Hz), -22.3 (d, 1P, $^2J_{P\text{-}P}$ = 27 Hz).

4.4.4.3 Reaction of **4.3**$_{\mathbf{BAC}}$ and **[*C*$_3$Cl]Cl** With Pyridine

A solution of ~50:50 mixture of **4.3**$_{\mathbf{BAC}}$ and **[*C*$_3$Cl]Cl** (50 mg, ~0.08 mmol each) was prepared in $CDCl_3$ (1 mL) in a nitrogen filled glovebox, and transferred into a J-young NMR tube. Pyridine (28 µL, 0.34 mmol) was added inside of the glovebox, then was sealed and monitored periodically by NMR spectroscopy. The NMR tube was heated in an oil bath at 50 °C when the sample was outside of the spectrometer. Negligible conversion was observed after multiple days of heating this sample.

The same procedure was also used for a regular NMR tube capped with a rubber septum. Trimeric species was observable after 1 h of heating this sample.

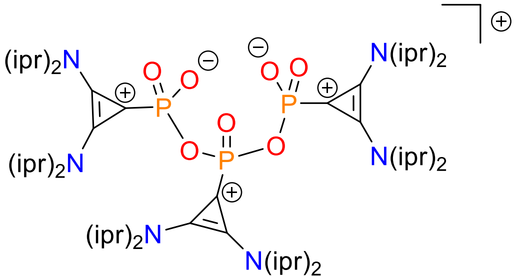

[4.21$_{tri}$]$^{2+}$

^{31}P{^{1}H} NMR (243 MHz, $CDCl_3$) δ = -21.2 (d, 2P, $^2J_{P\text{-}P}$ = 18 Hz), -26.0 (t, 1P, $^2J_{P\text{-}P}$ = 18 Hz).

4.4.4.4 Reaction Of **4.3**$_{\mathbf{BAC}}$ and **[*C*$_3$Cl]Cl** With Distilled Water

A solution of ~50:50 mixture of **4.3**$_{\mathbf{BAC}}$ and **[*C*$_3$Cl]Cl** (40 mg, ~0.06 mmol each) was prepared in $CDCl_3$ (1 mL) in a nitrogen filled glovebox, and transferred into an NMR tube sealed with a rubber septum. Outside of the glovebox, distilled water (5 µL, 0.3 mmol) was added *via* syringe through the septum then monitored periodically by NMR spectroscopy.

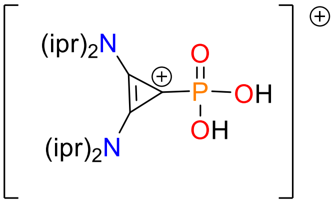

^{31}P{^{1}H} NMR (162 MHz, $CDCl_3$) δ = -9.3.

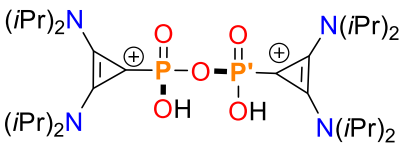

[4.21$_{di}$]$^{2+}$

$^{31}P\{^1H\}$ NMR (162 MHz, $CDCl_3$) δ = -20.6.

4.4.5 Synthesis and Characterization of **[4.17$_{DMAP}$]**Cl and **[4.24]Cl$_2$**

4.4.5.1 Reaction of **4.3$_{BAC}$** and **[*C*$_3$Cl]Cl** With DMAP

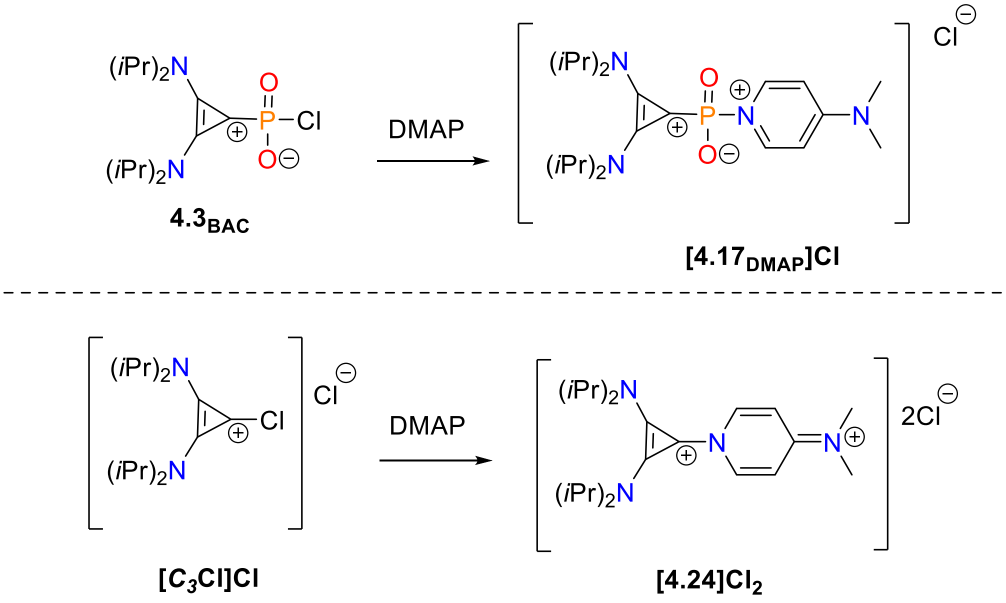

A solution of ~50:50 mixture of **4.3$_{BAC}$** and **[*C*$_3$Cl]Cl** (100 mg, approximately 0.16 mmol each) was prepared in CH_2Cl_2 (4 mL) in a nitrogen filled glovebox, a slight excess of DMAP (40 mg, 0.33 mmol) was added in one portion and allowed to stir for 24 h at ambient temperature. Volatiles were removed until an oily film was obtained, then then contents were then redissolved in CH_2Cl_2 (0.2 mL). Note: although the solids rapidly and completely dissolved, the concentrated mixture rapidly precipitated shortly afterwards. An additional portion of CH_2Cl_2 (2 mL) was then required to dissolve the material. The CH_2Cl_2 solution was then added dropwise to a rapidly stirred vial containing hexanes (10 mL). The mother liquor was decanted, and the solids were dried to a white powder *in vacuo*. The crude yield of 150 mg (higher than theoretical) indicated residual solvent was still present. A portion of this material was analyzed by NMR spectroscopy. The remining solids were then redissolved in a 2:1 ratio of CH_2Cl_2:hexanes, placed in a -30 °C freezer, and allowed to crystallize. After 2 days, the mother liquor was decanted from the solids, and a only minimal amount of solids had precipitated. The solids were dried under vacuum (6 mg, ca. 0.01 mmol, 8 % yield). ^1H NMR spectral analysis of this precipitate was approximately 93:7 ratio of **[4.17$_{DMAP}$]Cl** to DMAP.

4.4.5.2 Reaction of **4.3$_{BAC}$** With DMAP

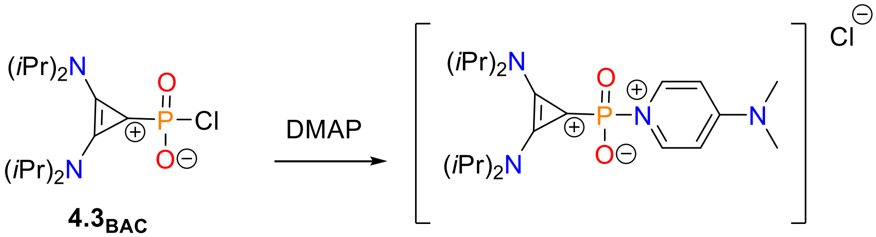

4.3$_{BAC}$

[4.17$_{DMAP}$]Cl

Handpicked crystals of **4.3$_{BAC}$** *via* Pasteur separation (4 mg, 0.01 mmol) were dissolved in $CDCl_3$ (1 mL) and then DMAP (1.9 mg, 0.015 mmol) was added. The reaction was tracked periodically by $^{31}P\{^1H\}$ NMR spectroscopy which only showed development of one new phosphorus species, at -16.2 ppm. Volatiles were removed and the solids were triturated with benzene (2 x 1 mL), then decanted. A white solid was collected after removal of volatiles *in-vacuo* for 45 min. 5.6 mg of solids were collected. Analysis of this material in $CDCl_3$ showed approximately 8 % unreacted DMAP by ^1H integration and 8 % unreacted **4.3$_{BAC}$** by $^{31}P\{^1H\}$ integration.

4.4.5.3 Characterization of **[4.17$_{DMAP}$]Cl**

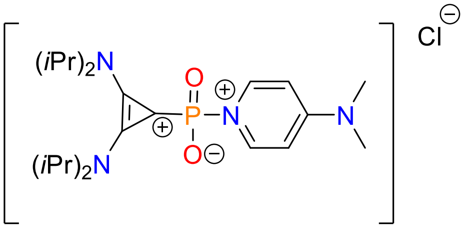

[4.17$_{DMAP}$]Cl

^1H NMR (400 MHz, $CDCl_3$) δ = 8.56 - 8.47 (m, 2H, P-N(C*H*)$_2$), 6.86 (d, 2H, $^3J_{H-H}$ = 7.3 Hz, P-N(CH-C*H*)$_2$), 4.11 (septet, 2H, $^3J_{H-H}$ = 6.8 Hz, *i*-Pr), 4.06-3.98 (br m, 2H, *i*-Pr), 3.24 (s, 6H, N*Me*$_2$), 1.39 (d, 12H, $^3J_{H-H}$ = 6.8 Hz, CH_3), 1.34 (d, 12H, $^3J_{H-H}$ = 6.8 Hz, CH_3). **$^{13}C\{^1H\}$ NMR (100.6 MHz,**

CDCl$_3$) δ = 157.4 (br s, *p*-DMAP) 141.70 (d, $^2J_{P\text{-}C}$ = 4.5 Hz, P-N(C)$_2$), 137.3 (d, $^2J_{P\text{-}C}$ = 5.5 Hz, P-C-*C*$_2$ 107.5 (d, $^3J_{P\text{-}C}$ = 5.1 Hz, P-N(C*C*)$_2$), 55.5 (br s, *i*-Pr), 51.2 (br s, *i*-Pr), 40.7 (s, N*Me*$_2$), 21.2 (s, CH$_3$), 20.8 (s, CH$_3$). Note: Could not detect P-*C* carbon. **^{31}P{^{1}H} NMR (162 MHz, CDCl$_3$)** δ = -16.2.

4.4.5.4 Characterization of **[4.24]Cl$_2$**

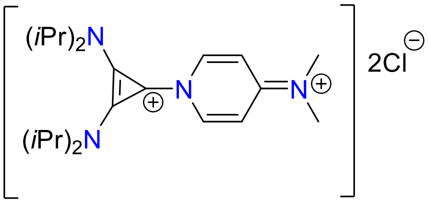

(iPr)2N
(iPr)2N
N
N
2Cl

[4.24]Cl$_2$

^{1}H NMR (400 MHz, CDCl$_3$) δ = 9.80 (d, 2H, ^3J=7.8 Hz, CN-(C*H*-CH)$_2$(CH$_3$)$_2$), 7.13 (d, 2H, ^3J=7.8 Hz, CN-(CH-C*H*)$_2$(CH$_3$)$_2$), 4.13 - 4.00 (overlapped with [(BAC)(DMAP)PO$_2$]Cl signals, supported by ^{1}H -^{1}H COSY, 2H, *i*-Pr), 3.72 (septet, 2H, $^3J_{H\text{-}H}$ = 6.8 Hz, *i*-Pr), 3.31 (s, 6H, NMe$_2$), 1.44 (d, 12H, $^3J_{H\text{-}H}$ = 6.8 Hz, CH$_3$), 1.26 (d, 12H, $^3J_{H\text{-}H}$ = 6.8 Hz, CH$_3$). **^{13}C{^{1}H} NMR (100.6 MHz, CDCl$_3$)** δ = 157.2 (*p*-DMAP), 143.5 (*o*-DMAP), 132.1 ((N*i*-Pr$_2$-*C*)$_2$) 109.1 (*m*-DMAP), 99.3 (N*i*-Pr$_2$-C-*C*-DMAP), 57.7 (*i*-Pr), 49.5 (*i*-Pr), 22.7 (CH$_3$), 21.0 (CH$_3$).

4.4.6 Reaction of **4.3$_{BAC}$** With LiBF$_4$

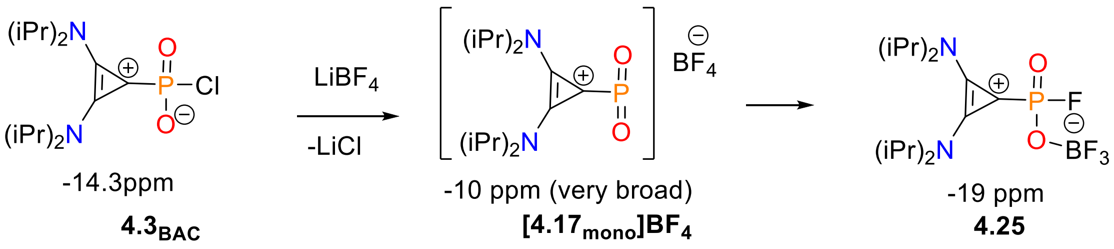

(iPr)2N
(iPr)2N
O
P
Cl
O
-14.3ppm
4.3BAC
LiBF4
-LiCl
(iPr)2N
(iPr)2N
O
P
O
BF4
-10 ppm (very broad)
[4.17mono]BF4
(iPr)2N
(iPr)2N
O
P
F
O
BF3
-19 ppm
4.25

Handpicked crystals of **4.3$_{BAC}$** (4 mg, 0.01 mmol) were dissolved in CDCl$_3$ (500 μL) then added to a J-Young tube. LiBF$_4$ (2 mg, 0.02 mmol) was weighed and then added to the NMR tube. The vial was then rinsed with more CDCl$_3$ (200 μL) and combined in the J-Young tube. The mixture was periodically monitored by NMR spectroscopy. Due to the instability of **[4.17$_{mono}$]BF$_4$** by ^{31}P{^{1}H} analysis and the difficulty of isolation of starting material (see **Figure 4-19**), full spectral characterization of the mixture of species was not performed.

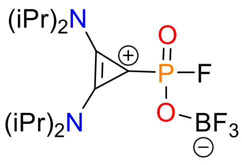

9

^{31}P{^{1}H} NMR (162 MHz, CDCl$_3$) δ = -13.2 (15 min); -10.2 (16 h). **^{31}P{^{1}H} NMR (162 MHz, CDCl$_3$)** δ = -19.0 (d, $^{1}J_{P\text{-}F}$ = 985 Hz). **^{19}F{^{1}H} NMR (376 MHz, CDCl$_3$)** δ = -53.9 (br d, 1F, $^{1}J_{P\text{-}F}$ = 985 Hz). -146.2 (d, 3F, $^{4}J_{F\text{-}F}$ = 8 Hz).

4.4.7 Synthesis and Characterization of **[4.17$_{mono}$]OTf** and **[*C*$_3$Cl]**OTf

4.4.7.1 Reaction of **4.3$_{BAC}$** and **[*C*$_3$Cl]Cl** With SiMe$_3$OTf

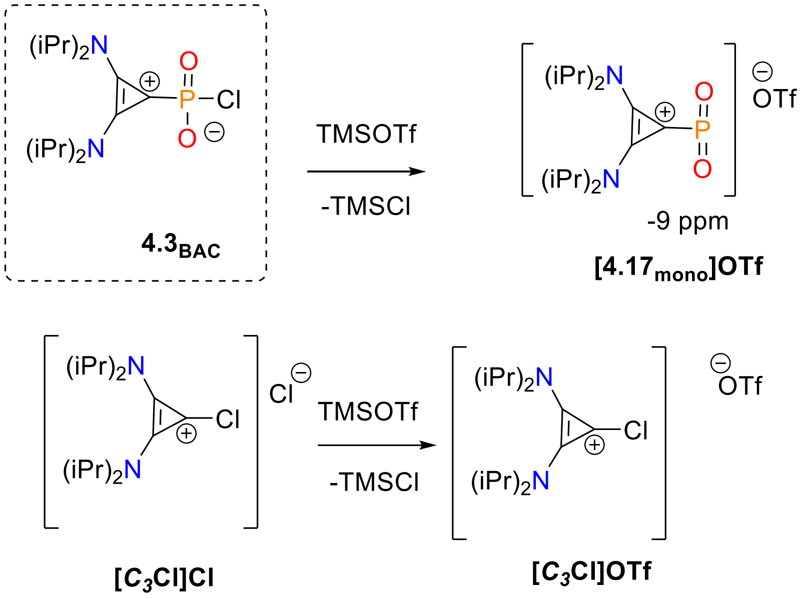

SiMe$_3$OTf (60 µL, 0.33 mmol) was added neat to a J-Young tube containing a 50:50 mixture of **4.3$_{BAC}$** and **[*C*$_3$Cl]Cl** (50 mg, ca. 0.08 mmol each) in CDCl$_3$ (1 mL). The NMR tube was sealed and taken for immediate NMR spectroscopic analysis. Within 10 min, all the starting material had been consumed and a single sharp, well-defined signal could be observed in the ^{31}P{^{1}H} NMR spectrum. Attempts to isolate as a solid resulted in decomposition of **[4.17$_{mono}$]OTf**.

4.4.7.2 Characterization of **[4.17$_{mono}$]OTf**

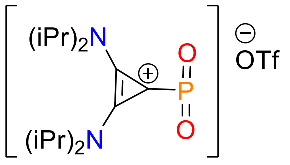

[4.17$_{mono}$]OTf

^{1}H NMR (400 MHz, CDCl$_3$) δ = 4.20 (septet, 2H, 6.7 Hz, *i*-Pr), 4.02 (septet, 2H, 6.8 Hz, *i*-Pr), 1.46 (d, 12H, 6.8 Hz, Me), 1.42 (d, 12H, 6.7 Hz, Me). **^{13}C{^{1}H} NMR (100.6 MHz, CDCl$_3$)** δ =

134.6 (d, N-C, ${}^{2}J_{\text{P-C}}$ = 5.8 Hz), 119.7 (q, ${}^{1}J_{\text{C-F}}$ = 320 Hz, CF_3), 96.0 (d, P-C, ${}^{1}J_{\text{P-C}}$ = 225.8 Hz), 59.9 (overlapped with **[*C*$_3$Cl]**OTf resonance), C*H*(CH_3)$_2$), 50.8 (C*H*(CH_3)2), 20.7 (CH_3), 20.4 (CH_3). **^{31}P{^{1}H} NMR (162 MHz, $CDCl_3$)** δ = -9.4 (${}^{1}J_{\text{P-C}}$ = 228 Hz). **^{19}F{^{1}H} NMR (376 MHz, $CDCl_3$)** δ = -77.9 (s, CF_3).

4.4.7.3 Characterization of **[*C*$_3$Cl]OTf**

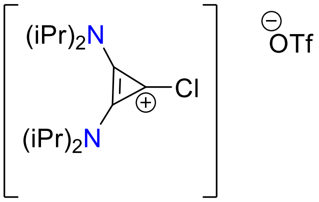

[*C*$_3$Cl]OTf

^{1}H NMR (400 MHz, $CDCl_3$) δ = 4.08 (septet, 2H, 6.5 Hz, *i*-Pr), 3.84 (septet, 2H, 6.5 Hz, *i*-Pr), 1.37 (d, 24H, 6.5 Hz, Me). **^{13}C{^{1}H} NMR (100.6 MHz, $CDCl_3$)** δ = 132.1 (N-C), 119.7 (q, ${}^{1}J_{\text{C-F}}$ = 320 Hz, CF_3), 93.3 (C-Cl), 57.9 (*i*-Pr), 48.4 (*i*-Pr), 22.4 (CH_3), 20.6 (CH_3).

4.4.8 Synthesis of **[4.21$_{\text{mono}}$]OTf**

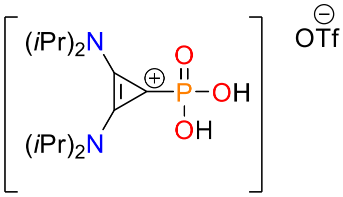

A J-Young NMR tube containing a solution of **4.3$_{\text{BAC}}$** (20 mg, 0.06 mmol) was mixed with TMsOTf (12 µL, 0.06 mmol) in $CDCl_3$ (1 mL) was opened to air and the compound was allowed to slowly hydrolyze, and was crystallized as the solvent evaporated.

4.4.9 Reactions of **4.3$_{\text{BAC}}$** and BCF

4.4.9.1 Reaction of **4.3$_{\text{BAC}}$** and BCF Performed Without Heating

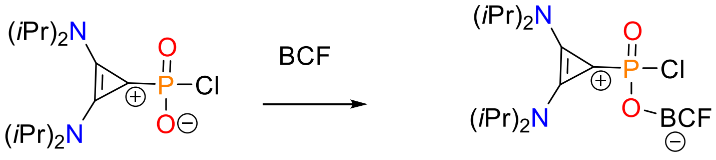

4.3$_{\text{BAC}}$ **4.26**

Handpicked crystals of **4.3$_{\text{BAC}}$** (4 mg, 0.01 mmol) and tris(pentafluorophenyl)borane (6 mg, 0.01 mmol) were mixed and dissolved in $CDCl_3$ (1 mL). The solution was transferred to an NMR tube and immediately analyzed. A boron resonance could not be identified in ^{11}B NMR spectroscopy experiments.

^{1}H NMR (600 MHz, CDCl$_3$) δ = 4.16 (br m, 4H, *i*-Pr), 1.43 (d, 12H, $^{3}J_{H-H}$ = 7 Hz, Me), 1.31 (br d, 12H, $^{3}J_{H-H}$ = 5.5 Hz, Me). **^{31}P{^{1}H} NMR (243 MHz, CDCl$_3$)** δ = -14.3 (br s). **^{19}F{^{1}H} NMR (564 MHz, CDCl$_3$)** δ = -133.5 (s), -158.9 (br s), -164.9.

4.4.9.2 Reaction of **4.3$_{BAC}$** and BCF Resulting in Isolation of **4.27** Crystal

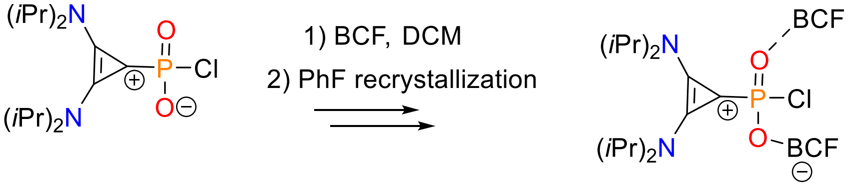

4.3$_{BAC}$

4.27

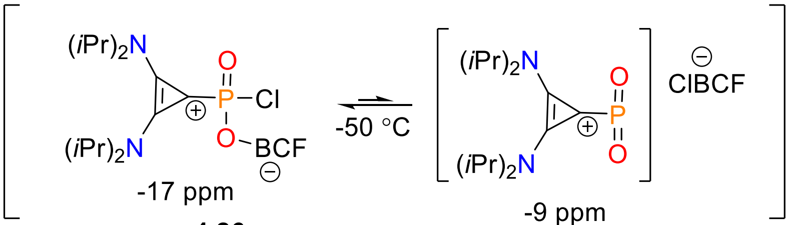

4.26

[4.17$_{mono}$]ClBCF

Handpicked crystals of **4.3$_{BAC}$** (20 mg, 0.06 mmol) and tris(pentafluorophenyl)borane (31 mg, 0.06 mmol) were dissolved in CH$_2$Cl$_2$ (1 mL) and sealed into a J-Young NMR tube. The solution was left undisturbed for 16 h, then volatiles were removed *in vacuo*. PhF (1 mL) was immediately added and the mixture was gently heated until all solids had dissolved. The tube was then resealed and left undisturbed for 24 h at room temperature to crystallize. The mother liquor was decanted and a few crystals were removed for SC-XRD, while the remaining solids contained within the NMR tube were rinsed with 1 mL pentane. Volatiles were removed again and CD$_2$Cl$_2$ (1 mL) was added, but did not result in significant dissolution of the solids. The J-Young tube was then used for NMR spectroscopic analyses.

^{1}H NMR (600 MHz, CD$_2$Cl$_2$, 25 °C) δ = 4.14 (br m, 4H, *i*-Pr), 1.41 (d, 12H, $^{3}J_{H-H}$ = 7 Hz, Me), 1.21 (br d, 12H, $^{3}J_{H-H}$ = 5.5 Hz, Me). **^{13}C{^{1}H} NMR (150 MHz, CD$_2$Cl$_2$, -75 °C)** δ = 21.9, 19.7, 18.9, 18.4 Note: only methyl signals were resolved after 2000 scans at

-75 °C. **$^{31}P\{^{1}H\}$ NMR (243 MHz, CD_2Cl_2, 25 °C)** δ = -15.0 (br s). **$^{31}P\{^{1}H\}$ NMR (243 MHz, CD_2Cl_2, -75 °C)** δ = -9.0 (br s; [4.17_{mono}]**ClBCF**), -16.4 (br s; **10**). **$^{19}F\{^{1}H\}$ NMR (564 MHz, CD_2Cl_2, 25 °C)** δ = -133.5 (s), -158.9 (br s), -164.9.

4.4.10 *In Situ* Generation of **4.18_{Ph}**

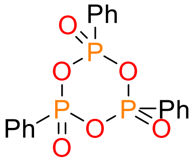

4.18_{Ph}

A solution of ***C_3O*** (0.100g, 0.4 mmol) was prepared in CH_2Cl_2 (6 mL), then $PhPOCl_2$ (120 μL, 0.96 mmol) was added neat and then allowed to stir at room temperature overnight. An aliquot of the reaction mixture after 16 h was analyzed by ^{1}H and $^{31}P\{^{1}H\}$ NMR spectroscopy. Complete consumption of ***C_3O*** was determined by ^{1}H NMR. The $^{31}P\{^{1}H\}$ NMR spectrum showed resonances for $PhPOCl_2$, and two new sets of resonances: a multiplet at 20 ppm, and **4.18_{Ph}**. Normalization of the signals for the unknown species and **4.22_{Ph}** reveals the reaction proceeded with 75 % selectivity for **4.18_{Ph}**. Separation of the species was not achieved.

^{1}H, and $^{31}P\{^{1}H\}$ NMR spectra containing **4.18_{Ph}** in $CDCl_3$ were consistent with previously reported data.[18]

4.4.11 Synthesis of **4.18_{Mes}**

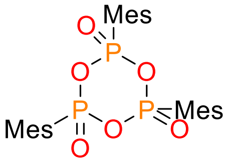

4.18_{Mes}

A solution of ***C_3O*** (0.252g, 1.00 mmol) was prepared in toluene (12 mL), while a second solution of $MesPOCl_2$ (238 mg, 1.00 mmol) was prepared in toluene (3 mL). The two solutions were combined and the vials were rinsed with an additional portion of toluene (2 mL). The solution rapidly went cloudy and was stirred for 30 min. An initial filtration was performed to separate a white powder (289 mg, **[*C_3*Cl]Cl)**, then the solution was allowed to continue stirring. Two more filtrations were performed at the 60 min and 80 min marks. The principle solution was allowed to continue stirring overnight as more precipitate was generated, then the solid was separated by decanting and was dried under reduced pressure to yield a white powder (130 mg; approximately 85:15 **4.18_{Mes}**: **[*C_3*Cl]Cl** by ^{1}H NMR integration).

^{1}H, ^{13}C{^{1}H}, and ^{31}P{^{1}H} NMR spectra obtained in either $CDCl_3$ or C_6D_6 containing **4.18$_{\mathbf{Mes}}$** were consistent with previously reported data.[18]

4.5 X-ray Crystallographic Data

A summary of X-ray diffraction collection and refinement data can be found in **Table 4-2**. Each sample was mounted on a Mitegen polyimide micromount with a small amount of Paratone N oil. X-ray measurements were made on a Bruker Kappa Axis Apex2 diffractometer at a temperature of -163 °C. The data collection strategy ω and φ scans, and data was collected up to 2θ values found in **Table 4-2**. The frame integrations were performed using SAINT.[43] The resulting raw data was scaled and absorption corrected using a multi-scan averaging of symmetry equivalent data using SADABS[43,44] or TWINABS.[45] Unless otherwise stated, the structures were solved by using a dual space methodology using the SHELXT program.[46] All non-hydrogen atoms were obtained from the initial solution. The hydrogen atoms were introduced at idealized positions and were allowed to ride on the parent atom. The structural models were fit to the data using full matrix least-squares based on F^2. The calculated structure factors included corrections for anomalous dispersion from the usual tabulation. **4.3$_{\mathbf{BAC}}$** possessed a fluorobenzene solvent molecule disordered over two positions where the fluorine atom rotated approximately 180° about an axis passing normal to the molecular plane through the centroid of the ring. The primary orientation refined to an occupancy factor of 0.891(3). The structures were refined using the SHELXL program from the SHELX suite of crystallographic software.[46] Graphic plots were produced using the Mercury program.[47]

Structure Solution and Refinement: Unless otherwise stated, the structures were solved by using a dual space methodology using the SHELXT program.[46] All non-hydrogen atoms were obtained from the initial solution. The hydrogen atoms were introduced at idealized positions and were allowed to ride on the parent atom. The structural models were fit to the data using full matrix least-squares based on F^2. The calculated structure factors included corrections for anomalous dispersion from the usual tabulation. The structures were refined using the SHELXL program from the SHELX suite of crystallographic software.[46] Graphic plots were produced using the Mercury program.[47]

Table 4-2. Summary of X-ray diffraction collection and refinement details for compounds in chapter 4.

Formula	$C_{15}H_{29}Cl_3N_2$ **[C_3Cl]ClHCl**	$C_{15}H_{28}Cl_5N_2P$ **[*C_3*Cl]PCl_4**	$C_{60}H_{35.50}B_2ClF_{31.50}N_2O_2P$ (**4.27**)	$C_{21}H_{33}ClFN_2O_2P$ (**4.3**$_{\mathbf{BAC}}$)	$C_{16}H_{30}F_3N_2O_6PS$ **[4.21$_{\mathbf{mono}}$]OTf**
Formula Weight (*g/mol*)	343.75	444.61	1502.94	430.91	466.45
Crystal System	monoclinic	orthorhombic	monoclinic	orthorhombic	monoclinic
Space Group	P 2_1/n	C m c m	C 2/c	P b c a	P 2_1/c
Temperature, K	110	110	110	110	110
***a*, Å**	12.556(7)	9.932(4)	42.882(17)	16.435(14)	10.556(4)
***b*, Å**	10.004(6)	12.620(4)	10.465(3)	16.169(15)	17.021(5)
***c*, Å**	15.044(9)	17.754(7)	27.165(9)	17.324(14)	25.567(8)
α,°	90	90	90	90	90
β,°	93.705(13)	90	101.287(8)	90	101.849(8)
γ,°	90	90	90	90	90
V, Å^3	1885.7(19)	2225.2(14)	11955(7)	4604(7)	4496(3)
Z	4	4	8	8	8
F(000)	736	928	6008	1840	1968
ρ (*g/cm^3*)	1.211	1.327	1.670	1.243	1.378
λ, Å, (MoKα)	0.71073	0.71073	0.71073	0.71073	0.71073
μ, (*cm^{-1}*)	0.480	0.724	0.237	0.262	0.273
Max 2θ for data collection, °	43.554	56.672	42.822	61.048	58.33
Measured fraction of data	0.995	0.999	0.994	1.000	0.998
R_{merge}	0.0998	0.0911	?	0.0735	0.1105
R_1	0.0366	0.0330	0.0421	0.0341	0.0396
wR_2	0.0880	0.0692	0.0836	0.0790	0.0913
R_1 (all data)	0.0522	0.0499	0.0667	0.0513	0.0531
wR_2 (all data)	0.0979	0.0757	0.0923	0.0882	0.0966
GOF	1.037	1.081	1.040	1.016	1.046

$R_1 = \Sigma \mid |F_o| - |F_c| \mid / \Sigma F_o$; $wR_2 = [\Sigma(w(F_o^2 - F_c^2)^2) / \Sigma w(F_o^4)]^{½}$; $GOF = [\Sigma(w(F_o^2 - F_c^2)^2) / (\text{No. of reflns. - No. of params.})]^{½}$

4.6 References

(1) Beattie, I. R.; Livingston, K. M. S.; Ozin, G. A.; Reynolds, D. J. Single-Crystal Raman Spectra of Arsenolite (As_4O_6) and Senarmonite (Sb_4O_6). The Gas-Phase Raman Spectra of P_4O_6, P_4O_{10}, and As_4O_6. *J. Chem. Soc. A* **1970**, No. 0, 449–451. https://doi.org/10.1039/J19700000449.

(2) Beagley, B.; Cruickshank, D. W. J.; Hewitt, T. G.; Haaland, A. Molecular Structures of P_4O_{10} and P_4O_9. *Trans. Faraday Soc.* **1967**, *63* (0), 836–845. https://doi.org/10.1039/TF9676300836.

(3) Beagley, B.; Cruickshank, D. W. J.; Hewitt, T. G.; Jost, K. H. Molecular Structures of P_4O_6 and P_4O_8. *Trans. Faraday Soc.* **1969**, *65* (0), 1219–1230. https://doi.org/10.1039/TF9696501219.

(4) Binnewies, M. Massenspektrometrische Untersuchung Des Gleichgewichts $POCl_g$ + 1/2 $O_{2,g}$ = PO_2Cl_g. *Z. Anorg. Allg. Chem.* **1983**, *507* (12), 77–80. https://doi.org/10.1002/zaac.19835071210.

(5) Ahlrichs, R.; Ehrhardt, C.; Lakenbrink, M.; Schunck, S.; Schnoeckel, H. Molecular PO_2Cl: Matrix IR Investigations and Ab Initio SCF Calculations. *J. Am. Chem. Soc.* **1986**, *108* (13), 3596–3602. https://doi.org/10.1021/ja00273a008.

(6) Scherer, O. J.; Braun, J.; Walther, P.; Heckmann, C.; Wolmershäuser, G. Phosphorus Monoxide (PO) as Complex Ligand. *Angew. Chem. Int. Ed.* **1991**, *30* (7), 852–854. https://doi.org/10.1002/anie.199108521.

(7) Dhara, D.; Pal, P. K.; Dolai, R.; Chrysochos, N.; Rawat, H.; Elvers, B. J.; Krummenacher, I.; Braunschweig, H.; Schulzke, C.; Chandrasekhar, V.; Priyakumar, U. D.; Jana, A. Synthesis and Reactivity of NHC-Coordinated Phosphinidene Oxide. *Chem. Commun.* **2021**, *57* (75), 9546–9549. https://doi.org/10.1039/D1CC04421D.

(8) Zeffert, B. M.; Coulter, P. B.; Macy, R. The Absence of Quaternary Salt

Formation between Phosphoryl Chloride and Pyridine[1]. *J. Am. Chem. Soc.* **1953**, *75* (3), 751–753. https://doi.org/10.1021/ja01099a514.

(9) Gutmann, V. Das Solvosystem Phosphoroxychlorid. V. *Monatsh. Chem.* **1954**, *85* (5), 1077–1081. https://doi.org/10.1007/BF00899855.

(10) Rovnaník, P.; Kapička, L.; Taraba, J.; Černík, M. Base-Induced Dismutation of $POCl_3$ and $POBr_3$: Synthesis and Structure of Ligand-Stabilized Dioxophosphonium Cations. *Inorg. Chem.* **2004**, *43* (7), 2435–2442. https://doi.org/10.1021/ic0354163.

(11) Bezgubenko, L. V; Pipko, S. E.; Shalimov, A. A.; Sinitsa, A. D. Nucleophilic Catalysis of Phosphorus Trichloride Oxygen Oxidation. *Heteroat. Chem.* **2008**, *19* (4), 408–411. https://doi.org/10.1002/hc.20439.

(12) Kuhn, N.; Ströbele, M.; Walker, M. A Stable Carbene Phosphenic Chloride Complex: First Structural Characterization of a PO_2Cl Base Adduct [1]. *Z. Anorg. Allg. Chem.* **2003**, *629* (2), 180–181. https://doi.org/10.1002/zaac.200390026.

(13) Teichmann, H.; Wilbrandt, D.; Schulz, J. Phosphorylations with $ROP(X)Cl_2$: A New Mechanistic Pathway. *Phosphorus, Sulfur Silicon Relat. Elem.* **1990**, *49/50*, 251. https://doi.org/10.1080/10426509008038953.

(14) Teichmann, H.; Schulz, J.; Wilbrandt, D. Ein Neuer Einfacher Zugang Zu Pyridinium-Phosphor-Betainen. *Z. Chem.* **1990**, *30*, 18. https://doi.org/10.1002/zfch.19900300104.

(15) Zhou, J.; Liu, L. L.; Cao, L. L.; Stephan, D. W. Base-Stabilized $[PO]^+/[PO_2]^+$ Cations. *Angew. Chem. Int. Ed.* **2019**, *58* (50), 18276–18280. https://doi.org/10.1002/anie.201912009.

(16) Diemert, K.; Kuchen, W.; Poll, W.; Sandt, F. A Convenient Synthesis of Phosphonic Anhydrides – Trimers $[RPO_2]_3$ (R = tert-Butyl, 2-Methylphenyl, 2,4,6-Trimethylphenyl): Their Structures and Reaction Products. *Eur. J. Inorg. Chem.* **1998**, *1998* (3), 361. https://doi.org/10.1002/(SICI)1099-

0682(199803)1998:3<361::AID-EJIC361>3.0.CO;2-T.

(17) Hettstedt, C.; Unglert, M.; Mayer, R. J.; Frank, A.; Karaghiosoff, K. Methoxyphenyl Substituted Bis(Picolyl)Phosphines and Phosphine Oxides. *Eur. J. Inorg. Chem.* **2016**, *2016* (9), 1405. https://doi.org/10.1002/ejic.201600032.

(18) Arz, M. I.; Annibale, V. T.; Kelly, N. L.; Hanna, J. V; Manners, I. Ring-Opening Polymerization of Cyclic Phosphonates: Access to Inorganic Polymers with a P^V–O Main Chain. *J. Am. Chem. Soc.* **2019**, *141* (7), 2894–2899. https://doi.org/10.1021/jacs.8b13435.

(19) Ranganathan, T.; Zilberman, J.; Farris, R. J.; Coughlin, E. B.; Emrick, T. Synthesis and Characterization of Halogen-Free Antiflammable Polyphosphonates Containing 4,4’-Bishydroxydeoxybenzoin. *Macromolecules* **2006**, *39* (18), 5974. https://doi.org/10.1021/ma0614693.

(20) Steinbach, T.; Ritz, S.; Wurm, F. R. Water-Soluble Poly(Phosphonate)s via Living Ring-Opening Polymerization. *ACS Macro Lett.* **2014**, *3* (3), 244–248. https://doi.org/10.1021/mz500016h.

(21) English, L. E.; Pajak, A.; McMullin, C. L.; Lowe, J. P.; Mahon, M. F.; Liptrot, D. J. A Terphenyl Supported Dioxophosphorane Dimer: The Light Congener of Lawesson’s and Woollins’ Reagents. *Chem. Eur. J.* **2022**, *28* (28), e202200376. https://doi.org/10.1002/chem.202200376.

(22) Henne, F. D.; Watt, F. A.; Schwedtmann, K.; Hennersdorf, F.; Kokoschka, M.; Weigand, J. J. Tetra-Cationic Imidazoliumyl-Substituted Phosphorus–Sulfur Heterocycles from a Cationic Organophosphorus Sulfide. *Chem. Commun.* **2016**, *52* (10), 2023–2026. https://doi.org/10.1039/C5CC08182C.

(23) Jochem, G.; Karaghiosoff, K.; Plank, S.; Schmidpeter, S. D. U. A. Ylidylphosphorsulfide, -Selenide, -Disulfide, -Sulfidselenide Und -Diselenide. *Chem. Ber.* **1995**, *128* (12), 1207–1219. https://doi.org/10.1002/cber.19951281212.

(24) Appel, R.; Knoch, F.; Kunze, H. The First Organodithioxophosphorane. *Angew. Chem. Int. Ed.* **1983**, *22* (12), 1004–1005. https://doi.org/10.1002/anie.198310041.

(25) Yde, B.; Yousif, N. M.; Pedersen, U.; Thomsen, I.; Lawesson, S.-O. Studies on Organophosphorus Compounds XLVII Preparation of Thiated Synthons of Amides, Lactams and Imides by Use of Some New p,s-Containing Reagents. *Tetrahedron* **1984**, *40* (11), 2047–2052. https://doi.org/10.1016/S0040-4020(01)88445-3.

(26) Gray, I. P.; Bhattacharyya, P.; Slawin, A. M. Z.; Woollins, J. D. A New Synthesis of $(PhPSe_2)_2$ (Woollins Reagent) and Its Use in the Synthesis of Novel P–Se Heterocycles. *Chem. Eur. J.* **2005**, *11* (21), 6221–6227. https://doi.org/10.1002/chem.200500291.

(27) Kuchenbeiser, G.; Donnadieu, B.; Bertrand, G. Stable Bis(Diisopropylamino)Cyclopropenylidene (BAC) as Ligand for Transition Metal Complexes. *J. Organomet. Chem.* **2008**, *693* (5), 899–904. https://doi.org/10.1016/j.jorganchem.2007.11.056.

(28) Bandar Tristan H., J. S. . L. Aminocyclopropenium Ions: Synthesis, Properties, and Applications. *Synthesis* **2013**, *45* (18), 2485–2498. https://doi.org/10.1055/s-0033-1338516.

(29) Bidal, Y. D.; Lesieur, M.; Melaimi, M.; Cordes, D. B.; Slawin, A. M. Z.; Bertrand, G.; Cazin, C. S. J. A Simple Access to Transition Metal Cyclopropenylidene Complexes. *Chem. Commun.* **2015**, *51* (23), 4778–4781. https://doi.org/10.1039/C4CC10375K.

(30) Konishi, H.; Matsumoto, S.; Kamitori, Y.; Ogoshi, H.; Yoshida, Z. Synthesis And Properties Of Diaminocyclopropenylidene Transition Metal Complexes. *Chem. Lett.* **1978**, *7* (3), 241–244. https://doi.org/10.1246/cl.1978.241.

(31) Gade, L. H.; Memmler, H.; Kauper, U.; Schneider, A.; Fabre, S.; Bezougli, I.; Lutz, M.; Galka, C.; Scowen, I. J.; McPartlin, M. Cooperative Reactivity of Early-

Late Heterodinuclear Transition Metal Complexes with Polar Organic Substrates. *Chem. Eur. J.* **2000**, *6* (4), 692–708. https://doi.org/10.1002/(SICI)1521-3765(20000218)6:4<692::AID-CHEM692>3.0.CO;2-2.

(32) Obata, N.; Takizawa, T. Novel Ring-Enlargement Reaction of Diphenylcyclopropenone with 2,6-Dimethylphenylisonitrile in the Presence of Triphenylphosphine. *Tetrahedron Lett.* **1970**, *11* (26), 2231–2234. https://doi.org/10.1016/S0040-4039(01)98196-1.

(33) Xin, T.; Cummins, C. C. Synthesis of Phosphet-2-One Derivatives via Phosphinidene Transfer to Cyclopropenones. *J. Am. Chem. Soc.* **2023**. https://doi.org/10.1021/jacs.3c11263.

(34) Alcarazo, M. α-Cationic Phosphines: Synthesis and Applications. *Chem. Eur. J.* **2014**, *20* (26), 7868–7877. https://doi.org/10.1002/chem.201402375.

(35) Strater, Z. M.; Rauch, M.; Jockusch, S.; Lambert, T. H. Oxidizable Ketones: Persistent Radical Cations from the Single-Electron Oxidation of 2,3-Diaminocyclopropenones. *Angew. Chem. Int. Ed.* **2019**, *58* (24), 8049–8052. https://doi.org/10.1002/anie.201902265.

(36) Weigand, J. J.; Feldmann, K.-O.; Henne, F. D. Carbene-Stabilized Phosphorus(III)-Centered Cations $[LPX_2]^+$ and $[L_2PX]^{2+}$ (L = NHC; X = Cl, CN, N_3). *J. Am. Chem. Soc.* **2010**, *132* (46), 16321–16323. https://doi.org/10.1021/ja106172d.

(37) Modern Aspects of ^{31}P NMR Spectroscopy. In *Organophosphorus Chemistry*; 2019; pp 457–498. https://doi.org/10.1002/9783527672240.ch9.

(38) Weiss, R.; Engel, S. Electrostatic Activation of Nucleofuges: Cationic Leaving Groups. *Angew. Chem. Int. Ed.* **1992**, *31* (2), 216–217. https://doi.org/10.1002/anie.199202161.

(39) Teichmann, H.; Schulz, J.; Costisella, B.; Habisch, D. Ammonium-Chlor(Thio)Phosphat-Betaine, Eine Klasse Koordinationsstabilisierter

Chlor(Thio)Metaphosphate. *Z. Anorg. Allg. Chem.* **1991**, *606* (1), 233–241. https://doi.org/10.1002/zaac.19916060125.

(40) Weiss, R.; Priesner, C.; Wolf, H. Structure and Formation of Triorganylphosphoniocyclopropenylium Ions. *Angew. Chem. Int. Ed.* **1979**, *18* (6), 472–473. https://doi.org/10.1002/anie.197904721.

(41) Kanters, J. A. N. A. Structure of the Pyridine Adduct of Dithiophosphoryl Monochloride. **1989**, No. 1979, 3–5. https://doi.org/10.1107/S010827018900452X.

(42) Dube, J. W.; Zheng, Y.; Thiel, W.; Alcarazo, M. α-Cationic Arsines: Synthesis, Structure, Reactivity, and Applications. *J. Am. Chem. Soc.* **2016**, *138* (21), 6869–6877. https://doi.org/10.1021/jacs.6b03500.

(43) Bruker-AXS, SAINT Version 2013.8, 2013, Bruker-AXS, Madison, WI 53711, USA.

(44) Bruker-AXS, SADABS Version 2012.1, 2012, Bruker-AXS, Madison, WI 53711, USA.

(45) Bruker-AXS. TWINABS Version 2012.1. Madison, WI 53711, USA 2012.

(46) Sheldrick, G. M. SHELXT - Integrated Space-Group and Crystal-Structure Determination. *Acta Cryst. A* **2015**, *71* (1). https://doi.org/10.1107/S2053273314026370.

(47) Macrae, C. F.; Bruno, I. J.; Chisholm, J. A.; Edgington, P. R.; McCabe, P.; Pidcock, E.; Rodriguez-Monge, L.; Taylor, R.; Van De Streek, J.; Wood, P. A. Mercury CSD 2.0 - New Features for the Visualization and Investigation of Crystal Structures. *J. Appl. Cryst*. **2008**. https://doi.org/10.1107/S0021889807067908.

Chapter 5

5 Conclusions and Future Work

5.1 Summary and Conclusions

This dissertation describes work done towards the formation of low-coordinate phosphinidene chalcogenide species, and explorations of chemistry of related species supported by either a strongly π-donating or a weakly π-donating ligand. Although the primary synthetic targets were not achieved, a novel family of isolable bis(azido)phosphines, and a new synthetic strategy for a chlorophosphonate and cyclic phosphonates were discovered. This work may be useful for the synthesis of easily modifiable electron rich phosphine chalcogenides, or for the synthesis of inorganic polymers with a $(P\text{-}O)_n$ backbone.

Chapter 2 described the strategies taken towards the generation of an elusive phosphinidene sulfide supported by a π-donating N-heterocyclic imine. Condensation reactions of $IPrNPCl_2$ with sodium sulfide (Na_2S) were extremely sluggish but consistently produced a very electron rich phosphorus species (**2.8**, $\delta_P = 310$) *in situ*. Qualitative evidence suggested the identity of this species to be phosphenium **[2.7]Cl**, but was not confirmed. Condensation reactions performed using $S(SiMe_3)_2$ instead were more rapid but lacked evidence of an electron-rich phosphinidene sulfide. Thermal and photolytic reductions of a novel bis(azido)phosphine sulfide were explored but found unsuitable for generating a phosphinidene sulfide. The structures of **2.10** and **2.13** serendipitously obtained revealed pervasive incorporation of oxygen, which likely due to solvent or trace oxygen exposure.

Chapter 3 reported the isolation of family of bis(azido)phosphines (**3.2**, **3.4S**, and **3.4Se**). Chemoselective reactions of bis(azido)phosphines **3.2** and **3.4S** with secondary or tertiary phosphines revealed a negative correlation of thermal stability and positive correlation of Staudinger reactivity with the oxidation state at phosphorus. Structurally characterized **3.5$_{Cy}$** supported the reactivity of **3.4S**, while sulfurization of the unstable species **3.7** to **3.5_{Me}** provided support for the identification of **3.7**. Computational analyses showed that energetically inaccessible azido antibonding orbital characters of the corresponding mono(azido)phosphines were responsible for the observed chemoselectivity. Thermogravimetric analysis of **3.2** suggested that thermolysis at 80 °C could effectively generate an NHI-stabilized phosphinidene. This expands the versatility of electron-rich bis(azido)phosphines, offering a new strategy for designing electron-rich phosphorus species.

Chapter 4 described a new method for the facile synthesis of a chlorophosphonate **4.3_{BAC}** and cyclic phosphonates using ***C_3O*** either to form a new P-C and P-O bond, or for the replacement of two chloride atoms. Methods of efficient separation of phosphorus species from the **[*C_3*Cl]Cl** by-product were not found, but significant progress was made in understanding the reaction and the formation of oligomeric species during reactions with Lewis bases. Structural verification of various **[*C_3*Cl]**$^+$ salts, chlorophosphonate **4.3_{BAC}**, hydrolysis product **[4.21_{mono}]OTf**, and BCF adduct **4.27** was obtained. Detection of an intermediate P(V) species **[4.6_{BAC}]Cl** in $CDCl_3$ provided insight towards a possible oxygen/chloride exchange mechanism. The sequence of hydrolysis steps was explored using NMR spectroscopy and supported by ESI-HRMS. **4.3_{BAC}** readily participated in substitution reactions with DMAP, or chloride abstraction reactions with $SiMe_3OTf$ to produce monomeric dioxophosphorane **[4.17_{mono}]OTf** *in situ*. The reactions of ***C_3O*** with dichlorophosphine oxides, generating cyclic phosphonates, highlighted the utility of oxygen/chloride exchange.

The work detailed in this thesis underscores the difficulty of isolating low-coordinate phosphorus chalcogenide species, and the inability of the IPrN ligand to provide adequate stabilization for a two-coordinate phosphinidene sulfide. The IPrN ligand conversely allowed for controlled Staudinger reactivity of bis(azido)phosphines to produce chiral mono(azido)phosphines. The versatility of this reactivity was shown for alkyl- and aryl- 3° phosphines, while reactions with a 2° phosphine resulted in the formation of two tautomers in a dynamic equilibrium. Additionally, a new method for the synthesis of either a PO_2 motif stabilized by a α-cationic BAC and chloride ligands, or a neutral cyclic phosphonates was also found. This method may be advantageous for further work exploring dioxophosphorane species, once an efficient separation method is established.

5.2 Future Work

Future work arising from this thesis can be sectioned into categories based on their respective chapters:

1) Continued efforts towards stabilization of a monomeric phosphinidene sulfide
2) Exploration of the chemistry of bis(azido)phosphines
3) Exploration of the chemistry of dichalcogoxo phosphoranes

5.2.1 Stabilization of Monomeric Phosphinidene Sulfide

5.2.1.1 Bulkier Ligand

The use of a bulkier ligand would be expected to address the challenges of self-reaction and stabilization of a phosphinidene sulfide. A more sterically encumbered phosphorus center would diminish its nucleophilic character, thereby reducing the formation of extended phosphazene decomposition species through self-reactions. This could also allow for the use of higher temperatures or more polar solvents to enhance Staudinger reactivity with external phosphines. One potential ligand class to explore is bulky aminopyridines reported by Kempe and co-workers (**Figure 5-1**).[1,2] Transition metal and main group complexes supported by this type of ligand have shown bidentate and arene-type coordination modes in the solid state,[1,3] potentially offering new stabilization for phosphinidene sulfides.

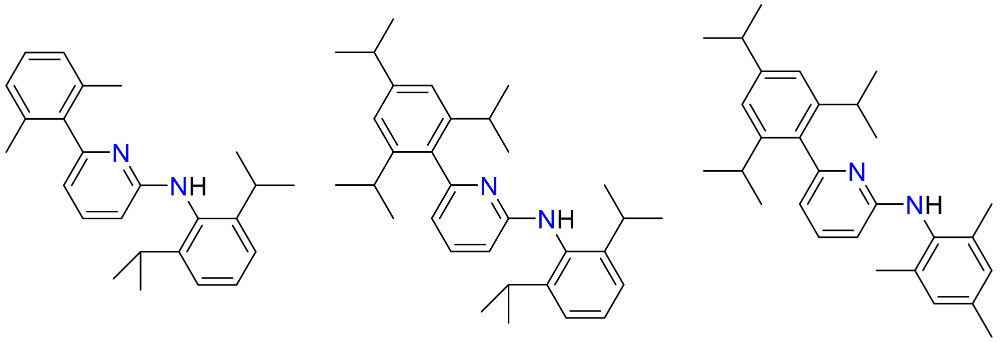

5.1a **5.1b** **5.1c**

Figure 5-1. Bulky bidentate aminopyridine ligands reported by Kempe and co-workers.[1,2]

5.2.2 Reactivity of Bis(azido)phosphines

5.2.2.1 Metal Coordination

Expanding the application of this chemistry could be achieved by demonstrating the ability of these compounds to form metal complexes, aiming to modulate reactivities of metal catalysts. Coordination adducts with simple group 13 Lewis acids or di-coordinate transition metals like gold or silver would provide a groundwork for such investigations. Alternatively, advancements in computer-aided techniques could be used towards targeted ligands and catalysts by predicting descriptors such as steric and electronic effects, Tolman cone angle, buried volume, and sterimol parameters.[4]

5.2.2.2 Alkylation Reactions

Further functionalization of the bis(azido)phosphines or mono(azido)phosphines may enable their use in metal coordination reactions. Preliminary evidence indicated that both the P(III) and P(V) bis(azido)phosphines reacted with methyltriflate, but produced mixtures of species. A solid-state structure of an S-methylated bis(azido)phosphine sulfide was also obtained, which demonstrated sulfur’s nucleophilic character. Alkylation could serve as a strategy to further tune reactivity and stability further by selecting appropriate alkylating agents. A P-alkylated species should enhance susceptibility to Staudinger reactivity.

5.2.2.3 Reactivity at Azide Functional Group

Functionalizing the azido groups *via* cycloaddition reactions offers the potential to tailor ligand properties at phosphorus. Such reactions, including copper-catalyzed[5] and metal-free variaints[6] with strained alkynes, have been reported. Azidophosphines are also known to undergo dipolar cycloadditions with dipolarphiles, forming six-membered rings,[78] with demonstrated ring contraction to a four-membered heterocycle upon heating.[7] As a demonstrable example, preliminary evidence of cycloaddition reactivity of **3.2** with dimethyl acetylenedicarboxylate produced a six-membered phosphorus heterocycle with a pendant azide (**5.2**), which was subsequently functionalized with PMe_3 (**5.3**, **Scheme 5-1**).

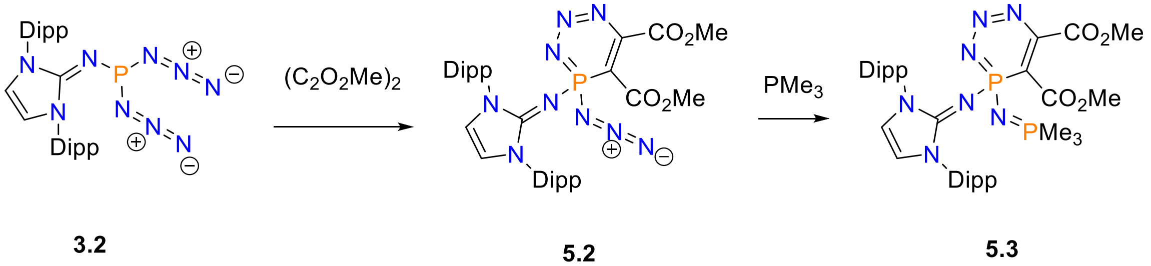

Scheme 5-1. Cycloaddition reaction of **3.2**, and subsequent Staudinger reaction.

5.2.3 Exploration of the Chemistry of Dichalcogoxophosphoranes and Dialkylcyclopropenones

5.2.3.1 Exploring Chemistry of Hydrolyzed Cationic Phosphonate

While much attention was devoted to isolating the highly reactive chlorophosphonate $\mathbf{4.3_{BAC}}$, the rapid hydrolysis in air was frequently encountered. However, efforts were not made to specifically investigate the isolation of the hydrolyzed phosphonate species $\mathbf{[4.21_{mono}]^+}$. Phosphonates have significant industrial and pharmaceutical relevance (*e.g.* herbicides, pesticides, fungicides),[9,10] can serve as metal chelating reagents,[10] and may be synthesized by mechanochemical synthesis in a ball-mill.[11] The phosphonic acid species is anticipated to remain stable in air and aqueous solutions across various pH levels (**Scheme 5-2**). Thus, these species could serve as precursors for a new range of metal-organic frameworks (MOFs) with oxophillic metals, act as phase-transfer catalysts,[12] allow for silica gel chromatographic separation, or be explored in interdisciplinary studies for their potential as herbicides/pesticides.[1]

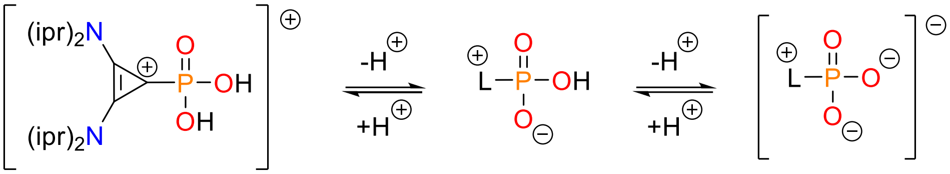

$[\mathbf{4.21}_{\mathbf{mono}}]^+$ $\mathbf{4.21}_{\mathbf{mono}}$ $[\mathbf{4.21}_{\mathbf{mono}}]^-$

Scheme 5-2. Suggested proton-transfer reactions of $[\mathbf{4.21}_{\mathbf{mono}}]^+$.

5.2.3.2 Deoxygenation Of Chlorophosphonate

Navech and coworkers previously reported that the reaction of a bulky dithioxophosphorane with PPh_3 resulted in the formation of trimeric $(Mes^*PS)_3$.[13] Preliminary evidence suggested that the excess use of PMe_3 may result in the formation of $OPMe_3$ as a by-product, along with an up-field shifted set of phosphorus resonances to a trimeric species (**Scheme 5-3**). Isolating such a heterocycle would represent the first instance of an organophosphorus heterocycle consisting solely of a (P(III)-O)$_n$ chain.

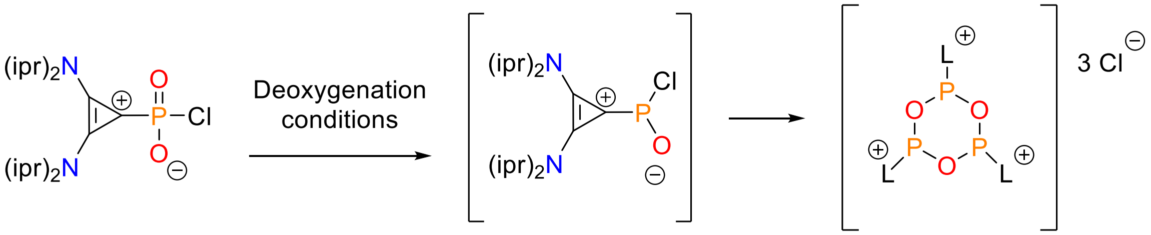

$\mathbf{4.3}_{\mathbf{BAC}}$ **5.4** **5.5**

Scheme 5-3. Deoxygenation of $\mathbf{4.3}_{\mathbf{BAC}}$ to produce polycationic P-O heterocycles.

5.2.3.3 Catalyst In Appel Reactions

Both triphenylphosphine oxide ($OPPh_3$)[14] and ***C₃O***[15] are effective catalysts for alcohol chlorodehydration reactions using $(COCl)_2$ as a chloride source and oxygen abstraction agent (**Figure 5-2**). They are believed to proceed *via* alcohol substitution reaction and Arbuzov-style elimination. Given the chloride substituent in $\mathbf{4.3}_{\mathbf{BAC}}$, it is anticipated to be a potent catalyst for this transformation.

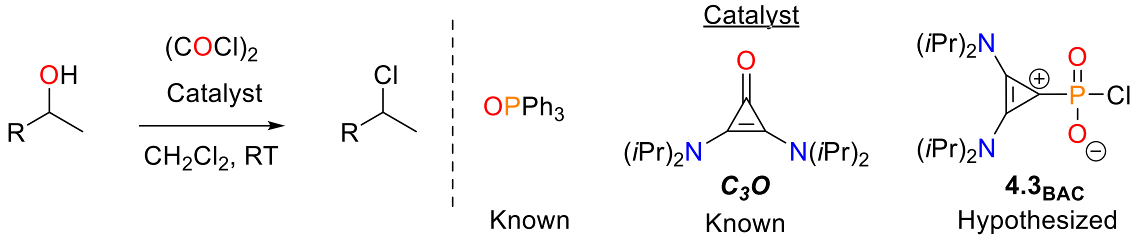
OH
R
(COCl)2
Catalyst
CH2Cl2, RT
Cl
R
Catalyst
OPPh3
Known
O
(iPr)2N
N(iPr)2
C3O
Known
(iPr)2N
(iPr)2N
O
P
Cl
O
4.3BAC
Hypothesized

Figure 5-2. Catalytic conversion of alcohols to chlorides.

5.2.3.4 Alkylation Of Chlorophosphonate

O-alkylation reactions of the **4.3$_{\mathbf{BAC}}$** could aid in separating **[C$_3$Cl]Cl** from the organophosphorus species, caution should be taken due to potential acute toxicity and its relation to organophosphorus nerve agents. Nerve agents such as tabun or sarin are highly toxic, containing a hydrolytically sensitive fluoride or pseudohalide substituent, and an O-alkyl group (**Figure 5-3**). The toxicity and rate of acetylcholine esterase inhibition by irreversible dealkylation are correlated with the stability of the alkyl cation formed.[16]

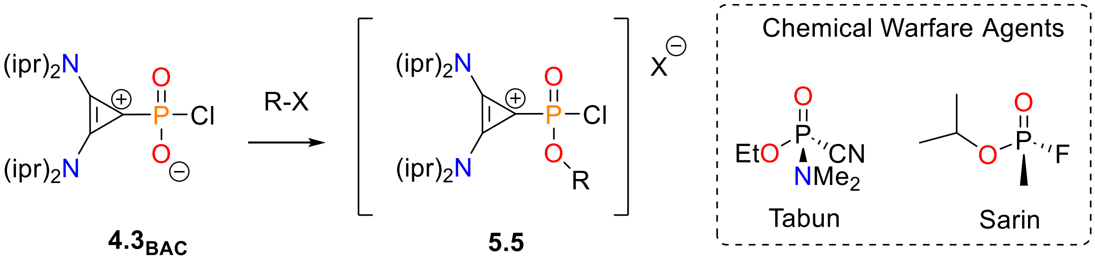
(ipr)2N
(ipr)2N
O
P
Cl
O
4.3BAC
R-X
(ipr)2N
(ipr)2N
O
P
Cl
O
R
X
5.5
Chemical Warfare Agents
O
EtO
P
CN
NMe2
Tabun
O
O
P
F
Sarin

Figure 5-3. Alkylation of **4.3$_{\mathbf{BAC}}$** (left) and structure of two acutely toxic chemical warfare agents (right).

5.2.3.5 Exploration Of Polymerization Reactions

The Lambert group previously functionalized of poly(methylamino)styrene with the BAC ligand to produce of polycationic polymer chains, yielding cationic polyelectrolytes.[17] Difficulties in isolating **[4.17$_{\mathbf{mono}}$]OTf** were likely due to oligomerization, suggesting it as an interesting monomer for further studies. Exploring polymerizations of either **4.3$_{\mathbf{BAC}}$** or **[4.17$_{\mathbf{mono}}$]OTf** may also result in the discovery of a more efficient separation of byproducts by their differences in solubilities.

5.2.3.6 Reactions Of Cyclopropenone Derivatives

Cyclopropenium species have been explored as ligands, catalysts, ionic liquids, and Brønsted Bases, showing a wide range of substitution patterns. This could aid in preparing chlorophosphonate derivatives, enhancing Chemoselectivity, or separating cyclic phosphonate products. Base adducts of "PCh_2Cl" are efficiently stabilized as sulfur derivatives.[18–21] Thus, reactions of the thiocyclopropenone derivative ***C_3S*** with PCl_3 may yield a cationic three-coordinate dithioxophosphorane (**Figure 5-4**). Mixed chalcogen phosphonates could be accessed *via* reactions of $RP(O)Cl_2$ with ***C_3S***, or $RP(S)Cl_2$ with ***C_3O***, potentially towards the construction of inorganic polymers of a general formula $(RPO_xS_{2-x})_n$.

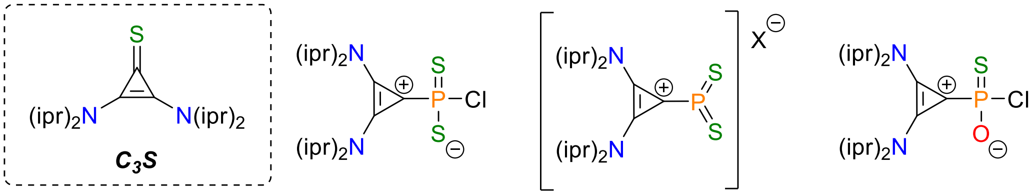

Figure 5-4. Possible organophosphorus products by reactions with ***C_3S***.

5.3 References

(1) Scott, N. M.; Schareina, T.; Tok, O.; Kempe, R. Lithium and Potassium Amides of Sterically Demanding Aminopyridines. *Eur. J. Inorg. Chem.* **2004**, *2004* (16), 3297–3304. https://doi.org/10.1002/ejic.200400228.

(2) Kretschmer, W. P.; Meetsma, A.; Hessen, B.; Schmalz, T.; Qayyum, S.; Kempe, R. Reversible Chain Transfer between Organoyttrium Cations and Aluminum: Synthesis of Aluminum-Terminated Polyethylene with Extremely Narrow Molecular-Weight Distribution. *Chem. Eur. J.* **2006**, *12* (35), 8969–8978. https://doi.org/10.1002/chem.200600660.

(3) Noor, A. Coordination Chemistry of Bulky Aminopryridinates with Main Group and Transition Metals. *Top. Curr. Chem.* **2021**, *379* (1), 6. https://doi.org/10.1007/s41061-020-00320-8.

(4) Falivene, L.; Cao, Z.; Petta, A.; Serra, L.; Poater, A.; Oliva, R.; Scarano, V.; Cavallo, L. Towards the Online Computer-Aided Design of Catalytic Pockets. *Nat. Chem.* **2019**, *11* (10), 872–879. https://doi.org/10.1038/s41557-019-0319-5.

(5) Meldal, M.; Tornøe, C. W. Cu-Catalyzed Azide−Alkyne Cycloaddition. *Chem. Rev.* **2008**, *108* (8), 2952–3015. https://doi.org/10.1021/cr0783479.

(6) Jewett, J. C.; Bertozzi, C. R. Cu-Free Click Cycloaddition Reactions in Chemical Biology. *Chem. Soc. Rev.* **2010**, *39* (4), 1272–1279. https://doi.org/10.1039/B901970G.

(7) Tejeda, J.; Reau, R.; Dahan, F.; Bertrand, G. Synthesis and Molecular Structure of a 1,2λ^5-Azaphosphete: A Cyclic 4-π-Electron Ylide. *J. Am. Chem. Soc.* **1993**, *115* (17), 7880–7881. https://doi.org/10.1021/ja00070a045.

(8) Kumaraswamy, S.; Kommana, P.; Satish Kumar, N.; Kumara Swamy, K. C. Novel Reactions of Phosphorus(III) Azides and Isocyanates: Unusual Modes of Cycloaddition with Dipolarophiles and an Unexpected Case of Ring Expansion. *Chem. Commun.* **2002**, No. 1, 40–41. https://doi.org/10.1039/B107087H.

(9) Casida, J. E. Organophosphorus Xenobiotic Toxicology. *Annu. Rev. Pharmacol. Toxicol.* **2017**, *57*, 309–327. https://doi.org/10.1146/annurev-pharmtox-010716-104926.

(10) Rathore, K.; Jangir, R. Insight into Synthesis, Properties and Applications of Metal Phosphonates: Emphasis on Catalytic Activities. *Inorganica Chim. Acta* **2024**, *559*, 121804. https://doi.org/10.1016/j.ica.2023.121804.

(11) Wilke, M.; Batzdorf, L.; Fischer, F.; Rademann, K.; Emmerling, F. Cadmium Phenylphosphonates: Preparation, Characterisation and in Situ Investigation. *RSC Adv.* **2016**, *6* (42), 36011–36019. https://doi.org/10.1039/C6RA01080F.

(12) Bandar, J. S.; Tanaset, A.; Lambert, T. H. Phase-Transfer and Other Types of Catalysis with Cyclopropenium Ions. *Chem. Eur. J.* **2015**, *21* (20), 7365–7368. https://doi.org/10.1002/chem.201500124.

(13) Navech, J.; Revel, M.; Kraemer, R. Etude de La Reactivite Du Tris(Tertiobutyl)Phenyldithiophosphorane. *Tetrahedron Lett.* **1985**, *26* (2), 207–210. https://doi.org/10.1016/S0040-4039(00)61881-6.

(14) Denton, R. M.; An, J.; Adeniran, B.; Blake, A. J.; Lewis, W.; Poulton, A. M. Catalytic Phosphorus(V)-Mediated Nucleophilic Substitution Reactions: Development of a Catalytic Appel Reaction. *J. Org. Chem.* **2011**, *76* (16), 6749–6767. https://doi.org/10.1021/jo201085r.

(15) Vanos, C. M.; Lambert, T. H. Development of a Catalytic Platform for Nucleophilic Substitution: Cyclopropenone-Catalyzed Chlorodehydration of Alcohols. *Angew. Chem. Int. Ed.* **2011**, *50* (51), 12222–12226. https://doi.org/10.1002/anie.201104638.

(16) Costanzi, S.; Machado, J.-H.; Mitchell, M. Nerve Agents: What They Are, How They Work, How to Counter Them. *ACS Chem. Neurosci.* **2018**, *9* (5), 873–885. https://doi.org/10.1021/acschemneuro.8b00148.

(17) Freyer, J. L.; Brucks, S. D.; Gobieski, G. S.; Russell, S. T.; Yozwiak, C. E.; Sun,

M.; Chen, Z.; Jiang, Y.; Bandar, J. S.; Stockwell, B. R.; Lambert, T. H.; Campos, L. M. Clickable Poly(Ionic Liquids): A Materials Platform for Transfection. *Angew. Chem. Int. Ed.* **2016**, *55* (40), 12382–12386. https://doi.org/10.1002/anie.201605214.

(18) Meisel, M.; Bock, H.; Solouki, B.; Kremer, M. Generation and Ionization Pattern of the Iso(Valence)Electronic Compounds $CIP(=O)_2$ and $CIP(=S)_2$. *Angew. Chem. Int. Ed.* **1989**, *28* (10), 1373–1376. https://doi.org/10.1002/anie.198913731.

(19) Teichmann, H.; Wilbrandt, D.; Schulz, J. Phosphorylations with $ROP(X)Cl_2$: A New Mechanistic Pathway. *Phosphorus, Sulfur Silicon Relat. Elem.* **1990**, *49/50*, 251. https://doi.org/10.1080/10426509008038953.

(20) Teichmann, H.; Schulz, J.; Wilbrandt, D. Ein Neuer Einfacher Zugang Zu Pyridinium-Phosphor-Betainen. *Z. Chem.* **1990**, *30*, 18. https://doi.org/10.1002/zfch.19900300104.

(21) Kuhn, N.; Ströbele, M.; Walker, M. A Stable Carbene Phosphenic Chloride Complex: First Structural Characterization of a PO_2Cl Base Adduct [1]. *Z. Anorg. Allg. Chem.* **2003**, *629* (2), 180–181. https://doi.org/10.1002/zaac.200390026.

Appendices

Appendix A. Supplementary Information for Chapter 2

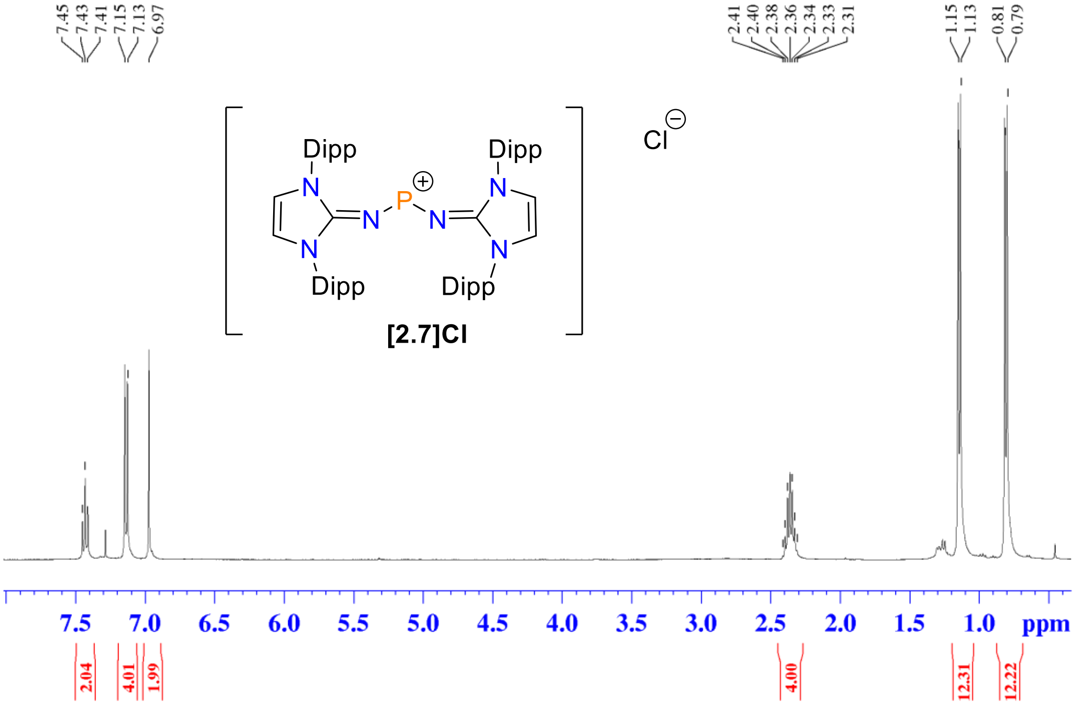

Appendix A-1. ^{1}H NMR spectrum of **[2.7]Cl** crystals redissolved in $CDCl_3$.

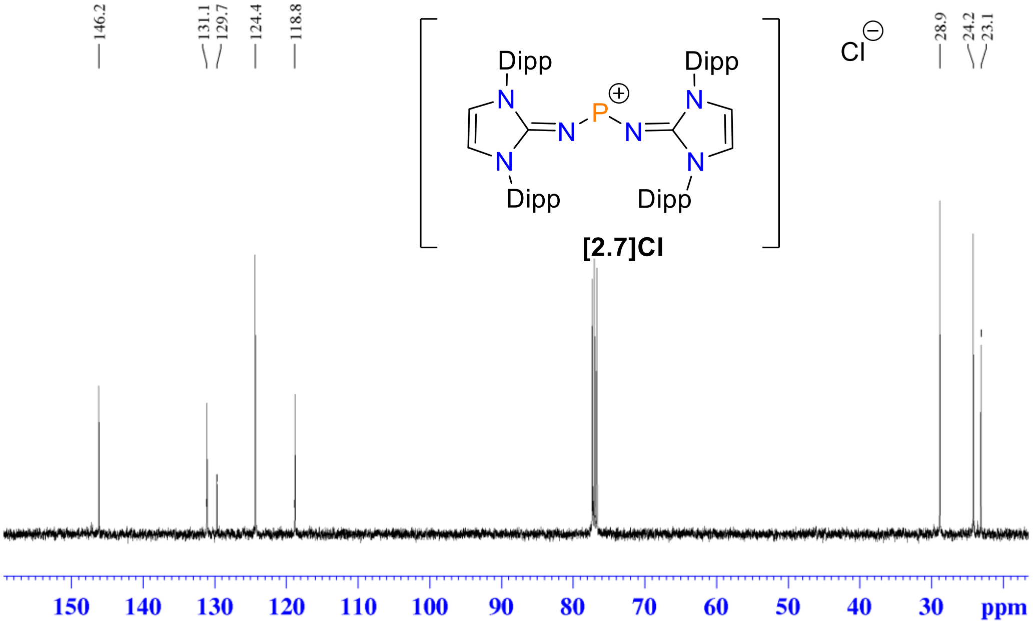

Appendix A-2. ^{13}C{^{1}H} NMR spectrum of **[2.7]Cl** crystals redissolved in $CDCl_3$.

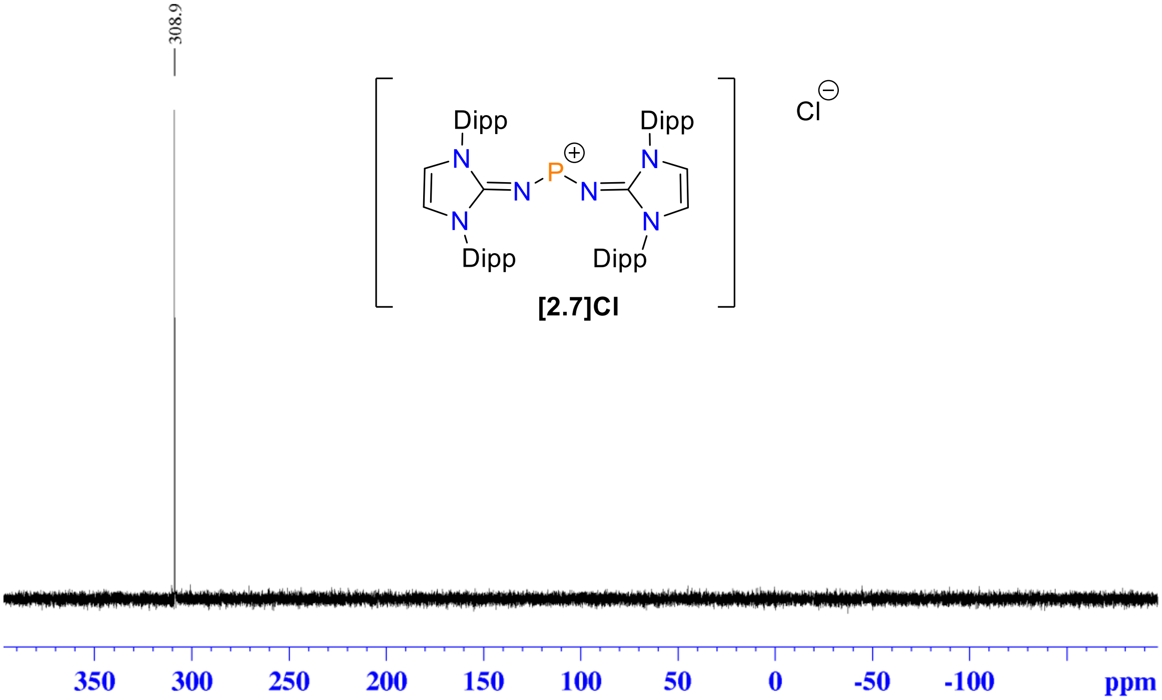

Appendix A-3. $^{31}P\{^1H\}$ NMR spectrum of **[2.7]Cl** crystals redissolved in $CDCl_3$.

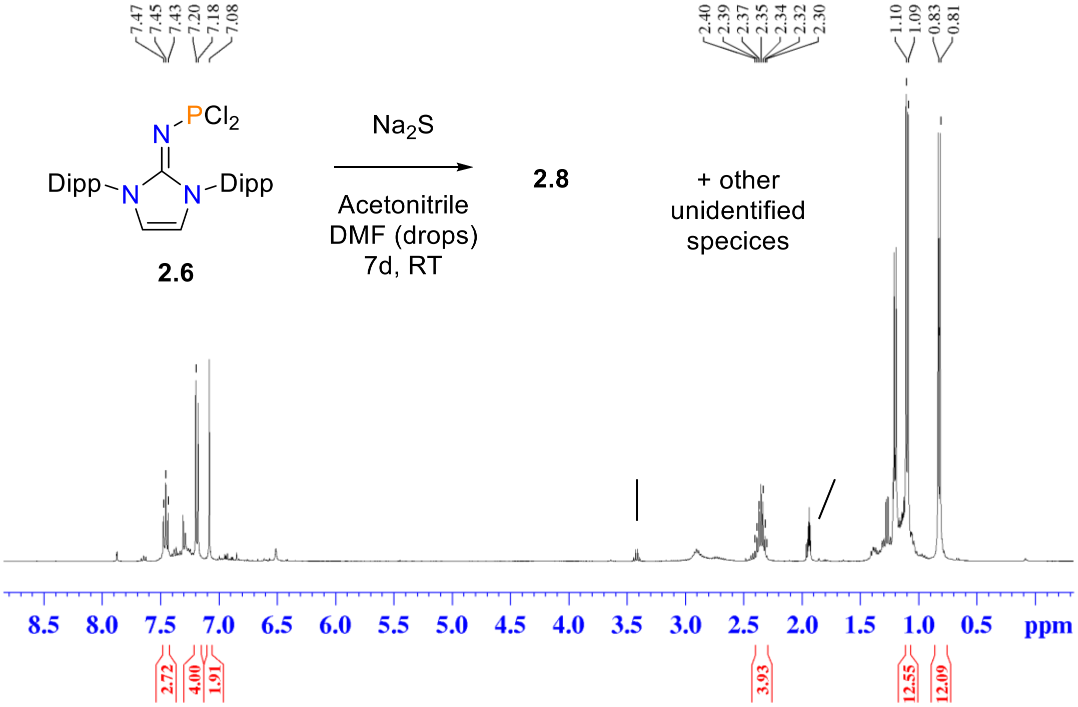

Appendix A-4. ^1H NMR spectrum (CD_3CN) of crude mixture forming **2.8**. † Denotes unidentified impurity.

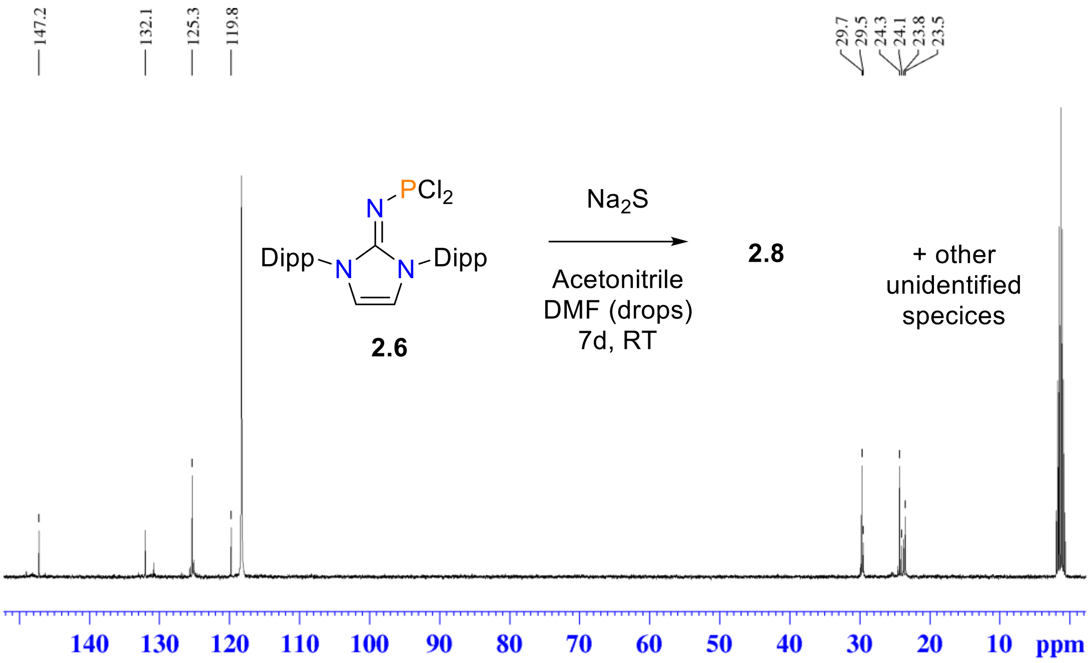

Appendix A-5. $^{13}C\{^1H\}$ NMR spectrum (CD_3CN) of crude mixture forming **2.8**.

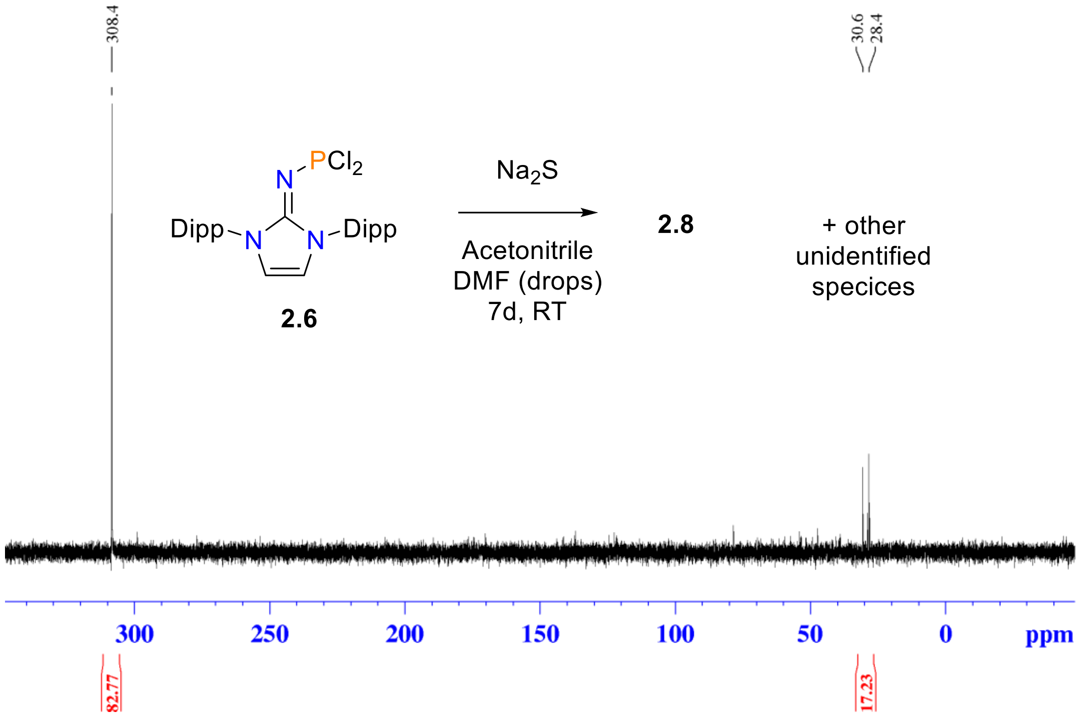

Appendix A-6. ^{31}P{^{1}H} NMR spectrum (CD$_3$CN) of crude mixture forming **2.8**. † Denotes unidentified impurities.

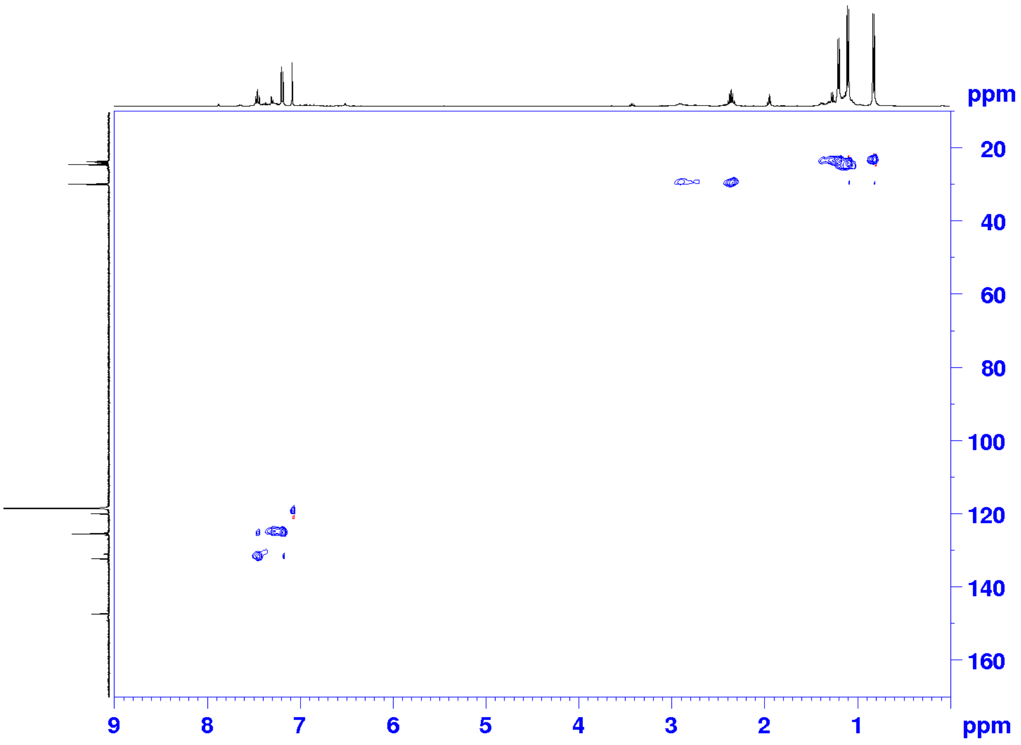

Appendix A-7. ^{1}H-^{13}C HSQC spectrum of crude mixture of **2.8** in CD_3CN.

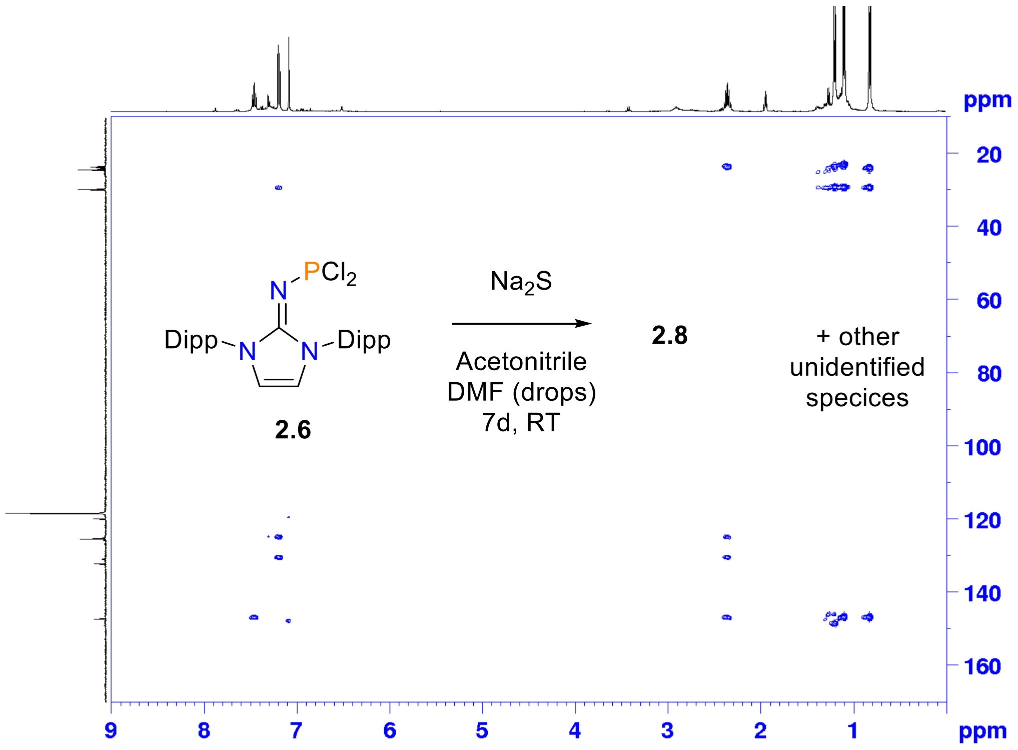

Appendix A-8. ^{1}H-^{13}C HMBC spectrum of crude mixture of **2.8** in CD_3CN.

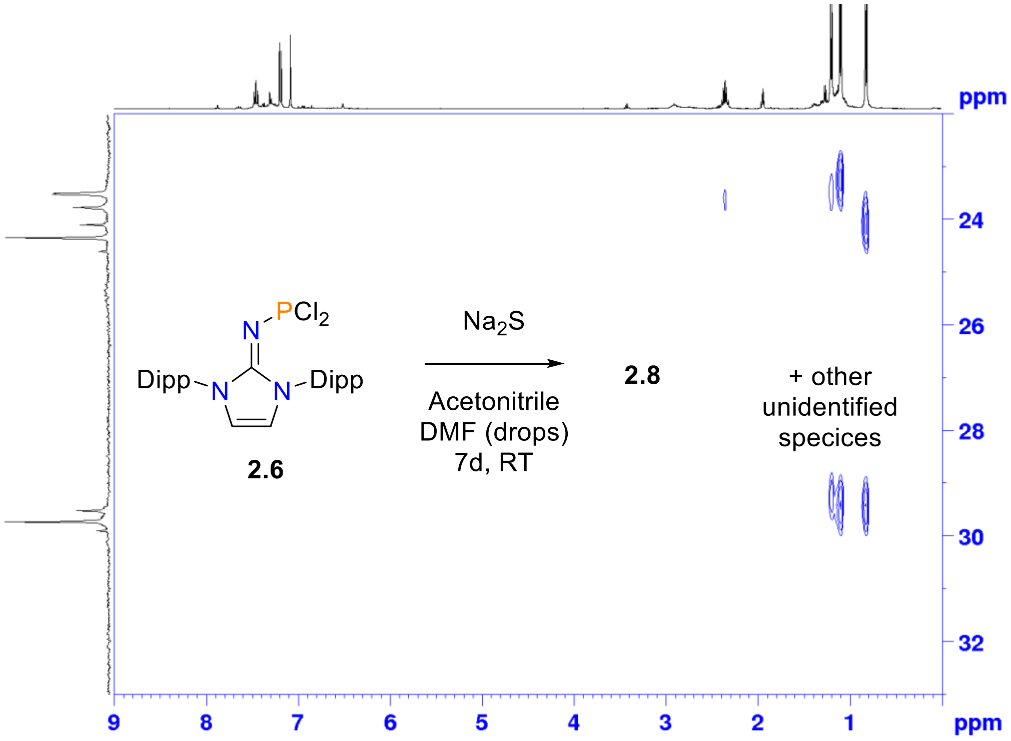

Appendix A-9. Zoomed in stacked HMBC spectra of crude mixture of **2.8** in CD_3CN.

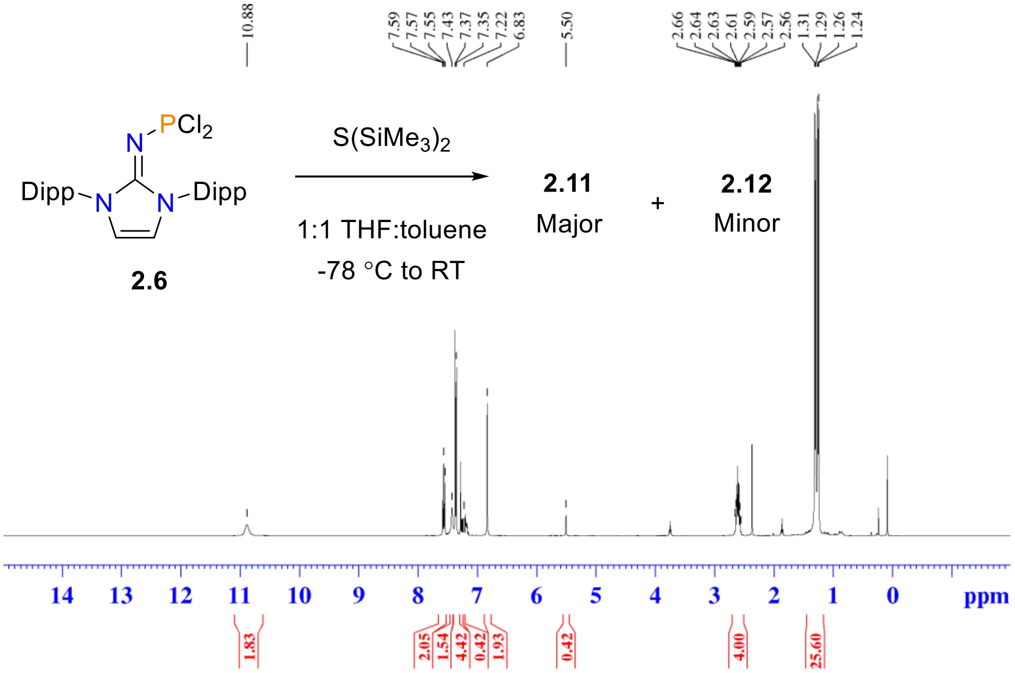

Appendix A-10. ^{1}H NMR spectrum of mixture of **2.11** and **2.12** in $CDCl_3$.

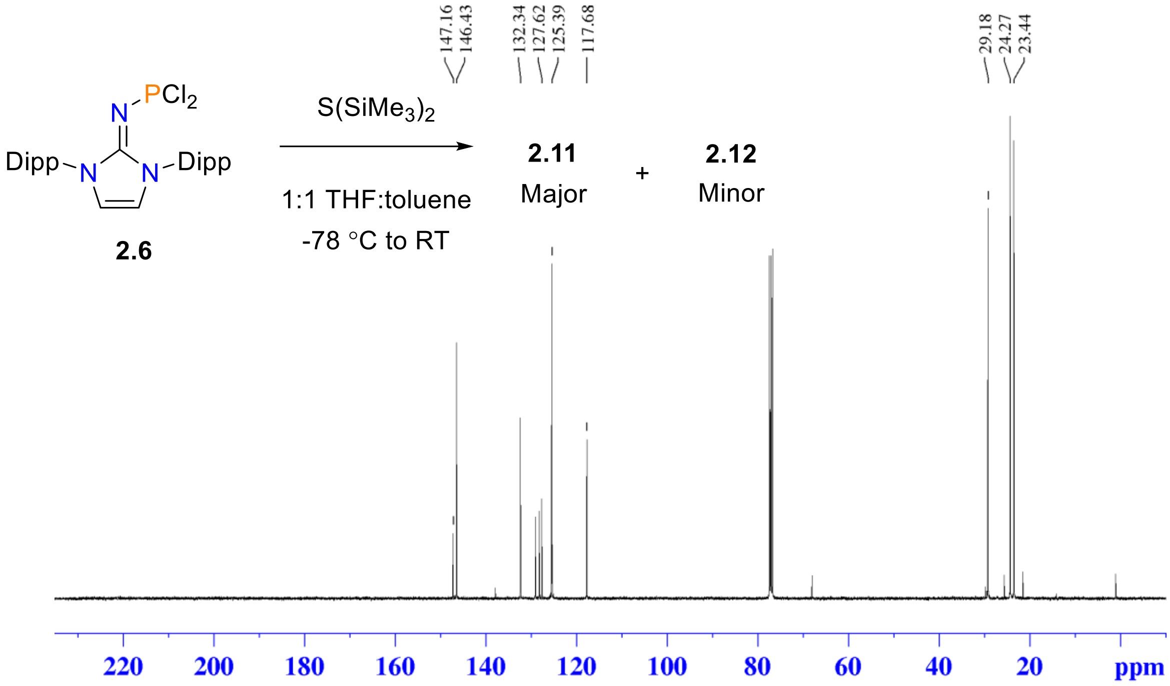

Appendix A-11. $^{13}C\{^1H\}$ NMR spectrum of mixture of **2.11** and **2.12** in $CDCl_3$.

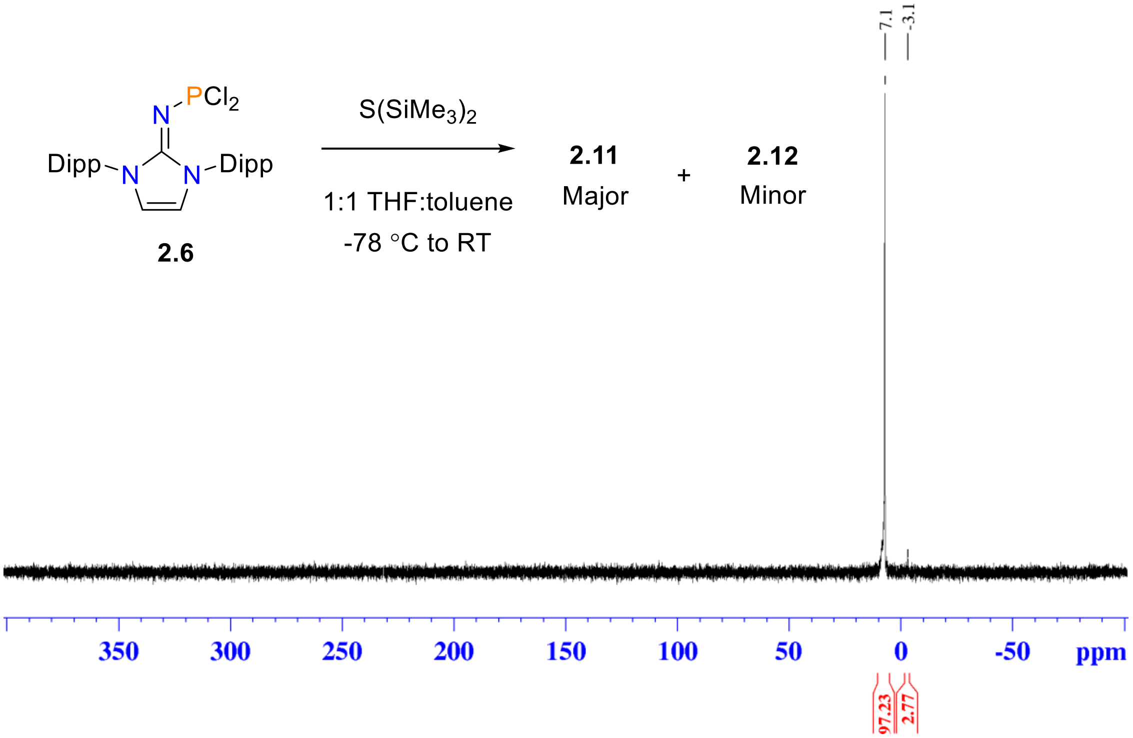

Appendix A-12. $^{31}P\{^1H\}$ NMR spectrum of mixture of **2.11** and **2.12** in $CDCl_3$.

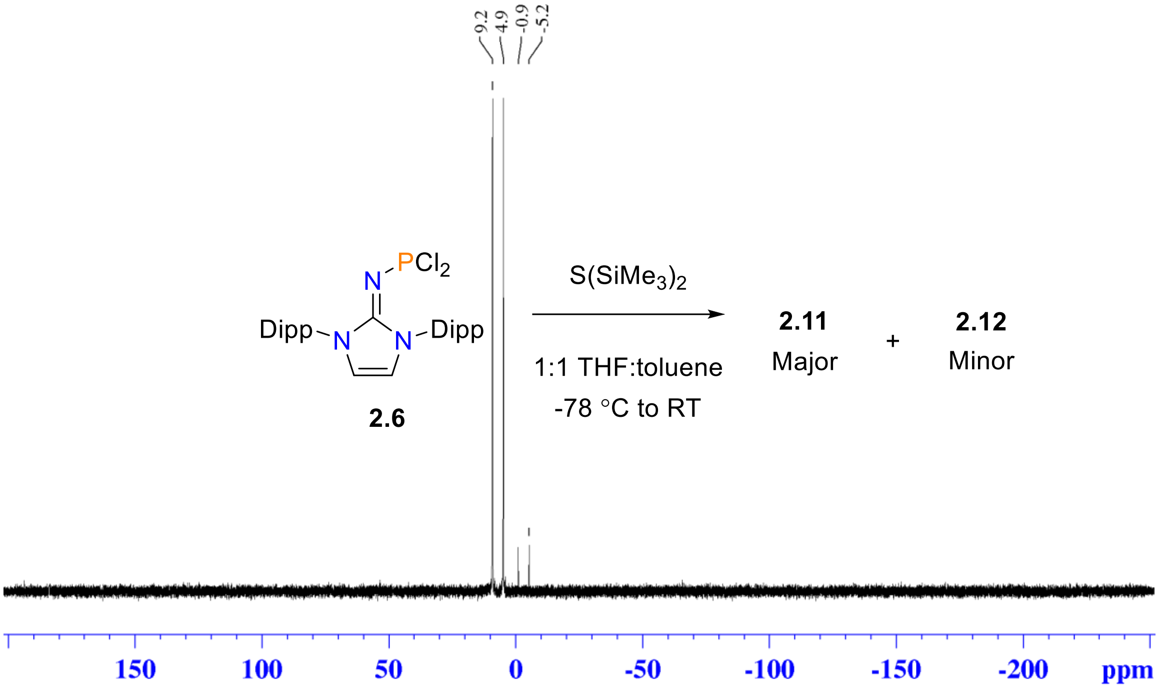

Appendix A-13. ^{31}P NMR spectrum of mixture of **2.11** and **2.12** in $CDCl_3$.

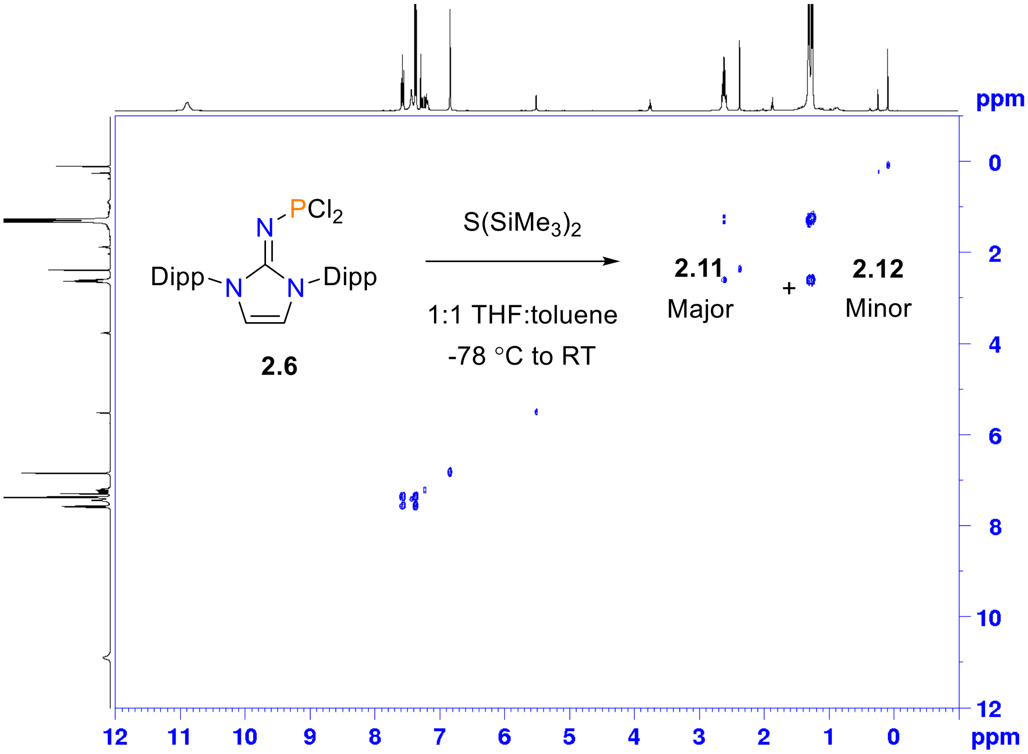

Appendix A-14. ^{1}H -^{1}H COSY NMR spectrum of mixture of **2.11** and **2.12** in $CDCl_3$.

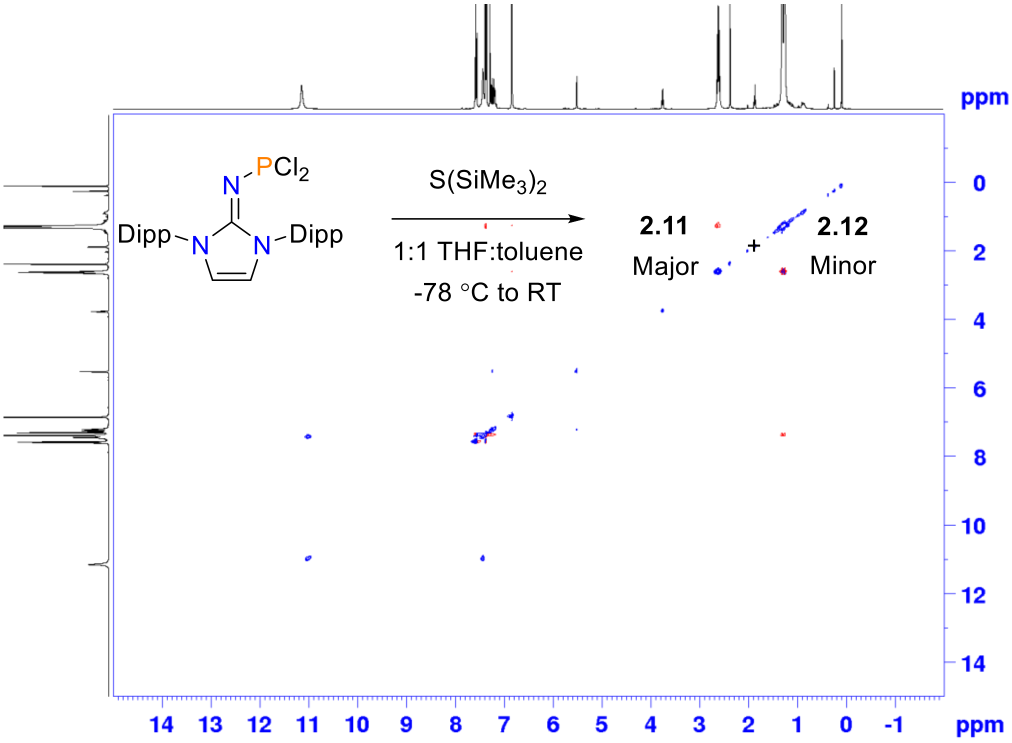

Appendix A-15. ^{1}H -^{1}H NOESY NMR spectrum of mixture of **2.11** and **2.12** in $CDCl_3$.

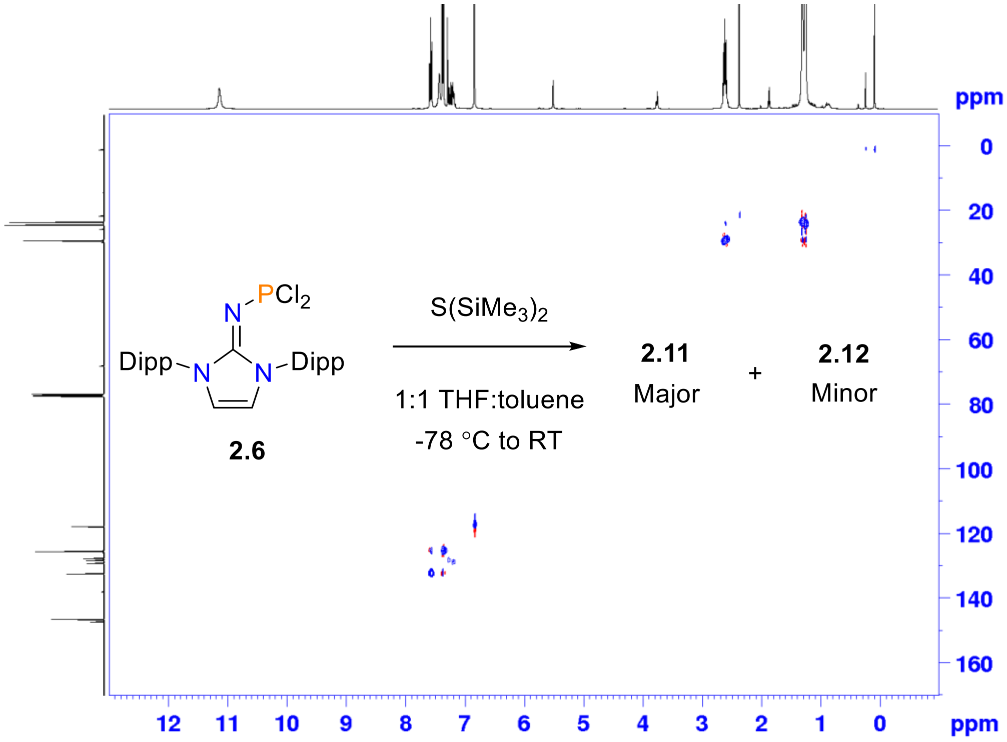

Appendix A-16. ^{1}H-^{13}C HSCQ NMR spectrum of **2.11** and **2.12** in $CDCl_3$.

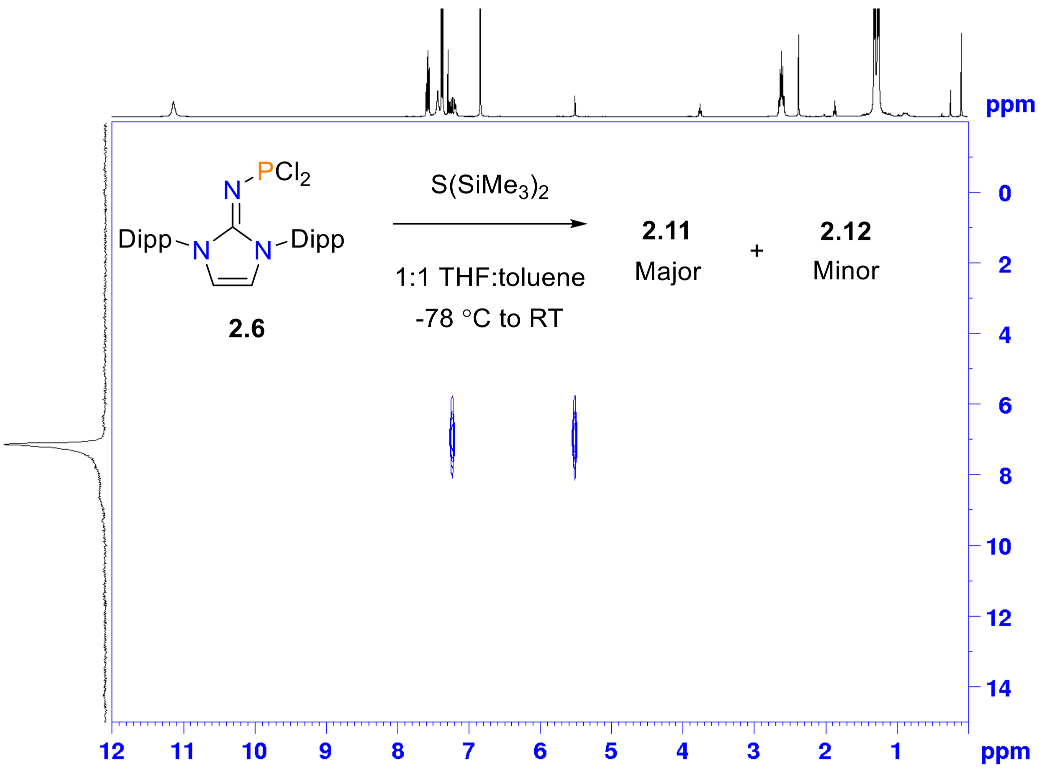

Appendix A-17. ^{1}H-^{31}P HMBC NMR spectrum of mixture of **2.11** and **2.12** in CDCl$_3$.

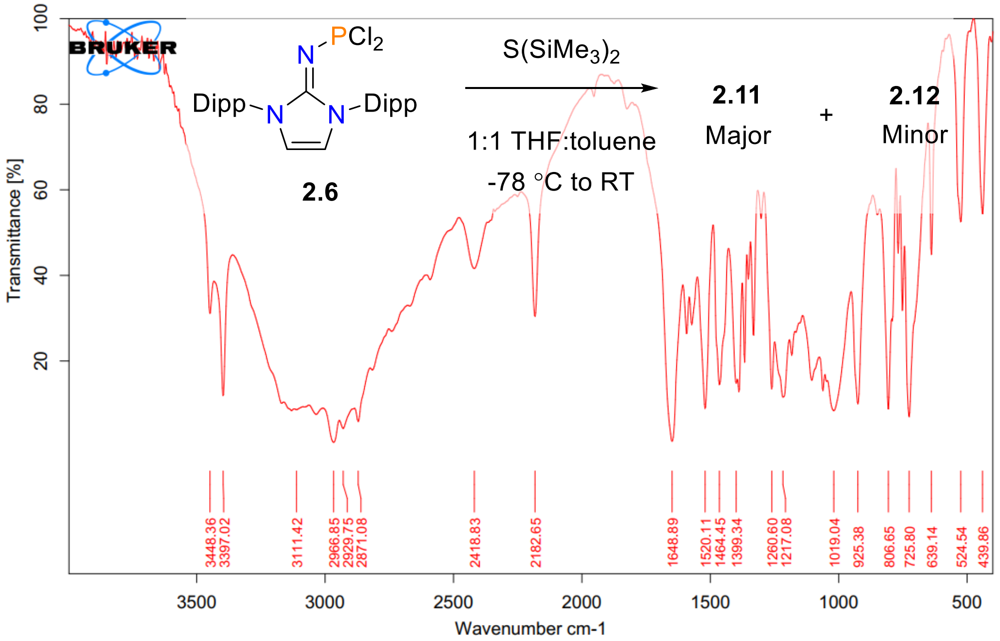

Appendix A-18. FT-IR spectrum of crude mixture containing **2.11** and **2.12**. [Transmission mode, KBr pellet].

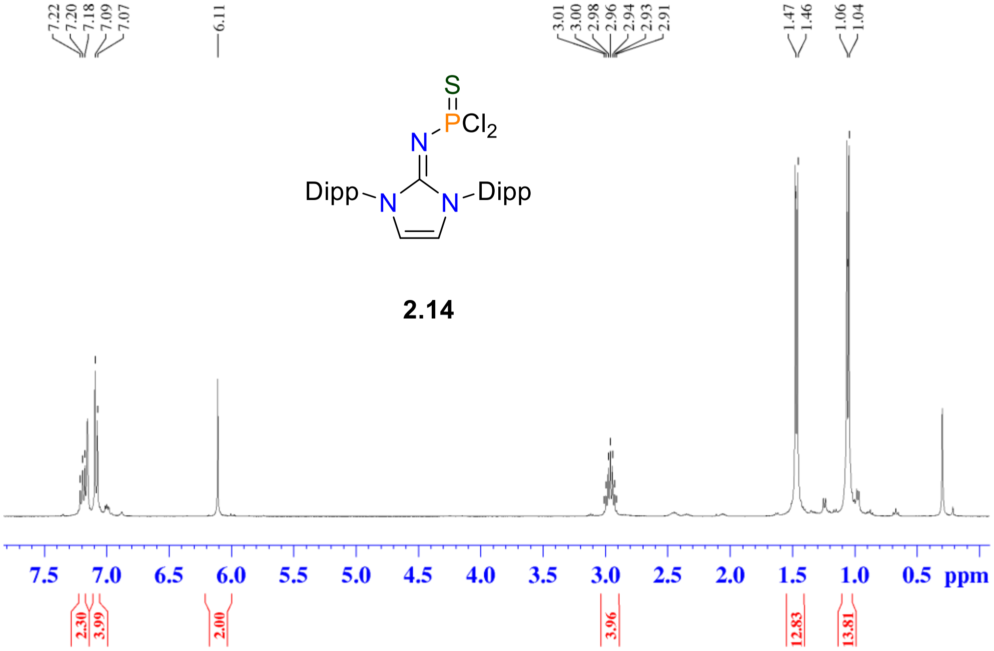

Appendix A-19. ^{1}H NMR spectrum (C_6D_6) of **2.14** isolated after toluene extraction from reaction mixture.

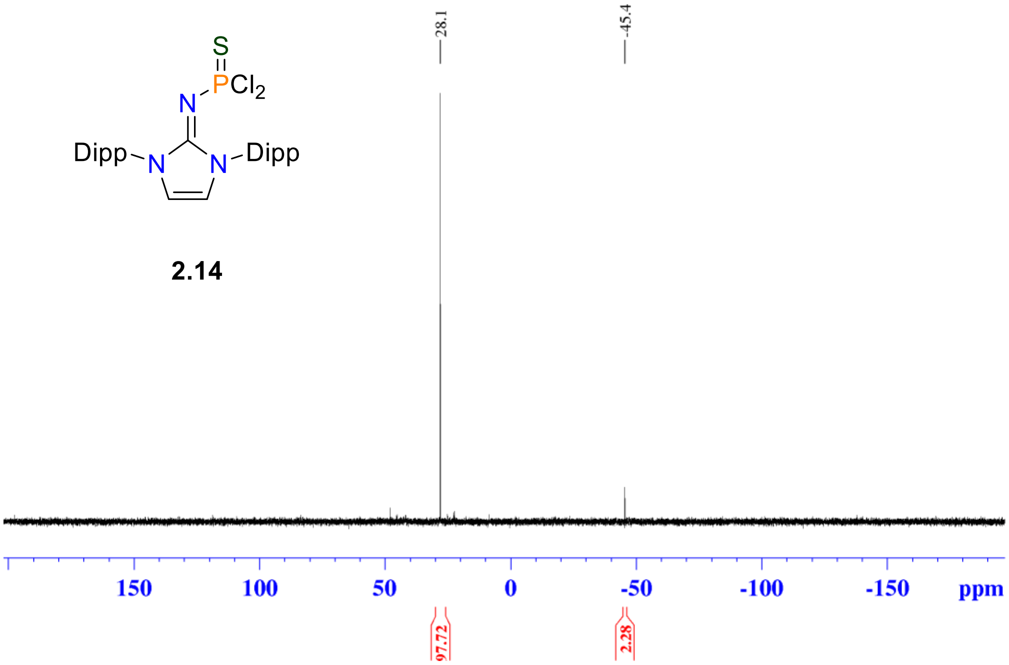

Appendix A-20. ^{31}P{^{1}H} NMR spectrum of IPrNPSCl$_2$ (**2.14**) in C_6D_6. † Denotes unidentified impurity.

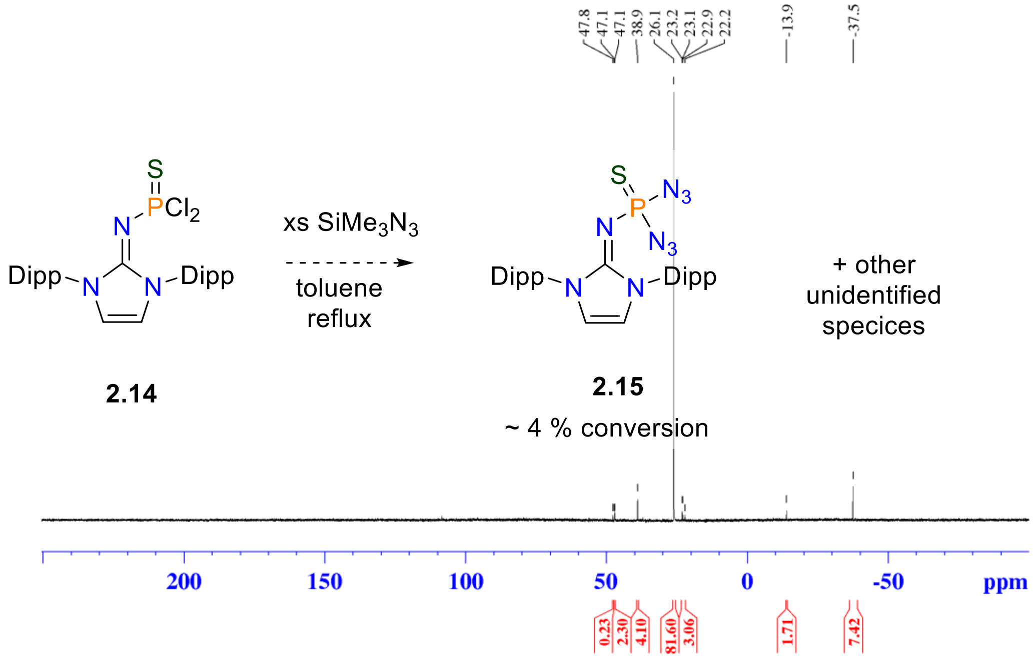

Appendix A-21. ^{31}P (^{1}H} NMR spectrum of the reaction of **2.14** (δ_P = 26) with $SiMe_3N_3$ at 60 °C after four h. Signal at 39 ppm is IPrNPS$(N_3)_2$ (*vide infra* Chapter 3).

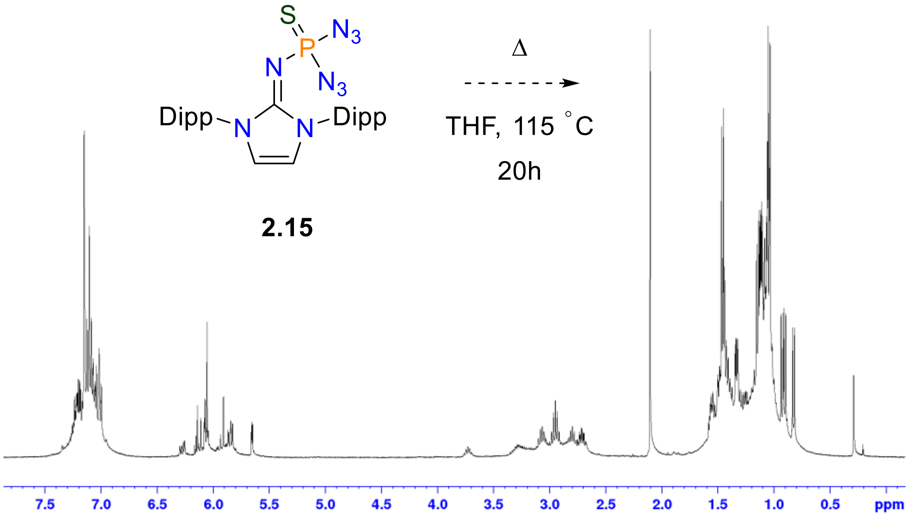

Appendix A-22. ^{1}H NMR spectrum (C_6D_6) of the crude residue obtained after 20 h of heating at 115 °C in pressure tube.

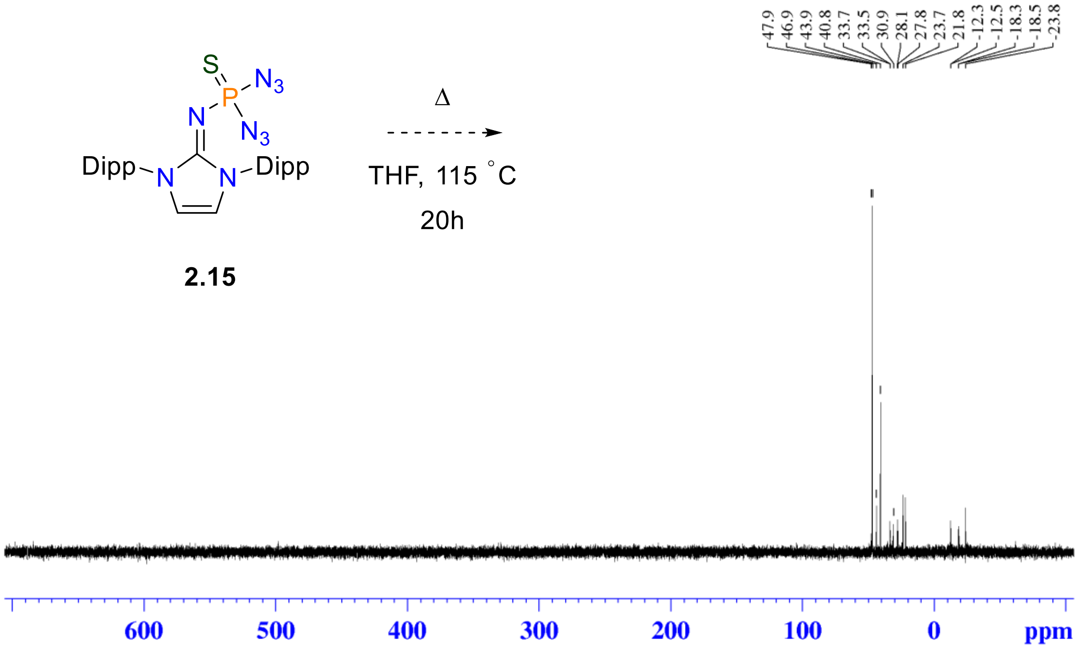

Appendix A-23. $^{31}P\{^1H\}$ NMR spectrum (C_6D_6) of the crude residue obtained after 20 h of heating at 115 °C in a pressure tube.

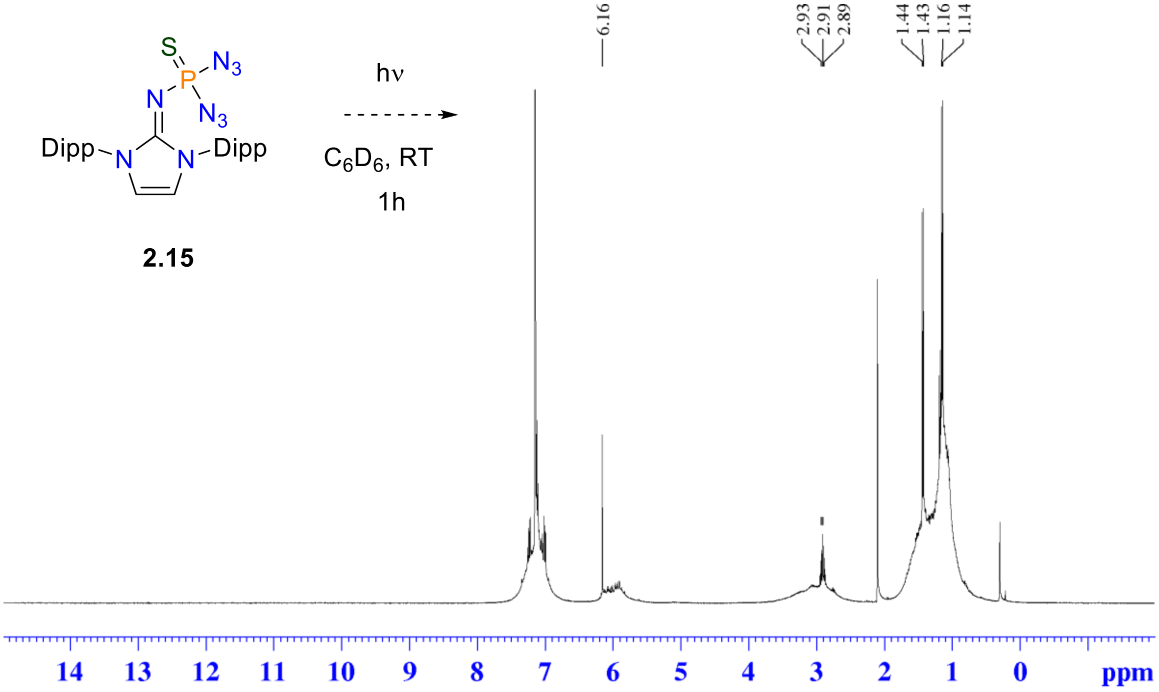

Appendix A-24. ^1H NMR spectrum of **2.15** photolyzed for 1 h in C_6D_6 in a quartz NMR tube.

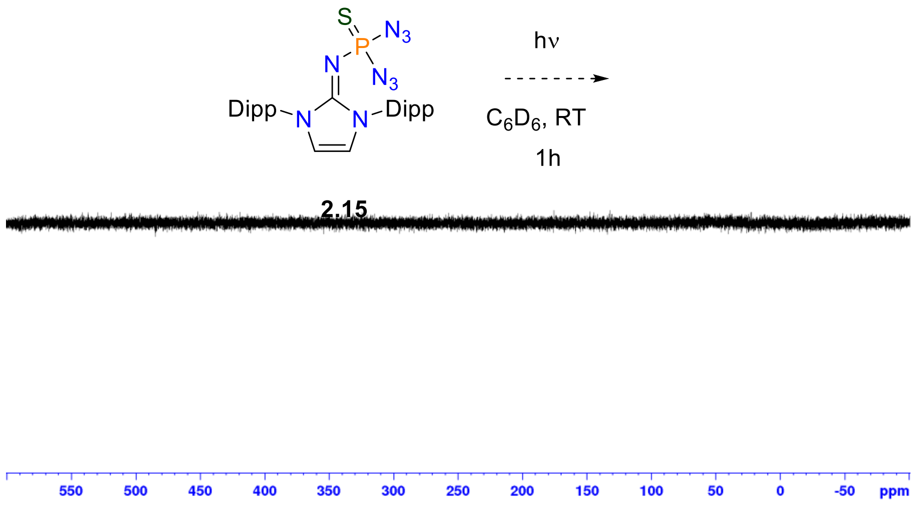

Appendix A-25. $^{31}P\{^{1}H\}$ NMR spectrum of **2.15** photolyzed for 1 h in C_6D_6 in a quartz NMR tube.

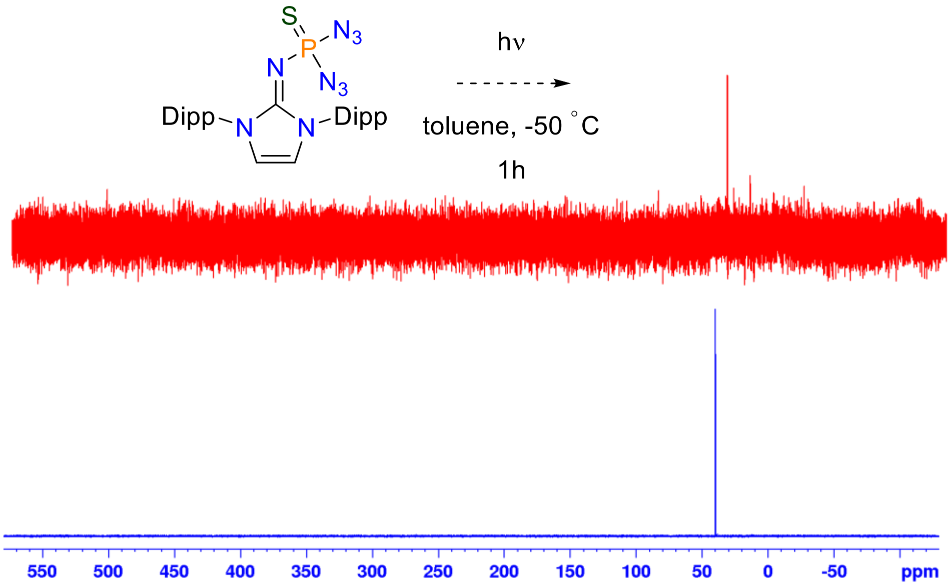

Appendix A-26. Stacked $^{31}P\{^{1}H\}$ spectra of **2.15** before (bottom) and after a 19 h low temperature photolysis experiment (top).

Note: Both NMR experiments in **Appendix A-26** were performed on the same J-Young tube sample with the same number of scans.

Appendix B. Supplementary Information for Chapter 3

B1. Spectral Data for Reported Compounds

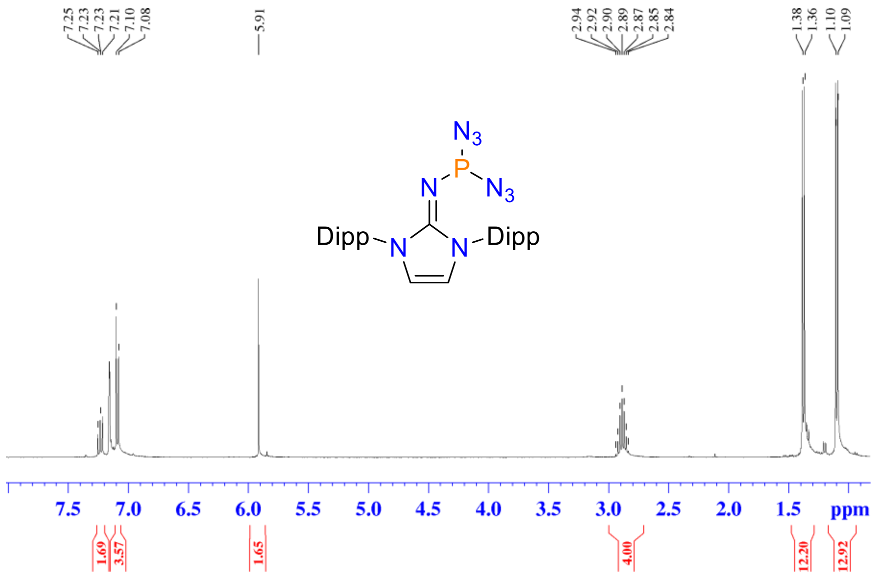

Appendix B-1. ^{1}H NMR spectrum of IPrNP(N$_3$)$_2$ (**3.2**) in C_6D_6.

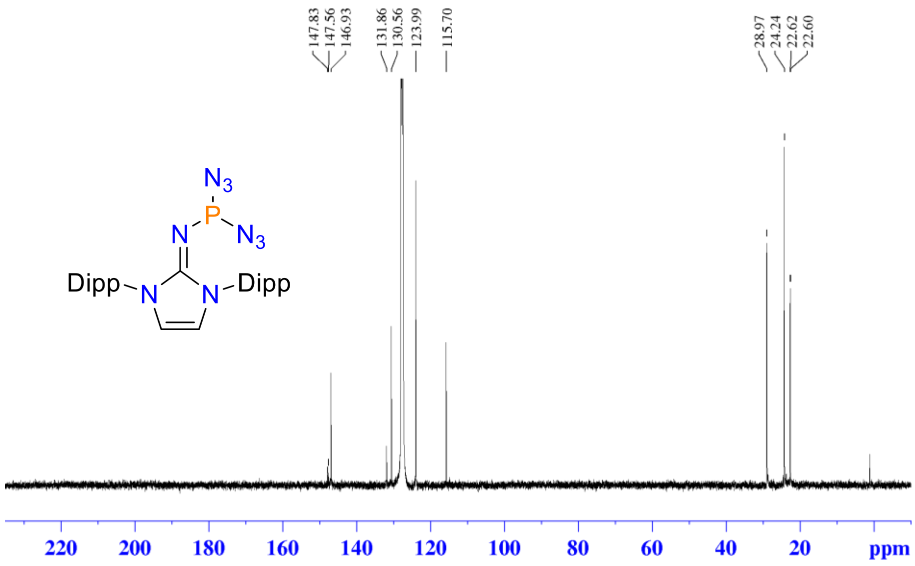

Appendix B-2. ^{13}C{^{1}H} NMR spectrum of IPrNP(N$_3$)$_2$ (**3.2**) in C_6D_6.

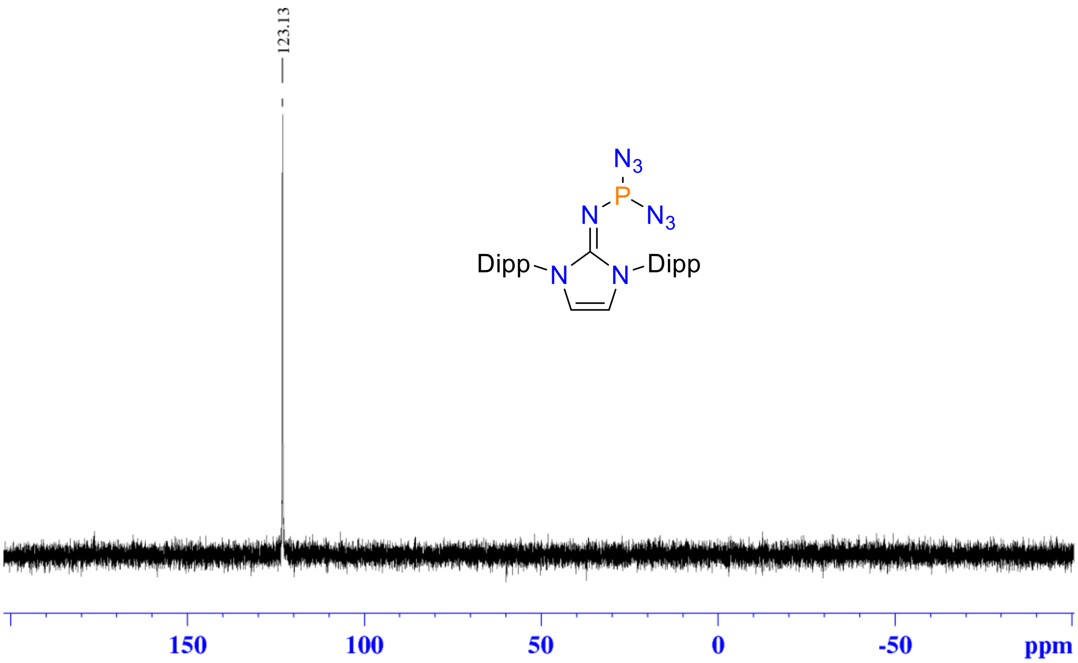

Appendix B-3. ${}^{31}P\{{}^{1}H\}$ NMR spectrum of IPrNP(N_3)$_2$ (**3.2**) in C_6D_6.

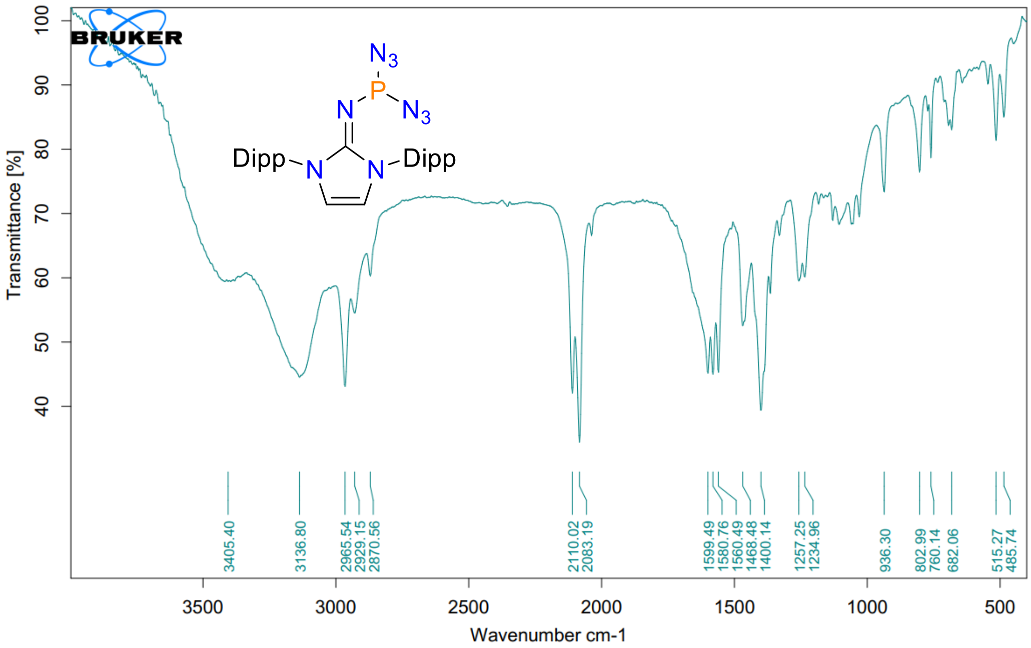

Appendix B-4. FT-IR spectrum of IPrNP(N_3)$_2$ (**3.2**) in KBr (Transmission mode).

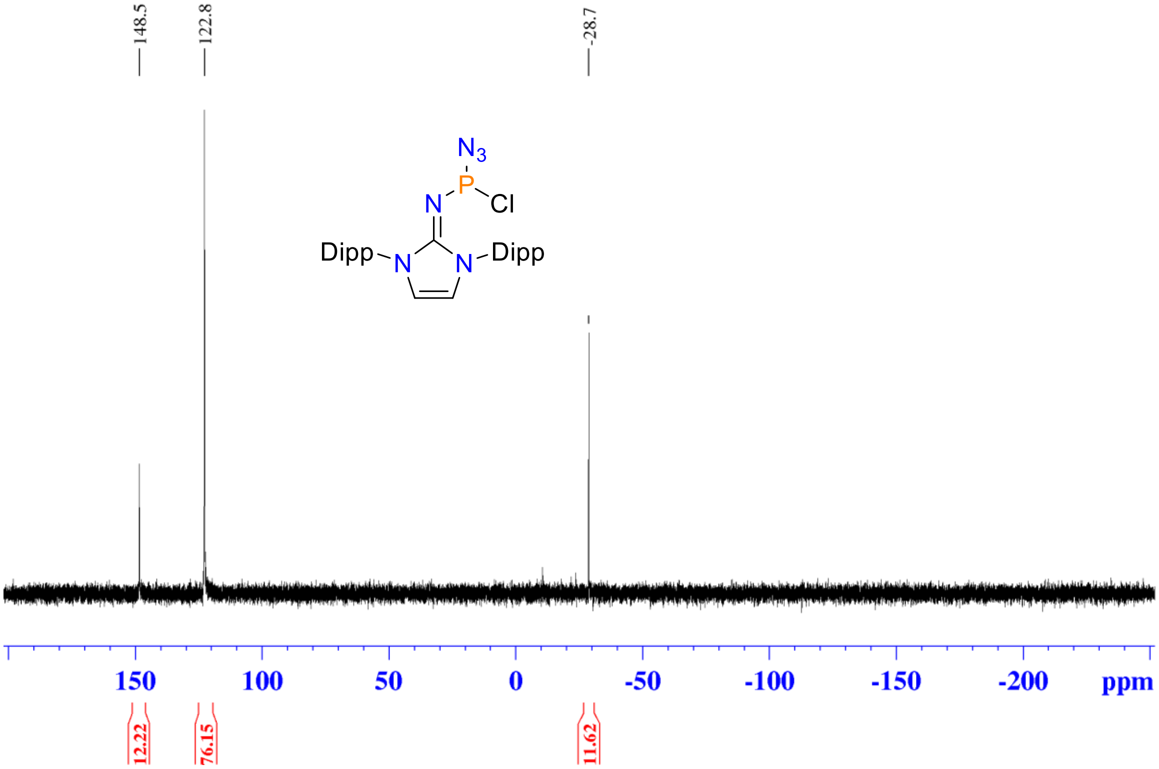

Appendix B-5. ^{31}P{^{1}H} NMR of reaction of **3.1** with two and a half equivalents of Me_3SiN_3 in toluene after complete consumption of **3.1**.

Note: Resonance for intermediate **3.2'** can be observed at 148.5 ppm, **3.2** at 122.8 ppm, and **3.4** at -28.7 ppm.

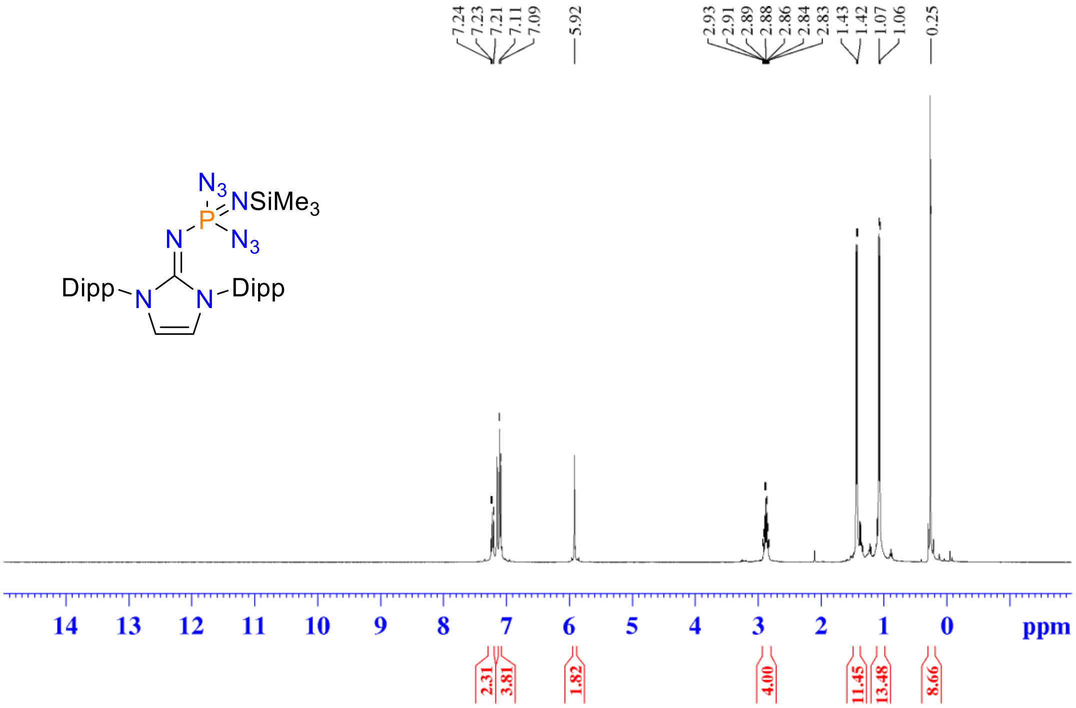

Appendix B-6. ^{1}H NMR spectrum of IPrNP(NSiMe$_3$)(N$_3$)$_2$ (**3.3**).

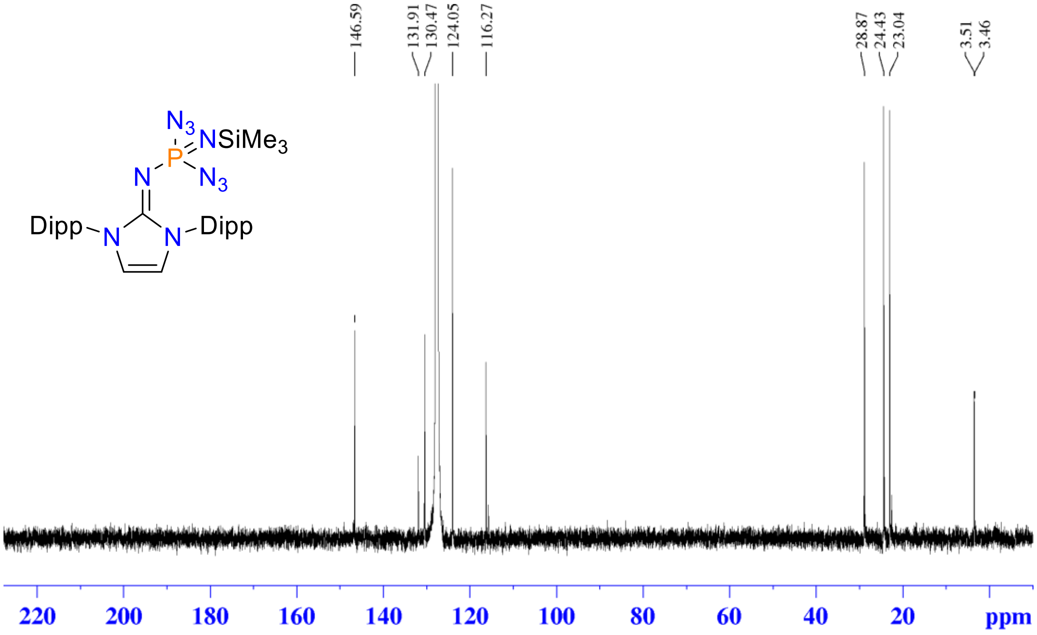

Appendix B-7. ^{13}C{^{1}H} NMR spectrum of compound IPrNP(NSiMe$_3$)(N$_3$)$_2$ (**3.3**).

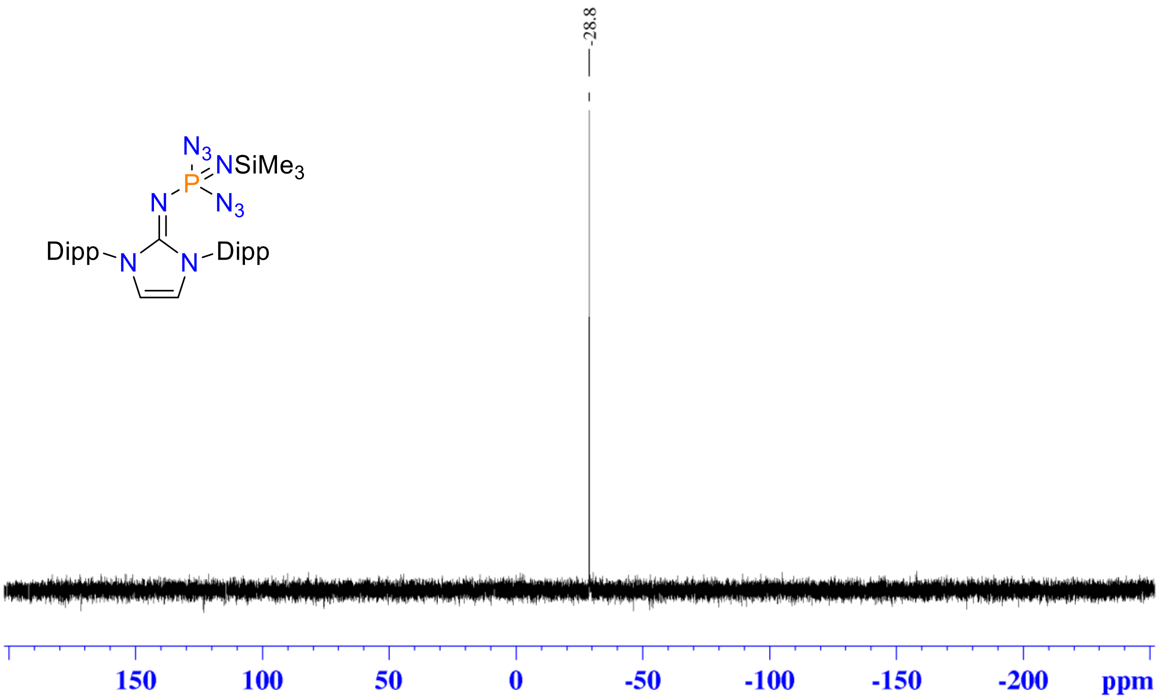

Appendix B-8. $^{31}P\{^{1}H\}$ NMR spectrum of compound IPrNP(NSiMe$_3$)(N$_3$)$_2$ (**3.3**) in C_6D_6.

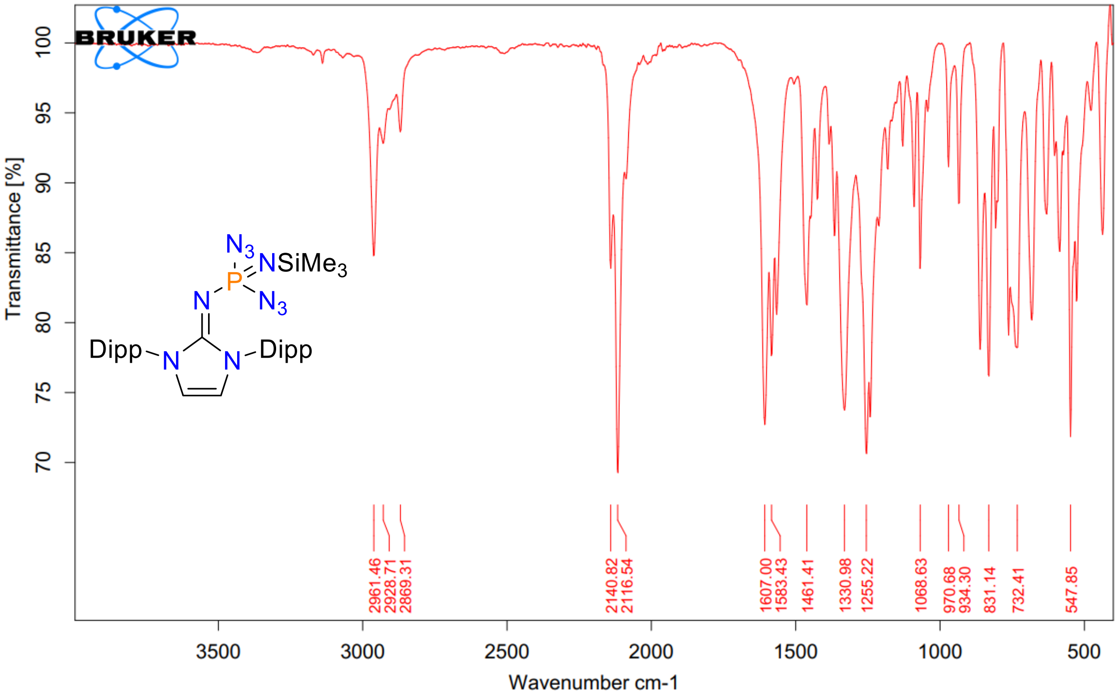

Appendix B-9. FT-IR spectrum of IPrNP(NSiMe$_3$)(N$_3$)$_2$ (**3.3**) (ATR mode).

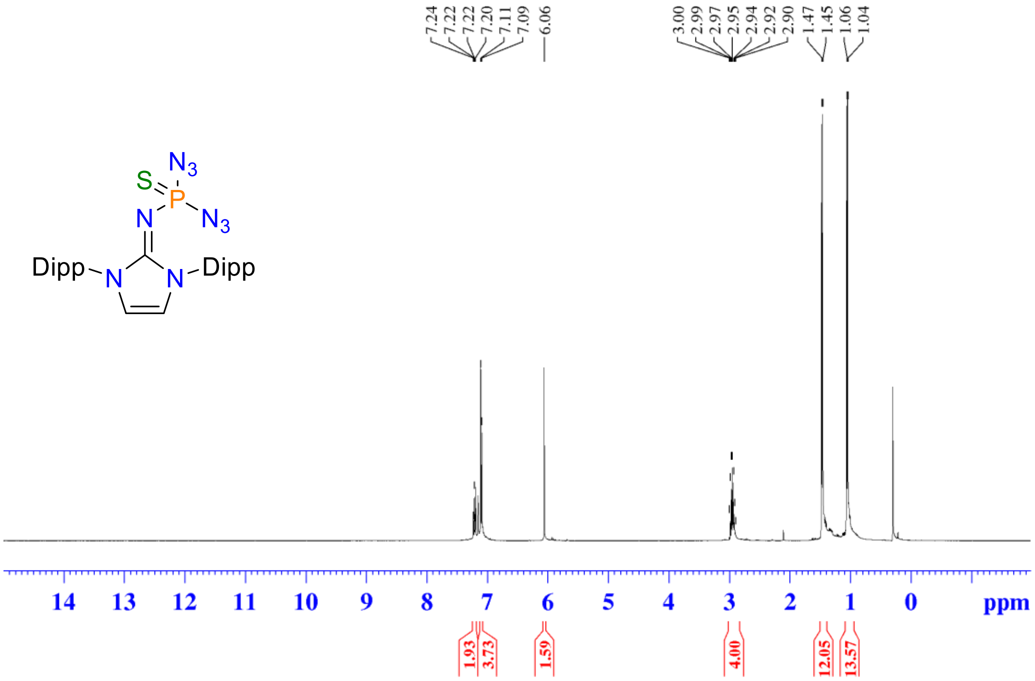

Appendix B-10. ^{1}H NMR of IPrNPS(N_3)$_2$ (**3.4S**) in C_6D_6.

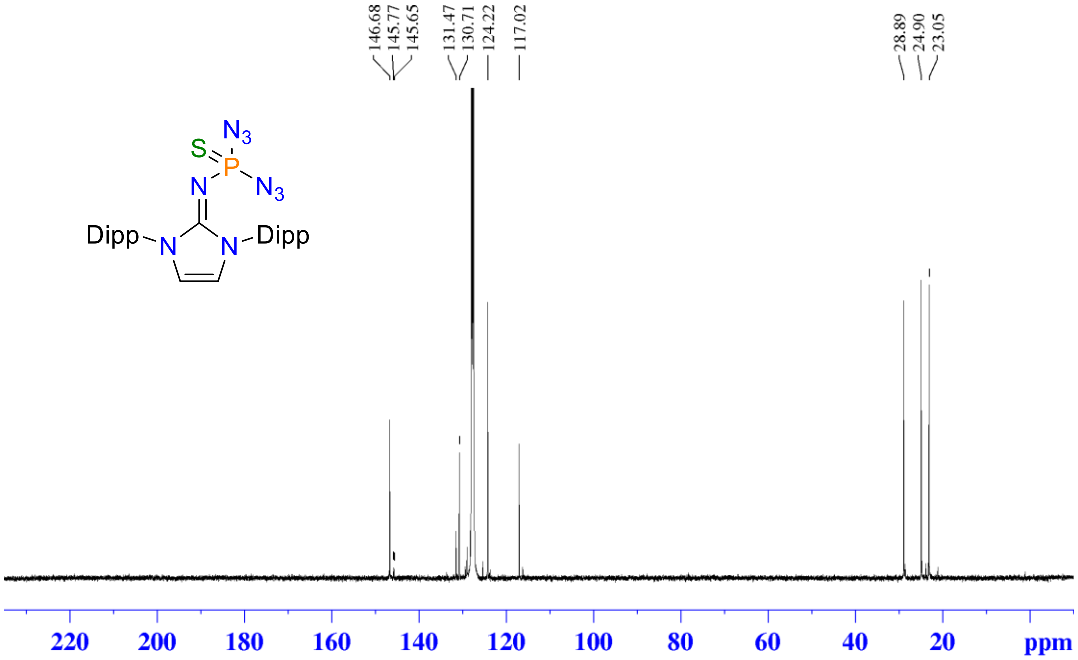

Appendix B-11. ^{13}C{^{1}H} NMR spectrum of IPrNPS(N_3)$_2$ (**3.4S**) in C_6D_6.

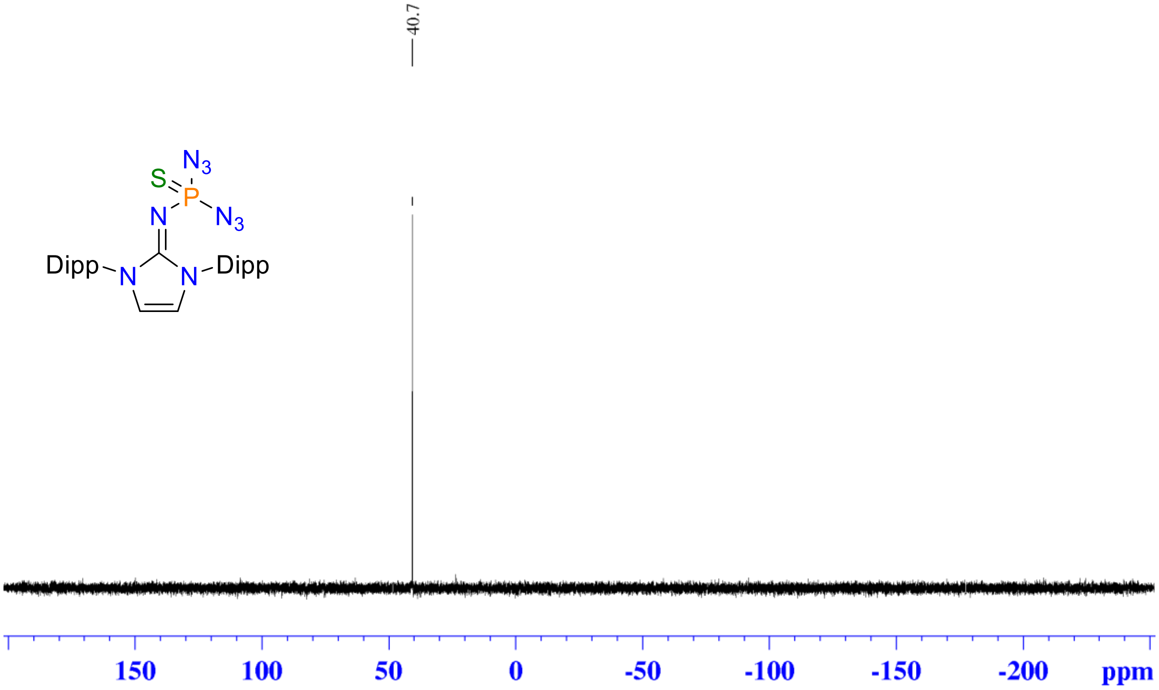

Appendix B-12. $^{31}P\{^1H\}$ NMR spectrum of IPrNPS(N_3)$_2$ (**3.4S**) in C_6D_6.

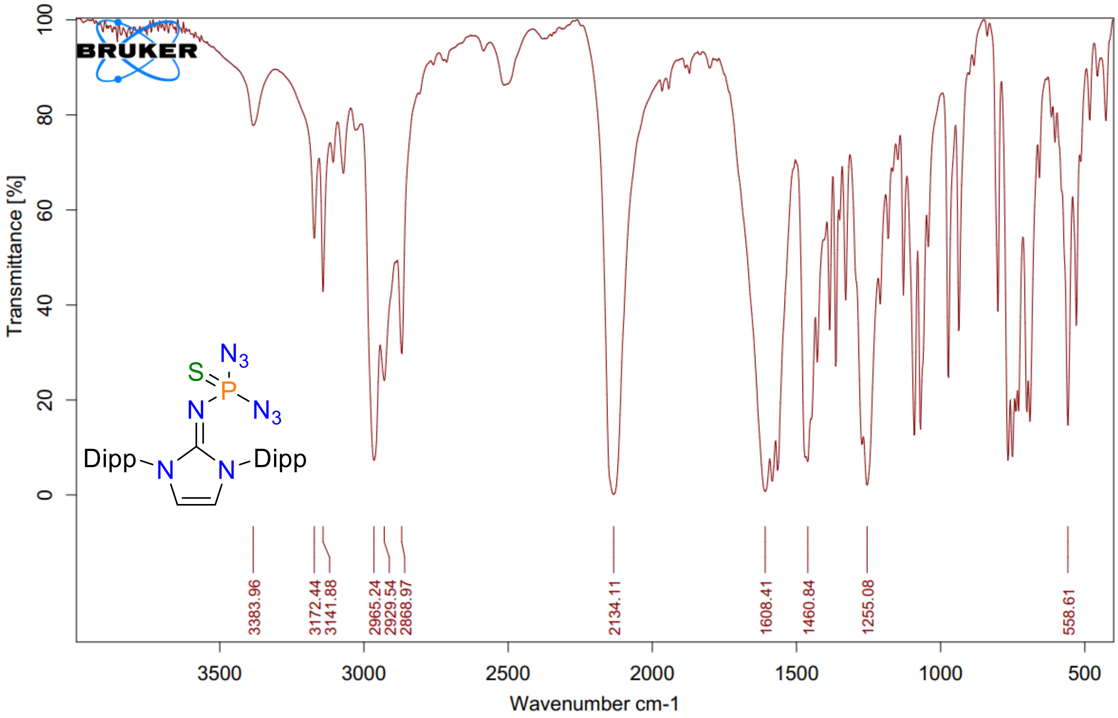

Appendix B-13. FT-IR spectrum of IPrNPS(N_3)$_2$ (**3.4S**) in air [ATR mode].

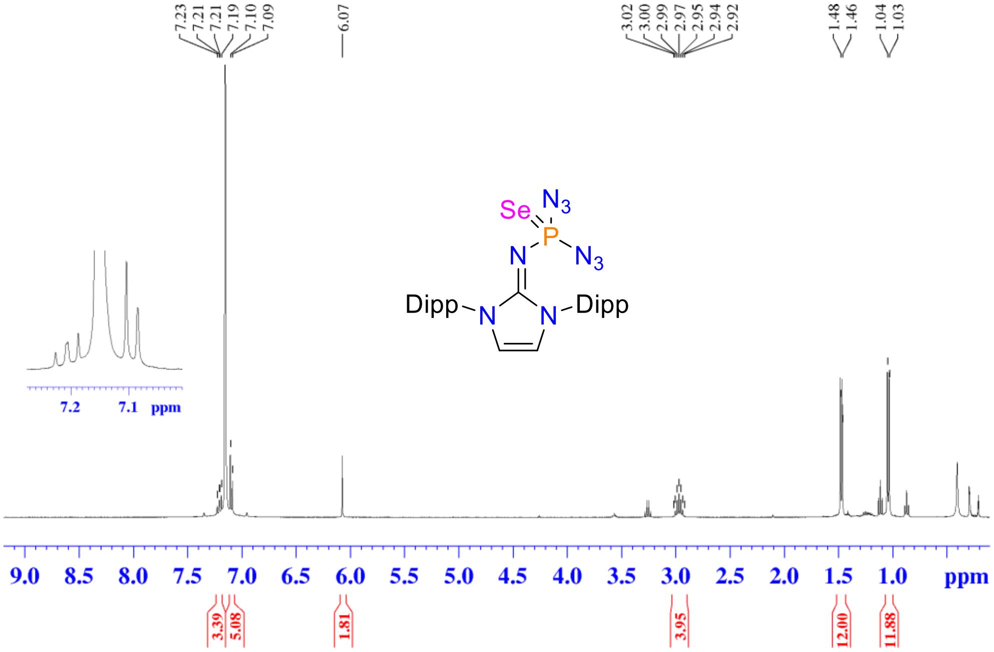

Appendix B-14. ^{1}H NMR spectrum of IPrNPSe(N$_3$)$_2$ (**3.4Se**) in C$_6$D$_6$. † denotes residual pentane. ‡ denotes residual Et$_2$O.

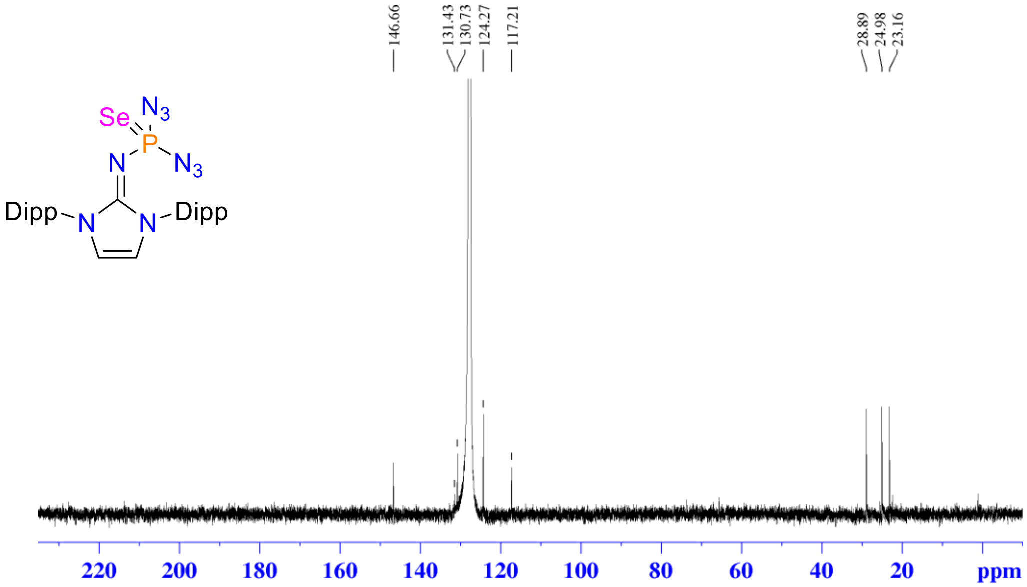

Appendix B-15. ^{13}C{^{1}H} NMR spectrum of IPrNPSe(N$_3$)$_2$ (**3.4Se**) in C$_6$D$_6$. N*C*N carbon not detected.

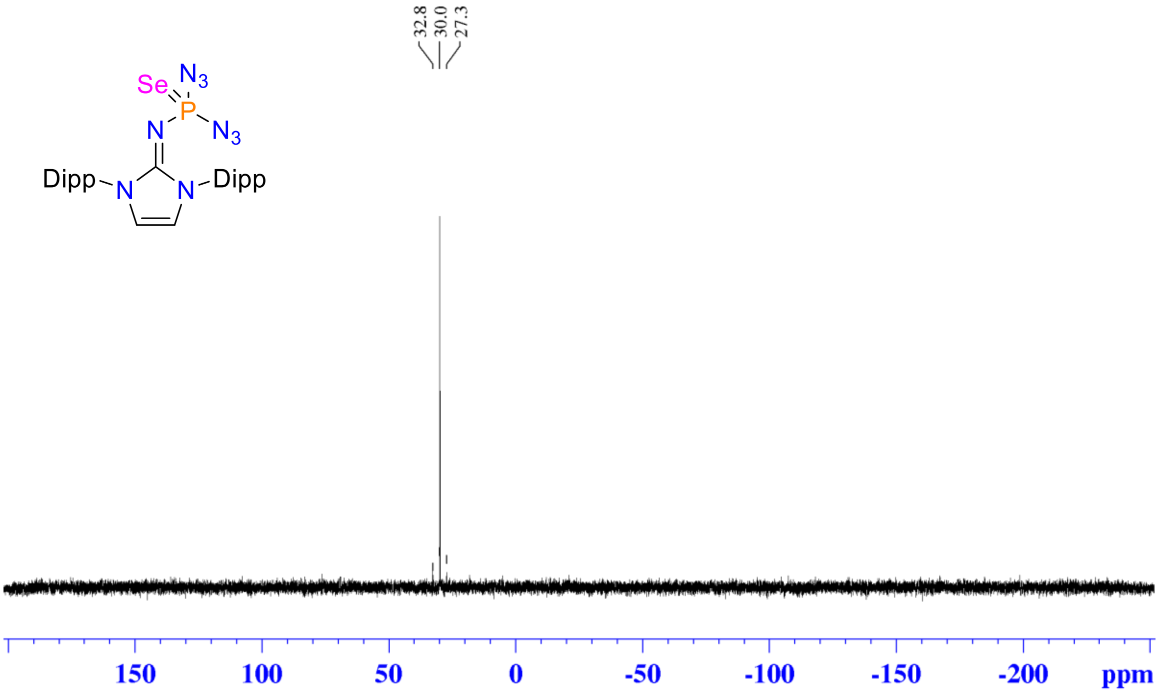

Appendix B-16. $^{31}P\{^{1}H\}$ NMR spectrum of IPrNPSe(N_3)$_2$ (**3.4Se**) in C_6D_6.

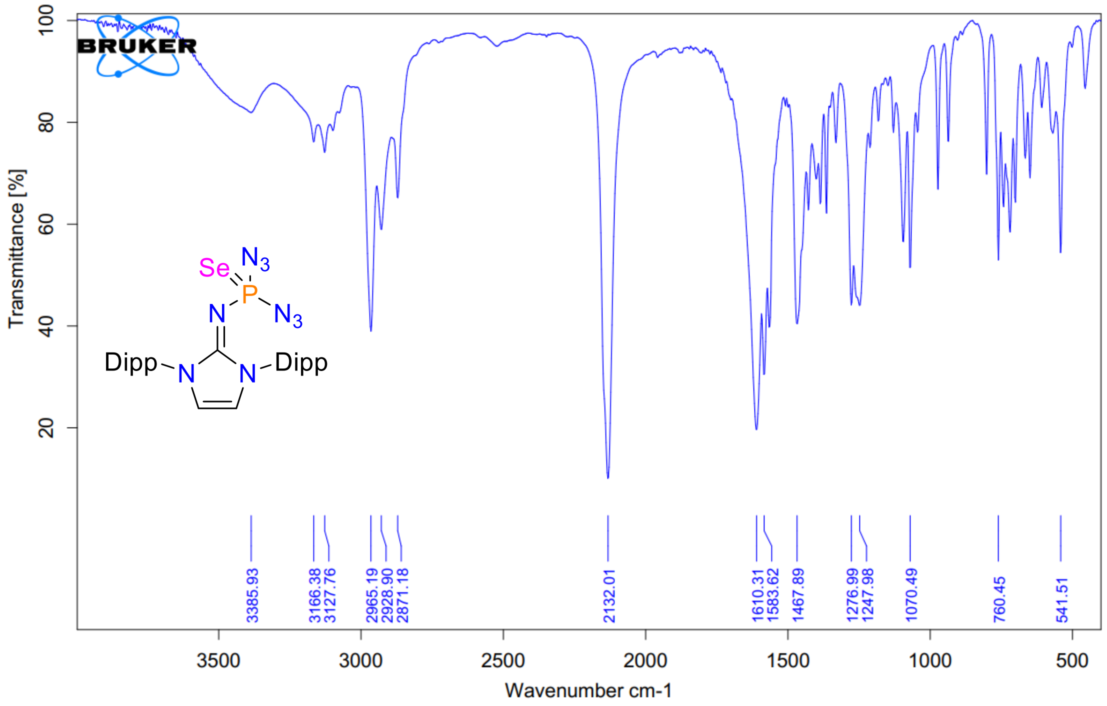

Appendix B-17. FT-IR spectrum of IPrNPSe(N_3)$_2$ (**3.4Se**) (transmission mode).

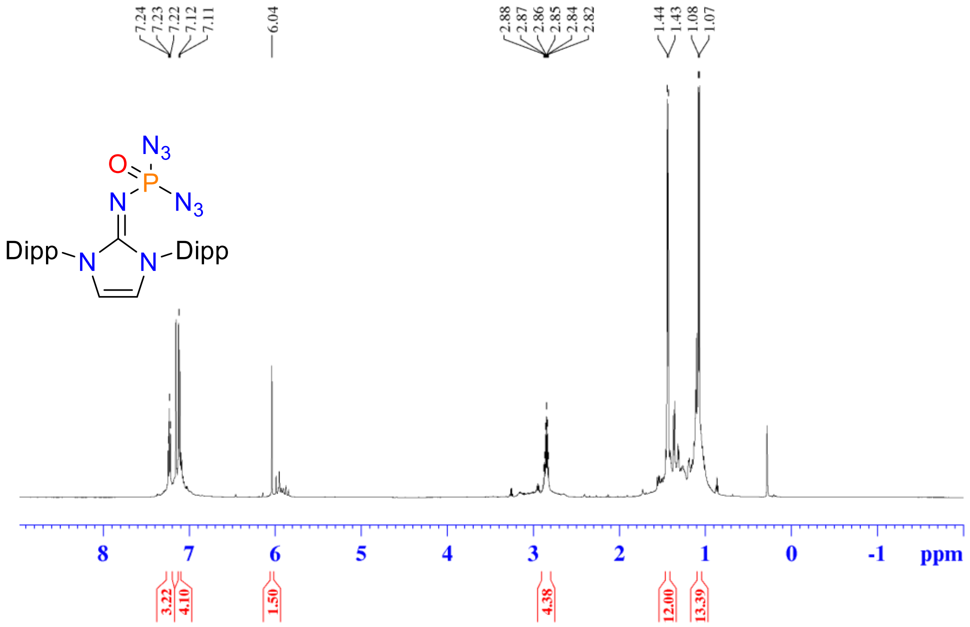

Appendix B-18. ^{1}H NMR spectrum of *in situ* formation of IPrNPO(N_3)$_2$ (**3.4O**) in C_6D_6 solution in O_2 (g) pressurized J-Young NMR tube after seven days.

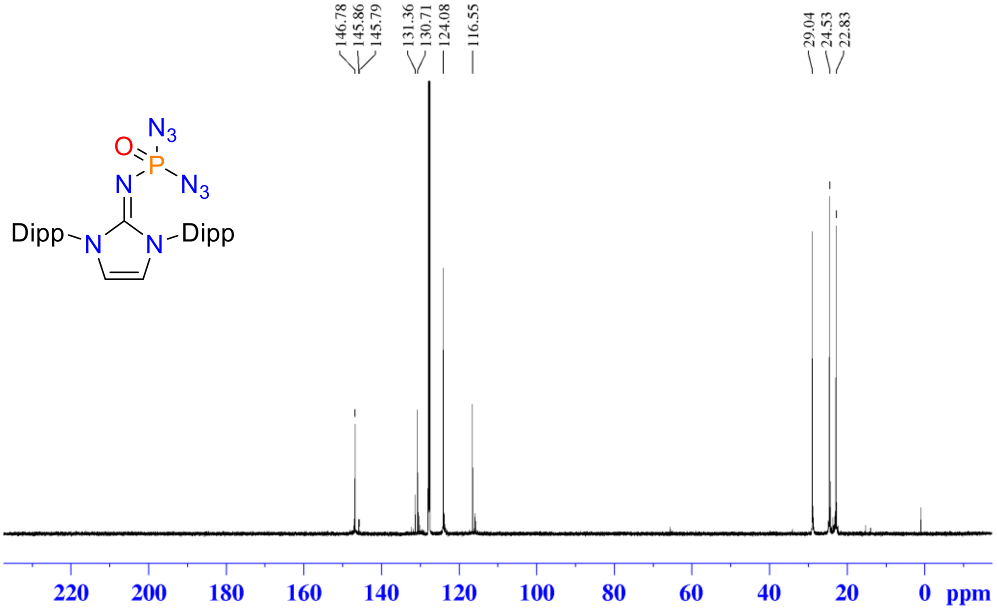

Appendix B-19. ^{13}C{^{1}H} NMR spectrum of *in situ* formation of IPrNPO(N_3)$_2$ (**3.4O**) in C_6D_6 solution in O_2 (g) pressurized J-Young NMR tube after seven days.

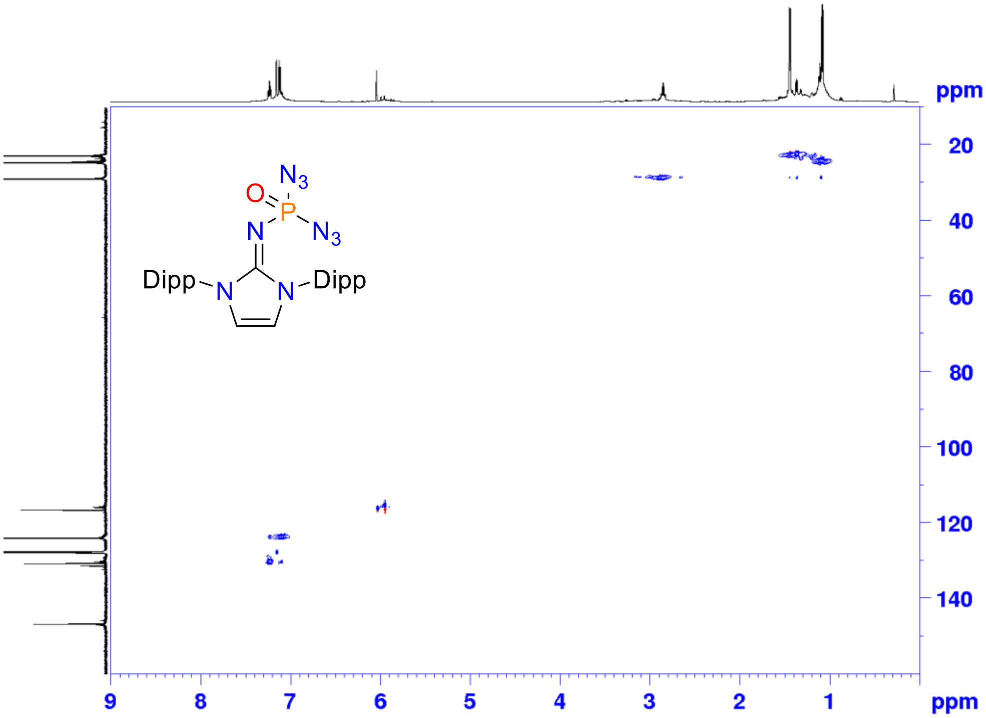

Appendix B-20. HSQC spectrum of IPrNPO(N_3)$_2$ (**3.4O**) in C_6D_6.

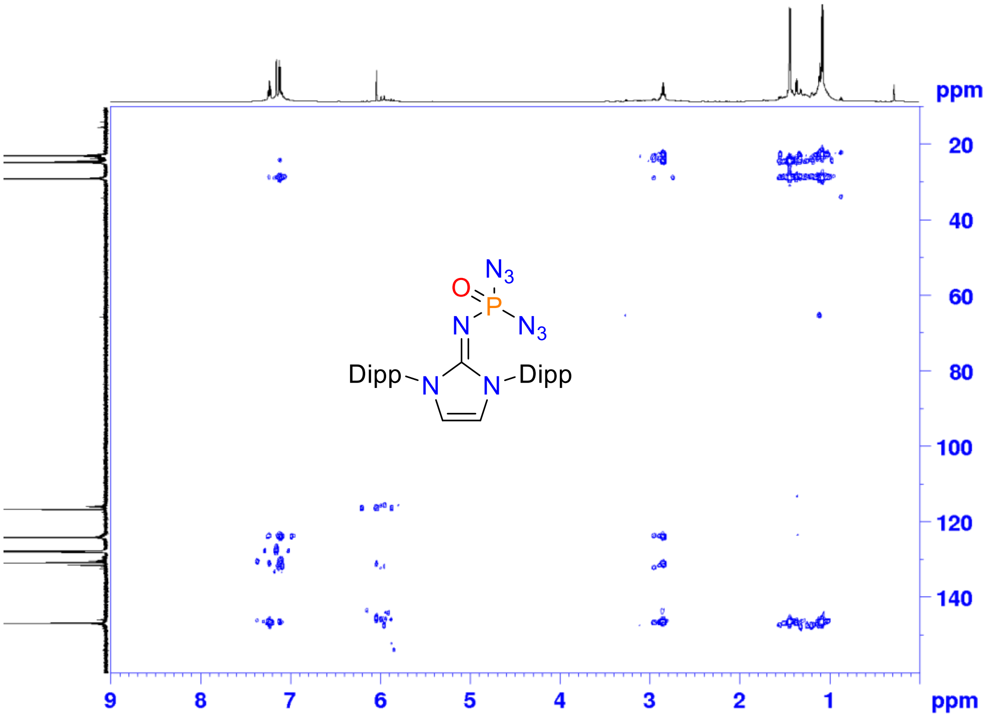

Appendix B-21. HMBC spectrum of IPrNPO(N_3)$_2$ (**3.4O**) in C_6D_6.

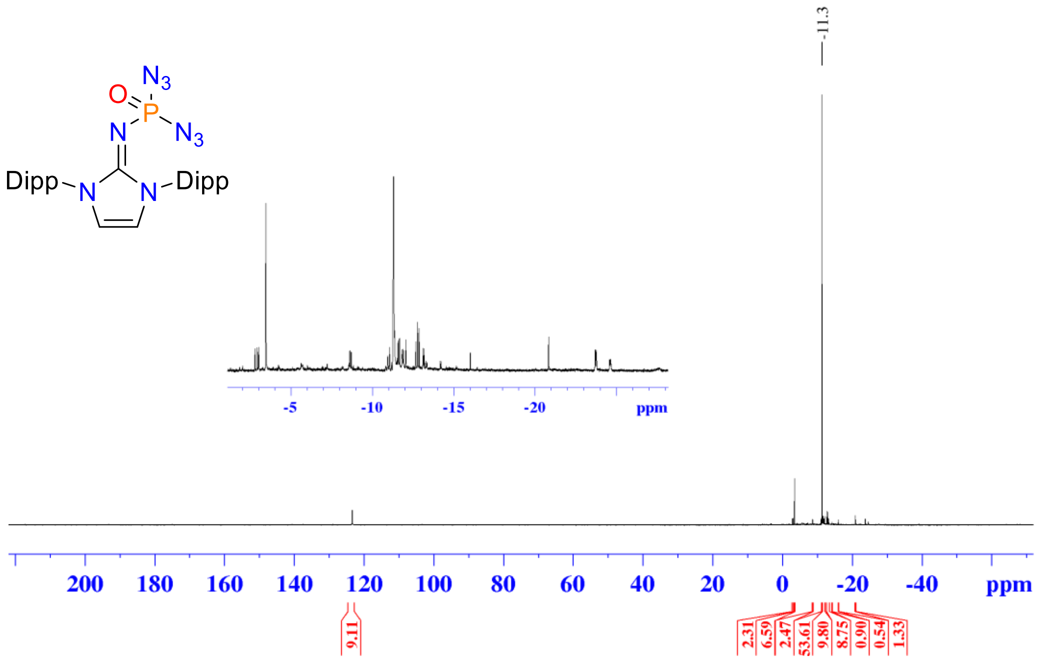

Appendix B-22. $^{31}P\{^1H\}$ NMR spectrum of *in situ* formation of IPrNPO(N_3)$_2$ (**3.4O**) by oxidation of **3.2** (*) with gaseous O_2 in C_6D_6 over six days at room temperature.

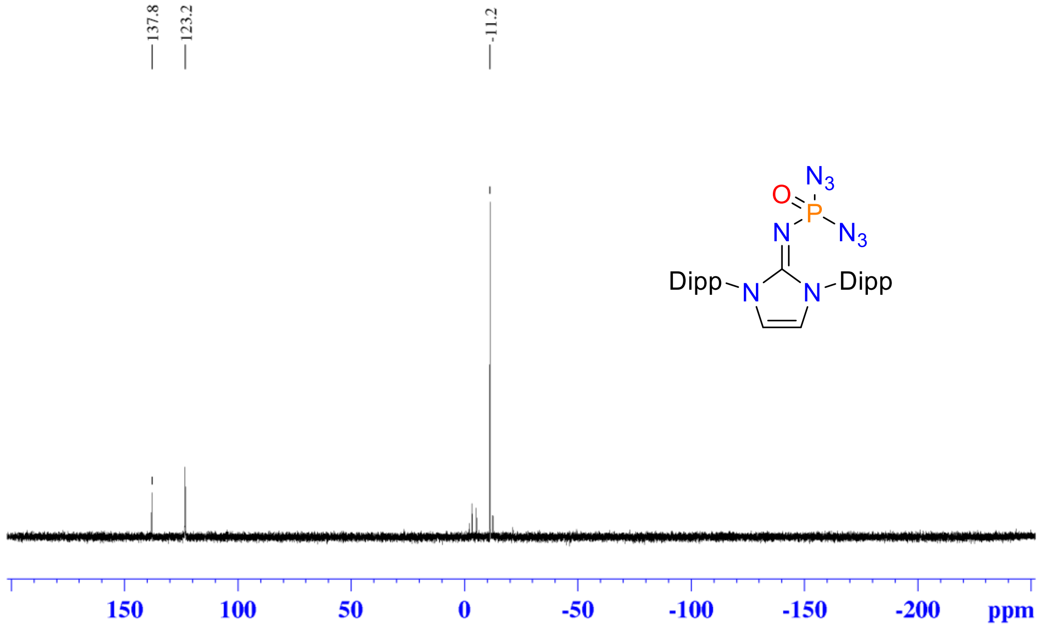

Appendix B-23. $^{31}P\{^1H\}$ NMR spectrum of reaction of **3.2** with few crystals *m*-CPBA in C_6D_6, after ten min. Unreacted **3.2** can be observed at 123 ppm and IPrNPO(N_3)$_2$ (**3.4O**) at -11.2 ppm. Unknown species at 137.8 ppm.

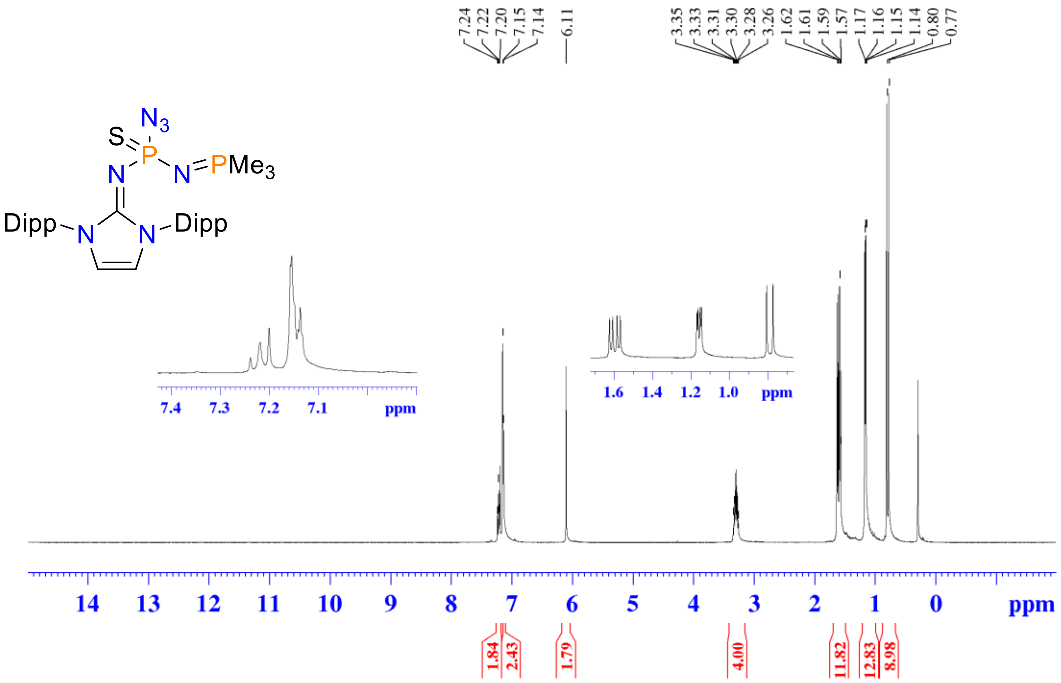

Appendix B-24. ^{1}H NMR spectrum of IPrNP(S)(N_3)($NPMe_3$) (**3.5$_{Me}$**) in C_6D_6.

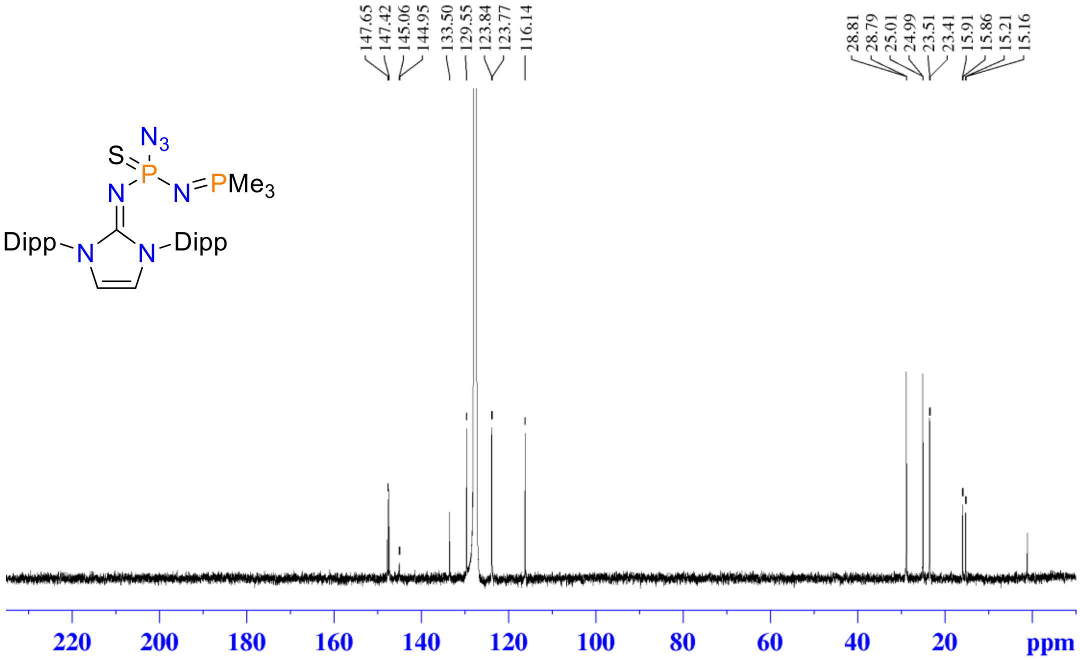

Appendix B-25. ^{13}C{^{1}H} NMR spectrum of IPrNP(S)(N_3)($NPMe_3$) (**3.5$_{Me}$**) in C_6D_6.

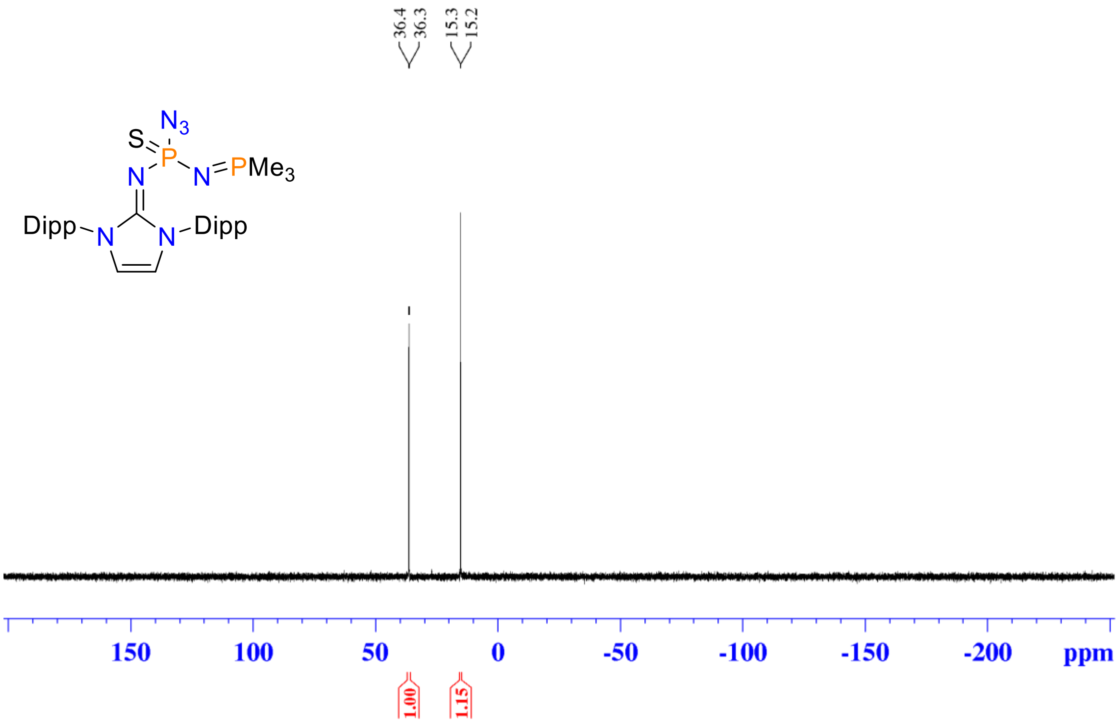

Appendix B-26. ^{31}P{^{1}H} NMR spectrum of IPrNP(S)(N$_3$)(NPMe$_3$) (**3.5$_{Me}$**) in C$_6$D$_6$.

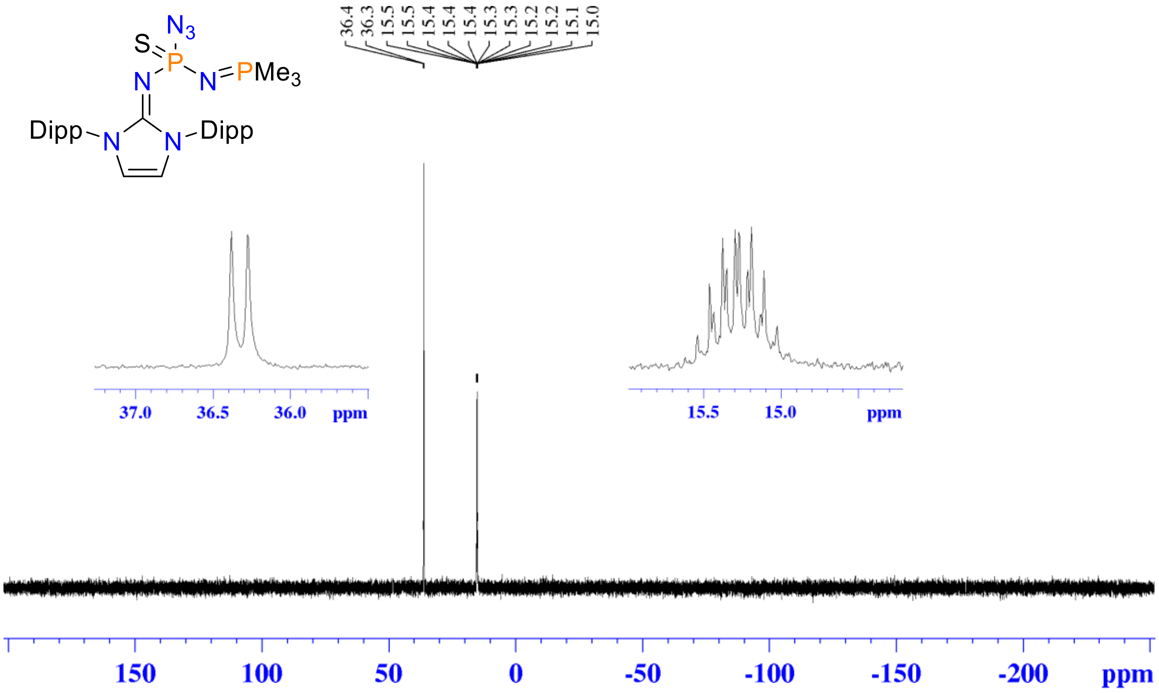

Appendix B-27. ^{31}P NMR spectrum of IPrNP(S)(N$_3$)(NPMe$_3$) (**3.5$_{Me}$**) in C$_6$D$_6$.

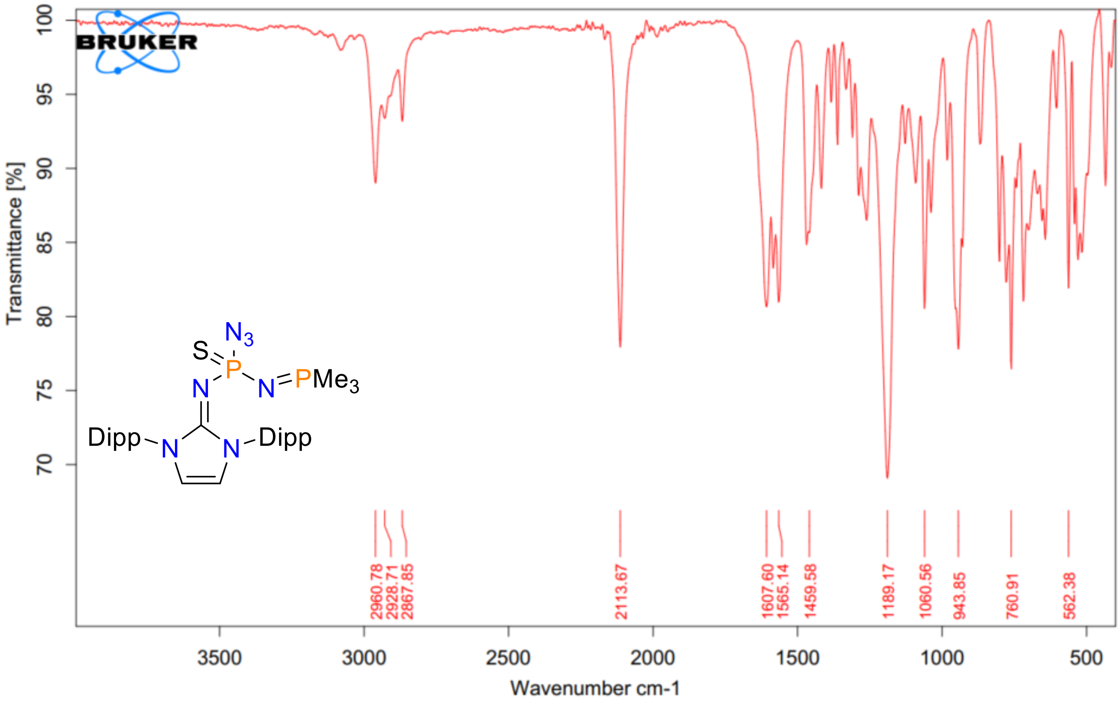

Appendix B-28. FT-IR spectrum of IPrNP(S)(N$_3$)(NPMe$_3$) (**3.5$_{Me}$**) (transmission mode).

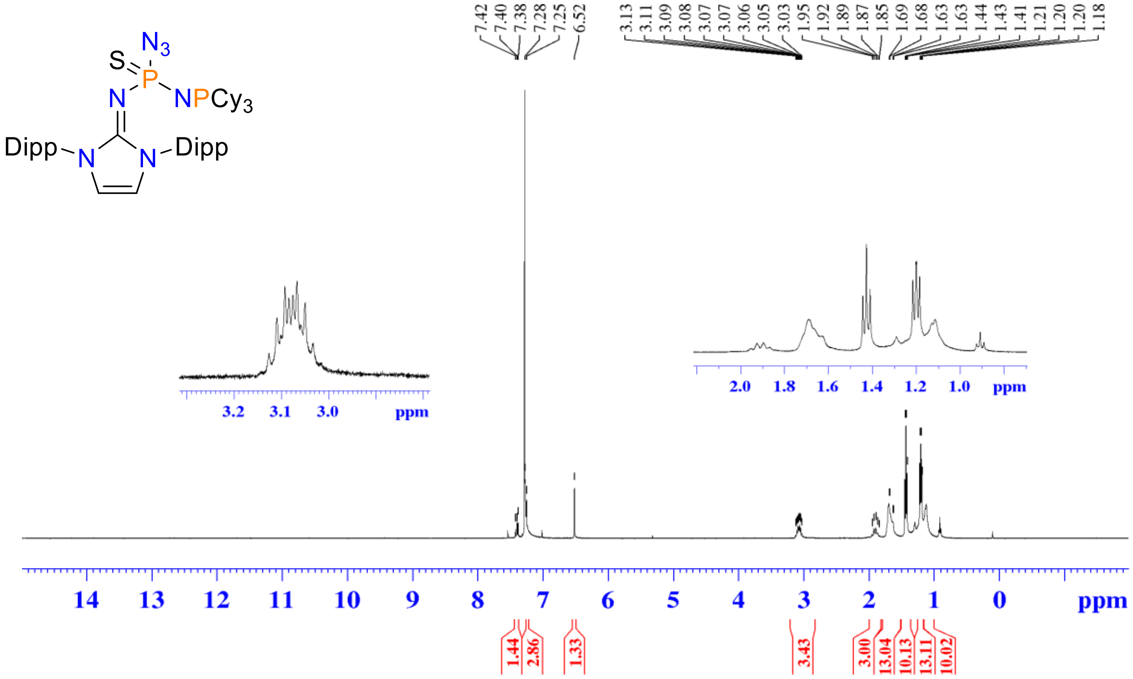

Appendix B-29. ^{1}H NMR spectrum of IPrNP(S)(N$_3$)(NPCy$_3$) (**3.5$_{Cy}$**) in CDCl$_3$. † denotes trace hexane.

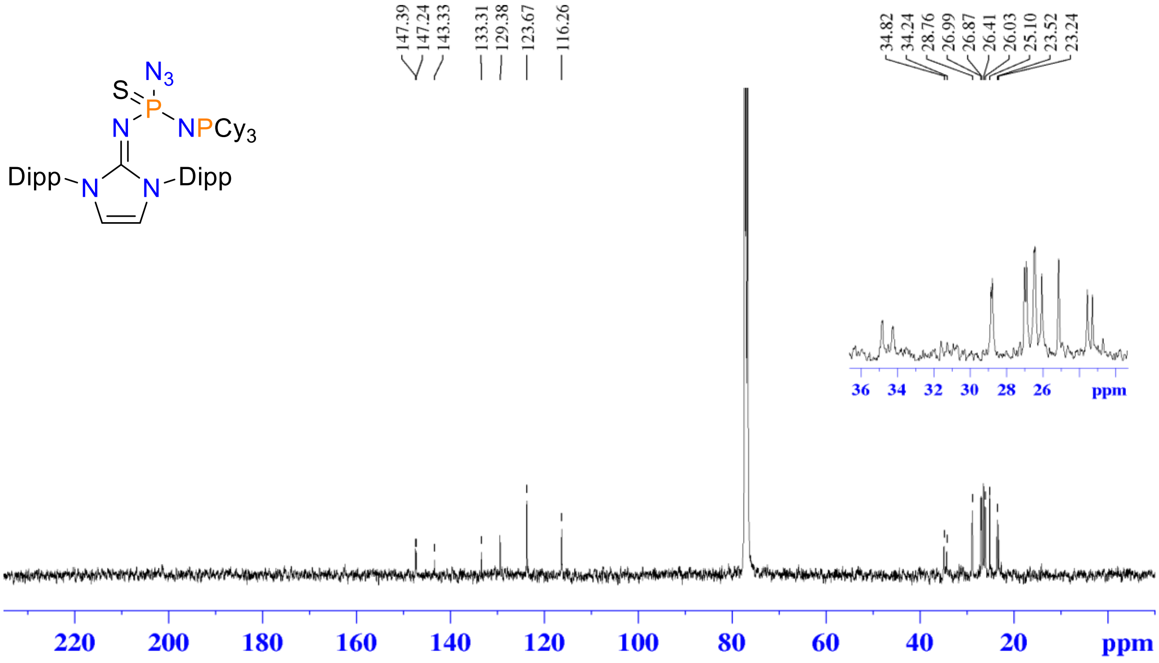

Appendix B-30. $^{13}C\{^1H\}$ NMR spectrum of IPrNP(S)(N$_3$)(NPCy$_3$) (**3.5$_{Cy}$**) in CDCl$_3$.

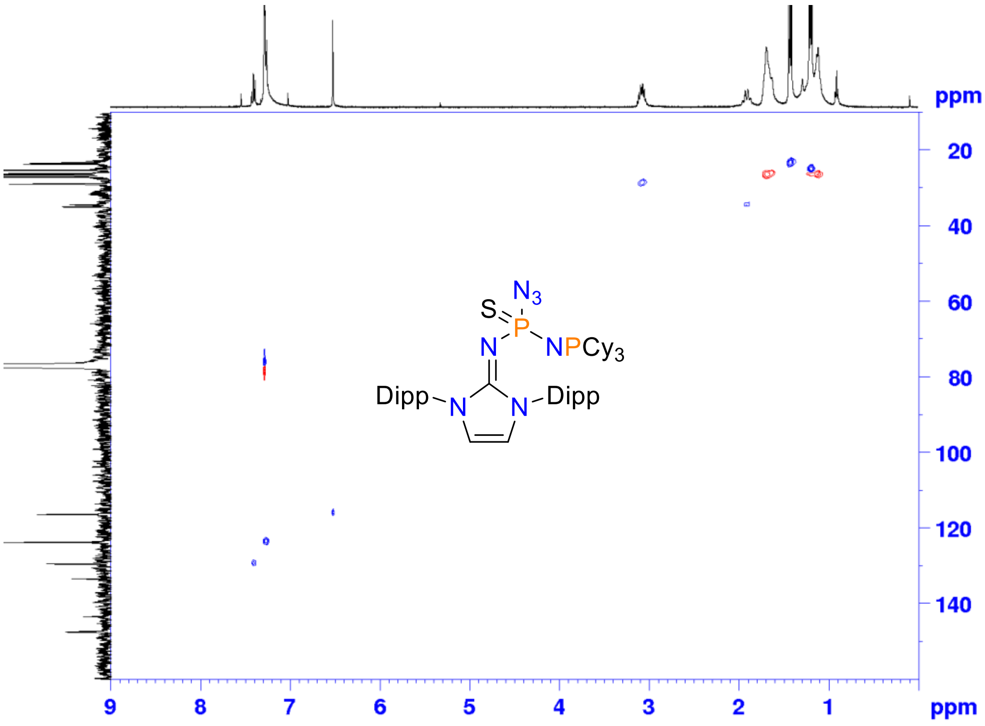

Appendix B-31. HSQC NMR spectrum of IPrNP(S)(N$_3$)(NPCy$_3$) (**3.5$_{Cy}$**) in CDCl$_3$.

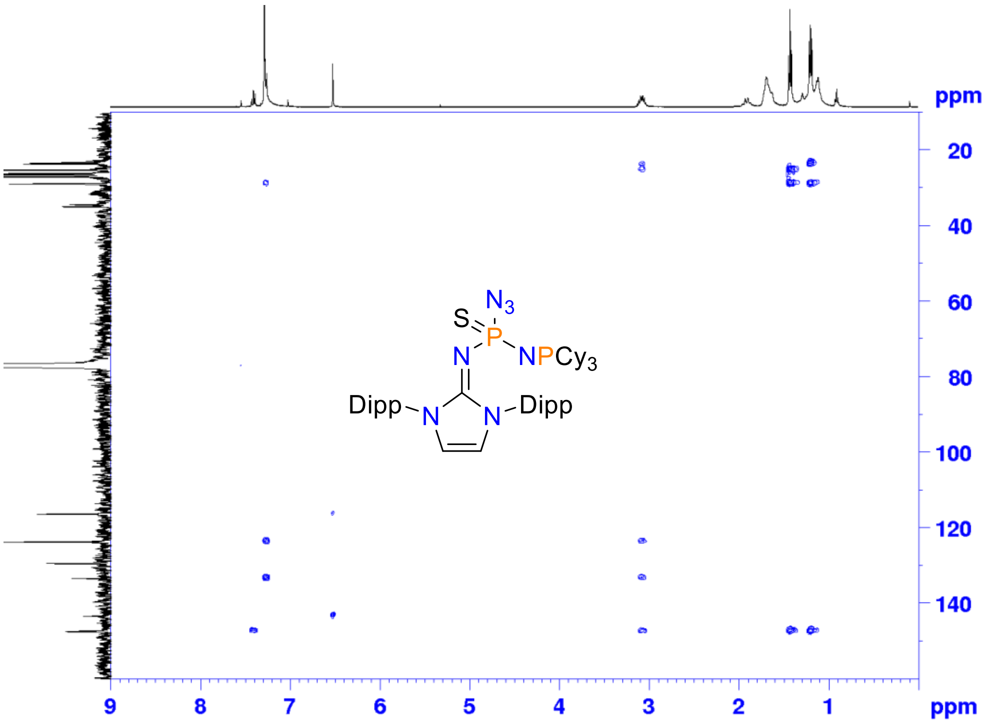

Appendix B-32. HMBC NMR spectrum spectrum of IPrNP(S)(N$_3$)(NPCy$_3$) (**3.5**$_{\mathbf{Cy}}$).

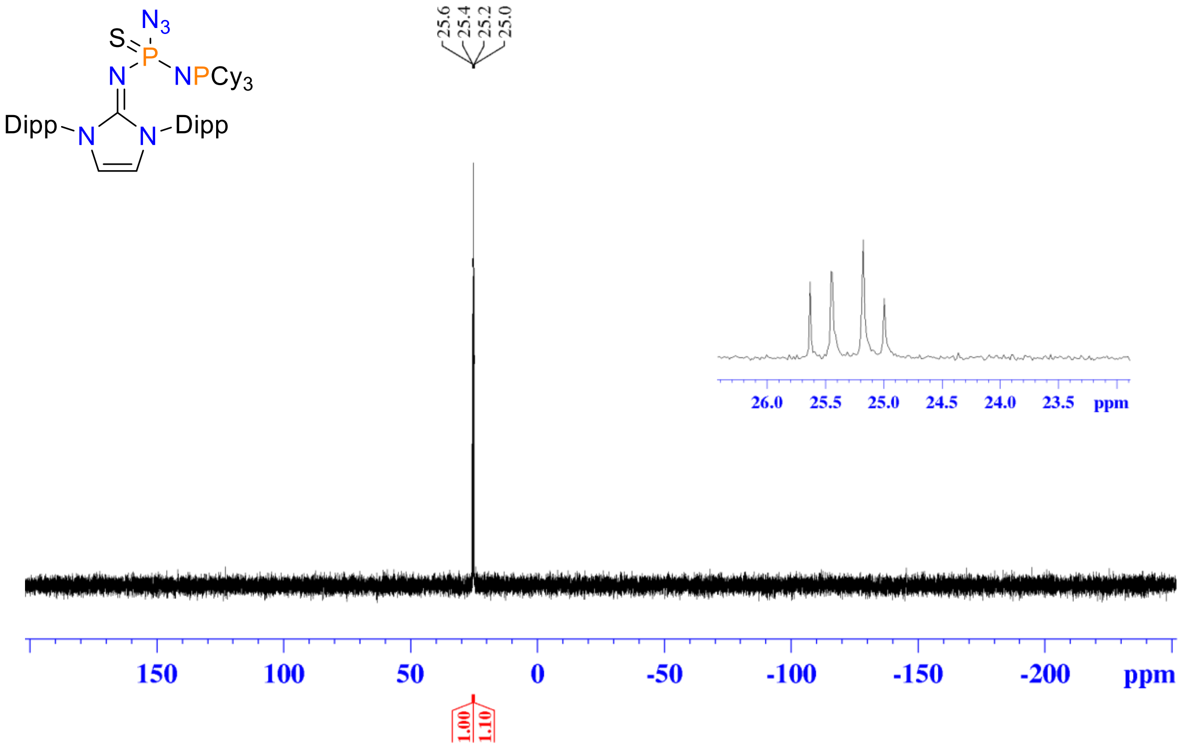

Appendix B-33. ^{31}P{^{1}H} NMR spectrum of IPrNP(S)(N$_3$)(NPCy$_3$) (**3.5**$_{\mathbf{Cy}}$) in CDCl$_3$.

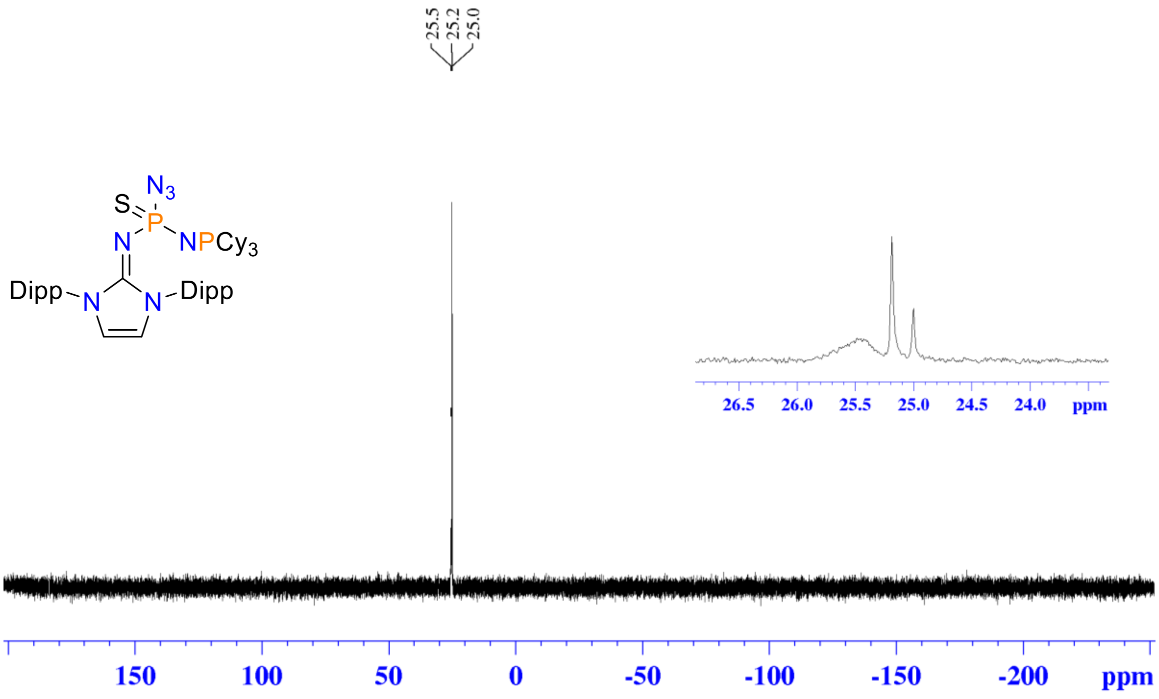

Appendix B-34. ^{31}P NMR spectrum of IPrNP(S)(N$_3$)(NPCy$_3$) (**3.5$_{Cy}$**), zoomed in.

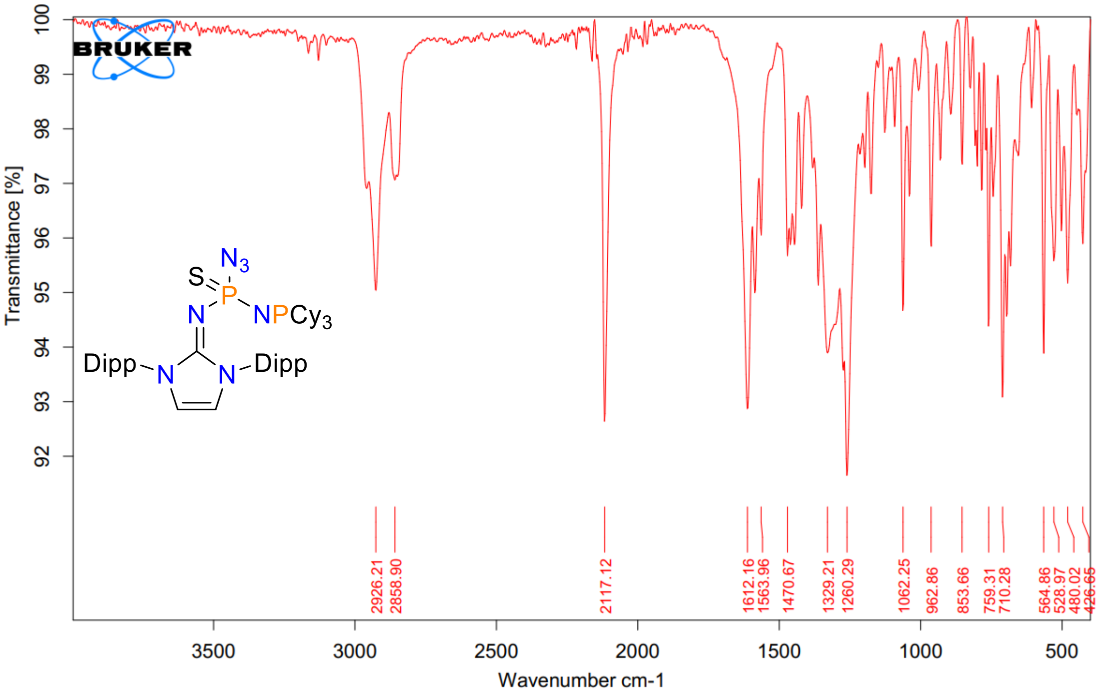

Appendix B-35. FT-IR spectrum of IPrNP(S)(N$_3$)(NPCy$_3$) (**3.5$_{Cy}$**) (transmission mode).

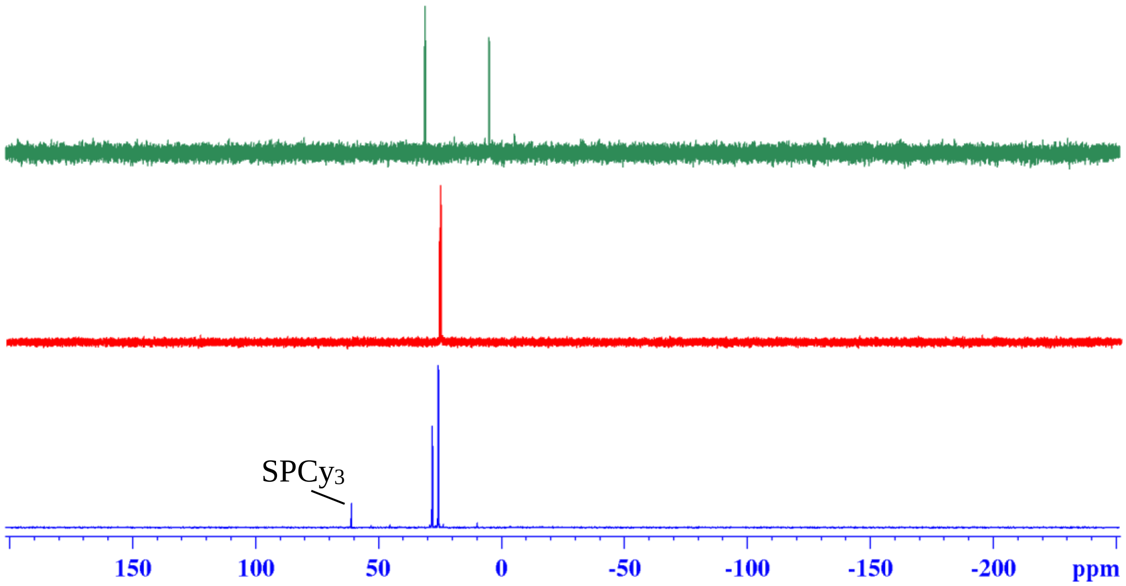

Appendix B-36. Stacked $^{31}P\{^{1}H\}$ NMR spectra of the reaction of **3.4S** (δ_P = 40.7) with PCy_3 (δ_P = 9.9). Blue: complete consumption shown here after four days at room temperature in toluene-h8. Red: After three volumes of one milliliter triturations with hexanes, solids redissolved in $CDCl_3$. Green: recrystallized **3.5_{Cy}** from hot hexanes, redissolved in C_6D_6.

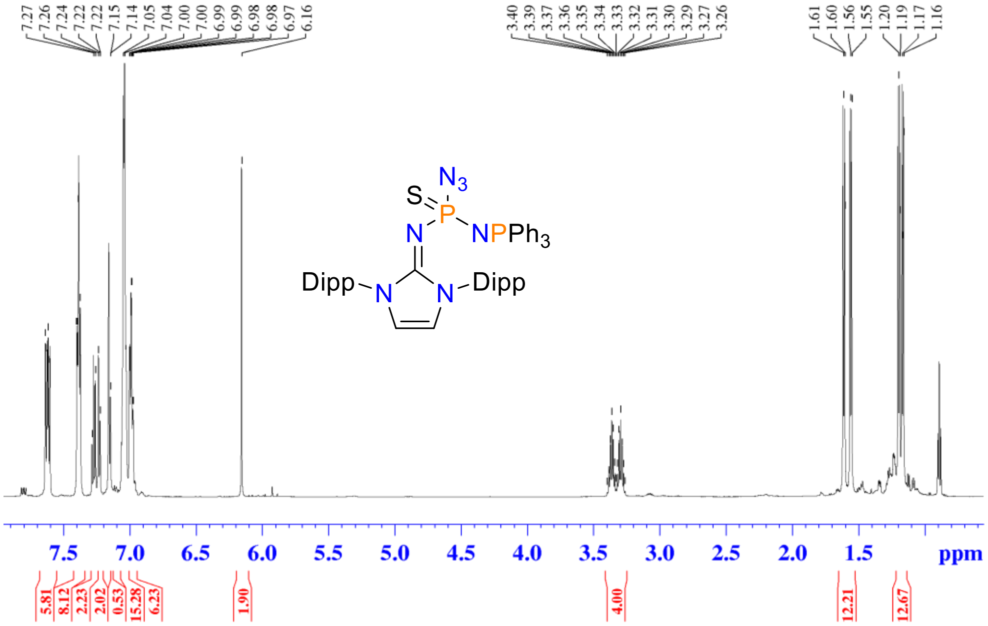

Appendix B-37. ^{1}H NMR spectrum of IPrNP(S)(N_3)($NPPh_3$) (**3.5_{Ph}**). Contains pentane and silicone grease impurities.

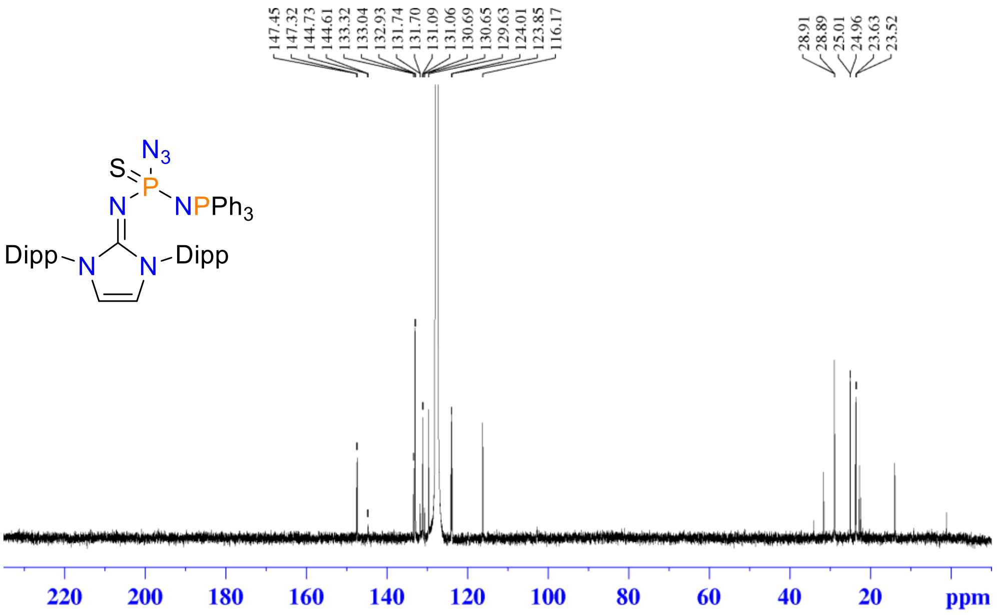

Appendix B-38. $^{13}C\{^{1}H\}$ NMR spectrum of IPrNP(S)(N_3)($NPPh_3$) (**3.5$_{Ph}$**). Pentane, hexane, and silicone grease impurities present in solvent.

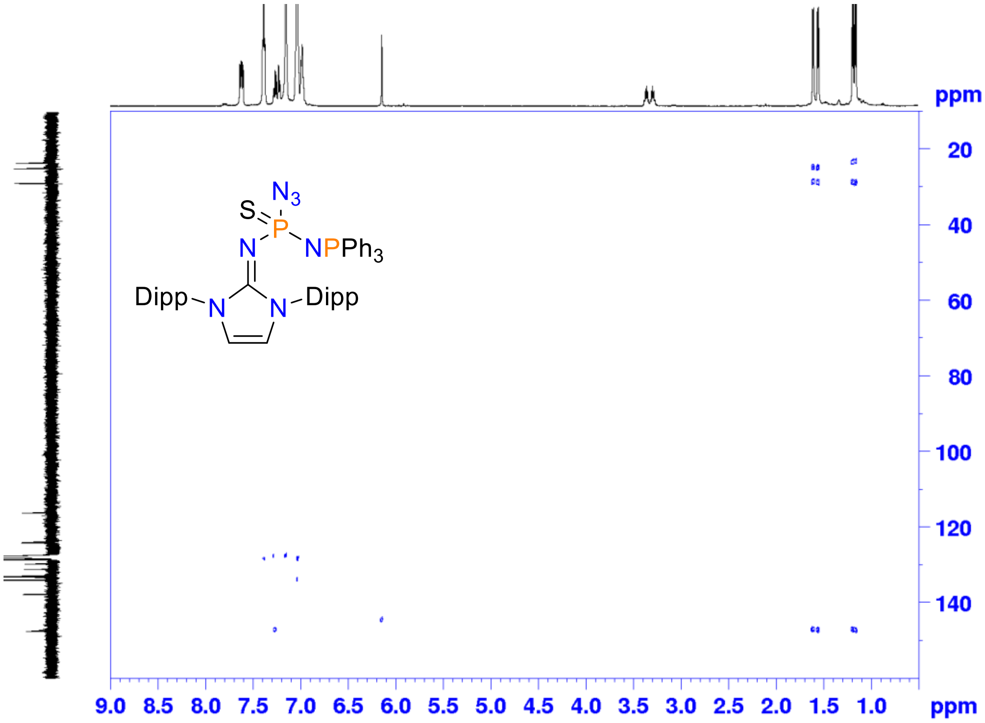

Appendix B-39. HMBC NMR spectrum of IPrNP(S)(N_3)($NPPh_3$) (**3.5$_{Ph}$**) for assignment of N*C*N carbon.

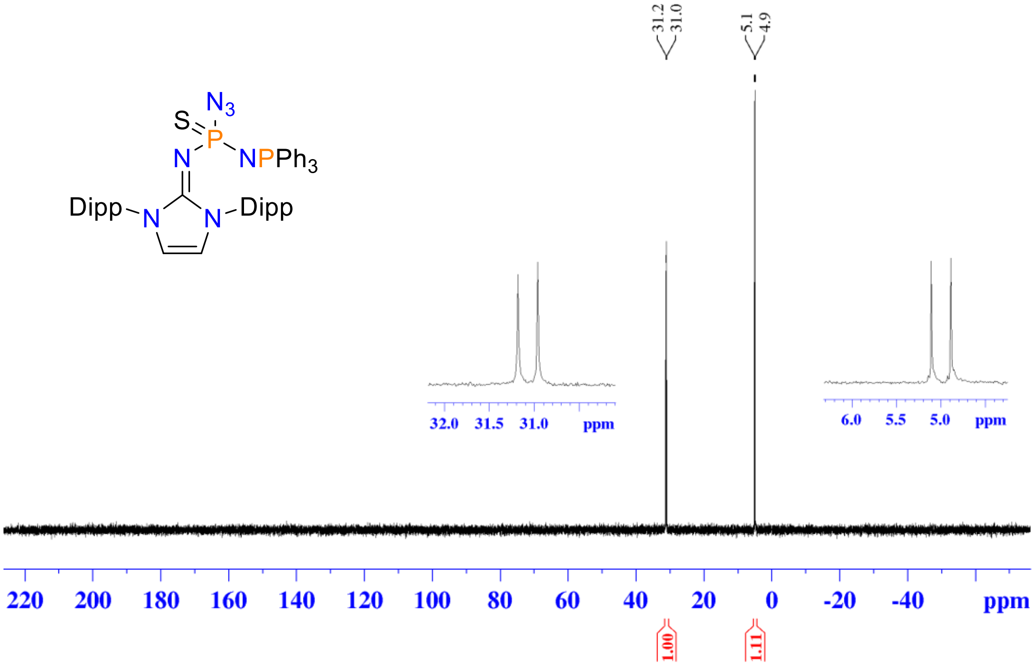

Appendix B-40. $^{31}P\{^{1}H\}$ NMR spectrum of IPrNP(S)(N_3)($NPPh_3$) (**3.5$_{Ph}$**) in C_6D_6.

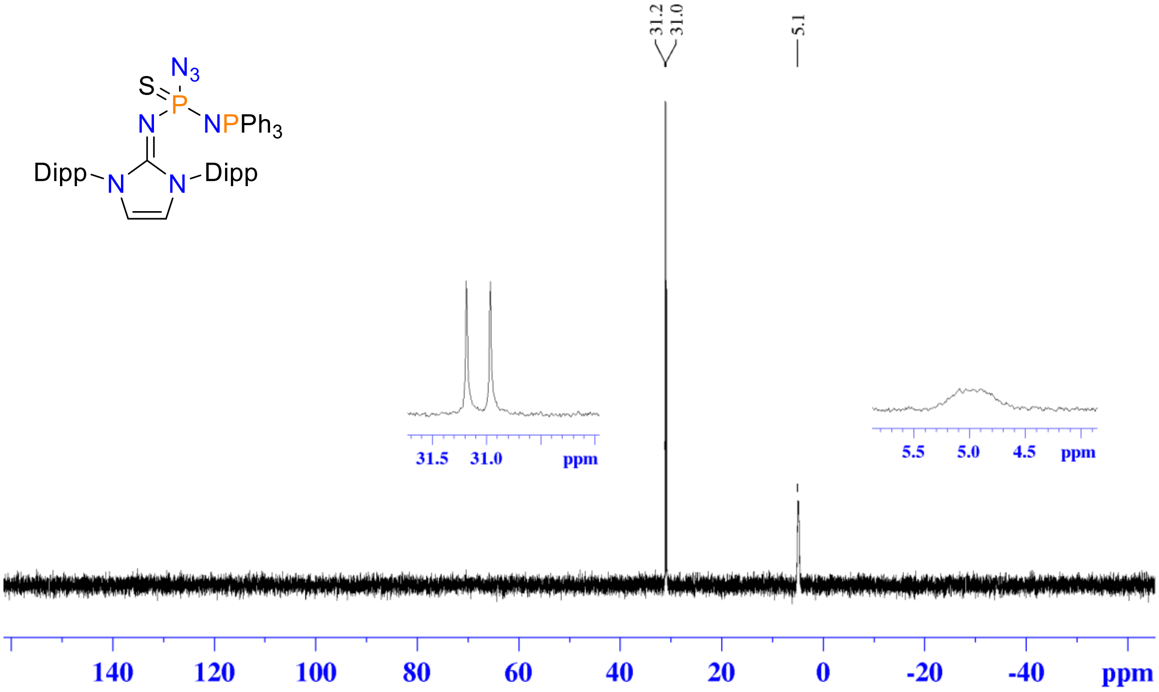

Appendix B-41. ^{31}P NMR spectrum of IPrNP(S)(N_3)($NPPh_3$) (**3.5$_{Ph}$**) in C_6D_6.

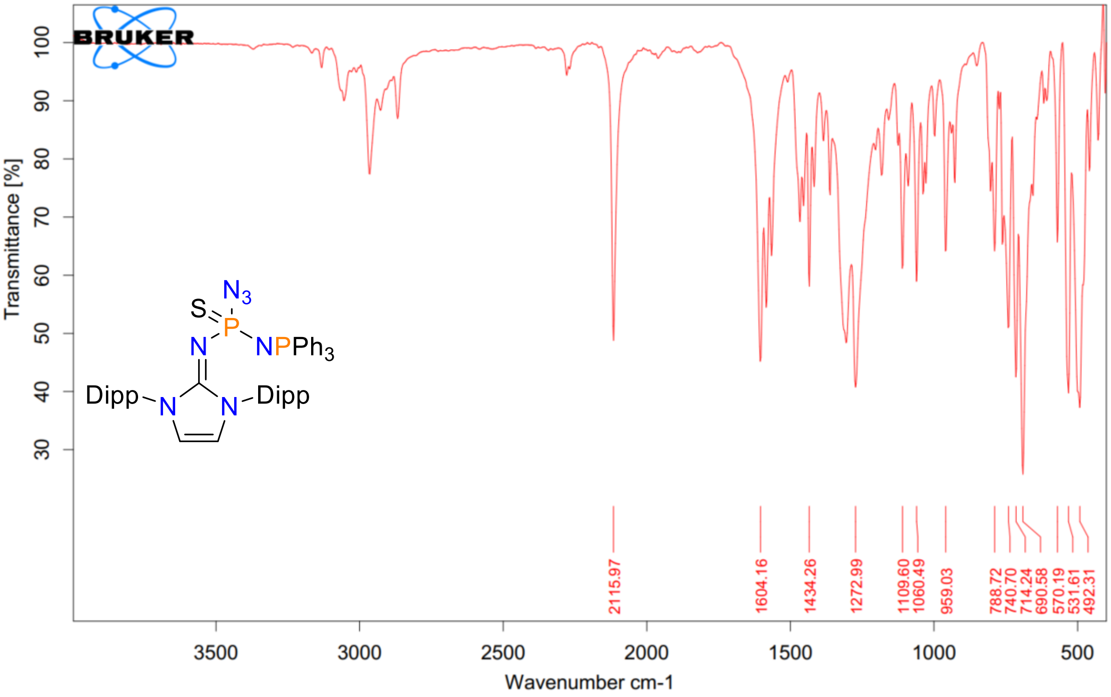

Appendix B-42. FT-IR spectrum of IPrNP(S)(N_3)($NPPh_3$) (**3.5_{Ph}**) (ATR mode).

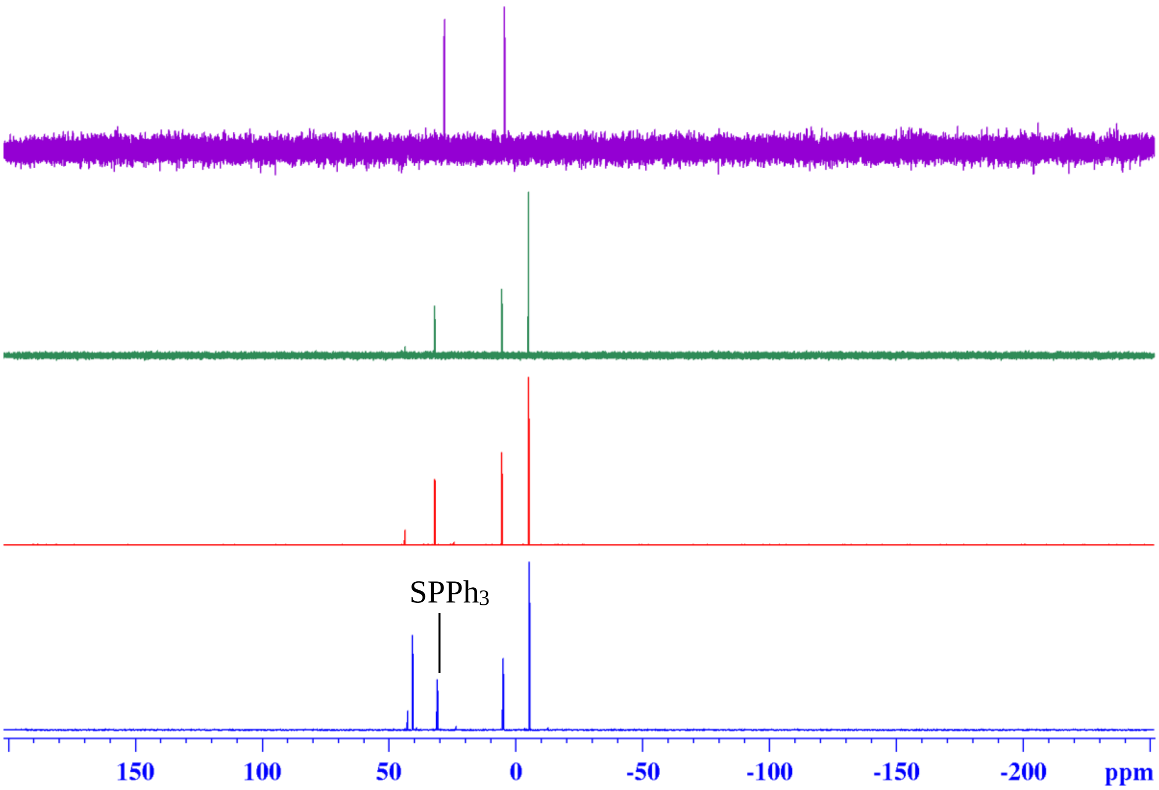

Appendix B-43. Stacked $^{31}P\{^1H\}$ NMR spectra of the reaction of **3.4S** (δ_P = 40.7) and PPh_3 (δ_P = -5.9). Blue: after four days at room temperature (1.05 eq PPh_3 used). Red: After an additional equivalent of PPh_3 added and two additional days at room temperature. Green: complete consumption after one week. Purple: PPh_3 and $SPPh_3$ removed after precipitation from Et_2O/pentane at -30 °C, and 3 x 0.5 mL pentane triturations.

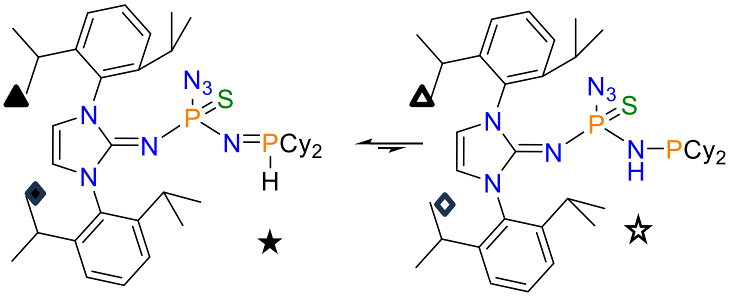

3.6a **3.6b**

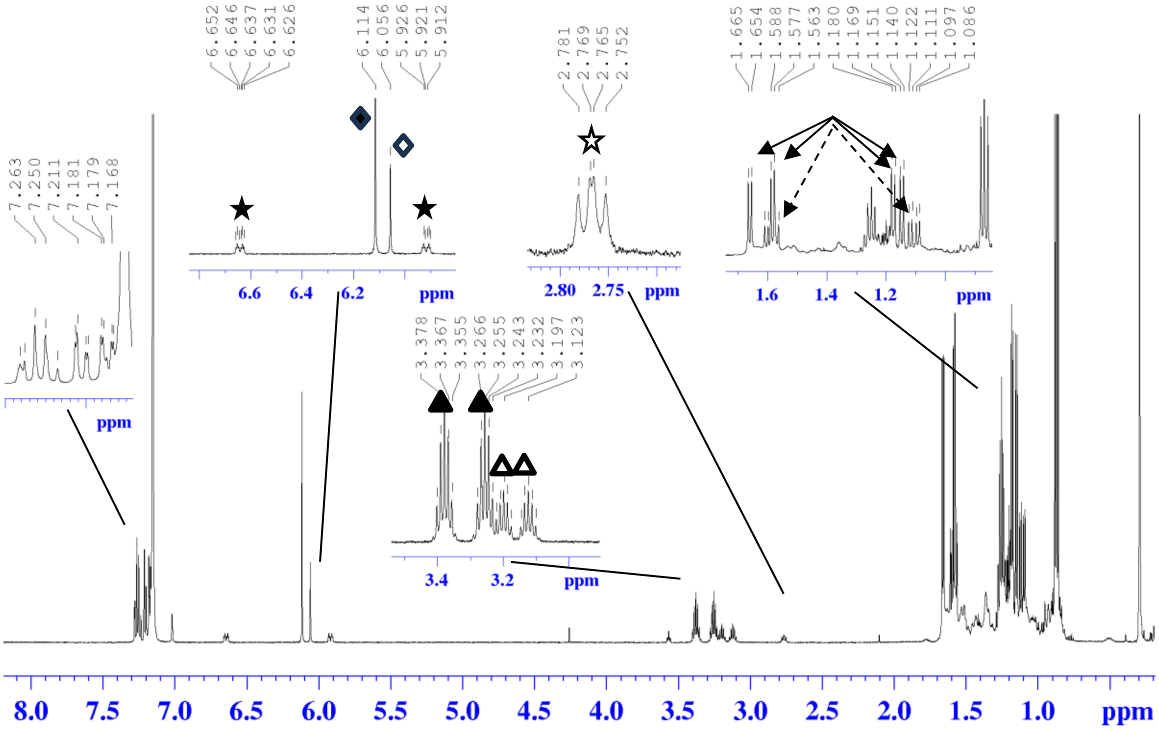

Appendix B-44. ^{1}H NMR spectrum of crystals of **3.6a**/**3.6b** dissolved in C_6D_6. Unambiguous assignment of aryl-, cyclohexyl-, and methyl- groups was not possible. Backbone, isopropyl, and P-H coupled protons have been explicitly labelled. Methyl groups have been assigned based on ^{1}H-^{1}H COSY. THF (*), pentane (‡), and silicone grease (†).

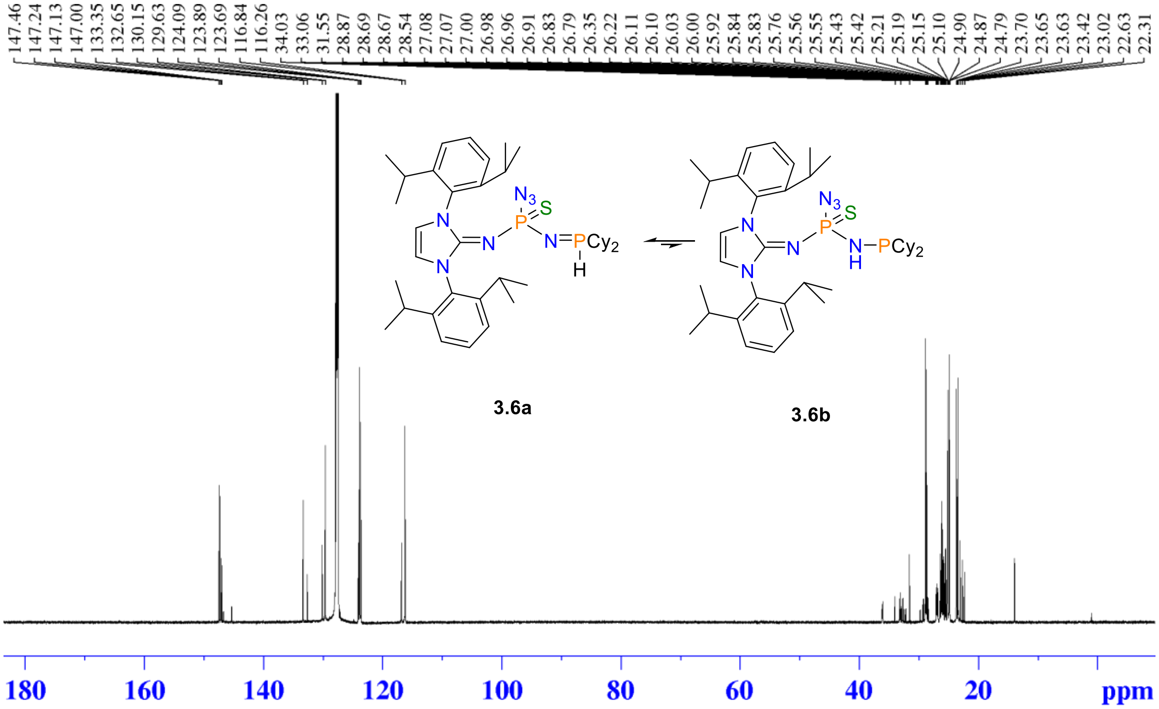

Appendix B-45. $^{13}C\{^1H\}$ NMR spectrum of **3.6a/3.6b** in C_6D_6 (full spectrum).

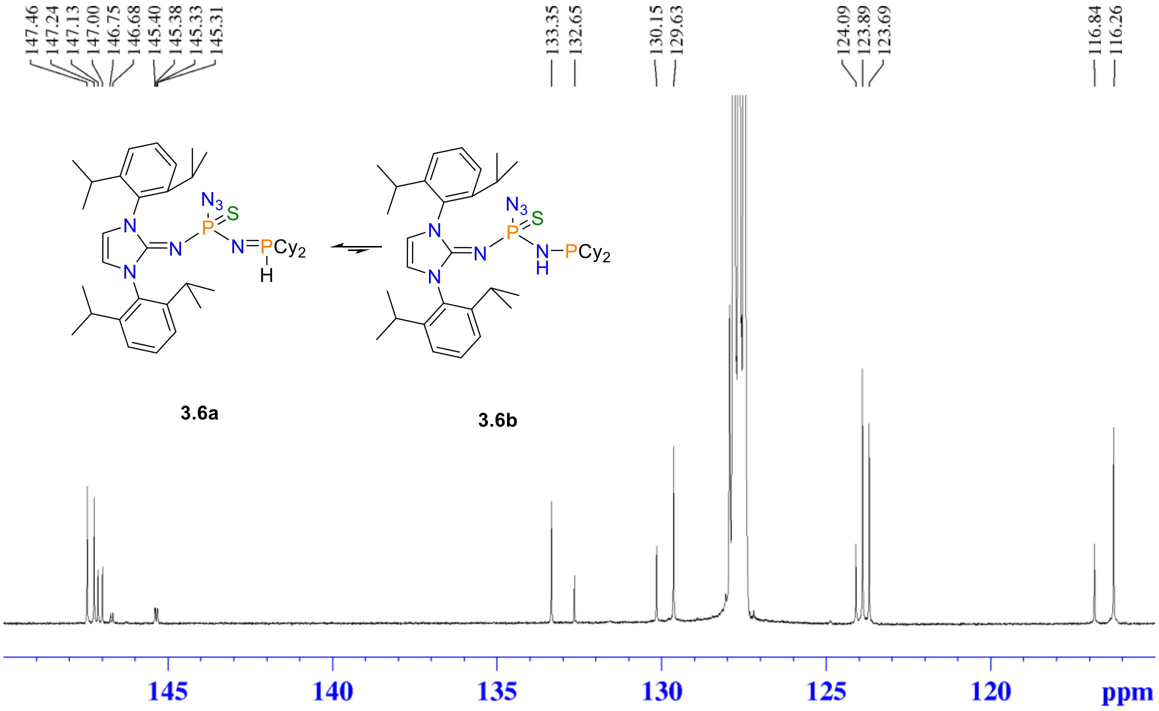

Appendix B-46. $^{13}C\{^1H\}$ NMR spectrum of **3.6a/3.6b** in C_6D_6 (zoomed in to 150 - 115 ppm).

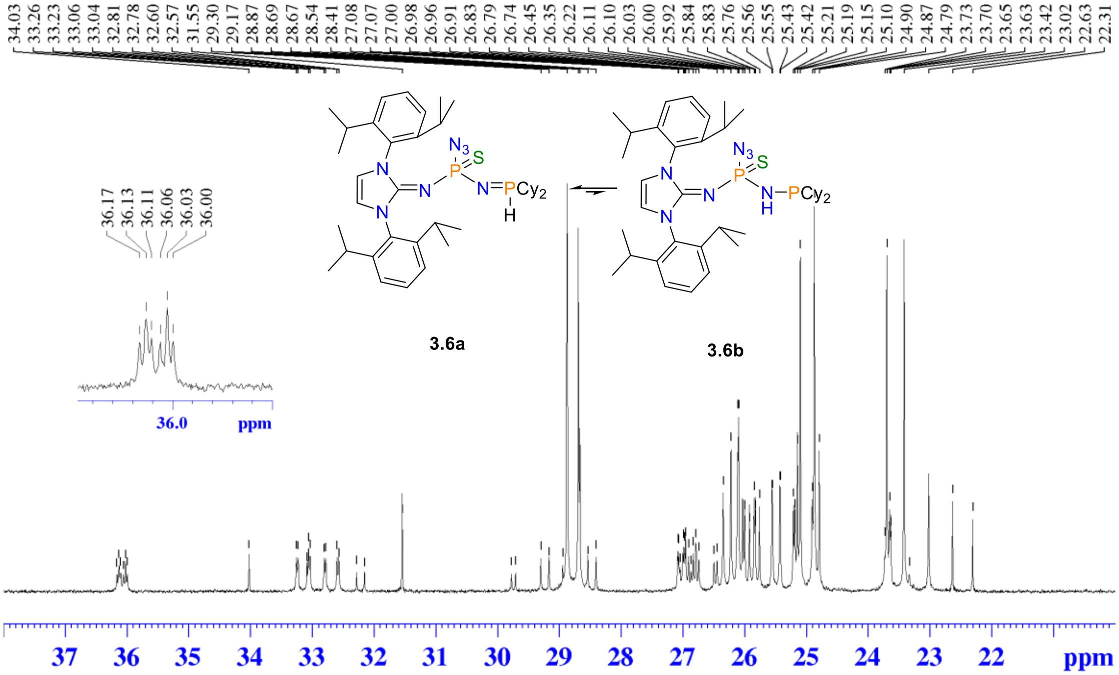

Appendix B-47. $^{13}C\{^1H\}$ NMR spectrum of **3.6a**/**3.6b** in C_6D_6 (zoomed into 38 – 22 ppm).

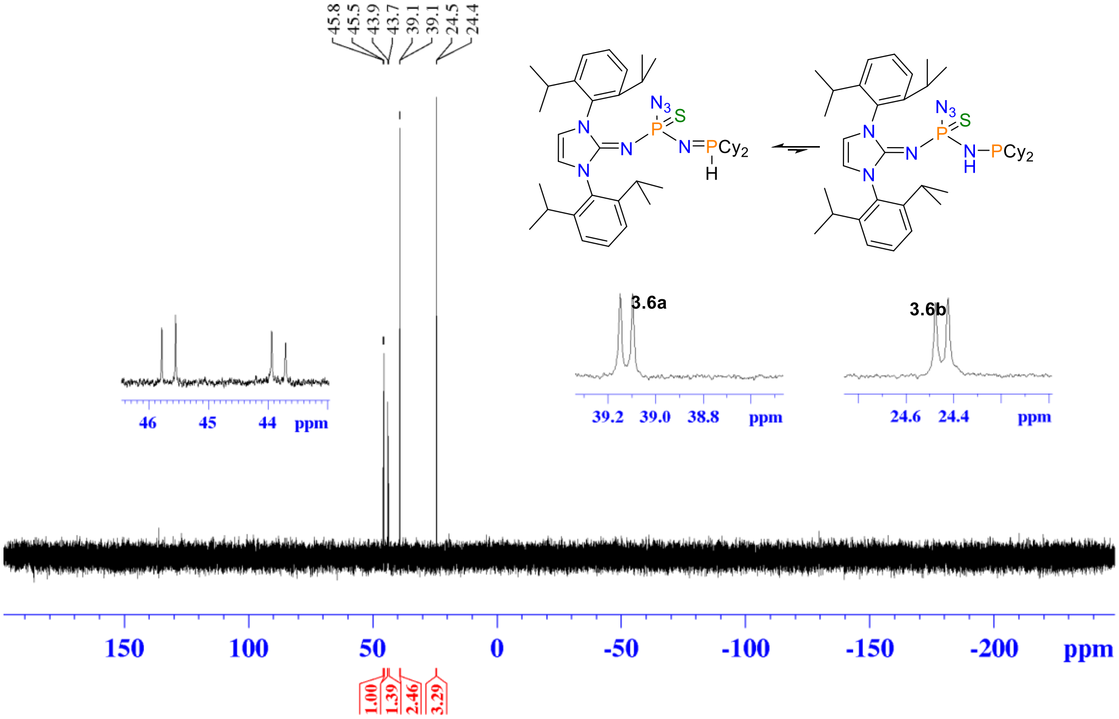

Appendix B-48. $^{31}P\{^{1}H\}$ NMR spectrum of crystals of **3.6a**/**3.6b** dissolved in C_6D_6. First delay time set to six seconds.

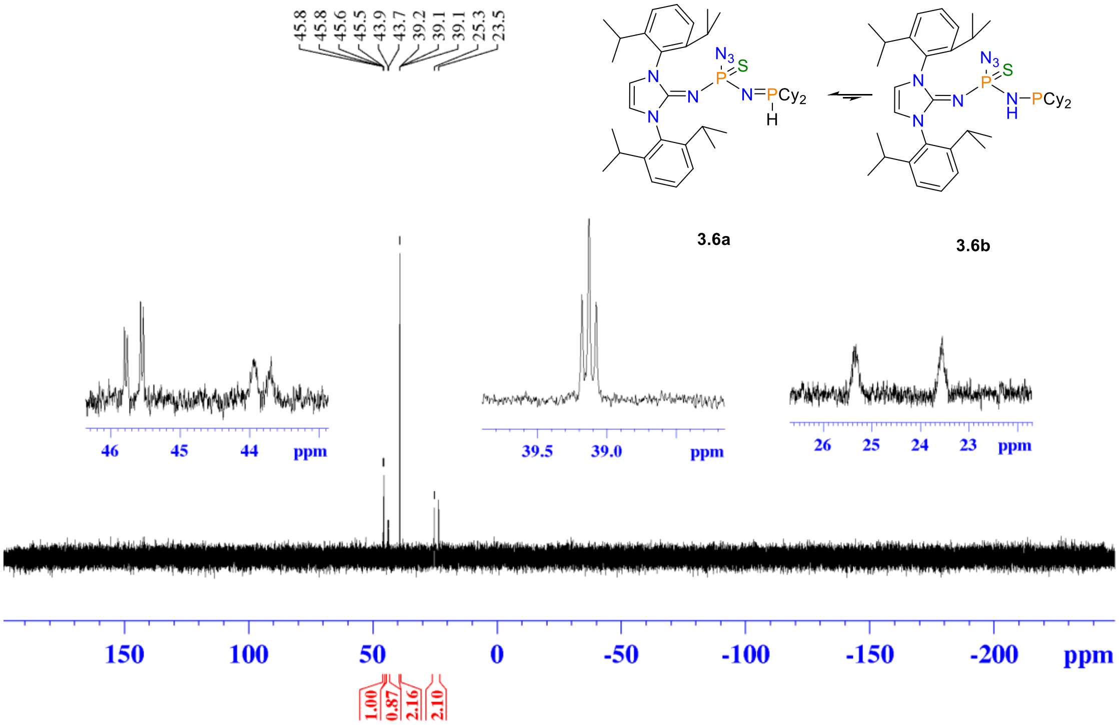

Appendix B-49. ^{31}P NMR spectrum of crystals of **3.6a**/**3.6b** dissolved in C_6D_6.

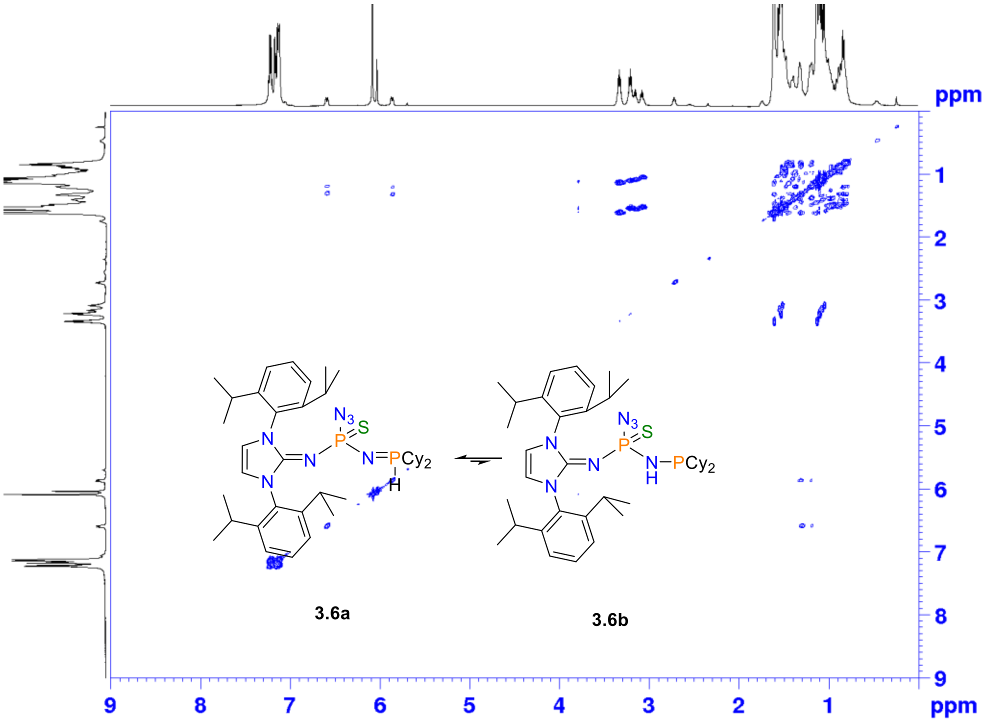

Appendix B-50. ^{1}H-^{1}H COSY NMR spectrum of **3.6a/3.6b** dissolved in C_6D_6.

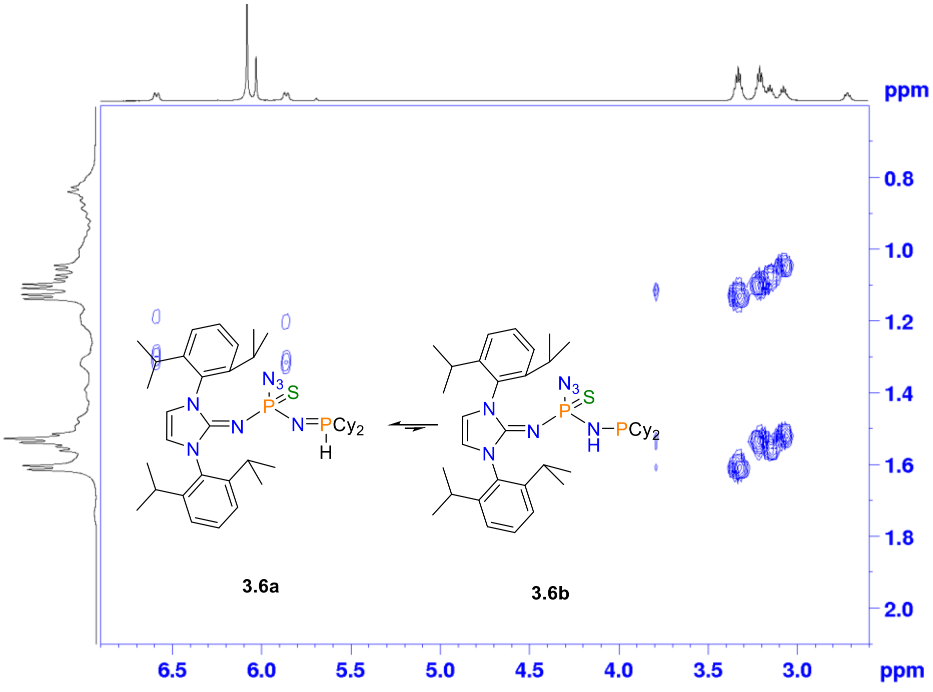

Appendix B-51. ^{1}H-^{1}H COSY NMR spectrum of **3.6a/3.6b** dissolved in C_6D_6 (zoomed in).

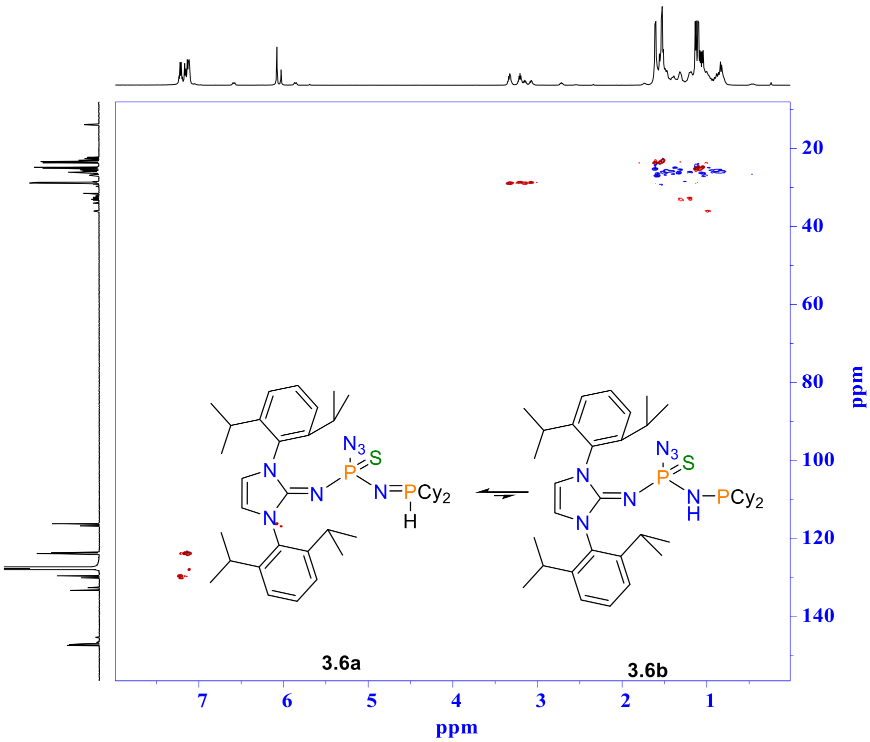

Appendix B-52. ^{1}H-^{13}C HSQC NMR spectrum of **3.6a**/**3.6b** dissolved in C_6D_6.

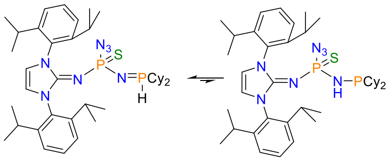
N3
S
P
N
N
N
N=PCy2
H
N-PCy2
H

3.6a

3.6b

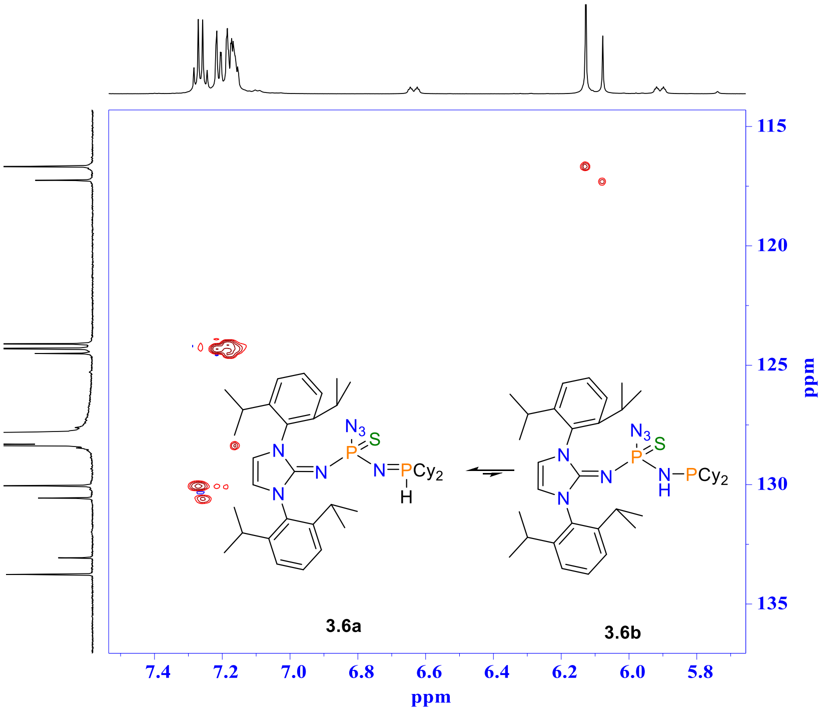

Appendix B-53. ^{1}H-^{13}C HSQC NMR spectrum of **3.6a**/**3.6b** dissolved in C_6D_6 (zoomed in).

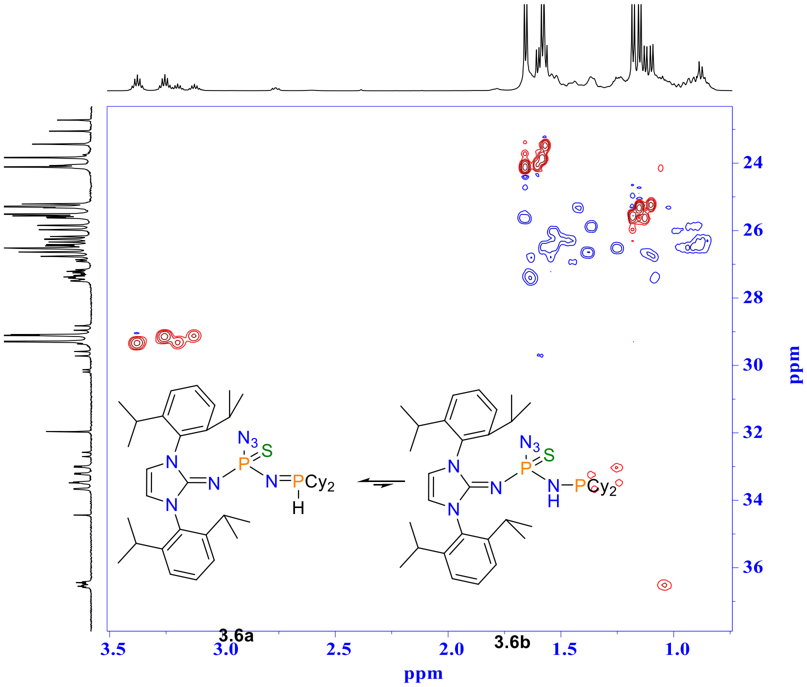

Appendix B-54. ^{1}H-^{13}C HSQC NMR spectrum of **3.6a**/**3.6b** dissolved in C_6D_6 (zoomed in).

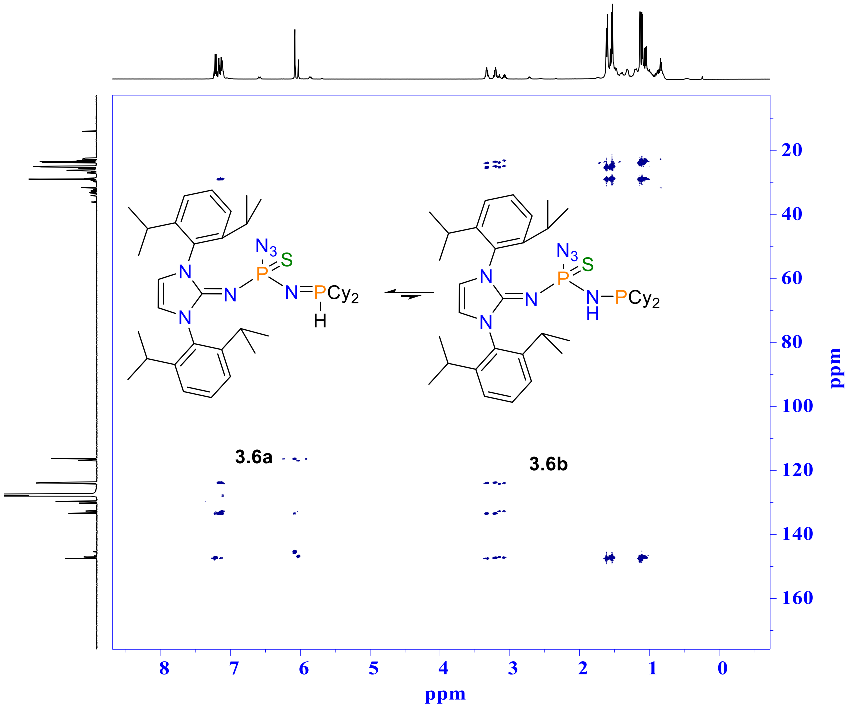

Appendix B-55. ^{1}H-^{13}C HMBC NMR spectrum of **3.6a**/**3.6b** dissolved in C_6D_6.

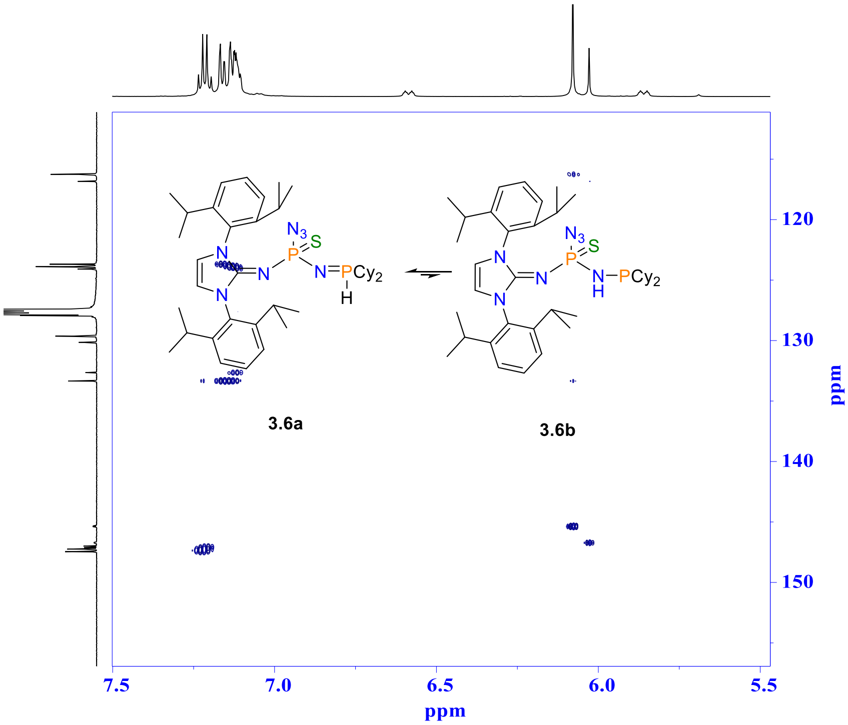

Appendix B-56. ^{1}H-^{13}C HMBC NMR spectrum of **3.6a/3.6b** dissolved in C_6D_6 (zoomed in).

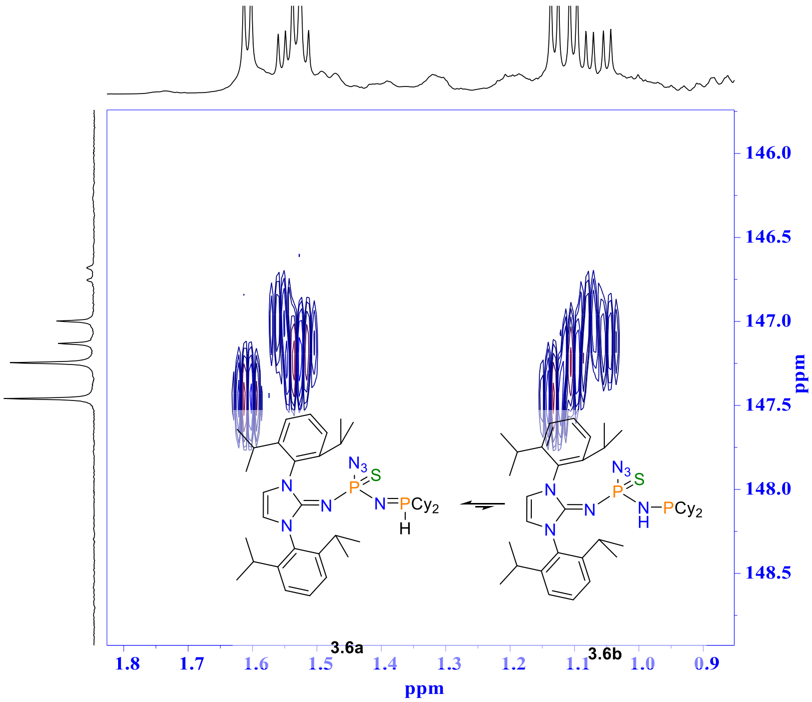

Appendix B-57. ^{1}H-^{13}C HMBC NMR spectrum of **3.6a/3.6b** dissolved in C_6D_6 (zoomed in).

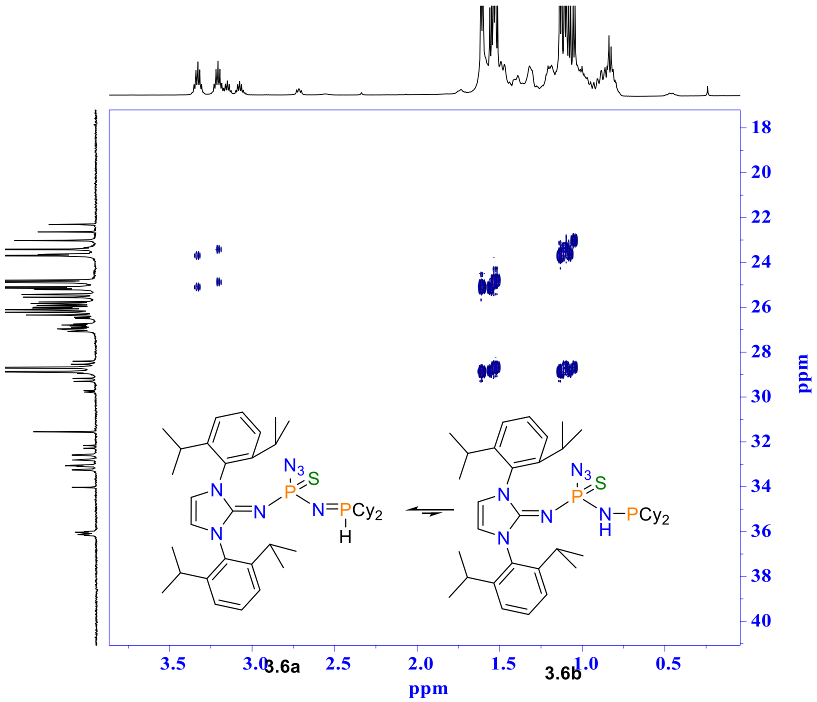

Appendix B-58. ^{1}H-^{13}C HMBC NMR spectrum of **3.6a/3.6b** dissolved in C_6D_6 (zoomed in).

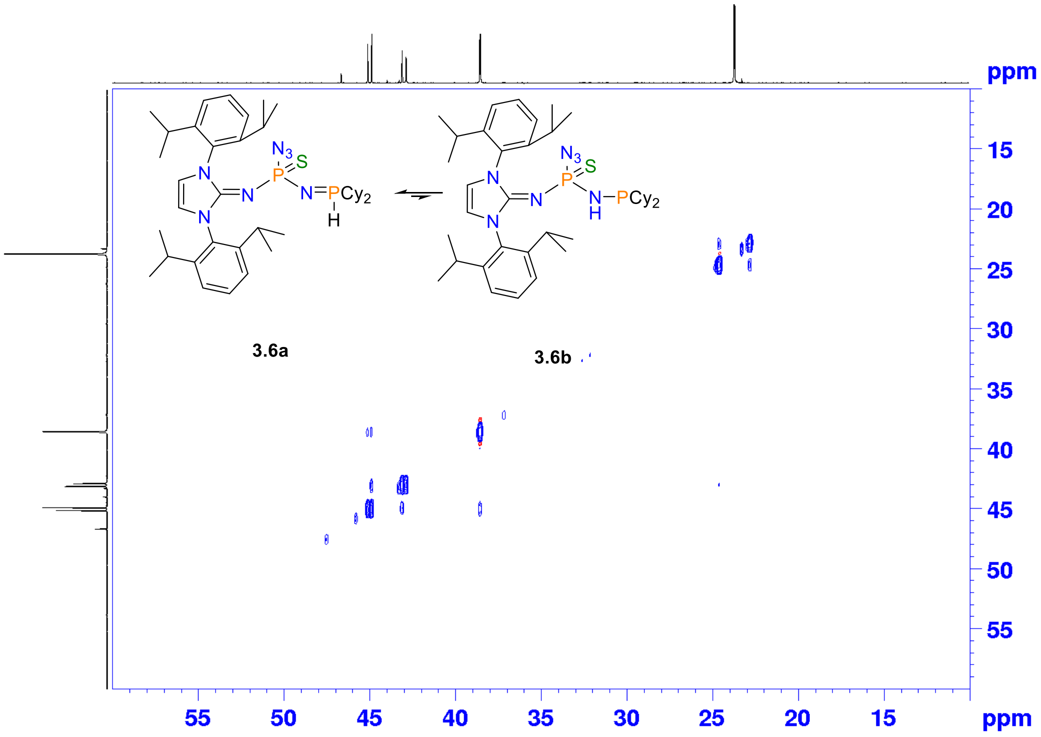

Appendix B-59. ^{31}P-^{31}P EXSY NMR spectrum of reaction mixture containing **3.6a**/**3.6b** and residual dicyclohexylphosphine.

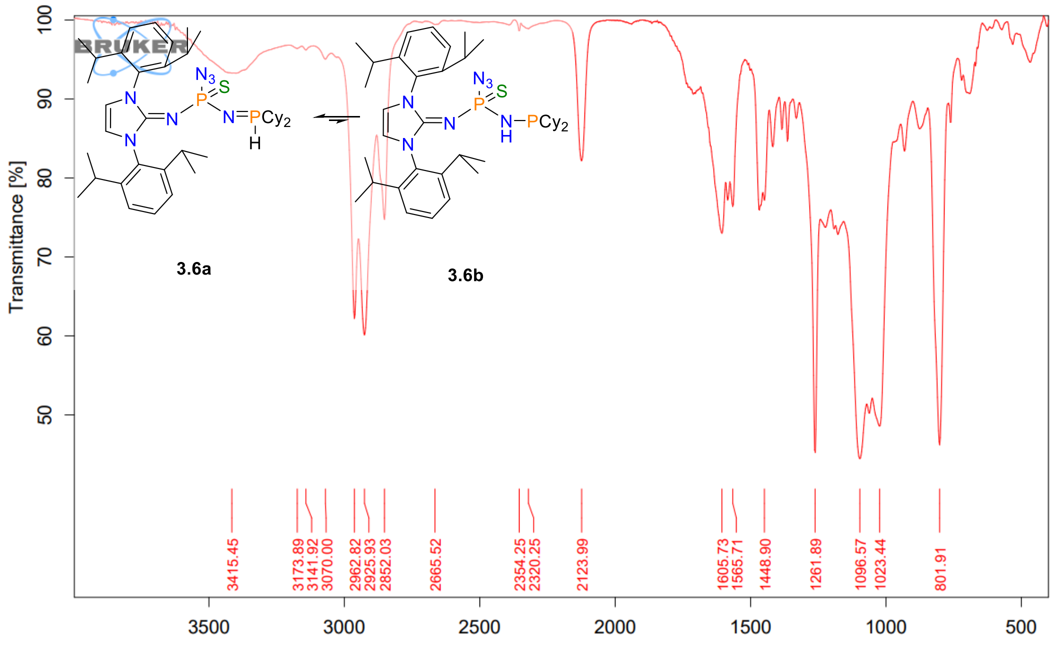

Appendix B-60. FT-IR spectrum of **3.6a**/**3.6b** (transmission mode).

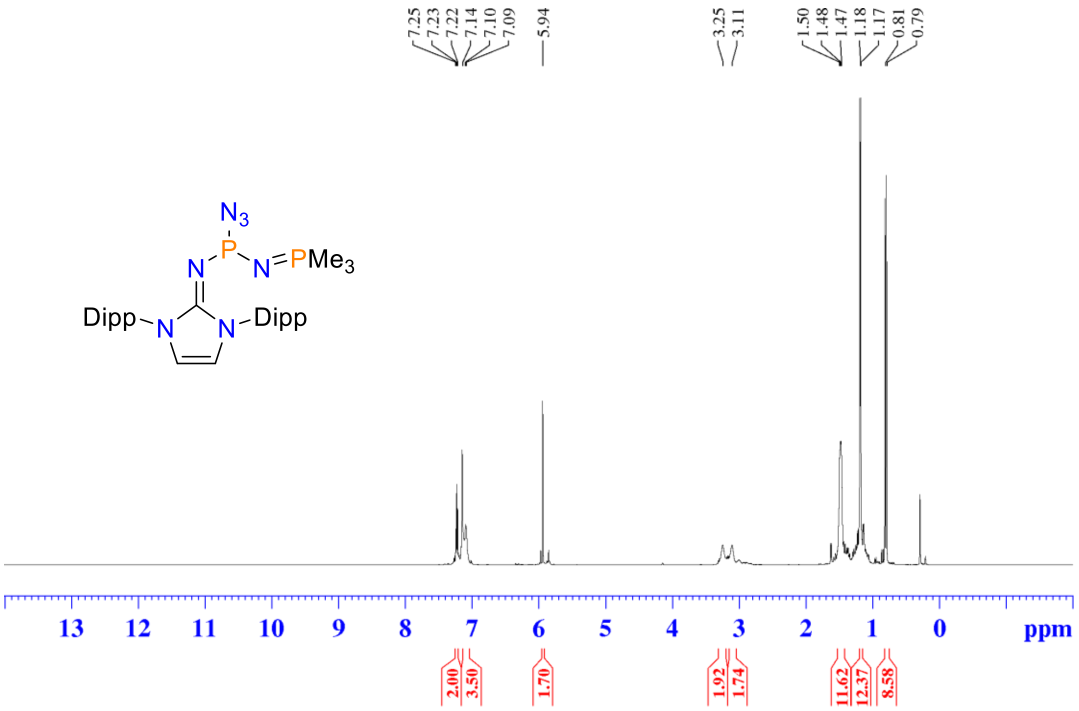

Appendix B-61. ^{1}H NMR spectrum of IPrNPN$_3$NPMe$_3$ (**3.7**) in C$_6$D$_6$.

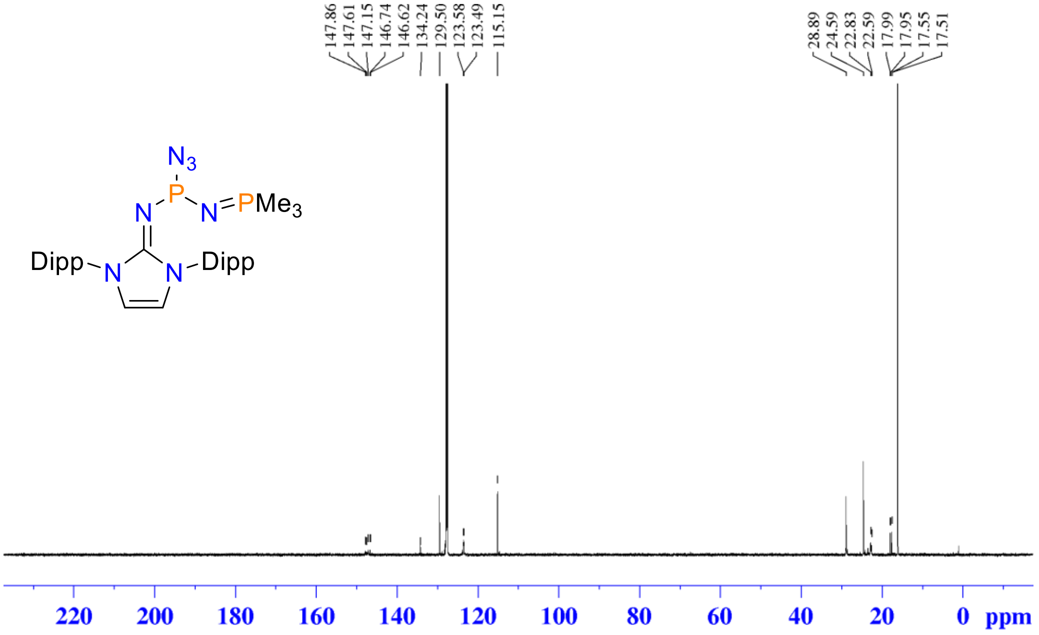

Appendix B-62. ^{13}C{^{1}H} NMR spectrum of IPrNPN$_3$NPMe$_3$ (**3.7**) in C$_6$D$_6$.

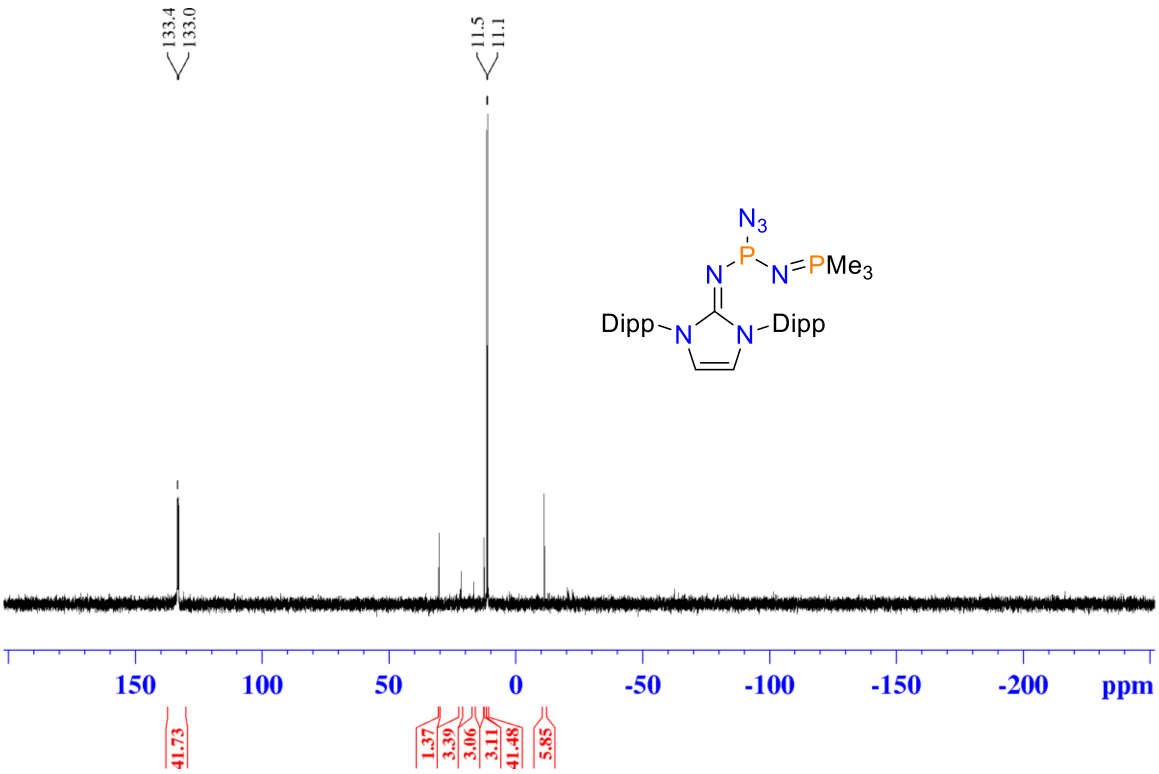

Appendix B-63. $^{31}P\{^1H\}$ NMR spectrum of IPrNPN$_3$NPMe$_3$ (**3.7**) in C_6D_6.

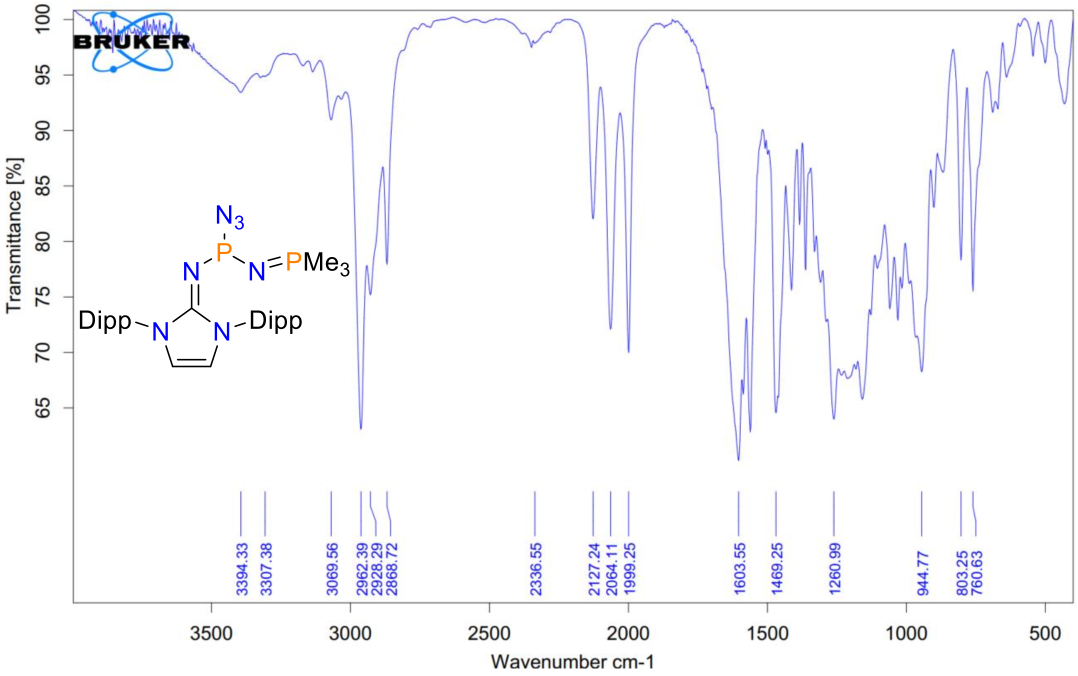

Appendix B-64. FT-IR spectrum of IPrNPN$_3$NPMe$_3$ (**3.7**) (transmission mode).

B2. Further Analysis of $IPrN_3NPMe_3$ (**3.7**)

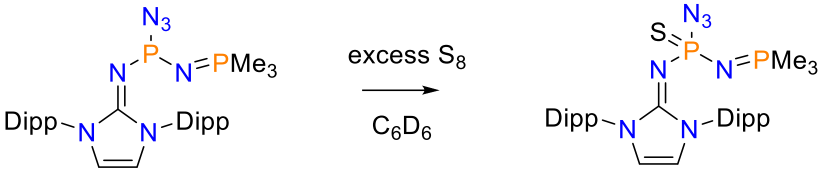

S_8 (12.0 mg, 0.0468 mmol) was weighed into a vial and was dissolved in one mL C_6D_6 then added to a vial containing minimally decomposed **3.7** (4.0 mg, 0.0071 mmol). This solution was transferred into an NMR tube and analyzed by ^1H and $^{31}P\{^1H\}$ NMR spectroscopy within 10 min of mixing.

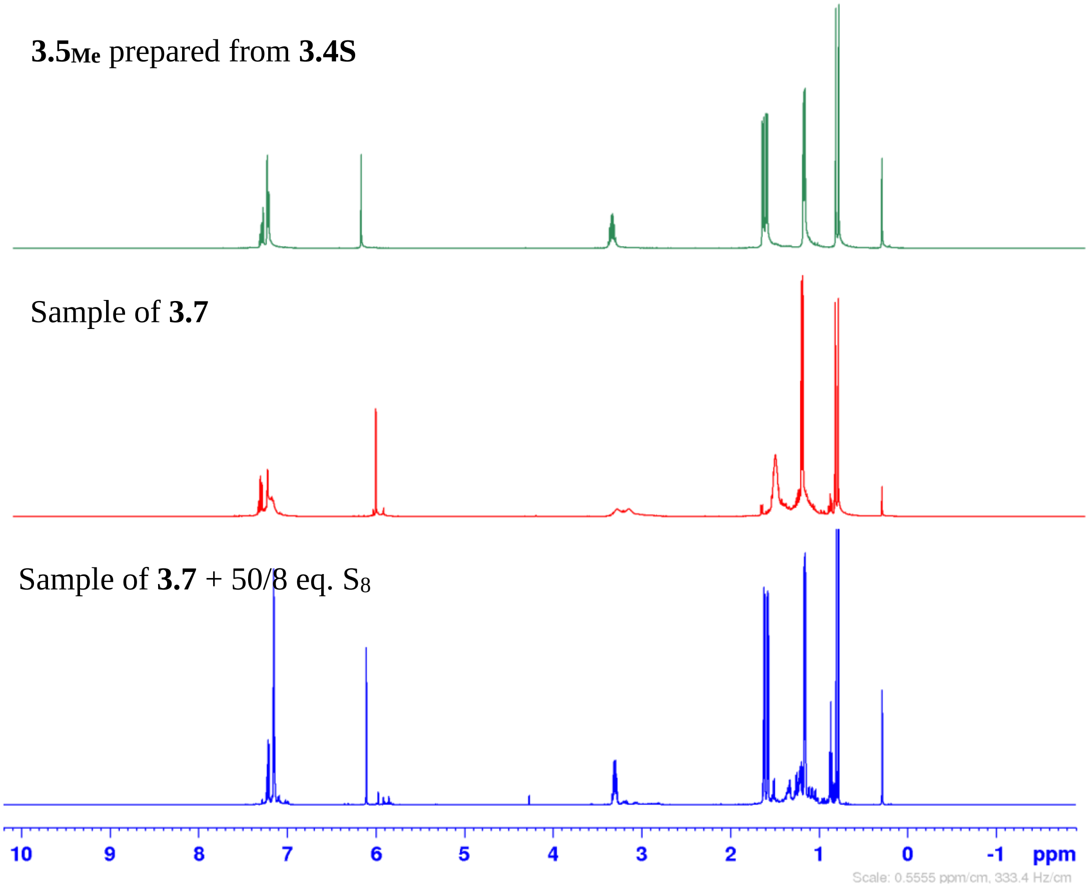

Appendix B-65. Stacked ^1H NMR spectra of **3.4S**, **3.7**, and the reaction of **3.7** with excess S_8.

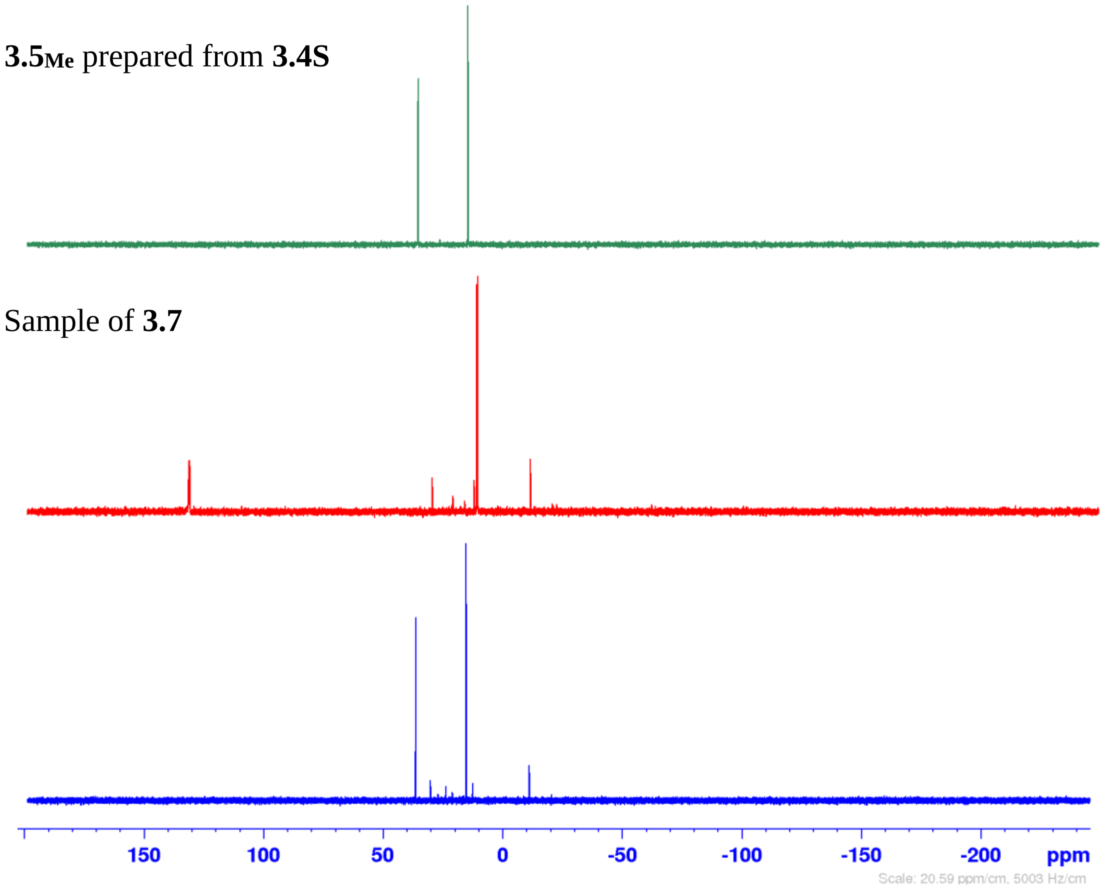

Appendix B-66. Stacked $^{31}P\{^{1}H\}$ NMR spectra of **3.4S**, **3.7**, and a reaction of **3.7** with excess S_8.

Appendix B-67. Table of comparisons of low error ions measured by high-resolution mass spectrometry of **3.5**$_{\mathbf{Me}}$ produced by different methods.

Ion	Expected mass-to-charge ratio (m/z)	Found mass-to-charge ratio (m/z)	
		3.4S + PMe_3	**3.7** + S_8
[3.5]$^{\cdot +}$	597.2927	-	597.2920
[3.5$_{Me}$+H]$^{+}$	598.3005	598.3006	598.2987
[3.5$_{Me}$·Na]$^{+}$	620.2825	620.2837	620.2802
[3.5$_{Me}$·K]$^{+}$	636.2564	636.2580	636.2560
[(3.5$_{Me}$)$_2$+H]$^{+}$	1195.5938	1195.5980	-
[(3.5$_{Me}$)$_2$·Na]$^{+}$	1217.5757	1217.5787	1217.5765
[(3.5$_{Me}$)$_2$·K]$^{+}$	1233.5496	1233.5496	-

B3. Decomposition of **3.7**

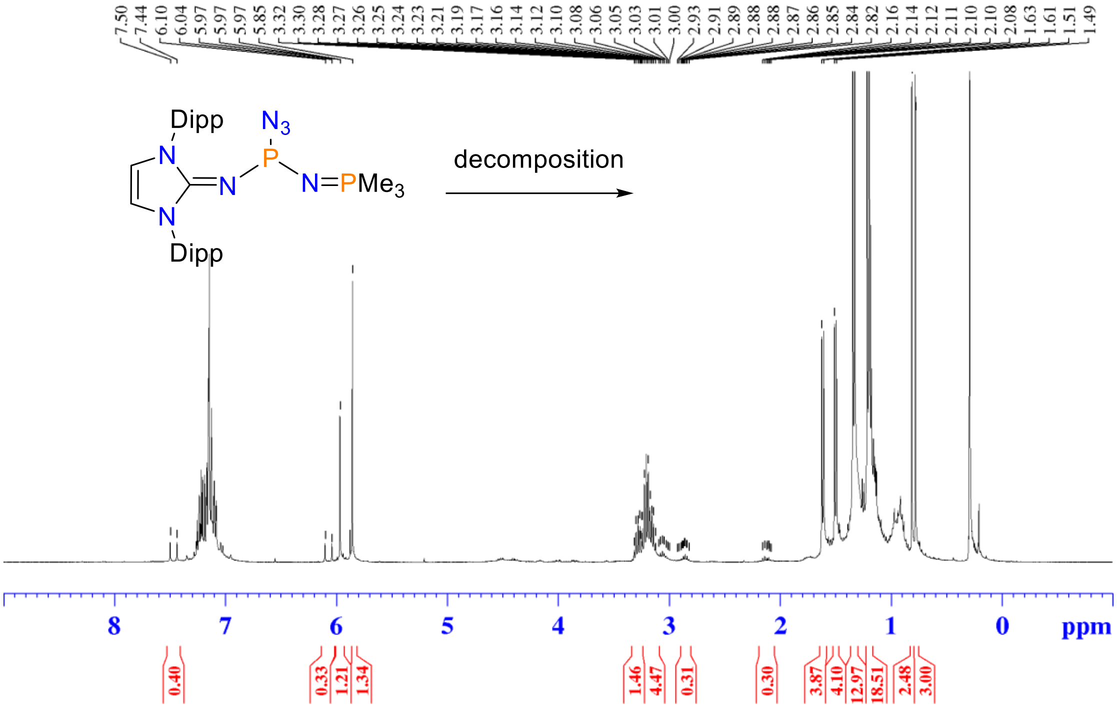

Appendix B-68. ^{1}H NMR spectrum of isolated decomposition product in C_6D_6.

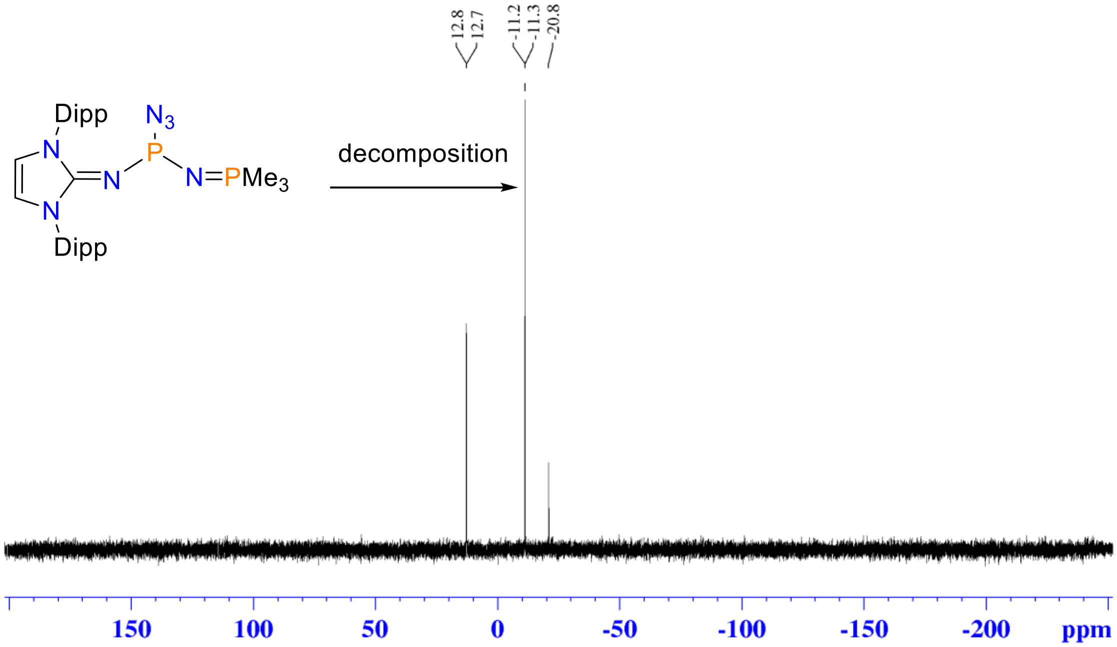

Appendix B-69. ^{1}H NMR spectrum of isolated decomposition product in C_6D_6.

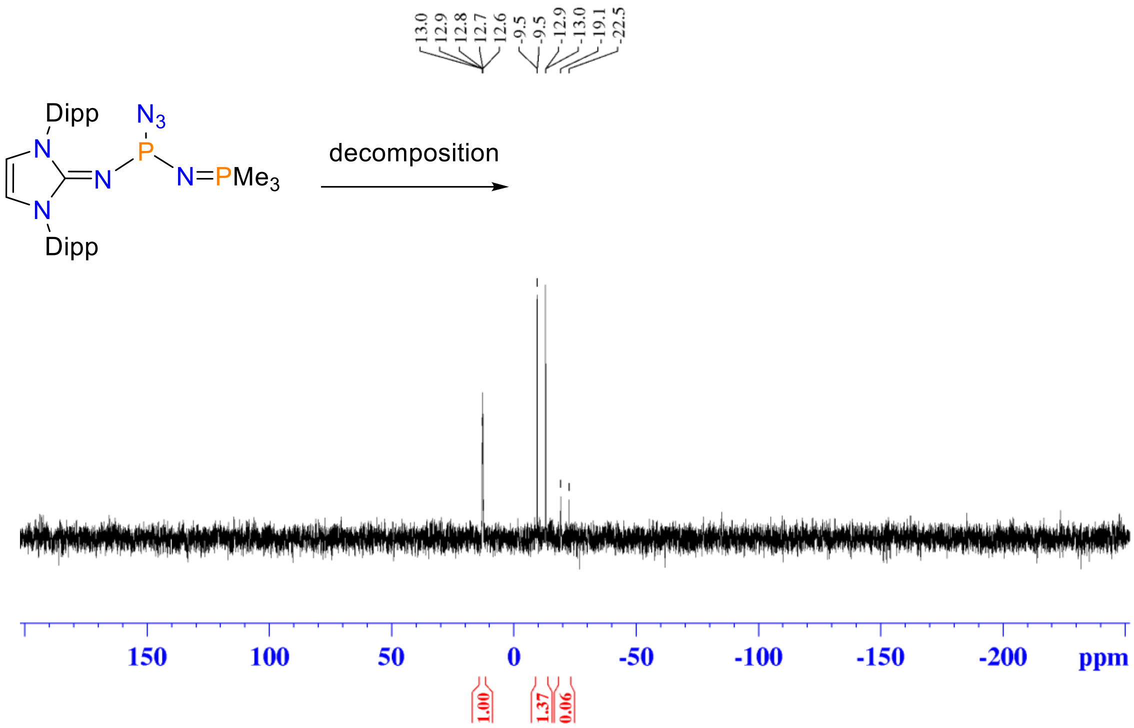

Appendix B-70. ^{31}P NMR spectrum of decomposition product in C_6D_6.

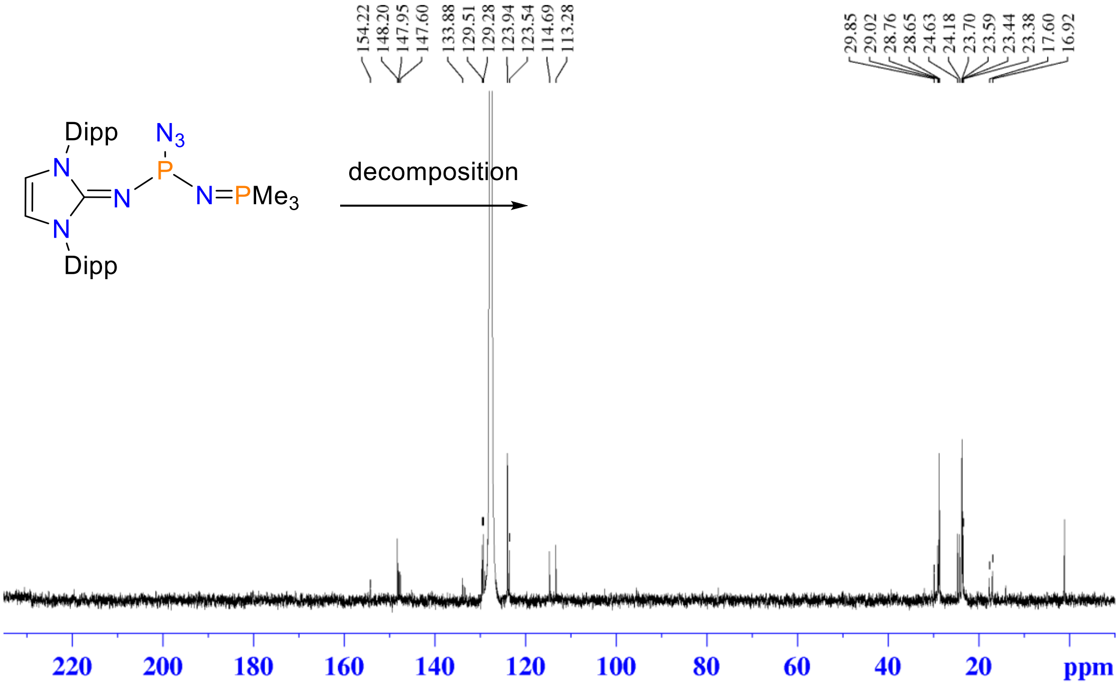

Appendix B-71. ^{13}C{^{1}H} NMR spectrum of decomposition product in C_6D_6.

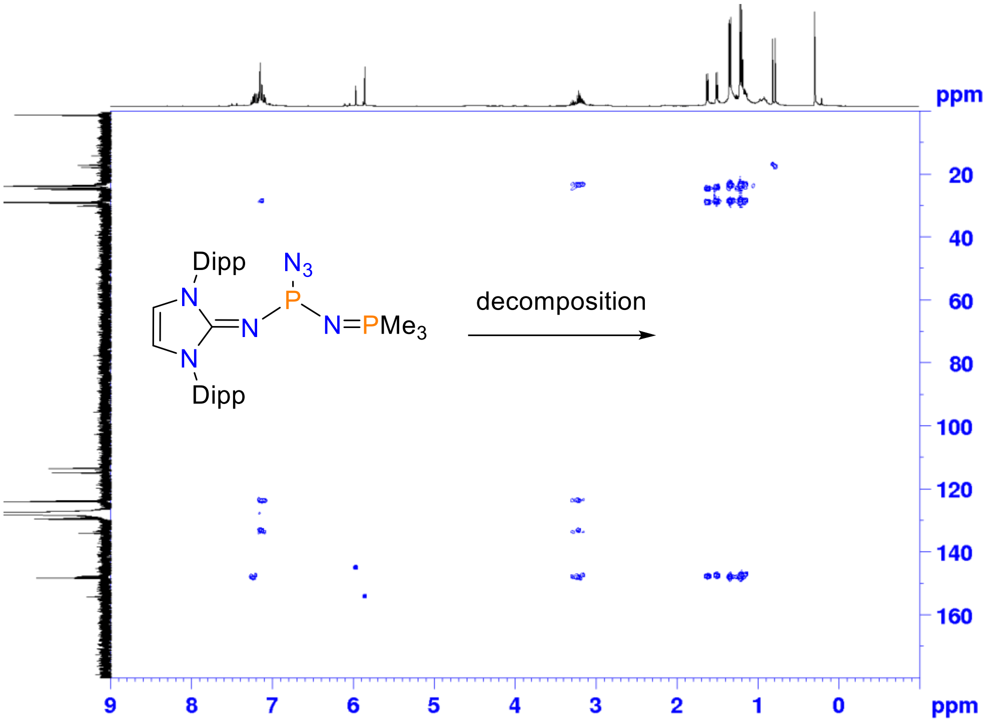

Appendix B-72. ^{1}H-^{13}C HMBC NMR spectrum spectrum of decomposition product in C_6D_6.

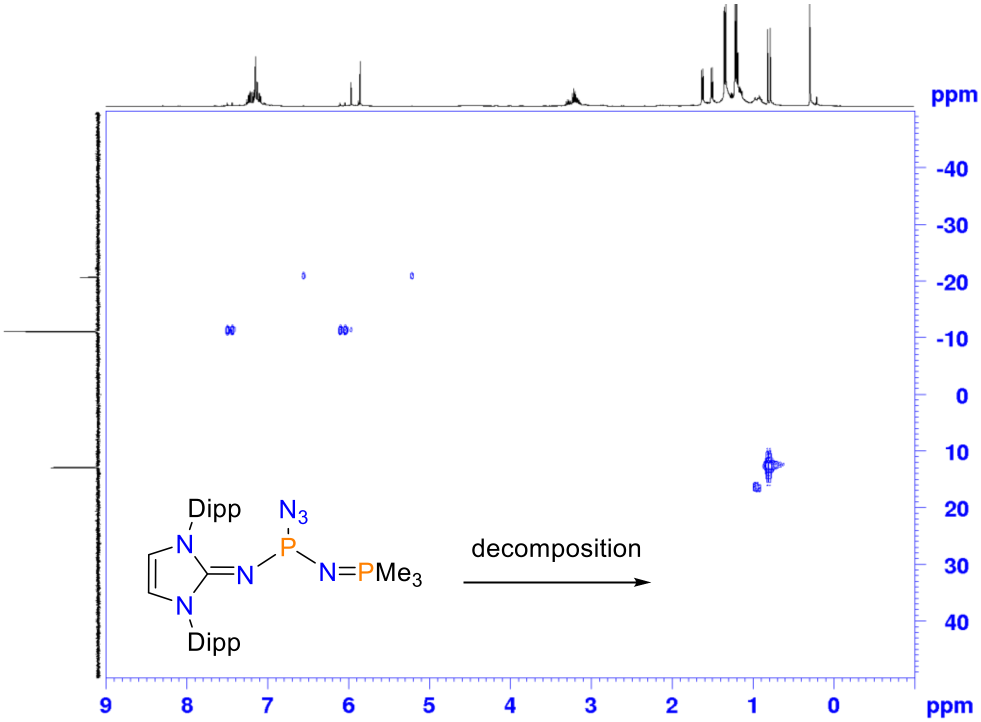

Appendix B-73. ^{1}H-^{31}P HMBC NMR spectrum of decomposition product.

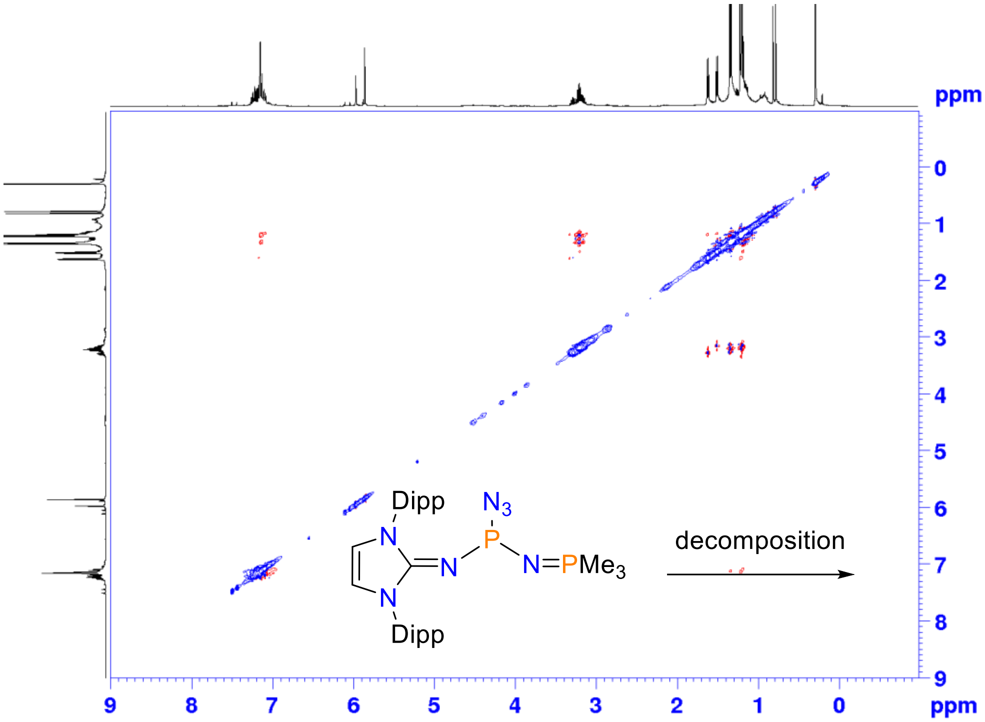

Appendix B-74. ^1H-^1H NOESY NMR spectrum of decomposition product in C_6D_6.

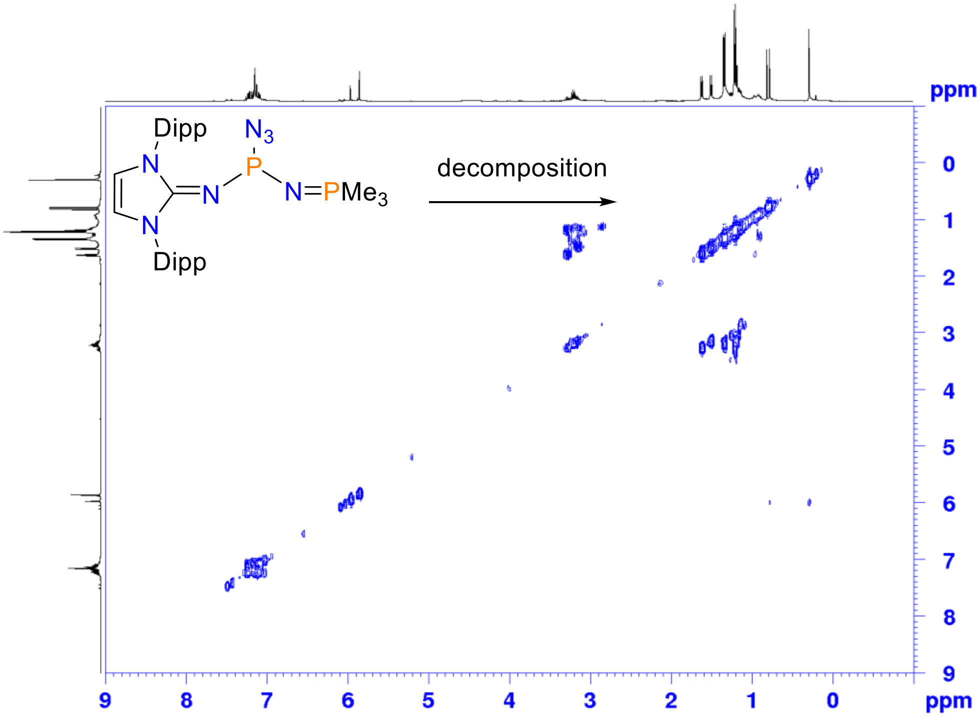

Appendix B-75. ^1H-^1H COSY NMR spectrum of decomposition product in C_6D_6.

B4. Computational Details

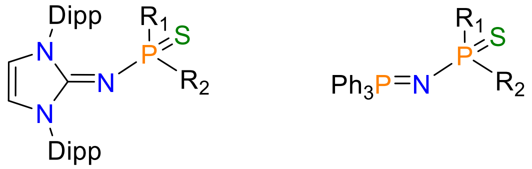

$R_1 = R_2 = N_3$; **I**
$R_1 = N_3$, $R_2 = NPMe_3$; **II**
$R_1 = R_2 = NPMe_3$; **III**

$R_1 = N_3$, $R_2 = NPPh_3$; **IV**

Appendix B-76. Structures investigated by DFT.

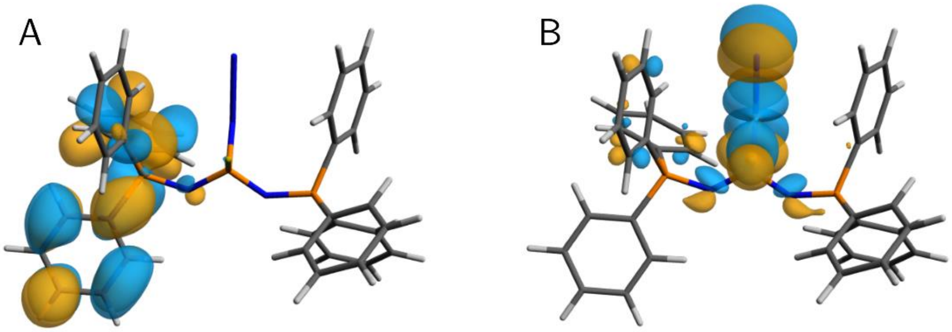

Appendix B-77. Visualized Kohn-Sham orbitals of **IV** corresponding to LUMO (A) and LUMO+12 (B). Yellow colour illustrates negative phase and blue illustrates positive phase of orbitals.

To test the hypothesis that the determining factor of the unavailability of an azide for further reaction was the LUMO level of the N_3 π* system, additional simulations of previously reported[21] species $SP(N_3)(NPPh_3)_2$ **(IV)** with an azide resilient from further Staudinger reactions were undertaken. This character was not seen in the LUMO (A, -1.268 eV) and did not appear until LUMO+12 (B, 0.081 eV) (**Appendix B-77**). This is in agreement with the results for the monoazide studied here.

Appendix B-78. Summary of calculated atomic charges for structures **I**, **II**, and **III** investigated by DFT.

	Hirshfield charges (e)			Mulliken charges (e)			Löwdin charges (e)			Becke dipole corrected charges (e^-)		
Atom	**I**	**II**	**III**	**I**	**II**	**III**	**I**	**II**	**III**	**I**	**II**	**III**
N γ	-0.1669	-0.1741	-	-0.3901	-0.4204	-	-0.1435	-0.1629	-	-0.5456	-0.9483	-
N β	0.17869	0.16149	-	0.39907	0.37806	-	0.06362	0.04325	-	0.88901	1.35945	-
N α	-0.0882	-0.1258	-	-0.1866	-0.2137	-	0.00057	-0.0344	-	-0.48	-0.726	-
P	0.3438	0.33791	0.34205	0.60883	0.62632	0.75512	0.10531	0.09111	0.07722	0.61314	0.70386	0.86003
S	-0.2948	-0.3304	-0.3882	-0.4063	-0.4873	-0.6243	-0.0743	-0.1125	-0.2368	-0.6087	-0.6754	-0.8683

B5. X-ray Crystallographic Data

B5.1 Compound **3.2**

The unit cell dimensions were determined from a symmetry constrained fit of 9919 reflections with 4.6° < 2θ < 62.7°. The N–P(N_3)$_2$ group was disordered about the crystallographic 2-fold axis.

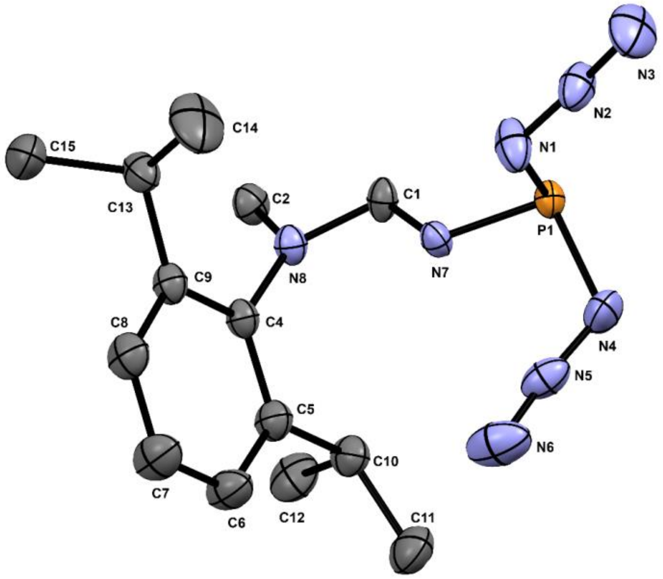
N3
N2
C14
N1
C15
C13
C2
C1
P1
N8
N7
C9
C8
C4
N4
N5
C5
C10
N6
C7
C6
C12
C11

Appendix B-79. ORTEP drawing of **3.2** asymmetric unit showing naming and numbering scheme. Ellipsoids are at the 50% probability level and hydrogen atoms were omitted for clarity.

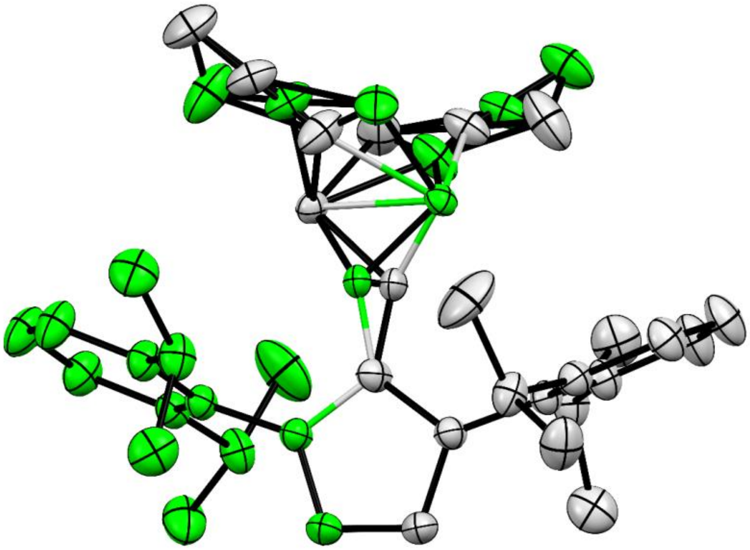

Appendix B-80. Mercury-rendered ORTEP style drawing of **3.2** coloured by symmetry operation. Ellipsoids are at the 50% probability level and hydrogen atoms were omitted for clarity.

B5.2 Compound **3.4S**

NOTE: It was apparent from the initial indexing that the sample crystal was comprised of at least two different lattices. Both lattices were indexed. However, this was not a case of non-merohedric twinning because the lattice parameters were significantly different and could not be reduced to a common set of basis vectors. The second phase could not be adequately refined, and in this report only the structural results of the predominant phase are reported. Some metrical relationships between the two phases co-grown phases (*vide infra*) are reported in **Appendix B-81**.

Data Collection and Processing. The unit cell dimensions were determined from a symmetry constrained fit of 9934 reflections with 4.8° < 2θ < 52.26°.

Analysis of co-grown Phases. The unit cell parameters for the co-grown phases are reported in the table below.

Appendix B-81. Summary of Unit Cell parameters of Predominant and Minor Phases of **3.4S**

Phase	**a** (Å)	**b** (Å)	**c** (Å)	**α** (º)	**β** (º)	**γ** (º)	**Vol.** (Å^3)
Predominant	9.016(5)	9.366(4)	21.187(9)	92.568(10)	99.542(7)	114.087(18)	1598.1(13)
Minor	8.991(5)	9.344(5)	19.526(10)	80.795(16)	86.307(13)	65.964(18)	1478.89

Scaling estimated the ratio of the predominant phase to the minor phase was 0.984/0.016. For the structure analyses, the intensity data for the two phases were integrated and scaled separately.

Structure Solution and Refinement. The structure contained a highly disordered n-pentane molecule which could not be adequately modelled. Therefore, the data were subjected to the SQUEEZE procedure as implemented in PLATON.[71]

B5.3 Compound **3.4Se**

The unit cell dimensions were determined from a symmetry constrained fit of 9917 reflections with 4.8° < 2θ < 57.14°.

Structure Solution and Refinement. The structure contained a highly disordered n-pentane molecule which could not be adequately modelled. Therefore, the data were subjected to the SQUEEZE procedure as implemented in PLATON.[71]

B5.4 Compound **3.5$_{Cy}$**

The unit cell dimensions were determined from a symmetry constrained fit of 9829 reflections with 4.82° < 2θ < 63.94°.

Appendix C. Supplementary Information for Chapter 4

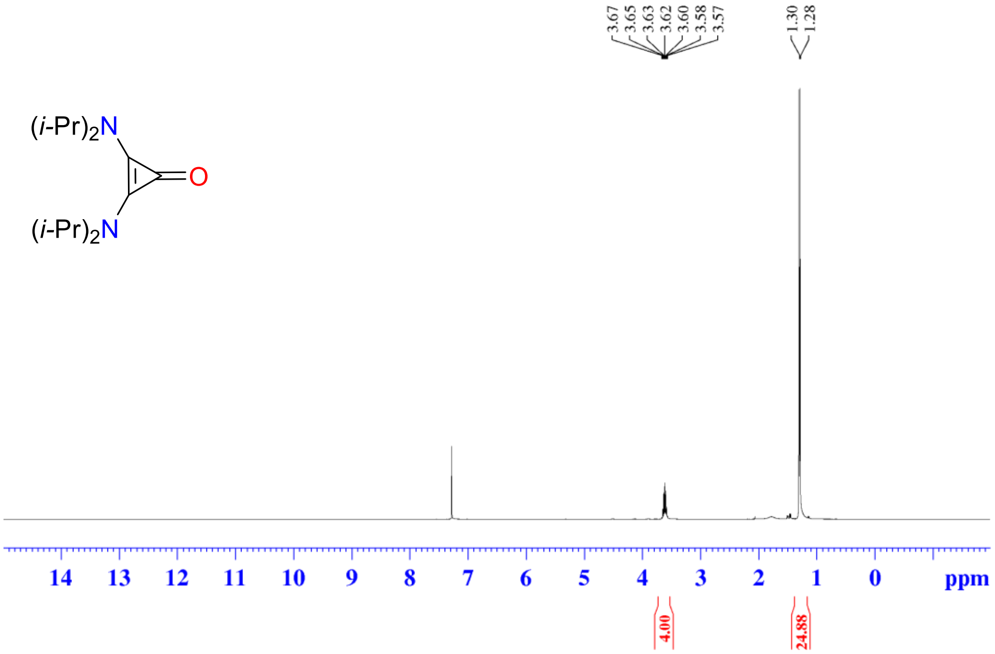

Appendix C-1. ^{1}H NMR spectrum of ***C_3O*** in $CDCl_3$.

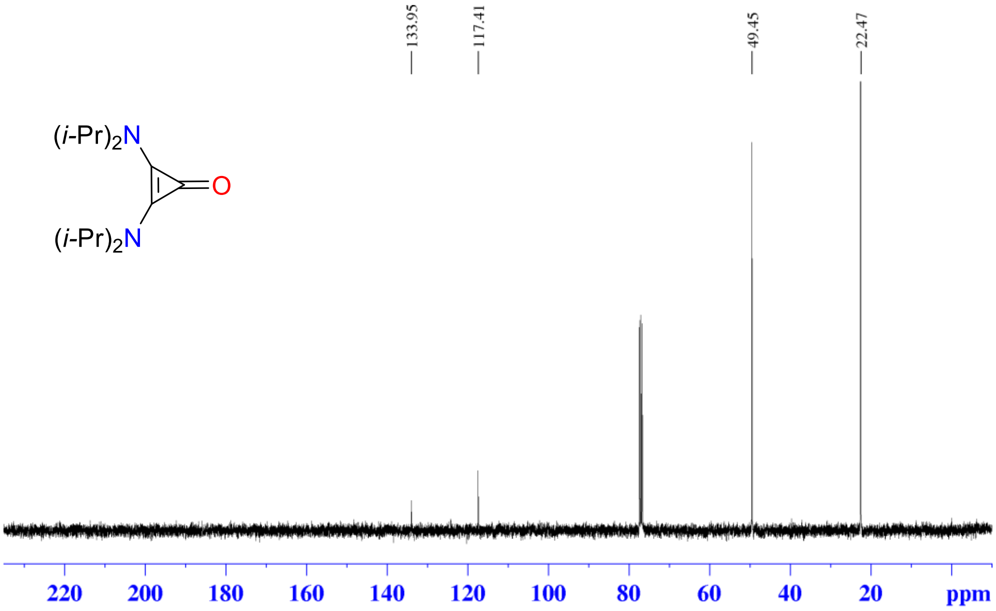

Appendix C-2. ^{13}C{^{1}H} NMR spectrum of ***C_3O*** in $CDCl_3$.

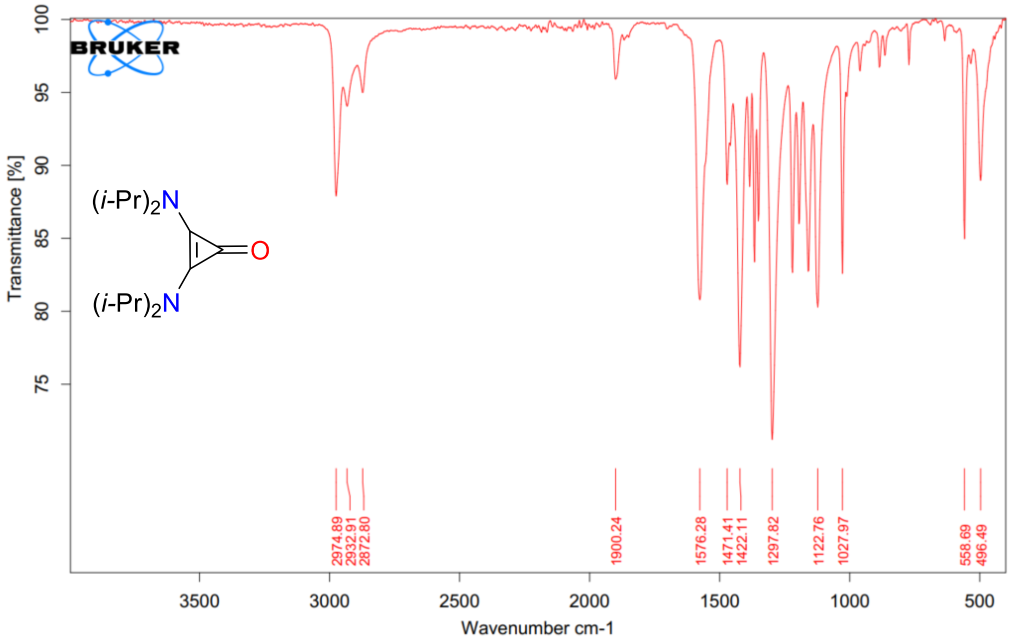

Appendix C-3. FT-IR spectrum of ***C_3O*** [ATR-mode].

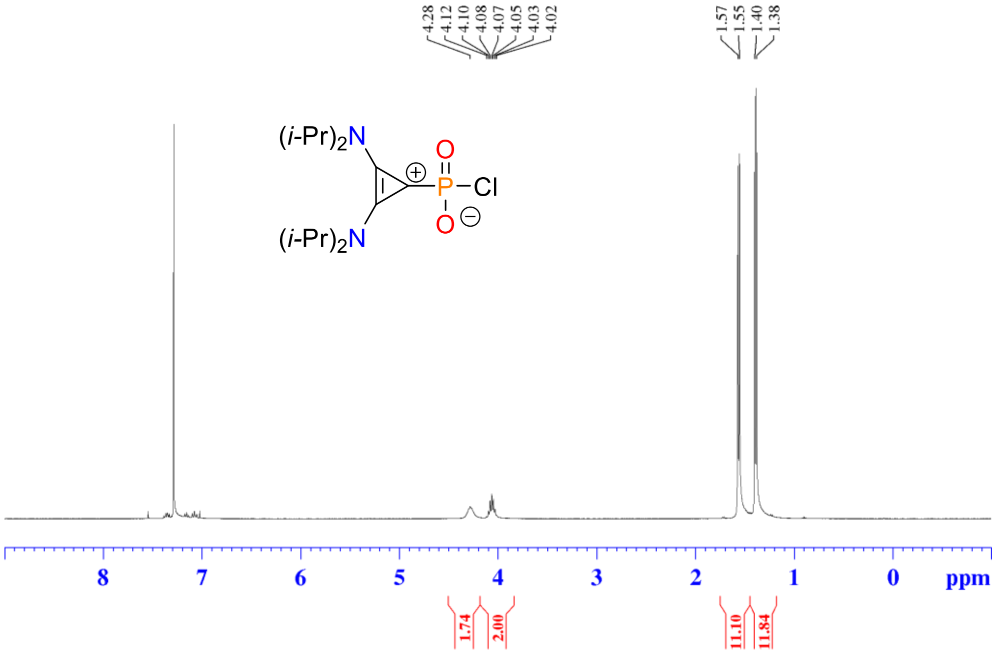

Appendix C-4. ^{1}H NMR ($CDCl_3$) spectrum of crystals of **4.3$_{\mathbf{BAC}}$** isolated by Pasteur separation.

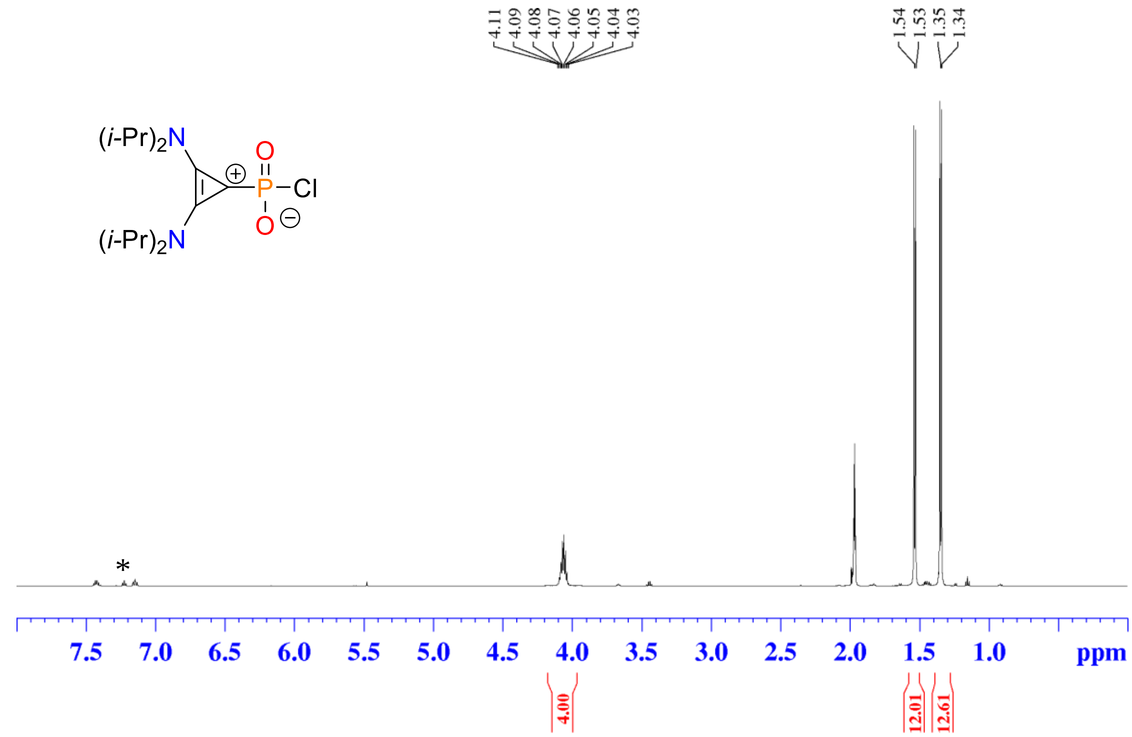

Appendix C-5. ^{1}H NMR spectrum of crystals of **4.3$_{\mathbf{BAC}}$** dissolved in CD_3CN. Residual PhF denoted with (*).

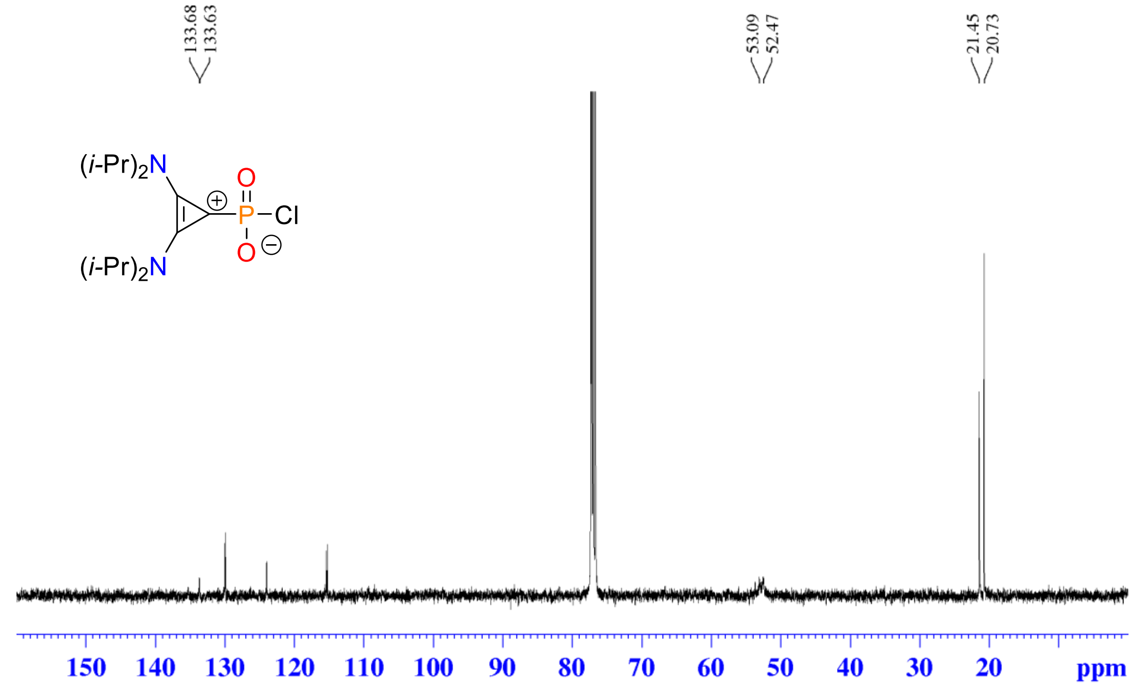

Appendix C-6. ^{13}C{^{1}H} NMR spectrum of isolated crystals of **4.3$_{\mathbf{BAC}}$** in $CDCl_3$.

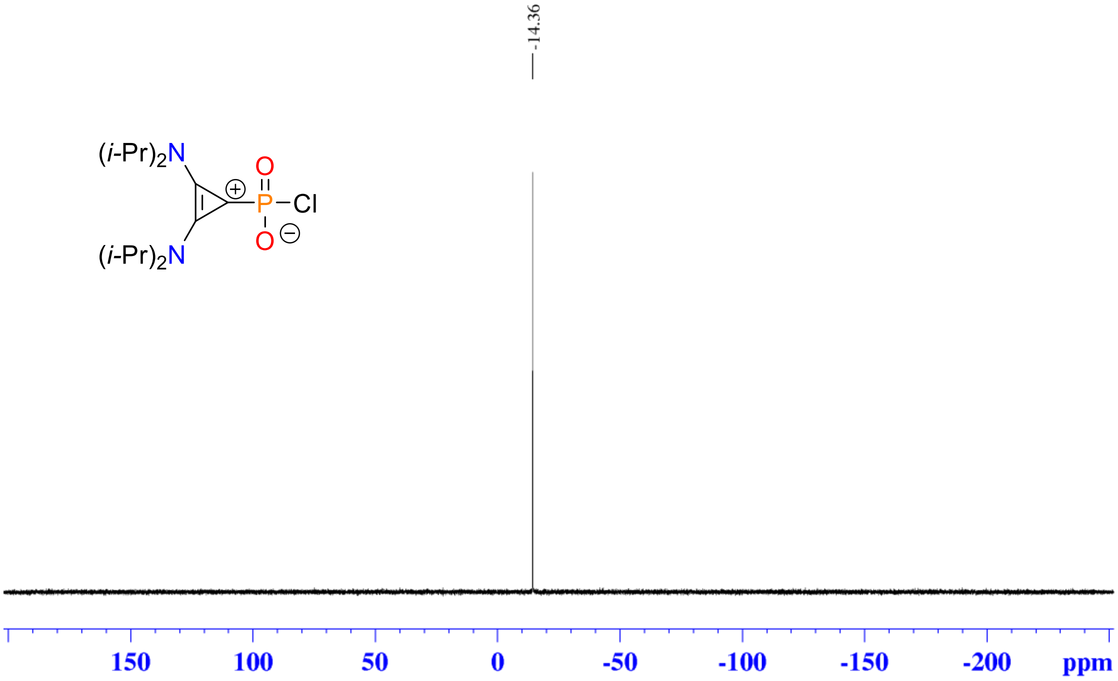

Appendix C-7. $^{31}P\{^{1}H\}$ NMR spectrum of isolated crystals of **4.3_{BAC}** in $CDCl_3$.

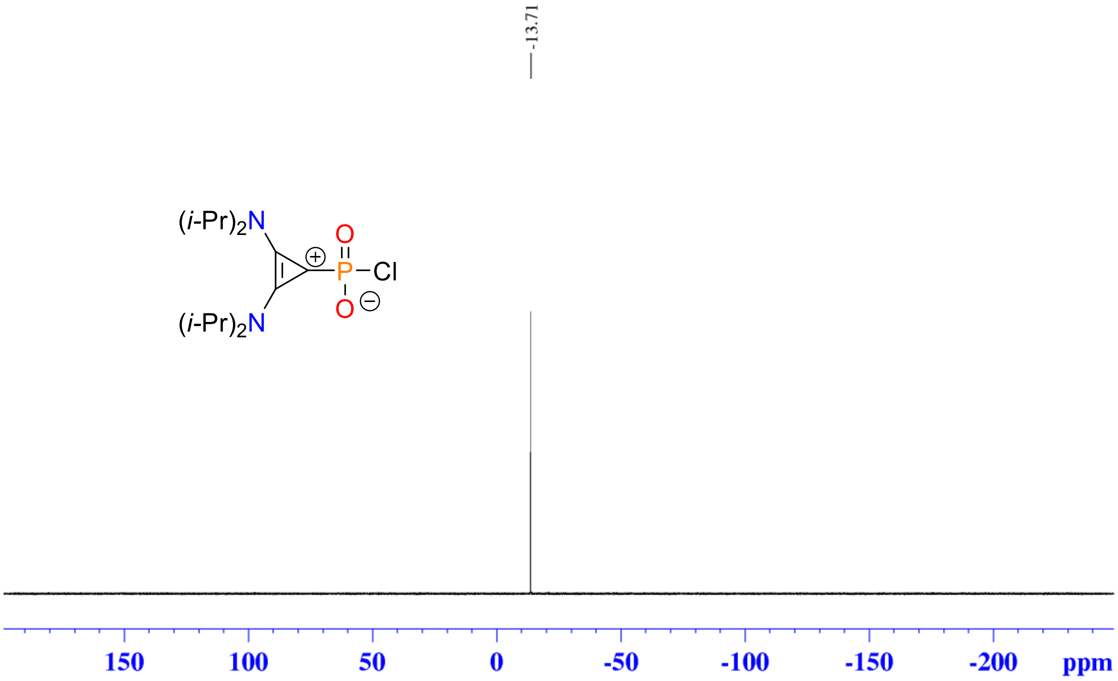

Appendix C-8. $^{31}P\{^{1}H\}$ NMR spectrum of **4.3_{BAC}** in CD_3CN.

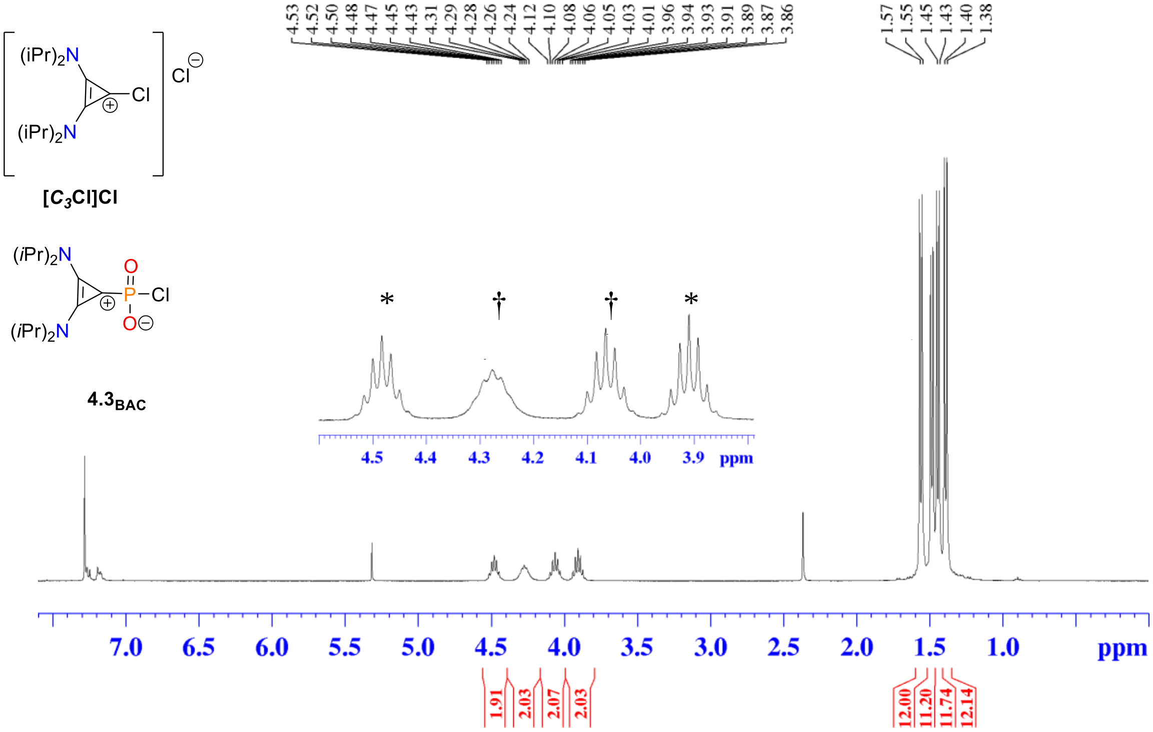

Appendix C-9. ^{1}H NMR spectrum of 50:50 mixture of **4.3BAC** (†) and **[C_3Cl]Cl** (*).

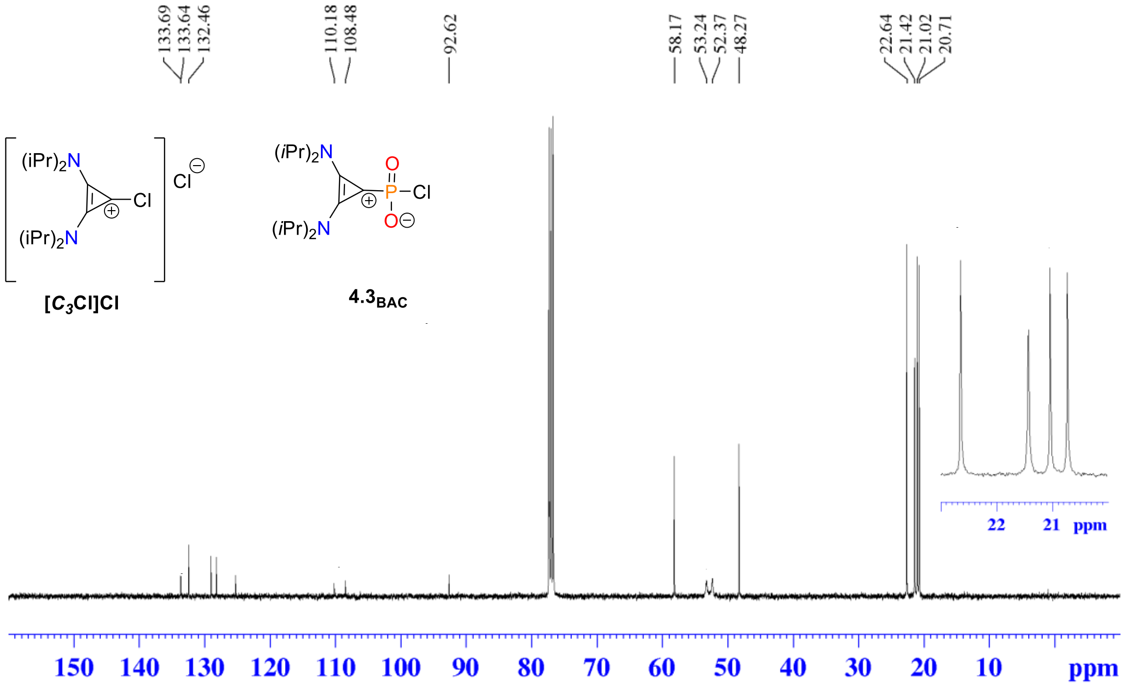

Appendix C-10. ^{13}C{^{1}H} NMR spectrum of 50:50 mixture of **4.3BAC** and **[C_3Cl]Cl**.

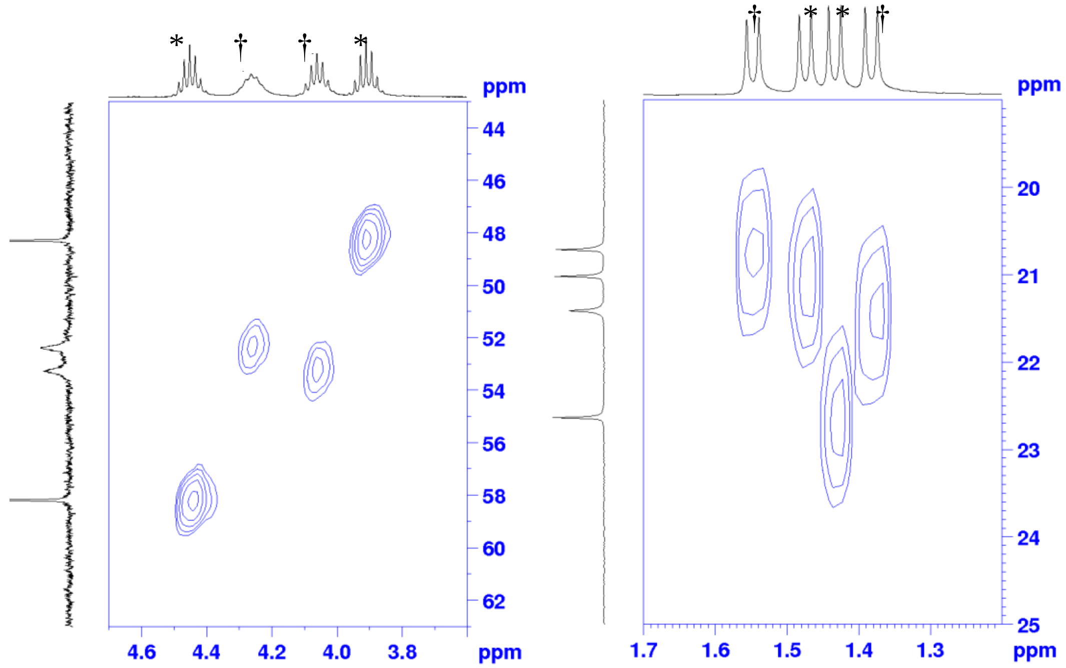

Appendix C-11. ^{1}H- ^{13}C HSQC NMR spectra of **4.3**$_{\textbf{BAC}}$ (†) and **[*C*$_3$Cl]Cl** (*) in CDCl$_3$. Left: Correlations of isopropyl groups. Right: Correlations of methyl groups.

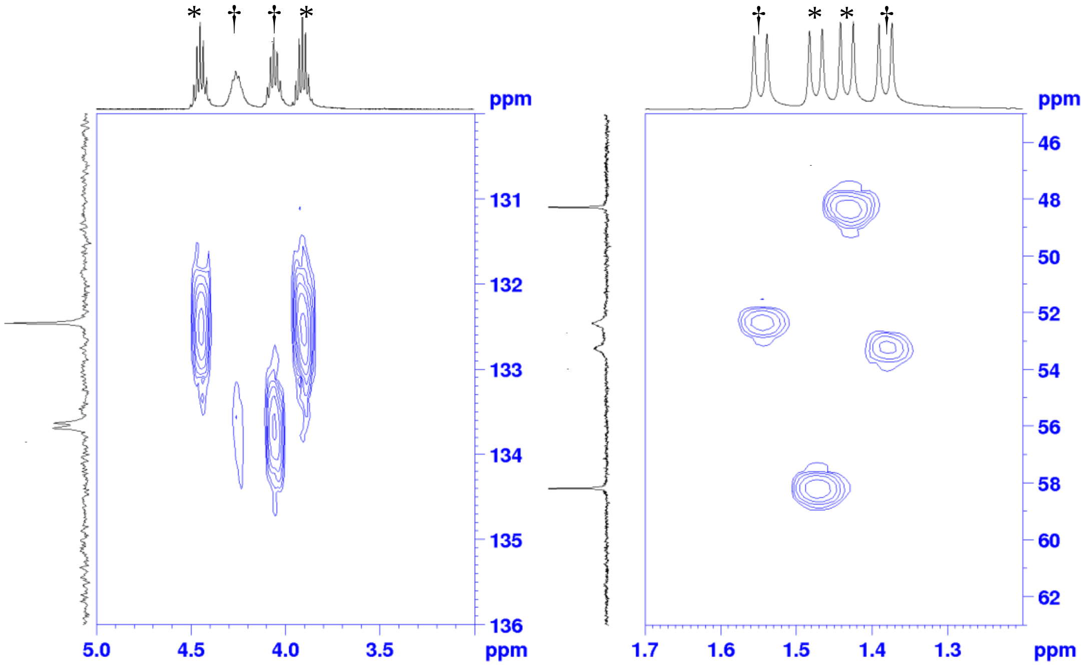

Appendix C-12. ^{1}H - ^{13}C HMBC NMR spectra of **4.3**$_{\textbf{BAC}}$ (†) and **[*C*$_3$Cl]Cl** (*) in CDCl$_3$. Left: correlations of isopropyl proton with cyclopropenium carbons. Right: correlations of isopropyl carbons with methyl protons.

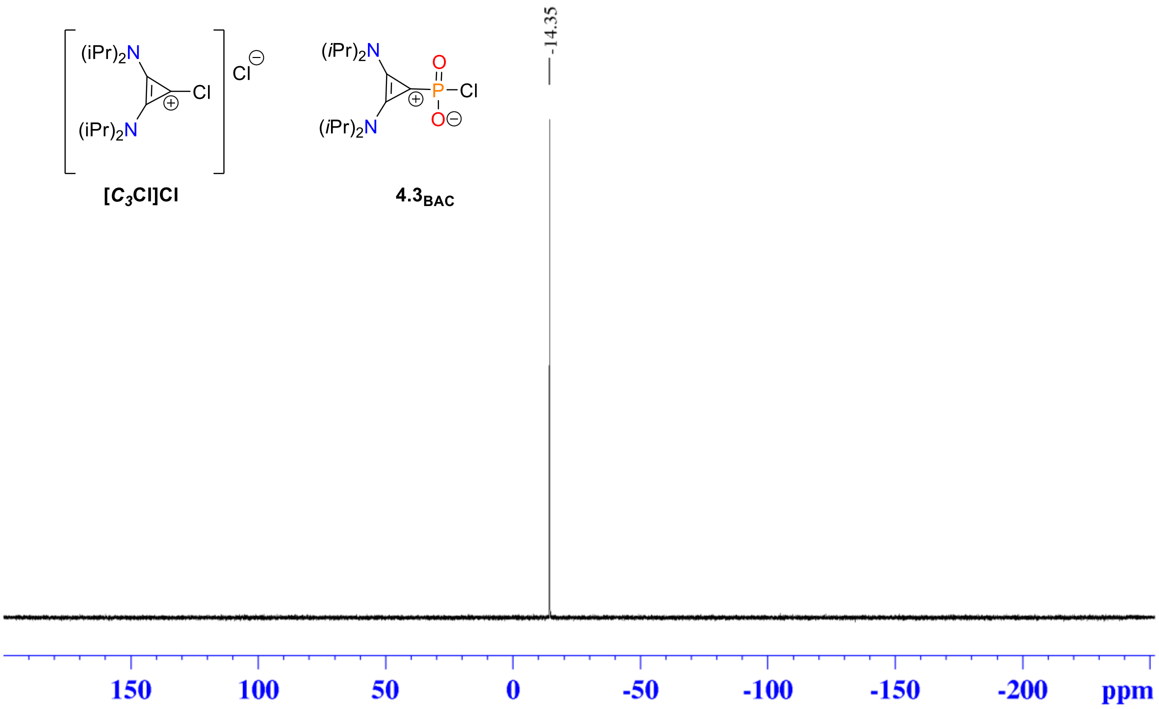

Appendix C-13. $^{31}P\{^{1}H\}$ NMR spectrum of 50:50 mixture of **4.3_{BAC}** and **[C_3Cl]Cl** in $CDCl_3$.

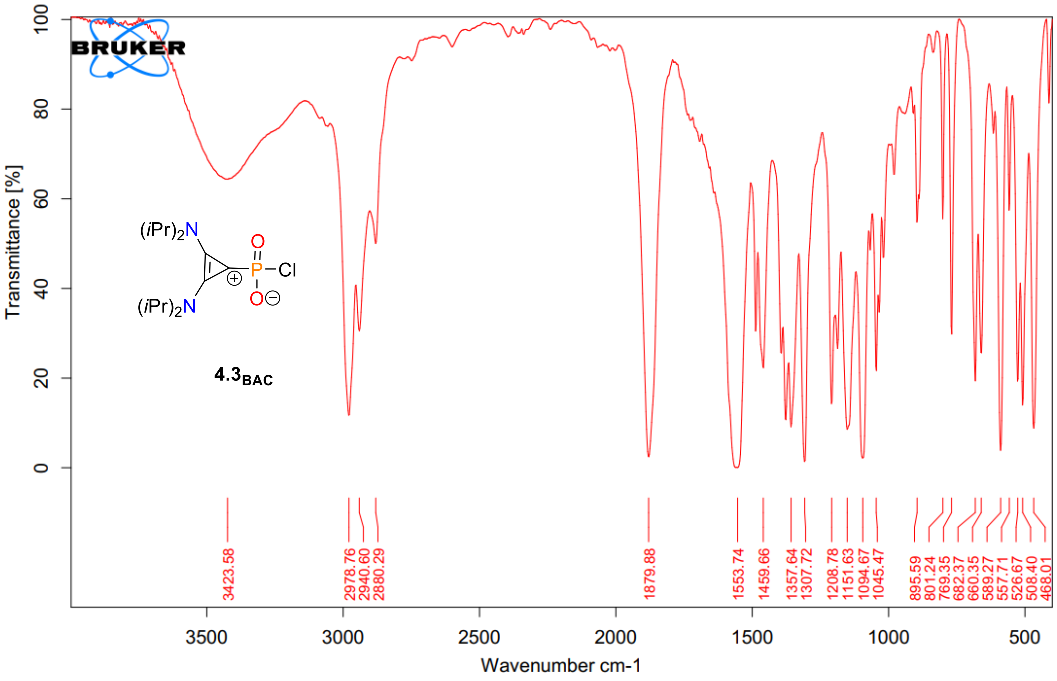

Appendix C-14. FT-IR spectrum of **4.3_{BAC}** [transmission mode].

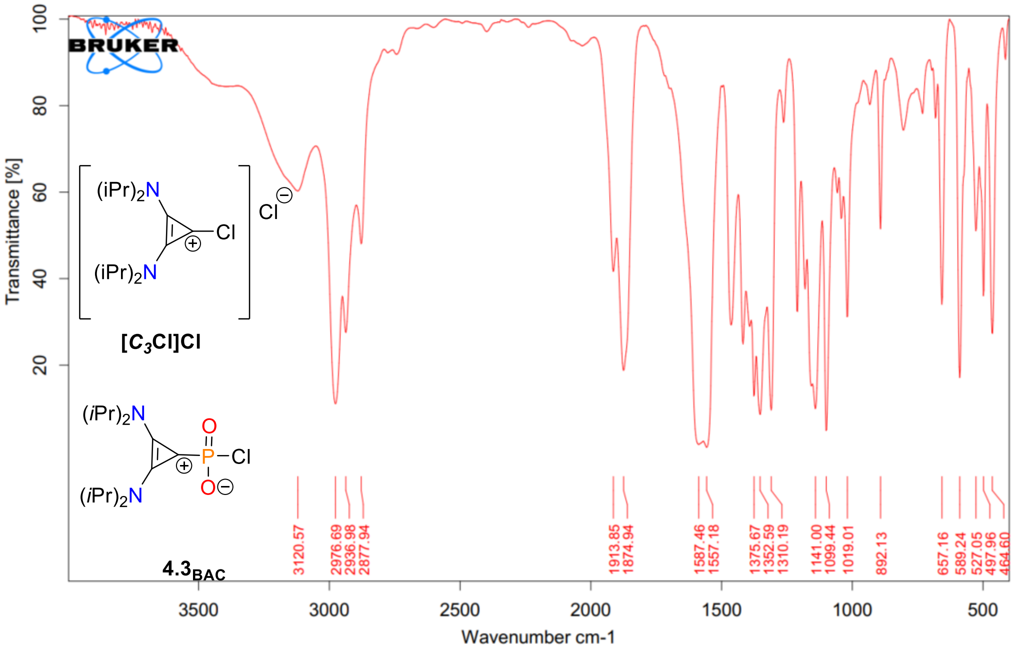

Appendix C-15. FT-IR spectrum of mixture of **4.3_{BAC}** and **[C_3Cl]Cl** [transmission mode].

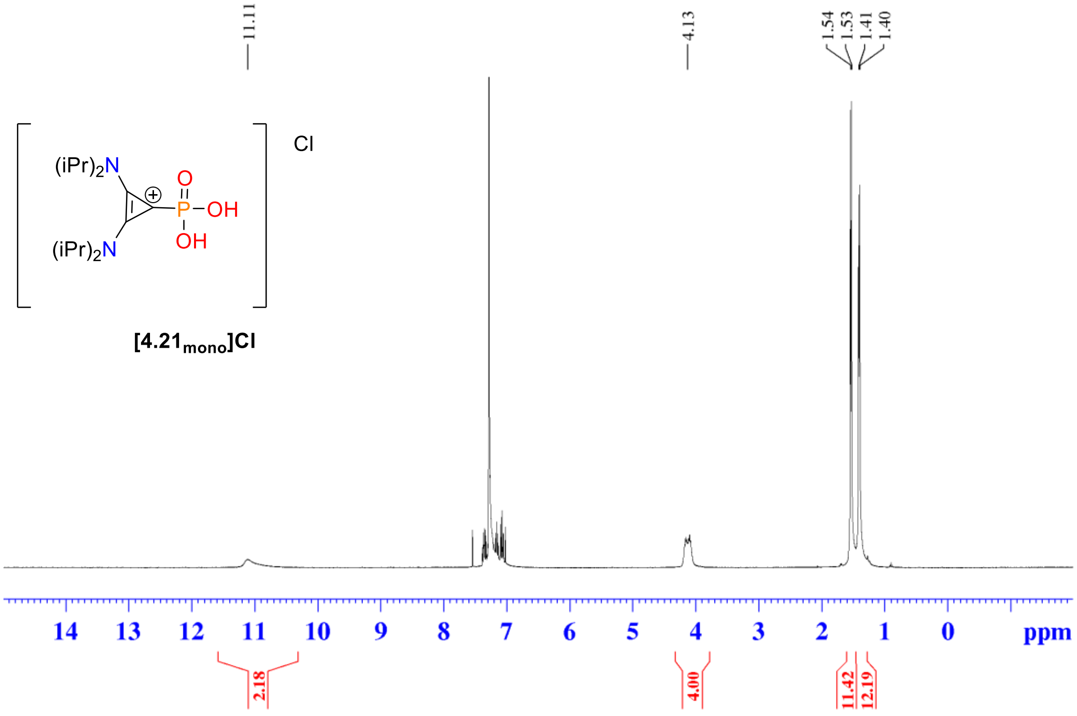

Appendix C-16. ^{1}H NMR spectrum of **[4.21_{mono}]Cl** in $CDCl_3$.

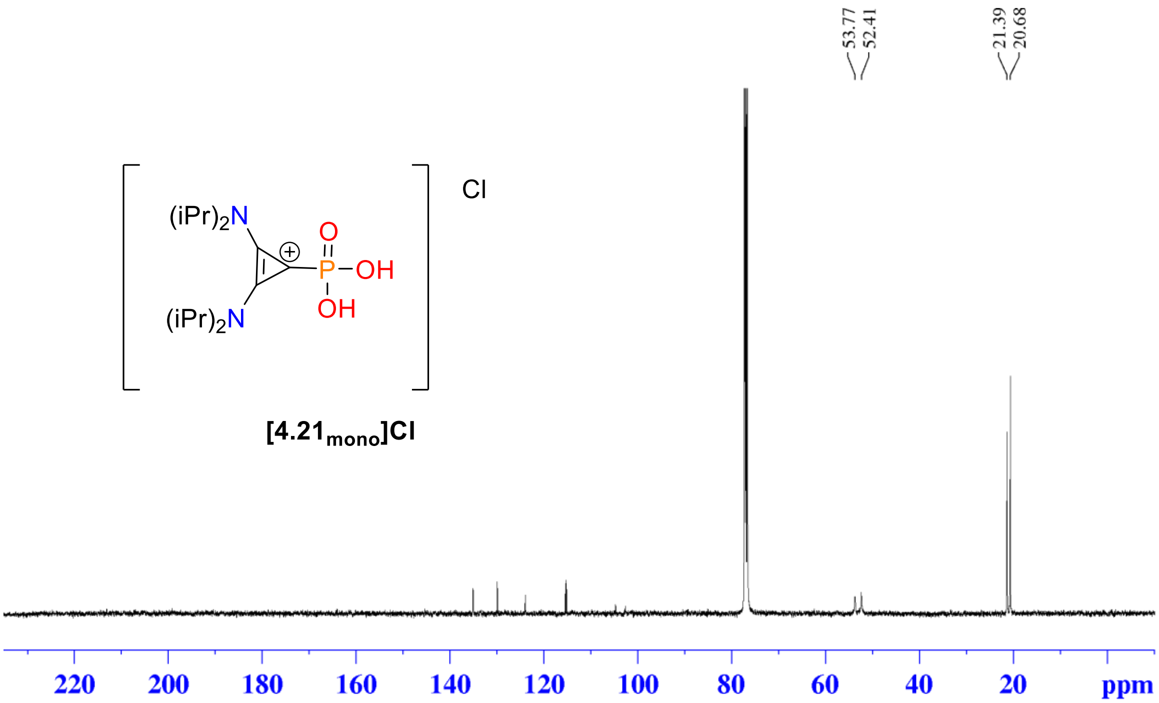

Appendix C-17. $^{13}C\{^{1}H\}$ NMR spectrum of **[4.21$_{mono}$]Cl** in $CDCl_3$. Contains PhF.

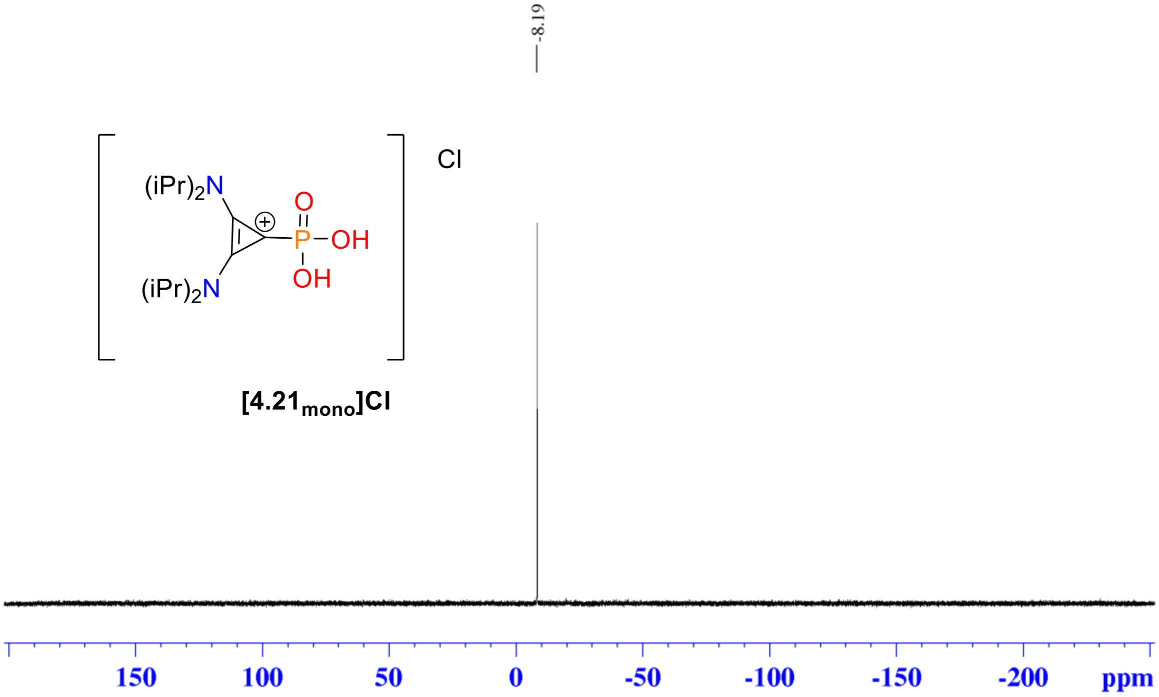

Appendix C-18. $^{31}P\{^{1}H\}$ NMR spectrum of **[4.21$_{mono}$]Cl** in $CDCl_3$.

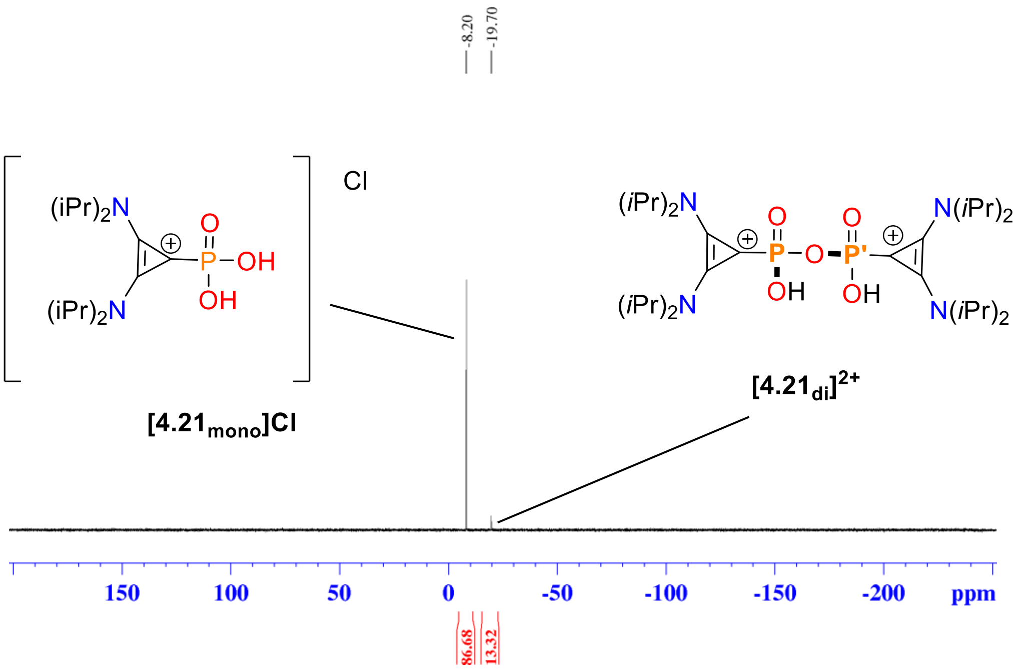

Appendix C-19. $^{31}P\{^{1}H\}$ NMR spectrum of partial hydrolysis of **4.3_{BAC}**. Intermediate hydrolysis species **$[4.21_{di}]^{2+}$** detected at -19.7 ppm.

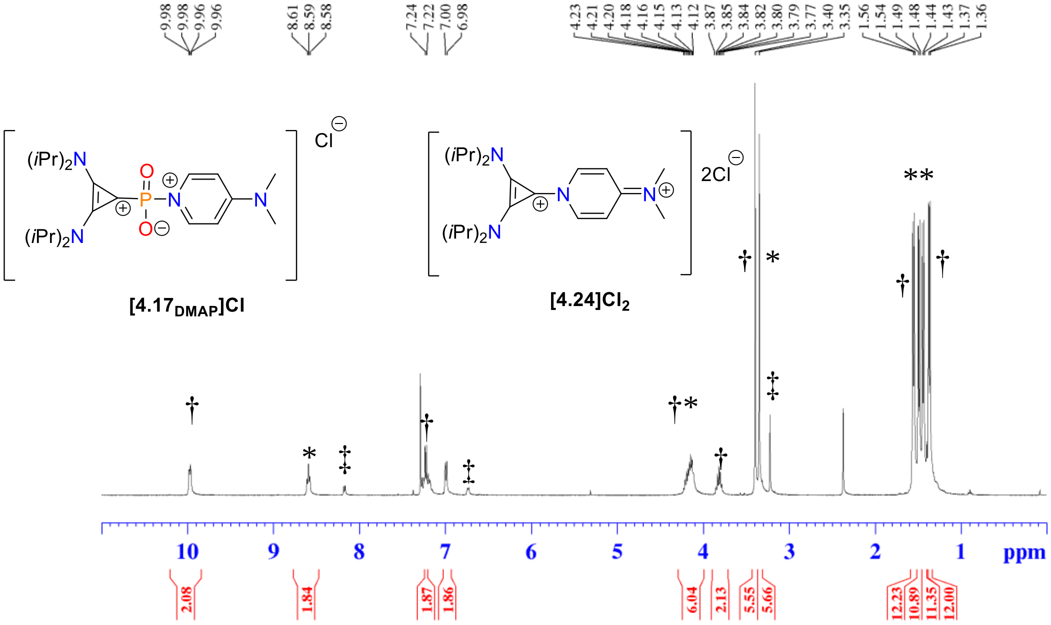

Appendix C-20. ^{1}H NMR spectrum of crude mixture of **$[4.17_{DMAP}]Cl$** (*), **$[4.24]Cl_2$** (†), and DMAP (‡) in $CDCl_3$.

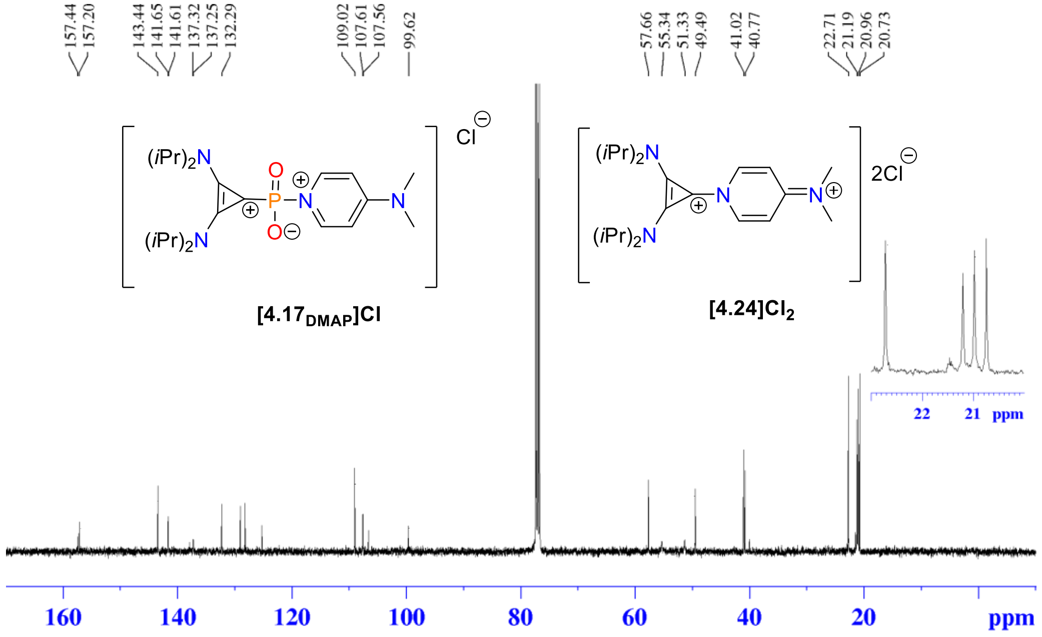

Appendix C-21. $^{13}C\{^{1}H\}$ NMR spectrum of mixture of **[4.17DMAP]Cl** and **[4.24]Cl** in $CDCl_3$.

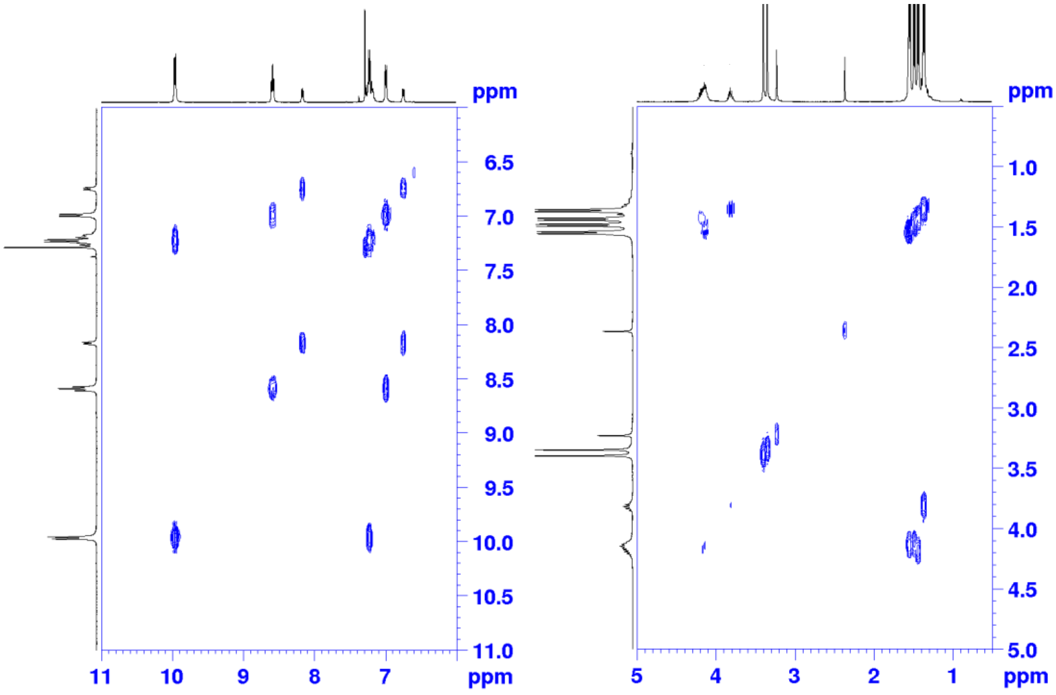

Appendix C-22. ^{1}H – ^{1}H COSY NMR spectra of **[4.17DMAP]Cl**, **[4.24]Cl2**, and DMAP ($CDCl_3$).

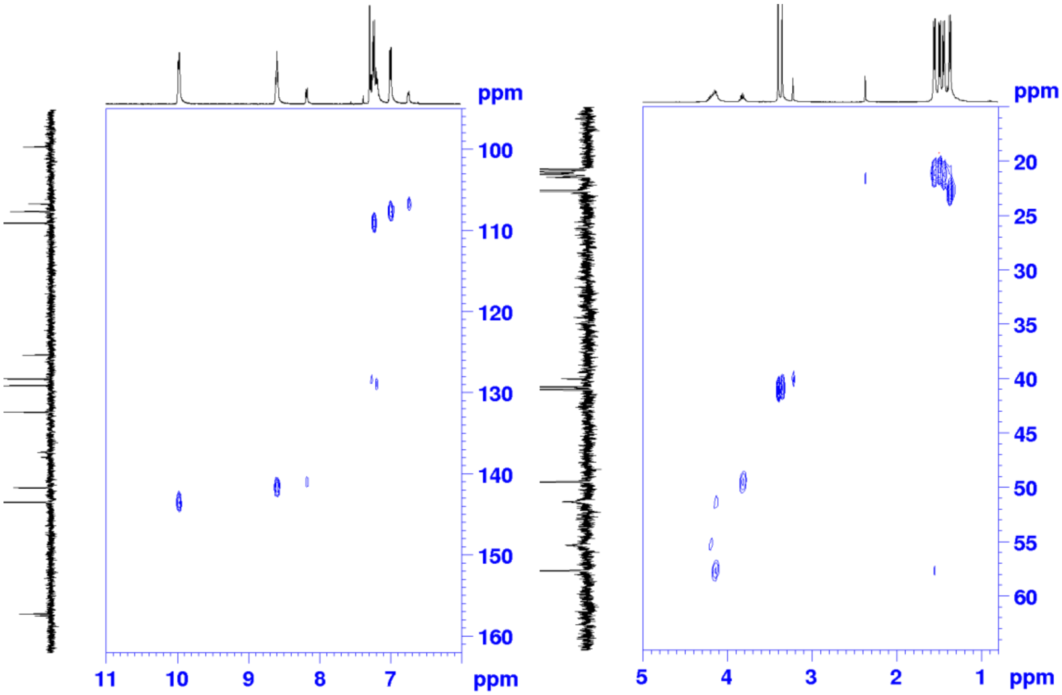

Appendix C-23. ^{1}H – ^{13}C HSQC NMR spectra of **[4.17$_{DMAP}$]Cl**, **[4.24]Cl$_2$**, and DMAP.

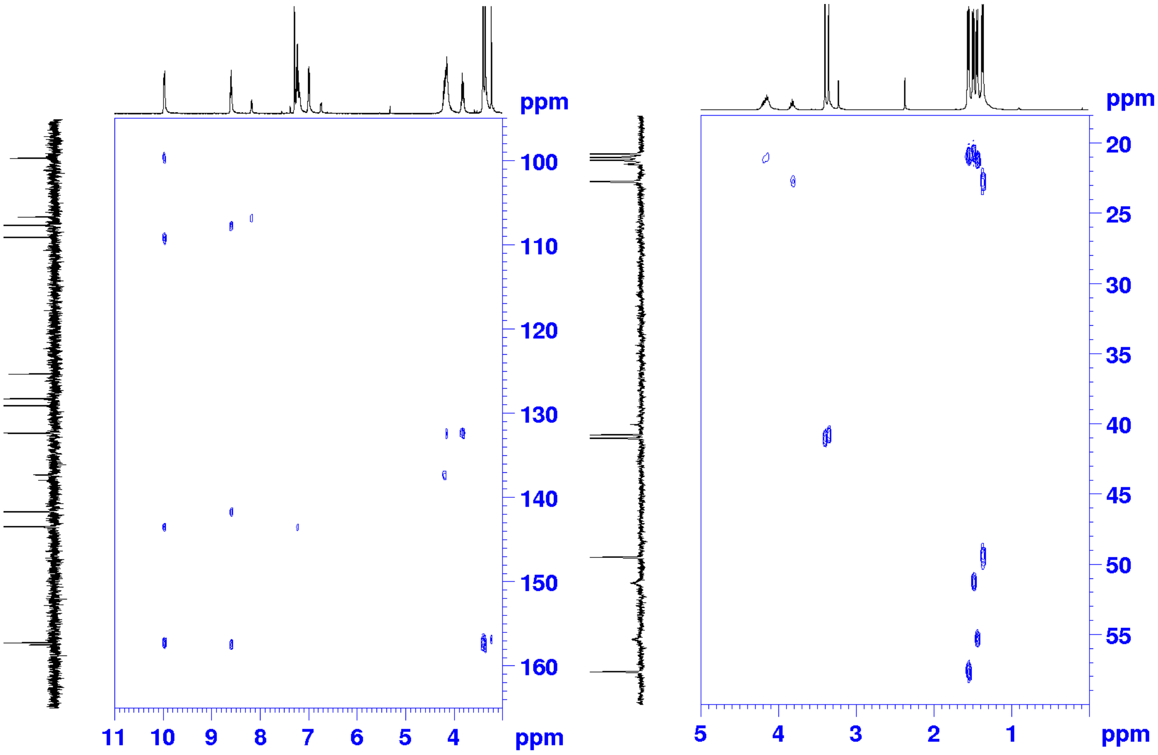

Appendix C-24. ^{1}H - ^{13}C HMBC NMR spectra of **[4.17$_{DMAP}$]Cl** and **[4.24]Cl$_2$**.

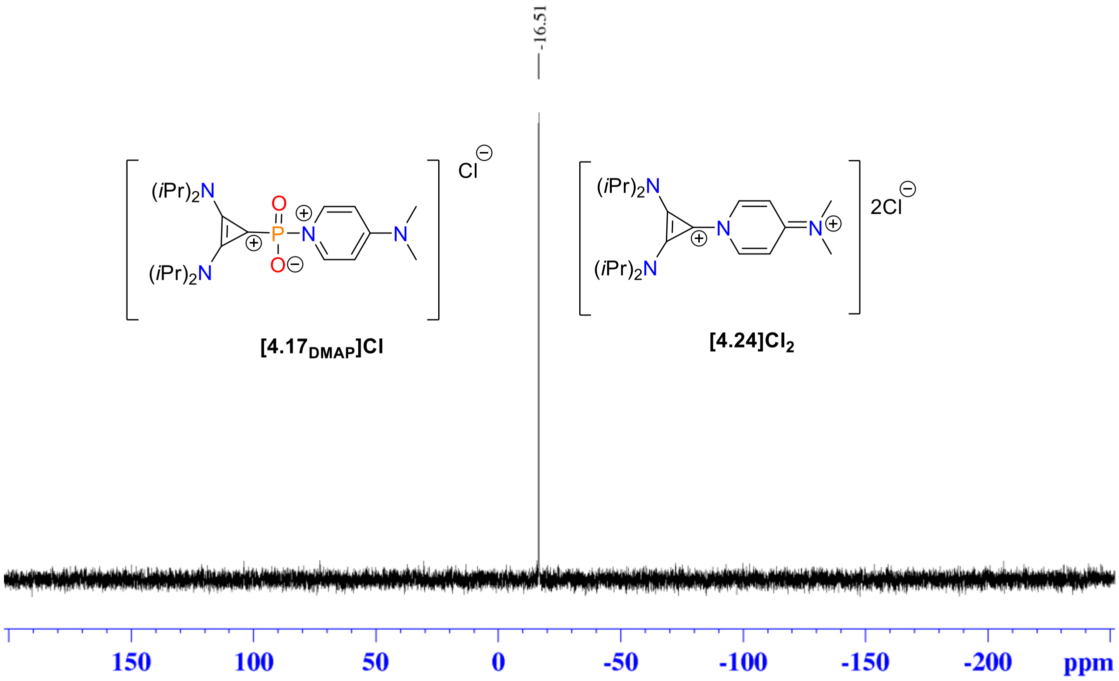

Appendix C-25. $^{31}P\{^{1}H\}$ NMR spectrum of crude reaction mixture containing **[4.17$_{\text{DMAP}}$]Cl**, **[4.24]Cl**, and slight excess DMAP.

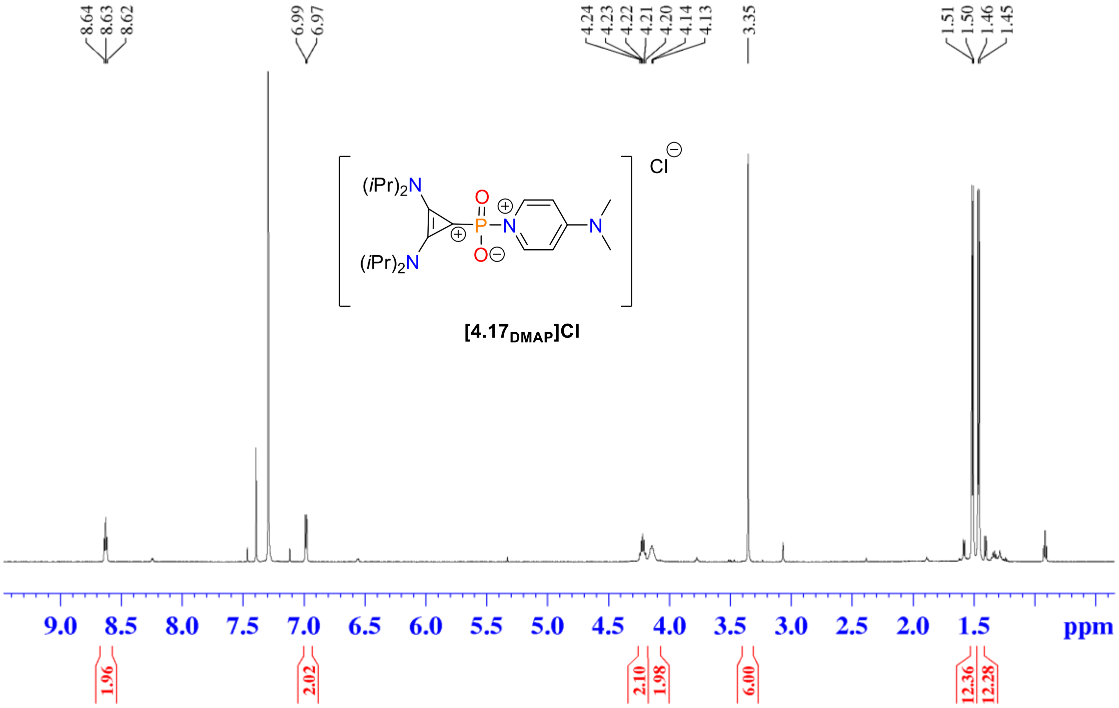

Appendix C-26. ^{1}H NMR spectrum of solids of **[4.17$_{\text{DMAP}}$]Cl** precipitated from CH_2Cl_2/hexanes.

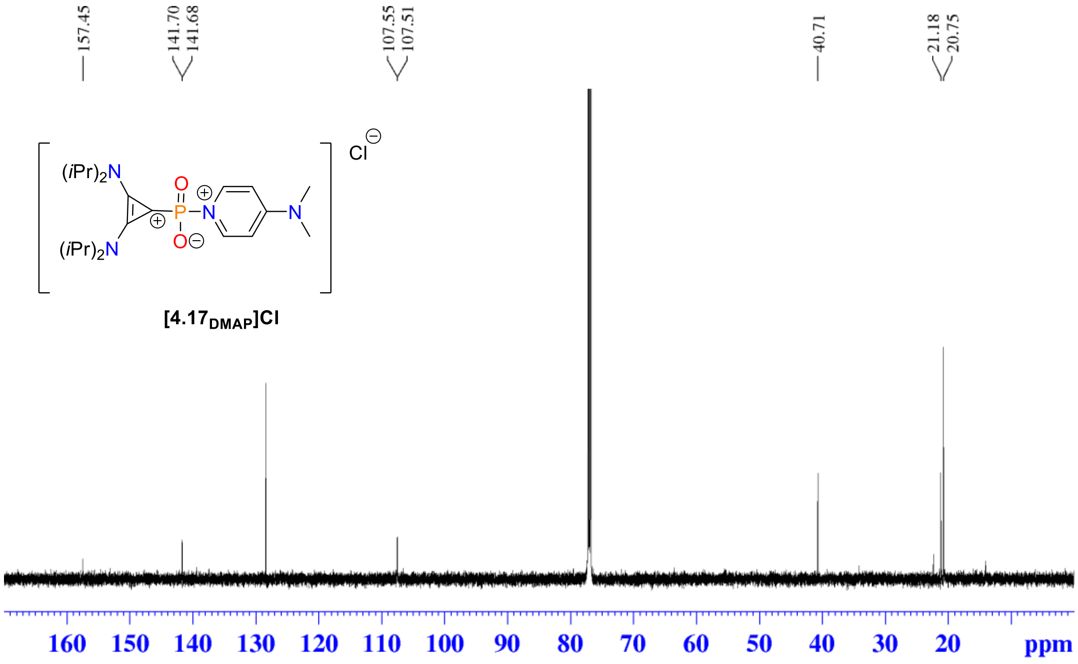

Appendix C-27. ^{31}C{^{1}H} NMR spectrum of isolated **[4.17$_{\text{DMAP}}$]Cl** in CDCl$_3$. Note: cyclopropenium carbons were not detected.

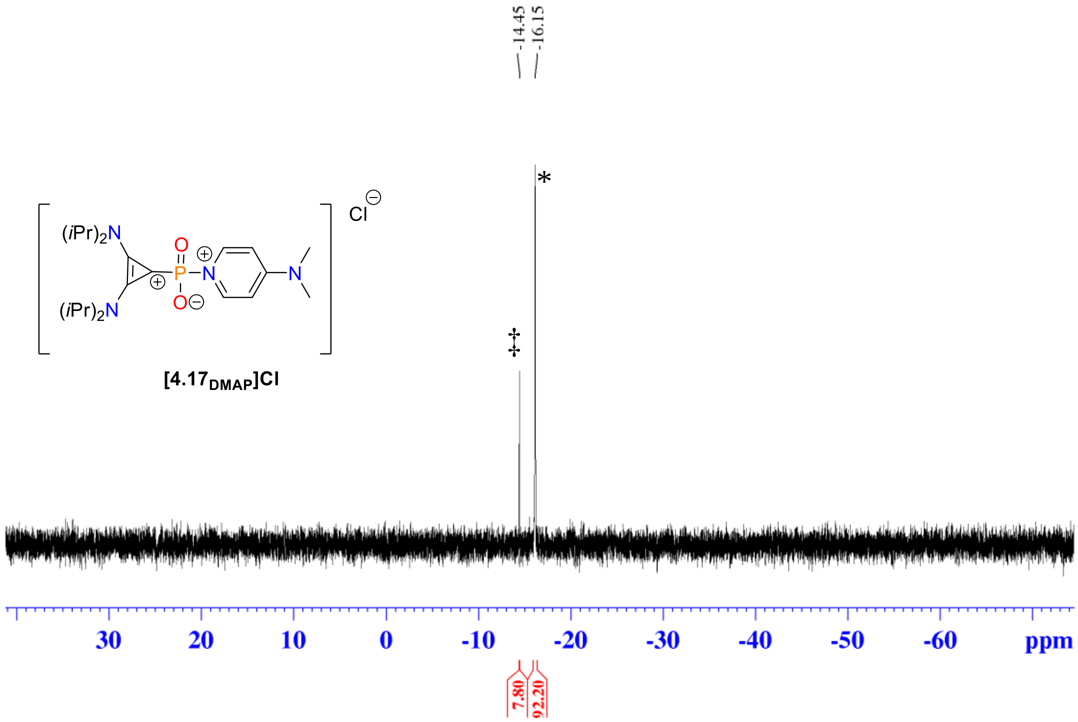

Appendix C-28. ^{31}P{^{1}H} NMR spectrum of isolated crystals of **[4.17$_{\text{DMAP}}$]Cl** (*) in CDCl$_3$. Spectrum contains free **4.3$_{\text{BAC}}$** (‡).

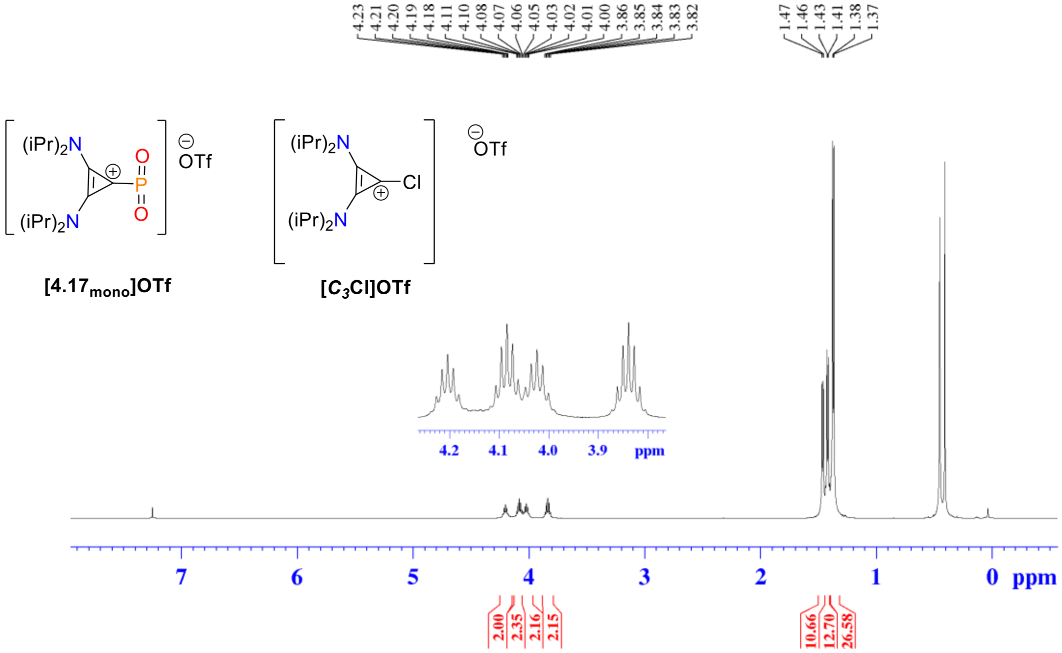

Appendix C-29. ^{1}H NMR spectrum of **[4.17$_{\text{mono}}$]OTf** and **[*C*$_{3}$Cl]OTf** in CDCl$_3$. Contains SiMe$_3$Cl and SiMe$_3$OTf.

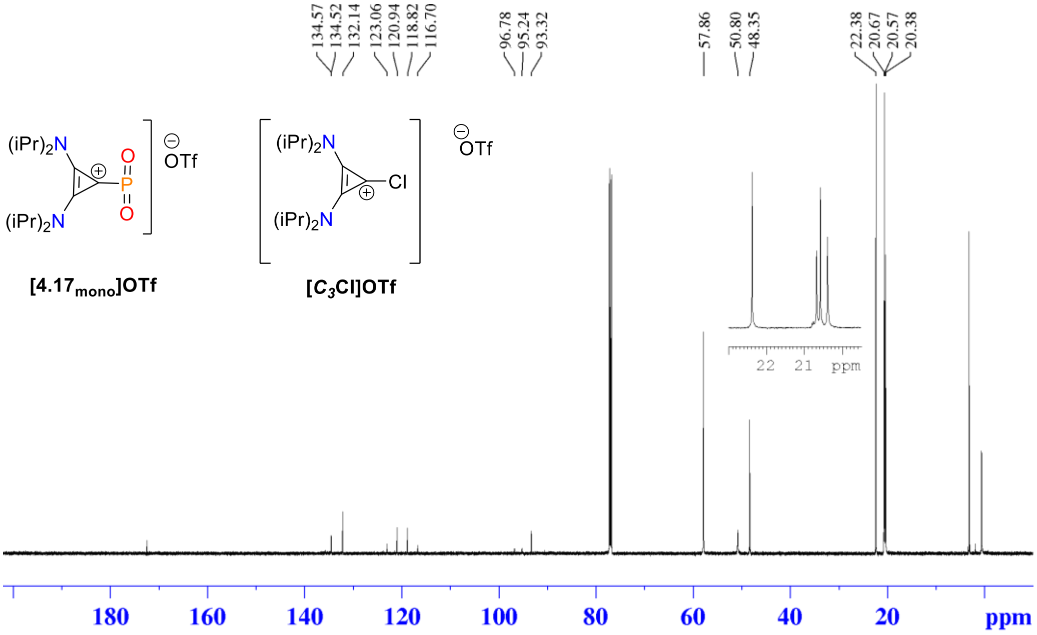

Appendix C-30. ^{13}C{^{1}H} NMR spectrum of **[4.17$_{\text{mono}}$]OTf** and **[*C*$_{3}$Cl]OTf** in CDCl$_3$. Sample contains SiMe$_3$OTf and SiMe$_3$Cl.

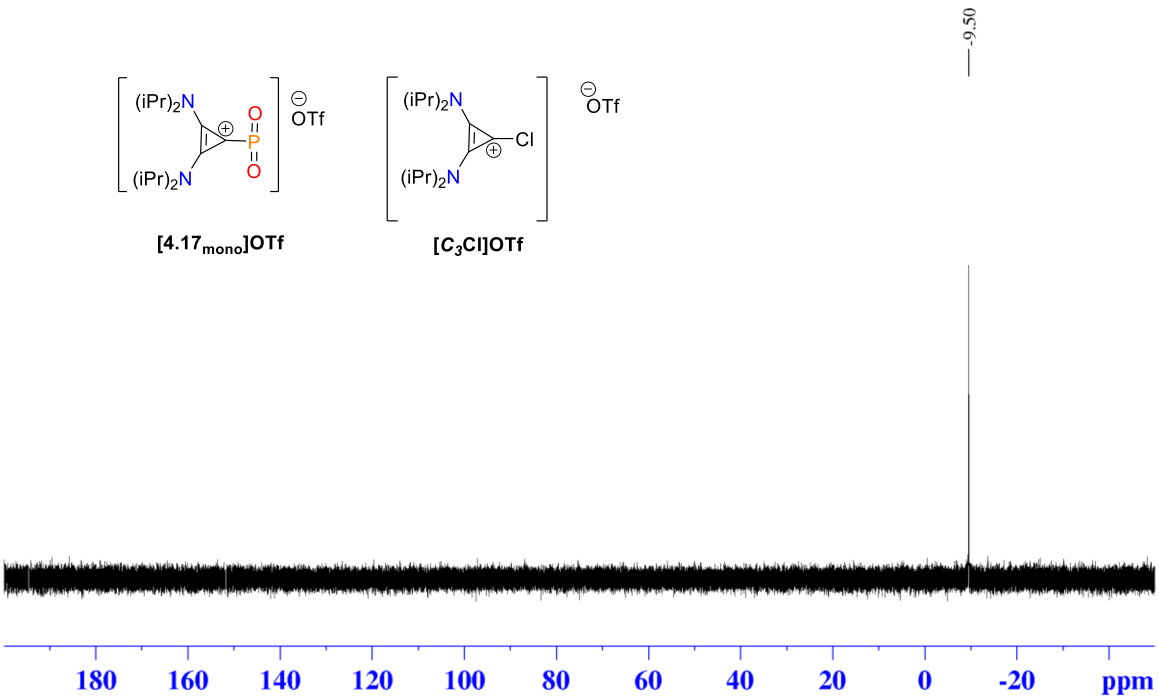

Appendix C-31. $^{31}P\{^1H\}$ NMR spectrum of **[4.17$_{mono}$]OTf** and **[*C*$_3$Cl]OTf** in CDCl$_3$.

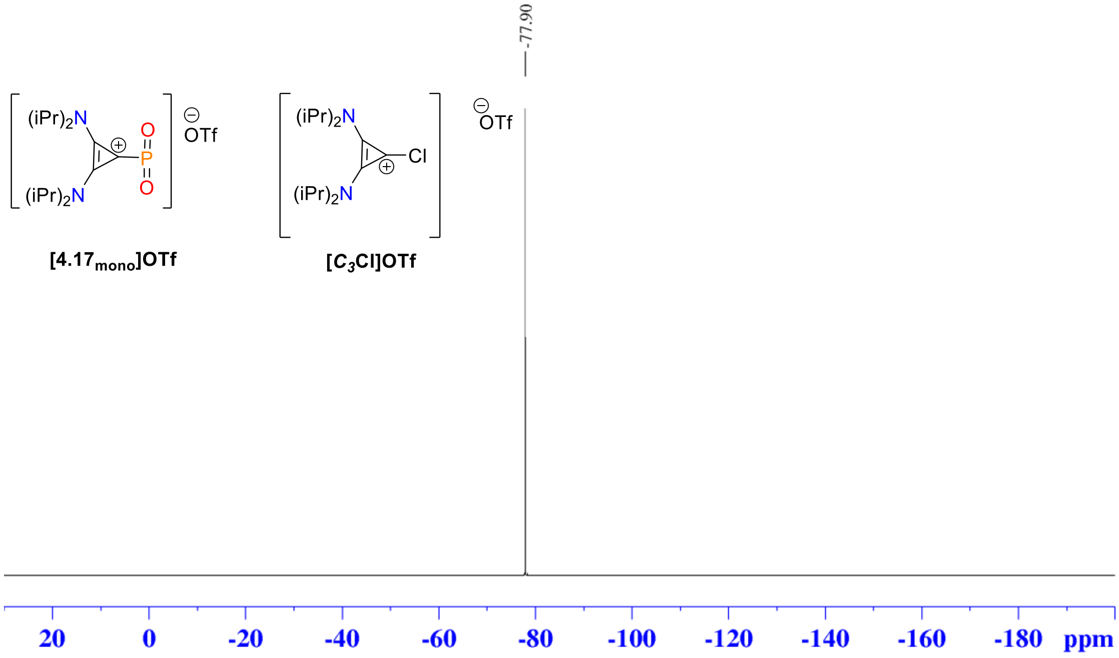

Appendix C-32. $^{19}F\{^1H\}$ NMR spectrum of **[4.17$_{mono}$]OTf** and **[*C*$_3$Cl]OTf** in CDCl$_3$.

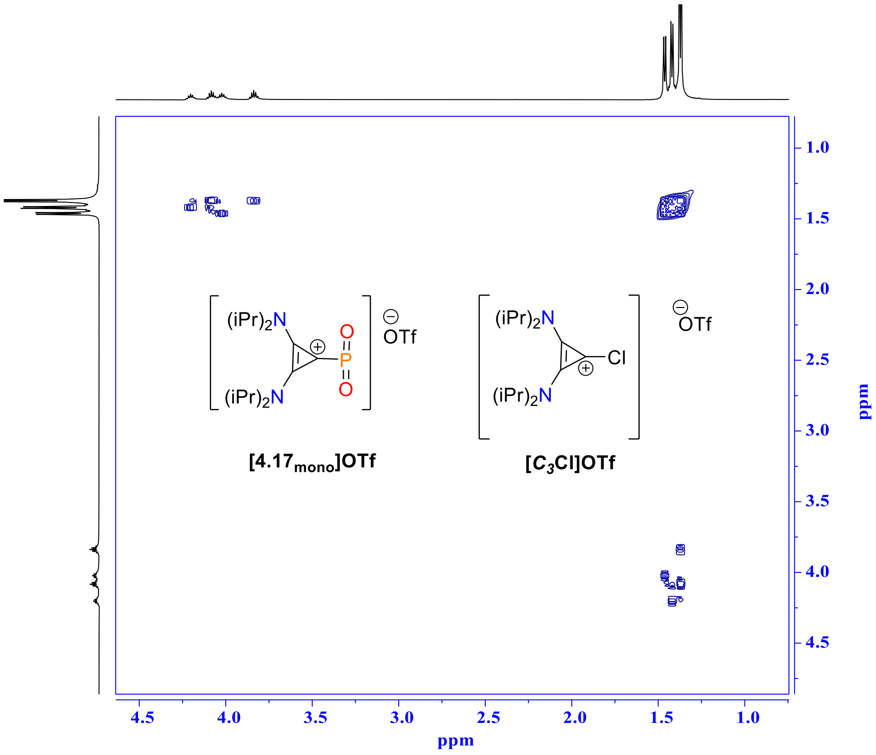

Appendix C-33. ^{1}H - ^{1}H COSY NMR spectra of **[*C$_3$*Cl]OTf** and **[4.17$_{mono}$]OTf**.

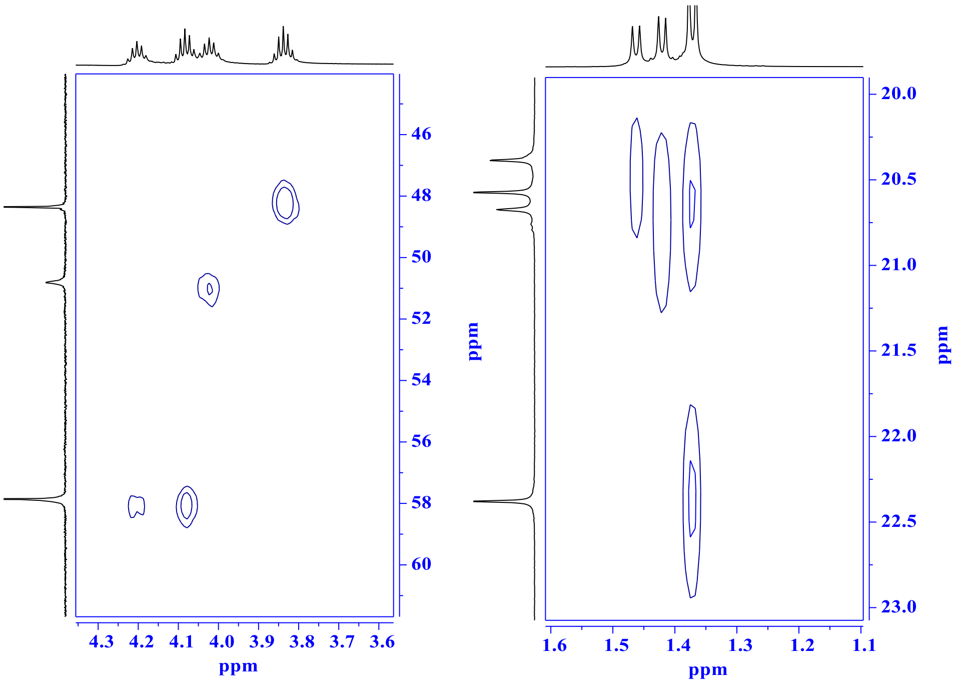

Appendix C-34. ^{1}H - ^{13}C HSQC NMR spectra of **[*C$_3$*Cl]OTf** and **[4.17$_{mono}$]OTf** in CDCl$_3$.

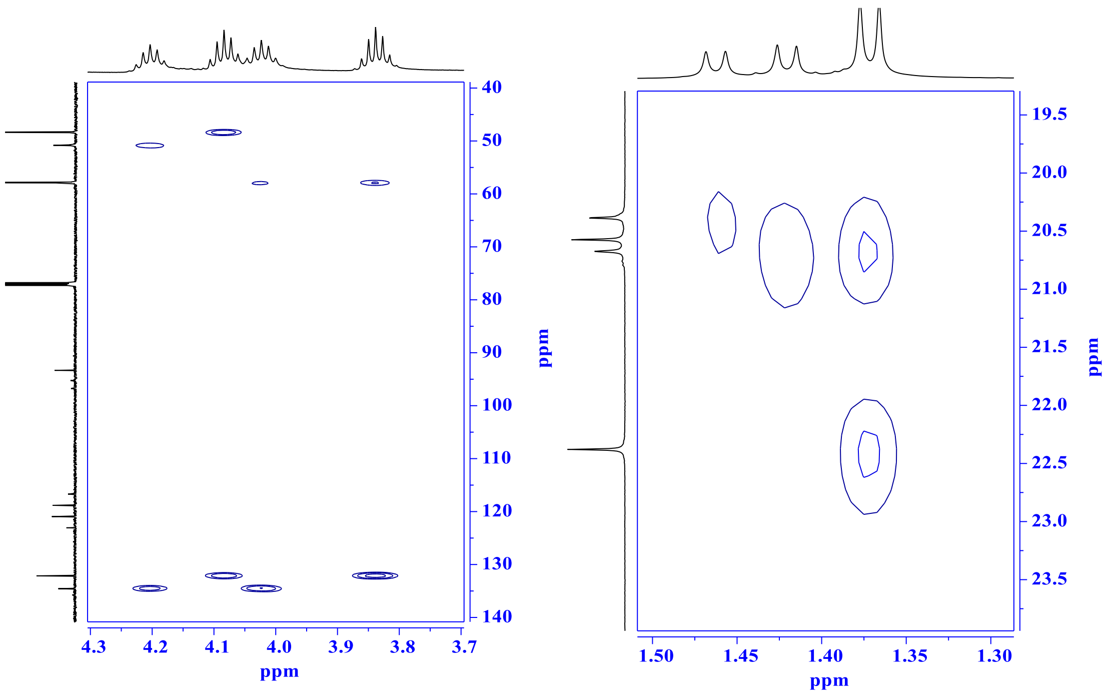

Appendix C-35. ^{1}H - ^{13}C HMBC NMR spectra of **[*C*$_3$Cl]OTf** and **[4.17$_{mono}$]OTf** in CDCl$_3$.

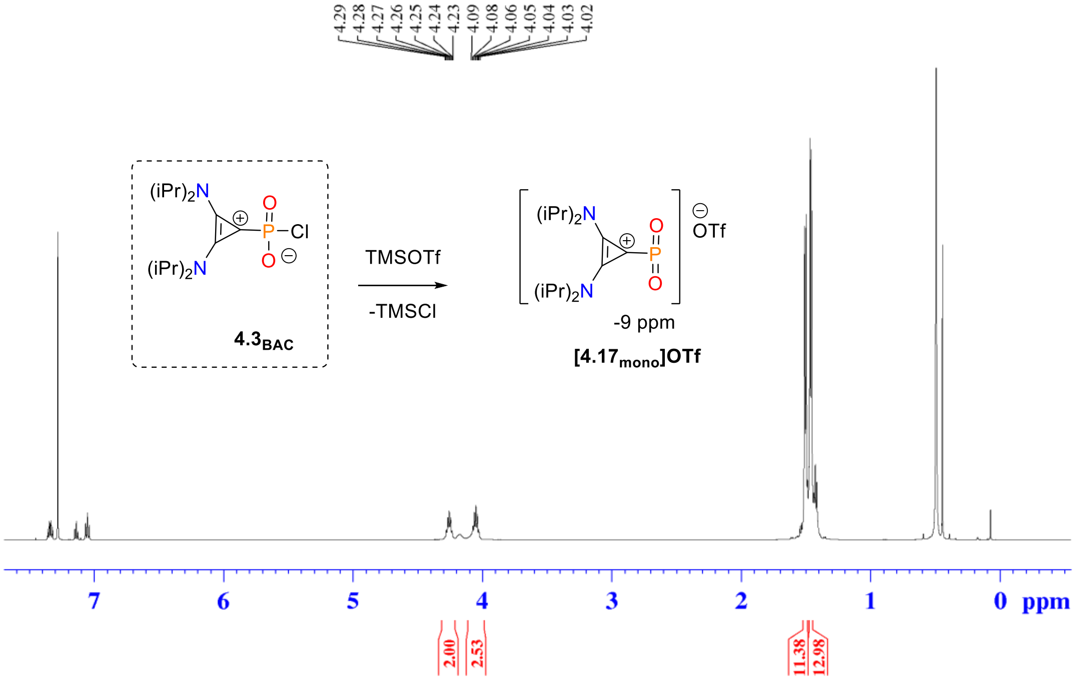

Appendix C-36. ^{1}H NMR spectrum of reaction of **4.3$_{BAC}$** with SiMe$_3$OTf. Contains SiMe$_3$Cl and SiMe$_3$OTf.

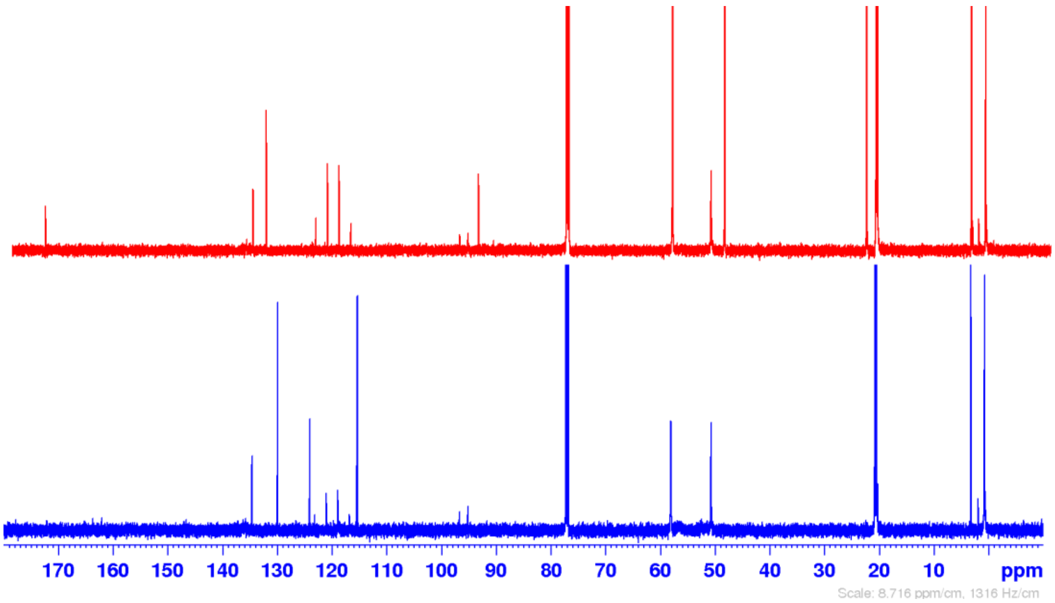

Appendix C-37. Stacked $^{13}C\{^1H\}$ NMR spectra of **[4.17$_{mono}$]OTf** generated *in situ*. Top: Mixture of **[4.17$_{mono}$]OTf** and **[*C*$_3$Cl]OTf**. Bottom: Prepared from isolated **4.3$_{BAC}$** (contains PhF).

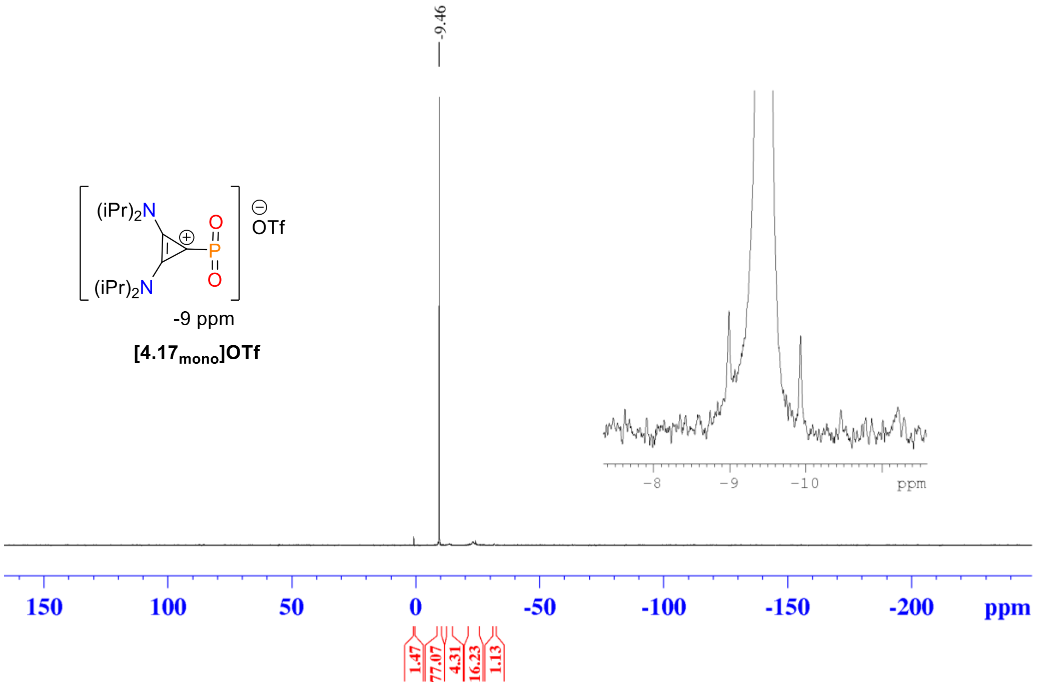

Appendix C-38. $^{31}P\{^1H\}$ NMR spectrum of crude reaction mixture of **4.3$_{BAC}$** with SiMe$_3$OTf. Inset contains zoomed in spectrum showing P-C coupling of monomeric **[4.17$_{mono}$]$^+$**.

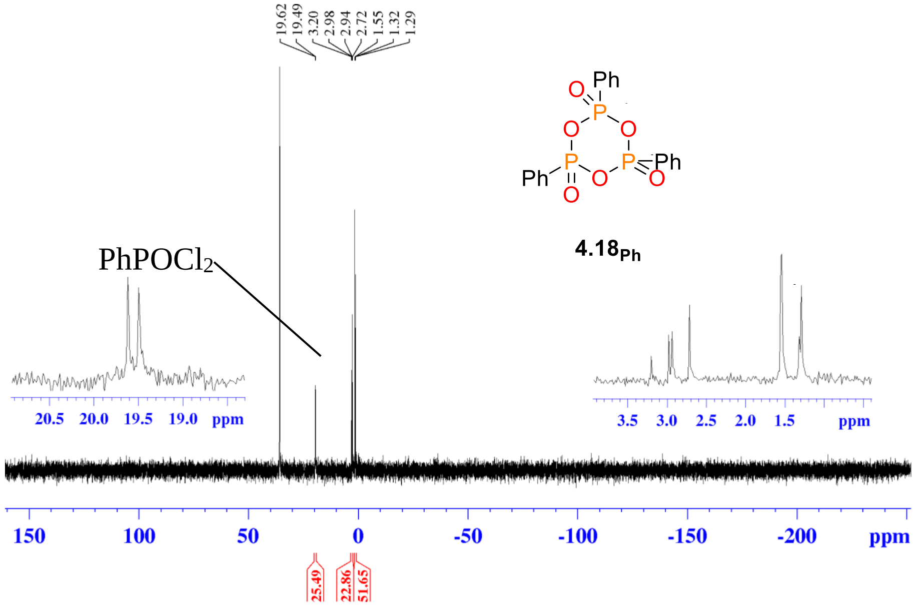

Appendix C-39. $^{31}P\{^1H\}$ NMR spectrum of crude reaction aliquot of ***C*₃*O*** and $PhPOCl_2$ to generate **4.18_{Ph}**.

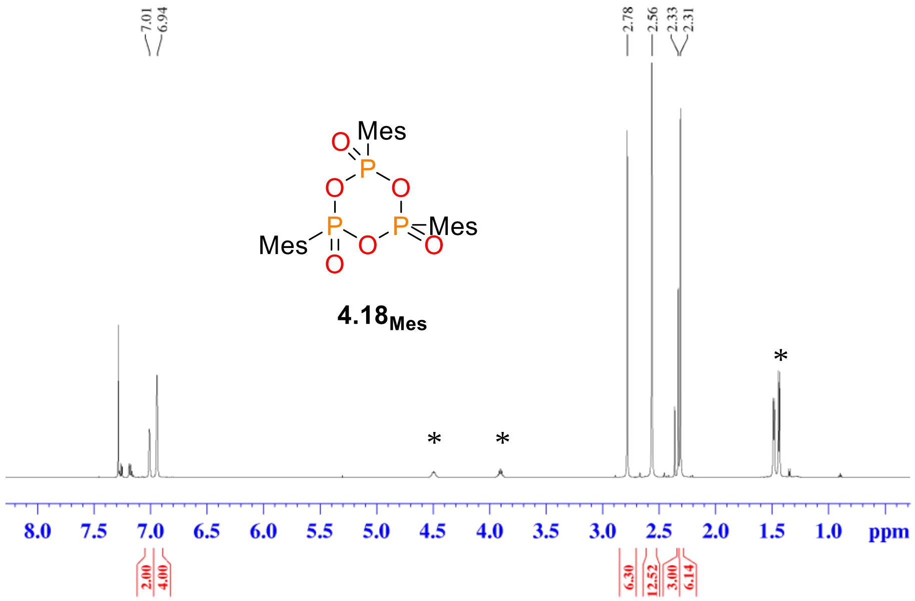

Appendix C-40. ^1H NMR spectrum of solids isolated after reaction of ***C_3O*** and $MesPOCl_2$, redissolved in $CDCl_3$. Contains **[*C_3*Cl]Cl** (*).

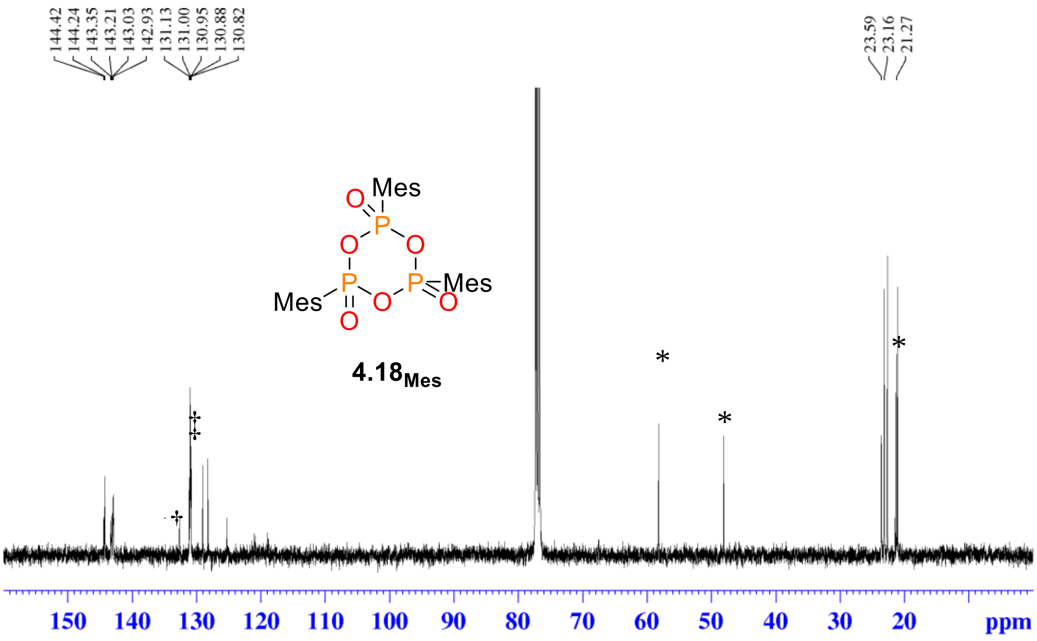

Appendix C-41. $^{13}C\{^1H\}$ NMR spectrum of solids isolated after reaction of ***C*₃*O*** and $MesPOCl_2$. Contains **[*C*₃Cl]Cl** (*) and toluene (‡).

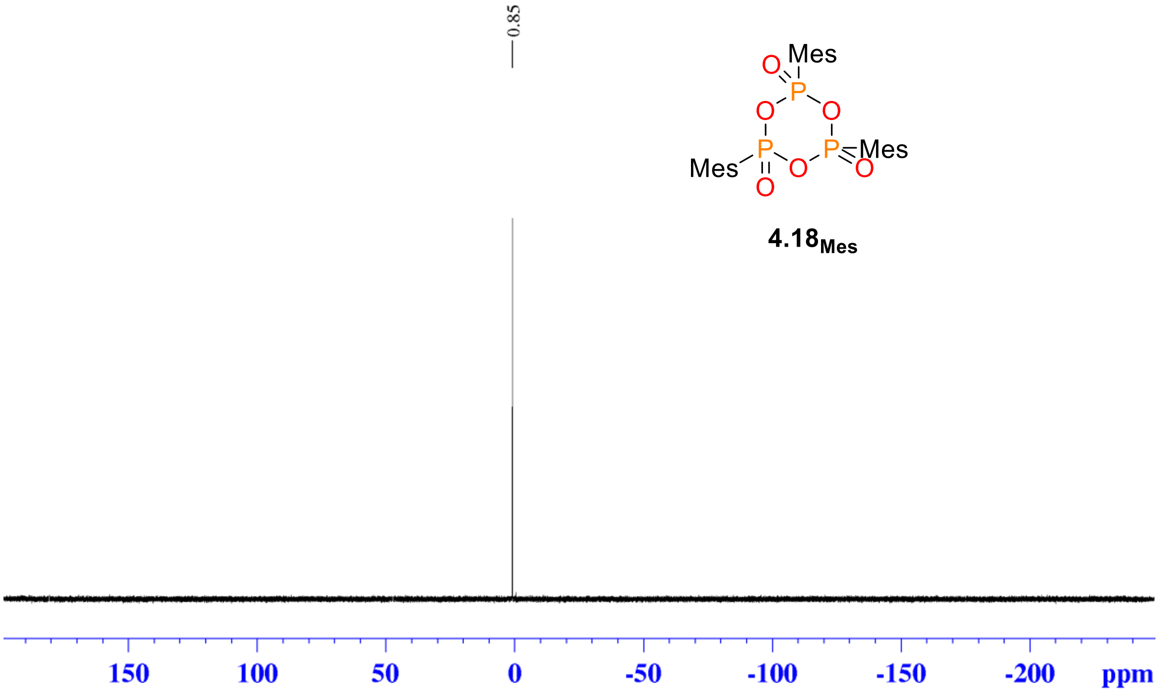

Appendix C-42. $^{31}P\{^1H\}$ NMR spectrum of precipitated **4.18Mes**, redissolved in $CDCl_3$.

.

Appendix D. Copyrights and Permissions

D1. American Chemical Society Permission

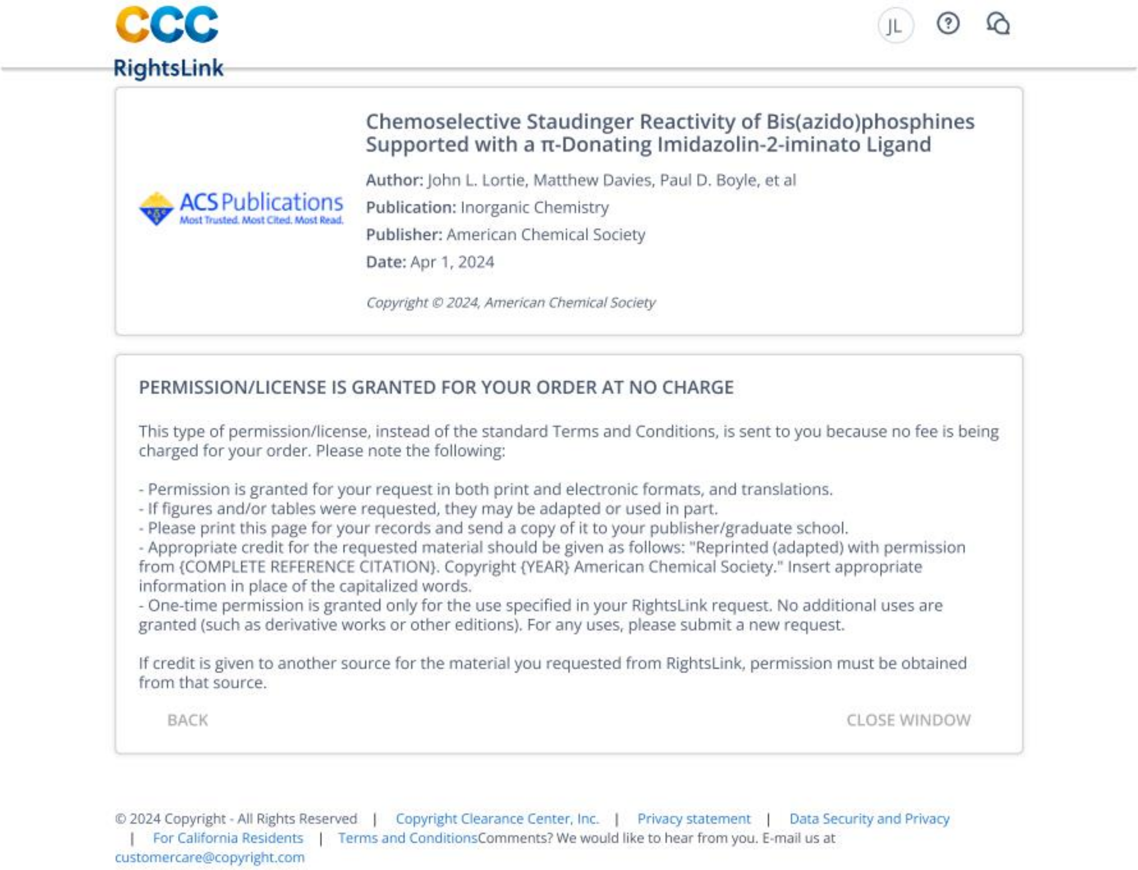

Chemoselective Staudinger Reactivity of Bis(azido)phosphines Supported with a π-Donating Imidazolin-2-iminato Ligand

Author: John L. Lortie, Matthew Davies, Paul D. Boyle, et al
Publication: Inorganic Chemistry
Publisher: American Chemical Society
Date: Apr 1, 2024

Copyright © 2024, American Chemical Society

PERMISSION/LICENSE IS GRANTED FOR YOUR ORDER AT NO CHARGE

This type of permission/license, instead of the standard Terms and Conditions, is sent to you because no fee is being charged for your order. Please note the following:

- Permission is granted for your request in both print and electronic formats, and translations.
- If figures and/or tables were requested, they may be adapted or used in part.
- Please print this page for your records and send a copy of it to your publisher/graduate school.
- Appropriate credit for the requested material should be given as follows: "Reprinted (adapted) with permission from {COMPLETE REFERENCE CITATION}. Copyright {YEAR} American Chemical Society." Insert appropriate information in place of the capitalized words.
- One-time permission is granted only for the use specified in your RightsLink request. No additional uses are granted (such as derivative works or other editions). For any uses, please submit a new request.

If credit is given to another source for the material you requested from RightsLink, permission must be obtained from that source.

© 2024 Copyright - All Rights Reserved | Copyright Clearance Center, Inc. | Privacy statement | Data Security and Privacy | For California Residents | Terms and ConditionsComments? We would like to hear from you. E-mail us at customercare@copyright.com

Appendix D-1. Screenshot of permission to use the previously published work, in chapter 3.

Curriculum Vitae

Education

Western University - London, ON 2019-present
PhD Inorganic Chemistry
Structure and Bonding of Phosphorus-chalcogenide Compounds
Supervisor: Dr. Paul Ragogna

Brock University - St. Catharines, ON 2016-2019
M.Sc. Inorganic Chemistry
N,S,N-tridentate Complexes of Zinc, Germanium, and Phosphorus
Supervisor: Dr. Georgii Nikonov

Brock University – St. Catharines, ON 2011-2016
B.Sc. Chemistry (Honours)
Zinc-hydride Catalyzed Hydrosilylation and Hydroboration of N-heterocycles
Supervisor: Dr. Georgii Nikonov

Publications

1. **John L. Lortie**, Travis Dudding, Bulat M. Gabidullin, Georgii I. Nikonov. "Zinc-Catalyzed Hydrosilylation and Hydroboration of N-Heterocycles", ACS Catalysis. 2017, 7, 8454-8459.
2. **John L. Lortie**, Matthew Davies, Paul D. Boyle, Paul J. Ragogna. "Chemoselective Staudinger Reactivity of Bis(azido)phosphines supported with a π-donating imidazolin-2-iminato ligand", *Manuscript accepted to ACS Inorganic Chemistry (March 1, 2024).*
3. **John L. Lortie**, Paul D. Boyle, Paul J. Ragogna. "Facile cyclopropenium Functionalization of PCl_3 and disproportionation of $RP(O)Cl_2$ species with Bis(diisopropylamino)cyclopropenone", *Manuscript in preparation*.

Conference Presentations

1. **John L. Lortie**, Matthew Davies, Paul D. Boyle, Paul J. Ragogna. "Exploring reactivity of N-heterocyclic imine-supported bis(azido)phosphine compounds". Canadian Chemistry Conference and Exhibition, National Conference [PhD work, Oral Presentation]
2. **John L. Lortie**, Paul D. Boyle, Paul J. Ragogna. "Facile Functionalization of Di and Trichlorophosphorus Species with Bis(diisopropylamino)cyclopropenone". Canadian Chemistry Conference and Exhibition, National Conference [PhD work, Poster Presentation]
3. **John L. Lortie**, Matthew Davies, Paul D. Boyle, Paul J. Ragogna. "Exploring reactivity of N-heterocyclic imine-supported bis(azido)phosphine compounds". 53th Annual Inorganic Discussion Weekend, Regional Conference [PhD work, Oral Presentation]

4. **John L. Lortie**, Georgii I. Nikonov. "Novel Tridentate N,S,N-Metal Complexes of Zinc, Germanium and Phosphorus". 102nd Canadian Chemistry Conference and Exhibition, National Conference [PhD work, Poster Presentation]
5. **John L. Lortie**, Georgii I. Nikonov. "Novel Tridentate N,S,N-Metal Complexes of Zinc, Germanium and Phosphorus". 51st Annual Inorganic Discussion Weekend, Regional Conference [MSc work, **Poster Presentation Award**]
6. **John L. Lortie**, Bulat M. Gabidullin, Georgii I. Nikonov. “Zinc Catalyzed Hydrosilylation and Hydroboration of N-Heterocycles”. 50th Annual Inorganic Discussion Weekend, Regional Conference [BSc work, Oral Presentation]
7. **John L. Lortie**, Georgii I. Nikonov. “Zinc Catalyzed Hydrosilylation and Hydroboration of N-Heterocycles”. 100th Canadian Chemistry Conference and Exhibition, National Conference. [BSc work, Poster Presentation]
8. **John L. Lortie**, Terry Chu, and Georgii I. Nikonov. “Zinc Hydride Catalyzed Regioselective Hydrosilylation and Hydroboration of N-Heterocycles”. 2016 Western New York American Chemical Society (WNYACS) Undergraduate Research Symposium, Regional Conference [BSc work, Oral Presentation]
9. **John L. Lortie**, Terry Chu, and Georgii I. Nikonov. “Zinc Hydride Catalyzed Regioselective Hydrosilylation and Hydroboration of N-Heterocycles”. 2016 Southern Ontario Undergraduate Student Chemistry Conference (SOUSCC), Regional Conference [BSc work, Oral Presentation]

Competitive Awards

Lipson-Baines Award in Chemistry, 2022, $1000

Queen Elizabeth II Award, 2021, $15,000 for 3 Term Tenure

Queen Elizabeth II Award, 2020, $15,000 for 3 Term Tenure

Poster Presentation Award at IDW Conference, 2018, $300

Match of Minds- Inquiring Minds, 2015, $4,500

Technology Group (Machine and Electronics Shop) Scholarship, 2012, $1,562

Teaching Experience

Western University: Lab Demonstrator and Resource Room Tutor*
Organic Chemistry I* and II, and 1st year general chemistry

Brock University: Lab Demonstrator, Seminar Leader, and Marker-Grader
Analytical Chemistry, Organic Chemistry I and II, Inorganic Chemistry I, 3rd year Organic Chemistry, and 1st year chemistry

Professional Development

Forest City Toastmasters 2021-2024

- 2022 International Speech Contest winner – Club Level
- Elected Roles on FCT Executive Committee:
    - Seargent-at-Arms, August 2023 – July 2024
    - Secretary, July 2021 - November 2021; August 2022 – July 2023
    - Vice President of Education, January 2022 - July 2022